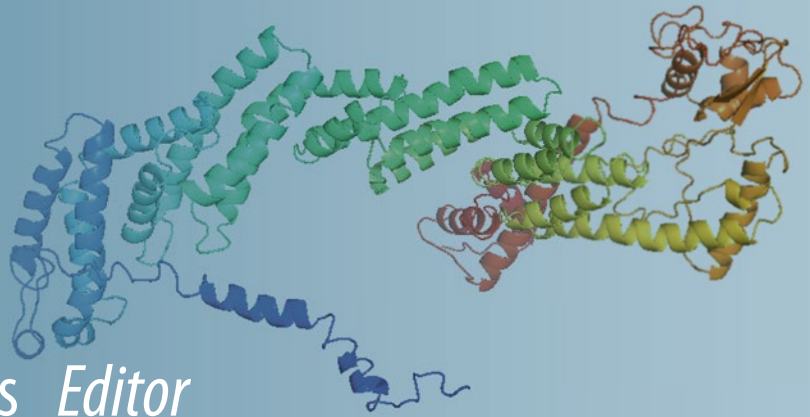


Methods in
Molecular Biology 2412

Springer Protocols



Sunil Thomas *Editor*

Vaccine Design

Methods and Protocols,
Volume 3: Resources for Vaccine
Development

Second Edition

 Humana Press

METHODS IN MOLECULAR BIOLOGY

Series Editor

John M. Walker

School of Life and Medical Sciences

University of Hertfordshire

Hatfield, Hertfordshire, UK

For further volumes:

<http://www.springer.com/series/7651>

For over 35 years, biological scientists have come to rely on the research protocols and methodologies in the critically acclaimed *Methods in Molecular Biology* series. The series was the first to introduce the step-by-step protocols approach that has become the standard in all biomedical protocol publishing. Each protocol is provided in readily-reproducible step-by-step fashion, opening with an introductory overview, a list of the materials and reagents needed to complete the experiment, and followed by a detailed procedure that is supported with a helpful notes section offering tips and tricks of the trade as well as troubleshooting advice. These hallmark features were introduced by series editor Dr. John Walker and constitute the key ingredient in each and every volume of the *Methods in Molecular Biology* series. Tested and trusted, comprehensive and reliable, all protocols from the series are indexed in PubMed.

Vaccine Design

**Methods and Protocols, Volume 3: Resources
for Vaccine Development**

Second Edition

Edited by

Sunil Thomas

Lankenau Institute for Medical Research, Wynnewood, Pennsylvania, USA

 **Humana Press**

Editor

Sunil Thomas
Lankenau Institute for Medical
Research
Wynnewood, Pennsylvania, USA

ISSN 1064-3745 ISSN 1940-6029 (electronic)
Methods in Molecular Biology
ISBN 978-1-0716-1891-2 ISBN 978-1-0716-1892-9 (eBook)
<https://doi.org/10.1007/978-1-0716-1892-9>

© The Editor(s) (if applicable) and The Author(s), under exclusive license to Springer Science+Business Media, LLC, part of Springer Nature 2022

This work is subject to copyright. All rights are solely and exclusively licensed by the Publisher, whether the whole or part of the material is concerned, specifically the rights of translation, reprinting, reuse of illustrations, recitation, broadcasting, reproduction on microfilms or in any other physical way, and transmission or information storage and retrieval, electronic adaptation, computer software, or by similar or dissimilar methodology now known or hereafter developed.

The use of general descriptive names, registered names, trademarks, service marks, etc. in this publication does not imply, even in the absence of a specific statement, that such names are exempt from the relevant protective laws and regulations and therefore free for general use.

The publisher, the authors, and the editors are safe to assume that the advice and information in this book are believed to be true and accurate at the date of publication. Neither the publisher nor the authors or the editors give a warranty, expressed or implied, with respect to the material contained herein or for any errors or omissions that may have been made. The publisher remains neutral with regard to jurisdictional claims in published maps and institutional affiliations.

This Humana imprint is published by the registered company Springer Science+Business Media, LLC, part of Springer Nature.

The registered company address is: 1 New York Plaza, New York, NY 10004, U.S.A.

Dedication

The healthcare and frontline workers who worked tirelessly taking care of COVID-19 patients.

Researchers who studied diligently the biology of SARS-CoV-2 and developed vaccines to protect against COVID-19.

Preface

*“A healthy society should not have just one voice.”—Li Wenliang (1986–2020)
(the first physician to recognize the outbreak of COVID-19 in Wuhan, China)*

Vaccinations have greatly reduced the burden of infectious diseases. Aggressive vaccination strategies have helped eradicate smallpox in humans and rinderpest, a serious disease of cattle. Vaccination has greatly reduced many pediatric infectious diseases. Vaccines not only protect the immunized but can also reduce disease among unimmunized individuals in the community through “herd protection.” Vaccines have also led to increased production of fish and farm animals, thereby improving food security.

The development of vaccines has improved our understanding of immunology and the principles of immunity. This has led to the research and development of vaccines for cancer and neurodegenerative diseases.

The world’s health and economy deteriorated since the first report of COVID-19 in China in December 2019. The pandemic has resulted in a huge interest in the development of vaccines. Even the skeptics were clamoring for early development of vaccines. Generally, vaccines take around 10–15 years to reach the clinic. Advances in the knowledge of molecular biology, immunology, and bioinformatics have led to the development of mRNA and adenovirus vector vaccines that are more efficacious than conventional vaccines. Collaboration at multiple levels led to the development and quick employment of COVID-19 vaccines in the clinic within a year of the observation of the disease, making it the quickest vaccines ever to be developed and deployed.

In 2016, we published the first edition of the book *Vaccine Design: Methods and Protocols*. Volume 1: *Vaccines for Human Diseases* and Volume 2: *Vaccines for Veterinary Diseases*. The books were a tremendous success.

The *Methods in Molecular Biology*TM series, *Vaccine Design: Methods and Protocols*, Second Edition, contains 87 chapters in three volumes. Volume 1: *Vaccines for Human Diseases* has an introductory section on future challenges for vaccinologists, the immunological mechanism of vaccines, and the principles of vaccine design. The design of human vaccines for viral, bacterial, fungal, and parasitic diseases as well as vaccines for tumors is also described in this volume. Volume 2: *Vaccines for Veterinary Diseases* includes vaccines for farm animals and fishes. Volume 3: *Resources for Vaccine Development* includes chapters on vaccine adjuvants, vaccine vectors and production, vaccine delivery systems, vaccine bioinformatics, vaccine regulation, and intellectual property.

It has been 225 years since Edward Jenner vaccinated his first patient in 1796 to protect against smallpox. This book is a tribute to the pioneering effort of his work. The job of publishing the second edition of the book *Vaccine Design: Methods and Protocols* was assigned at a tough time. Most of the universities were closed due to COVID-19 immediately after I took up the assignment. Several of the authors, their collaborators, and families were infected with the virus while contributing to the book. Nevertheless, the authors completed their chapters within the stipulated time. I am extremely grateful to the authors for completing the task in spite of the hardship faced while contributing to the books. My sincere thanks to all the authors for contributing to *Vaccine Design: Methods and Protocols* (Edition 2); Volume 1: *Vaccines for Human Diseases*; Volume 2: *Vaccines for Veterinary Diseases*; and Volume 3: *Resources for Vaccine Development*. I would also like to thank the series editor of *Methods in Molecular Biology*TM, Prof. John M. Walker, for giving me the opportunity to edit this book. My profound thanks to my parents Thomas and Thresy, wife

Jyothi for the encouragement and support, and also our twins Teresa and Thomas for patiently waiting for me while preparing the book. Working on the book was not an excuse for staying away from the laboratory. I made sure that my children were told about new exciting data generated in the laboratory and the advances in science published daily before bedtime.

Wynnewood, PA, USA

Sunil Thomas

Contents

<i>Dedication</i>	<i>v</i>
<i>Preface</i>	<i>vii</i>
<i>Contributors</i>	<i>xiii</i>

PART I TRENDS IN VACCINE DEVELOPMENT

1 Artificial Intelligence for Vaccine Design	3
<i>Peter McCaffrey</i>	
2 Progress in the Development of Structure-Based Vaccines	15
<i>Sunil Thomas and Ann Abraham</i>	
3 Polymer–Peptide Conjugate Vaccine for Oral Immunization	35
<i>Mohammad Omer Faruck, Mariusz Skwarczynski, and Istvan Toth</i>	
4 An Update on “Reverse Vaccinology”: The Pathway from Genomes and Epitope Predictions to Tailored, Recombinant Vaccines.....	45
<i>Marcin Michalik, Bardya Djabanshiri, Jack C. Leo, and Dirk Linke</i>	

PART II VACCINE VECTORS AND PRODUCTION SYSTEM

5 Phage T7 as a Potential Platform for Vaccine Development	75
<i>Chuan Loo Wong, Chean Yeah Yong, and Khai Wooi Lee</i>	
6 Plant-Based Systems for Vaccine Production	95
<i>Mattia Santoni, Elisa Gecchele, Roberta Zampieri, and Linda Avesani</i>	
7 Production of a Hepatitis E Vaccine Candidate Using the <i>Pichia pastoris</i> Expression System	117
<i>Jyoti Gupta, Amit Kumar, and Milan Surjit</i>	

PART III VACCINE ADJUVANTS

8 Developments in Vaccine Adjuvants	145
<i>Farrhana Ziana Firdaus, Mariusz Skwarczynski, and Istvan Toth</i>	
9 Adjuvants: Engineering Protective Immune Responses in Human and Veterinary Vaccines	179
<i>Bassel Akache, Felicity C. Stark, Gerard Agbayani, Tyler M. Renner, and Michael J. McCluskie</i>	
10 Cationic Nanostructures as Adjuvants for Vaccines	233
<i>Ana Maria Carmona-Ribeiro, Beatriz Ideriha Mathiazzi, and Yunys Pérez-Betancourt</i>	

11	Emulsion Adjuvants for Use in Veterinary Vaccines	247
	<i>Rachel Madera, Yulia Burakova, and Jisbu Shi</i>	
12	Generation of a Liposomal Vaccine Adjuvant Based on Sulfated S-Lactosylarchaeol (SLA) Glycolipids	255
	<i>Bassel Akache, Yimei Jia, Vandana Chandan, Lise Deschatelets, and Michael J. McCluskie</i>	
13	Glucan Particles: Choosing the Appropriate Size to Use as a Vaccine Adjuvant	269
	<i>Mariana Colaço, João Panão Costa, and Olga Borges</i>	

PART IV VACCINE DELIVERY SYSTEMS

14	Use of Optical In Vivo Imaging to Monitor and Optimize Delivery of Novel Plasmid-Launched Live-Attenuated Vaccines	283
	<i>Sapna Sharma and Kai Dallmeier</i>	
15	Liposomes for the Delivery of Lipopeptide Vaccines	295
	<i>Jieru Yang, Armira Azuar, Istvan Toth, and Mariusz Skwarczynski</i>	
16	Current Prospects in Peptide-Based Subunit Nanovaccines	309
	<i>Prashamsa Koirala, Sahra Bashiri, Istvan Toth, and Mariusz Skwarczynski</i>	
17	Design and Synthesis of Protein-Based Nanocapsule Vaccines	339
	<i>Ivana Skakic, Jasmine E. Francis, and Peter M. Smooker</i>	
18	Design and Preparation of Solid Lipid Nanoparticle (SLN)-Mediated DNA Vaccines	355
	<i>Jasmine E. Francis, Ivana Skakic, and Peter M. Smooker</i>	
19	Nano-Particulate Platforms for Vaccine Delivery to Enhance Antigen-Specific CD8 ⁺ T-Cell Response	367
	<i>Jhanvi Sharma, Carcia S. Carson, Trevor Douglas, John T. Wilson, and Sebastian Joyce</i>	
20	PilVax: A Novel Platform for the Development of Mucosal Vaccines	399
	<i>Catherine (Jia-Yun) Tsai, Jacelyn M. S. Loh, and Thomas Proft</i>	

PART V VACCINE BIOINFORMATICS

21	Bioinformatic Techniques for Vaccine Development: Epitope Prediction and Structural Vaccinology	413
	<i>Peter McCaffrey</i>	
22	Immunoinformatic Approaches for Vaccine Designing for Pathogens with Unclear Pathogenesis	425
	<i>Naina Arora, Anand K. Kesbri, Rimanpreet Kaur, Suraj Singh Rawat, and Amit Prasad</i>	
23	In Silico Identification of the B-Cell and T-Cell Epitopes of the Antigenic Proteins of <i>Staphylococcus aureus</i> for Potential Vaccines	439
	<i>Sunil Thomas and Irini Doytchinova</i>	

24	Computational Mining and Characterization of Hypothetical Proteins of <i>Mycobacterium bovis</i> Toward the Identification of Probable Vaccine Candidates.	449
	<i>Bhaskar Ganguly</i>	
25	Recombinant Vaccine Design Against <i>Clostridium</i> spp. Toxins Using Immunoinformatics Tools	457
	<i>Rafael Rodrigues Rodrigues, Marcos Roberto Alves Ferreira, Frederico Schmitt Kremer, Rafael Amaral Donassolo, Clóvis Moreira Júnior, Mariliana Luiza Ferreira Alves, and Fabricio Rochedo Conceição</i>	
26	Searching Epitope-Based Vaccines Using Bioinformatics Studies.	471
	<i>Marlet Martínez-Archundia, G. Lizbeth Ramírez-Salinas, Jazmin García-Machorro, and José Correa-Basurto</i>	
PART VI VACCINE SAFETY AND REGULATION		
27	The Regulatory Evaluation of Vaccines for Human Use	483
	<i>Norman W. Baylor</i>	
PART VII VACCINE INTELLECTUAL PROPERTY		
28	Intellectual Property Rights and Vaccines	505
	<i>Penny Gilbert, Richard Fawcett, Joel Coles, and William Hillson</i>	
29	Vaccine Intellectual Property	519
	<i>Ana Santos Rutschman, Joshua D. Sarnoff, and Timothy L. Wiemken</i>	
PART VIII PATHWAYS TO VACCINE COMMERCIALIZATION		
30	Resources for Starting a Company	529
	<i>Ann Abraham, Jude Mathew, and Sunil Thomas</i>	
	<i>Index</i>	543

Contributors

- ANN ABRAHAM • *Lankenau Institute for Medical Research, Wynnewood, PA, USA*
- GERARD AGBAYANI • *Human Health Therapeutics, National Research Council Canada, Ottawa, ON, Canada*
- BASSEL AKACHE • *Human Health Therapeutics, National Research Council Canada, Ottawa, ON, Canada*
- MARILIANA LUIZA FERREIRA ALVES • *Centro de Desenvolvimento Tecnológico, Universidade Federal de Pelotas, Pelotas, Rio Grande do Sul, Brazil*
- NAINA ARORA • *School of Basic Sciences, Indian Institute of Technology Mandi, Mandi, Himachal Pradesh, India*
- LINDA AVESANI • *Department of Biotechnology, University of Verona, Verona, Italy*
- ARMIRA AZUAR • *School of Chemistry and Molecular Biosciences, The University of Queensland, St Lucia, QLD, Australia*
- SAHRA BASHIRI • *School of Chemistry and Molecular Biosciences, The University of Queensland, Brisbane, QLD, Australia*
- NORMAN W. BAYLOR • *Biologics Consulting Group, Inc., Alexandria, VA, USA*
- OLGA BORGES • *Center for Neurosciences and Cell Biology, Coimbra, Portugal; Faculty of Pharmacy, University of Coimbra, Coimbra, Portugal*
- YULIA BURAKOVA • *Department of Anatomy and Physiology, Kansas State University, College of Veterinary Medicine, Manhattan, KS, USA*
- ANA MARIA CARMONA-RIBEIRO • *Biocolloids Laboratory, Departamento de Bioquímica, Instituto de Química, Universidade de São Paulo, São Paulo, Brazil*
- CARCIA S. CARSON • *Department of Biomedical Engineering, Vanderbilt University, Nashville, TN, USA*
- VANDANA CHANDAN • *Human Health Therapeutics, National Research Council Canada, Ottawa, ON, Canada*
- MARIANA COLAÇO • *Center for Neurosciences and Cell Biology, Coimbra, Portugal; Faculty of Pharmacy, University of Coimbra, Coimbra, Portugal*
- JOEL COLES • *Powell Gilbert LLP, London, UK*
- FABRICIO ROCHEDO CONCEIÇÃO • *Centro de Desenvolvimento Tecnológico, Universidade Federal de Pelotas, Pelotas, Rio Grande do Sul, Brazil*
- JOSÉ CORREA-BASURTO • *Laboratorio de Diseño y Desarrollo de Nuevos Fármacos e Innovación Biotecnológica (Laboratory for the Design and Development of New Drugs and Biotechnological Innovation), Escuela Superior de Medicina, Instituto Politécnico Nacional, México City, Mexico*
- KAI DALLMEIER • *KU Leuven Department of Microbiology, Immunology and Transplantation, Rega Institute, Virology and Chemotherapy, Molecular Vaccinology and Vaccine Discovery, Leuven, Belgium*
- LISE DESCHATELETS • *Human Health Therapeutics, National Research Council Canada, Ottawa, ON, Canada*
- BARDYA DJAHANSCHIRI • *Institute of Cell Biology and Neuroscience, Goethe University, Frankfurt, Germany*
- RAFAEL AMARAL DONASSOLO • *Centro de Desenvolvimento Tecnológico, Universidade Federal de Pelotas, Pelotas, Rio Grande do Sul, Brazil*

- TREVOR DOUGLAS • *Department of Chemistry, Indiana University, Bloomington, IN, USA*
- IRINI DOYTCHINOVA • *Department of Chemistry, Faculty of Pharmacy, Medical University of Sofia, Sofia, Bulgaria*
- MOHAMMAD OMER FARUCK • *School of Chemistry and Molecular Biosciences, The University of Queensland, St Lucia, QLD, Australia*
- RICHARD FAWCETT • *Powell Gilbert LLP, London, UK*
- MARCOS ROBERTO ALVES FERREIRA • *Centro de Desenvolvimento Tecnológico, Universidade Federal de Pelotas, Pelotas, Rio Grande do Sul, Brazil*
- FARRHANA ZIANA FIRDAUS • *School of Chemistry and Molecular Biosciences, The University of Queensland, St Lucia, QLD, Australia*
- JASMINE E. FRANCIS • *School of Science, RMIT University, Bundoora, VIC, Australia*
- BHASKAR GANGULY • *Department of Clinical Research, Research and Development Division, Ayurved Limited, Baddi, Himachal Pradesh, India; D-04, Alliance Kingston Estate, Rudrapur, Uttarakhand, India*
- JAZMIN GARCÍA-MACHORRO • *Laboratorio de medicina de Conservación, Escuela Superior de Medicina, Instituto Politécnico Nacional, México City, Mexico*
- ELISA GECHELE • *Diamante srl, Verona, Italy*
- PENNY GILBERT • *Powell Gilbert LLP, London, UK*
- JYOTI GUPTA • *Virology Laboratory, Translational Health Science and Technology Institute, NCR Biotech Science Cluster, Faridabad, Haryana, India*
- WILLIAM HILLSON • *Powell Gilbert LLP, London, UK*
- YIMEI JIA • *Human Health Therapeutics, National Research Council Canada, Ottawa, ON, Canada*
- SEBASTIAN JOYCE • *Department of Pathology, Microbiology and Immunology, Vanderbilt University School of Medicine, Nashville, TN, USA; Department of Veterans Affairs, Tennessee Valley Healthcare System, Nashville, TN, USA*
- CLÓVIS MOREIRA JÚNIOR • *Centro de Desenvolvimento Tecnológico, Universidade Federal de Pelotas, Pelotas, Rio Grande do Sul, Brazil*
- RIMANPREET KAUR • *School of Basic Sciences, Indian Institute of Technology Mandi, Mandi, Himachal Pradesh, India*
- ANAND K. KESHRI • *School of Basic Sciences, Indian Institute of Technology Mandi, Mandi, Himachal Pradesh, India*
- PRASHAMSA KOIRALA • *School of Chemistry and Molecular Biosciences, The University of Queensland, Brisbane, QLD, Australia*
- FREDERICO SCHMITT KREMER • *Centro de Desenvolvimento Tecnológico, Universidade Federal de Pelotas, Pelotas, Rio Grande do Sul, Brazil*
- AMIT KUMAR • *Virology Laboratory, Translational Health Science and Technology Institute, NCR Biotech Science Cluster, Faridabad, Haryana, India*
- KHAI WOOL LEE • *School of Biosciences, Faculty of Health and Medical Sciences, Taylor's University, Subang Jaya, Selangor, Malaysia*
- JACK C. LEO • *Department of Biosciences, Nottingham Trent University, Nottingham, UK*
- DIRK LINKE • *Department of Biosciences, University of Oslo, Oslo, Norway*
- JACELYN M. S. LOH • *Department of Molecular Medicine and Pathology, School of Medical Sciences and Maurice Wilkins Centre for Biomolecular Discovery, The University of Auckland, Auckland, New Zealand*
- RACHEL MADERA • *Department of Anatomy and Physiology, Kansas State University, College of Veterinary Medicine, Manhattan, KS, USA*

- MARLET MARTÍNEZ-ARCHUNDIA • *Laboratorio de Diseño y Desarrollo de Nuevos Fármacos e Innovación Biotecnológica (Laboratory for the Design and Development of New Drugs and Biotechnological Innovation), Escuela Superior de Medicina, Instituto Politécnico Nacional, México City, Mexico*
- JUDE MATHEW • *Lebow College of Business, Drexel University, Philadelphia, PA, USA*
- BEATRIZ IDERIHA MATHIAZZI • *Biocolloids Laboratory, Departamento de Bioquímica, Instituto de Química, Universidade de São Paulo, São Paulo, Brazil*
- PETER MCCAFFREY • *Department of Pathology, University of Texas Medical Branch, Galveston, TX, USA*
- MICHAEL J. MCCLUSKIE • *Human Health Therapeutics, National Research Council Canada, Ottawa, ON, Canada*
- MARCIN MICHALIK • *Department of Biosciences, University of Oslo, Oslo, Norway*
- JOÃO PANÃO COSTA • *Center for Neurosciences and Cell Biology, Coimbra, Portugal; Faculty of Pharmacy, University of Coimbra, Coimbra, Portugal*
- YUNYS PÉREZ-BETANCOURT • *Biocolloids Laboratory, Departamento de Bioquímica, Instituto de Química, Universidade de São Paulo, São Paulo, Brazil*
- AMIT PRASAD • *School of Basic Sciences, Indian Institute of Technology Mandi, Mandi, Himachal Pradesh, India*
- THOMAS PROFT • *Department of Molecular Medicine and Pathology, School of Medical Sciences and Maurice Wilkins Centre for Biomolecular Discovery, The University of Auckland, Auckland, New Zealand*
- G. LIZBETH RAMÍREZ-SALINAS • *Laboratorio de Diseño y Desarrollo de Nuevos Fármacos e Innovación Biotecnológica (Laboratory for the Design and Development of New Drugs and Biotechnological Innovation), Escuela Superior de Medicina, Instituto Politécnico Nacional, México City, Mexico*
- SURAJ SINGH RAWAT • *School of Basic Sciences, Indian Institute of Technology Mandi, Mandi, Himachal Pradesh, India*
- TYLER M. RENNER • *Human Health Therapeutics, National Research Council Canada, Ottawa, ON, Canada*
- RAFAEL RODRIGUES RODRIGUES • *Centro de Desenvolvimento Tecnológico, Universidade Federal de Pelotas, Pelotas, Rio Grande do Sul, Brazil*
- ANA SANTOS RUTSCHMAN • *Saint Louis University School of Law, St. Louis, MO, USA*
- MATTIA SANTONI • *Department of Biotechnology, University of Verona, Verona, Italy; Diamante srl, Verona, Italy*
- JOSHUA D. SARNOFF • *DePaul University College of Law, Chicago, IL, USA*
- JHANVI SHARMA • *Department of Pathology, Microbiology and Immunology, Vanderbilt University School of Medicine, Nashville, TN, USA*
- SAPNA SHARMA • *KU Leuven Department of Microbiology, Immunology and Transplantation, Rega Institute, Virology and Chemotherapy, Molecular Vaccinology and Vaccine Discovery, Leuven, Belgium*
- JISHU SHI • *Department of Anatomy and Physiology, Kansas State University, College of Veterinary Medicine, Manhattan, KS, USA*
- IVANA SKAKIC • *School of Science, RMIT University, Bundoora, VIC, Australia*
- MARIUSZ SKWARCZYNSKI • *School of Chemistry and Molecular Biosciences, The University of Queensland, St Lucia, QLD, Australia*
- PETER M. SMOOKER • *School of Science, RMIT University, Bundoora, VIC, Australia*
- FELICITY C. STARK • *Human Health Therapeutics, National Research Council Canada, Ottawa, ON, Canada*

- MILAN SURJIT • *Virology Laboratory, Translational Health Science and Technology Institute, NCR Biotech Science Cluster, Faridabad, Haryana, India*
- SUNIL THOMAS • *Lankenau Institute for Medical Research, Wynnewood, PA, USA*
- ISTVAN TOTH • *School of Chemistry and Molecular Biosciences, The University of Queensland, St Lucia, QLD, Australia; Institute of Molecular Biosciences, The University of Queensland, St Lucia, QLD, Australia; School of Pharmacy, The University of Queensland, Woolloongabba, QLD, Australia*
- CATHERINE (JIA-YUN) TSAI • *Department of Molecular Medicine and Pathology, School of Medical Sciences and Maurice Wilkins Centre for Biomolecular Discovery, The University of Auckland, Auckland, New Zealand*
- TIMOTHY L. WIEMKEN • *Saint Louis University School of Medicine, St. Louis, MO, USA*
- JOHN T. WILSON • *Department of Biomedical Engineering, Vanderbilt University, Nashville, TN, USA*
- CHUAN LOO WONG • *Faculty of Biotechnology and Biomolecular Sciences, Universiti Putra Malaysia, Serdang, Selangor, Malaysia*
- JIERU YANG • *School of Chemistry and Molecular Biosciences, The University of Queensland, St Lucia, QLD, Australia*
- CHEAN YEAH YONG • *Faculty of Biotechnology and Biomolecular Sciences, Universiti Putra Malaysia, Serdang, Selangor, Malaysia*
- ROBERTA ZAMPIERI • *Diamante srl, Verona, Italy*

Part I

Trends in Vaccine Development



Chapter 1

Artificial Intelligence for Vaccine Design

Peter McCaffrey

Abstract

Often likened to “the new electricity,” artificial intelligence (AI) has broad and sweeping impact in many areas. Perhaps most exciting among these are in bioinformatics as AI allows for new and increasingly powerful ways of understanding genomics, proteomics, and immunology, just to name a few areas. Also exciting is a parallel growth in high-throughput assays including sequencing which will further accelerate the development and use of AI in biomedicine. In this chapter, we will discuss artificial intelligence and deep learning in particular, and we will review how such approaches are enhancing and even reshaping vaccine design in terms of epitope detection and optimization. Moreover, we discuss how AI is particularly valuable to the design of mRNA vaccines including in research and production. Finally, we will discuss several additional areas across trials and operations where AI will have pervasive impact on the development of vaccines going forward.

Key words Artificial intelligence, Deep learning, Neural network

1 Introduction

Artificial intelligence (AI) is a broad term used to represent a diverse collection of research and applied endeavors. Strictly speaking, artificial intelligence describes the design of nonhuman agents that perceive and respond to their environment, and this theme has encompassed efforts in autonomous vehicles, robotics, image recognition, and language understanding just to name a few areas. Importantly, artificial intelligence encompasses many technical implementations and could broadly be defined to include machine learning of any variety. That being said, most modern uses of the term artificial intelligence imply the use of neural network models and, specifically, the use of deep learning. Deep learning is a form of machine learning wherein neural network models are built to consist of many sequential, smaller models referred to as “layers”. We discuss this in greater detail below but the general advantage of having many such sequential models—that is, being “Deep” in terms of how many layers a neural network

has—is that it allows for increasingly nuanced and complex data to be distinguished and effectively modeled upon in useful ways. At the risk of overfitting, such deep learning models have demonstrated exceptional power in assessing complex inputs such as images, text, and sequence data and being able to successfully achieve classification and prediction performance directly from these source data without requiring extensive human-engineered pre-processing. While the history of AI and even deep learning reaches back to the first half of the twentieth century, meaningful applications are a relatively recent phenomenon. To consider biomedical informatics in particular, machine learning generally was a later evolution of the field prevented in large part by a relative scarcity of data and higher cost to data acquisition than in many other domains. Progress in next-generation sequencing and many other high-throughput assays has worked to resolve this and create volumes of publicly and privately held data for which machine learning and deep learning can prove useful.

A common theme in the evolution of AI as a practice is that adjacent technological advancements bring new techniques which spread to other areas. Deep learning, which exists really as a specific engineering approach aimed at achieving AI through the creation of robust neural network models, really achieved its flagship successes in domains of image analysis with convolutional networks and work done by leaders such as LeCun, Hinton, and Bengio demonstrating that image classification could be successfully performed by models that required very little prior information about how such problems should be solved [1]. As we will discuss in greater detail below, many successful applications of deep learning in biomedical informatics apply image or language models to analogous problems in sequence analysis. Deep learning is also an increasingly popular term at the time of this writing with seemingly every project, paper, and company alluding to its use in some way, and it is increasingly important to understand what this term really describes. Strictly speaking, deep learning refers to the use of neural networks that contain many “layers,” thereby giving them the ability to represent functions that describe often semi-structured and complex inputs such as images and sequences. This capability is imparted by this layering architecture which can be thought of as a system of models each of which learns how to interpret the output of other models that precede it. Ultimately, this results in classification and prediction behavior that can capably summarize patterns and accommodate nonlinear relationships in input data. With regard to vaccine design in particular, neural networks have an established history of success in epitope prediction, often outperforming alternative modeling approaches as with NetMHCpan. More recently, these network approaches have grown to involve more heterogeneous inputs and more advanced network architectures, and they have shown promise in improving important areas

such as MHC II [2] and linear B-cell epitope prediction [3]. This chapter will hopefully clarify some of the reasons why neural networks perform well in this regard and to establish intuitions around neural networks and deep learning as a strategy for solving certain bioinformatic challenges.

2 Overview of Artificial Intelligence and Deep Learning

To describe the design of neural networks, we will first consider a far more conventional logistic regression model. In the case of logistic regression, the model attempts to identify a linear separation between the features of some collection of input samples. More specifically, such a model will look to apply a single weight to each feature describing its inputs and will look to establish some linear function of those features that constitutes a meaningful distinction for labeling, prediction, or classification. Although appealing in its simplicity, this approach suffers from an inability to accommodate “nonlinear” behavior, meaning that such models cannot effectively describe situations where the relationship between a feature and some outcome label is different at different values of that feature or where features may interact with each other such that they become mutually more or less influential in making a prediction at different points across the range feature values. By contrast, neural networks represent “nonlinear” models in that they can accommodate situations where the importance of features differ depending upon the value and context of those features. In technical terms, this is achieved by the fact that neural network models implement a linear mapping between the outputs of one layer and the inputs of another where each layer is allowed to learn weights and biases to parameterize this mapping. Thus, examples such as the “not-or” function can be aptly represented by a neural network, whereas they cannot be represented by a linear model because there is no dividing line between the two categories represented by this function. For example, we can imagine a plot with two axes and four points at x,y coordinates (0,0), (0,1), (1,0), and (1,1). In the not-or function, we may categorize those points that have a 1 or 0 but not both as opposed to those that do. Thus, (1,0) and (0,1) would be blue for example but (0,0) and (1,1) would be red. In such a plot, there is no possible line separating blue from red points, thus they are not linearly separable. Deep learning, therefore, exists as a mode of implementing neural networks wherein models contain many layers allowing them to accommodate increasingly more complex relationships between features and some target outcome.

A second important point about neural networks and one that applies especially to convolutional networks is that feature representation within such models takes a form that is often better suited

to bioinformatic tasks than other approaches. Convolutional networks apply the aforementioned linear mappings to a collection of features that are first abstracted through the use of varying layers of convolution operators that process adjacent windows of some input matrix (often an image). The potent effect of doing this is that these networks are able to abstract generalized patterns and detect them in subsequent images without relying upon those patterns occurring in specific locations of an image. In bioinformatic tasks, sequence analysis offers a meaningful analogy where it may be desirable to model local nucleotide or amino acid motifs wherever they may occur within a sequence and then to use an abstract feature generated from these patterns in order to make a potent classification or prediction model. Convolutional networks are a very popular approach for solving challenges in imaging and genomics where local patterns may emerge within a broader feature space. Importantly, these are not the only successful model architectures used within modern deep learning with recurrent networks serving to capture important features that appear across elements in a sequence whether they be at different timepoints or locations.

3 Artificial Intelligence in Epitope Prediction

To bring this discussion of neural networks more directly into focus, we will consider its applications to epitope prediction. The goal of epitope prediction is likely familiar to the reader but, in short, its purpose is to identify protein sequences which have specific immunogenic properties. As it is infeasible to annotate every possible protein sequence experimentally, this process involved modeling the relationship between amino acid sequence and immune function on a sample data set and then using such models to predict the immunogenicity of new protein sequences. As proteins can assume complex three-dimensional structures driving their immunogenicity, this prediction can be challenging as it may need to account for key subsequences (i.e., motifs) located at variable positions within a given protein sequence. Considering the task of predicting linear B-cell epitopes, feed forward neural network architectures have been shown to offer improved predictive power [3]. Liu et al. examined this by first downloading 408,251 epitope sequences from the Immune Epitope Database (IEDB) of which approximately 240,000 were labeled as epitopes or non-epitopes. Features of each peptide included the sequence, position, host, and immunogenicity. Authors then truncated epitopes at various lengths from 11 to 50 amino acids, training models for each length to predict whether a given sequence was an epitope, and they used two third-party data sets with non-overlapping peptide sequences to test model performance. To accommodate class imbalance, namely that there are often many more non-epitope

sequences than there are epitope sequences in any given database, authors created equally balanced training data sets by randomly sampling 20,000 peptides from the epitope and non-epitope groups. This resulted in 11 sampled data sets each representing a partially overlapping sample of the entire training data from IEDB. Finally, each of these 11 training data sets was used to train a model resulting in 11 different models each trained on one of these sub-sampled data sets. Test data peptides, then were scored by each of the 11 models—each of which learned a slightly different strategy for distinguishing epitope from non-epitope—resulting in 11 scores for each test peptide sequence. The prediction score for a test peptide sequence was the sum of the binary output—either 1 or 0—of each of the underlying models, resulting in a score ranging from 0 (if no models scored a peptide as an epitope) to 11 (if all models scored a peptide as an epitope). This may seem somewhat tedious to cover such details of data organization for training, but these are actually quite important to understand. As mentioned previously, one of the key advantages of neural networks and deep learning in particular is that such models do not require deliberately crafted features in many cases, and, instead, they can identify complex features directly from input data. The downside of such behavior is that they are reliant upon lots of data in order to do this effectively, and they can accumulate bias and overfitting behavior quickly and sometimes in nonobvious ways. Thus, balancing training data among classes (e.g., epitope and non-epitope) is important in facilitating models to develop a generalizable hypothesis as much as possible.

As for the model itself, the aforementioned authors employed a feed forward neural network, meaning that the model consists of a stack of layers wherein each layer consists of multiple “neurons,” each capable of learning a mapping between its respective inputs from its upstream layer to its respective outputs to its downstream layer. In this model, the initial input consists of 400 features consisting of the dipeptide composition for an input peptide. More specifically, the feature space consists of all two-amino-acid combinations achievable from among 20 amino acids, resulting in 400 possible dipeptides. Then each input peptide sequence was divided into overlapping dipeptides, and each such dipeptide was tallied and calculated as a percentage over all dipeptides in the sequence. These proportions were then used to populate corresponding dipeptide features resulting in a vector of 400 values some of which were 0 if a given dipeptide was not present in an input sequence and some of which were non-zero where there was a given proportion to a dipeptide. The final output of the model was simply a 1 or 0 corresponding to whether a peptide was an epitope or not. The layers in this network were successively smaller going from 400 at input to 200, then 100, then 40, then 20, and finally 2 at output. Thus, to continue our description of networks as

linear mappings, what this network is doing is first learning key dipeptide abundances that indicate an epitope, then learning key groups of those abundances, and then groups of those groups, and so forth. Although there are many potential ways in which neural network models can be constructed, this approach is—at its core—representative of the power of this approach and of deep learning more broadly in detecting biologically relevant sequence motifs and composing those into increasingly more complex patterns. Given that the identity of a motif, its position in a sequence, or its relationship to other motifs need not be known a priori in order to do this—and in many cases such information cannot be known in advance—such approaches are clearly powerful for learning relevant patterns from biological data where we know, for mechanistic reasons, that function results from sequence but where the explicit features are often yet to be discovered. Accuracy as measured by area under the ROC curve (AUC) ranged from 0.88 to 0.95 depending upon the length of input peptide sequence used and performed well when compared to many other epitope prediction models.

Artificial intelligence may have many valuable roles in vaccine design—some of which we will cover below—but one key area where such models demonstrate value is in the critical task of epitope prediction where identifying complex and hierarchical signatures from amino acid sequences is both biologically valid and amenable to neural network models. Another important point to make is that model inspection, and explainability is a rapidly growing domain and one which will likely see numerous significant advancements following the publication of this chapter. As a general forward-looking statement, the advancement of high-throughput technologies to identify peptide sequences and host interaction creates a fertile environment for deep learning to operate effectively. A parallel maturation in model inspection would then allow for such large data investigations to be used not just for the development of a predictive tool but for the development and extraction of the underlying model as a means to identify previously unknown motif sequences or other key biological indicators.

4 Artificial Intelligence with Additional Data Sources

Much of the discussion thus far has rightfully focused on sequence-based methods, namely epitope prediction from peptide sequences, but there are multiple emerging areas for artificial intelligence to advance vaccine development. One such area is adjacent to epitope prediction but concerns population targeting. Predicting whether a sequence is an epitope is one challenge but another is predicting which epitope may be the most useful to target and for which

patient population. Recent work from Liu et al. demonstrated such optimization by examining the proteome of SARS-CoV-2 first identifying likely MHC-I and MHC-II epitopes, then scoring from among that list for the optimal collection of epitopes that would grant broad population coverage given the underlying HLA distribution of various patient populations [4]. The authors developed a model that takes as an input an HLA-peptide pair and outputs a corresponding HLA-peptide binding affinity in nanomolar units. The authors then developed a model termed “OptiVax,” the aim of which was to select a minimal set of peptides such that, for a target population, there would be a threshold of at least n predicted HLA hits. Thus, the optimization objective is to identify the minimal set of peptides such that at least 5 or 10 or 15 peptides would bind to that population’s HLA profile. OptiVax achieved this using beam search which is a search algorithm that begins with an empty peptide set and iteratively adds one peptide, scoring the population-specific HLA binding profile of the entire set, and keeps the top 10 highest-scoring versions of the set before moving on to the next iteration where an additional peptide is added. Thus, at each iteration, the size of the peptide set grows from 0 to 1, to 2 and up to the final target while the highest scoring peptide composition is carried over from iteration to iteration. This is an efficient search algorithm that does not explore the complete combinatorial space of peptides—which would be infeasible—but instead builds upon the top scoring sets from the previous step, efficiently arriving at an optimal peptide set. OptiVax also de-prioritizes peptide sequences that are similar to those already in the current set, thus reducing the likelihood of redundant peptides in the set.

Using this approach, authors developed a peptide set of 19 peptides that achieves 99% coverage over Asian, Black, and White ethnic groups with at least one HLA-peptide hit per patient and 93% coverage with at least five hits per patient. Perhaps more interestingly, the authors used this model to evaluate various publicly available vaccine designs for SARS-CoV-2. Starting with whole protein vaccines, the authors sample peptide subsequences to generate inputs from which to compose optimized peptide sets. Overall, they noted that many published vaccines had narrow coverage when compared to the optimized peptide set produced by OptiVax, and importantly, since the results of OptiVax are an optimal set of peptide sequences, such results can be used to suggest specific additional peptides that should be included in existing formulations to increase coverage, something that is a practical value-add to existing vaccine efforts. Of course, the efficacy of such an approach should be tested further and should be tested on indications outside of SARS-CoV-2, but this is indicative of a broadening role for AI in the vaccine development process where it may offer enhancements or optimizations atop human efforts.

Equally important is also the use of AI for the development of mRNA vaccines. Much of the attention in bioinformatic design has been in selecting protein epitopes, but the advent of mRNA vaccines introduces new variables that double as opportunities for AI to deliver value. When designing such a vaccine, many questions around how mRNA stability, specificity, conformation, and protein product can be controlled through enhance analysis and prediction [5]. Also important, the ability to sequence and synthesize RNA allows for the systematic collection of large-scale data for developing such approaches. Baidu, in collaboration with Oregon State University and the University of Rochester, announced the development of LinearDesign, an AI which can design mRNA sequences with optimal stability, enhancing the yield and efficacy of mRNA vaccine design efforts. This is an example of many opportunities for AI to improve vaccine design processes by tackling areas with especially high risk or areas where a lack of foreknowledge can incur significant cost [6]. LinearDesign models the mRNA design problem in light of a desired target peptide (one which may be selected or optimized by other AI algorithms). Given this desired outcome, the algorithm then considers all possible mRNA sequences which could translate into the target peptide and optimized for the mRNA sequence with the minimum folding free energy change. This is an exponentially large search space, and so, the authors use deterministic finite automaton (DFA) which is a directed graph wherein each edge represents a potential nucleotide selection and the end-to-end sequence represents a peptide transcript as triplet codons. This approach can learn preferential weighting of paths through this graph based upon desired peptide properties and results in improved mRNA stability when compared to random selection or codon-based design with the added benefit of maintaining efficient computation time even when considering long peptide sequences. Importantly, these sorts of advancements which improve the efficiency and precision of mRNA vaccine design may have more far-reaching effects in improving the production process and advancing mRNA-based vaccine design as a paradigm.

5 Potential Future Uses of Artificial Intelligence in Vaccine Design

Reaching beyond the use of epitope detection and binding, artificial intelligence offers the ability to enhance vaccine development and monitoring in other aspects of the process. An important point to be made here is that neural networks and really any machine learning algorithm benefit greatly from dense numerical data. What this means is that assays that can describe biology in the form of standardized measurements that produce continuous numerical values with consistent dimensionality will effectively pave the way for enhanced expansion of artificial intelligence to deliver value. A

useful example of this is in patient phenotyping and immunologic monitoring itself where techniques such as RNA-seq and high-throughput immunologic measurement with tools such as O-Link and Luminex allow for the rapid generation of consistent, numerical features describing cytokines, immune cell populations, and functional impacts of vaccine products. These technologies will facilitate more granular phenotyping and systematic modeling amenable to neural network techniques and will likely lead to increased reliance on artificial intelligence at multiple points in the vaccine development process. As a technical enabler, assays that can generate continuous, numerical features such as a table of proteome abundances, gene abundances, or cytokine levels are deeply compatible with neural networks as these models operate by learning to place various weights upon numerical inputs in order to achieve optimal model outputs and are trained most effectively when both correct and incorrect model outputs can be attributed to and modified by incremental adjustment of feature weights and where features can be consistently measured in light of different output classifications. Thus, these assays allow for the collection of large amounts of data and the consistent capture of these measurements in multiple contexts, creating a useful substrate upon which artificial intelligence may operate.

Shifting to a slightly broader case is that of side effect surveillance which becomes especially challenging when effects are subtle both because they may be harder to detect but also because they require increasingly larger populations in order to detect them. In its ability to efficiently featurize and compute large-scale data sets, artificial intelligence offers multiple potential advantages in this arena. More specifically, abstracting patient phenotypes is challenging for numerous reasons and is generally infeasible to do manually at a production scale. Thus, automating the process of phenotype identification (often termed “computational phenotyping”) across patients, providers, and institutions is critical [7]. Unfortunately, documentation of such phenotypes is typically inconsistent and to such a degree that implementation of standard queries and formal rules is often impractical. For example, one key challenge in the domain of side effect surveillance is to deploy a nuanced patient phenotyping process at the scale of a computer-automated system. Artificial intelligence and natural language processing in particular have advanced significantly in the 24 months leading up to this writing of this chapter with Facebook, Google, and OpenAI—just to name a few companies—having developed increasingly advanced models capable of detecting complex nuances and accommodating variability in language. Thus, abstracting phenotypic characteristics from the volumes of healthcare data that exist as free text is a challenge suited for natural language processing. Multiple works have demonstrated the ability to create vector representations of text known as embeddings and to use these as features for deep

learning to develop nuanced classification and detection models. In the case of computational phenotyping in particular, this has been demonstrated to outperform many other methods of disease detection and symptom detection using free text notes such as admission and discharge summaries [8, 9].

Lastly, artificial intelligence has several use cases throughout the development and distribution supply chain, offering to reduce the time, cost, and risk of developing a vaccine program. In the case of the SARS-CoV-2 vaccine, this specifically looks like optimization of distribution channels, recipient populations, and transportation routes. More internal to the discovery process itself, this can look like optimization for clinical trial cohorts and eligibility not to mention efficacy and capability to produce vaccine candidates themselves. While this may seem somewhat oblique as a discussion of artificial intelligence in vaccine design, the broader impact of such advancements is important as a general reduction in time, cost, and risk for program development also reduces the risk of upstream innovation, making vaccine programs potentially more numerous and more specific to target populations which can be identified, enrolled, tested, and ultimately marketed in a more efficient manner. General operational enhancements across the supply chain would be a good sign for vaccine discovery as it would possibly reduce barriers to the timely creation of vaccines and make the funding and commercialization climate more receptive to potentially novel vaccines and vaccine technology.

Most immediately, however, the impact of AI on vaccine design is likely to result in the proliferation of mRNA-based programs and the reconfiguration of the emphasis placed at different program steps. With an ability to sequence pathogen or cancer genomes and transcriptomes and the ability to generate larger high-throughput data sets describing proteomes, their binding affinities, and their immunologic impact, it would stand to reason that these steps will increasingly move toward systematic screening efforts at scale. Should this be true, then much of the vaccine design phase would likely focus on the identification of optimal epitopes from high-throughput screening data followed by the proliferation of a collection of optimal vaccine components such as mRNAs which have been generated by AI with optimized stability and which encode a desired epitope. In the case of mRNA vaccines in particular, since such algorithms can be developed and validated at scale through high-throughput synthesis and testing of AI-designed transcripts, this step is likely to grow rapidly in its performance and yield. Finally, this is likely to also pair with an increase in personalized vaccines whether at the level of individualized cancer vaccines or even vaccine cocktails optimized for a given subpopulation based upon HLA alleles for example. This may further increase the variety and velocity of vaccine programs and lead toward smaller clinical trial cohorts with more specific indications and a shorter time to market for such programs.

6 Conclusions

In this chapter, we discussed a range of potential applications of artificial intelligence from those with more immediate and specific use cases, such as epitope detection to those with more abstract or theoretical use cases such as broad supply chain optimization. In any case, one key theme to capture is that there are many and various areas for the application of artificial intelligence to vaccine development. Second, it is important to understand that artificial intelligence and deep learning especially offer the ability to grapple with bioinformatic data in unique ways especially with the convergent advancement techniques for model evaluation and explanation. As an overall trend, increases in data volume brought about by efficient assay technologies and a very active research space advancing the capability of deep learning models depicts a bright and increasingly relevant future for this technology.

References

1. Lecun Y, Bengio Y, Hinton G (2015) Deep learning. *Nature* 521(7553):436–444. <https://doi.org/10.1038/nature14539>
2. Chen B, Khodadoust MS, Olsson N et al (2019) Predicting HLA class II antigen presentation through integrated deep learning. *Nat Biotechnol* 37(11):1332–1343. <https://doi.org/10.1038/s41587-019-0280-2>
3. Liu T, Shi K, Li W (2020) Deep learning methods improve linear B-cell epitope prediction. *BioData Min* 13(1):1. <https://doi.org/10.1186/s13040-020-00211-0>
4. Liu G, Carter B, Bricken T et al (2020) Computationally optimized SARS-CoV-2 MHC class I and II vaccine formulations predicted to target human haplotype distributions. *Cell Syst* 11(2):131–144.e6. <https://doi.org/10.1016/j.cels.2020.06.009>
5. Mauger DM, Joseph Cabral B, Presnyak V et al (2019) mRNA structure regulates protein expression through changes in functional half-life. *Proc Natl Acad Sci U S A* 116(48):24075–24083. <https://doi.org/10.1073/pnas.1908052116>
6. Zhang H, Zhang L, Li Z, et al. LinearDesign: Efficient Algorithms for Optimized mRNA Sequence Design arXiv Published online April 21, 2020. Accessed December 29, 2020. <http://arxiv.org/abs/2004.10177>
7. Zeng Z, Deng Y, Li X, Naumann T, Luo Y. Natural Language Processing for EHR-Based Computational Phenotyping. Published 2019. Accessed December 29, 2020. <https://ieeexplore.ieee.org/stamp/stamp.jsp?arnumber=8395074>
8. Gehrmann S, Dernoncourt F, Li Y, et al. Comparing Rule-Based and Deep Learning Models for Patient Phenotyping arXiv Published online March 25, 2017. Accessed December 29, 2020. <http://arxiv.org/abs/1703.08705>
9. Teixeira PL, Wei W-Q, Cronin RM et al (2017) Evaluating electronic health record data sources and algorithmic approaches to identify hypertensive individuals. *J Am Med Informatics Assoc* 24(1):162–171. <https://doi.org/10.1093/jamia/ocw071>



Progress in the Development of Structure-Based Vaccines

Sunil Thomas and Ann Abraham

Abstract

The immune response elicited by vaccines against microorganisms makes it the most successful medical interventions against infectious diseases. Conventional vaccines have limitations in inducing immunity against many types of pathogenic microorganism. The genetic diversity of microorganisms, coupled with the high degree of sequence variability in antigenic proteins, presents a challenge to developing broadly effective conventional vaccines. Atomic-resolution structure determination is crucial for understanding antigenic protein function. Cryo-electron microscopy, nuclear magnetic resonance spectroscopy coupled with bioinformatics provide three-dimensional structure of the antigenic proteins and provide a wealth of information about the organization of individual atoms and their chemical makeup. The atomic detail information of proteins offers enormous potential to rationally engineer proteins to enhance their properties and act as effective immunogens to induce immunity. The observation that whole protein antigens are not necessarily essential for inducing immunity has led to the emergence “structural vaccinology.” Structure-based vaccines are designed on the rationale that protective epitopes should be sufficient to induce immune responses and provide protection against pathogens. In 2013 we published a review on structure-based vaccines (Thomas and Luxon. *Expert Rev Vaccines* 12 1301–11, 2013). This review states the progress in development of structure-based vaccines since the first review.

Key words Structure-based vaccines, Structural biology, Antigen, Epitope

1 Introduction

Vaccines have revolutionized global health and have greatly reduced the spread of infectious diseases. Conventional vaccines rely on the induction of immune responses against antigenic proteins to be effective. However, conventional and recombinant vaccines have not provided efficacious solutions against several infectious diseases. The genetic diversity of microorganisms, coupled with the high degree of sequence variability in antigenic proteins, presents a challenge to developing broadly effective conventional vaccines. The observation that whole protein antigens are not necessarily essential for inducing immunity has led to the emergence of a new branch of vaccine design termed “structural

vaccinology.” Structure-based vaccines are designed on the rationale that protective epitopes should be sufficient to induce immune responses and provide protection against pathogens. Recent studies demonstrated that designing structure-based vaccine candidates with multiple epitopes induce a higher immune response. As yet no commercial vaccines are available based on structure-based design, and most of the structure-based vaccine candidates are in the preclinical stages of development [1].

Structure-based vaccine design seeks to create surfaces on immunogens that will elicit protective antibody responses against the target pathogen. Enabled by new approaches for rapid identification and selection of human monoclonal antibodies, atomic-level structural information for viral surface proteins, and capacity for precision engineering of protein immunogens and self-assembling nanoparticles, a new era of antigen design and display options has evolved. Defining the atomic-level details of key surfaces on antigens accessible on pathogens is a primary requirement for structure-based vaccine design. Knowing which proteins to target, and which specific sites on those proteins to target with antibodies, is fundamental to initiating a structure-based vaccine project. Therefore, structure-based design often begins by identifying pathogen-specific antibodies with specific properties such as potent neutralization. Geometry of antibody binding to an antigen can be an important factor in vaccine design. There are some epitopes or antigenic sites on proteins that can be bound by antibodies from multiple lineages using multiple angles of approach or degrees of rotation. However, there are other critical targets that require an antibody to approach at a particular angle or rotation. Viruses also tend to protect sites of vulnerability by frequently mutating surrounding surfaces and adding or removing glycans. These immune evasion mechanisms can therefore require long CDR loops to reach sites of vulnerability or short CDR loops to avoid clashes and allow closer proximity. Structure-based design must account for these immune-evasion mechanisms. Neutralizing activity implies that an antibody will reduce the frequency of pathogen-infected cells. To neutralize, the antibody must bind to a vulnerable site on a surface-exposed pathogen protein. The strength or potency of neutralization is determined by site of protein binding, strength of binding, accessibility of the binding site, and extent of occupancy on the available sites [2].

The field of structure-based vaccine design is rapidly maturing and can be applied to a wide variety of pathogens when antibodies with desirable properties are discovered and structures are then solved in complex with their antigens. These are the starting points for generating immunogens, or series of immunogens, that immunofocus antibody responses to sites of vulnerability. Excitingly, new antigenic targets are still being uncovered, providing new opportunities to apply this rational approach. Researchers are on the

verge of molecular control of immune responses using rationally designed immunogens, and there are tools to probe such responses in humans, thereby circumventing the need for large empirical efficacy trials. As technology continues to improve, atomic-level knowledge of antibody-antigen recognition and modes of interaction remains the linchpin of immunogen design and should provide opportunities for novel vaccines beyond those for pathogens including cancer, autoimmunity, and neurodegeneration [3].

Previously, we published a paper on structure-based vaccines [1]. This paper is an update on the progress in the development of structure-based vaccines.

2 Structure-Based Vaccines to Protect Against HIV

The advent of atomic-level structures for lead antigens has raised the notion of precise structure-based antigen design to elicit protective immune responses, as guided by known antibodies [4]. Human immunodeficiency virus (HIV) is a continual raging pandemic that is affecting millions of people globally and is a serious threat to public health. The virus is known since the early 1980s and is responsible for 32.7 million deaths since the start of the epidemic (Source: UNAIDS.org). Approximately, 38 million people are living with HIV around the globe [5]. Antibodies and cytotoxic T lymphocytes are produced upon infection with HIV-1. However, the virus has evolved several features that undermine immunological control and eradication of infection, most notably, very high antigenic diversity and the establishment of a latent viral reservoir. If left untreated, HIV-1 infection results in diminished numbers of CD4+ T cells (the major viral target cell), causing acquired immune deficiency syndrome (AIDS) and death. While treatment with antiretroviral drugs can extend the life expectancy of infected individuals to near-normal, drug resistance and side effects have been documented for every class of antiretroviral currently in use. Furthermore, cessation of therapy results in rapid viral rebound. As yet there are no vaccines for HIV and AIDS. Despite significant efforts, a vaccine capable of eliciting a protective response against the human immunodeficiency virus type 1 (HIV-1) has proved elusive [6].

Due to the integration of the virus into the DNA of the host cell, the HIV is undetectable to the immune system. Therefore, the opportunities to eradicate the virus through an immune response is formidable. The structure of the HIV is uniquely complex due to its mutability and genetic diversity, which in turn adds to the challenge of inducing an immune response in the host. HIV-1 is an enveloped, single-stranded RNA retrovirus, which, like the coronaviruses, is highly glycosylated [7]. HIV quickly integrates itself

into the host's DNA, where in some cells will remain invisible to the immune system. Within day or weeks, the virus becomes latent in the cells which limits the opportunity to eradicate the virus in its most vulnerable state [8]. To date, it has been difficult to eradicate the virus once latency is established. Due to the complexities of the HIV structure, the new mutations allow the virus to evade the immune system. The HIV-1 Envelope has genetic plasticity and antigenic variability, extensive glycosylation, and immunodominance problems that have only been explored with very limited knowledge [7].

The enormous diversity of human immunodeficiency virus (HIV)-1 strains is a major obstacle for the development of a broadly protective vaccine. Diversity is highest in the envelope glycoprotein complex (Env), the target for neutralizing antibodies (NAbs), where amino acid sequences can differ by up to 35% between subtypes. Thus, HIV-1 diversity makes it extremely difficult to induce broadly reactive NAbs (bNAbs) by an Env immunogen from any one particular HIV-1 isolate. Sliepen et al. [9] generated a native-like Env (SOSIP) trimer based on a consensus sequence of all HIV-1 group M isolates (ConM). The ConM trimer displays the epitopes of most known bNAbs and several germline bNAb precursors. The crystal structure of the ConM trimer at 3.9 Å resolution resembles that of the native Env trimer and its antigenic surface displays few rare residues. The ConM trimer elicits strong NAb responses against the autologous virus in rabbits and macaques that are significantly enhanced when it is presented on ferritin nanoparticles. The dominant NAb specificity was directed against an epitope at or close to the trimer apex. Immunogens based on consensus sequences have utility in engineering vaccines against HIV-1 and other viruses.

An approach to elicit broadly neutralizing antibodies against HIV-1 is to stabilize the structurally flexible HIV-1 envelope (Env) trimer in a conformation that displays predominantly broadly neutralizing epitopes and few to no non-neutralizing epitopes. The prefusion-closed conformation of HIV-1 Env has been identified as one such preferred conformation, and a current leading vaccine candidate is the BG505 DS-SOSIP variant, comprising two disulfides and an Ile-to-Pro mutation of Env from strain BG505. Additional mutations were introduced to further stabilize BG505 DS-SOSIP in the vaccine-preferred prefusion-closed conformation. In guinea pigs, the best mutant, DS-SOSIP.4mut, elicited a significantly higher ratio of autologous versus V3-directed neutralizing antibody responses than the SOSIP-stabilized form; the changes also resulted in an improvement in thermostability and a reduction in CD4 affinity. With improved antigenicity, stability, and immunogenicity, DS-SOSIP.4mut-stabilized trimers may have utility as HIV-1 immunogens or in other antigen-specific contexts, such as

with B-cell probes [10]. Zhang et al. [11] locked the HIV-1 Env trimer in a pre-fusion configuration, resulting in impaired CD4 binding and enhanced binding to broadly neutralizing antibodies. This design was achieved via structure-guided introduction of neo-disulfide bonds bridging the gp120 inner and outer domains and was successfully applied to soluble trimers and native gp160 from different HIV-1 clades. Thus, interdomain stabilization provides a widely applicable template for the design of Env-based HIV-1 vaccines.

The RV144 clinical trial has been the only human clinical trial to show that vaccination can provide protection from HIV infection. The RV144 vaccination protocol consisted of immunization with the ALVAC (VCP1521) canarypox virus vector, designed to elicit a robust cell-mediated immune response, followed by co-immunization with the bivalent AIDSVAX B/E gp120 vaccine, designed to elicit an anti-gp120 antibody response. This regimen provided statistically significant protection over 3.5 years, with up to 60% efficacy within the first year after vaccination. The protection of the HIV vaccine correlated with antibodies to the V2 domain of gp120, high levels of antibody-dependent cellular cytotoxicity (ADCC), and HIV-1-specific IgG3 antibodies, but not with gp120-specific CD8+ T-cell responses. The studies indicated a role for anti-gp120 antibodies in the modest but significant level of protection afforded by the vaccine. The studies associating protection with anti-gp120 antibodies provided a rationale for further development of gp120-based immunogens. Doran et al. [12] reported improving the antigenic structure of the rgp120 immunogens used in the vaccine by optimizing glycan-dependent epitopes recognized by multiple bN-mAbs. Their data demonstrated that by shifting the location of one PNGS in A244-rgp120, and by adding two PNGS to MN-rgp120, in conjunction with the production of both proteins in a cell line that favors the incorporation of oligomannose glycans, they could significantly improve the binding by three major families of bN-mAbs. The immunogens described represent a second generation of gp120-based vaccine immunogens.

Epitope-specific immunogens targeting the glycan-V3 site have been successful of eliciting antibodies capable of neutralizing HIV-1. Fusion peptide-directed antibodies have also been a target against diverse and natively glycosylated viral isolates. Clinical studies are currently being performed to elicit neutralizing responses from fusion peptide-directed antibodies [13]. New epitopes and target antibodies are being identified. However, due to the complexity of the epitopes and the mutability of the HIV, it still poses a challenge for vaccine design.

3 Structure-Based Vaccines Against Respiratory Syncytial Virus

Respiratory syncytial virus (RSV) is a non-segmented negative stranded RNA virus in the family *Pneumoviridae* that causes severe respiratory diseases in infants as well as the elderly [13]. It is a leading cause of the highest rates of childhood mortality [14]. The virus is recognized as the most important viral agent of lower respiratory tract infection worldwide, responsible for up to 199,000 deaths each year [14].

The fusion (F) glycoprotein is the antigen target for RSV, which exists in two major conformational states: prefusion (pre-F) and postfusion (post-F) [13]. The only FDA-approved regime to prevent HRSV-mediated disease is pre-exposure administration of a humanized HRSV-specific monoclonal antibody, which, although being effective, is not in widespread usage due to its cost. Currently, efforts to develop a licensed vaccine have been unsuccessful [15]. Structure-based design has been used to generate an RSV fusion glycoprotein stabilized in its prefusion conformation (DS-Cav1). This immunogen is highly effective in mice and macaques. A phase I vaccine clinical trial used the stabilized prefusion DS-Cav1 molecule. Four weeks after immunization, these vaccines elicited substantially more high-quality antibody titers than those typically generated using earlier RSV immunogens. The findings provide a proof of concept for how structural biology can contribute to precision vaccine design [7].

Clinical trials of F subunit vaccine candidates have shown an increase in neutralizing activity and ~10- to 30-fold increase in F-protein binding antibody levels; however, a large portion of the antibodies elicited are non- or poorly neutralizing, and trials have shown no or minimal efficacy [13]. Significant epitopes associated with high neutralizing activity in human sera were preserved by stabilized pre-F trimers with protein engineering. Clinical trials show that RSV pre-F vaccines induced higher titers of neutralizing activity than vaccines based on post-F proteins.

4 Structure-Based Vaccines Against Influenza

The influenza virus is a human viral pathogen that causes infections and remains a serious health threat. In the United States alone, in 2017–2018 season, there were 959,000 hospitalizations related to influenza illness, and 79,400 deaths [16]. Worldwide, the annual influenza epidemics cause 3–5 million cases of severe disease, with 290,000–650,000 of these severe cases resulting in death [17]. The delayed availability of vaccine during the 2009 H1N1 influenza pandemic created a sense of urgency to better prepare for the next influenza pandemic [18]. The influenza virus is characterized by its ability to evade immune surveillance through rapid genetic

drift and reassortment [19]. Influenza vaccine comprises two influenza A strains and one influenza B strain. Despite current vaccine production for influenza, there is an urgent need to develop a novel structure-based vaccine that is quicker and cheaper to manufacture.

Moise et al. [18] described a novel vaccine design strategy called immune engineering in the context of H7N9 influenza vaccine development. The approach combines immunoinformatic and structure modeling methods to promote protective antibody responses against H7N9 hemagglutinin (HA) by engineering whole antigens to carry seasonal influenza HA memory CD4+ T-cell epitopes—without perturbing native antigen structure—by galvanizing HA-specific memory helper T cells that support sustained antibody development against the native target HA.

The polyepitope strategy is a promising approach for successfully creating a broadly protective flu vaccine, which targets T-lymphocytes (both CD4+ and CD8+) to recognize the most conserved epitopes of viral proteins. Bazhan et al. [20] employed a computer-aided approach to develop several artificial antigens potentially capable of evoking immune responses to different virus subtypes. These antigens included conservative T-cell epitopes of different influenza A virus proteins. To design epitope-based antigens, they used experimentally verified information regarding influenza virus T-cell epitopes from the Immune Epitope Database (IEDB) (<http://www.iedb.org>). Amino acid sequences of target polyepitope antigens were designed using TEpredict/Poly-CTLDesigner software. Immunogenic and protective features of DNA constructs encoding “murine” target T-cell immunogens were studied in BALB/c mice. The authors showed that mice groups immunized with a combination of computer-generated “murine” DNA immunogens had a 37.5% survival rate after receiving a lethal dose of either A/California/4/2009 (H1N1) virus or A/Aichi/2/68 (H3N2) virus, while immunization with live flu H1N1 and H3N2 vaccine strains provided protection against homologous viruses and failed to protect against heterologous viruses. These results demonstrate that mechanisms of cross-protective immunity may be associated with the stimulation of specific T-cell responses. This study demonstrated that computer-aided approach may be successfully used for rational designing artificial polyepitope antigens capable of inducing virus-specific T-lymphocyte responses and providing partial protection against two different influenza virus subtypes.

5 Structure-Based Vaccines to Protect Against Hepatitis C Virus

Hepatitis C is a viral infection that causes liver inflammation, sometimes leading to serious liver damage. The hepatitis C virus (HCV) spreads through contaminated blood. HCV accounts for approximately 15–20% cases of acute hepatitis. After acute infection,

around 50–80% of HCV patients will develop chronic infection. Globally, HCV infects 170 million individuals. Chronic hepatitis C (CHC) patients are at high risk to develop life-threatening complications, including cirrhosis in 20% of cases and hepatocellular carcinoma (HCC) at an incidence of 45% per year in cirrhotic patients. Epidemiological studies also indicate that HCV is associated with a number of extrahepatic manifestations including insulin resistance, type 2 diabetes mellitus, glomerulopathies, oral manifestations, etc. HCV also causes liver cancer [21]. As yet there are no effective vaccines to protect against HCV.

Due to its extremely high sequence variability, HCV can readily escape the immune response; thus, an effective vaccine must target conserved, functionally important epitopes. Hepatitis C virus (HCV) envelope glycoproteins E1 and E2 are responsible for cell entry, with E2 being the major target of neutralizing antibodies (NAbs). Using the structure of a broadly neutralizing antibody in complex with a conserved linear epitope from the HCV E2 envelope glycoprotein (residues 412–423; epitope I), Pierce et al. [22] performed structure-based design of immunogens to induce antibody responses to this epitope. This resulted in epitope-based immunogens based on a cyclic defensin protein, as well as a bivalent immunogen with two copies of the epitope on the E2 surface. Mice vaccinated with the designed immunogens produced robust antibody responses to epitope I, and their serum could neutralize HCV. Notably, the cyclic designs induced greater epitope-specific responses and neutralization than the native peptide epitope.

The same authors further designed a vaccine targeting HCV envelope glycoprotein E2 (Pierce et al. [23]). They designed immunogens to modulate the structure and dynamics of E2 and favor induction of broadly neutralizing antibodies (bNAbs) in the context of a vaccine. These designs include a point mutation in a key conserved antigenic site to stabilize its conformation, as well as redesigns of an immunogenic region to add a new *N*-glycosylation site and mask it from antibody binding. Designs were experimentally characterized for binding to a panel of human monoclonal antibodies (HMABs) and the coreceptor CD81 to confirm preservation of epitope structure and preferred antigenicity profile. Selected E2 designs were tested for immunogenicity in mice, with and without hypervariable region 1, which is an immunogenic region associated with viral escape. One of these designs showed improvement in polyclonal immune serum binding to HCV pseudoparticles and neutralization of isolates associated with antibody resistance. These results indicate that antigen optimization through structure-based design of the envelope glycoproteins is a promising route to an effective vaccine for HCV. Whereas, He et al. [24] redesigned variable region 2 in a truncated form (tVR2) on E2 cores derived from genotypes 1a and 6a, resulting in improved stability and antigenicity. Crystal structures of three optimized E2

cores with human cross-genotype NAb (AR3s) revealed how the modified tVR2 stabilizes E2 without altering key neutralizing epitopes. They then displayed these E2 cores on 24- and 60-meric nanoparticles and achieved substantial yield and purity, as well as enhanced antigenicity. In mice, these nanoparticles elicited more effective NAb responses than soluble E2 cores.

6 Structure-Based Vaccines Against Coronaviruses

Coronaviruses belong to the order *Nidovirales* and are positive-strand RNA viruses that affect respiratory function. The spike glycoprotein is the major target of neutralizing antibodies; however, it is highly glycosylated and antigenically variable [25]. It is built of a receptor-binding subunit (S1) and a membrane-fusing subunit (S2). Within two decades, there have emerged three highly pathogenic and deadly human coronaviruses, namely SARS-CoV, Middle East respiratory syndrome coronavirus (MERS-CoV), and SARS-CoV-2. The economic burden and health threats caused by these coronaviruses are extremely dreadful and getting more serious as the increasing number of global infections and attributed deaths of SARS-CoV-2 and MERS-CoV [26, 27].

Middle East respiratory syndrome coronavirus (MERS-CoV) is a lineage C betacoronavirus that since its emergence in 2012 has caused outbreaks in human populations with case-fatality rates of ~36%. As in other coronaviruses, the spike (S) glycoprotein of MERS-CoV mediates receptor recognition and membrane fusion and is the primary target of the humoral immune response during infection. Pallesen et al. [28] used structure-based design to develop a generalizable strategy for retaining coronavirus S proteins in the antigenically optimal prefusion conformation and demonstrated that the engineered immunogen is able to elicit high neutralizing antibody titers against MERS-CoV. They also determined high-resolution structures of the trimeric MERS-CoV S ectodomain in complex with G4, a stem-directed neutralizing antibody. The structures reveal that G4 recognizes a glycosylated loop that is variable among coronaviruses, and they define four conformational states of the trimer wherein each receptor-binding domain is either tightly packed at the membrane-distal apex or rotated into a receptor-accessible conformation. The studies suggest a potential mechanism for fusion initiation through sequential receptor-binding events and provide a foundation for the structure-based design of coronavirus vaccines.

The CoV spike receptor-binding domain (RBD) is an attractive vaccine target for coronaviruses but is undermined by limited immunogenicity. However, a dimeric form of MERS-CoV RBD can overcome this limitation. Dai et al. [29] demonstrated that the RBD-dimer significantly increased neutralizing antibody (NAb)

titers compared to conventional monomeric form and protected mice against MERS-CoV infection. Crystal structure showed RBD-dimer fully exposed dual receptor-binding motifs, the major target for NAbs. Structure-guided design further yielded a stable version of RBD-dimer as a tandem repeat single-chain (RBD-sc-dimer) which retained the vaccine potency.

Walls et al. [30] described the structure-based design of self-assembling protein nanoparticle immunogens that elicit potent and protective antibody responses against SARS-CoV-2 in mice. The nanoparticle vaccines display 60 SARS-CoV-2 spike receptor-binding domains (RBDs) in a highly immunogenic array and induce neutralizing antibody titers tenfold higher than the prefusion-stabilized spike despite a fivefold lower dose. Antibodies elicited by the RBD nanoparticles target multiple distinct epitopes, suggesting they may not be easily susceptible to escape mutations and exhibit a lower binding:neutralizing ratio than convalescent human sera, which may minimize the risk of vaccine-associated enhanced respiratory disease. The high yield and stability of the assembled nanoparticles suggest that manufacture of the nanoparticle vaccines will be highly scalable.

Apart from vaccines, monoclonal antibodies can also be generated based on structure-based design. Recently, a humanized monoclonal antibody, H014, that efficiently neutralizes SARS-CoV-2 and SARS-CoV pseudoviruses as well as authentic SARS-CoV-2 at nanomolar concentrations by engaging the spike (S) receptor binding domain (RBD) was developed. H014 administration reduced SARS-CoV-2 titers in infected lungs and prevented pulmonary pathology in a human angiotensin-converting enzyme 2 mouse model. Cryo-electron microscopy characterization of the SARS-CoV-2 S trimer in complex with the H014 Fab fragment unveiled a previously uncharacterized conformational epitope, which was only accessible when the RBD was in an open conformation. Biochemical, cellular, virological, and structural studies demonstrated that H014 prevents attachment of SARS-CoV-2 to its host cell receptors. Epitope analysis of available neutralizing antibodies against SARS-CoV and SARS-CoV-2 uncovered broad cross-protective epitopes. The data highlight a key role for antibody-based therapeutic interventions in the treatment of COVID-19 [31].

7 Structure-Based Vaccines Against *Neisseria meningitidis*

N. meningitidis is an aerobic or facultative anaerobic, Gram-negative diplococcus that exclusively infects humans. There are at least 12 serotypes based on unique capsular polysaccharides of *N. meningitidis* with serotypes A, B, C, W, X, and Y, causing

most of the meningococcal infections. *N. meningitidis* causes significant morbidity and mortality in children and young adults worldwide through epidemic or sporadic meningitis and/or septicemia [32]. Common symptoms of meningococcal meningitis include sudden fever, headache, and stiff neck. Other symptoms may include nausea, vomiting, increased sensitivity to light, and confusion. Children and infants may show different signs and symptoms, such as inactivity, irritability, vomiting, or poor reflexes [33].

Factor H binding protein (fHbp) is a key antigen that elicits protective immunity against the meningococcus and recruits the host complement regulator, fH. As the high affinity interaction between fHbp and fH could impair immune responses, Johnson et al. [34] sought to identify non-functional fHbps that could act as effective immunogens. This was achieved by alanine substitution of fHbps from all three variant groups (V1, V2, and V3 fHbp) of the protein; while some residues affected fH binding in each variant group, the distribution of key amino underlying the interaction with fH differed between the V1, V2, and V3 proteins. To develop transgenic models to assess the efficacy of non-functional fHbps, they determined the structural basis of the low level of interaction between fHbp and murine fH; in addition to changes in amino acids in the fHbp binding site, murine fH has a distinct conformation compared with the human protein that would sterically inhibit binding to fHbp. Non-functional V1 fHbps were further characterized by binding and structural studies, and shown in non-transgenic and transgenic mice (expressing chimeric fH that binds fHbp and precisely regulates complement system) to retain their immunogenicity. The study provides a catalog of non-functional fHbps from all variant groups that can be included in new generation meningococcal vaccines, and establish proof-in-principle for clinical studies to compare their efficacy with wild-type fHbps.

Hollingshead et al. [35] generated chimeric antigens (ChAs) against serogroup B *N. meningitidis* (MenB). MenB ChAs exploit factor H binding protein (fHbp) as a molecular scaffold to display the immunogenic VR2 epitope from the integral membrane protein PorA. Structural analyses demonstrate fHbp is correctly folded and the PorA VR2 epitope adopts an immunogenic conformation. In mice, immunization with ChAs generates fHbp and PorA antibodies that recognize the antigens expressed by clinical MenB isolates; these antibody responses correlate with protection against meningococcal disease. Application of ChAs is therefore a potentially powerful approach to develop multivalent subunit vaccines, which can be tailored to circumvent pathogen diversity.

8 Structure-Based Vaccines Against Lyme Disease

Lyme disease is a multisystem illness caused by the spirochete *Borrelia burgdorferi* sensu lato. It is the most common vector-borne illness in the United States. Spirochetes have a wavelike body and flagella enclosed between the outer and inner membranes. Three genospecies of *B. burgdorferi* cause most human disease: *B. burgdorferi* sensu stricto, *Borrelia garinii*, and *B. afzelii*. *B. burgdorferi* sensu stricto is the only genospecies associated with human disease in the United States, whereas all three genospecies occur in Europe, and *B. garinii* and *B. afzelii* occur in Asia. *B. garinii* and *B. afzelii* are antigenically distinct from *B. burgdorferi* sensu stricto, and these differences may account for the variation in clinical presentation in different geographic regions [36].

Nayak et al. [37] applied a structure-based surface shaping approach for the development of a Lyme disease vaccine. The surface of the C-terminal fragment of outer surface protein A (OspA) was marked as distinct regions, based on binding sites of monoclonal antibodies. In order to target the six clinically most relevant OspA serotypes (ST) in a single protein, exposed amino acids of the individual regions were exchanged to corresponding amino acids of a chosen OspA serotype. Six chimeric proteins were constructed, and, based on their immunogenicity, four of these chimeras were tested in mouse challenge models. Significant protection could be demonstrated for all four proteins following challenge with infected ticks (OspA ST1, OspA ST2, and OspA ST4) or with in vitro-grown spirochetes (OspA ST1 and OspA ST5). Two of the chimeric proteins were linked to form a fusion protein, which provided significant protection against in vitro-grown spirochetes (OspA ST1) and infected ticks (OspA ST2).

A multivalent OspA-based vaccine was designed by Comstedt et al. [38]. The vaccine includes three proteins, each containing the C-terminal half of two OspA serotypes linked to form a heterodimer. In order to stabilize the C-terminal fragment and thus preserve important structural epitopes at physiological temperature, disulfide bonds were introduced. The immunogenicity was increased by introduction of a lipidation signal which ensures the addition of an N-terminal lipid moiety. Three immunizations with 3.0 µg adjuvanted vaccine protected mice from a challenge with spirochetes expressing either OspA serotype 1, 2, or 5. Mice were protected against both challenge with infected ticks and in vitro grown spirochetes. Immunological analyses (ELISA, surface binding, and growth inhibition) indicated that the vaccine can provide protection against the majority of *Borrelia* species pathogenic for humans.

Outer surface protein C (OspC) is a major antigen on the surface of *B. burgdorferi*. Experimental Osp C-based subunit chimeritope vaccinogens for Lyme disease were assessed by Izac et al. [39] for immunogenicity, structure, ability to elicit antibody (Ab) responses to divergent OspC proteins, and bactericidal activity. Chimeritopes are chimeric epitope-based proteins that consist of linear epitopes derived from multiple proteins or multiple variants of a protein. An inherent advantage to chimeritope vaccinogens is that they can be constructed to trigger broadly protective Ab responses. Three OspC chimeritope proteins Chv1, Chv2, and Chv3 were comparatively assessed. All Chv proteins were immunogenic in mice and rats eliciting high titer Ab. Immunoblot and ELISA demonstrated that the Chv proteins elicit IgG that recognizes a diverse array of OspC type proteins. The study highlighted the ability of OspC chimeritopes to serve as vaccinogens that trigger potentially broadly protective Ab responses.

9 Structure-Based Vaccines to Protect Against *Streptococci*

Streptococcus pyogenes (group A streptococcus) are Gram-positive, nonmotile, non-spore forming, catalase-negative cocci that occur in pairs or chains. Older cultures may lose their Gram-positive character. Most Streptococci are facultative anaerobes, and some are obligate anaerobes. Group A strep, sometimes called GAS, tends to affect the throat and the skin. People may carry GAS yet may not show any symptoms of illness. Most strep A infections cause relatively mild illness, but on rare occasions, these bacteria can lead to severe and even life-threatening disease [40].

A major obstacle to the development of broadly protective M protein-based group A streptococcal (GAS) vaccines is the variability within the N-terminal epitopes that evoke potent bactericidal antibodies. M protein sequences (AA 16–50) from the E4 cluster containing 17 emm types of GAS were analyzed using de novo 3D structure prediction tools and the resulting structures subjected to chemical diversity analysis to identify sequences that were the most representative of the 3D physicochemical properties of the M peptides in the cluster. The synthetic vaccine rabbit antisera reacted with all 17 E4 M peptides and demonstrated bactericidal activity against 15/17 E4 GAS. A recombinant hybrid vaccine containing the E4 peptides elicited antibodies that cross-reacted with all E4 M peptides [41].

Loh et al. [42] generated a multivalent vaccine called TeeVax1, a recombinant protein that consists of a fusion of six T-antigen domains. Vaccination with TeeVax1 produces opsonophagocytic antibodies in rabbits and confers protective efficacy in mice against invasive disease. Two further recombinant proteins TeeVax2 and TeeVax3 were constructed to cover 12 additional T-antigens.

Combining TeeVax1–3 produced a robust antibody response in rabbits that was cross-reactive to a full panel of 21 T-antigens, expected to provide over 95% vaccine coverage. The study demonstrated the potential for a T-antigen-based vaccine to prevent GAS infections.

Kuo et al. [43] developed a vaccine using the polyvalence epitope recombinant FSBM protein (rFSBM), which contains four different epitopes, including the fibronectin-binding repeats domain of streptococcal fibronectin binding protein Sfb1, the C-terminal immunogenic segment of streptolysin S, the C3-binding motif of streptococcal pyrogenic exotoxin B, and the C-terminal conserved segment of M protein. Vaccination with the rFSBM protein successfully prevented mortality and skin lesions caused by several emm strains of GAS infection. Anti-FSBM antibodies collected from the rFSBM-immunized mice were able to opsonize at least six emm strains and can neutralize the hemolytic activity of streptolysin S. The internalization of GAS into nonphagocytic cells is also reduced by anti-FSBM serum. The study suggested that rFSBM can be applied as a vaccine candidate to prevent different emm strains of GAS infection.

Streptococcus agalactiae (group B streptococcus) or GBS can cause illness in people of all ages, though it can be particularly severe in newborns, most commonly causing sepsis, pneumonia, and meningitis. In adults, the most common health issues caused by GBS include urinary tract infections, skin infections, bloodstream infections, pneumonia, skin and soft-tissue infections, and bone and joint infections [44]. Currently, there are no licensed vaccines for GBS infections.

Based on the structural epitope of the capsular polysaccharide from type III Group B *Streptococcus* (GBSIII), Oldrini et al. [45] designed a conjugate vaccine. Using X-ray crystallographic structure of the polysaccharide fragment–mAb complex, they synthesized a hexasaccharide comprising exclusively the relevant positions involved in binding. Combining competitive surface plasmon resonance and saturation transfer difference NMR spectroscopy as well as in silico modeling, they demonstrated that this synthetic glycan was recognized by the mAb similarly to the dimer. The hexasaccharide conjugated to CRM197, a mutant of diphtheria toxin, elicited a robust functional immune response that was not inferior to the polysaccharide conjugate, indicating that it may suffice as a vaccine antigen.

10 Structure-Based Vaccines to Protect Against *Staphylococcus aureus*

Staphylococcus aureus is a Gram-positive bacteria that cause a wide variety of clinical diseases. Infections caused by this pathogen are common both in community-acquired and hospital-acquired settings. The treatment remains challenging due to the emergence of

multi-drug resistant strains such as MRSA (Methicillin-Resistant *Staphylococcus aureus*). *S. aureus* does not normally cause infection on healthy skin; however, if it is allowed to enter the internal tissues or bloodstream, these bacteria may cause a variety of potentially serious infections [46].

Efforts to develop effective vaccines against *S. aureus* have been largely unsuccessful, in part due to the variety of virulence factors produced by this organism. *S. aureus* alpha-hemolysin (Hla) is a pore-forming toxin expressed by most *S. aureus* strains and reported to play a key role in the pathogenesis of SSTI and pneumonia. Adhikari et al. [47] reported a recombinant subunit vaccine candidate for Hla, rationally designed based on the heptameric crystal structure. This vaccine candidate, denoted by AT-62aa, was tested in pneumonia and bacteremia infection models using *S. aureus*. The authors reported significant protection from lethal bacteremia upon vaccination with AT-62aa. Passive transfer of rabbit immunoglobulin against AT-62aa (AT62-IgG) protected mice against intraperitoneal and intranasal challenge with USA300 and produced significant reduction in bacterial burden in blood, spleen, kidney, and lungs. AT62-IgG and sera from vaccinated mice effectively neutralized the toxin in vitro and AT62-IgG inhibited the formation of Hla heptamers, suggesting antibody-mediated neutralization as the primary mechanism of action.

S. aureus thwarts the host defense by secreting a myriad of virulence factors, including bicomponent, pore-forming leukotoxins. While all vaccine development efforts that aimed at achieving opsonophagocytic killing have failed, targeting virulence by toxoid vaccines represents a novel approach to preventing mortality and morbidity that are caused by SA. Leukotoxin LukAB kills human phagocytes and monocytes, and it is present in all known *S. aureus* clinical isolates. While using a structure-guided approach, Kailasan et al. [48] generated a library of mutations that targeted functional domains within the LukAB heterodimer to identify attenuated toxoids as potential vaccine candidates. The mutants were evaluated based on expression, solubility, yield, biophysical properties, cytotoxicity, and immunogenicity, and several fully attenuated LukAB toxoids that were capable of eliciting high neutralizing antibody titers were identified. Rabbit polyclonal antibodies against the lead toxoid candidate provided potent neutralization of LukAB. While the neutralization of LukAB alone was not sufficient to fully suppress leukotoxicity in supernatants of *S. aureus* USA300 isolates, a combination of antibodies against LukAB, α -toxin, and Pantone-Valentine leukocidin completely neutralized the cytotoxicity of these strains. These data strongly support that the inclusion of LukAB toxoids in a multivalent toxoid vaccine for the prevention of *S. aureus* disease.

The antigenic proteins coproporphyrinogen III oxidase (CgoX) and triose phosphate isomerase (TPI) fulfil essential housekeeping functions in heme synthesis and glycolysis, respectively. Immunization with rCgoX and rTPI elicited protective immunity against *S. aureus* bacteremia. Two monoclonal antibodies (mAb), CgoX-D3 and TPI-H8, raised against CgoX and TPI, efficiently provided protection against *S. aureus* infection. MAb-CgoX-D3 recognized a linear epitope spanning 12 amino acids, whereas TPI-H8 recognized a larger discontinuous epitope. The CgoX-D3 epitope conjugated to BSA elicited a strong, protective immune response against *S. aureus* infection. The CgoX-D3 epitope is highly conserved in clinical *S. aureus* isolates, indicating its potential wide usability against *S. aureus* infection. The data suggest that immunofocusing through epitope-based immunization constitutes a strategy for the development of a *S. aureus* vaccine with greater efficacy and better safety profile [49].

11 Conclusion

In spite of vaccinations, infectious diseases still take a heavy toll on the global population, and that provides strong rationale for broadening vaccine development repertoire. Hence, there is a need for novel vaccination strategies to protect against infectious diseases. Structural vaccinology, in which protein structure information is utilized to design immunogens, has promise to provide new vaccines against traditionally difficult targets. Crystal structures of antigens containing one or more protection epitopes, especially when in complex with a protective antibody, are the starting point for immunogen design. To develop vaccines that protect against antigenically variable pathogens, pioneering structure-based work demonstrated that multiple strain-specific epitopes could be engineered onto a single immunogen [50].

References

1. Thomas S, Luxon BA (2013) Vaccines based on structure-based design provide protection against infectious diseases. *Expert Rev Vaccines* 12:1301–1311
2. Graham BS, Gilman MSA, McLellan JS (2019) Structure-based vaccine antigen design. *Annu Rev Med* 70:91–104
3. Ward AB, Wilson IA (2020) Innovations in structure-based antigen design and immune monitoring for next generation vaccines. *Curr Opin Immunol* 65:50–56
4. Kwong PD, DeKosky BJ, Ulmer JB (2020) Antibody-guided structure-based vaccines. *Semin Immunol* 50:101428
5. UN AIDS (2020) Global HIV & AIDS statistics—2020 fact sheet. Retrieved from. <https://www.unaids.org/en/resources/fact-sheet>
6. Seabright GE, Doores KJ, Burton DR, Crispin M (2019) Protein and glycan mimicry in HIV vaccine design. *J Mol Biol* 431(12):2223–2247
7. Crank MC, Ruckwardt TJ, Chen M, Morabito KM, Phung E, Costner PJ, Holman LA, Hickman SP, Berkowitz NM, Gordon IJ, Yamshchikov GV, Gaudinski MR, Kumar A, Chang LA, Moin SM, Hill JP, AT DP, Schwartz RM, Kueltzo L, Cooper JW, Chen P, Stein JA, Carlton K, Gall JG, Nason MC, Kwong PD,

- Chen GL, Mascola JR, JS ML, Ledgerwood JE, Graham BS, VRC 317 Study Team (2019) A proof of concept for structure-based vaccine design targeting RSV in humans. *Science* 365(6452):505–509
8. Chun TW, Engel D, Berrey MM, Shea T, Corey L, Fauci AS (1998) Early establishment of a pool of latently infected, resting CD4(+) T cells during primary HIV-1 infection. *Proc Natl Acad Sci U S A* 95:8869–8873
 9. Sliepen K, Han BW, Bontjer I, Mooij P, Garcés F, Behrens AJ, Rantalainen K, Kumar S, Sarkar A, Brouwer PJM, Hua Y, Tolazzi M, Schermer E, Torres JL, Ozorowski G, van der Woude P, de la Peña AT, van Breemen MJ, Camacho-Sánchez JM, Burger JA, Medina-Ramírez M, González N, Alcami J, LaBranche C, Scarlatti G, van Gils MJ, Crispin M, Montefiori DC, Ward AB, Koopman G, Moore JP, Shattock RJ, Bogers WM, Wilson IA, Sanders RW (2019) Structure and immunogenicity of a stabilized HIV-1 envelope trimer based on a group-M consensus sequence. *Nat Commun* 10(1):2355
 10. Chuang GY, Geng H, Pancera M, Xu K, Cheng C, Acharya P, Chambers M, Druz A, Tsybovsky Y, Wanninger TG, Yang Y, Doria-Rose NA, Georgiev IS, Gorman J, Joyce MG, O'Dell S, Zhou T, McDermott AB, Mascola JR, Kwong PD (2017) Structure-based design of a soluble prefusion-closed HIV-1 Env trimer with reduced CD4 affinity and improved immunogenicity. *J Virol* 91(10):e02268–e02216
 11. Zhang P, Gorman J, Geng H, Liu Q, Lin Y, Tsybovsky Y, Go EP, Dey B, Andine T, Kwon A, Patel M, Gururani D, Uddin F, Guzzo C, Cimburo R, Miao H, McKee K, Chuang GY, Martin L, Sironi F, Malnati MS, Desaire H, Berger EA, Mascola JR, Dolan MA, Kwong PD, Lusso P (2018) Interdomain stabilization impairs CD4 binding and improves immunogenicity of the HIV-1 envelope trimer. *Cell Host Microbe* 23(6):832–844.e6
 12. Doran RC, Tatsuno GP, O'Rourke SM, Yu B, Alexander DL, Mesa KA, Berman PW (2018) Glycan modifications to the gp120 immunogens used in the RV144 vaccine trial improve binding to broadly neutralizing antibodies. *PLoS One* 13(4):e0196370
 13. Kwong D (2020) Antibody-guided structure-based vaccines. *Semin Immunol*:101428
 14. Graham G (2019) Structure-based vaccine antigen design. *Annu Rev Med* 70(1):91–104
 15. Muniyandi S, Pangratiou G, Edwards TA, Barr JN (2018) Structure and function of the human respiratory syncytial virus M2-1 protein. *Subcell Biochem* 88:245–260
 16. Centers for Disease Control and Prevention (2018) Estimated Influenza Illnesses, Medical Visits, Hospitalizations, and Deaths in the United States — 2017–2018 Influenza Season | CDC. Available online at: <https://www.cdc.gov/flu/about/burden/estimates.htm>
 17. Sherman AC, Mehta A, Dickert NW, Anderson EJ, Roupheal N (2019) The future of flu: a review of the human challenge model and systems biology for advancement of influenza vaccinology. *Front Cell Infect Microbiol* 9:107
 18. Moise L, Biron BM, Boyle CM, Yilmaz NK, Jang H, Schiffer C, Ross TM, Martin WD, De Groot AS (2018) T cell epitope engineering: an avian H7N9 influenza vaccine strategy for pandemic preparedness and response. *Hum Vaccin Immunother* 14(9):2203–2207
 19. Ekiert DC, Bhabha G, Elsliger MA, Friesen RH, Jongeneelen M, Throsby M, Goudsmit J, Wilson IA (2009) Antibody recognition of a highly conserved influenza virus epitope. *Science* 324:246–251
 20. Bazhan SI, Antonets DV, Starostina EV, Ilyicheva TN, Kaplina ON, Marchenko VY, Volkova OY, Bakulina AY, Karpenko LI (2020) In silico design of influenza a virus artificial epitope-based T-cell antigens and the evaluation of their immunogenicity in mice. *J Biomol Struct Dyn*:1–17
 21. Li HC, Lo SY (2015) Hepatitis C virus: virology, diagnosis and treatment. *World J Hepatol* 7(10):1377–1389
 22. Pierce BG, Boucher EN, Piepenbrink KH, Ejemel M, Rapp CA, Thomas WD Jr, Sundberg EJ, Weng Z, Wang Y (2017) Structure-based Design of Hepatitis C Virus Vaccines that Elicit Neutralizing Antibody Responses to a conserved epitope. *J Virol* 91(20):e01032–e01017
 23. Pierce BG, Keck ZY, Wang R, Lau P, Garagusi K, Elkholy K, Toth EA, Urbanowicz RA, Guest JD, Agnihotri P, Kerzic MC, Marin A, Andrianov AK, Ball JK, Mariuzza RA, Fuerst TR, Founng SKH (2020) Structure-based design of hepatitis C virus E2 glycoprotein improves serum binding and cross-neutralization. *J Virol* 94(22):e00704–e00720
 24. He L, Tzarum N, Lin X, Shapero B, Sou C, Mann CJ, Stano A, Zhang L, Nagy K, Giang E, Law M, Wilson IA, Zhu J (2020) Proof of concept for rational design of hepatitis C virus E2 core nanoparticle vaccines. *Sci Adv* 6(16):eaaz6225
 25. Buchholz U (2004) Contributions of the structural proteins of severe acute respiratory syndrome coronavirus to protective immunity. *Proc Natl Acad Sci U S A* 101:9804–9809

26. Zhu Z, Lian X, Su X et al (2020) From SARS and MERS to COVID-19: a brief summary and comparison of severe acute respiratory infections caused by three highly pathogenic human coronaviruses. *Respir Res* 21:224
27. Thomas S (2020) The structure of the membrane protein of SARS-CoV-2 resembles the sugar transporter SemiSWEET. *Pathog Immun* 5(1):342–363
28. Pallesen J, Wang N, Corbett KS, Wrapp D, Kirchdoerfer RN, Turner HL, Cottrell CA, Becker MM, Wang L, Shi W, Kong WP, Andres EL, Kettenbach AN, Denison MR, Chappell JD, Graham BS, Ward AB, McLellan JS (2017) Immunogenicity and structures of a rationally designed prefusion MERS-CoV spike antigen. *Proc Natl Acad Sci U S A* 114(35):E7348–E7357
29. Dai L, Zheng T, Xu K, Han Y, Xu L, Huang E, An Y, Cheng Y, Li S, Liu M, Yang M, Li Y, Cheng H, Yuan Y, Zhang W, Ke C, Wong G, Qi J, Qin C, Yan J, Gao GF (2020) A universal design of betacoronavirus vaccines against COVID-19, MERS, and SARS. *Cell* 182(3):722–733.e11
30. Walls AC, Fiala B, Schäfer A, Wrenn S, Pham MN, Murphy M, Tse LV, Shehata L, O'Connor MA, Chen C, Navarro MJ, Miranda MC, Pettie D, Ravichandran R, Kraft JC, Ogohara C, Palsler A, Chalk S, Lee EC, Guerriero K, Kepl E, Chow CM, Sydeman C, Hodge EA, Brown B, Fuller JT, Dinnon KH 3rd, Gralinski LE, Leist SR, Gully KL, Lewis TB, Guttman M, Chu HY, Lee KK, Fuller DH, Baric RS, Kellam P, Carter L, Pepper M, Sheahan TP, Veesler D, King NP (2020) Elicitation of potent neutralizing antibody responses by designed protein nanoparticle vaccines for SARS-CoV-2. *Cell* 183(5):1367–1382.e17
31. Lv Z, Deng YQ, Ye Q, Cao L, Sun CY, Fan C, Huang W, Sun S, Sun Y, Zhu L, Chen Q, Wang N, Nie J, Cui Z, Zhu D, Shaw N, Li XF, Li Q, Xie L, Wang Y, Rao Z, Qin CF, Wang X (2020) Structural basis for neutralization of SARS-CoV-2 and SARS-CoV by a potent therapeutic antibody. *Science* 369(6510):1505–1509
32. Nguyen N, Ashong D (2020) *Neisseria Meningitidis*. In: StatPearls [internet]. Treasure Island (FL): StatPearls publishing. Retrieved from. <https://www.ncbi.nlm.nih.gov/books/NBK549849/>
33. Centers for Disease Control and Prevention (2020) Meningococcal Disease (*Neisseria meningitidis*). Retrieved from. <https://wwwnc.cdc.gov/travel/diseases/meningococcal-disease>
34. Johnson S, Tan L, van der Veen S, Caesar J, Goicoechea De Jorge E, Harding RJ, Bai X, Exley RM, Ward PN, Ruivo N, Trivedi K, Cumber E, Jones R, Newham L, Staunton D, Ufret-Vincenty R, Borrow R, Pickering MC, Lea SM, Tang CM (2012) Design and evaluation of meningococcal vaccines through structure-based modification of host and pathogen molecules. *PLoS Pathog* 8(10):e1002981
35. Hollingshead S, Jongerius I, Exley RM, Johnson S, Lea SM, Tang CM (2018) Structure-based design of chimeric antigens for multivalent protein vaccines. *Nat Commun* 9:1–10
36. Marques AR (2010) Lyme disease: a review. *Curr Allergy Asthma Rep* 10:13–20
37. Nayak A, Schüler W, Seidel S, Gomez I, Meinke A, Comstedt P, Lundberg U (2020) Broadly protective multivalent OspA vaccine against Lyme Borreliosis, developed based on surface shaping of the C-terminal fragment. *Infect Immun* 88(4):e00917–e00919
38. Comstedt P, Hanner M, Schüler W, Meinke A, Lundberg U (2014) Design and development of a novel vaccine for protection against Lyme borreliosis. *PLoS One* 9(11):e113294
39. Izac JR, O'Bier NS, Oliver LD Jr, Camire AC, Earnhart CG, LeBlanc Rhodes DV, Young BF, Parnham SR, Davies C, Marconi RT (2020) Development and optimization of OspC chimeritope vaccinogens for Lyme disease. *Vaccine* 38(8):1915–1924
40. Cunningham MW (2000) Pathogenesis of Group A streptococcal infections. *Clin Microbiol Rev* 13(3):470–511
41. Dale JB, Smeesters PR, Courtney HS, Penfound TA, Hohn CM, Smith JC, Baudry JY (2017) Structure-based design of broadly protective group A streptococcal M protein-based vaccines. *Vaccine* 35(1):19–26
42. Loh JMS, Rivera-Hernandez T, McGregor R et al (2021) A multivalent T-antigen-based vaccine for Group A *Streptococcus*. *Sci Rep* 11:4353
43. Kuo C-F, Tsao N, Hsieh I-C, Lin Y-S, Wu J-J, Hung Y-T (2017) Immunization with a streptococcal multiple-epitope recombinant protein protects mice against invasive group A streptococcal infection. *PLoS One* 12(3):e0174464
44. Raabe VN, Shane AL (2019) Group B Streptococcus (*Streptococcus agalactiae*). *Microbiol Spectr* 7(2). <https://doi.org/10.1128/microbiolspec.GPP3-0007-2018>
45. Oldrini D, Del Bino L, Arda A, Carboni F, Henriques P, Angiolini F, Quintana JI,

- Calloni I, Romano MR, Berti F, Jimenez-Barbero J, Margarit I, Adamo R (2020) Structure-guided Design of a Group B Streptococcus Type III synthetic glycan-conjugate vaccine. *Chemistry* 26(31):7018–7025
46. Taylor TA, Unakal CG (2020) *Staphylococcus Aureus*. In: StatPearls [internet]. Treasure Island (FL): StatPearls publishing. Retrieved from. <https://www.ncbi.nlm.nih.gov/books/NBK441868/>
47. Adhikari RP, Karauzum H, Sarwar J, Abaandou L, Mahmoudieh M, Boroun AR et al (2012) Novel structurally designed vaccine for *S. aureus* α -Hemolysin: protection against bacteremia and pneumonia. *PLoS One* 7(6):e38567
48. Kailasan S, Kort T, Mukherjee I, Liao GC, Kanipakala T, Williston N, Ganjbaksh N, Venkatasubramaniam A, Holtsberg FW, Karauzum H, Adhikari RP, Aman MJ (2019) Rational design of toxoid vaccine Candidates for *Staphylococcus aureus* Leukocidin AB (LukAB). *Toxins (Basel)* 11(6):339
49. Klimka A, Mertins S, Nicolai AK et al (2021) Epitope-specific immunity against *Staphylococcus aureus* coproporphyrinogen III oxidase. *NPJ Vaccines* 6:11
50. Kulp DW, Schief WR (2013) Advances in structure-based vaccine design. *Curr Opin Virol* 3(3):322–331



Polymer–Peptide Conjugate Vaccine for Oral Immunization

Mohammad Omer Faruck, Mariusz Skwarczynski, and Istvan Toth

Abstract

The copper-catalyzed azide-alkyne cycloaddition (CuAAC) reaction, well-known as “click” reaction, is widely used in organic synthesis, medicinal chemistry, and polymer science for the conjugation of molecular entities of all sizes. In this protocol, B-cell epitope J8, derived from group A *Streptococcus* (GAS) M protein, and universal T-helper epitope PADRE were conjugated to poly(methyl acrylate) (PMA) to form a self-assembled nanoparticle vaccine candidate (PMA-P-J8). The vaccine construct was orally administered to mice in a single dose of 30 µg, resulting in the production of a high number of serum (IgG) and salivary (IgA) antibodies.

Key words Single immunization, Copper-catalyzed alkyne-azide cycloaddition click reaction, Self-assembly, Dialysis, Poly(methyl acrylate)

1 Introduction

Vaccines are designed to protect a host against a specific disease. They are usually safe, stable, reproducible, and inexpensive. Traditionally, vaccines have been produced using live-attenuated or killed whole microorganisms. However, these vaccines can revert to a virulent state or induce allergies and autoimmune responses [1]. Furthermore, traditional vaccines need cold chain for transportation and storage, which is often impractical in developing countries or remote areas [2]. To overcome these disadvantages, subunit vaccines, including protein and peptide-based vaccines, have been extensively investigated.

Peptide-based vaccines are composed of minimal immunologic components (known as epitopes) [3]. They are easy to synthesize in a pure state and at large scale. The exclusion of redundant components from these vaccines eliminates or reduces the risk of adverse post-immunization reactions; however, it also greatly reduces vaccine immunogenicity. Therefore, adjuvants (immune stimulants) are usually incorporated into peptide-based vaccines to augment immune responses [4].

Recently, polymers have shown great promise as vaccine delivery systems with self-adjuncting properties. Polymers can be given either as a physical mixture with antigen or conjugated to the antigen. Various polymer-based antigen delivery systems have been designed, including polymer-coated liposomes [5], nanoparticles [6, 7], polyelectrolytes [8, 9], hydrogels [10], microparticles [11], and microspheres [12].

Oral administration is the preferred delivery route for pharmaceuticals, due to high patient compliance and elimination of the need for professional personnel during therapy or vaccination [13, 14]. However, peptide antigens are extremely labile in the gastrointestinal tract (GIT) and are promptly degraded by proteases. In addition, antigens become highly diluted upon oral administration due to the large surface area of the GIT. This leads to the requirement for multiple, high doses of the vaccine, and strong adjuvants to avoid the induction of immune tolerance [15].

Streptococcus pyogenes is a Gram-positive *coccus* bacterium that colonizes the pharynx and skin. It is often referred to as group A *Streptococcus* (GAS). GAS is responsible for a variety of diseases, as well as deadly postinfectious complications [16, 17]. Currently, no vaccines are available for GAS infection.

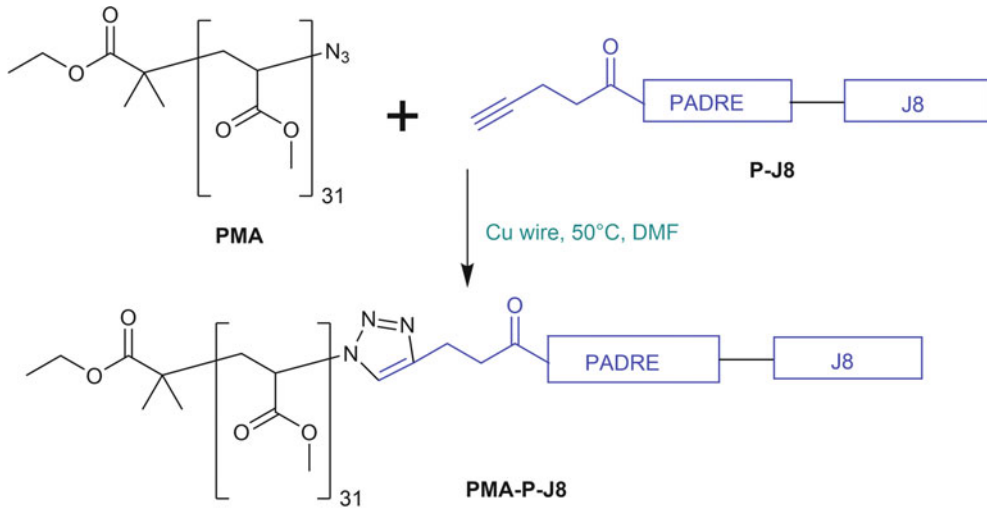
In this protocol, conjugation between P-J8 peptide, covering B-cell epitope J8 derived from GAS M protein, together with universal T-helper epitope PADRE (P), and commercial poly (methyl acrylate) (PMA) was performed using copper-catalyzed alkyne-azide 1,3-dipolar cycloaddition (CuAAC) reaction in the presence of copper wires to produce PMA-P-J8 (Fig. 1) [18]. P-J8 was synthesized according to solid-phase peptide synthesis methods presented previously in this book series [19–21]. The produced conjugate (PMA-P-J8) was self-assembled into nanoparticles using the solvent exchange method, dialyzed, and analyzed by elemental analysis. Mice were orally immunized with PMA-P-J8, and antigen-specific antibody production was analyzed by ELISA.

2 Materials

All solutions should be prepared using peptide synthesis/chromatography grade chemicals and ultrapure water (from a MilliQ water system with a sensitivity of 18.1 M cm at 25 °C) at room temperature.

2.1 Polymer–Peptide Conjugation

1. *N,N*-Dimethylformamide (DMF).
2. Poly(methyl acrylate) with azide terminal (molecular weight 2500–3000).
3. Copper wire.



J8= QAEDKVKQSREAKKQVEKALKQLEDKVQ

PADRE (P)=AKFVAAWTLKAAA

Fig. 1 Schematic illustration of the peptide-polymer conjugation

4. Sulfuric acid (ACS reagent, 95–98%).
5. Round-bottom flask (2 mL).
6. Balance.
7. Vortex machine.
8. Magnetic stirrer.
9. Beaker (1000 mL).
10. Rubber stopper for the 2-mL flask.
11. Aluminum foil.
12. Oil bath.
13. Magnetic stirrer mixer with hot plate.
14. Porcelain filter funnel.
15. Syringe (5 mL).
16. Needles (21G 1 TW, 0.8 mm × 25 mm).
17. Scintillation vial (20 mL).
18. Microfilter (pore size 0.45 μm, volume 12 mL).
19. Thermometer.
20. Dialysis bag (Pierce snakeskin, MWCO 10 K).
21. Dialysis clips.
22. Syringe pump.

23. Zetasizer—Malvern Panalytical, for dynamic light scattering measurement.
24. Long metal needle.

2.2 Immunization

1. Black mice (C57BL/6, 4–6 weeks old, female).
2. Pilocarpine.
3. Ear puncher/notcher.
4. Eppendorf tubes.
5. Phenylmethylsulfonylfluoride (PMSF) protease inhibitor.
6. Cholera endotoxin subunit: B (CTB).

3 Methods

3.1 Polymer–Peptide Conjugation

1. Weigh 7.0 mg (2.54 μmol , 1.4 equivalent) of the peptide, P-J8, in an Eppendorf tube using a microbalance (*see Note 1*).
2. Weigh 5.0 mg (1.82 μmol , 1.0 equivalent) of PMA in a separate Eppendorf tube using a microbalance.
3. Add 1 mL DMF into the tube with P-J8 and dissolve properly using the vortex.
4. Add 1 mL DMF into the tube with PMA and dissolve properly using the vortex (*see Note 2*).
5. Transfer both peptides/polymer into a 2-mL round-bottom flask.
6. Add 60 mg of Cu wire and a stirring bar into the flask (*see Note 3*).
7. Seal the flask with a rubber stopper.
8. Insert a needle with attached nitrogen balloon into the stopper, then insert a second empty/open needle to allow nitrogen flow through the flask for 15–30 s (*see Note 4*).
9. Cover the reaction mixture with aluminum foil and stir at 50 °C under nitrogen atmosphere (Fig. 2) (*see Note 5*).
10. Filter the reaction mixture using a 0.12- μm nylon filter; wash the remaining wires with 0.5 mL DMF and filter again.
11. Transfer the 2.5 mL filtered reaction mixture into a 5-mL plastic syringe.
12. Add 5 mL distilled water into a 20-mL scintillation vial equipped with a 1-cm stirring bar.
13. Attach a long, bent metal needle to the 5-mL syringe (*see Note 6*).
14. Insert the bent needle into the 20-mL scintillation vial.
15. Set the flow rate on the syringe pump to 0.7 mL/hour and add the conjugated solution dropwise to the water (Fig. 3).

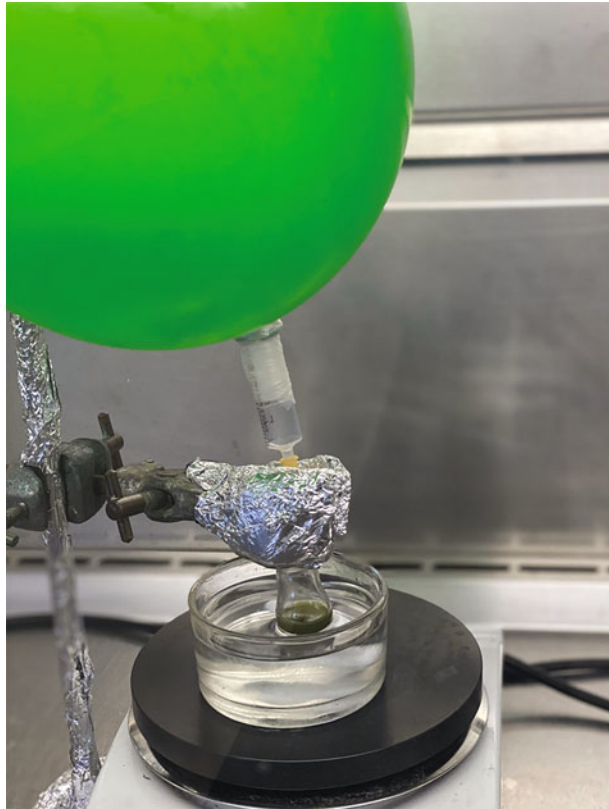


Fig. 2 The conjugation reaction upon completion (bluish/green solution)

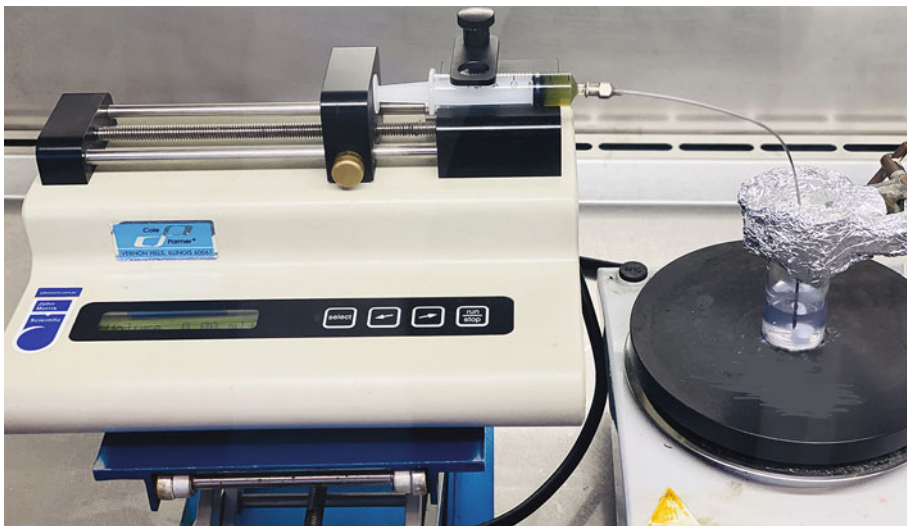


Fig. 3 Self-assembly of the particles

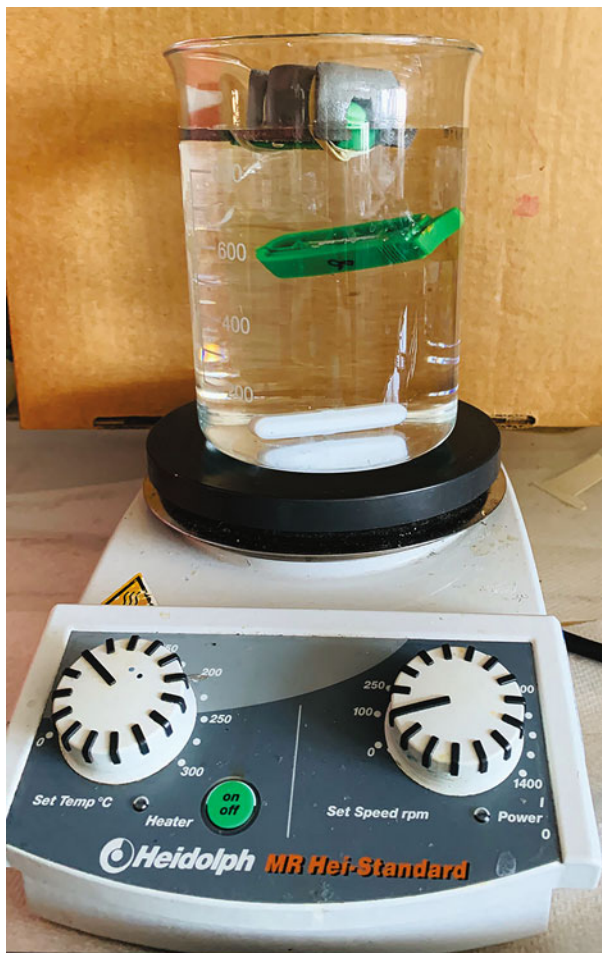


Fig. 4 Dialysis against water

16. Transfer the produced solution from the scintillation vial to a dialysis bag.
17. Close the dialysis bag from both sides using dialysis clips and use a sponge support to keep the bag in the water. Put bag in the beaker with water (Fig. 4).
18. Dialyze against water for 3 days with a stirring speed of 250 rpm. Change the water frequently: at least three times per day (*see Note 7*).
19. Transfer the conjugated solution from the dialysis bag to a clean scintillation vial.
20. Check the particle size and polydispersity index (PDI) using dynamic light scattering (DLS).
21. Freeze-dry half of the PMA-P-J8 solution (~3 mL) to quantify conjugation efficacy and yield (*see Note 8*).
22. Use the freeze-dried product to perform elemental analysis and calculate the substitution ratio (Fig. 5) (*see Note 9*).

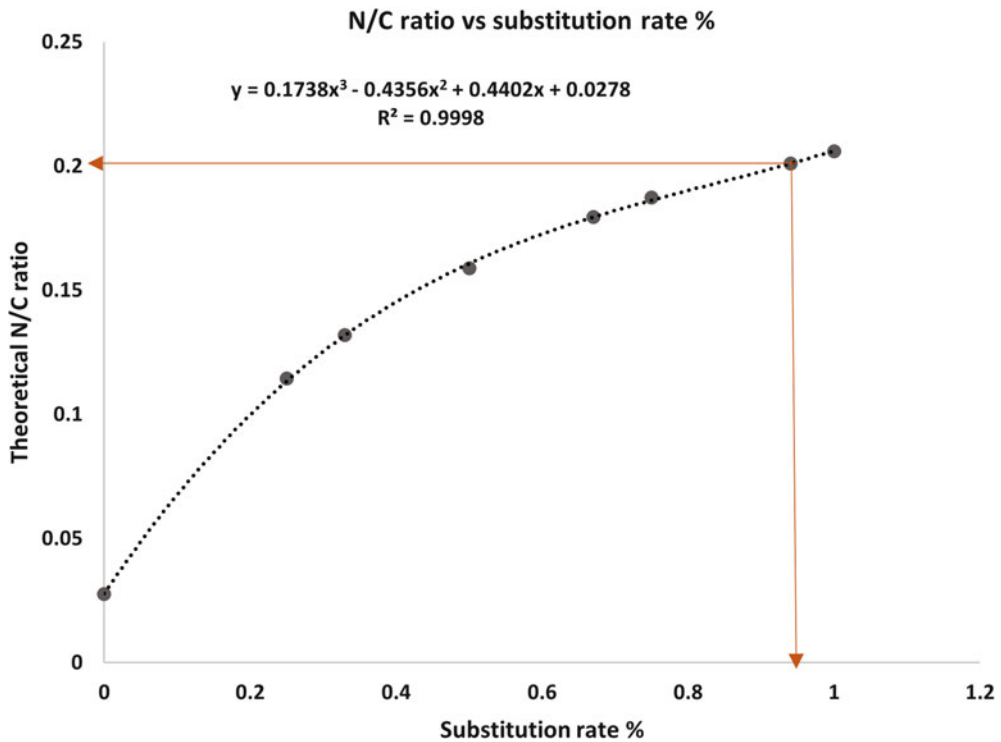


Fig. 5 The curve of the theoretical substitution ratio of the peptide conjugated to polymer compared to the N/C ratio. The brown line represents experimental values for PMA-P-J8

3.2 Immunization

1. Maintain all mice in clean cages.
2. Divide the mice into three groups: PBS (negative control group), PMA-P-J8, PMA-P-J8 + CTB (positive control group).
3. Collect a blood sample (10 μ L) via tail bleed (day 0) for naïve serum.
4. Dilute all blood serum samples with PBS (1 \times).
5. Centrifuge blood for 10 min at 4300 $\times g$.
6. Collect the serum supernatant.
7. Store the supernatant at -80°C for further analysis.
8. Collect saliva (naïve controls) before immunization (day 0) (*see Note 10*).
9. Store the saliva samples in tubes pretreated with the protease inhibitor, phenylmethylsulfonylfluoride (PMSF).
10. Orally administer 30 μ g of PMA-P-J8 solution (freshly prepared peptide-polymer conjugation) in 30 μ L of water to each mouse in the PMA-P-J8 group (day 1).
11. Orally administer 30 μ L of 1 \times PBS to each mouse in the negative control group (day 1).

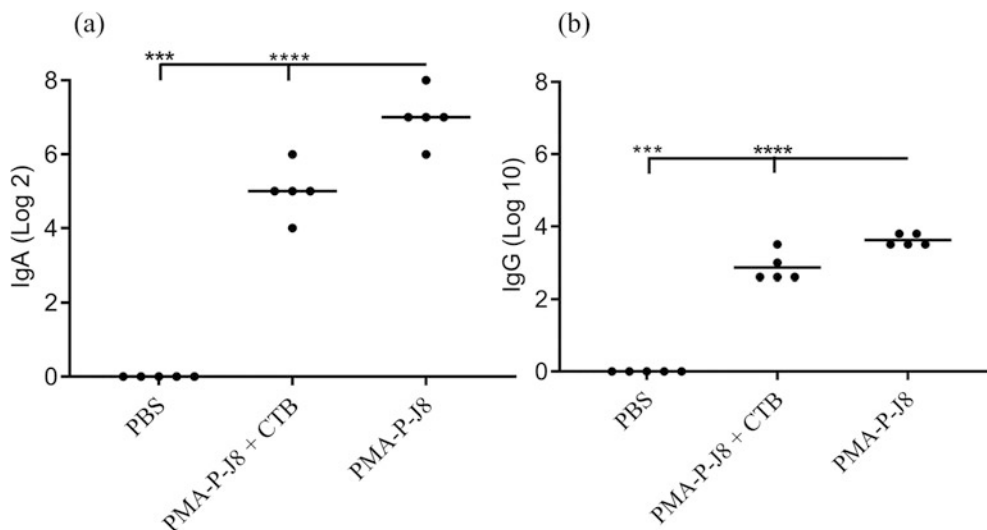


Fig. 6 J8-specific antibody responses, as determined by ELISA. (a) J8-specific saliva IgA titers after single immunization; (b) J8-specific serum IgG titers after single immunization

12. Orally administer 30 μg of the vaccine solution plus CTB (10 μg) to each mouse in the positive control group (day 1).
13. Euthanize all mice on day 15 and collect cardiac blood (500–1000 μL).
14. Screen the samples via ELISA, according to the previously reported procedure [22] (Fig. 6).

4 Notes

1. Molecular weight of P-J8 is 5831.70, as it includes trifluoroacetic acetic acid ($\text{MW} = 114.02 \times 10$), which forms a salt with arginine and lysine amine side chains.
2. Methanol can be used as a replacement for DMF.
3. If the copper wires are not shiny, they should be submerged in concentrated sulfuric acid for 1–2 min, then washed in a glass filter funnel with MilliQ water (5 times), and methanol (5 times) before drying under a stream of nitrogen.
4. Do not remove the air (oxygen) completely. The complete removal of air can cause a substantial delay or cease the reaction as a small amount of oxygen is needed to oxidize copper metal into copper I; this is essential for catalyzing the CuAAC reaction. In contrast, an excessive amount of oxygen can trigger the undesired formation of a large quantity of copper II.
5. After 12 h, the reaction mixture should change from colorless to green (or bluish-green), indicating the occurrence of the

reaction. If the reaction mixture remains transparent, extend the reaction time.

6. The needle must be washed three times with methanol and dried using nitrogen gas before use. The needle should be set in the middle of the water and should not touch the scintillation vial wall. The scintillation vial and magnet need to be washed three times with endotoxin-free water before use. Confirm that the magnet is rotating in the middle of the solution and not touching the wall of the vial. The flow rate of DMF into the water needs to be adjusted so that self-assembly is complete within 3–4 h.
7. During dialysis, shake the dialysis bag at least three times per day to avoid precipitation of the polymer.
8. The toxicity of copper is well established; however, at the same time, copper is an essential element for human health. Therefore, the level of copper traces present in the biologically relevant material needs to be precisely determined. Normally, copper level after click reaction and dialysis is below 100 ppb [23].
9. Calculate the theoretical value of the N/C (nitrogen/carbon) ratio of the conjugated peptide–polymer. For PMA-P-J8, the theoretical values are: C = 49.88 (%), H = 6.48 (%), N = 10.29 (%). Thus, the N/C ratio is 0.206 for 100% substitution. Draw a standard curve for the N/C ratios using different theoretical substitution values. For PMA-P-J8, substitutions at 0%, 25%, 50%, 67%, and 75% correspond to N/C ratios of 0.0276, 0.114, 0.132, 0.159, 0.187, respectively. Use experimental N/C ratio values to calculate the substitution ratio, for example, *see* Fig. 5.
10. Prior to saliva collection, intraperitoneally inject each mouse with 50 μ L of 0.1% pilocarpine solution to stimulate saliva secretion.

References

1. Nevagi RJ, Toth I, Skwarczynski M (2018) Peptide-based vaccines, peptide applications in biomedicine, biotechnology and bioengineering. Elsevier, Amsterdam, pp 327–358
2. Ren Q, Xiong H, Li Y, Xu R, Zhu C (2009) Evaluation of an outside-the-cold-chain vaccine delivery strategy in remote regions of western China. *Public Health Rep* 124 (5):745–750
3. Skwarczynski M, Toth I (2016) Peptide-based synthetic vaccines. *Chem Sci* 7(2):842–854
4. Azmi F, Ahmad Fuaad AAH, Skwarczynski M, Toth I (2014) Recent progress in adjuvant discovery for peptide-based subunit vaccines. *Hum Vaccin Immunother* 10(3):778–796
5. Marasini N, Giddam AK, Ghaffar KA, Batzloff MR, Good MF, Skwarczynski M, Toth IJN (2016) Multilayer engineered nanoliposomes as a novel tool for oral delivery of lipopeptide-based vaccines against group A *Streptococcus*. *Nanomedicine* 11(10):1223–1236
6. Skwarczynski M, Zhao G, Boer JC, Ozberk V, Azuar A, Cruz JG, Giddam AK, Khalil ZG, Pandey M, Shibu MA (2020) Poly (amino acids) as a potent self-adjuncting delivery

- system for peptide-based nanovaccines. *Sci Adv* 6(5):eaax2285
7. Skwarczynski M, Toth I (2014) Recent advances in peptide-based subunit nanovaccines. *Nanomedicine* 9:2657–2669
 8. Zhao L, Skwarczynski M, Toth I (2019) Polyelectrolyte-based platforms for the delivery of peptides and proteins. *ACS Biomater Sci Eng* 5(10):4937–4950
 9. Zhao L, Jin W, Cruz JG, Marasini N, Khalil ZG, Capon RJ, Hussein WM, Skwarczynski M, Toth I (2020) Development of polyelectrolyte complexes for the delivery of peptide-based subunit vaccines against group A streptococcus. *Nanomaterials* 10:823. <https://doi.org/10.3390/nano10050823>
 10. Wu Y, Wei W, Zhou M, Wang Y, Wu J, Ma G, Su Z (2012) Thermal-sensitive hydrogel as adjuvant-free vaccine delivery system for H5N1 intranasal immunization. *Biomaterials* 33(7):2351–2360
 11. O'Hagan DT (1998) Microparticles and polymers for the mucosal delivery of vaccines. *Adv Drug Deliv Rev* 34(2-3):305–320
 12. Eyles J, Carpenter Z, Alpar H, Williamson E (2003) Immunological aspects of polymer microsphere vaccine delivery systems. *J Drug Target* 11(8-10):509–514
 13. Skwarczynski M, Toth I (2020) Non-invasive mucosal vaccine delivery: advantages, challenges and the future. Taylor & Francis, Milton Park, Abingdon-on-Thames
 14. Vela Ramirez JE, Sharpe LA, Peppas NA (2017) Current state and challenges in developing oral vaccines. *Adv Drug Deliv Rev* 114:116–131
 15. Marasini N, Skwarczynski M, Toth I (2014) Oral delivery of nanoparticle-based vaccines. *Expert Rev Vaccines* 13(11):1361–1376
 16. Watkins DA, Johnson CO, Colquhoun SM, Karthikeyan G, Beaton A, Bukhman G, Forouzanfar MH, Longenecker CT, Mayosi BM, Mensah GA (2017) Global, regional, and national burden of rheumatic heart disease, 1990–2015. *N Engl J Med* 377(8):713–722
 17. Azuar A, Jin W, Mukaida S, Hussein WM, Toth I, Skwarczynski M (2019) Recent advances in the development of peptide vaccines and their delivery systems against group A streptococcus. *Vaccines (Basel)* 7(3):58
 18. Faruck MO, Zhao L, Hussein WM, Khalil ZG, Capon RJ, Skwarczynski M, Toth IJV (2020) Polyacrylate–peptide antigen conjugate as a single-dose oral vaccine against Group A *Streptococcus*. *Vaccines (Basel)* 8(1):23
 19. Dai C, Stephenson RJ, Skwarczynski M, Toth I (2020) Application of Fmoc-SPPS, thiol-Malimide conjugation, and copper (I)-catalyzed alkyne–Azide cycloaddition “click” reaction in the synthesis of a complex peptide-based vaccine candidate against group A streptococcus, peptide synthesis. Springer, New York, pp 13–27
 20. Amblard M, Fehrentz J-A, Martinez J, Subra G (2006) Methods and protocols of modern solid phase peptide synthesis. *Mol Biotechnol* 33(3):239–254
 21. Fuaad AAA, Skwarczynski M, Toth I (2016) The use of microwave-assisted solid-phase peptide synthesis and click chemistry for the synthesis of vaccine candidates against hookworm infection, vaccine design. Springer, New York, pp 639–653
 22. Lin AV (2015) Indirect ELISA. In: Hnasko R (ed) *ELISA: methods and protocols*. Springer New York, New York, NY, pp 51–59
 23. Hussein WM, Liu TY, Jia Z, McMillan NA, Monteiro MJ, Toth I, Skwarczynski M (2016) Multiantigenic peptide-polymer conjugates as therapeutic vaccines against cervical cancer. *Bioorg Med Chem* 24(18):4372–4380



Chapter 4

An Update on “Reverse Vaccinology”: The Pathway from Genomes and Epitope Predictions to Tailored, Recombinant Vaccines

Marcin Michalik, Bardya Djahanschiri, Jack C. Leo, and Dirk Linke

Abstract

In this chapter, we review the computational approaches that have led to a new generation of vaccines in recent years. There are many alternative routes to develop vaccines based on the concept of reverse vaccinology. They all follow the same basic principles—mining available genome and proteome information for antigen candidates, and recombinantly expressing them for vaccine production. Some of the same principles have been used successfully for cancer therapy approaches. In this review, we focus on infectious diseases, describing the general workflow from bioinformatic predictions of antigens and epitopes down to examples where such predictions have been used successfully for vaccine development.

Key words Reverse vaccinology, Vaccine design, Epitope prediction, Surface proteins, Peptide epitopes, Core genome

1 Introduction

The successful removal of a pathogen from the human body by the adaptive immune system requires the recognition of the pathogen’s molecules as “foreign.” Molecular patterns can be recognized by both branches of the mammalian immune system, innate immunity and adaptive immunity. The innate immune system recognizes widely conserved molecular features common to many pathogens (so-called pathogen-associated molecular patterns), allowing this branch of the system to mount a rapid response to early signs of infection. The adaptive immune response is more specific, and the molecular patterns allowing the adaptive immune system to detect pathogens are called antigenic or immunogenic. Furthermore, the site of the antigen to which the antigen-binding receptors actually

Marcin Michalik and Bardya Djahanschiri contributed equally to this work.

Sunil Thomas (ed.), *Vaccine Design: Methods and Protocols, Volume 3: Resources for Vaccine Development*, Methods in Molecular Biology, vol. 2412, https://doi.org/10.1007/978-1-0716-1892-9_4, © The Author(s), under exclusive license to Springer Science+Business Media, LLC, part of Springer Nature 2022

bind is called the antigenic determinant or epitope. In most cases, antigens possess several different epitopes; however, they can vary in immunogenicity, which leads to the phenomenon of so-called immunodominant epitopes.

The two branches of the immune system work on different principles. The innate immune system is inherited from the parents and is genetically fixed for life, while the adaptive branch is key to the recognition of new pathogenic structures. The adaptive immune system again is composed of two arms: the humoral and the cellular immune responses. These responses are mediated by two classes of lymphocytes, called B and T cells, respectively. B cells are able to express unique immunoglobulin receptors localized on the cell surface. These immunoglobulin receptors possess a variable antigen-binding site permitting vertebrates to specifically recognize and bind potentially billions of different epitopes. B cells are activated upon contact with an antigen, with or without the help of T-helper cells (see below). Protein antigens typically activate B cells directly [1]. As soon as an antigen binds to the immunoglobulin receptor of a naïve B cell, the B-cell is stimulated to proliferate and differentiate into an antibody-producing plasma cell (effector cell) [2] with the sole task of amplifying a single type of antibody that specifically binds its cognate antigen while circulating freely within the blood and lymph.

As soon as an immunoglobulin binds to a pathogen, the activity of the pathogen is reduced, and it is marked (opsonized) for elimination by cells of the innate immune system, neutrophils and macrophages, capable of phagocytosis and subsequent killing and degradation of the pathogen. Some B cells, however, differentiate into a different cell type, so-called memory B cells. In case of the same antigen entering the host again, these cells are promptly activated to accelerate a stronger, secondary immune response. Memory B cells have the ability to persist in the host for several years, thereby allowing a long-lasting protection [3]. It is this memory of the immune system that is exploited when vaccines are used.

The cellular immune response is mediated by a second type of equally important immune cells called T cells. T cells, like B cells, are stimulated to proliferate and differentiate into the mature state by specifically binding to antigens. However, antigen recognition by T-cell receptors (TCRs) is only possible if the epitopes are presented as protein fragments on the surface of cells. The presentation of protein fragments requires distinct processing pathways, which include the partial degradation of proteins within host cells. Finally, after several enzymatic processing steps, some of the resulting fragments are displayed in the context of co-stimulators on the cell surface by proteins of the major histocompatibility complex (MHC) [4]. Upon activation, naïve T cells can develop into two major classes of effector cells. Each of them maintains the ability to

bind the same MHC-peptide complexes that had led to their activation. Cytotoxic T cells (CTLs or CD8⁺ cells¹) destroy nearby infected or malignant/transformed cells. T-helper cells (T_h cells or CD4⁺) are a decisive factor in the activation of various immune reactions of T-dependent B cells, CTLs, macrophages, and dendritic cells. In analogy to B cells, subpopulations of both CD4⁺ as well as CD8⁺ cells are capable of differentiating into memory T cells similarly enabling long-term protection. MHC proteins are key to these processes. There are two classes of MHC proteins, named MHC Class I and Class II. While MHC Class I proteins are found on the surface of all nucleated cells, MHC Class II proteins are exclusively found on the surface of professional antigen-presenting cells (APCs), which are part of the innate immune system, mainly dendritic cells, macrophages, and B cells. Both MHC classes have variable binding pockets which specifically bind previously processed peptides in an extended linear conformation with high affinity. In both cases, the loaded MHC receptors are subsequently translocated from the endoplasmic reticulum (where the loading takes place) to the cell surface of the APC, where these peptides are presented to bind TCRs [3]. Nevertheless, there are important differences between these two classes, as explained in the following paragraphs.

2 Reverse Vaccinology

Since the British physician Edward Jenner introduced his smallpox vaccine to the Western world in the late eighteenth century, classical vaccinology became one of the most successful counter-measures in the constant battle against infectious diseases. In many cases, governmental programs for exhaustive vaccination were able to push the number of new infections per year of previously prevalent diseases to almost zero [5]. Prominent examples include the vaccination against smallpox that effectively eradicated the disease, and against polio, where incidence rates have dropped by more than 99% since the late 1980s. Despite the ongoing success of classical vaccination strategies, a number of infectious diseases have remained recalcitrant to vaccine development, largely due to the inherent constraints of classical vaccine technology.

Usually the vaccine administered is a biological suspension of either inactivated or killed cells, polysaccharide capsules or toxoids [6]. However, in many cases, it is challenging to prepare a potent

¹ CD8 and CD4 are transmembrane glycoproteins. They function as co-receptors of T-cell receptors on the surface of T cells. “CD” is an abbreviation for cluster of differentiation: a superscripted plus or minus sign indicates whether this type of cell actually does or does not express the specific receptor. CTLs do not possess a CD4 receptor and are therefore unable to bind to the MHC II-peptide complex. In contrast, T-helper cells are unable to bind MHC I as they do not express CD8 receptors on their cell surfaces.

vaccine against a specific pathogen. Non-culturable microorganisms, antigens that are not expressed *in vitro*, pathogens with antigenic determinants that can trigger detrimental autoimmune reactions, as well as extremely heterogeneous strains are only a few of the severe difficulties classical vaccinologists are confronted with today.

Recently, a new impetus was given to current vaccine research thanks to the growing number of available complete pathogen genomes. Based on the assumption that all (protein) antigens a pathogen can express at any time are encoded in its genome (and therefore available to the scientist without cultivation), the idea is to combine bioinformatics and biotechnology to identify protein candidates for vaccine development. As this approach begins with the genome sequence, in contrast to starting from an entire living microorganism, it is called “reverse vaccinology” [7, 8]. The first projects based on this approach used genome information only to naïvely select surface-localized proteins as a pool of possible candidates for subsequent classical animal experiments. In their pioneering work for the development of a vaccine against *Neisseria meningitidis* B (MenB), R. Rappouli and colleagues collected the sequences of 570 surface-localized proteins, of which about 350 could successfully be cloned and expressed in *Escherichia coli*. The purified proteins were then used to immunize mice, and the resulting sera were subjected to various immunoassays to test for the candidate protein’s efficacy as a vaccine. The researchers found 28 proteins which showed consistently positive results in all immunoassays and were able to induce antibodies with bactericidal activity [9]. Furthermore, five of these candidates were also highly conserved in the genome of distantly related strains. A subset of these candidates became the basis for the development of a vaccine called “4CMenB,” which contains three recombinant protein antigens combined with outer membrane vesicles derived from the meningococcal strain NZ98/254 and has obtained market authorization for the European Union in January 2013 (Bexsero, Novartis International AG [10]). Reverse vaccinology has since developed enormously [11, 12], in particular by using increasingly sophisticated bioinformatic methods to mine the large quantities of information provided by pathogen genomes and proteomes. In addition, the complexity of the immune system and the vast amount of data generated from systematic characterization of the human genome and of immune cells along with clinical and epidemiological parameters have required the development of bioinformatics data structures, tools and algorithms to handle and analyze them efficiently [13]. These tools have proved invaluable for reverse vaccinology.

In this chapter, we review the computational approaches that have integrated this data and that have led to new vaccines in recent years. We also briefly summarize the mode of action of antigens and

vaccines, and how vaccines are able to provide long-term protection. We want to emphasize that there are many alternative routes to success in reverse vaccinology—thus, we focus on prominent examples of infectious diseases. We show the general workflow from bioinformatics predictions of antigens and epitopes down to examples where such predictions have been used for vaccines successfully.

3 Software Pipelines for Reverse Vaccinology

An ideal protein vaccine candidate (PVC) has key attributes such as its accessibility by the host immune system. Identifying such proteins within a larger initial dataset, e.g., a bacterial proteome, is a recurring task in many reverse vaccinology workflows. Over the past 15 years, several software pipelines have been designed specifically to automatize this process. Commonly, they integrate an array of tools for identifying and annotating features to the individual proteins. However, they differ in the way they exploit this information for collating an output subset of candidates. Filtering-based programs filter the proteins stepwise for those having desirable and lacking non-desirable features. Machine-learning (ML)-based programs, in contrast, have been trained a priori to correctly classify the input proteins into “candidates” and “non-candidates” based on the vector of their annotated features.

Table 1 lists the most popular pipelines together with the feature annotation tools they employ. Regardless of the method, most of the pipelines focus on the same type of features and, thus, show some overlap in the tools they employ. Usually, desirable features fall into four basic categories: (1) high conservation across all strains of the pathogen, (2) (predicted) subcellular localization outside the cell/envelope (surface exposure), (3) functional characterization (including on domain level) as a virulence factor or as a protein involved in host–pathogen interactions, and (4) antigenicity/immunogenicity, i.e., one or more predicted epitope(s) of cellular immune receptor classes. Likewise, non-desirable features are: (1) high sequence similarity to human or commensal bacterial proteins (or of a model host system, due to possible autoimmunity effects) and (2) the presence of transmembrane helices which hamper the protein’s purification and cloning.

In 2019, Dalsass et al. [14] benchmarked six pipelines for their ability to find protein vaccine candidates within the proteomes of 11 bacterial species. Intriguingly, the authors described a large variance in the number of proteins each pipeline outputs as PVCs. In addition, despite the similarities in feature prediction described earlier, the predictions were largely in disagreement (with the exception of NERVE and Vaxign which are nearly identical). Moreover, none of the pipelines could recover more than 76% of a set of

Table 1
Software pipelines for reverse vaccinology

Pipeline	Year	Tools and attributes used to identify key protein features				Undesirable protein features			
		Conserved (Pan-genome analysis)	Surface localization	Virulence-related function	Immunogenic epitopes	Other	Host protein similarity	Many TM-helices	Other
NERVE	2006 [15]		pSORTb	SPAAN, BLASTp (vs. UniProt)			BLASTp (vs. MHC Pep [16])	HMMTOP	
VaxiJen	2007 [17]					Physicochemical properties			
Vaxign	2010 [18]	OrthoMCL	pSORTb	SPAAN	Vaxitope (MHC I, MHC II)		OrthoMCL	HMMTOP	
Jenner-predict	2013 [19]	BLASTp	pSORTb	PFAM	IEDB (search)		BLASTp (vs. human genome)	HMMTOP	
Vaccine	2014 [20]		WoLF, PSORT, SignalP, TargetP, Phobius, TMHMM		IEDB (search)			Phobius, TMHMM	
Bowman-Heinson	2017 [21]		NetSurfP, NetAcet, TargetP, PSORTb, LipoP	SPAAN	GPS-CCD, GPS-ARM, Net Chop, CBTOPE (B cell), BepiPred (B cell), GPS-MBA	Glycosylation, Phosphorylation, PUPylation, SUMOylation, S-nitrosylation, Furin cleavage sites,		HMMTOP	

				(specific MHC II allele), PickPocket (MHC I), NetMHCpan (MHC I)	Physicochemical properties				
VacSol	2017 [22]	DEG	PSORTb, CELLO2GO	Mvir CELLO2GO	VFDB, Mvir	ABCpred (B-cell), Propred-I (MHC I), Propred (MHC II)	BlastP (vs. human genome)	HMMTOP	
PanRV	2019 [23]	Roary, BLASTp, DEG	PSORTb	VFDB, COG, UniProt	VFDB, COG, UniProt	ABCpred (B-cell), PropredI (MHC I), Propred (MHC II), VaxiJen	BlastP (vs. human genome/gut microbiome)	HMMTOP	Mol. Weight
ReVac	2019 [24]	PanOCT, OrthoMCL, LS-BSR, Custom orthology prediction	LipoP, SignalP, PFAM, PSORTb, TMHMM	GO, SPAAN	GO, SPAAN	IEDB (search), NetCTLpan (MHC I), IEDB-AR consensus prediction (MHC I/II), IEDB-AR consensus prediction (linear B cell)		TMHMM	IslandPath, SSR finder
Vaxign-ML (Vaxign2)	2020 [25]		PSORTb, SignalP, TMHMM	SPAAN	SPAAN	IEDB-AR (MHC I only)	BlastP (vs. human/mouse/pig genome)	TMHMM	Compositional and physicochemical properties

known protective bacterial antigens extracted from the Protegen database. The best performing pipeline, Bowman/Heinson, is an optimized ML-based approach, which extends the set of features and annotation tools to include predictions for surface exposure, proteasomal cleavage, and a range of posttranslational modifications. This suggests that careful exploration of the feature space by increasing the number of features and annotation tools might help to increase the sensitivity. This approach is pursued by the more recently developed pipelines PanRV and especially by Vaxign-ML (module of Vaxign2) and ReVac.

The benchmark results further underline how each pipeline's performance depends on the input proteome and the feature annotation tools it employs. Filtering-based approaches rely on tool-specific, predetermined thresholds to accurately decide whether the desirable feature is present or is not. These thresholds, however, are rarely optimal for all inputs, i.e., they could be too strict for one species yet too permissive for another. Consequently, false-negative and false-positive feature predictions could lead to accumulation of less suitable PVCs in the output. Hence, avoiding parametrization with predetermined thresholds is a promising approach pursued by ML-based pipelines. Unfortunately, these approaches are still limited by the diversity, quality, and quantity of available training data as both types, protective and non-protective antigens, ideally require rigorous *in vivo* testing.

In conclusion, feature acumen paired with a conceptual understanding of the employed annotation tools is pivotal for choosing the appropriate pipeline in a new RV project. Only then are troubleshooting problems and circumventing them by pipeline-independent analyses possible. In the following paragraphs, we discuss the basic feature types as well as some of tools for their annotation.

4 Pan-Genomic Analysis

Apart from being a valuable approach to investigating the characteristics of a specific phylogenetic clade, pan-genomic analysis is indispensable for identifying conserved target proteins within a set of genomes of pathogenic strains within a single clade. The term, first coined by Tettelin [27], is defined as the entire genomic repertoire accessible to the clade studied. It encompasses two subsets: the “core genome” and the “dispensable” or “accessory genome.” While the former describes the intersection of genes (or open reading frames [ORFs]) shared by all strains of the clade, the latter comprises genes only found in subsets of strains. Such a classification is biologically meaningful as it allows us to differentiate between (core) genes considered essential for growth and (accessory) genes encoding, e.g., for supplementary pathways

and functions which confer a selective advantage, such as antibiotic resistance or virulence genes that are limited to certain strains [28].

Similarity between genes or proteins is usually determined by pairwise sequence alignment. Particular thresholds are set for the percentage of sequence identity over a percentage of pairwise aligned sequence length. However, depending on the phylogenetic resolution and the available quality and quantity of genomes, it might be necessary to increase sensitivity. This can be done by incorporating additional methods such as orthology prediction [29], i.e., the prediction of genes among species or strains that originated by vertical descent from a single gene of their last common ancestor, as well as structural alignments. Relying solely on pairwise sequence alignments on the protein level, Tettelin [27] chose a minimum of 50% identity over 50% of the sequence lengths, while Hiller [30] chose 70% to identify similar proteins within strains of *Streptococcus agalactiae* and *S. pneumoniae*, respectively. At such levels of overall identity scores, it can be assumed that the identified proteins have identical functions (and are true orthologues). For the purpose of identifying target proteins, it is nonetheless beneficial to choose considerably higher threshold values to exclude false positives early on in the workflow. The potential loss of immunogenic sequences due to the high threshold values is relatively low, as at least locally, epitopes need to be very highly conserved to be effective. Given the high specificity of the immune system's receptors, this is a good trade-off for the reduction of the number of proteins to analyze in subsequent steps.

To be even more conservative, some studies and pipelines [31] use databases to filter for so-called essential genes, i.e., genes indispensable for the survival and successful reproduction of the organism. The rationale behind this is that these genes are part of the core genome, are typically constitutively expressed, and so slowly evolving that they are highly conserved across all the strains of a pathogen. However, there are several problems with this approach in the context of reverse vaccinology. On the one hand, genome-wide identification of essential genes is labor-intensive as it requires elaborate mutagenesis or knockdown experiments. Consequently, available experimental data is scarce. Even the most used database, DEG [32], comprises only 66 genome-wide experiments on bacteria, covering an even smaller number of different species. Moreover, most studies conduct the experiments with organisms suspended in standard nutritional medium. Gene essentiality, however, is highly context-dependent and significantly influenced by the particular genome or strain studied as well as the experimental settings like medium composition, and environmental and growth conditions. Simple mapping of a target pathogen's gene set against a database of essential genes, therefore, could result in a considerable number of incorrectly classified genes and should be interpreted cautiously.

5 Surface Localization

To perform their functions at their native subcellular localization (SCL), newly synthesized proteins must be sorted and transported to their respective subcellular compartments. The SCL of proteins not only provides important clues to their function in the cell but is also important for judging their potential as vaccine targets. Surface-localized proteins are typically the first molecular patterns of pathogens that are in contact with the host immune system and are generally considered the best candidates for recombinant vaccines.

Determining the SCL of proteins by experimental means, such as subcellular fractionation combined with mass spectrometry, is accurate but time-consuming and expensive [33]. Bioinformatics methods are an increasingly comprehensive and reliable way to determine the SCL of proteins in large datasets, as they contain defined (and thus detectable) signals in their sequence.

There are two basic types of prediction tools for subcellular localization. One predicts very specific sequence features such as signal peptides for the Sec, Tat, or lipoprotein pathways using TargetP, SignalP and related tools [34], or transmembrane segments [35]. The other type predicts the exact localization of a protein by combining various localization-specific features [36, 37] or general features like amino acid composition [38], evolutionary information [39], structure conservation information [36], or gene ontology [40]. The combination of different prediction tools in a pipeline increases the quality of the overall prediction significantly and can reduce false-positive and false-negative results [41]. Last but not least, limiting the huge amount of protein sequence data to only the interesting, surface-localized vaccine candidates significantly reduces the workload for later immunogenicity prediction steps in the reverse vaccinology pipeline. Alternatively, experimental data such as proteomics approaches can be used to narrow down the number of candidates for further analysis [42].

6 Immunoinformatics: The Prediction of Epitopes

Ideal vaccine candidates are not only localized on the surface of the pathogen but will also contain multiple epitopes that elicit strong immune responses within the host organism. However, experimental identification of epitopes within a set of proteins is a very resource- and time-intensive task, making a computer-aided, complementary approach especially attractive.

While “reverse vaccinology” describes the overall approach in opposition to classical—entirely wet-lab-based—vaccine development, a new branch of bioinformatics emerged around the same

time, termed immunoinformatics or computational immunology—defined as the application of informatics techniques to molecules relevant to the immune system [43, 44]. The ability to predict immunogenicity on the level of epitopes is a key tool for computer-aided vaccine design. Numerous tools exist for such predictions, for both MHC I and MHC II, as well as B-cell-mediated immunity. This chapter can only provide a crude overview of the different obstacles all prediction tools face and gives a brief overview of the general strategies they pursue. As for all bioinformatics tools, it is advisable to use multiple tools in parallel and to compare the results to minimize false-positive and false-negative predictions. In fact, recent publications have shown that combining prediction tools to produce a consensus-like output can achieve superior predictive performances [45, 46].

7 MHC I and MHC II Binding Predictions

Generally speaking, MHC I binds and presents epitopes which are derived from proteolytically degraded intracellular proteins (e.g., from intracellular pathogens) and are 8–10 residues long. By contrast, MHC II epitopes are derived from extracellular sources (e.g., from extracellular pathogens) and are much longer on average (up to 25 residues [47]). Originally, it was thought that these peptide epitopes would be recognized at least in part by their secondary structure, but structural data suggest that they are presented mostly in an extended form. Early prediction tools working under the wrong assumption accordingly gave inconsistent results [6]. Additionally, MHC I and MHC II bind peptides very differently: as the molecular structure of MHC II requires longer peptides, due to its “open” binding pocket, the residues extending the binding pocket on both sides contribute to the overall peptide binding affinity [47, 48]. To address this finding, modern MHC II epitope prediction tools often identify a binding core, i.e., a shorter subsequence within the longer peptide sequences of the query, which is predicted to bind to the pocket.

To use prediction tools efficiently for vaccine design, one has to consider that the human MHC molecules are encoded in a highly polymorphic locus called the human leukocyte antigen (HLA) locus on chromosome 6. There are profuse amounts of HLA alleles with different binding affinities to the same epitope sequence: more than ten thousand different human alleles have been identified, and, to complicate things even further, within different populations, different alleles (i.e., variants) of the MHC genes are present in different ratios.

Various online methods are available for the prediction of epitopes, ranging from sequence-based to structure-based (using, e.g., homology modelling or docking) methods. Table 2 shows a

Table 2

Methods: QM: quantitative matrix-based methods (QM combine a matrix-based approach with a strategy to quantify the prediction scores), A/DNN: artificial/deep neural networks, $T_{1/2}(h)$: half-life of the antigen-MHC-I complex in hours at 37 °C

Authors	Method	Publication	Output
MHC I			
Bui et al.	QM	[49]	IC ₅₀ (nM)
Sidney et al.	QM	[50]	
Nielsen et al.	ANN	[51]	IC ₅₀ (nM)
Peters et al.	QM	[52]	IC ₅₀ (nM)
Kim et al.	QM	[53]	IC ₅₀ (nM)
Moutaftsi et al.	QM	[54]	Percentile rank
Nielsen et al.	ANN, Pan-specific	[55]	IC ₅₀ (nM)
<u>Karosiene et al.</u>	ANN, Pan-specific	[46]	IC ₅₀ (nM)
<u>Zhang et al.</u>	QM	[45]	IC ₅₀ (nM)
<u>Rasmussen et al.</u>	ANN, Pan-specific	[56]	$T_{1/2}(h)$ and IC ₅₀ (nM)
<u>O'Donnell et al.</u>	ANN, Pan-specific	[57]	IC ₅₀ (nM)
<u>Bassani-Sternberg et al.</u>	Probabilistic mixture model	[58]	Binding score
<u>Jurtz et al.</u>	ANN, Pan-specific	[59]	IC ₅₀ (nM)
<u>Singh et al.</u>	QM	[60]	Binding score
MHC II			
Bui et al.	QM	[49]	IC ₅₀ (nM)
Jensen et al.	ANN, Pan-specific	[61]	IC ₅₀ (nM)
Reynisson et al.	ANN, Pan-specific	[62]	IC ₅₀ (nM)
Sidney et al.	QM	[50]	IC ₅₀ (nM)
<i>Singh et al.</i>	QM	[63]	Binding score
Nielsen et al.	QM	[64]	IC ₅₀ (nM)
Hoof et al.	ANN, Pan-specific	[65]	IC ₅₀ (nM)
Sturniolo et al.	QM	[38]	IC ₅₀ (nM)
Wang et al.	ANN, QM	[26]	Probability
Racle et al.	Probabilistic mixture model	[66]	Binding score
Chen et al.	DNN	[67]	Probability
Liu et al.	DNN	[68]	IC ₅₀ (nM)

selection of sequence-based bioinformatics tools used for MHC I or MHC II predictions, which have the advantage of speed over structure-based methods and are therefore more favorable for large-scale analysis of peptides.

State-of-the-art sequence-based approaches attempt to predict the binding quality of a query sequence by abstracting from the sequence information of peptides with experimentally determined binding affinities. By doing so, they are able to generate models for each individual MHC variant. Matrix-based methods try to derive position-specific binding coefficients for each residue from a database of known binders of the same length. For the prediction, each position of a query sequence is evaluated individually, yielding a score of congruousness to its respective position in the abstract model of a binding sequence. To predict the binding quality of the complete query sequence, the final score is given as the sum of the scores of the individual positions. This approach can be modified by adding weights to certain positions (so-called anchor positions) to increase their impact on the final score.

The second group of prediction tools relies on machine learning approaches or stochastic models like support vector machines, artificial neural networks, or Hidden Markov models to predict the binding quality of a query sequence. Generally speaking, all of these approaches attempt to refine a model by adjusting internal parameters to the sequence information provided by a collection of known binders. Therefore, a set of known binders is used to train the model, i.e., to adjust internal parameters in such a way as to enable accurate prediction of binding quality based on empirical data (supervised learning).

Some tools in both groups also include strategies to quantitatively predict the binding of a query sequence. By incorporating either position-specific affinity contributions (matrix-based approaches) or statistical regression analysis (machine learning approaches), the user can readily compare experimentally determined IC_{50} or K_d values with predicted ones. However, there are no predefined absolute threshold values clearly separating query sequences into either binders or nonbinders. Rather, it is advisable to define cut-off values for each MHC allele individually [69] using percentile ranks.

It is important to note that all the tools, regardless of approach, heavily rely on experimental data on the measured binding affinities of peptide sequences for a specific MHC variant. Therefore, the quality of the prediction is determined by how well the binding space of a particular MHC variant is explored by the available data. Unfortunately, for many alleles data are scarce; this has led to the development of pan-specific methods for MHC binding prediction. These use known MHC binders to known MHC alleles to infer binding for unknown pairs. Typically, such approaches are based on structural data where alleles with similar physico-chemical attributes in the binding-pocket are classed together using machine-learning approaches [70–72].

In recent years, data from MHC ligand elution assays have emerged as a second source of training data for the development

of MHC epitope predictors. Using high-throughput mass spectrometry, it is possible to detect large quantities of MHC ligands from a pool of extracted, surface presented epitopes, i.e., MHC ligands. In contrast to affinity values obtained from binding assay data, elution data does not provide a quantitative value to rank the epitopes relative to each other. Nevertheless, the large amount of data still helps to characterize binding motifs of different alleles and thereby increase the sensitivity of epitope prediction. In fact, recent developments such as NetMHC(II)pan 4.0 [59, 62], MARIA [67], MHCFlurry 2.0 [57], and MixMHC [2]Pred 2.0 [58, 66], all rely on a combination of binding assay and elution data for training, which has contributed to their significantly improved performance—especially in the more challenging prediction of MHC II epitopes—over former state-of-the-art tools.

8 B-Cell Epitope Binding Predictions

B-cell (or antibody) epitopes are 16 residues long on average but are not presented in the context of MHC molecules. Therefore, they are especially hard to predict as crystallographic studies have shown that B-cell receptors (BCRs) are capable of binding discontinuous protein epitopes as well as specific peptide sequences. Epitopes are called discontinuous if they are composed of distant sequence segments which are brought into close proximity due to the protein's tertiary structure. Contemporary tools for identifying B-cell epitopes can be divided into those relying solely on primary structure information and those additionally incorporating structural data. The first group of tools calculate a prediction by considering a set of descriptors such as the propensity for a sequence segment to form a continuous, linear secondary structure, physico-chemical attributes, surface-accessibility, and amino acid composition [73]. In general, these tools yield reasonable accuracy for continuous (linear) epitopes, but fall short when identifying discontinuous epitopes [74]. To surmount this shortcoming, prediction calculations by the second group of tools include secondary structure information, calculated surface accessibilities, and/or protrusion indices, in addition to information about the protein's three-dimensional structure and the structure of known antigen-BCR complexes. Popular sequence-based tools are BepiPred [75] and BepiPred 2.0 [76], ABCpred [77], BEST [78], LBTope [79], and EpiDope [80]. Commonly used structure-based tools are CBTOPE [81], ElliPro [82], Paratome [83], PEPOP [84], BEE-Pro [85], and DiscoTope 2.0 [74]. It is even claimed that benchmarking has shown that the latter two tools are able to achieve high accuracy levels similar to MHC prediction tools [75].

Many of the tools for MHC I, II, and BCR epitope prediction offer web interfaces which allow thorough testing of their

predictive powers before applying them in a larger scale. A very useful analytical resource is the Immune Epitope Database (IEDB), funded by the National Institute of Health [52]. In addition to providing a database of binding epitopes and their affinities (where available, also including elution data), the IEDB furnishes a regularly updated compilation of self-developed and newly implemented popular prediction tools accessible via a single intuitive web interface.

9 Methods for Using Full-Length Antigens (Proteins) as Vaccines

All vaccines work in a similar way: by presenting foreign antigens to the immune system in order to activate a specific immune response. The aim of vaccination is usually to induce long-term protection through memory B cells [86]. The composition of vaccines can be diverse. Traditional formulations include live attenuated vaccines, which are composed of live viruses or bacteria that have been weakened in the lab to lower virulence by long-term passaging or genetic engineering (deletions in genes required for virulence) but are still able to activate the immune system. They elicit a strong response that can result in lifelong immunity with a minimal number of doses. Despite their advantages, live attenuated vaccines can have many drawbacks. Potential problems include difficulties with storage and transportation, where inappropriate handling may cause loss of vaccine efficacy. In addition, there are cases where this type of vaccine cannot be used, e.g., when patients take anti-infective drugs or are immunocompromised for any reason. There is a risk that attenuated vaccines can revert to a fully virulent pathogen (e.g., oral poliovirus vaccine [87]). Last but not least, the attenuation process itself is lengthy and depends on random events out of the control of the researchers (examples: BCG tuberculosis vaccine, Yellow fever rotavirus vaccine) [88, 89].

An alternative method is to inactivate the pathogens before use as a vaccine. This method is safer compared to the live attenuated vaccines, but is less potent in inducing immune responses. In short, such vaccines contain pathogens killed by heat or chemical treatment (i.e., formaldehyde). Risks related to such vaccines include errors in the inactivation. Because the inactivated pathogen does not reproduce in the host organism, there is a need for one or more “boosters,” i.e., administration of additional doses of the vaccine after defined intervals (examples: Cholera vaccine, Hepatitis A vaccine, Rabies) [86].

With better biochemical and immunological methods available, it has been possible to engineer vaccine formulations by only using active antigens (rather than complete pathogens). This is referred to as a subunit vaccine. It uses only specific parts of a pathogen to immunize against disease. The search for such components is typically focused on surface-exposed or secreted antigens, which

provide the best accessibility for antibodies and other immune mechanisms [86, 90]. Using purified proteins as a vaccine component is a widely used technique today. With bioinformatics, it is possible to select ideal antigen candidates for subunit vaccines, which have many advantages over the “whole-pathogen” approaches [91]. Subunit vaccine production is a safe process as it does not require the culturing of dangerous pathogens. The final product is also safer to use [92, 93]: there is no infectious material, and thus no risk of the vaccine strain reverting to a harmful pathogen. In addition, it is possible to control all ingredients of the vaccine. Traditional vaccines induce very strong immunological responses with a very small dose; often this high response is not really necessary and does not always translate into later protection. In subunit vaccines, antigens are tested individually, and the kinds of responses they provide are known. Thus, it is in principle possible to customize vaccines for specific patient groups (e.g., immunocompromised patients or patients already suffering from an infectious disease) [88].

10 Examples of Protein Subunit Vaccines

A vaccine against pertussis containing purified proteins was first created in 1981 in Japan by Sato and Sato, who purified the antigenic proteins by classical biochemical methods from cultures of the pathogen—with the obvious problems in biological safety and with upscaling of the procedure [94]. Another example is the hepatitis B vaccine which contains one of the proteins from the viral envelope—the hepatitis B surface antigen (HBsAg). This was one of the first protein-based vaccines, and while at first the protein was obtained from natural human plasma, it was later successfully expressed recombinantly in yeast cells. Today, this is the production method of choice for human vaccines (Table 3) [95]. Another example of a subunit vaccine on the market is the one against

Table 3
Advantages of protein-based vaccines [92, 105]

- | |
|---|
| <ul style="list-style-type: none"> • No need to culture dangerous pathogens • Problems with toxic or oncogenic parts of the pathogen, or with antigens potentially causing allergies or autoimmune diseases, can be avoided • Proteins can be altered by adding different chemical groups to improve immunogenicity, stability, or solubility • Quality of the final vaccine is higher and is more reproducible • Distribution and storage are improved (high stability, e.g., in freeze-dried form) • No risk of reversion to a more virulent strain (in contrast to live attenuated vaccines) • Using computational and bioinformatics methods potentially lowers the costs of initial research • Production methods are comparatively easy to scale up |
|---|

Bacillus anthracis. Although the components are still collected from pathogen cultures, which raises concerns about the safety of the procedure, the strength of the initial immune response, and long-term efficacy are high [96].

Some studies have included production of plasmid-derived antigens using attenuated, avirulent *Bacillus* strains. Expressing these proteins in a *Bacillus* strain ensures properly processed and folded protein. The product is then purified from fermentation cultures and adsorbed onto an aluminum adjuvant. Preclinical studies showed that the vaccine as such is safe and well-tolerated and can induce an immune reaction with long-term immunity. Researchers are also looking for new targets using of bioinformatics, now that the complete genome of the clinical strain is available [97, 98].

Two new vaccines against human papillomavirus (HPV) have been brought to the market recently—Cervarix and Gardasil (Silgard). Both contain proteins from the capsids of different virus strains—HPV16, 18 and HPV6, 11, 16, 18, respectively—and differ in the formulation of enhancers and adjuvants. In 2014, the US Food and Drug Administration approved another new HPV vaccine from Merck, Gardasil 9, which protects against nine subtypes of the virus (HPV6, [11, 16, 18, 31, 33, 45, 52, 58]). These vaccines are all produced recombinantly using yeast cells (or insect cells for Cervarix) [99–101].

In ongoing Phase III clinical trials (NCT01563263), promising results have been obtained for a vaccine against *Pseudomonas aeruginosa* (IC43) (Table 4). This is an outer membrane protein-based vaccine containing an OprF/OprI fusion with a His tag. The product is expressed in *E. coli* from a plasmid. The vaccine gives good immune responses with and without an alum adjuvant [102–104].

11 Methods for Using Predicted Epitopes/Peptides as Vaccines

Producing complete proteins in a stable form for vaccines or other purposes is not always straightforward. Many potential vaccine targets are membrane proteins, are otherwise insoluble, or are prone to degradation or aggregation. Short peptide epitopes taken from vaccine target proteins are a promising alternative, as they can still be efficiently recognized and displayed by either MHC I or MHC II. In some cases, reducing a subunit vaccine to a single epitope has the additional advantage of removing deleterious further epitopes; examples where this can be important are epitopes that can cause cross-reactivity leading to autoimmune responses.

In principle, an unlimited number of defined peptide epitopes can be combined to create multi-epitope vaccines. To obtain such epitopes, both reverse vaccinology approaches based on

Table 4
Selected list of ongoing clinical trials with subunit vaccines

Vaccine	Target	Notes	Stage	Active compound	References
Improvac	Boar taint	Stimulation of the (pig) immune system to produce antibodies that ultimately block and reverse the accumulation of compounds responsible for boar taint	On market (animal use)	Synthetic incomplete analog of gonadotropin-releasing factor (GnRF) (without hormone activity) linked with carrier protein	[128]
Recombitec WNV	West Nile virus	Combination of existing canarypox vaccine (ALVAC) with genes expressing two proteins from West Nile virus	On market (animal use)	<i>prM/E</i> genes	[129]
Vacc-4×	HIV	Synthetic peptides targeting HIV protein p24	Phase III	Peptides with adjuvants	[130]
Vacc-C5	HIV	Synthetic peptides targeting HIV glycoprotein gp120 (C5)	Phase II/III	Peptides with adjuvants	[130]
RECOMBIVAX HB	Hepatitis B virus	Recombinantly produced HBsAg protein in yeast cells	On market	Protein with aluminum adjuvant	[101]
IC43	<i>Pseudomonas aeruginosa</i>	Recombinant outer membrane protein-based vaccine	Phase II/III	OprF/OprI hybrid vaccine with N-terminal His tag	[102, 104, 127]
NDV-3	<i>Candida</i> sp.	Recombinant vaccine	Phase I/II	Agglutinin-like sequence 3 protein (Als3p) from <i>Candida albicans</i> with aluminum hydroxide adjuvant	[131, 132]
SA4Ag	<i>Staphylococcus aureus</i>	Recombinant vaccine containing 2 different capsular polysaccharides	Phase I/II	Polysaccharides CP5 and CP8; recombinant surface protein clumping factor A	[127, 133]

(continued)

Table 4
(continued)

Vaccine	Target	Notes	Stage	Active compound	References
		and 2 surface proteins		(rmClfA) and recombinant manganese transporter protein C (rP305A)	
PreviThrax	<i>Bacillus anthracis</i>	Recombinant protective antigen protein	Phase II	Purified recombinant protective antigen protein	[134]
Respiratory syncytial virus (RSV) vaccine	Respiratory syncytial virus (RSV)	F glycoprotein produced recombinantly in insect cells with a recombinant baculovirus	Phase II	Purified recombinant RSV F oligomers	[135]
Cenv3	Hepatitis C	Selected 3 peptides from 2 envelope proteins. Each was synthesized in 8 multiple antigenic peptides (MAPs)	Phase II	3 envelope peptides derived from 2 envelope proteins E1 and E2	[127, 136]
NeuroVax	Multiple sclerosis	Vaccine contains three peptides which correspond to potentially pathogenic TCRs on T cells (which are overexpressed in 90% of multiple sclerosis patients)	Phase II/III	3 TCR peptides in aqueous solution and IFA	[137]
IC41	Hepatitis C	Vaccine contains 5 peptides derived from hepatitis C virus genotype 1 core. There are 4 cytotoxic T lymphocyte (CTL) epitopes and 3 helper epitopes	Phase I/II	5 synthetic peptides with Poly-L-arginine as adjuvant	[127, 138]

bioinformatics predictions (see above) or more traditional techniques based on antisera can be used to fish for epitopes [88]. One approach to using predicted peptide epitopes is to fuse them to a previously chosen protein scaffold as a carrier. This scaffold can itself play additional important roles in enhancing the immunological response, e.g., due to the presence of T-helper cell epitopes in its own sequence. A distinct advantage of this method is that multiple epitopes from different target proteins or even from diverse pathogen strains can be combined to obtain wider spectrum of protection [92]. Production and handling can also be improved in the process as the scaffold can be chosen according to desired properties (water solubility, non-toxicity, stability at room temperature, etc.).

An example for using predicted epitopes conjugated to a carrier scaffold is an ongoing study using *Aeromonas hydrophila* epitopes from outer membrane proteins (OmpF, OmpC) with the heat-labile enterotoxin B (LTB) of *Escherichia coli* as a scaffold [106]. LTB has been reported to be an efficient adjuvant capable of eliciting a strong immune response [73]. In four out of five cases (five different fusions), the authors found that the recombinant fusion proteins induce antibody production. The antisera generated by this process were able to recognize the native proteins from which epitopes were taken. All epitopes in the study were predicted as B-cell epitopes using bioinformatics approaches and tools as described above.

There are also potential problems with using peptide-based epitopes as vaccines: removing an epitope from its native context risks losing immunogenic efficacy and, as a result, general response to the vaccination [105]. Examples for such context-dependent recognition by the immune system are the loss of secondary structure, or the fact that especially B-cell antigens are known to be mostly (90%) discontinuous, nonlinear antigens—they derive from different protein regions localized closely in space due to the three-dimensional structure. Such conformation-dependent recognition cannot always be achieved using only a linear peptide/epitope [107]. Using suitable scaffold proteins for peptide epitopes can solve some of these problems, e.g., by adding sequences which will enhance binding and the stability of the peptide-MHC complex [108]. Another option for optimization is to modify epitopes using β -amino acids instead of natural ones, which can increase the binding affinity to MHC dramatically. Such recombinant epitopes maintain the properties of natural epitopes because the side chains of the amino acids are identical between the α - and β -type. However, the modification improves resistance to proteases as the epitopes do not have the same peptide backbone, so that the epitope is protected from digestion before it is loaded on the MHC. Even changing one amino acid to its β -variant has dramatic effects on the overall stability of the peptide [109–111].

Another, less well understood disadvantages of using subunit vaccines is that they can be less efficient in inducing long-lasting immunity [112, 113]. Peptide vaccines often lack T-helper epitopes, especially when just a mix of peptides is used as a vaccine [114]. To improve the response, vaccine formulations are modified with different immunostimulants (adjuvants) and also by conjugation of the peptides to carrier proteins which will enhance immunogenicity and immune system activation [88]. The most common general adjuvant is an aluminum salt that can be found in many existing vaccines and is still used in new formulations in clinical trials and in preclinical phases [115]. Many novel adjuvants are being tested currently, with the aim of finding adjuvants that are safe to use, can enhance the immune response of even of weakly binding peptides or proteins, and can play a direct role as a delivery system at the same time. Typically, these are different types of emulsions (water-in-oil and oil-in-water), e.g., MF59 which is composed of squalene (licensed for influenza vaccines in Europe), polymeric particles like PLA (polylactic acid), or PLGA (poly[lactide-*co*-glycolide] acid), liposomes (which can protect peptides from enzymatic digestion, keep the folded structure of antigen, and elicit a high cellular immune response), virus-like particles (VLPs, self-assembling proteins which mimic the conformation of native viruses), inorganic nanoparticles, and carbon nanotubes [105, 116, 117]. Other adjuvants include flagellin-based adjuvants, lipopolysaccharide, and other bacterial structures that co-stimulate the immune system [91], as well as complete avirulent (and thus safe) living cells expressing the foreign antigen on the surface. Examples include the use of a type III secretion system [118–120], and the use of autodisplay systems based on type V secretion systems [121, 122]. As described above, in cases where the immunological memory is not lifelong, there is a need for additional “boosting” to increase and maintain the protectivity of a vaccine [123].

The most recent developments in reverse vaccinology include personalized vaccines, which are aimed at specific patient groups or even individuals. This is particularly relevant for anticancer vaccines, where the targets (cancer cells) are highly variable from patient to patient. As an example, GAPVAC, with a promising results from Phase I clinical trials [124], is a vaccine that uses patient-specific genes expressed in brain tumors and is based on peptides as well as cancer-specific mutations [125]. A similar study is currently being performed using HEPAVAC, a patient-specific vaccine against liver cancer [126].

Currently, no peptide-based vaccine is licensed for human use, but there are currently over 400 clinical trials of peptide vaccines in progress [92, 127]. A number of promising examples of peptide-based and other subunit vaccines are shown in Table 4.

There is an obvious need for more basic research and clinical trials and especially for long-term studies to demonstrate that reverse vaccinology approaches can yield vaccines that are potentially safer and at least as efficient as traditional vaccines. With increasing numbers of antibiotic-resistant bacteria, and with old and new viral diseases such as Ebola, Middle-East Respiratory Syndrome (MERS), most recently SARS-CoV-2, and others emerging or re-emerging, tailored vaccines are promising solutions to the continuous problem of infectious diseases. The great potential of patient-specific vaccines, especially for use in cancer therapy, where traditional approaches cannot be used at all, has barely been tapped.

References

1. Janeway CAJ, Travers P, Walport M et al (2001) *Immunobiology*. Garland Science, New York
2. Alberts B, Johnson A, Walter P et al (2007) *Molecular biology of the cell*. Francis, Taylor &
3. Neumann J (2008) *Immunbiologie*. Springer-Lehrbuch, Berlin, Heidelberg
4. Saha B (2001) *Encyclopedia of life sciences*. John Wiley & Sons, Ltd, Chichester, UK
5. WHO UNICEF World Bank (2009) *State of the world's vaccines and immunization*. World Health Organization, Geneva
6. Flower DR (2009) *Bioinformatics for vaccinology*. John Wiley & Sons, Ltd, Chichester, UK
7. Rinaudo CD, Telford JL, Rappuoli R et al (2009) Vaccinology in the genome era. *J Clin Invest* 119:2515–2525
8. Seib KL, Zhao X, Rappuoli R (2012) Developing vaccines in the era of genomics: A decade of reverse vaccinology. *Clin Microbiol Infect* 18:109–116
9. Pizza M, Scarlato V, Masignani V et al (2000) Identification of vaccine candidates against serogroup B meningococcus by whole-genome sequencing. *Science* 287:1816–1820
10. Medicinal Products and Human Use. Bexsero. Technical report, European Medicines Agency. http://www.ema.europa.eu/docs/en_GB/document_library/EPAR_
11. Rappuoli R, Bottomley MJ, D'Oro U et al (2016) Reverse vaccinology 2.0: human immunology instructs vaccine antigen design. *J Experiment Med* 13(4):469–481
12. Burton DR (2017) What are the Most powerful immunogen design vaccine strategies? Reverse vaccinology 2.0 shows great promise. *Cold Spring Harb Perspect Biol* 9(11):a030262
13. Hegde NR, Gauthami S, Sampath Kumar HM et al (2018) The use of databases, data mining and immunoinformatics in vaccinology: where are we? *Expert Opin Drug Discovery* 13:117–130
14. Dalsass M, Brozzi A, Medini D et al (2019) Comparison of open-source reverse vaccinology programs for bacterial vaccine antigen discovery. *Front Immunol* 10:113
15. Vivona S, Bernante F, Filippini F (2006) NERVE: new enhanced reverse vaccinology environment. *BMC Biotechnol* 6:35
16. Brusic V (1998) MHCPEP, a database of MHC-binding peptides: update 1997. *Nucleic Acids Res* 26:368–371
17. Doytchinova IA, Flower DR (2007) VaxiJen: a server for prediction of protective antigens, tumour antigens and subunit vaccines. *BMC Bioinformatics* 8:4
18. He Y, Xiang Z, Mobley HLT (2010) Vaxign: the first web-based vaccine design program for reverse vaccinology and applications for vaccine development. *J Biomed Biotechnol* 2010:297505
19. Jaiswal V, Chanumolu SK, Gupta A et al (2013) Jenner-predict server: prediction of protein vaccine candidates (PVCs) in bacteria based on host-pathogen interactions. *BMC Bioinformatics* 14:211
20. Goodswen SJ, Kennedy PJ, Ellis JT (2014) Vaxceed: a high-throughput in silico vaccine candidate discovery pipeline for eukaryotic pathogens based on reverse vaccinology. *Bioinformatics* (Oxford, England) 30:2381–2383
21. Heinson AI, Gunawardana Y, Moesker B et al (2017) Enhancing the biological relevance of

- machine learning classifiers for reverse vaccinology. *Int J Mol Sci* 18:312
22. Rizwan M, Naz A, Ahmad J et al (2017) VacSol: a high throughput in silico pipeline to predict potential therapeutic targets in prokaryotic pathogens using subtractive reverse vaccinology. *BMC Bioinformatics* 18:106
 23. Naz K, Naz A, Ashraf ST et al (2019) PanRV: Pangenome-reverse vaccinology approach for identifications of potential vaccine candidates in microbial pangenome. *BMC Bioinformatics* 20:123
 24. D’Mello A, Ahearn CP, Murphy TF et al (2019) ReVac: a reverse vaccinology computational pipeline for prioritization of prokaryotic protein vaccine candidates. *BMC Genomics* 20:981
 25. Ong E, Wang H, Wong MU et al (2020) Vaxign-ML: supervised machine learning reverse vaccinology model for improved prediction of bacterial protective antigens. *Bioinformatics* 36:3185–3191
 26. Goodswen SJ, Kennedy PJ, Ellis JT (2021) Computational antigen discovery for eukaryotic pathogens using vacceed. *Methods Mol Biol* 2183:29–42
 27. Tettelin H, Masignani V, Cieslewicz MJ et al (2005) Genome analysis of multiple pathogenic isolates of *Streptococcus agalactiae*: Implications for the microbial “pan-genome”. *Proc Natl Acad Sci U S A* 102:13950–13955
 28. Vernikos G, Medini D, Riley DR et al (2015) Ten years of pan-genome analyses. *Curr Opin Microbiol* 23:148–154
 29. Nichio BTL, Marchaukoski JN, Raittz RT (2017) New tools in Orthology analysis: a brief review of promising perspectives. *Front Genet* 8:165
 30. Hiller NL, Janto B, Hogg JS et al (2007) Comparative genomic analyses of seventeen *Streptococcus pneumoniae* strains: insights into the pneumococcal Supragenome. *J Bacteriol* 189:8186–8195
 31. Vilela Rodrigues TC, Jaiswal AK, de Sarom A et al (2019) Reverse vaccinology and subtractive genomics reveal new therapeutic targets against *Mycoplasma pneumoniae*: a causative agent of pneumonia. *R Soc Open Sci* 6:190907
 32. Luo H, Lin Y, Gao F et al (2014) DEG 10, an update of the database of essential genes that includes both protein-coding genes and non-coding genomic elements. *Nucleic Acids Res* 42:D574–D580
 33. Thein M, Sauer G, Paramasivam N et al (2010) Efficient subfractionation of Gram-negative bacteria for proteomics studies. *J Proteome Res* 9:6135–6147
 34. Emanuelsson O, Brunak S, von Heijne G et al (2007) Locating proteins in the cell using TargetP, SignalP and related tools. *Nat Protoc* 2:953–971
 35. Punta M, Forrest LR, Bigelow H et al (2007) Membrane protein prediction methods. *Methods* 41:460–474
 36. Su EC-Y, Chiu H-S, Lo A et al (2007) Protein subcellular localization prediction based on compartment-specific features and structure conservation. *BMC Bioinformatics* 8:330
 37. Yu NY, Wagner JR, Laird MR et al (2010) PSORTb 3.0: improved protein subcellular localization prediction with refined localization subcategories and predictive capabilities for all prokaryotes. *Bioinformatics* 26:1608–1615
 38. Yu C-S, Chen Y-C, Lu C-H et al (2006) Prediction of protein subcellular localization. *Proteins* 64:643–651
 39. Rashid M, Saha S, Raghava GP (2007) Support vector machine-based method for predicting subcellular localization of mycobacterial proteins using evolutionary information and motifs. *BMC Bioinformatics* 8:337
 40. Chou KC, Shen HB (2006) Large-scale predictions of gram-negative bacterial protein subcellular locations. *J Proteome Res* 5:3420–3428
 41. Paramasivam N, Linke D (2011) Clubsub-P: cluster-based subcellular localization prediction for gram-negative bacteria and archaea. *Front Microbiol* 2:218
 42. Dunston CR, Herbert R, Griffiths HR (2015) Improving T cell-induced response to subunit vaccines: opportunities for a proteomic systems approach. *J Pharm Pharmacol* 67 (3):290–299
 43. Flower DR, Doytchinova IA (2002) Immunoinformatics and the prediction of immunogenicity. *Appl Bioinforma* 1:167–176
 44. De Groot AS, Sbai H, Saint AC et al (2002) Immuno-informatics: mining genomes for vaccine components. *Immunol Cell Biol* 80:255–269
 45. Zhang H, Lund O, Nielsen M (2009) The PickPocket method for predicting binding specificities for receptors based on receptor pocket similarities: application to MHC-peptide binding. *Bioinformatics* 25:1293–1299
 46. Karosiene E, Lundegaard C, Lund O et al (2012) NetMHCcons: a consensus method for the major histocompatibility complex

- class I predictions. *Immunogenetics* 64:177–186
47. Wang P, Sidney J, Dow C et al (2008) A systematic assessment of MHC class II peptide binding predictions and evaluation of a consensus approach. *PLoS Comput Biol* 4:e000048
 48. Zhang L, Udaka K, Mamitsuka H et al (2012) Toward more accurate pan-specific MHC-peptide binding prediction: a review of current methods and tools. *Brief Bioinform* 13:350–364
 49. Bui H-H, Sidney J, Peters B et al (2005) Automated generation and evaluation of specific MHC binding predictive tools: ARB matrix applications. *Immunogenetics* 57:304–314
 50. Sidney J, Assarsson E, Moore C et al (2008) Quantitative peptide binding motifs for 19 human and mouse MHC class I molecules derived using positional scanning combinatorial peptide libraries. *Immun Res* 4:2
 51. Nielsen M, Lundegaard C, Worning P et al (2003) Reliable prediction of T-cell epitopes using neural networks with novel sequence representations. *Protein Sci* 12:1007–1017
 52. Peters B, Sette A (2005) Generating quantitative models describing the sequence specificity of biological processes with the stabilized matrix method. *BMC Bioinformatics* 6:132
 53. Kim Y, Sidney J, Pinilla C et al (2009) Derivation of an amino acid similarity matrix for peptide:MHC binding and its application as a Bayesian prior. *BMC Bioinformatics* 10:394
 54. Moutaftsi M, Peters B, Pasquetto V et al (2006) A consensus epitope prediction approach identifies the breadth of murine T (CD8⁺)-cell responses to vaccinia virus. *Nat Biotechnol* 24:817–819
 55. Nielsen M, Lundegaard C, Blicher T et al (2007) NetMHCpan, a method for quantitative predictions of peptide binding to any HLA-A and -B locus protein of known sequence. *PLoS One* 2:e796
 56. Rasmussen M, Fenoy E, Harndahl M et al (2016) Pan-specific prediction of peptide-MHC class I complex stability, a correlate of T cell immunogenicity. *J Immunol* 197:1517–1524
 57. O'Donnell TJ, Rubinsteyn A, Laserson U (2020) MHCflurry 2.0: improved pan-allele prediction of MHC class I-presented peptides by incorporating antigen processing. *Cell Syst* 11:42–48.e7
 58. Bassani-Sternberg M, Chong C, Guillaume P et al (2017) Deciphering HLA-I motifs across HLA peptidomes improves neo-antigen predictions and identifies allosteric regulating HLA specificity. *PLoS Comput Biol* 13:e1005725
 59. Jurtz V, Paul S, Andreatta M et al (2017) NetMHCpan-4.0: improved peptide-MHC class I interaction predictions integrating eluted ligand and peptide binding affinity data. *J Immunol* 199:3360–3368
 60. Singh H, Raghava GPS (2003) ProPred1: prediction of promiscuous MHC class-I binding sites. *Bioinformatics* 19:1009–1014
 61. Jensen KK, Andreatta M, Marcatili P et al (2018) Improved methods for predicting peptide binding affinity to MHC class II molecules. *Immunology* 154:394–406
 62. Reynisson B, Alvarez B, Paul S et al (2020) NetMHCpan-4.1 and NetMHCIIpan-4.0: improved predictions of MHC antigen presentation by concurrent motif deconvolution and integration of MS MHC eluted ligand data. *Nucleic Acids Res* 48:W449–W454
 63. Singh H, Raghava GPS (2001) ProPred: prediction of HLA-DR binding sites. *Bioinformatics* 17:1236–1237
 64. Nielsen M, Lundegaard C, Blicher T et al (2008) Quantitative predictions of peptide binding to any HLA-DR molecule of known sequence: NetMHCIIpan. *PLoS Comput Biol* 4:e1000107
 65. Hoof I, Peters B, Sidney J et al (2009) NetMHCpan, a method for MHC class I binding prediction beyond humans. *Immunogenetics* 61:1–13
 66. Racle J, Michaux J, Rockinger GA et al (2019) Robust prediction of HLA class II epitopes by deep motif deconvolution of immunopeptidomes. *Nat Biotechnol* 37:1283–1286
 67. Chen B, Khodadoust MS, Olsson N et al (2019) Predicting HLA class II antigen presentation through integrated deep learning. *Nat Biotechnol* 37:1332–1343
 68. Liu Z, Jin J, Cui Y, et al. (2019) DeepSeqPanII: an interpretable recurrent neural network model with attention mechanism for peptide-HLA class II binding prediction, *bioRxiv* 817502
 69. Paul S, Weiskopf D, Angelo M a, et al. (2013) HLA class I alleles are associated with peptide-binding repertoires of different size, affinity, and immunogenicity. *J Immunol* 191:5831–5839
 70. Doytchinova IA, Guan P, Flower DR (2004) Identifying human MHC supertypes using bioinformatic methods. *J Immunol* 172:4314–4323

71. Sidney J, Peters B, Frahm N et al (2008) HLA class I supertypes: a revised and updated classification. *BMC Immunol* 9:1
72. Doytchinova IA, Flower DR (2005) In silico identification of supertypes for class II MHCs. *J Immunol* 174:7085–7095
73. Ponomarenko J V., Marc H. V. van Regenmortel (2009) B-cell epitope prediction, In: Gu, J. and Bourne, P.E. (eds.) *Structural bioinformatics*, Wiley-Blackwell Hoboken, New Jersey
74. Kringelum JV, Lundegaard C, Lund O et al (2012) Reliable B cell epitope predictions: impacts of method development and improved benchmarking. *PLoS Comput Biol* 8:e1002829
75. Larsen JEP, Lund O, Nielsen M (2006) Improved method for predicting linear B-cell epitopes. *Immun Res* 2:2
76. Jespersen MC, Peters B, Nielsen M et al (2017) BepiPred-2.0: improving sequence-based B-cell epitope prediction using conformational epitopes. *Nucleic Acids Res* 45:W24–W29
77. Saha S, Raghava GPS (2006) Prediction of continuous B-cell epitopes in an antigen using recurrent neural network. *Proteins Struct Funct Genet* 65:40–48
78. Gao J, Faraggi E, Zhou Y et al (2012) BEST: improved prediction of B-cell epitopes from antigen sequences. *PLoS One* 7:e40104
79. Singh H, Ansari HR, Raghava GPS (2013) Improved method for linear B-cell epitope prediction using Antigen's primary sequence. *PLoS One* 8:e62216
80. Collatz M, Mock F, Barth E et al (2020) EpiDope: a deep neural network for linear B-cell epitope prediction. *Bioinformatics* 37(4):448–455
81. Ansari HR, Raghava GP (2010) Identification of conformational B-cell epitopes in an antigen from its primary sequence. *Immun Res* 6:6
82. Ponomarenko J, Bui H-H, Li W et al (2008) ElliPro: a new structure-based tool for the prediction of antibody epitopes. *BMC Bioinformatics* 9:514
83. Kunik V, Ashkenazi S, Ofra Y (2012) Paratome: an online tool for systematic identification of antigen-binding regions in antibodies based on sequence or structure. *Nucleic Acids Res* 40:W521–W524
84. Moreau V, Fleury C, Piquier D et al (2008) PEPPOP: computational design of immunogenic peptides. *BMC Bioinformatics* 9:71
85. Lin SY, Cheng C, Su EC (2013) Prediction of B-cell epitopes using evolutionary information and propensity scales. *BMC Bioinformatics* 14:S10
86. Patronov A, Doytchinova I (2013) T-cell epitope vaccine design by immunoinformatics. *Open Biol* 3:120139
87. Shimizu H, Thorley B, Paladin FJ et al (2004) Circulation of type 1 vaccine-derived poliovirus in the Philippines in 2001. *J Virol* 78:13512–13521
88. Moyle PM (2015) Progress in vaccine development. *Curr Protoc Microbiol* 36:1–17
89. Centers for Disease Control and Prevention (2012) *Epidemiology and prevention of vaccine-preventable diseases*. Public Health Foundation, Washington DC
90. Plotkin S (2014) History of vaccination. *Proc Natl Acad Sci U S A* 2014:1–5
91. Moyle PM, Toth I (2013) Modern subunit vaccines: development, components, and research opportunities. *ChemMedChem* 8:360–376
92. Purcell AW, McCluskey J, Rossjohn J (2007) More than one reason to rethink the use of peptides in vaccine design., *nature reviews. Drug Discov* 6:404–414
93. Moyle PM, Toth I (2008) Self-adjuvanting lipopeptide vaccines. *Curr Med Chem* 15:506–516
94. Sato Y, Sato H (1999) Development of acellular pertussis vaccines. *Biologicals* 27:61–69
95. Michel M-L, Tiollais P (2010) Hepatitis B vaccines: protective efficacy and therapeutic potential. *Pathol Biol* 58:288–295
96. Cybulski RJ, Sanz P, O'Brien AD (2009) Anthrax vaccination strategies. *Mol Asp Med* 30:490–502
97. Chun JH, Hong KJ, Cha SH et al (2012) Complete genome sequence of *Bacillus anthracis* H9401, an isolate from a Korean patient with anthrax. *J Bacteriol* 194:4116–4117
98. Keitel WA (2006) Recombinant protective antigen 102 (rPA102): profile of a second-generation anthrax vaccine. *Expert Rev Vaccines* 5:417–430
99. McKee SJ, Bergot A-S, Leggatt GR (2015) Recent progress in vaccination against human papillomavirus-mediated cervical cancer. *Rev Med Virol* 25:54–71
100. Khallouf H, Grabowska A, Riemer A (2014) Therapeutic vaccine strategies against human papillomavirus. *Vaccine* 2:422–462
101. Merck, <http://www.merck.com>
102. Rello J, Krenn C-G, Locker G et al (2017) A randomized placebo-controlled phase II

- study of a pseudomonas vaccine in ventilated ICU patients. *Crit Care* 21:22
103. Vincent J-L (2014) Vaccine development and passive immunization for *Pseudomonas aeruginosa* in critically ill patients: a clinical update. *Future Microbiol* 9:457–463
 104. Westritschnig K, Hochreiter R, Wallner G et al (2014) A randomized, placebo-controlled phase I study assessing the safety and immunogenicity of a *Pseudomonas aeruginosa* hybrid outer membrane protein OprF/I vaccine (IC43) in healthy volunteers. *Hum Vaccin Immunother* 10:170–183
 105. Skwarczynski M, Toth I (2014) Recent advances in peptide-based subunit nanovaccines. *Nanomedicine* 9:2657–2669
 106. Sharma M, Dixit A (2015) Identification and immunogenic potential of B cell epitopes of outer membrane protein OprF of *Aeromonas hydrophila* in translational fusion with a carrier protein. *Appl Microbiol Biotechnol* 99(15):6277–6291
 107. Van Regenmortel MHV (1996) Mapping epitope structure and activity: from one-dimensional prediction to four-dimensional description of antigenic specificity. *Methods* 9:465–472
 108. Sette A, Fikes J (2003) Epitope-based vaccines: an update on epitope identification, vaccine design and delivery. *Curr Opin Immunol* 15:461–470
 109. Guichard G, Zerbib A, Le Gal FA et al (2000) Melanoma peptide MART-1(27-35) analogues with enhanced binding capacity to the human class I histocompatibility molecule HLA-A2 by introduction of a β -amino acid residue: implications for recognition by tumor-infiltrating lymphocytes. *J Med Chem* 43:3803–3808
 110. Reinelt S, Marti M, Dédier S et al (2001) β -Amino acid scan of a class I major histocompatibility complex-restricted Alloreactive T-cell epitope. *J Biol Chem* 276:24525–24530
 111. Webb AI, Dunstone MA, Williamson NA et al (2005) T cell determinants incorporating β -amino acid residues are protease resistant and remain immunogenic in vivo. *J Immunol* 175:3810–3818
 112. Brito LA, Malyala P, O'Hagan DT (2013) Vaccine adjuvant formulations: A pharmaceutical perspective. *Semin Immunol* 25:130–145
 113. Pulendran B, Ahmed R (2011) Immunological mechanisms of vaccination. *Nat Immunol* 12:509–517
 114. Berti F, Adamo R (2013) Recent mechanistic insights on glycoconjugate vaccines and future perspectives. *ACS Chem Biol* 8:1653–1663
 115. Plotkin S a. (2009) Vaccines: the fourth century. *Clin Vaccine Immunol* 16:1709–1719
 116. Azmi F, Fuaad AAHA, Skwarczynski M et al (2014) Recent progress in adjuvant discovery for peptide-based subunit vaccines. *Hum Vaccin Immunother* 10:778–796
 117. Lua LHL, Connors NK, Sainsbury F et al (2014) Bioengineering virus-like particles as vaccines. *Biotechnol Bioeng* 111:425–440
 118. Wieser A, Magistro G, Nörenberg D et al (2012) First multi-epitope subunit vaccine against extraintestinal pathogenic *Escherichia coli* delivered by a bacterial type-3 secretion system (T3SS). *Int J Med Microbiol* 302:10–18
 119. Bumann D, Hueck C, Aebischer T et al (2000) Recombinant live salmonella spp. for human vaccination against heterologous pathogens. *FEMS Immunol Med Microbiol* 27:357–364
 120. Garmory HS, Leary SEC, Griffin KF et al (2003) The use of live attenuated bacteria as a delivery system for heterologous antigens. *J Drug Target* 11:471–479
 121. Nicolay T, Vanderleyden J, Spaepen S (2015) Autotransporter-based cell surface display in gram-negative bacteria. *Crit Rev Microbiol* 41:109–123
 122. van den Berg van Saparoea HB, Houben D, de Jonge MI et al (2018) Display of recombinant proteins on bacterial outer membrane vesicles by using protein ligation. *Appl Environ Microbiol* 84(8):e02567–e02517
 123. Demento SL, Siefert AL, Bandyopadhyay A et al (2011) Pathogen-associated molecular patterns on biomaterials: a paradigm for engineering new vaccines. *Trends Biotechnol* 29:294–306
 124. Hilf N, Kuttruff-Coqui S, Frenzel K et al (2019) Actively personalized vaccination trial for newly diagnosed glioblastoma. *Nature* 565:240–245
 125. GAPVAC. <http://gapvac.eu/>
 126. HepaVac. <http://www.hepavac.eu/>
 127. A service of the U.S. National Institutes of Health. <https://clinicaltrials.gov/>
 128. Improvac. <http://improvac.com>
 129. El Garch H, Minke JM, Rehder J et al (2008) A West Nile virus (WNV) recombinant canarypox virus vaccine elicits WNV-specific neutralizing antibodies and cell-mediated

- immune responses in the horse. *Vet Immunol Immunopathol* 123:230–239
130. Bionorpharma. <http://www.bionorpharma.com>
 131. NovaDigm Therapeutics. <http://www.novadigm.net/>
 132. Schmidt CS, White CJ, Ibrahim AS et al (2012) NDV-3, a recombinant alum-adjuvanted vaccine for *Candida* and *Staphylococcus aureus*, is safe and immunogenic in healthy adults. *Vaccine* 30:7594–7600
 133. Anderson AS, Miller AA, RGK D et al (2012) Development of a multicomponent *Staphylococcus aureus* vaccine designed to counter multiple bacterial virulence factors. *Hum Vaccin Immunother* 8:1585–1594
 134. Emergent Biosolutions. <http://emergentbiosolutions.com/>
 135. Raghunandan R, Lu H, Zhou B et al (2014) An insect cell derived respiratory syncytial virus (RSV) F nanoparticle vaccine induces antigenic site II antibodies and protects against RSV challenge in cotton rats by active and passive immunization. *Vaccine* 32:6485–6492
 136. El-Awady MK, El Gendy M, Waked I et al (2013) Immunogenicity and safety of HCV E1E2 peptide vaccine in chronically HCV-infected patients who did not respond to interferon based therapy. *Vaccine* (paper was withdrawn later)
 137. Immune Response BioPharma, Inc. <http://www.immuneresponsebiopharma.com>
 138. Wedemeyer H, Schuller E, Schlaphoff V et al (2009) Therapeutic vaccine IC41 as late add-on to standard treatment in patients with chronic hepatitis C. *Vaccine* 27:5142–5151

Part II

Vaccine Vectors and Production System



Phage T7 as a Potential Platform for Vaccine Development

Chuan Loo Wong, Chean Yeah Yong, and Khai Wooi Lee

Abstract

Bacteriophages have been explored for their uses in vaccine development, due to the ease of propagation while displaying epitopes in high density. Bacteriophage T7 has been demonstrated to be useful in the production of potential vaccine candidates for various diseases, including influenza A, foot-and mouth disease (FMD), and cancers. In this chapter, we described the use of phage T7 to display potential foot-and-mouth disease virus (FMDV) epitope, from cloning to expression, purification, and immunization in a mouse model.

Key words Bacteriophage T7, Phage T7 display, Phage vaccine, Foot-and-mouth disease virus (FMDV), Mice immunization

1 Introduction

Vaccines against various diseases are consistently under study. Traditionally, vaccines are prepared by purification and inactivation of the disease-causing agent, such as a virus. However, such methods are often costly and tedious, and is greatly limited by the source of the disease-causing agent. With advances in the field of genetics and genome, recombinant vaccines have gained increasing popularity, as the genome of a newly emerging virus can be obtained within days or weeks [1, 2]. Through bioinformatics, immunogenic epitopes can be predicted and produced in various expression systems, such as yeasts, bacteria, cell culture, and bacteriophage.

Bacteriophages are viruses that infect bacteria. As phages have developed friendly relationship with eukaryotes, it is highly unlikely to cause pathogenesis in mammals [3, 4]. In addition, safe application of phages in humans have also been demonstrated [5–7]. Apart from safety perspective, phage display is also known to improve the immunogenicity of the displayed foreign epitopes through high-density display of the epitopes [8, 9]. The coat proteins of bacteriophages have also been reported to function as an adjuvant, further

enhancing the immunogenicity of the displayed epitopes [10–12]. Taken together, phage display is a highly potential platform for vaccine development.

Bacteriophage T7 is a lytic phage of the *Podoviridae* family. The icosahedral head of the virus is made of 415 copies of the gp10 proteins. Through genetic engineering, any desired foreign epitopes of up to 50 amino acid residues can be cloned and expressed on the surface of the phage capsid [13]. As phage T7 is lytic in nature, additional lysis step can be omitted, as the recombinant phages will be released to the culture media via host lysis. Additionally, T7 phage particle is extremely robust and is stable in harsh conditions that would inactivate other phages [13], thereby lowering the cost for storage and transport of T7-based vaccines. The potential of phage T7 as a vaccine platform has been demonstrated against influenza A virus [14], breast cancer [15, 16], lung cancer [17, 18], and foot-and-mouth disease virus (FMDV) [9], all of which showed promising results.

Here, we display FMDV VP1 epitope (amino acid residue 131–170) on the surface of the bacteriophage T7 via DNA cloning, followed by phage propagation and purification. We then use the recombinant phage, namely T7-FOVPI_{131–170}, to immunize the BALB/c mice. The serum samples of mice immunized with T7-FOVPI_{131–170} interacted strongly with T7-FOVPI_{131–170} in contrast to the wild-type phage T7, suggesting that the displayed epitope is immunogenic. Similarly, the method presented in this chapter can be modified easily to display other epitope of interest, where the recombinant bacteriophages can be further studied as potential vaccine candidates.

2 Materials

All materials are prepared at room temperature unless stated otherwise.

2.1 Cloning

1. Restriction endonucleases (EcoRI and HindIII) (*see Note 1*).
2. Tris–EDTA (TE) buffer: 10 mM Tris–Cl, 1 mM EDTA; pH 8.0. Sterilize solution by autoclaving for 15 min at 15 psi on liquid cycle. Store the buffer at room temperature (RT).
3. T7Select[®] Cloning kit: T7Select 415-1 EcoRI/HindIII vector arms, T7Select control DNA insert, T7 Select packaging extract, T7Select packaging control DNA, *E. coli* BL21 [*F⁻ omp hsd_B (r_B⁻ m_B) gal dcm*] glycerol stocks, T7 Select Up primer, T7 Select Down primer.
4. T4 DNA ligase and 10× ligase buffer (*see Note 2*).

5. 1% (w/v) TAE: Dissolve 1 g of agarose in 1× TAE buffer (40 mM Tris–acetate, 1 mM EDTA; pH 8.0).
6. Luria–Bertani (LB) broth: Dissolve 10 g Bacto-tryptone, 5 g yeast extract, and 10 g NaCl in 800 mL of deionized water. Adjust the pH to 7.5 with 1N NaOH and top up the broth to 1 L. Sterilize the broth by autoclaving for 15 min. For LB agar plates, add 15 g of bacteriological agar in 1 L of LB broth.
7. Top agarose: Dissolve 1 g Bacto-tryptone, 0.5 g yeast extract, 0.5 g NaCl, and 0.6 g agarose powder in 100 mL of deionized water.
8. SM medium: In 1 L of solution, add 5.8 g NaCl, 2 g $\text{MgSO}_4 \cdot 7\text{H}_2\text{O}$, 50 mL of 1 M Tris–Cl; pH 7.5, 5 mL of 2% (w/v) gelatin solution and top up to 1 L with deionized water. Sterilize the buffer by autoclaving for 15 min at 15 psi. SM medium can be stored at RT.
9. 10 mM EDTA, pH 8.0.
10. 100 mM DNTP mix.
11. Taq DNA polymerase (5 U/ μL) and its complementary 10× amplification buffer.

2.2 Phage Amplification and Precipitation with Polyethylene Glycol (PEG)

1. DNase I (20 mg/mL).
2. 10% (w/v) PEG 8000: Add 10 g of PEG 8000 to 100 mL of respective phage supernatants.
3. 10% (w/v) PEG/TE: Dissolve 10 g of PEG 8000 in 100 mL of Tris–EDTA (TE), pH 8.0.
4. 1 M (w/v) NaCl/TE: Dissolve 5.85 g of NaCl in 100 mL of Tris–EDTA (TE), pH 8.0.

2.3 Phage Purification with Cesium Chloride (CsCl) Step Gradient Ultracentrifugation

1. 62.5% (w/v) CsCl: Weigh 25 g of CsCl and dissolve it with 15 mL deionized water.
2. Tris–EDTA (TE) buffer: 10 mM Tris–Cl, 1 mM EDTA; pH 8.0. Sterilize solution by autoclaving for 15 min at 15 psi on liquid cycle. Store the buffer at RT.
3. 13.2 mL open-top thin wall ultra-clear tube 14 × 89 mm.
4. Phage dialysis buffer: 0.1 M NaCl, 0.1 M Tris–HCl; pH 8.0. Sterilize solution by autoclaving for 15 min at 15 psi on liquid cycle. Store the buffer at RT.

2.4 Western Blotting

1. *N,N,N,N'*-Tetramethylethylenediamine (TEMED).
2. 10% (w/v) ammonium persulfate (APS): Dissolve 1 g of APS in 10 mL deionized water (*see Note 3*).
3. Polyacrylamide mixture: Weigh 29.2 g of acrylamide monomer and 0.8 g of bis-acrylamide (29.2:0.8) and dissolve in 100 mL deionized water. Filter the mixture through a 0.45- μm

cellulose acetate syringe filter. Store at 4 °C, in a bottle wrapped with aluminum foil.

4. 4× upper buffer: 0.5 M Tris-HCl, 0.4% (w/v) SDS; pH 6.8.
5. 4× lower buffer: 1.5 M Tris-HCl, 0.4% (w/v) SDS; pH 8.8.
6. Gel cassette (7.25 cm × 10 cm × 1.5 mm).
7. 6× sample buffer: 62.5 mM Tris-HCl; pH 6.8, 30% (v/v) glycerol, 5% SDS (w/v), 0.01% (w/v) bromophenol blue, and 5% (v/v) mercaptoethanol.
8. SDS-PAGE running buffer: 3% (w/v) Tris-base, 14.4% (w/v) glycine 0.1% (w/v) SDS; pH 8.4 (*see Note 4*).
9. Nitrocellulose membrane and blotting paper.
10. Towbin transfer buffer: 25 mM Tris-base, 190 mM glycine, 20% (v/v) methanol.
11. Tris-buffered saline (TBS): 50 mM Tris-Cl, 150 mM NaCl; pH 7.4.
12. TBS containing 0.05% Tween-20 (TBST).
13. Blocking solution: 10% (w/v) of skim milk powder dissolved in TBS.
14. Anti-T7 monoclonal antibody.
15. Anti-mouse IgG conjugated to alkaline phosphatase.
16. Nitro blue tetrazolium (NBT)/5-bromo-4-chloro-3-indolyl phosphate (BCIP): Dissolve 1 g NBT in 20 mL of 70% dimethylformamide (DMF). Dissolve 1 g BCIP in 20 mL of 100% DMF.
17. Alkaline phosphatase buffer: 100 mM Tris-HCl, 100 mM NaCl, 1 mM MgCl₂; pH 9.5.

2.5 Mice Immunization

1. Female BALB/c mice (6–8 weeks old).
2. Mouse cages, feed, and water bottles.
3. Complete Freund's adjuvant.
4. Incomplete Freund's adjuvant.
5. 1 mL syringe.
6. 16 G and 26 G needles.

2.6 Enzyme-Linked Immunosorbent Assay (ELISA)

1. Round-bottom 96-well ELISA plate.
2. Sodium bicarbonate buffer: 50 mM sodium bicarbonate and adjust to pH 9.6 with 0.1N NaOH.
3. Tris-buffered saline (TBS): 50 mM Tris-Cl, 150 mM NaCl; pH 7.4.
4. TBS containing 0.05% Tween-20 (TBST).
5. Blocking solution: 5% (w/v) of milk in TBS.

6. Goat anti-mouse IgG conjugated to alkaline phosphatase.
7. *p*-nitrophenyl phosphate (pNPP) substrate: Dissolve 10 mg of pNPP in 10 mL of pNPP buffer (10 mM diethanolamine, 0.55 mM MgCl₂; pH 9.8).

3 Methods

All the procedures are performed at room temperature unless specified otherwise.

3.1 Cloning into Phage T7 Vectors

In this cloning method, T7 bacteriophage display system (T7Select415-1; Novagen Merck KGaA, Darmstadt, Germany) is used to display FMDV VP1 peptide. The coding sequence for the peptide is cloned within the multiple cloning site (MCS) following amino acid 348 of the 10B protein. The linearized vector is 37,314 bp in size. Refer to the Novagen's T7Select[®] System Manual for vector map.

3.1.1 Preparation of Foreign DNA

1. Generate individual restriction fragments of foreign DNA (nucleotide sequence encoding the FMDV VP1 amino acid residues 131–170, flanked by EcoRI and HindIII restriction sites) by cleavage with the EcoRI and HindIII restriction endonucleases (*see Note 5*).
2. The digested DNA fragment was then electrophoresed on 1% (w/v) agarose gel electrophoresis and purified using QIAquick[®] gel extraction kit (*see Note 6*).
3. Dissolve the foreign DNA in appropriate volume of TE buffer (pH 8.0) or water at a concentration that yield about 0.02–0.06 pmol/μL (*see Note 7*).

3.1.2 Ligation of Phage T7 Arms to Foreign Genomic DNA

When ligating DNAs with complementary cohesive termini, follow **Steps 1–8** below.

1. In a 1.5-mL microcentrifuge tube (Tube A), mix 0.5 μL of T7Select EcoRI/HindIII vector arms containing 0.5 μg of vector DNA (0.02 pmol) and one- to threefold molar excess of the foreign DNA fragment(s) (0.02–0.06 pmol) (*see Note 8*). The combined volume of the two DNAs should not exceed 5 μL.
2. As controls, set up another two ligation reactions in parallel with Tube A as described below (*see Note 9*):

Tube DNA	
B	Same amount of vector DNA with 1 μL of positive control DNA insert (0.04 pmol)
C	Same amount of vector DNA with no DNA insert

3. Add 0.5 μL of 10 \times ligase buffer and 0.5 μL of 10 mM ATP to all reactions (Tubes A–C). Omit the use of ATP if using commercial buffer which consists of ATP.
4. Add 0.4–0.6 Weiss units of T4 DNA ligase to all the tubes (*see Note 10*).
5. Add sterile water to each of the tubes to a final volume of 5 μL (*see Note 11*).
6. Gently mix the component by pipetting the mixtures up and down.
7. Incubate the ligation reactions for 3–16 h at room temperature (RT).
8. Store at 4 $^{\circ}\text{C}$ until use.

3.1.3 In Vitro Packaging

1. Allow 25 μL of the T7 Select packaging extract to thaw on ice. This extract allows the packaging of up to 1 μg of vector DNA (*see Note 12*).
2. Add 5 μL ligation reactions per 25 μL extract. Mix gently by stirring with a pipette tip. Do not vortex.
3. To test the packaging efficiency, add 0.5 μg of the T7Select packaging control DNA to 25 μL extract.
4. Incubate the reaction for 2 h at RT.
5. Stop the reaction by adding 270 μL sterile Luria Bertani (LB) broth. Add 20 μL chloroform to the packaging mixture if the mixture will be kept more than 24 h prior to amplification. Invert the tubes gently (*see Note 13*).
6. Perform a phage titration assay using *E. coli* BL21 [F^{-} *omp hsdS_B (r_B⁻m_B) gal dcm*] as the host strain to determine the number of recombinants generated.

3.1.4 Titration Assay

1. Inoculate a single colony of BL21 host cells into 5 mL of LB broth and incubate the culture at 37 $^{\circ}\text{C}$ overnight with shaking at 180 rpm until the culture reach a density of about 1 at OD₆₀₀.
2. Perform tenfold serial dilutions on the packaging mixture using SM medium as the diluent. The initial 1:10 dilution can be prepared by adding 100 μL of the sample to 900 μL of the diluent and following serial dilutions can be made by adding 100 μL of the 1:10 dilution to 900 μL of diluent to yield a 10² dilution, and so on (*see Note 14*).
3. Melt the top agarose (at least 3 mL per phage dilution) by microwaving, and cool to 45–50 $^{\circ}\text{C}$ in a water bath or incubator.
4. For each phage dilution, aliquot 250 μL of host cells along with 100 μL of the packaging mixture into a sterile glass test tube

(75 × 10 mm). Replace new pipette tip between each dilution to prevent sample contamination.

5. Add 3 mL of top agarose to each tube, vortex and dispense uniformly over the surface of a 20 mL prewarmed LB agar.
6. Allow the top agarose overlay to solidify at RT.
7. Invert the plates and incubate at 37 °C for 3–4 h.
8. Plaques should appear as relatively clear disc against a lawn of cells. Count the plaques and calculate the phage titer in plaque-forming unit (pfu) per unit volume (*see Note 15*).

3.1.5 Screening of Selected Phage Recombinants

For the screening of positive putative transformants, a pair of primers, namely T7SelectUP (5'-GGAGCTGTTCGATTCCAGTC-3') and T7SelectDOWN primers (5'-AACCCCTCAA GACCCGTTTA-3'), are used for the amplification of the region that includes the MCS.

1. Apply a mild suction to the chosen individual plaques using a sterile 200- μ L pipette tip and disperse it in a 1.5-mL microcentrifuge tube containing 100 μ L of 10 mM EDTA, pH 8.0.
2. Vortex the tube briefly and incubate the tubes at 65 °C for 10 min.
3. Allow the samples to cool to RT and centrifuge the tubes at 10,000 × *g* for 3 min.
4. Set up the following reactions as described below:

Reaction component	Standard reaction (μ L)	Negative control (μ L)
Phage lysate	0.5	–
100 mM dNTP mix	0.5	0.5
10× amplification buffer	2.5	2.5
T7 select up primer (5 pmol/ μ L)	0.5	0.5
T7 select down primer (5 pmol/ μ L)	0.5	0.5
Nuclease-free water	20.25	20.75
<i>Taq</i> DNA polymerase (5 U/ μ L)	0.25	0.25
Total volume	25.0	25.0

5. Amplify the nucleic acids using the PCR. The PCR cycle conditions were denaturation at 94 °C for 1 min followed by a 30-cycle reaction (94 °C, 50 s; 50 °C, 1 min; 72 °C, 1 min) and a final elongation at 72 °C for 5 min.

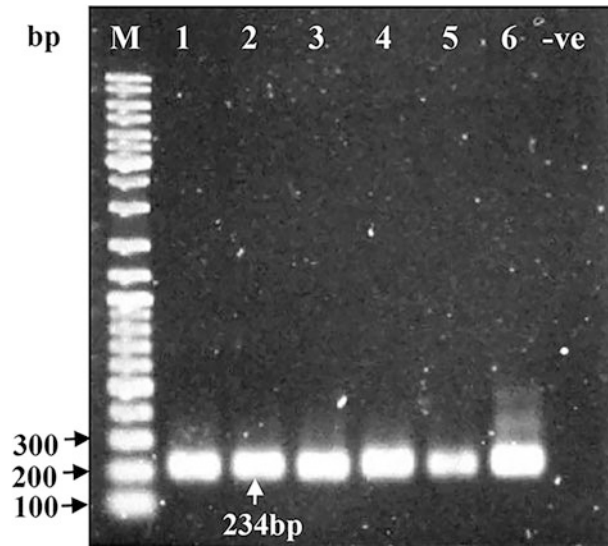


Fig. 1 PCR amplification of the recombinant phage T7 DNA. Lane M is the DNA markers in base pair (bp). Recombinant T7-FOVP1₁₃₁₋₁₇₀ phage (lanes 1–6), and no template control (–ve). Arrows indicate the estimated PCR product size after amplification with T7SelectUP and T7SelectDOWN primers

6. Analyze the PCR amplified product on a 1% (w/v) TAE agarose gel.
7. Stain the gel with ethidium bromide (1 µg/mL) and visualize it using a gel imaging system under the transillumination of UV light (Fig. 1) (*see Note 16*).

3.2 Amplification and Concentration of Phage by Precipitation with Polyethylene Glycol

1. Inoculate a single colony of BL21 host cells into 5 mL of LB broth and incubate the culture at 37 °C overnight with shaking at 180 rpm until the culture reach a density of about 1 at OD₆₀₀.
2. The next day, add 2 mL of the fresh overnight culture each to four flasks containing 500 mL LB media and shake at 180 rpm at 37 °C until OD₆₀₀ reaches 0.6–0.8.
3. Add the high-titer infectious phage T7 particles at the MOI of 0.1 (*see Note 17*) and continue shaking at 37 °C at 180 rpm to ensure the inoculum is dispersed rapidly throughout the culture until lysis is observed, usually within 1–1.5 h (*see Note 18*).
4. Upon lysis, add 5 µL of DNase (20 mg/mL) to the bacterial lysate and continue shaking at 37 °C for 15 min (*see Note 19*). Dissolve solid NaCl into the bacteriophage suspension to a final concentration of 0.5 M and swirl to dissolve.
5. Pour the lysate into centrifuge bottles and remove bacterial debris by centrifugation at 13,000 × *g* for 10 min at 4 °C.

6. Transfer and combine the phage-containing supernatants into a clean flask.
7. Add 10% (w/v) PEG 8000 and slowly stir at RT until all the PEG is completely dissolved. For more effective precipitation of phage particles, let it stand at 4 °C for overnight.
8. Sediment the precipitated phage at $13,000 \times g$ for 10 min at 4 °C and carefully discard the supernatant (*see Note 20*).
9. Turn the centrifuge bottles over on paper towels and drain the pellet for 5–10 min. Remove the liquid as much as possible by wiping the inside rims of the centrifuge bottles.
10. Gently resuspend the pellets in a combined volume of about 40 mL of sterile 10% (w/v) PEG in TE buffer.
11. Transfer the resuspended mixture into two Falcon tube and centrifuge at $7500 \times g$ for 10 min at 4 °C.
12. Decant the supernatant and drain the washed pellets as completely as possible.
13. Resuspend each pellet in 5 mL of 1 M of NaCl in TE buffer and vortex vigorously to extract the phage particles.
14. Centrifuge at $7500 \times g$ for 10 min at 4 °C to recover the supernatant which consist of extracted phages. The pellets can be re-extracted again with another 5 mL of 1 M NaCl/TE as in **step 17** and pool the resultant supernatants.
15. Determine the titer of the phage by the titration assay mentioned in Subheading **3.1.4**.

The phage precipitation with PEG itself is a purification procedure, which can be sufficient for several applications depending on the purity required for phage preparation. In other more sensitive downstream experiments, this PEG-purified phages can be further purified by centrifugation in a cesium chloride (CsCl) step gradient.

3.3 Cesium Chloride (CsCl) Purification of the Concentrated Phage T7

Rapid elimination of most bacterial debris and contaminants to obtain a highly pure and concentrated phage particles can be achieved via centrifugation of phage suspensions in CsCl gradients. This CsCl gradients centrifugation is suitable for the purification of large-scale phage preparations. It remains the most widely used methods to achieve high degree of purity. Nevertheless, some bacteriophages can also be purified by centrifugation on sucrose gradients or by ion exchange chromatography (*see Note 21*).

1. Prepare the CsCl gradients by mixing the stock solution of 62.5% (w/v) CsCl (25 g CsCl +15 mL deionized water) with TE buffer in the following different ratios:

Gradient volume (mL)	CsCl:TE
2	1:2
2	1:1
2	2:1
1	1:0

- Set up the gradient in an open-top thin wall ultra-clear tube 14 × 89 mm by carefully layering the above CsCl:TE solutions, starting from the ratio of 1:0 at the bottom of the tube, followed by 2:1, 1:1, and 1:2 (*see Note 22*).
- Layer 5 mL of the PEG purified phage suspension onto the CsCl density gradient.
- Collect the phage band after centrifugation for 1 h at 209,700 × *g* in a Beckman SW41 rotor (Fig. 2) (*see Note 23*).
- Dialyze the CsCl-purified phage against dialysis buffer for four times over 1 h at RT with a minimum of 100 volumes of buffer each round.
- Store the dialyzed CsCl-purified phage at 4 °C until further usage (*see Note 24*).

3.4 Western Blotting

- Prepare the resolving gel and stacking gel for 12% (w/v) SDS-polyacrylamide gel according to the recipe listed below:

Components	Stacking gel (μL)	Resolving gel (μL)
Distilled water	1460	1315
Polyacrylamide mixture	415	1500
4× upper buffer	625	–
4× lower buffer	–	940
TEMED	3.5	3.8
APS	16.7	23.5

- Cast the resolving gel within a 7.25 cm × 10 cm × 1.5 mm gel cassette. Allow space for stacking gel and gently overlay with isobutanol or water.
- After the resolving gel is solidified, cast the stacking gel and insert gel combs immediately.
- Mix the phage/protein samples with 6× sample buffer.
- Denature the protein sample by boiling in water bath for 5 min and load onto the SDS-PAGE.

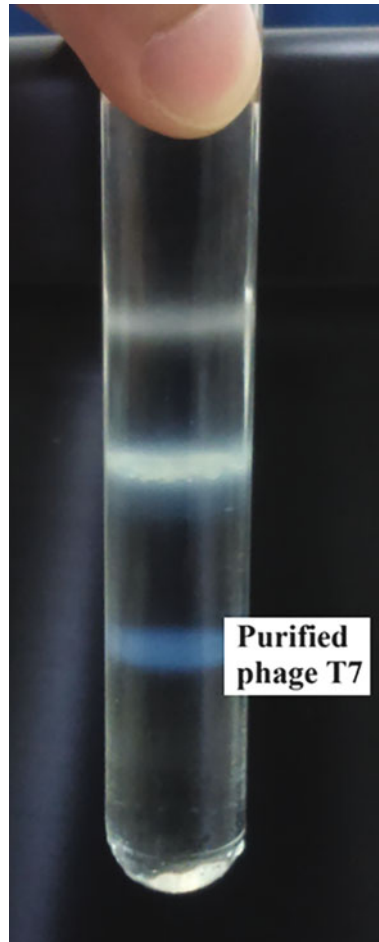


Fig. 2 Purification of phage T7 by CsCl ultracentrifugation. Recombinant phage T7 (5 mL) was layered over a CsCl step gradient performed in a thin wall ultraclear tube (No. 334509 from Beckman-Coulter). After centrifugation for 1 h at $209,700 \times g$ in a Beckman SW41 rotor, the phage particles formed an opalescent bluish band while the empty phage capsid and the thick layer of debris appeared as a white-yellow zone

6. Electrophorese at a constant current of 16 mA (for 1 gel) for 1 h in SDS-PAGE running buffer, or until the front dye reach the bottom of the gel (*see Note 25*).
7. Following SDS-PAGE, remove the stacking gel and rinse the gel with deionized water to remove traces of SDS-PAGE running buffer.
8. Electrotransfer the proteins on the gel to a nitrocellulose membrane sandwiched between blotting paper through a semi-dry electro-trans blotter with Towbin transfer buffer at a constant voltage of 24 V for 40 min.

9. Block the membrane with blocking solution for 2 h on a rotary shaker.
10. Wash 3× with TBST buffer, 10 min each on rotary shaker.
11. Incubate the nitrocellulose membrane in 10 mL of TBS buffer containing anti-T7 tag monoclonal antibody (1:10,000 dilution, Novagen Merck KGaA, Darmstadt, Germany) for 1 h with shaking (*see Note 26*).
12. Repeat the washing step as in **step 10**.
13. Incubate the membrane with the anti-mouse IgG conjugated to alkaline phosphatase (1:5000 dilution in TBS, Chemicon, MA, USA) for another 1 h (*see Note 27*).
14. Repeat the washing step as in **step 10** and lastly rinse the membrane with deionized water (*see Note 28*).
15. Add substrate solution containing 66 μL of nitro-blue tetrazolium (NBT) and 33 μL of 5-bromo-4-chloro-3'-indoyl phosphate toluidinium salt (BCIP) in alkaline phosphatase buffer for color development (Fig. 3) (*see Note 29*).

3.5 Immunization

1. Assign 6- to 8-week-old female BALB/c mice (17–20 g) into groups consisting 4 mice ($n = 4$). Acclimate the mice for 1 week.
2. After acclimation, inject the mice with 100 μL of 3×10^{11} pfu of recombinant phage T7 emulsified with complete Freund's adjuvant (CFA), subcutaneously at the neck (Fig. 4) (*see Note 30*).
3. Administer booster with recombinant phages emulsified with incomplete Freund's adjuvant (ICFA), subcutaneously at 3 weeks after primary injection.
4. After another 3 weeks, administer the second booster with incomplete Freund's adjuvant.
5. Bleed mice at day 63 through a small cut at the sub-mandibular vascular bundles below their cheeks, with the tip of a 16G needle [19] (Fig. 5) (*see Note 31*).
6. Prepare serum samples by incubating blood samples at RT for 1 h and centrifuge at $1500 \times g$ for 10 min. Transfer the supernatant (serum) to a clean microcentrifuge tube and store at -20°C .
7. Pool the sera from four individual mice for experiments utilizing serum samples.

3.6 Enzyme-Linked Immunosorbent Assay (ELISA)

1. Coat a round-bottom 96-well ELISA plate with $\sim 10^{12}$ pfu/mL of purified recombinant phage T7 carrying the FMDV epitope, wild-type T7 phage, and skimmed milk diluted to a total amount of 2 μg in 100 μL sodium bicarbonate buffer (pH 9.6).

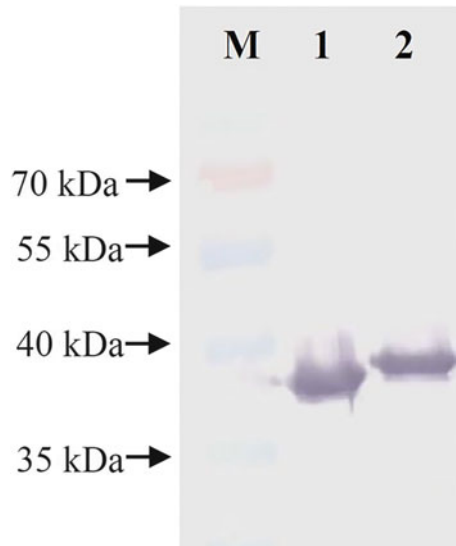


Fig. 3 Western blot analysis of wild-type and recombinant T7 phages. Lane M: molecular weight markers in kDa. Wild-type T7 phage (lane 1) and recombinant T7-FOVP1₁₃₁₋₁₇₀ phage (lane 2) were probed with anti-T7 monoclonal antibody



Fig. 4 Subcutaneous injection of vaccine candidate into mouse. As the skin at the back of the neck is very loose, injection at this site results in minimal struggle from the mouse

2. Incubate the plate for 20 h at 4 °C.
3. Discard the unbound antigen by inverting and flicking the plate over a sink.
4. Wash the coated wells with TBST buffer and leave for at least 5 min at RT before discarding it. Repeat for 3× consecutively.



Fig. 5 Sub-mandibular bleeding on mouse. A swift but shallow penetration near the indicated position will cause extensive bleeding. Collect up to 0.5 mL from a \pm 22 g mouse and stop the bleeding by applying pressure with gauze wet with ethanol

5. Add 200 μ L of blocking buffer to each well [5% (w/v) skimmed milk in TBS]. Incubate at RT for 2 h.
6. Discard blocking buffer and wash plate 3 \times as described in **step 4**.
7. Prepare a titration of serum in TBS buffer to the final dilution of 1:50, 1:150, and 1:500 (*see Note 32*).
8. Load 100 μ L of diluted serum samples in TBS buffer into wells and incubate at RT for at least 1 h.
9. Wash plates 3 \times as described in **step 4**.
10. Dilute the goat anti-mouse IgG-alkaline phosphatase conjugate to the ratio 1:5000 in TBS buffer. Incubate at RT for 1 h.
11. Wash plates 3 \times as described in **step 4**.
12. Add 100 μ l of *p*-nitrophenyl phosphate (pNPP) diluted in pNPP buffer, pH 9.8.
13. Allows color to develop for 30 min.
14. Read absorbances at 405 nm using a microtiter plate reader (**Fig. 6**).

4 Notes

1. Whenever possible, use the 10 \times reaction buffer provided by the manufacturer of the restriction enzymes used.
2. Thaw by vortexing the T4 DNA ligase buffer until there is no precipitate observed at the bottom of the tube (typically

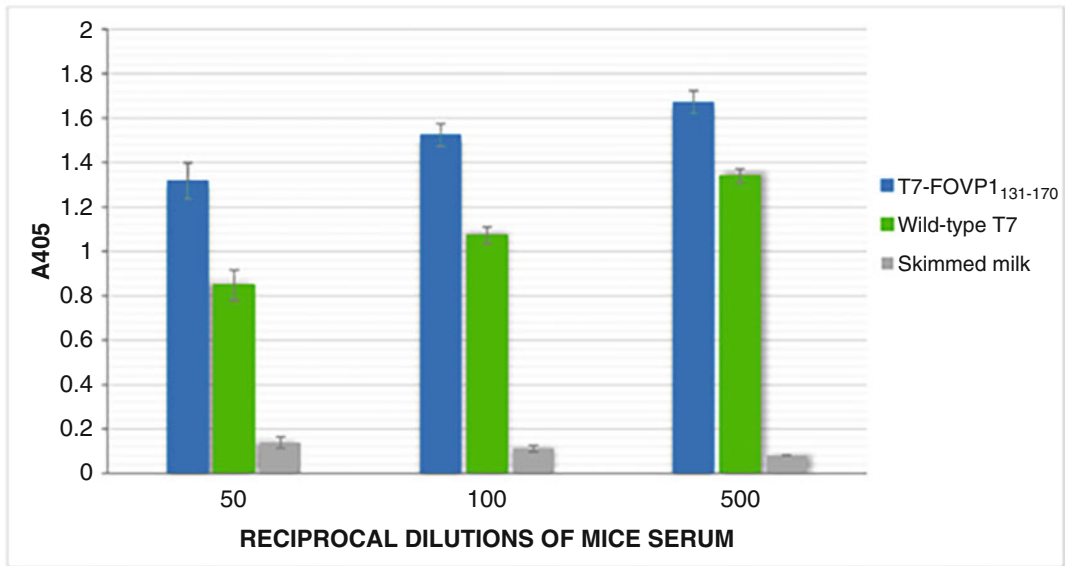


Fig. 6 Immunogenicity of the FMDV VP1 residue 131–170 displayed on bacteriophage T7. Serum samples from mice immunized with recombinant T7-FOVP1_{131–170} phage were used in enzyme-linked immunosorbent assay (ELISA) against T7-FOVP1_{131–170} and wild-type phage T7. The antiserum demonstrated higher affinity toward T7-FOVP1_{131–170} compared to the wild-type phage, suggesting that the displayed VP1 epitope is indeed immunogenic. Assays were performed in triplicates and error bars represent standard deviation from the arithmetic mean

1–2 min). This is because the DTT in the ligase buffer may precipitate upon freezing. Divide the buffer in small aliquots and store at -20°C to minimize the degradation of ATP and DTT.

3. Prepare the APS solution fresh each time. Alternatively, divide the APS solution into small aliquots and store at -20°C .
4. Prepare $10\times$ Tris-glycine buffer (0.25 M Tris-HCl, 1.92 M glycine) as stock solution. Weigh 30.3 g Tris-HCl and 144 g glycine, mix, and add deionize water to 1 L. Prepare SDS-PAGE running buffer freshly before use by diluting 100 mL of $10\times$ Tris-glycine buffer in 0.9 L of water, add 5 mL of 20% (w/v) SDS, and top up to 1 L. Using SDS-PAGE running buffer that had been stored for a week or longer could cause improper migration of the protein bands across the gel, resulting in smear or crocked protein bands.
5. Any gene of interest can be used to replace the FMDV VP1 encoding sequence specified in the methodology. In addition, C-terminal polyhistidine-tag can be added to the insertion nucleotide sequence before HindIII restriction site to ease the purification process with immobilized metal affinity chromatography.

6. Other commercially available gel extraction and purification kit can also be used.
7. Calculate the conversion of μg to pmol of a double-stranded DNA using the equation below:

$$\text{DNA in pmol} = \mu\text{g DNA} \times 1 \text{ pmol} \\ \times 10^6 \text{ pg}/(660 \text{ pg} \times 1 \mu\text{g} \times N)$$

where N is the total base pairs (bp) of the double-stranded DNA.

8. More than threefold increase in the molar amount of the foreign DNA fragment will increase the chance of the DNA inserts to be ligated to the T7Select EcoRI/HindIII vector arms.
9. Set up both positive and background controls in parallel to test the efficiency of ligation and to determine the background of non-recombinant phage.
10. When the ligase concentration is increased to 3 Weiss unit, the number of phages packaged will increase substantially.
11. Addition of water in a ligation reaction can sometimes be omitted. In place of the water, increase the amount of vector and DNA inserts in a reaction tube.
12. Divide the extract into several other pre-chilled tubes if smaller scale of packaging tests is performed simultaneously. However, the amount of ligation mixture should be reduced proportionately.
13. Chloroform is commonly used in a conventional phage isolation and enrichment procedures. Chloroform is added to lyse any infected cells that contain the intracellular phages. Nevertheless, it is not recommended to add chloroform in a lipid-enveloped or filamentous phage.
14. Serial dilutions on the packaging mixture and other phage samples can be performed using LB or TB media according to the T7Select System Manual. The appropriate dilution for the recombinant phage is typically around 10^3 to 10^6 .
15. Pfu is a quantitative measurement of number of infectious virus particles in a known volume of solution and is expressed as pfu per mL. The following formula is used to determine the phage titer (pfu/mL):

$$\text{pfu/mL} = \text{number of plaques}/[\text{dilution factor} \times \text{volume (in mL) of packaging mixture}]$$

16. Staining step is not required if PCR buffer contains DNA staining solution. Alternatively, non-toxic DNA stains such as Atlas ClearSight can be added directly to the agarose gel while in molten form.

17. Ratio of infectious virions to cells in a culture is commonly defined as the multiplicity of infection (MOI). In order to obtain a high titer of infectious phage, a small scale of phage liquid lysate amplification (30 mL) can be performed by transferring a plug containing a single T7 plaque from an agar plate into a mid-log phase bacteria culture ($OD_{600} = 0.6$) and continue shaking until lysis is observed. Upon lysis, centrifuge the 30 mL mixture and the resultant supernatant is then used for this large-scale phage amplification.
18. Lysis of culture can also be indicated by the presence of strings of translucent bacteria cell debris.
19. This step completes the degradation of the residual bacterial DNA and unpackaged phage DNA.
20. The pellet forms a film, which sticks to the wall of the centrifuge bottles.
21. Ultracentrifugation in CsCl gradients may not be able to purify certain recombinant phages due to the extreme centrifugal force which disrupts the phage structure and infectivity. Hence, anion exchange chromatography has been described as an alternative method for purification of phages [20, 21].
22. The gradient gets mixed up very easily so extra care is needed to slowly layer the lower density gradient on top of the higher density gradient.
23. The bluish color phage particles banded atop the 2:1 layer and a thick layer of debris and empty phage heads are observed above the 1:2 layer.
24. Purified phage stocks will gradually lose infectivity over time. It is advisable to perform a phage titration assay to determine the phage titer right before use if absolute quantity is important.
25. For multiple gels, multiply constant current by $16 \text{ mA} \times \text{number of gels}$. If current cannot achieve the desired level, check for buffer leakage, and increase the cap level for voltage (V) and power (W).
26. It is preferable to use an antibody that targets the displayed epitope compared to the anti-T7 monoclonal antibody, as the antigenicity of the displayed epitope can be confirmed directly from the Western blot. In general, monoclonal is preferred over polyclonal antibody, followed by antisera.
27. Secondary antibody should bind to the primary antibody that is being used. If the primary antibody is antiserum from swine, the secondary antibody should be antiserum antibody tagged with enzyme such as alkaline phosphatase or horseradish peroxidase.
28. Rinsing the membrane strips with deionized water will help to remove bulk of the nonspecific antibodies and other contaminants binding to the membrane.

29. BCIP/NBT in ready-to-use solution and tablet forms are available. Occasionally, there are protein samples that are not running at their expected molecular weight on SDS-PAGE. If the phage protein band appears to be smaller or larger than expected compared to the protein marker, it is recommended to use another unstained or pre-stained protein marker for comparison. In addition, it is also advisable to go for N-terminal or C-terminal protein sequencing for the confirmation of the protein sequences as well as the protein molecular weight.
30. Freund's adjuvant can be replaced with any other adjuvants, as its use in human is not allowed. The phage itself can also function as adjuvant; therefore, recombinant phage without adjuvant could be sufficient in inducing immunity.
31. Sub-mandibular bleeding is much easier with the use of a bleeding lancet, as the use of needle could over-penetrates and cause blood to enter into ear and/or mouth canal of the mouse. If the mouse exhibit symptoms of breathing difficulty, massage its thorax to prevent choking by its own blood.
32. Different dilutions of serum can be performed to attain the optimum absorbance readings as serum with high viscosity tend to inhibit the protein interactions and eventually lower the signal generated.

References

1. WHO (2020) Archived: WHO Timeline—COVID-19. <https://www.who.int/news-room/detail/27-04-2020-who-timeline%2D%2D-covid-19>. Accessed Aug 2020
2. Maurier F, Beury D, Fléchon L, Varré J-S, Touzet H, Goffard A, Hot D, Caboche S (2019) A complete protocol for whole-genome sequencing of virus from clinical samples: application to coronavirus OC43. *Virology* 531:141–148. <https://doi.org/10.1016/j.virol.2019.03.006>
3. Salmond GPC, Fineran PC (2015) A century of the phage: past, present and future. *Nat Rev Microbiol* 13(12):777–786. <https://doi.org/10.1038/nrmicro3564>
4. Loc-Carrillo C, Abedon ST (2011) Pros and cons of phage therapy. *Bacteriophage* 1(2):111–114. <https://doi.org/10.4161/bact.1.2.14590>
5. Bruttin A, Brüssow H (2005) Human volunteers receiving *Escherichia coli* phage T4 orally: a safety test of phage therapy. *Antimicrob Agents Chemother* 49(7):2874–2878. <https://doi.org/10.1128/AAC.49.7.2874-2878.2005>
6. Shukla GS, Krag DN, Peletskaya EN, Pero SC, Sun Y-J, Carman CL, McCahill LE, Roland TA (2013) Intravenous infusion of phage-displayed antibody library in human cancer patients: enrichment and cancer-specificity of tumor-homing phage-antibodies. *Cancer Immunol Immunother* 62(8):1397–1410. <https://doi.org/10.1007/s00262-013-1443-5>
7. Krag DN, Shukla GS, Shen GP, Pero S, Ashikaga T, Fuller S, Weaver DL, Burdette-Radoux S, Thomas C (2006) Selection of tumor-binding ligands in cancer patients with phage display libraries. *Cancer Res* 66(15):7724–7733. <https://doi.org/10.1158/0008-5472.can-05-4441>
8. Tan GH, Yusoff K, Seow HF, Tan WS (2005) Antigenicity and immunogenicity of the immunodominant region of hepatitis B surface antigen displayed on bacteriophage T7. *J Med Virol* 77(4):475–480. <https://doi.org/10.1002/jmv.20479>
9. Xu H, Bao X, Lu Y, Liu Y, Deng B, Wang Y, Xu Y, Hou J (2017) Immunogenicity of T7 bacteriophage nanoparticles displaying G-H

- loop of foot-and-mouth disease virus (FMDV). *Vet Microbiol* 205:46–52. <https://doi.org/10.1016/j.vetmic.2017.04.023>
10. March JB, Clark JR, Jepson CD (2004) Genetic immunisation against hepatitis B using whole bacteriophage λ particles. *Vaccine* 22(13):1666–1671. <https://doi.org/10.1016/j.vaccine.2003.10.047>
 11. Bartolacci C, Andreani C, Curcio C, Occhipinti S, Massaccesi L, Giovarelli M, Galeazzi R, Iezzi M, Tilio M, Gambini V, Wang J, Marchini C, Amici A (2018) Phage-based anti-HER2 vaccination can circumvent immune tolerance against breast cancer. *Cancer Immunol Res* 6(12):1486. <https://doi.org/10.1158/2326-6066.CIR-18-0179>
 12. Tao P, Mahalingam M, Zhu J, Moayeri M, Sha J, Lawrence WS, Leppla SH, Chopra AK, Rao VB (2018) A bacteriophage T4 nanoparticle-based dual vaccine against anthrax and plague. *mBio* 9(5):e01926–e01918. <https://doi.org/10.1128/mBio.01926-18>
 13. Rosenberg AH, Griffin K, Washington MT, Patel SS, Studier FW (1996) Selection, identification, and genetic analysis of random mutants in the cloned primase/helicase gene of bacteriophage T7. *J Biol Chem* 271(43):26819–26824
 14. Hashemi H, Pouyanfard S, Bandehpour M, Noroozbabaei Z, Kazemi B, Saelens X, Mokhtari-Azad T (2012) Immunization with M2e-displaying T7 bacteriophage nanoparticles protects against influenza a virus challenge. *PLoS One* 7(9):e45765. <https://doi.org/10.1371/journal.pone.0045765>
 15. Pouyanfard S, Bamdad T, Hashemi H, Bandehpour M, Kazemi B (2012) Induction of protective anti-CTL epitope responses against HER-2-positive breast cancer based on multivalent T7 phage nanoparticles. *PLoS One* 7(11):e49539. <https://doi.org/10.1371/journal.pone.0049539>
 16. Shadidi M, Sørensen D, Dybwad A, Furset G, Sioud M (2008) Mucosal vaccination with phage-displayed tumour antigens identified through proteomics-based strategy inhibits the growth and metastasis of 4T1 breast adenocarcinoma. *Int J Oncol* 32(1):241–247
 17. Liu D, Tang L, Zhou C, Tan L (2006) Immunotherapy of EGFR-positive tumor based on recombinant EGFR phage vaccine. *Chin-Ger J Clin Oncol* 5(3):189–193. <https://doi.org/10.1007/s10330-006-0474-1>
 18. Li X-H, Tang L, Liu D, Sun H-M, Zhou C-C, Tan L-S, Wang L-P, Zhang P-D, Zhang S-Q (2006) Antitumor effect of recombinant T7 phage vaccine expressing xenogenic vascular endothelial growth factor on Lewis lung cancer in mice. *Ai Zheng* 25(10):1221–1226
 19. Golde WT, Gollobin P, Rodriguez LL (2005) A rapid, simple, and humane method for submandibular bleeding of mice using a lancet. *Lab Anim* 34(9):39–43. <https://doi.org/10.1038/labani1005-39>
 20. Adriaenssens EM, Lehman SM, Vandersteegen K, Vandenheuvel D, Philippe DL, Cornelissen A, Clokie MRJ, García AJ, De Proft M, Maes M, Lavigne R (2012) CIM® monolithic anion-exchange chromatography as a useful alternative to CsCl gradient purification of bacteriophage particles. *Virology* 434(2):265–270. <https://doi.org/10.1016/j.virol.2012.09.018>
 21. Monjezi R, Tey BT, Siew CC, Tan WS (2010) Purification of bacteriophage M13 by anion exchange chromatography. *J Chromatogr B* 878(21):1855–1859. <https://doi.org/10.1016/j.jchromb.2010.05.028>



Plant-Based Systems for Vaccine Production

Mattia Santoni, Elisa Gecchele, Roberta Zampieri, and Linda Avesani

Abstract

Plant systems have been used as biofactories to produce recombinant proteins since 1983. The huge amount of data, collected so far in this framework, suggests that plants display several key advantages over existing traditional platforms when they are intended for therapeutic uses, including safety, scalability, and the speed in obtaining the final product.

Here, we describe a method that could be applied for the expression and production of a candidate subunit vaccine in *Nicotiana benthamiana* plants by transient expression, defining all the protocols starting from plant cultivation to target recombinant protein purification.

Key words Molecular farming, Transient expression, *Nicotiana benthamiana*, Downstream processing, Biofactories, Biopharmaceutical, Design-of-experiment

1 Introduction

Since the first successful transformation of plant cell cultures in 1983 [1], plants provide a viable alternative for recombinant protein production to conventional systems, mainly based on bacteria, yeast, and mammalian cells.

The term plant molecular farming was coined for such an application, and it comprises a range of diverse platforms with the potential of producing different proteins, ranging from technical enzymes to biopharmaceutical proteins and by exploiting a variety of expression technologies from stable nuclear transformation (transgenic plants) or plastid transformation (transplastomic plants) to transient expression without stable transgene integration [2]. Transient expression is achieved by the infiltration of adult wild-type plants—usually tobacco (*Nicotiana tabacum*) or its relative *Nicotiana benthamiana*—with strains of *Agrobacterium tumefaciens* carrying either a plant-expression plasmid or recombinant full or deconstructed plant viral vectors containing the appropriate transgene cassette [3].

There are significant regional differences in current regulatory guidelines covering the production of biopharmaceuticals by molecular farming using transient expression systems. The FDA recommendations have always been flexible, accommodating all whole plant systems and those based on plant organs [4]. Several companies in the USA and Canada now base their business model on GMP manufacturing by transient expression in tobacco and/or *N. benthamiana*, while in Europe there is only one facility, to our knowledge, that has been GMP certified in this framework [5, 6].

The use of transient expression systems in plants to synthesize a biopharmaceutical has peculiar advantages over other systems; for example, the use of transient expression allows production to be scaled up much more quickly than any other fermenter-based platform [7, 8]. Furthermore, specific vectors for transient expression systems, mainly those based on full or deconstructed plant viruses, mediate high expression levels of recombinant proteins [9].

The first proof-of-concept of a plant-made vaccine was the production of hepatitis B surface antigen (HBsAg) [10], that was followed by many other examples (reviewed in [11]) with a major focus on virus-like particles [12] and subunit vaccines [13]. This technology has been recently adopted by Medicago for developing a candidate vaccine for COVID-19, with Phase 2 Clinical Trials planned to initiate by November 2020 (<https://www.medicago.com/en/newsroom/medicago-signs-agreements-with-the-government-of-canada-to-supply-up-to-76-million-doses-of-its-recombinant-plant-derived-covid-19-vaccine/>) and for a seasonal influenza vaccine currently under review by Health Canada after the successful completion of the clinical trials.

Here we describe a detailed protocol of the process relying on the production of recombinant proteins by using transient expression in *N. benthamiana* leaves, starting from plant cultivation to recombinant protein purification (Fig. 1). To make the protocol broadly applicable, we consider the use of a 6× His-tag fused either at the N- or C-terminus of the candidate vaccine. The use of a tag allows also a simple preliminary evaluation of the plant-made candidate vaccine. It is important to underline that the His-tag is not allowed in the final candidate vaccine product, and it should be removed before performing clinical trials.

The downstream processing (DSP) here described, starting from plant material expressing the target recombinant protein, comprises the use of design-of-experiment to guide the set-up of the soluble protein extraction buffer, which is a crucial step in DSP. This approach could easily be transferred to any system involving multiple parameters and their interactions to be evaluated to obtain reliable data and response optimization (e.g., characterization of protein expression in plant systems, optimization of the incubation temperature and bacterial OD_{600nm} for leaf infiltration, plant age, and harvest schemes [14], or investigation of effects of extraction process variables on bioactive compound yield [15]).

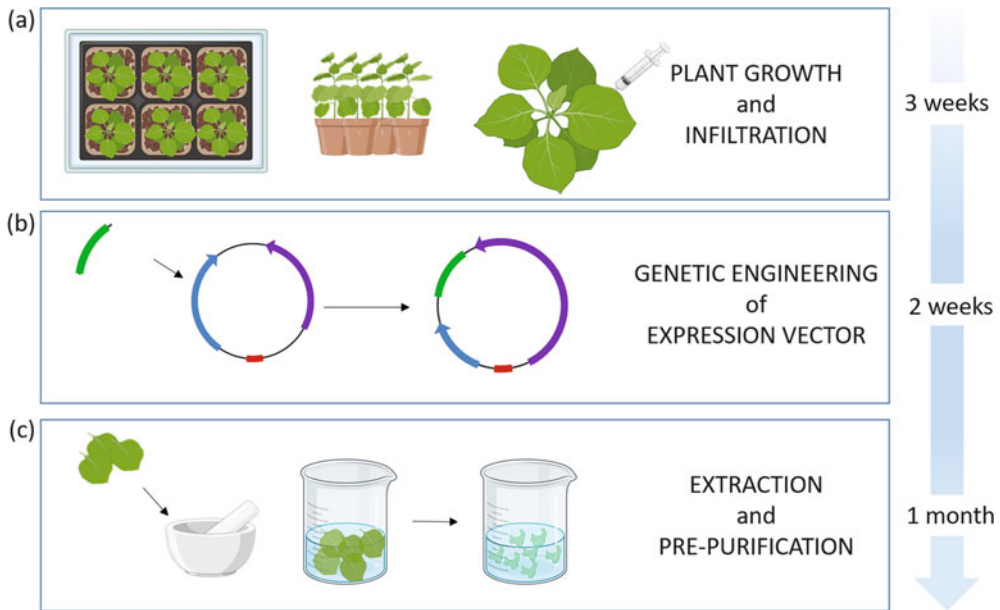


Fig. 1 Timeline of (a) plant growth and infiltration, (b) genetic engineering of plant-specific expression vector, and (c) extraction and pre-purification steps

2 Materials

2.1 Genetic Engineering of Plant Expression Vectors

1. TE buffer: 10 mM Tris-HCl, pH 7.5, 1 mM EDTA.
2. Taq Polymerase.
3. Nucleotides (dNTPs).
4. Primers: M13 forward and reverse for the entry vector (M13 forward: TGT AAA ACG ACG GCC AC and M13 reverse: CAG GAA ACA GCT ATG AC) (*see step 6* of Subheading 3.1).
5. PCR product and agarose gel purification kits (e.g., Wizard[®] SV Gel and PCR Clean-Up System).
6. Plasmid DNA extraction.
7. Plasmids: pENTR/D-TOPO (ThermoFisher), destination vectors (*see Table 1*).
8. Recombination: LR clonase II enzyme mix.
9. Shrimp Alkaline Phosphatase.
10. *Escherichia coli* TOP10 heat shock competent cells.
11. *A. tumefaciens* strains (*see Table 1*).
12. LB media (Luria-Bertani): 5 g/L yeast extract, 10 g/L Tryptone, 10 g/L NaCl, pH 7.5 [21].
13. Super Optimal broth with Catabolite repression (S.O.C) [22].
14. Glycerol.
15. Gene Pulser 0.2 cm gap (Bio-Rad).

Table 1
Frequently used combinations of *A. tumefaciens* strains and plant-specific expression vectors

Agrobacterium strain	Marker gene	Ti plasmid	Marker gene	Vector used	Marker gene	Protein expressed	Host	Yields obtained (mg/g)	References
LBA4404	rif	pAL4404	spec and strep	pEAQ-HT-DEST	kan	GFP	<i>N. benthamiana</i>	0.7-1.25	[16]
GV2260	rif	pGV2260 (pTiB6S3ΔT-DNA)	carb						
C58C1	-	Cured	-	pPHASHGW	kan	GAD67	<i>A. thaliana</i>	1.4-4.5	[17]
GV33100	-	Cured	-	-	-	-	-	-	-
A136	rif and nal	Cured	-	-	-	-	-	-	-
GV3101	rif	Cured	-	pPVXGAT (A)	kan	Bet v 1	<i>N. benthamiana</i>	0.05	[18]
GV3850	rif	pGV3850 (pTiC58Δonc. genes)	carb	-	-	-	-	-	-
GV3101:: pMP90	rif	pMP90 (pTiC58ΔT-DNA)	gent	-	-	-	-	-	-
GV3101:: pMP90RK	rif	pMP90RK (pTiC58ΔT-DNA)	gent and kan	-	-	-	-	-	-
EHA101	rif	pEHA101 (pTiBo542ΔT-DNA)	kan	-	-	-	-	-	-
EHA105	rif	pEHA105 (pTiBo542ΔT-DNA)	-	pAAmy3Dst pK7WG2	hygro spectro	mGMCSF Bet v 1	Rice cell culture <i>N. benthamiana</i>	24 mg/L 0.002	[19] [18]
AGL-1	rif, carb	pTiBo542ΔT-DNA	-	pDEST-PN-T	Amp	GFP	<i>N. tabacum</i> chloroplasts		[20]

2.2 Plants Growth

1. Universal fine soil.
2. Sand.
3. *N. benthamiana* seeds.
4. Multi-pot tray.
5. Nonwoven fabric.
6. 12 cm diameter pots.

2.3 Plants Infiltration and Recombinant Protein Expression Analysis

2.3.1 Syringe Infiltration

1. LB broth with antibiotics (depending on the vector used for transformation, *see* Table 1).
2. MMA solution: MES 10 mM pH 5.5, MgCl₂ 1 M, and Acetosyringone 100 μM.
3. 2.5 mL Needleless syringe.

2.3.2 Vacuum Infiltration

1. LB broth with antibiotics (depending on the vector used for transformation, *see* Table 1).
2. MMA solution: MES 10 mM pH 5.5, MgCl₂ 1 M, and Acetosyringone 100 μM.
3. Vacuum pump and chamber.

2.3.3 Time Course Recombinant Protein Expression Analysis

1. PBS buffer: NaCl 8 g/L, KCL 2 g/L, Na₂HPO₄ 1.44 g/L, KH₂PO₄ 0.24 g/L.
2. R sample buffer: Tris-HCl 1.5 M, SDS 3%, glycerol 15%, 2-mercaptoethanol 4%.
3. 12% acrylamide pre-cast gels: SurePage—Genscript.
4. Nitrocellulose blotting membrane: 0.45 μm.
5. Antibody: anti-His.

2.4 Extraction and Pre-purification Steps

2.4.1 Identification of the Best Extraction Buffer Composition

1. DoE software Design Expert (State-Ease, MN, USA).

2.4.2 Recombinant Protein Extraction and Clarification

1. Extraction buffer: Prepare the solutions as calculated by the DoE software, including buffer, detergent (optional), reducing agent and excipient, such as sugars, polyamines, alkylamines, or specific amino acids.
2. Protease inhibitors (Protease Inhibitor Cocktail, SIGMA).

- 2.4.3 Pre-purification**
1. Saturated ammonium sulfate solution (add 100 g ammonium sulfate to 100 mL distilled water, stir to dissolve).
- Fractional Precipitation
2. 1 M Tris-HCl, pH 8.0.
 3. Extraction buffer for first purification step.
- Desalting Procedure
1. PD-10 desalting column.
 2. Equilibration buffer: buffer of choice.
- Ion Exchange
1. DEAE-based anion exchange chromatographic resin.
 2. Equilibration buffer: binding buffer (*see Note 1*).
 3. Elution buffers prepared adding NaCl in a step gradient way from 0 to 1 M concentration.
- 2.5 Immobilized Metal Ion Affinity Chromatography (IMAC)**
1. Imidazole 1 M solution.
 2. Ascorbic acid 100 mM solution.
 3. Filter paper.
 4. Ni-NTA agarose resin.
 5. Disposable polypropylene 1 mL columns.
 6. Mortar and pestle.
 7. Liquid nitrogen.
 8. Cheese cloth.
 9. Bi-chambered gradient maker.
 10. Peristaltic pump.

3 Methods

3.1 Genetic Engineering of Expression Vectors

To assess the production, the correct folding of the protein of interest and its biological activity, it is important to perform preliminary analysis. For this purpose, a tag is added to the candidate vaccine to facilitate its detection and purification.

Different tags are available, here we describe the use of the six histidine tag (6× His) that can be fused at the C- or N-termini of the target sequence, bearing in mind that the tag and its position can affect the expression and accumulation of the protein [23].

1. Choose the protein of interest and retrieve its nucleotide and aminoacidic sequences, on common databases (e.g., NCBI Gene Bank, <https://www.ncbi.nlm.nih.gov/genbank/>). Add to the target sequence the nucleotides coding for 6× His either at the N- or at the C-terminus.
2. Choose a destination vector (*see Table 1*).

Design an appropriate nucleotide sequence for cloning the gene of interest. Codon optimize the sequence for

N. benthamiana (IDT, <https://eu.idtdna.com/CodonOpt>), to the resulting sequence add at the 5'-end of the CACC sequence necessary for TOPO directional cloning. Order the resulting sequence from companies that synthesize custom DNA strings (double strands of linear synthetic DNA).

3. To generate the entry vector, prepare the TOPO cloning mix following manufacturer's instructions (*see* **Note 2**).
4. Transform *E. coli* chemical competent cells: use 2 μL of cloning product to transform a 100 μL aliquot of TOP 10.
 - 4a. Add 2 μL of mix to the TOP 10 and incubate in ice for 15 min.
 - 4b. Heat Shock the cells at 42 °C 30 s.
 - 4c. Incubate the cells on ice for 2 min and finally resuspend them in 250 μL (*see* **Note 3**) of SOC media.
 - 4d. Recover the cells incubating them at 37 °C for 1 h in horizontal shaking.
 - 4e. Seed 50 and 200 μL of the transformation product on two LB plates added with 50 $\mu\text{g}/\text{mL}$ of Kanamycin (*see* **Note 4**).
 - 4f. Incubate at 37 °C overnight (o/n).
5. Screen Positive Clones by Colony PCR Using M13 Primers (*see* **Note 5**).
 - 5a. Prepare the PCR mix and dispense it in clean 0.2-mL tubes.
 - 5b. Pick colonies from the plate, dissolve them in the PCR mix. Use the same toothpick/tip to spread it on a fresh selective plate as a backup and, finally, in 4 mL of liquid LB with antibiotics.
 - 5c. Run the PCR cycle. A standard PCR cycle with M13 primers is:

95 °C 5 min	
95 °C 30 s	} x 35 cycles
48 °C 30 s	
72 °C 1 min/ 1 kb	
72 °C 7 min	

- 5d. Run 10 μL of the reaction on agarose gel.
- 5e. Incubate the colonies streaked plate and the liquid cultures at 37 °C o/n.
6. Extract the plasmid DNA from one of the positive colonies using plasmid mini kit extraction, following the manufacturer instructions, and perform a PCR in order to check for the presence of the insert (*see* **Note 6**).

7. Sequence the extracted plasmid with forward and reverse primers to check the presence of the insert (*see* **Note 6**).
8. Different destination vectors can be used as reported in Table 1. Here two examples of LR reactions are described:
 - 8a. When using a high transformation yields vector, for example, pK7WG2, the LR reaction can be carried out according to the manufacturer's instructions.
 - 8a1. Prepare the recombination mix in a final volume of 10 μL .
 - 8a2. Mix 100 ng of entry vector with 150 ng of destination vector (*see* **Note 7**).
 - 8a3. Thaw LR clonase mix II on ice and add 2 μL then mix briefly.
 - 8a4. Top up the volume with TE buffer to 9 μL and incubate the mix at 25 °C for 1 h (*see* **Note 8**).
 - 8a5. After the incubation, add 1 μL of proteinase K and incubate at 37 °C for 15 min.
 - 8a6. Transform TOP 10 with 5 μL of recombination product as already described in **step 5**. For pK7WG2, plate on Spectinomycin 75 $\mu\text{g}/\text{mL}$ and incubate at 37 °C o/n.
 - 8b. When using a low transformation yields vector, like the pG PVX GATEWAY(A), some additional steps should be considered to increase transformation yields:
 - 8b1. Perform a digestion to linearize the entry vector, with a single cutter restriction enzyme (for example using ApaI).
 - (i) Digest at least 1 μg of pENTR/D-TOPO.
 - (ii) Set up the digestion mix following the manufacturer instructions. Incubate for at least 1 h.
 - (iii) Add an appropriate quantity of loading die to the reaction.
 - (iv) Run the whole reaction on a 0.7% agarose gel using an aliquot of the non-digested plasmid as a negative control.
 - (v) Excise the linearized plasmid band.
 - (vi) Purify the band from the gel using a kit Wizard[®] SV Gel and PCR Clean-Up System.
 - (vii) A de-phosphorylation step should be performed here to prevent the re-circularization of the linearized plasmid; this can be done with Shrimp Alkaline Phosphatase.
 - (viii) Purify the reaction with Wizard[®] SV Gel and PCR Clean-Up System.

- 8b2. Use the linearized pENTR/D-TOPO as entry vector for the LR reaction to be performed as described above (*see Note 8*).
- 8b3. Transform TOP 10 cells using 5 μ L of the recombination product, as already described in **step 5**, in the pG PVX GAT (A) example plate on Kanamycin 50 μ g/mL.
9. Perform a colony PCR on 10 colonies with vector backbone-specific primers (*see Note 5*).
10. Extract plasmid DNA from one of the positive liquid cultures with EZNA plasmid mini kit according to **step 7**.
11. Prepare *A. tumefaciens* competent cells [24]:
 - 11a. Streak *A. tumefaciens* from a glycerol stock on a selective LB plate and incubate it at 28 °C for 48 h.
 - 11b. Pick a single colony and propagate it in 5 mL of selective LB (in Table 1 antibiotics are reported based on the *A. tumefaciens* strain used), incubate with gentle shaking at 28 °C for 48 h.
 - 11c. Pellet the 1.5 mL of liquid culture, $5000 \times g$ for 1 min at 4 °C.
 - 11d. Discard the supernatant and wash the pellet with 500 μ L of cold 10% glycerol.
 - 11e. Repeat the previous step for three times.
 - 11f. Re-suspend the pellet in 40 μ L of cold 10% glycerol.
 - 11g. Freeze the competent cells in liquid nitrogen and store them at -80 °C until usage.
12. *A. tumefaciens* transformation:
 - 12a. Dilute the destination vector at a concentration of 10 ng/ μ L.
 - 12b. Add 2 μ L of the vector to the *A. tumefaciens* competent cells and keep it on ice.
 - 12c. Transfer the 42 μ L of the transformation mix in the Gene pulser (*see Note 9*).
 - 12d. Assemble the electroporation apparatus and apply the charge which should be 2.5 kV with a time constant between 4 and 5 ms.
 - 12e. Quickly transfer the *A. tumefaciens* in a tube, add 400 μ L of S.O.C. medium (*see Note 10*).
 - 12f. Recover the cell incubating them at 28 °C for at least 1 h with gentle shaking.

12g. Plate 50 and 250 μL of the transformation mix on selective LB and incubate at 28 °C for 48 h.

13. To check the presence of the plasmid, perform a colony PCR (see **Notes 5** and **11**).
14. To confirm transformation, extract the plasmid DNA and perform a PCR and a digestion.

3.2 Plant Growth

1. Prepare the growing substrate, mixing 2/3 of universal fine soil with 1/3 of sand.
2. Fill a multi-pot tray with the growing substrate and dampen it with water.
3. Hand out one *N. benthamiana* seed per each plot and incubate tray in growth chamber at 24 °C relative humidity of 70% and 14/10 light/dark cycle.
4. Lay a nonwoven fabric on the tray to keep the humidity until the seed germination and water every 2 days to prevent the soil to shrink.
5. After a week (Fig. 2) transfer a single bud in an independent pot (see **Note 12**) previously filled with the growing substrate and water it every 2 days (see **Note 13**).

3.3 Plant Infiltration and Time-Course Recombinant Protein Expression Analysis.

3.3.1 Syringe Infiltration

1. Inoculate a single transformed *A. tumefaciens* colony in 5 mL of selective LB broth.
2. Incubate at 28 °C o/n in 180 rpm agitation.
3. Transfer 1 mL of the grown culture in 50 mL of selective broth and incubate o/n at 28 °C in 180 rpm agitation.
4. Precipitate the bacterial cells by centrifugation at 3000 $\times g$ for 20 min.
5. Resuspend the pellet in MMA solution until an OD₆₀₀ of 0.8 and incubate 2–3 h at room temperature (RT).
6. Choose and label leaves (three per plant) (see **Note 14**) to be infiltrated.

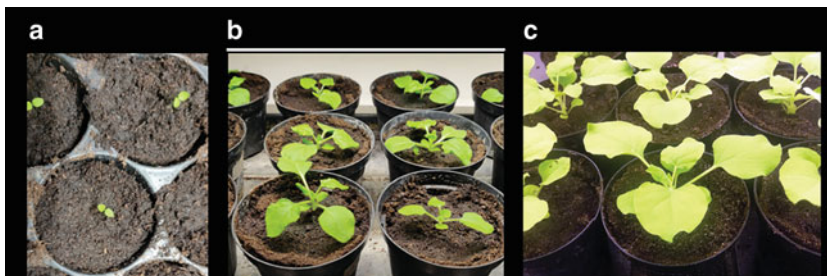


Fig. 2 *Nicotiana benthamiana* plants 1-week (a), 3-weeks (b), and 4-week old (c)

7. Take up resuspended *A. tumefaciens* sample in a 1- or 5-mL syringe (no needle).
8. Place the tip of syringe against the underside of the selected leaf and press down gently on the plunger supporting the upper side of the leaf with a finger until the liquid diffuses throughout the leaf (*see Note 15*).
9. Harvest infiltrated leaves of three plants per day (biological replicates) starting from 3 to 14 days post infiltration (dpi).

3.3.2 Vacuum Infiltration

1. Inoculate a single transformed *A. tumefaciens* colony in 250 mL of selective LB broth.
2. Incubate at 28 °C o/n in 180 rpm agitation.
3. Precipitate the bacterial cells by centrifugation at $4500 \times g$ for 20 min.
4. Resuspend the pellet in 1 L MMA solution until an OD₆₀₀ of 0.8 and incubate 2–3 h at RT.
5. Vacuum infiltrate the aerial parts of *N. benthamiana* by dipping the plants in the infiltration suspension in a vacuum chamber applying vacuum for 3 min with a pressure of 90 mBar.
6. Release the vacuum for 45 s.
7. Harvest infiltrated leaves of three plants per day (a biological replicate) starting from 3 to 14 dpi.

3.3.3 Time-Course Recombinant Protein Expression Analysis

1. Freeze the harvested leaves and homogenize 100 mg of frozen plant material with 3 volumes (w/v) PBS buffer (*see Note 16*).
2. Clarify by centrifugation at $10,000 \times g$ for 10 min.
3. Add 5 μ L of $3 \times R$ sample buffer to 10 μ L of supernatant and incubate in a heat block for 10 min at 100 °C.
4. Load the sample onto 12% acrylamide gel and run samples at 200 V for 1 h.
5. Transfer the proteins to a nitrocellulose blotting membrane and analyze them by Western blot using a specific antibody to identify the day of highest expression (*see Note 17*).

3.4 Total Soluble Protein Extraction and Recombinant Protein Detection

3.4.1 Identification of the Best Extraction Buffer Composition

This protocol discusses a design-of-experiment (DoE) approach for the definition of the best extraction buffer composition to enhance recombinant protein recovery from *N. benthamiana* tissue.

1. Define responses suitable for the evaluation of the outcomes of the study. Here we define as a case-of-study example to produce an antigen in *N. benthamiana*, these responses: recombinant protein yield (μ g of recombinant protein/g of leaf fresh weight, LFW) and aggregate prevention.

2. Select the relevant components (factors) for the screening study: buffer concentration, pH value, detergent type and its concentration, reducing agent type and its concentration (*see Notes 18–22*).
3. Select ranges within which the factors will be varied during the DoE investigation: 50–200 mM concentration for buffer substance, from 4.0 to 8.0 pH value, maximum 5 or 2.5% V/V concentration for mild detergent agents (Tween-20 or Triton X-100, respectively), maximum 10 or 20 mM concentration for reducing agents (DTT or Na₂S₂O₅, respectively).
4. Set up a RSM (response surface method) for a DoE approach to be used for building predictive models.
5. Test all the 50 different solutions calculated by the DoE predictive model for the recombinant protein extraction maximization in *N. benthamiana* leaves (*see Subheading 3.4.2*).
6. Perform a recombinant protein analyses, considering the parameters set in 1 (*see Note 23*).
7. Transfer the analyzed response data (here the recombinant protein extraction yield and presence/absence of protein aggregate/s) into the design-of-experiment. Make sure that response data are correctly assigned to the corresponding factor settings.
8. Investigate the model and the included factors by analyzing the responses obtained from the extraction experiments to obtain information about factors that are important for the system under investigation.
9. Model predictions for maximal extraction efficiency are verified in five additional runs for design points that are of major interest.

3.4.2 Recombinant Protein Detection

1. Collect agroinfiltrated leaves at the maximum expression dpi, depending on the recombinant protein accumulation and freeze them in liquid nitrogen. Store plant tissue at –80 °C.
2. Grind the frozen plant material to fine powder in liquid nitrogen using mortar and pestle. Transfer the powder into a new tube.
3. Add three volumes of an appropriate extraction buffer (*see Note 24*), supplemented with protease inhibitors to block protease degradation during extraction and following procedures.
4. Homogenize the mixture by vortexing for 1 min.
5. Centrifuge the mixture (10,000 × *g*) at 4 °C (*see Note 25*).
6. Collect the clarified supernatant in a clean tube (*see Note 26*) and store it at –20 °C. The pellet is discarded.

3.5 Pre-purification

Additional specific sample preparation steps may be evaluated to remove contaminants, from the clarified *N. benthamiana* extract, that can interfere with subsequent purification. Various methods are available as pre-purification treatments, such as fractional precipitation (*see* Subheading 3.5.1), desalting (*see* Subheading 3.5.2), or ion exchange (*see* Subheading 3.5.3).

3.5.1 Fractional Precipitation

Precipitation techniques separate fractions by the principle of differential solubility and can be applied to remove gross impurities. Here the protocol for the most common precipitation method using ammonium sulfate is reported (*see* **Note 27**).

1. Add 1 part 1 M Tris-HCl, pH 8.0–10 parts sample volume to maintain the pH of the clarified extract.
2. Stir gently. Add ammonium sulfate solution, drop by drop. Add up to 50% saturation (*see* **Note 28**). Stir for 1 h.
3. Centrifuge 20 min at $10,000 \times g$.
4. Remove supernatant. Wash the pellet twice by resuspension in an equal volume of ammonium sulfate solution of the same concentration (i.e., a solution that will not resuspend the precipitated protein or cause further precipitation). Centrifuge again (repeat **step 3**).
5. Dissolve the pellet in a small volume of the buffer to be used for the next step.
6. Ammonium sulfate could be removed during clarification/buffer exchange steps using desalting columns (*see* **Note 29**).
7. Check the presence of the recombinant protein performing a Western blot on the resuspended pellets.

3.5.2 Desalting Procedure

The desalting procedure is a simple and very fast method to remove low molecular weight contaminants and to change a buffer.

1. Cut off bottom tip, remove top cap, and pour off excess liquid.
2. Equilibrate the column with approximately 25 mL of buffer. Discard the flow-through (use the plastic tray to collect flow-through). To ensure optimal results, it is critical to equilibrate the column with a total of 25 mL of equilibration buffer to completely remove the storage solution.
3. Add sample to a final volume of 2.5 mL. If the sample is less than 2.5 mL, add buffer until the total volume of 2.5 mL is achieved. Discard the flow-through.
4. Elute with 3.5 mL of buffer and collect the flow-through.
5. Check the presence of the recombinant protein performing a Western blot on the collected fractions: loaded extract, flow-through, and eluted fraction.

3.5.3 Ion Exchange Chromatography

Ion exchange chromatography can be used as a pre-purification method for removing contaminants. Different ion exchanger and ion exchange ligand are suitable for this application. Here the protocol for a DEAE-based anion exchange chromatography performing the elution by increasing salt concentration is reported.

1. Equilibrate the resin with approximately five column volumes with equilibration buffer (*see Note 30*).
2. Add the clarified extract (*see Note 31*) and collect flow-through sample.
3. Wash the column with at least five volumes of extraction buffer. Collect the flow-through.
4. Perform protein elution using the most common salt, NaCl, in a step gradient way from 0 to 1 M concentration. Collect all the eluted fractions.
5. Check the presence of the recombinant protein by performing a Western blot on the collected fractions: loaded extract, flow-through, wash, and eluted fractions.

3.6 Immobilized Metal Ion Affinity Chromatography (IMAC)

The protocol is intended for the use of gravity disposable columns; however, the same protocol can be applied to other system that relies on a FLPC system (e.g., AKTA start). Bear in mind that each protein has its own characteristics and consequently will need an optimized purification protocol. For example, the imidazole concentration described in this section is a standard example: it could be modified after experimental evidence of the pattern of target protein elution.

1. Prepare a solution of protein extract from *N. benthamiana* leaves as described in Subheading 3.4.1.
2. Add to the supernatant NaCl and imidazole at a final concentration of 500 and 5 mM, respectively. Adjust the pH of the solution to 8.
3. Incubate for 1 h on ice by gentle shaking.
4. Clarify the solution by centrifugation at $30,000 \times g$ for 30 min at 4 °C (*see Note 32*).
5. Column preparation:
 - 5a. Set up the stand, attach the disposable column to the stand, and check if the screw cap is closed properly.
 - 5b. Vortex briefly the resin bottle to resuspend the 50% Ni-NTA solution.
 - 5c. To pack the resin, add about two times the final column volume (e.g., for a 1 mL column volume, add 2 mL of resin).
 - 5d. Remove the screw cap.

- 5e. Allow the resin to settle and discard the eluate.
- 5f. To equilibrate the column, use the extraction buffer adding NaCl and imidazole at a final concentration of 500 and 5 mM, respectively. Adjust the pH to 8. Use about 5–10 column volumes (*see Note 33*).
6. Load the extract on the column and collect the flow-through for further analysis (*see Notes 34 and 35*). Allow the extract to flow completely.
7. Prepare the wash buffer using the same extraction buffer and adding NaCl at a final concentration of 500 mM and imidazole at a final concentration of 10 mM, pH 8 (*see Note 36*).
8. Wash the column with at least 20 column volumes of washing buffer, until the flow-through OD₂₈₀ reaches 0. Keep the eluted wash solution for further analysis (*see Note 36*).
9. Standard elution protocol: Use this protocol for preliminary analysis. Keep in mind that the elution buffer is always the same, the only variable that changes is the imidazole concentration.
 - 9a. Prepare the elution buffer raising the imidazole concentration to 50 mM. Perform the first elution adding five column volumes (*see Notes 36 and 37*) and allow the elution buffer to flow completely out of the disposable column.
 - 9b. Collect the eluted solution in a clean tube.
 - 9c. Prepare the elution buffers raising the imidazole concentration to 100, 150, and 200 mM and perform the other elution steps repeating **9a** and **9b**.
 - 9d. Check the presence of the His-tag protein performing a Western blot on the fractions collected: loaded extract, flow-through, wash, and purification elution.
 - 9e. Check the purity of the elution performing an SDS-PAGE with silver staining [25].
10. If the elution step optimization (*see Note 37*) is not enough to obtain a purified protein, the elution gradient protocol can be exploited. Like in the previous steps, a protocol based on a gravity flow column is described, but the same protocol can be used in an FPLC system.
 - 10a. Prepare the low imidazole concentration buffer (1 × PBS 500 mM, NaCl 20 mM, imidazole pH 8) and a high imidazole concentration buffer (1 × PBS 500 mM, NaCl 200 mM, imidazole pH 8).
 - 10b. Set up the gradient maker:

- 10b1. Close the nozzle between the two tanks.
- 10b2. Fill the tanks with the same volume of elution buffer, low imidazole concentration in the wired one, and high imidazole concentration in the close one.
- 10b3. Connect the low imidazole concentration containing tank to the peristaltic pump.
- 10c. Follow the protocol described above for the column preparation until **step 8**.
- 10d. Once the load is completely bound to the resin, it is possible to start the gradient elution.
 - 10d1. Set the peristaltic pump to a 0.2 mL/min flow and check the absence of air bubbles in the tubes.
 - 10d2. Connect the pump tube to the column.
 - 10d3. Open the nozzle between the two tanks.
 - 10d4. Start the elution (*see Note 37*).
 - 10d5. Collect about 1.5 mL fractions in clean tubes.
- 10e. Check the presence of the His-tag protein performing a Western blot on the collected fractions: loaded extract, flow-through, wash, and purification elution.
- 10f. Check the purity of the eluted recombinant protein performing an SDS-PAGE with silver staining.

4 Notes

1. The binding buffer must contain the same ion that is present in the ion exchanger.
2. To optimize the cloning, different molar ratio Insert: pENTR/D-TOPO vector should be tested, ranging from 0.5:1 to 3:1.
3. It is possible to raise or lower the SOC volume leading to a more diluted or a more concentrated transformation product and consequently resulting in a lower or higher number of colonies.
4. Plate two or three different quantities of transformation product (e.g., 50, 100, and 200 μ L).
5. Picking the colonies directly from plates can lead to false-positive screening. Pick the colony and set up a liquid culture in selective LB, incubate o/n at 37 °C and perform a PCR using 1 μ L of the liquid culture as a template. Plasmid DNA can be directly extracted from liquid cultures of PCR-positive colonies.

6. Design different primers to cover the insert flanking region, on the vector backbone and the insert as well.
7. To increase the efficiency of the protocol:
 - (a) Change the molar ratio between entry and destination vector, from 1:2 to 1:20. Molar ratio can be calculated as the moles of the entry vector divided by the moles of the destination vector.
 - (b) Sometimes a high background given by the entry vector can be experienced. To reduce it, try the LR reaction with a PCR product from the pENTR.
8. To increase the yield of positive colonies perform the LR reaction o/n.
9. Cuvette should be cold and dry: put it at $-20\text{ }^{\circ}\text{C}$ for at least 1 h before the transformation.
10. Directly add the SOC in the cuvette and transfer the product in a new tube.
11. The template is prepared picking a colony and dissolving it in $10\text{ }\mu\text{L}$ of sterile water and incubate it at $95\text{ }^{\circ}\text{C}$ for 10 min, in order to break the cell membrane of *A. tumefaciens* $5\text{ }\mu\text{L}$ are enough as a template to perform the PCR.
12. The pot diameter is 12 cm.
13. A fertilizer (N/P/K 15/15/15) can be used on 2-week-old plants to improve the plant growth.
14. The selected leaves should be the first three leaves from the apical meristem excluding the cotyledons.
15. The agrobacterium suspension should fill completely mesophyll air spaces of the leaf; then, if necessary, repeat **step 8** in more spots of the leaf.
16. If the subcellular localization of the target protein is not cytosolic add a detergent and reducing agent to the PBS buffer.
17. Use anti-His antibody if the protein has a His-tag otherwise use a protein-specific antibody.
18. The buffer substance should have a $\text{p}K_{\text{a}}$ value as close as possible to the selected pH, to give maximum buffer capacity. A typical concentration of buffer substance is 20–200 mM.
19. The pH value should be selected so that it matches the pH optimum of the target protein. The solubility of a protein is often lowest at its pI [26]. To obtain good solubility of the target protein, select a pH that is not near the pI.
20. Detergents are used in membrane protein purification but can also be applied to decrease aggregation or adsorption for water-soluble proteins. The hydrophobic interactions can be reduced by the addition of moderate concentrations of mild

detergents (e.g., non-ionic Tween-20 or Triton X-100) that interact with hydrophobic regions on the target protein and other sample components.

21. Reducing agents are added to the buffer to keep the environment in a reduced state, thus minimizing interactions between proteins and phenolic compounds thereby preventing oxidation that may alter the target protein structure [27].
22. The aggregate formation of some proteins can be prevented by using excipients [28, 29] such as sugars [30–32], polyamines or alkylamines [33], and specific amino acids [34].
23. The recombinant protein concentration can be estimated by densitometric evaluation of target protein band in SDS-PAGE. This type of analysis allows also to estimate the presence of possible target protein aggregates and their quantity respect to the monomeric form.
24. The selected ratio of plant tissue weight (g) to buffer volume (mL) is 1:3.
25. Centrifugation is the most common clarification method for extracts on a laboratory scale. It removes most particulate matter and cell debris, but depending on source and extraction procedure, there may be various amounts of particles that cannot be sedimented or that float on top.
26. If the sample is still not clear after centrifugation, use a filter as clarification step.
27. Fractional precipitation can be applied using different precipitation agents, such as dextran sulfate, polyvinylpyrrolidone (PVPP), polyethylene glycol (PEG), acetone, etc. Sometimes thermal or pH precipitation can be performed.
28. The percentage saturation can be adjusted either to precipitate a target molecule or to precipitate contaminants.
29. It may be practical to use HIC (hydrophobic interaction chromatography) as capture step after an initial ammonium sulfate precipitation, as the sample contains a high salt concentration and can be applied directly to the HIC column.
30. Before starting a run, make sure that the medium has reached equilibrium. This is done by loading equilibration buffer through the column until the pH of the effluent is the same as that of the in-going start buffer.
31. The ratio between clarified extract volume and resin volume must be optimized.
32. If the insoluble material does not pellet during centrifugation and remains in suspension, it is possible to remove it by passing the supernatant through cheesecloth.

33. The column should be considered equilibrated when the pH of the flow-through reaches the pH of the equilibrating buffer.
34. Normally the first column volume of every step that flows through belongs to the preceding fraction (e.g., the first column volume of the load goes in the waste, the first column volume of the wash goes in the flow-through, the first column volume of the elution goes in the wash, etc.).
35. In every purification step take an aliquot to keep track of the protein of interest.
36. If the protein needs a more selective environment, it is possible to raise the concentration of imidazole in the wash buffer to 20 mM.
37. Sometimes protein can co-elute in the same fraction: changing the imidazole concentration or raising the number of elutions can overcome this problem. If not, the protocol can be performed eluting the protein with an imidazole gradient. The imidazole gradient can be generated with a gradient maker or with an FLPC machine.

Acknowledgments

This work was supported by the Pharma-Factory project (number 774078) in the framework of the call H2020-BB-2017-1.

References

1. Fraley RT, Rogers SG, Horsch RB et al (1983) Expression of bacterial genes in plant cells. *Proc Natl Acad Sci* 80:4803–4807. <https://doi.org/10.1073/pnas.80.15.4803>
2. Fischer R, Buyel JF (2020) Molecular farming—the slope of enlightenment. *Biotechnol Adv* 40:107519. <https://doi.org/10.1016/j.biotechadv.2020.107519>
3. McDonald KA, Holtz RB (2020) From farm to finger prick—a perspective on how plants can help in the fight against COVID-19. *Front Bioeng Biotechnol* 8:782. <https://doi.org/10.3389/fbioe.2020.00782>
4. FDA (2002) Guidance for industry: drugs, biologics, and medical devices derived from bioengineered plants for use in humans and animals [draft guidance]. United States Food and Drug Administration, Rockville
5. Tremblay R, Wang D, Jevnikar AM, Ma S (2010) Tobacco, a highly efficient green bioreactor for production of therapeutic proteins. *Biotechnol Adv* 28:214–221. <https://doi.org/10.1016/j.biotechadv.2009.11.008>
6. Whaley KJ, Hiatt A, Zeitlin L (2011) Emerging antibody products and Nicotiana manufacturing. *Hum Vaccin* 7:349–356. <https://doi.org/10.4161/hv.7.3.14266>
7. Hiatt A, Pauly M, Whaley K et al (2015) The emergence of antibody therapies for Ebola. *Hum Antibodies* 23:49–56. <https://doi.org/10.3233/HAB-150284>
8. Holtz BR, Berquist BR, Bennett LD et al (2015) Commercial-scale biotherapeutics manufacturing facility for plant-made pharmaceuticals. *Plant Biotechnol J* 13:1180–1190. <https://doi.org/10.1111/pbi.12469>
9. Hefferon K (2014) Plant virus expression vector development: new perspectives. *BioMed Res Int* 2014:785382. <https://www.hindawi.com/journals/bmri/2014/785382/>. Accessed 29 Oct 2020
10. Mason HS, Lam DM, Arntzen CJ (1992) Expression of hepatitis B surface antigen in transgenic plants. *Proc Natl Acad Sci U S A* 89:11745–11749. <https://doi.org/10.1073/pnas.89.24.11745>

11. Rybicki EP (2014) Plant-based vaccines against viruses. *Virology* 11:205. <https://doi.org/10.1186/s12985-014-0205-0>
12. D'Aoust M-A, Lavoie P-O, Couture MM-J et al (2008) Influenza virus-like particles produced by transient expression in *Nicotiana benthamiana* induce a protective immune response against a lethal viral challenge in mice. *Plant Biotechnol J* 6:930–940. <https://doi.org/10.1111/j.1467-7652.2008.00384.x>
13. Mbewana S, Mortimer E, Pêra FFPG et al (2015) Production of H5N1 influenza virus matrix protein 2 ectodomain protein bodies in tobacco plants and in insect cells as a candidate universal influenza vaccine. *Front Bioeng Biotechnol* 3:197. <https://doi.org/10.3389/fbioe.2015.00197>
14. Buyel JF, Fischer R (2014) Characterization of complex systems using the design of experiments approach: transient protein expression in tobacco as a case study. *J Vis Exp* (83): e51216. <https://doi.org/10.3791/51216>
15. Kadam SU, Tiwari BK, O'Donnell CP (2015) Extraction, structure and biofunctional activities of laminarin from brown algae. *Int J Food Sci Technol* 50:24–31. <https://doi.org/10.1111/ijfs.12692>
16. Sainsbury F, Thuenemann EC, Lomonosoff GP (2009) pEAQ: versatile expression vectors for easy and quick transient expression of heterologous proteins in plants. *Plant Biotechnol J* 7:682–693. <https://doi.org/10.1111/j.1467-7652.2009.00434.x>
17. Morandini F, Avesani L, Bortesi L et al (2011) Non-food/feed seeds as biofactories for the high-yield production of recombinant pharmaceuticals. *Plant Biotechnol J* 9:911–921. <https://doi.org/10.1111/j.1467-7652.2011.00605.x>
18. Santoni M, Ciardiello MA, Zampieri R et al (2019) Plant-made Bet v 1 for molecular diagnosis. *Front Plant Sci* 10:1273. <https://doi.org/10.3389/fpls.2019.01273>
19. Liu Y-K, Huang L-F, Ho S-L et al (2012) Production of mouse granulocyte-macrophage colony-stimulating factor by gateway technology and transgenic rice cell culture. *Biotechnol Bioeng* 109:1239–1247. <https://doi.org/10.1002/bit.24394>
20. Gottschamel J, Waheed MT, Clarke JL, Lössl AG (2013) A novel chloroplast transformation vector compatible with the Gateway® recombination cloning technology. *Transgenic Res* 22:1273–1278. <https://doi.org/10.1007/s11248-013-9726-3>
21. Bertani G (1951) Studies on lysogenesis. I The mode of phage liberation by lysogenic *Escherichia coli*. *J Bacteriol* 62:293–300. <https://doi.org/10.1128/JB.62.3.293-300.1951>
22. Hanahan D (1983) Studies on transformation of *Escherichia coli* with plasmids. *J Mol Biol* 166:557–580. [https://doi.org/10.1016/S0022-2836\(83\)80284-8](https://doi.org/10.1016/S0022-2836(83)80284-8)
23. Pinnola A, Ghin L, Gecchele E et al (2015) Heterologous expression of moss light-harvesting complex stress-related 1 (LHCSR1), the chlorophyll a-xanthophyll pigment-protein complex catalyzing non-photochemical quenching, in *Nicotiana sp.* *J Biol Chem* 290:24340–24354. <https://doi.org/10.1074/jbc.M115.668798>
24. Kámán-Tóth E, Pogány M, Dankó T et al (2018) A simplified and efficient *Agrobacterium tumefaciens* electroporation method. *3 Biotech* 8:148. <https://doi.org/10.1007/s13205-018-1171-9>
25. Mortz E, Krogh TN, Vorum H, Görg A (2001) Improved silver staining protocols for high sensitivity protein identification using matrix-assisted laser desorption/ionization-time of flight analysis. *Proteomics* 1:1359–1363. [https://doi.org/10.1002/1615-9861\(200111\)1:11<1359::AID-PROT1359>3.0.CO;2-Q](https://doi.org/10.1002/1615-9861(200111)1:11<1359::AID-PROT1359>3.0.CO;2-Q)
26. Balasubramaniam D, Wilkinson C, Van Cott K, Zhang C (2003) Tobacco protein separation by aqueous two-phase extraction. *J Chromatogr A* 989:119–129. [https://doi.org/10.1016/s0021-9673\(02\)01900-3](https://doi.org/10.1016/s0021-9673(02)01900-3)
27. Holler C, Zhang C (2008) Purification of an acidic recombinant protein from transgenic tobacco. *Biotechnol Bioeng* 99:902–909. <https://doi.org/10.1002/bit.21638>
28. Wang W (2000) Lyophilization and development of solid protein pharmaceuticals. *Int J Pharm* 203:1–60. [https://doi.org/10.1016/s0378-5173\(00\)00423-3](https://doi.org/10.1016/s0378-5173(00)00423-3)
29. Lerbret A, Bordat P, Affouard F et al (2007) How do trehalose, maltose, and sucrose influence some structural and dynamical properties of lysozyme? Insight from molecular dynamics simulations. *J Phys Chem B* 111:9410–9420. <https://doi.org/10.1021/jp071946z>
30. Arora A, Ha C, Park CB (2004) Inhibition of insulin amyloid formation by small stress molecules. *FEBS Lett* 564:121–125. [https://doi.org/10.1016/S0014-5793\(04\)00326-6](https://doi.org/10.1016/S0014-5793(04)00326-6)
31. Liu R, Barkhordarian H, Emadi S et al (2005) Trehalose differentially inhibits aggregation and neurotoxicity of beta-amyloid 40 and 42. *Neurobiol Dis* 20:74–81. <https://doi.org/10.1016/j.nbd.2005.02.003>

32. Gecchele E, Schillberg S, Merlin M et al (2014) A downstream process allowing the efficient isolation of a recombinant amphiphilic protein from tobacco leaves. *J Chromatogr B Analyt Technol Biomed Life Sci* 960C:34–42. <https://doi.org/10.1016/j.jchromb.2014.04.004>
33. Yasui K, Uegaki M, Shiraki K, Ishimizu T (2010) Enhanced solubilization of membrane proteins by alkylamines and polyamines. *Protein Sci* 19:486–493. <https://doi.org/10.1002/pro.326>
34. Arakawa T, Prestrelski SJ, Kenney WC, Carpenter JF (2001) Factors affecting short-term and long-term stabilities of proteins. *Adv Drug Deliv Rev* 46:307–326. [https://doi.org/10.1016/s0169-409x\(00\)00144-7](https://doi.org/10.1016/s0169-409x(00)00144-7)



Production of a Hepatitis E Vaccine Candidate Using the *Pichia pastoris* Expression System

Jyoti Gupta, Amit Kumar, and Milan Surjit

Abstract

Hepatitis E virus (HEV) is associated with acute hepatitis disease, which may lead to chronic disease in immunocompromised individuals. The disease is particularly severe among pregnant women (20–30% mortality). No vaccine is available to combat the HEV except Hecolin, which is available only in China. Virus-like particle (VLP) generated from the capsid protein (ORF2) of HEV is known to be a potent vaccine antigen against HEV. Hecolin consists of 368–606 amino acid (aa) region of the capsid protein of HEV, which forms a VLP. It is expressed and purified from the inclusion bodies of *E. coli*. Here, we describe a method to express the 112–608aa region of the capsid protein (ORF2) of genotype-1 HEV in *Pichia pastoris* (*P. pastoris*) and purify VLPs from the culture medium. 112–608aa ORF2 VLPs are secreted into the culture medium in a methanol inducible manner. The purified VLPs are glycosylated and induce robust immune response in Balb/c mice. Further, 112–608aa ORF2 VLPs are bigger than the 368–606 VLP present in Hecolin, which may help them in inducing a superior immune response. *P. pastoris* offers a robust and economical heterologous expression system to produce large quantities of glycosylated 112–608aa ORF2 VLP, which appears to be a promising vaccine candidate against the HEV.

Key words Hepatitis E virus, Virus-like particle, Open reading frame 2, *Pichia pastoris*

1 Introduction

1.1 Hepatitis E Virus

Hepatitis E virus (HEV) is a small, non-enveloped, single-stranded, positive-sense RNA virus with a genome size of approximately 7.2 kb [1]. HEV is a predominant cause of acute icteric viral hepatitis and responsible for large outbreaks in developing as well as developed countries [2, 3]. The viral infection is usually self-limiting but can lead to chronic hepatitis in immunocompromised and organ transplant or chemotherapy recipients [4]. The elderly people, pregnant women, and individuals with liver disease have been reported to have lethal cases of acute viral hepatitis [5, 6]. This virus is not only a prime cause of hepatitis but also express the extrahepatic manifestations, such as kidney failure and neurological

abnormalities [7]. According to WHO report, HEV infection burden is distributed worldwide, and there are around 20 million cases with approximately 3.3 million symptomatic cases every year [8]. In pregnant women, HEV infection has a poor prognosis, mainly in the third trimester, that lead to a mortality rate up to 30% [9–11]. HEV is mainly transmitted through the fecal–oral route (infection by drinking contaminated water), zoonotic route (infection by consumption of raw or undercooked meat), and ingestion of infected dairy products including close contact with infected animals [12]. Additional routes include blood transfusion and organ transplantation processes [13, 14]. There are eight genotypes (genotype 1 to genotype 8) of HEV reported until now. Though different genotypes of HEV demonstrate heterogeneous nature, they share single serotype, which make sense for the development of a monovalent HEV vaccine [15].

The HEV genome consists of three open reading frames (ORFs). ORF1 encodes a nonstructural multiprotein, consisting of seven different domains, such as methyltransferase (Met), Y domain (Y), papain-like cysteine protease (PCP), V domain (V), X domain (X), helicase (Hel), and RNA-dependent RNA polymerase (RdRp). ORF1 is followed by ORF2, which encodes the capsid protein; and ORF3, which overlaps with the ORF2 and encodes a phosphoprotein that plays an important role in virus release and participate in multiple signal transduction processes [1]. Genotype 1-HEV (g1-HEV) has an additional ORF4 that is expressed under endoplasmic reticulum (ER) stress and promotes the virus replication [16, 17]. ORF2 protein consists of 660 amino acids (aa) and early studies reveal that the N-terminal 111 residues of ORF2 protein are likely to be involved in RNA encapsidation and 112–608aa has ability to self-assemble into virus-like particle (VLP) [18, 19]. ORF2 protein has three functional domains: shell (S), middle (M), and protruding (P) with three N-linked glycosylation sites [20, 21]. Schematic of HEV genome and ORF2 protein is shown in Fig. 1. The 112–608aa region retains the immunodominant epitopes including neutralization epitope that shows protective efficacy in primates against HEV infection. Thus the complete and truncated capsid proteins are considered as vaccine candidate against HEV infection in humans [22–24].

1.2 VLP-Based Vaccine

VLPs consist of subunit viral capsid proteins that assemble into enclosed core–shell morphology. These subunits oligomerize into highly ordered structures which have been shown to be highly immunogenic, especially in relation to their corresponding non-oligomeric proteins [25, 26]. The self-assembled VLPs without being infectious agent allow the display of conformational epitopes similar to the intrinsic virus and are capable of stimulating innate immune response [27]. VLPs maintain the repetitive antigen display and are considered safer as potential vaccine candidates

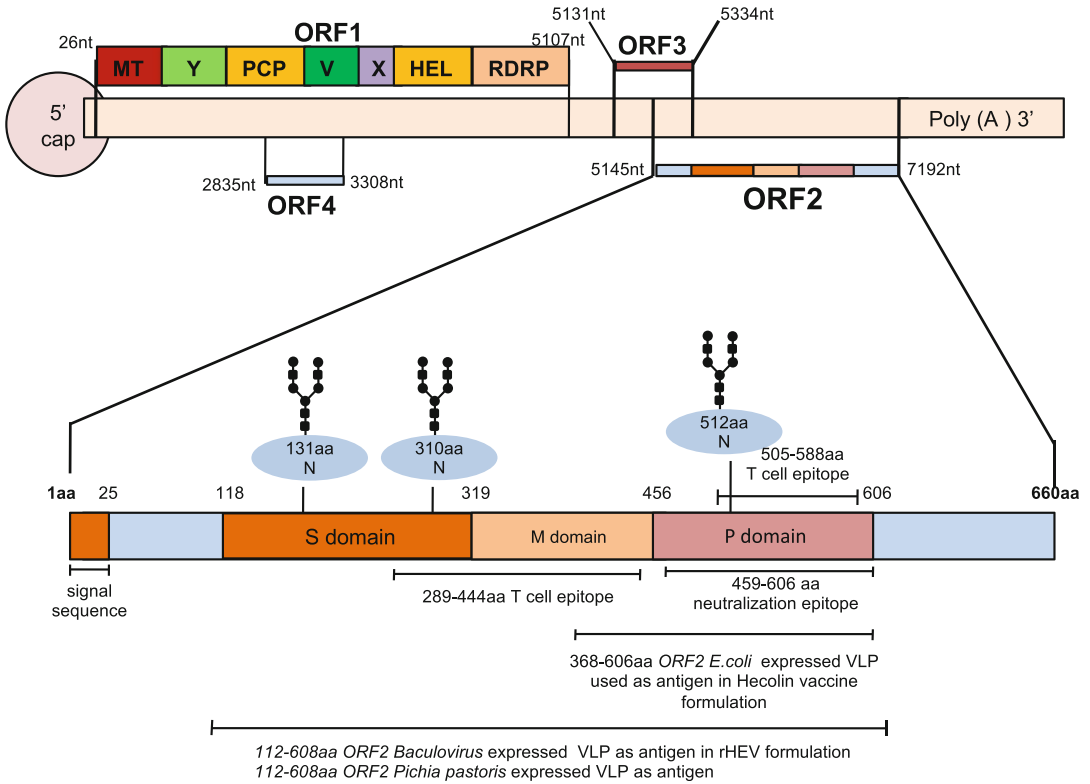


Fig. 1 Genome organization of genotype 1 hepatitis E virus and schematic representation of ORF2 protein.

compared to traditional live, attenuated, or inactivated viruses since they do not contain a genome. Advancement in expression technology has enabled production of the VLPs for more than 30 different pathogens infecting humans and animals. The success of this approach is well illustrated by the worldwide commercial availability of the vaccines against the hepatitis B virus and human papillomavirus, named as Engerix[®] (hepatitis B virus, GlaxoSmithKline), Recombivax HB[®] (hepatitis B virus, Merck), and Cervarix[®] (human papillomavirus, GlaxoSmithKline), Gardasil[®] (human papillomavirus, Merck) [28, 29]. The licensed HEV vaccine available in China is also a VLP-based vaccine (Hecolin, Xiamen Innovax Biotech).

1.3 Pichia pastoris (P. pastoris) Expression System

Out of hundreds of yeast species, *Saccharomyces cerevisiae* (*S. cerevisiae*) and *Pichia pastoris* (*P. pastoris*) are commonly used hosts for the production of heterologous proteins [30–32]. Although many heterologous proteins have been expressed in *S. cerevisiae*, low yield and hyperglycosylation of proteins limit the use of *S. cerevisiae* as a suitable host. *P. pastoris*, on the other hand, shows high growth rate, the ease of genetic manipulation, and high yield of heterologous proteins and permits mammalian

cell like glycosylation to some extent. Therefore, it is possible to produce high quantity of soluble, correctly folded, and functional recombinant protein in *P. pastoris* [33]. A number of pathogen-encoded proteins purified using *Pichia* expression system are summarized in Table 1.

P. pastoris is a methylotrophic yeast which is capable of metabolizing methanol as its sole carbon source. The first step in the metabolism of methanol is the oxidation of methanol to formaldehyde using molecular oxygen by the enzyme alcohol oxidase. Alcohol oxidase has a poor affinity for O₂, and *P. pastoris* compensates by generating large amounts of the enzyme. The promoter (P_{AOX}) regulating the production of alcohol oxidase is used to drive heterologous protein expression in *Pichia* expression system [52, 53]. *P. pastoris* has two genes to encode alcohol oxidase: *AOX1* and *AOX2*, the expression of both genes is regulated by the availability of methanol. The expression of the *AOX1* gene is tightly regulated and induced by methanol to very high levels, while low level of methanol promotes the *AOX2* expression. There are three phenotypes for *P. pastoris*, namely Mut⁺ (methanol utilization wide-type), Mut^s (methanol utilization slow), and Mut⁻ (methanol utilization deleted). Mut⁺ strains containing intact and active both *AOX* genes are characterized by a higher growth rate on methanol than Mut^s strains composed of variants lacking *AOX1* gene and Mut⁻ strains are unable to grow on methanol as the sole carbon source due to the knock-out of both *AOX* genes [52].

All *P. pastoris* expression strains are derived from the wild-type strain NRRL-Y11430 (Northern Regional Research Laboratories, Peoria, Ill). Auxotrophic mutants (GS115) and protease-deficient strains (SMD1163, SMD1165, and SMD1168) are frequently used. KM71 (*his4 arg4 aox1Δ::ARG4*), which shows Mut^s phenotype, is a strain in which the chromosomal *AOX1* gene is largely deleted and replaced with the *S. cerevisiae ARG4* gene. As a result, this strain must rely on the much weaker *AOX2* gene for AOX and grows on methanol at a slow rate (methanol utilization slow or Mut^s phenotype) [31, 52].

Different plasmid vectors have been designed for heterologous protein expression in *P. pastoris*. They contain different antibiotic resistance genes. pPIC3K and pPIC9K vectors contain the bacterial kanamycin-resistance gene and confers resistance to high levels of G418 (neomycin sulfate). Another set of vectors, the pPICZ series vectors, contain *Sh ble* gene from *Streptoalloteichus hindustanus*. This gene is small (375 bp) and confers resistance to the antibiotic zeocin in *E. coli*, *P. pastoris*, and other eukaryotes. Because the *ble* gene serves as the selectable marker in both *E. coli* and *P. pastoris*, the ZeoR vectors are much smaller (~3 kb) and easier to manipulate than other *P. pastoris* expression vectors [53–55]. These vectors also have sequences encoding the His6X and myc epitopes, so that foreign proteins can be easily tagged at their carboxyl termini, if desired.

Table 1
Expression and purification of recombinant protein antigens of indicated pathogens using the *P. pastoris* expression system

Pathogen	Disease	Antigen	Expression strategy	References
A. Viral proteins expressed in <i>P. pastoris</i>				
Hepatitis E virus	Hepatitis	112-608aa ORF2	VLP	[34]
Dengue virus	Dengue	DENV envelope protein domain III (EDIII)	VLP	[35]
Rock bream iridovirus (RBIV)	Morbidity and mortality in fish	Recombinant major capsid protein (rMCP)	WRY	[36]
Coxsackievirus A	Hand, foot, and mouth disease (HFMD)	P1 and 3CD	VLP	[37]
Hepatitis C virus	Hepatitis	HCV CoreE1E2 protein	Protein subunit	[38]
Influenza virus	Flu	H5 hemagglutinin	Protein subunit	[39]
Influenza virus	Flu	Alpha agglutinin	Yeast Surface display	[40]
B. Protozoan proteins expressed in <i>P. pastoris</i>				
<i>P. falciparum</i>	Malaria	Apical membrane antigen 1 (PfAMA1)	Protein subunit	[41]
<i>P. berghei</i>	Malaria	Circumsporozoite surface antigen	Yeast whole cell lysate	[42]
<i>Babesia bovis</i>	Bovine babesiosis	MSA-2a1, MSA-2b and MSA-2c	Protein subunit	[43]
<i>T. congolense</i>	Trypanosomosis	Protease (congopain)	Protein subunit	[44]
C. Bacterial proteins expressed in <i>P. pastoris</i>				
<i>C. botulinum</i>	Botulism	Recombinant C-terminus heavy chain fragment from botulinum neurotoxin serotype C [rBoNTC (H(c))]	Protein subunit	[45]
Influenza A	Flu	Me2-HSP70 fusion protein	Protein subunit	[46]
<i>M. tuberculosis</i>	Tuberculosis	Recombinant heparin-binding haemagglutinin	Purified protein	[47]
<i>Leptospira interrogans</i>	Leptospirosis	LigANI	Protein subunit	[48]
D. Nematode and tick proteins expressed in <i>P. pastoris</i>				
<i>Schistosoma mansoni</i>	Intestinal schistosomiasis	Tetraspanin surface antigen protein (Sm-TPS2)	Protein subunit	[49]
<i>Schistosoma mansoni</i>	Intestinal schistosomiasis	Sm14 antigen	Protein subunit	[50]

(continued)

Table 1
(continued)

Pathogen	Disease	Antigen	Expression strategy	References
E. Tumor-associated antigen expressed in <i>P. pastoris</i>				
Human papillomavirus	Cervical cancer	HPV16 L1 antigen	Whole recombinant yeast	[51]

*VLP virus-like particle, *WRT whole recombinant yeast, *YSD yeast surface display

Additional features of *P. pastoris* expression vectors serve as tools for specialized functions. For secretion of foreign proteins, vectors have been constructed that contain a DNA sequence immediately following the AOX1 promoter that encodes a secretion signal. Out of them, the most frequently used sequence is *S. cerevisiae* α factor prepro signal sequence, which leads to the production of higher amounts of a foreign protein than using its native signal peptide [56]. Since *P. pastoris* secretes very low levels of native proteins, the secreted heterologous proteins constitute the majority of the total proteins in the medium.

1.4 Hepatitis E-VLP (HEVLP) Expression System

Different expression systems have been used to express HEVLP as described below:

1.4.1 *E. coli* Expressed HEVLPs

Escherichia coli (*E. coli*) is an economical and commonly used expression system for the production of heterologous proteins. However, it has the limitation of lack of posttranslational modification of the recombinant protein. Hecolin is produced by expressing 368–606aa region of ORF2 protein, which self assembles to form VLPs of 23 nm size. In clinical trial, this vaccine showed an efficacy of >99% in preventing clinical hepatitis E. Immunization with Hecolin induced antibodies against HEV and provided protection against hepatitis E for up to 4.5 years [57–60].

1.4.2 Insect Cell Line Expressed VLPs

The HEV capsid antigen expressed in Baculovirus-infected insect cell system has been proposed as a candidate subunit vaccine against the hepatitis E. Different regions of ORF2 protein have been expressed in Sf21, Sf9, Tn5, and Spodoptera Litura Larvae insect cell lines [19, 61]. The 56 kDa (112–608aa ORF2) vaccine candidate showed high immunogenicity when administered to rhesus monkeys and protected them from hepatitis E when challenged with a large intravenous dose of homologous or heterologous HEV [62]. Oral administration of the baculovirus expressed

112-660aa ORF2 VLP candidate to the cynomolgus monkeys protected them against subsequent HEV challenge, supporting the utility of 112-660 ORF2 VLP as an oral hepatitis E vaccine [23].

1.4.3 *P. pastoris* Expressed HEVLPs

Our group has developed a method to produce HEVLPs using 112-608aa region of ORF2 protein of g1-HEV in *P. Pastoris* expression system [34]. Here, we describe the method of 112-608aa ORF2 VLP production in *P. pastoris*. The chapter explains the cloning strategy of 112-608aa region of ORF2 into pPICZ α vector and expression of protein in KM71H strain of *Pichia*. The recombinant protein is secreted into the culture medium, which is subsequently purified and characterized. We also describe the method for evaluation of immunogenic properties of the 112-608 ORF2 VLP. As the first approach, a simple immunization protocol is recommended to analyze if the produced particles are able to trigger an antigen-specific antibody response in mice. Different doses of antigen with or without adjuvant were used to immunize the mice to validate the dose-dependent antibody response. Further, the cell proliferation response was assessed to evaluate the memory response. The overall strategy of 112-608 ORF2 VLP expression and purification is shown in Fig. 2.

2 Materials and Reagents

2.1 Cloning of 112-608 ORF2 into pPICZ α

2.1.1 Instruments Required

1. Centrifuge.
2. Thermocycler.
3. 16, 37 °C water baths.
4. 30 and 37 °C shaking and non-shaking incubators.
5. Standard horizontal agarose gel electrophoresis apparatus.
6. Spectrophotometer nanodrop 2000.

2.1.2 Materials Required

1. PCR tubes.
2. 50-mL conical centrifuge tubes.
3. 15-mL polypropylene tubes.
4. 1.5-mL microcentrifuge tubes.
5. 90-mm plates.

2.1.3 Reagents for Molecular Biology Experiment

1. *E. coli* (Top'10) (Thermo scientific, USA).
2. *P. pastoris* KM71H (Thermo scientific, USA).
3. pPICZ α vector (Thermo Fisher Scientific, USA).
4. 112-608 ORF2 Primer for PCR amplification.

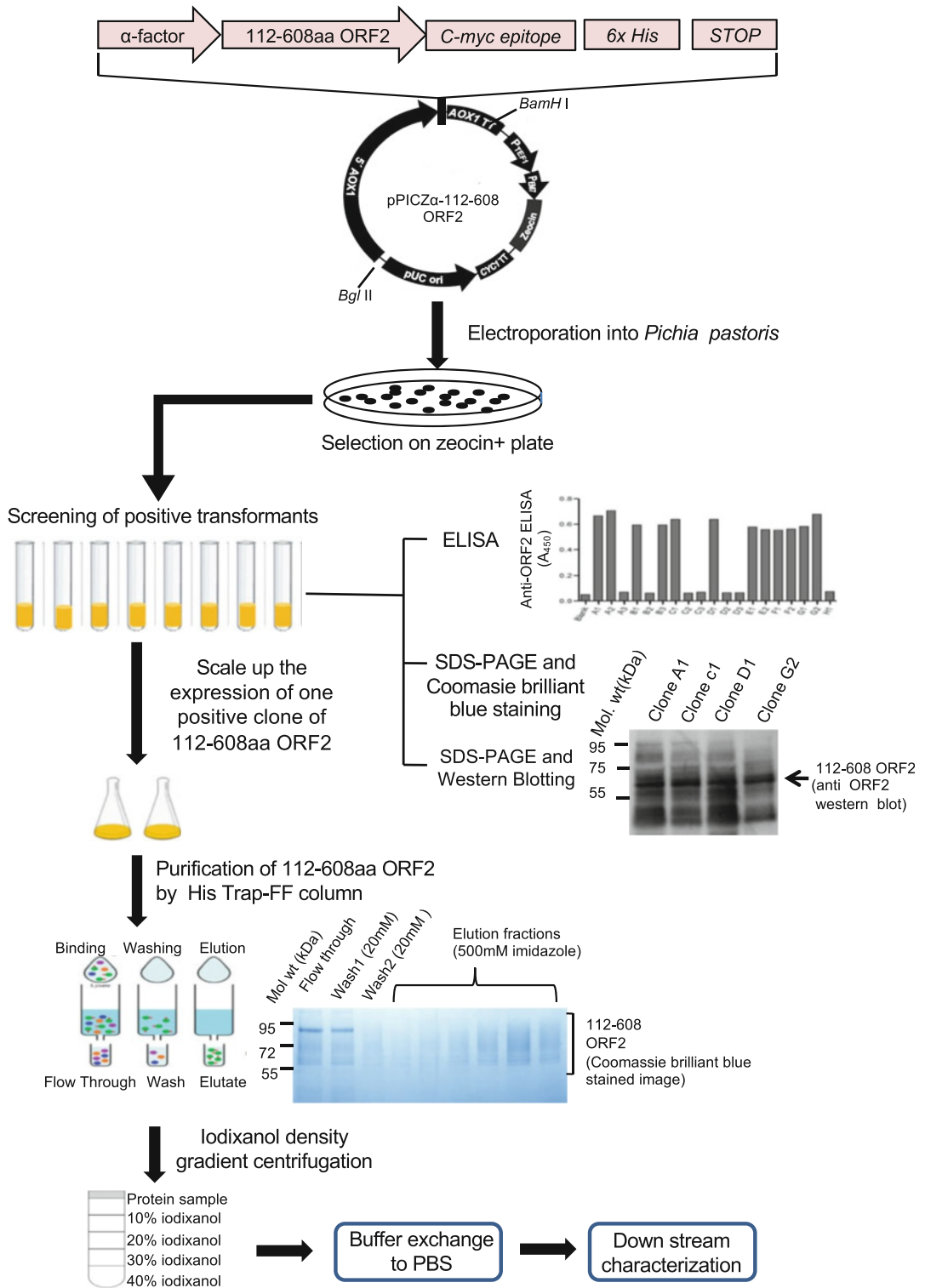


Fig. 2 Strategy of 112-608 ORF2 VLP expression and purification from *P. pastoris*.

Forward Primer 5' AGCCGCGGCGGCCGCGCGGTCCG
CTCCGGC 3' and Reverse Primer 5' CATTGTTCTA
GAAATGCTAGCACAGAGTGG3'.

5. pSKHEV2 plasmid (Genbank No. AF444002.1) [63].
6. 10 mM dNTP mixture containing 10 mM each of dATP, dTTP, dCTP, and dGTP in nuclease-free water.
7. 5× HF buffer.
8. Phusion DNA polymerase.
9. Nuclease-free water.
10. Agarose.
11. 1× TAE buffer: 40 mM Tris (pH 7.6), 20 mM acetic acid, 1 mM EDTA.
12. *NotI*-HF, *XbaI*-HF restriction enzyme.
13. *BstXI*-HF restriction enzyme.
14. Cutsmart 10× buffer.
15. Plasmid isolation miniprep kit.
16. PCR purification kit.
17. 6× Gel loading dye: 0.03% bromophenol (w/v), Tris-Cl (1 M, pH 8.0) 50 mM, EDTA (0.5 M, pH 8.0) 25 mM, glycerol 60%.
18. Gene ruler 1 kb plus DNA ladder.
19. 10× T4 DNA ligase buffer.
20. T4 DNA ligase.
21. Luria Broth (LB).
22. Ampicillin.

2.2 Generation of *Pichia* Transformants Expressing 112-608 ORF2 Protein

2.2.1 Instruments Required

1. Electroporator.
2. 30 °C shaking and non-shaking incubators.

2.2.2 Materials Required

1. 0.2 cm cuvettes.
2. Baffled flask.

2.2.3 Medium and Buffers

1. **10× YNB:**
13.4% yeast nitrogen base with ammonium sulfate, without amino acids. Dissolve 134 g of yeast nitrogen base (YNB) with ammonium sulfate and without amino acids in 1000 mL of water. Heat the solution to dissolve YNB completely in water. Filter sterilize and store at 4 °C.

2. **500× biotin (0.02% biotin):**
Dissolve 20 mg biotin in 100 mL of water and filter sterilize. Store at 4 °C.
3. **10× dextrose (20% dextrose):**
Dissolve 200 g of D-glucose in 1000 mL of water. Autoclaves for 15 min or filter sterilize.
4. **10× methanol (5% methanol):**
Mix 5 mL of methanol with 95 mL of water. Filter sterilize and store at 4 °C.
5. **10× GY (10% glycerol):**
Mix 100 mL of glycerol with 900 mL of water. Sterilize either by filtering or autoclaving and store at room temperature.
6. **1 M potassium phosphate buffer, pH 6.0:**
Combine 132 mL of 1 M K₂HPO₄, 868 mL of 1 M KH₂PO₄ and confirm that the pH = 6.0. Sterilize by autoclaving and store at room temperature.
7. **YPD media (yeast extract peptone dextrose medium):**
1% yeast extract, 2% peptone, 2% dextrose (glucose). Dissolve 10 g yeast extract, 20 g of peptone in 900 mL of water. For making YPD plates, add 20 g (2%) of agar in media. Autoclave for 20 min on liquid cycle. Cool solution to ~60 °C and add 100 mL of 10× Dextrose. Store YPD plates at 4 °C.
8. **YPD zeocin media:**
1% yeast extract, 2% peptone, 2% dextrose (glucose), 100 µg/mL of zeocin. Dissolve 10 g yeast extract, 20 g of peptone in 900 mL of water. Autoclave for 20 min on liquid cycle. Cool solution to ~60 °C and add 100 mL of 10× dextrose. Add 1.0 mL of 100 mg/mL zeocin.
9. **YPDS media agar (yeast extract peptone dextrose medium):**
1% yeast extract, 2% peptone, 2% dextrose (glucose), 1 M sorbitol, 2% agar, 100 µg/mL zeocin. Dissolve 10 g yeast extract, 182.2 g sorbitol, 20 g of peptone. Add 20 g of agar in 900 mL of water, autoclave for 20 min on liquid cycle. Add 100 mL of 10× dextrose. Cool solution to ~60 °C and add 1.0 mL of 100 mg/mL zeocin.
10. **BMGY- and BMMY-buffered glycerol complex medium buffered methanol complex medium (1 L):**
11. 1% yeast extract, 2% peptone, 100 mM potassium phosphate, pH 6.0, 1.34% YNB, 4×10^{-5} % biotin, 1% glycerol, or 1.5% methanol. Dissolve 10 g of yeast extract, 20 g peptone in 700 mL water. Autoclave 20 min on liquid cycle. Cool to room temperature, and add the following and mix well: 100 mL 1 M potassium phosphate buffer, pH 6.0, 100 mL

10× YNB, 2 mL 500× B, 100 mL 10× glycerol. For BMMY, add 30 mL 10× methanol instead of glycerol. Store media at 4 °C.

2.3 Enzyme Linked Immunosorbent Assay (ELISA), SDS-PAGE, and Western Blot

2.3.1 Instruments Required

1. Gel documentation system.
2. Micro plate reader.

2.3.2 Materials Required

1. Mini PROTEAN 3 System glass plates.
2. PVDF (polyvinylidene fluoride) membrane.
3. Whatman filter paper.
4. Blotting paper.
5. High protein binding 96 microtiter immunoplate.

2.3.3 Reagents and Buffers

1. **Coating buffer:**
(0.05 M carbonate-bicarbonate, pH 9.6)
Dissolve 3.7 g of sodium bicarbonate (NaHCO_3) and 0.64 g of sodium carbonate (Na_2CO_3) in 1000 mL of distilled water.
2. **Wash buffer:**
PBS, 0.1% Tween20, pH 7.4.
3. **Blocking buffer:**
PBS, 1% BSA, pH 7.4.
4. **Assay buffer:**
PBS, 0.1% Tween20, 0.2%BSA, pH 7.4.
5. **Enzyme substrate:**
TMB substrate (3,3',5,5'-tetramethylbenzidine).
Stop solution:
1 M H_2SO_4 .
6. **1× SDS-PAGE running buffer:**
0.025 M Tris-HCl, pH 8.3, 0.192 M glycine, 0.1% SDS.
7. **2× Laemmli buffer:**
50 mM Tris-HCl, 100 mM dithiothreitol, 4% SDS, 0.2% bromophenol blue, and 20% glycerol.
8. **Coomassie staining solution:**
50 mL methanol + 40 mL AMQ + 10 mL glacial acetic acid + 0.1 g Coomassie Brilliant Blue R250.
9. **Destaining solution:**
50 mL methanol: 40 mL AMQ + 10 mL glacial acetic acid.

10. **Transfer buffer:**
0.025 M Tris-HCl, 0.192 M glycine.
11. **Blocking solution:**
5% milk in PBS.
12. **Wash buffer:**
PBS containing 0.05% Tween-20 (PBST).
13. **Diluent solution:**
5% milk in PBST.
14. **Anti-ORF2 polyclonal rabbit antibody [16].**
15. **Anti-rabbit IgG Horseradish peroxidase(HRPO).**
16. **Clarity Western ECL blotting substrate.**
17. **1 mM phenyl methyl sulfonyl fluoride (PMSF).**
18. **Buffer A:**
50 mM Tris-Cl, 500 mM NaCl, pH 7.5.
19. **Buffer B:**
50 mM Tris-Cl, 500 mM NaCl, 500 mM imidazole, pH 7.5.
20. **Bradford assay reagent.**

2.4 Protein Purification and Characterization

2.4.1 Instruments Required

2.4.2 Materials Required

1. FPLC (fast protein liquid chromatography) system.
2. Ultracentrifuge and SW 55Ti rotor (Beckman Coulter, USA).
3. Tecnai F20 electron microscope (FEI, Oregon, USA).

2.4.3 Reagents and Buffers

1. HisTrap FF 1 mL column.
 2. 10 kDa centrifugal filter device.
 3. Formvar-coated 300-mesh copper grids for electron microscopy.
 4. Tweezers.
 5. 0.22 μ m filtered distilled water.
 6. Filter papers.
1. Iodixanol.
 2. Endoglycosidase H and PNGase F enzymes.
 3. 2.2% Uranyl acetate solution.
 4. TEN Buffer (1 \times TE, 150 mM NaCl).

2.5 Immunogenicity Assessment of 112-608 ORF2 VLP

2.5.1 Instruments Required

1. Micro plate reader.
2. Biological safety cabinet.
3. Centrifuge.
4. Adjustable pipettors and tips (0.5–1000 μ L) and multipipettors (50–200 μ L).
5. Hemocytometer.
6. Microscope.

2.5.2 Materials Required

1. ALUM adjuvant.
2. 1-mL syringe and needles for animal injection.
3. Capillaries for blood collection.
4. Scissors.
5. Forceps.
6. Cell strainer, 70 μ m pore size.
7. Petri dish, 60 mm.

2.5.3 Animals

1. Male 6–8 weeks old BALB/c mice.

2.5.4 Reagents and Buffers

1. **Ketamine/xylazine cocktail:**
87.5 mg/kg ketamine and 12.5 mg/kg xylazine.
Mixing instructions: For a 10-mL vial using ketamine 100 mg/mL and xylazine 100 mg/mL, add the following: 1.75 mL ketamine (100 mg/mL), 0.25 mL xylazine (100 mg/mL), 8 mL saline or sterile water for injection. Dosage: 0.1 mL/20 g IP.
2. **RPMI 1640 medium:**
Add 10% fetal bovine serum (FBS) prior to use the FBS is heat inactivated for 30 min at 56 °C.
3. **Antibiotic cocktail** (100 U/mL penicillin, 100 μ g/mL streptomycin).
4. **ACK Lysis buffer:**
150 mM NH_4Cl , 1 mM KHCO_3 , 0.1 mM Na_2EDTA .
5. **Cell Titer 96 Aqueous Non-Radioactive Cell Proliferation Assay Kit.**

3 Methods

3.1 Cloning of 112-608aa in pPICZ α Vector

3.1.1 PCR Amplification of 112-608aa Region of ORF2

1. Set up the reaction to amplify the 112-608aa coding region of ORF2 of g1-HEV (*see* **Note 1**).

Component name	Test sample (μ L)
F/R primer (10 pmol each)	1.0
10 mM dNTP	1.0
5 \times Buffer	4.0
Template 10 ng (pSKHEV2 plasmid DNA)	1.0
Phusion polymerase II	0.2
Nuclease-free water	12.8
Total volume	20.0

2. The following PCR amplification cycle is used: (1) 1 cycle at 95 °C for 2 min, (2) 30 cycles at 95 °C for 30 s; 55 °C for 30 s; and 72 °C for 1 min, (3) 1 cycle at 72 °C for 10 min.
3. Verify the size (1500 bp) of gene by agarose gel electrophoresis.
4. Purify the amplified product using PCR purification kit and quantify the concentration by spectrophotometer, following manufacturer's instructions.

3.1.2 Restriction Digestion and Ligation of Amplified Product

Set up the reaction to digest the amplified product and pPICZ α vector with NotI and XbaI restriction enzymes [3 μ L 10 \times buffer, 1 μ g (10 μ L) DNA, 1 μ L NotI, 1 μ L XbaI enzymes and 25 μ L water].

1. Incubate the reaction mix at 37 °C for 2 h and check for complete digestion by agarose gel electrophoresis.
2. Purify the digested product and quantify by spectrophotometry followed by ligation.
3. Ligate the digested PCR product into pPICZ α A vector using T4 DNA ligase enzyme in 1:3 vector:insert molar ratio. Assemble the following reaction:
vector DNA (30 ng), insert DNA (37.5 ng), ligase 10 \times buffer (1 μ L), T4 DNA ligase (1 μ L), and nuclease-free water to final volume of 10 μ L.
4. Incubate the reaction at 16 °C for 16 h.
5. Transform the ligation mixtures into competent TOP10 *E. coli* strain and plate the cells on LB media with 25 μ g/mL zeocin and incubate overnight at 37 °C for 12 h.
6. Pick the zeocin-resistant transformants and inoculate into 5 mL LB medium with 25 μ g/mL zeocin. Grow overnight at 37 °C with shaking.

7. Isolate plasmid DNA by miniprep for restriction mapping analysis and confirm the resulting pPICZ α 112-608aa ORF2 construct by sequencing the insert containing region.

3.2 Preparation of *P. pastoris* Competent Cells

1. Streak out the *P. pastoris* strain KM71H on YPD plate and incubate at 30 °C for 2–3 days.
2. Pick a single colony and grow in 5 mL of YPD broth in a 50-mL conical tube at 30 °C overnight, 270 rpm.
3. Inoculate 500 mL of fresh medium in a 2-L baffled flask using 1% primary culture and grow overnight till OD₆₀₀ of ~1.3 to 1.5.
4. Centrifuge the cells at 1500 $\times g$ for 5 min at 4 °C. Resuspend the pellet with 500 mL of ice-cold, sterile water.
5. Centrifuge the cells as in **step 4**, and resuspend the pellet with 250 mL of ice-cold, sterile water.
6. Centrifuge the cells as in **step 4** and resuspend the pellet in 20 mL of ice-cold 1 M sorbitol.
7. Centrifuge the cells as in **step 3** and resuspend the pellet in 1 mL of ice-cold 1 M sorbitol and prepare the aliquots of 50 μ L.

3.3 Electroporation and Generation of *Pichia* Transformant Containing pPICZ α -112-608 ORF2

1. Linearize 20 μ g of pPICZ α vector and pPICZ α 112-608 ORF2 plasmid using BstXI enzyme in 50 μ L reaction mix (5 μ L 10 \times buffer, 20 μ L DNA, 2.5 μ L enzyme, and 22.5 μ L water).
2. Purify both the linearized DNA using PCR purification kit; verify the size and integrity of the DNA by agarose gel electrophoresis.
3. Mix 50 μ L of KM71H competent cells with 10 μ g of linearized DNA and transfer them to an ice-cold 0.2 cm electroporation cuvette and incubate them on ice for 5 min.
4. Electroporate the cells (conditions: $V = 1500$ V, $C = 25$ μ F, $R = 200$ Ω , time 5 ms/pulse) and add immediately 1 mL of ice-cold 1 M sorbitol, followed by 1 mL of media (1:1 ratio of YPD broth and 1 M sorbitol) and incubate the tubes at 30 °C for 1 h at 250 rpm with shaking. Centrifuge the cells at 17,000 $\times g$ for 1 min and plate 100 μ L of each on YPDS plates containing 100 μ g/mL zeocin.
5. Incubate the plate at 30 °C for 2–3 days till colonies appear.

3.4 Screening of Transformants and Selection of 112-608 ORF2 Protein Expressing *P. pastoris* Clones

1. Select 20–30 colonies along with 10 pPICZ α vector transformants and grow in BMGY medium at 28.5 °C, 270 rpm for 48 h.
2. Measure the level of ORF2 protein in the culture medium by ELISA using anti-ORF2 antibody, following the protocol mentioned below.

3. Coat the 96-well micro-titer plate with 50 μL of culture medium mixed with 50 μL of bicarbonate buffer (pH 9.6) and incubate at 4 $^{\circ}\text{C}$ for 12 h.
4. Next day wash the plate thrice in 200 μL /well of wash buffer and block with 200 μL /well of blocking buffer at 37 $^{\circ}\text{C}$ for 2 h.
5. Wash the plates with wash buffer and incubate with anti-ORF2 rabbit polyclonal antibody at a dilution of 1:1000 in assay buffer at 37 $^{\circ}\text{C}$ for 2 h.
6. Wash the plate thrice in 200 μL /well of wash buffer and incubate with HRP-conjugated anti-rabbit IgG in assay buffer for 1 h at 37 $^{\circ}\text{C}$ and wash three times in wash buffer.
7. Add the TMB substrate (100 μL /well), incubate for 15 min at 25 $^{\circ}\text{C}$. Stop the reaction by adding 1 M H_2SO_4 and measure the absorbance at 450 nm using a multimode microplate reader.

3.5 Confirmation of 112-608 ORF2 Protein Expression in *P. pastoris* Culture Medium

3.5.1 Mini Scale Expression of 112-608 ORF2 Protein

1. Inoculate few 112-608 ORF2 protein expression of positive colonies from identified clones and one pPICZ α transformed colony in 40 mL of BMGY media in baffled flask and grow at 28.5 $^{\circ}\text{C}$ in shaking incubator at 270 rpm for 16–18 h till A_{600} reaches ~ 2 .
2. Harvest the cells by centrifugation at $3000 \times g$ for 5 min at RT, followed by resuspending the pellet in 8 mL of BMMY medium supplemented with 1% methanol for 48 h. Centrifuge the culture medium at $10,000 \times g$ for 2–3 min at room temperature (RT) and collect the supernatant.
3. Compare the expression of 112-608 ORF2 protein in an aliquot of culture medium of different clones by SDS-PAGE Coomassie blue staining and Western blot using anti-ORF2 antibody as mentioned below.
4. Select the clone showing maximum expression of 112-608 ORF2 (illustrated in Fig. 2), and optimize the following conditions to maximize protein expression: different concentration of methanol (0–4%), duration of methanol induction (24–98 h), pH of the culture medium (0–8), and cell density of induced culture ($A_{600} = 0$ –100) (*see Note 2*).

3.5.2 SDS-PAGE and Western Blot Analysis of 112-608 ORF2 Protein

1. Mix the samples with $2 \times$ Laemmli buffer, incubate for 5 min at 95 $^{\circ}\text{C}$, and resolve on 10% SDS-PAGE gels.
2. Stain the gel with Coomassie Brilliant Blue to visualize the protein bands.
3. For Western blot, transfer the protein from gel to 0.45- μm PVDF membrane.
4. Block the membrane using 5% BSA in $1 \times$ PBS for 45 min at RT.

5. Incubate overnight (16 h) with 1:1000 anti-ORF2 polyclonal rabbit antibody diluted in 5% skimmed milk in $1 \times$ PBST at 4°C .
6. Wash $3 \times$ in PBST, incubate with 1:5000 anti-rabbit IgG HRP secondary antibody diluted in 5% skimmed milk in $1 \times$ PBST at room temperature.
7. Wash $3 \times$ in PBST.
8. Add enhanced chemiluminescence substrate and acquire the image using chemi doc-MP gel documentation system. A band of approximately 56 kDa should be visible (Fig. 2, [34]).

3.6 Expression and Purification of 112-608 ORF2 Protein

3.6.1 Large-Scale Expression of 112-608 ORF2 Protein

1. Inoculate single colony of 112-608 ORF2 protein expressing transformant in 100 mL of YPDS medium in a 1-L baffled flask and incubate in a rotatory shaker for a period of 16–18 h at 28.5°C , 270 rpm till A_{600} reaches ~ 2.0 .
2. Centrifuge the culture at $3000 \times g$ for 5 min at room temperature. Remove supernatant and resuspend the cell pellet in BMGY media (6 L) and incubate for a period of 16–18 h under similar conditions till the A_{600} reaches ~ 6.0 .
3. Harvest the cells by centrifugation at $3000 \times g$ for 5 min at room temperature. Remove supernatant and resuspend the cell pellet in 500 mL of BMMY and continue to incubate till A_{600} reaches ~ 60 –70.
4. Add 1.5% methanol at 24 h interval for 72 h, 270 rpm, 28.5°C .
5. Centrifuge the culture at $10,000 \times g$ and collect the supernatant.
6. Use an aliquot of culture media to confirm the 112-608 ORF2 protein expression and store the remaining medium at -80°C .
7. Confirm the presence of 112-608 ORF2 protein by SDS-PAGE Coomassie blue staining and Western blot using anti-ORF2 antibody, as mentioned above.

3.6.2 112-608 ORF2 Protein Purification by Immobilized Metal Ion Affinity Chromatography

1. Filter the above stored culture media and buffers using a $0.45\text{-}\mu\text{m}$ filter unit.
2. Equilibrate the 500 mL culture medium in buffer A containing 1 mM PMSF and 5 mM imidazole.
3. Connect 1 mL HisTrap FF Global Ni-Sepharose column to an AKTA purifier FPLC and equilibrate the column with 5 mL buffer A. Run at a flow rate of 1 mL/min, and maintain pressure below 0.5 psi.
4. Load the sample on to the column at 0.5 mL/min flow rate.
5. Wash the unbound protein by washing in 5–50 mM gradient of imidazole.

6. Elute the bound protein in a gradient of 50–500 mM imidazole.
7. Monitor the purification procedure by UV absorption of the protein at 280 nm, solution pH, and conductivity. Data are collected using Unicorn software.
8. Collect the fractions showing protein peaks.
9. Analyze aliquots of different fractions by SDS-PAGE and Western blot.
10. Pool the fractions containing 112-608 ORF2 protein and exchange the imidazole buffer to PBS (pH 7.4) using 10 kDa centrifugal filter device.
11. Estimate protein concentration by serial dilutions by Bradford assay.

3.6.3 Purification of 112-608 ORF2 Protein by Iodixanol Density Gradient

1. Prepare 10–40% iodixanol gradient in 5 mL SW 55Ti ultracentrifuge tube, diluted in $1 \times$ TEN buffer.
2. Layer 112-608 ORF2 protein (from Subheading 3.6.2) over the density gradient and centrifuge in SW 55Ti rotor in an ultracentrifuge (Beckman Coulter, Indianapolis, USA) for 16 h at $100,000 \times g$ without braking.
3. Collect equal fractions from top and analyze aliquots by SDS-PAGE and Western blot.
4. Pool the fractions containing VLPs and buffer exchange to PBS using 10 kDa centrifugal filter device.

3.7 Characterization of 112-608 ORF2 VLP

3.7.1 Glycosylation Status Verification (See Note 3)

1. Mix the purified protein with $10 \times$ glycoprotein denaturation buffer and incubate at 95°C for 5 min, chill on ice and centrifuge for 10 s.
2. Prepare the reaction mixture 2 (2 μL of $10 \times$ glycobuffer + 2 μL 10% NP40 + 6 μL H_2O) and incubate at 37°C .
3. Incubate the denatured protein sample with reaction mixture 2 and add 1 μL endoglycosidase H or PNGase F enzymes.
4. Incubate the mixture for 4 h at 37°C . Analyze the aliquots of the enzyme treated and mock samples on SDS-PAGE by Coomassie Brilliant Blue staining and Western blot using anti-ORF2 antibody (Fig. 3a).

3.7.2 Transmission Electron Microscopy (TEM)

1. Filter the purified VLPs and buffer through 0.45 μm filter.
2. Adsorb 5 μL of purified VLP in suspension, at a concentration of 0.5 mg/mL on to a glow discharged formvar-coated 300-mesh copper grid for 2 min.
3. Wash the grid with PBS three times, followed by staining with 2% uranyl acetate.
4. Air-dry the grid and examine in a Tecnai F20 electron microscope (FEI, Oregon, USA) operating at 200 kV (Fig. 3b).

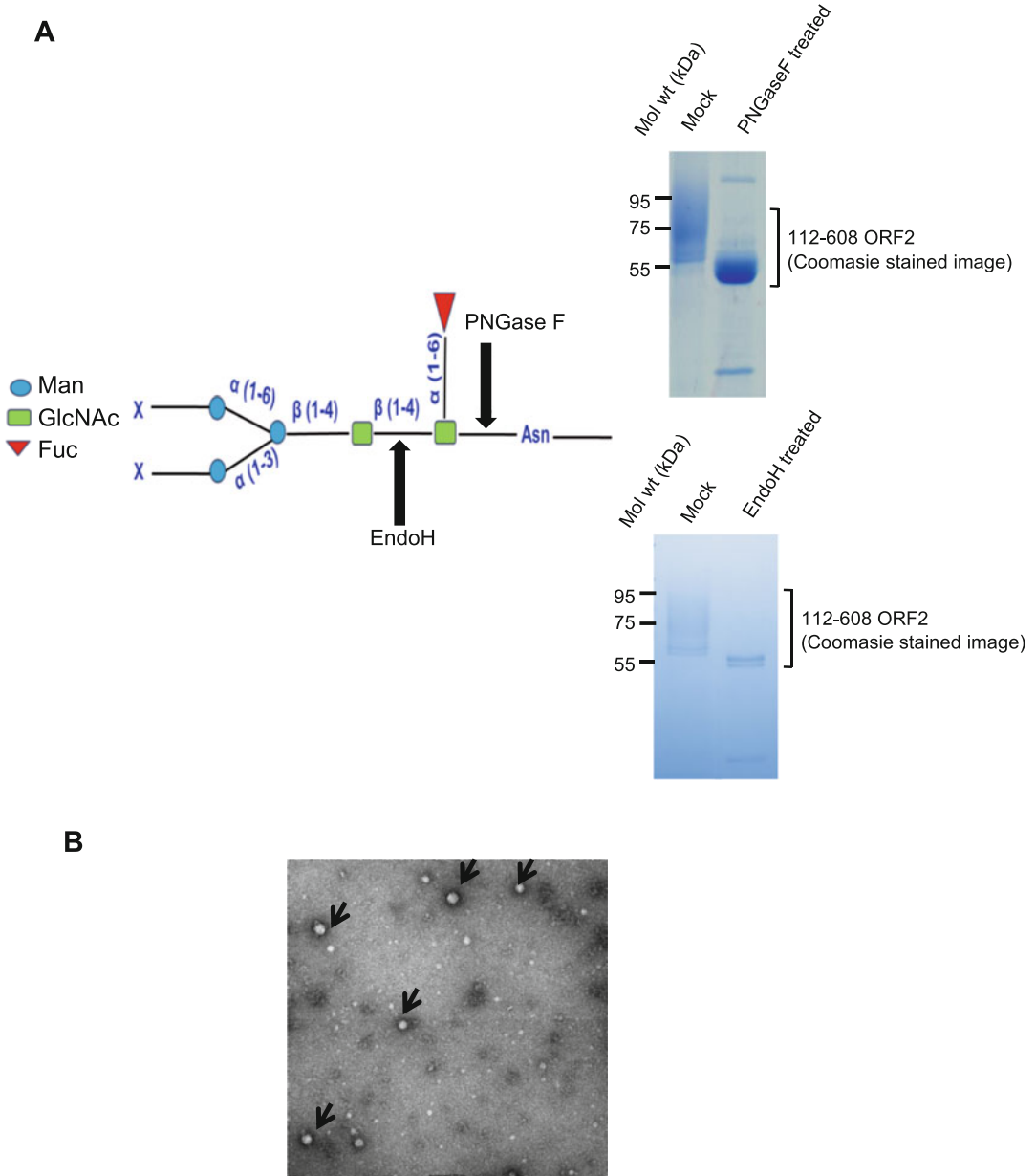


Fig. 3 Characterization of 112-608 ORF2 VLP: **(a)** Functional sites of glycosidase enzymes are indicated by arrow and the respective Coomassie Brilliant Blue-stained image of the glycosidase-treated purified ORF2 protein. **(b)** Transmission electron micrograph of the purified ORF2 protein (scale: 50 nm, magnification: 100k \times). Arrow indicates VLPs

3.8 Immunogenicity Assessment of 112-608 ORF2 VLP

3.8.1 Immunization of Mice

1. Divide 6- to 8-week-old male mice ($n = 5$) into 8 groups.
2. Collect blood sample to obtain pre-immune sera.
3. Mix 1, 3, and 5 μg of 112-608 ORF2 VLP in PBS; as well as with ALUM adjuvant (1:1 volumetric ratio) to a volume of 100 μL /mouse and intraperitoneally inject into mice on day 1.
4. Give two booster doses with the same dose of immunogen at 2 weeks.
5. Collect blood sample before each immunization, separate sera and store at $-80\text{ }^{\circ}\text{C}$ (*see Note 4*).

3.8.2 Antibody Titration

1. Calculate the titer of antibodies in mice sera by indirect ELISA.
2. For ELISA, coat the 96-well microtiter plates with 100 ng of purified VLP in 100 μL of bicarbonate buffer (pH 9.6) and incubate at $4\text{ }^{\circ}\text{C}$ overnight.
3. Block the plate as described in Subheading 3.4.
4. Wash the plate with wash buffer and incubate with twofold serially diluted sera obtained from each mouse at indicated time points starting from 1:100 dilutions.
5. Next, wash the plate thrice in 200 μL /well of wash buffer and incubate with HRP conjugated anti-mouse IgG in assay buffer for 1 h at $37\text{ }^{\circ}\text{C}$ and wash three times in wash buffer as described in Subheading 3.4.
6. Measure A_{450} in microplate reader.
7. Calculate the end-point dilution of each sample and the final titer value as given below:

$$\text{Antibody titer} = \log_2 (\text{reciprocal of highest dilution showing two times absorbance of control mice})$$
 (*see Note 5*).

3.8.3 Splenocyte Proliferation Assay

Preparation of Splenocyte Suspension

The following protocol describes the preparation of spleen cells to be used in proliferation assay. Post-dissection procedures should be performed under sterile conditions in a biosafety cabinet.

1. Sacrifice the mouse on day 43 of immunization by asphyxiation and excise the spleen using scissors and forceps.
2. Immediately put the spleen in a 1.5-mL centrifuge tube containing 1 mL of RPMI medium.
3. Make single-cell suspension by teasing the spleen with the plunger of a 1-mL syringe in 70 μM cell strainer placed in a petri-dish.
4. Transfer the cell suspension to a new 15-mL Falcon tube, wash the cell strainer with 5 mL of complete RPMI medium and collect the wash in the same tube.
5. Centrifuge for 5 min at $450 \times g$ at $4\text{ }^{\circ}\text{C}$.

6. Discard the supernatant and resuspend the pellet in the remaining medium.
7. Add 1 mL of ACK lysis buffer and incubate at room temperature for 1 min (*see Note 6*).
8. Add 10 mL of PBS to the Falcon tube to inactivate the ACK lysis buffer and proceed immediately with centrifugation for 5 min at $450 \times g$, 4 °C.
9. Discard the supernatant and resuspend the cell pellet in 2 mL of complete medium.
10. Prepare cells for counting by mixing 10 μ L cell suspension + 90 μ L trypan blue stains 0.4%.
11. Count cells in a Hemocytometer.

Splenocyte
Proliferation Assay

1. Plate 1×10^6 splenocytes/well isolated from the immunized and control mice and culture in 96-well plates for 24 h, followed by stimulation with 5 μ g of purified 112-608 ORF2 VLPs.
2. After 24 h of stimulation, perform the cell proliferation assay by using Cell Titer 96 Aqueous Non-Radioactive Cell Proliferation Assay Kit.
3. Add 20 μ L MTS dye in each well and incubated for 4 h, followed by measurement of the absorbance at A_{490} nm.
4. Assess the proliferation by the stimulation index (SI), calculated according to the formula:

$$SI = (\text{experimental OD} - \text{control OD}) / \text{control OD}.$$

4 Notes

1. The gene-specific primers having Not I and XbaI restriction enzyme sites in forward and reverse primers, respectively, were synthesized to clone in pPICZ α A vector.
2. To get the optimum protein expression, the conditions of protein expression must be optimized. In the present study, clone D1 was selected for the optimization and the highest ORF2 yield was obtained by 72-h incubation with 1.5% methanol. pH analysis of the culture medium demonstrated that pH 3.0 is optimal for the maximum yield of the ORF2 and cell density of 80 ($A_{600} = 80$) favors maximum yield [34].
3. ORF2 protein contains three N-linked glycosylation sites. Susceptibility to glycosidase enzymes, endoglycosidase H (endo H), and PNGase F is used to determine the glycosylation status of the purified protein. Endo H cleaves the N-linked glycans between the two *N*-acetylglucosamine (GlcNAc) residues in

the core region of the glycan chain on high mannose glycans, leaving one GlcNAc still bound to the protein while PNGase F is a glycoamidase that cleaves the bond between the innermost GlcNAc and asparagine residues, releasing the entire sugar chain.

4. To collect the blood sample, mice are injected with 100 μ L ketamine/xylazine cocktail by intraperitoneal route and blood is taken by puncturing the retro-orbital plexus using glass capillary.
5. The reciprocal of the highest dilution which has two times absorbance value of control mice is considered as positive titer and negative titer value is set as log value 2.0 for statistical analysis. Data is represented as log₂ transformed antibody titers.
6. Shorter incubation time will result in insufficient lysis of the red blood cells. Longer incubation time will affect the viability of the splenocytes and may result in low cell yield.

References

1. Nan Y, Zhang YJ (2016) Molecular biology and infection of hepatitis E virus. *Front Microbiol* 7:1419
2. Donnelly MC, Scobie L, Crossan CL, Dalton H, Hayes PC, Simpson KJ (2017) Review article: hepatitis E—a concise review of virology, epidemiology, clinical presentation and therapy. *Aliment Pharmacol Ther* 46:126–141
3. Primadharsini PP, Nagashima S, Okamoto H (2019) Genetic variability and evolution of hepatitis E virus. *Viruses* 11:456
4. Lhomme S, Marion O, Abravanel F, Chapuy-Regaud S, Kamar N, Izopet J (2016) Hepatitis E pathogenesis. *Viruses* 8:212
5. Kamar N, Izopet J, Pavio N, Aggarwal R, Labrique A, Wedemeyer H, Dalton HR (2017) Hepatitis E virus infection. *Nat Rev Dis Primers* 3:1–6
6. Hoofnagle JH, Nelson KE, Purcell RH (2012) Hepatitis E. *N Engl J Med* 367:1237–1244
7. Kamar N, Marion O, Abravanel F, Izopet J, Dalton HR (2016) Extrahepatic manifestations of hepatitis E virus. *Liver Int* 36:467–472
8. World Health Organization. Hepatitis E. Available online: <https://www.who.int/news-room/fact-sheets/detail/hepatitis>
9. Nimgaonkar I, Ding Q, Schwartz RE, Ploss A (2018) Hepatitis E virus: advances and challenges. *Nat Rev Gastroenterol Hepatol* 15:96
10. Boccia D, Guthmann JP, Klovstad H, Hamid N, Tatay M, Ciglenecki I, Nizou JY, Nicand E, Guerin PJ (2006) High mortality associated with an outbreak of hepatitis E among displaced persons in Darfur, Sudan. *Clin Infect Dis* 42:1679–1684
11. Pérez-Gracia MT, Suay-García B, Mateos-Lindemann ML (2017) Hepatitis E and pregnancy: current state. *Rev Med Virol* 27:e1929
12. Teixeira J, Mesquita JR, Pereira SS, Oliveira RM, Abreu-Silva J, Rodrigues A, Myrnel M, Stene-Johansen K, Øverbø J, Gonçalves G, Nascimento MS (2017) Prevalence of hepatitis E virus antibodies in workers occupationally exposed to swine in Portugal. *Med Microbiol Immunol* 206:77–81
13. Boxall E, Herborn A, Kochethu G, Pratt G, Adams D, Ijaz S, Teo CG (2006) Transfusion-transmitted hepatitis E in a ‘non-hyperendemic’ country. *Transfus Med* 16:79–83
14. Kamar N, Selves J, Mansuy JM, Ouezzani L, Péron JM, Guitard J, Cointault O, Esposito L, Abravanel F, Danjoux M, Durand D (2008) Hepatitis E virus and chronic hepatitis in organ-transplant recipients. *N Engl J Med* 358:811–817
15. Okamoto H (2017) Genetic variability and evolution of hepatitis E virus. *Virus Res* 127:216–228

16. Nair VP, Anang S, Subramani C, Madhvi A, Bakshi K, Srivastava A, Nayak B, Kumar CTR, Surjit M (2016) Endoplasmic reticulum stress induced synthesis of a novel viral factor mediates efficient replication of genotype-1 hepatitis E virus. *PLoS Pathog* 12:e1005521
17. Subramani C, Nair VP, Anang S, Mandal SD, Pareek M, Kaushik N, Srivastava A, Saha S, Nayak B, Ranjith-Kumar CT, Surjit M (2018) Host-virus protein interaction network reveals the involvement of multiple host processes in the life cycle of hepatitis E virus. *mSystems* 3(1):e00135–e00117
18. Chandra V, Taneja S, Kalia M, Jameel S (2008) Molecular biology and pathogenesis of hepatitis E virus. *J Biosci* 33:451–464
19. Robinson RA, Burgess WH, Emerson SU, Leibowitz RS, Sosnovtseva SA, Tsarev S, Purcell RH (1998) Structural characterization of recombinant hepatitis E virus ORF2 proteins in baculovirus-infected insect cells. *Protein Expr Purif* 12:75–84
20. Zafrullah M, Ozdener MH, Kumar R, Panda SK, Jameel S (1999) Mutational analysis of glycosylation, membrane translocation, and cell surface expression of the hepatitis E virus ORF2 protein. *J Virol* 73:4074–4082
21. Cao D, Meng XJ (2012) Molecular biology and replication of hepatitis E virus. *Emerg Microbes Infect* 1(8):e17
22. Li TC, Yoshimatsu K, Yasuda SP, Arikawa J, Koma T, Kataoka M, Ami Y, Suzaki Y, Mai LT, Hoa NT, Yamashiro T (2011) Characterization of self-assembled virus-like particles of rat hepatitis E virus generated by recombinant baculoviruses. *J Gen Virol* 92:2830
23. Li TC, Suzaki Y, Ami Y, Dhole TN, Miyamura T, Takeda N (2004) Protection of cynomolgus monkeys against HEV infection by oral administration of recombinant hepatitis E virus-like particles. *Vaccine* 22:370–377
24. Xing L, Li TC, Mayazaki N, Simon MN, Wall JS, Moore M, Wang CY, Takeda N, Wakita T, Miyamura T, Cheng RH (2010) Structure of hepatitis E virion-sized particle reveals an RNA-dependent viral assembly pathway. *J Biol Chem* 285:33175–33183
25. Crisci E, Bárcena J, Montoya M (2012) Virus-like particles: the new frontier of vaccines for animal viral infections. *Vet Immunol Immunopathol* 148:211–225
26. Murata K, Lechmann M, Qiao M, Gunji T, Alter HJ, Liang TJ (2003) Immunization with hepatitis C virus-like particles protects mice from recombinant hepatitis C virus-vaccinia infection. *Proc Natl Acad Sci* 100:6753–6758
27. Grgacic EV, Anderson DA (2006) Virus-like particles: passport to immune recognition. *Methods* 40:60–65
28. Keating GM, Noble S (2003) Recombinant hepatitis B vaccine (Engerix-B (R))—a review of its immunogenicity and protective efficacy against hepatitis B. *Drugs* 63:1021–1051
29. Bryan JT, Buckland B, Hammond J, Jansen KU (2016) Prevention of cervical cancer: journey to develop the first human papillomavirus virus-like particle vaccine and the next generation vaccine. *Curr Opin Chem Biol* 32:34–47
30. Ahmad M, Hirz M, Pichler H, Schwab H (2014) Protein expression in *Pichia pastoris*: recent achievements and perspectives for heterologous protein production. *Appl Microbiol Biotechnol* 98:5301–5317
31. Baghban R, Farajnia S, Rajabibazl M, Ghasemi Y, Mafi A, Hoseinpoor R, Rahbarnia L, Aria M (2019) Yeast expression systems: overview and recent advances. *Mol Biotechnol* 61:365–384
32. Darby RA, Cartwright SP, Dilworth MV, Bill RM (2012) Which yeast species shall I choose? *Saccharomyces cerevisiae* versus *Pichia pastoris* (review). *Methods Mol Biol* 866:11–23
33. Spohner SC, Müller H, Quitmann H, Czermak P (2015) Expression of enzymes for the usage in food and feed industry with *Pichia pastoris*. *J Biotechnol* 202:118–134
34. Gupta J, Kaul S, Srivastava A, Kaushik N, Ghosh S, Sharma C, Batra G, Banerjee M, Nayak B, Ranjith-Kumar CT, Surjit M (2020) Expression, purification and characterization of the hepatitis E virus like-particles in the *Pichia pastoris*. *Front Microbiol* 11:141
35. Ramasamy V, Arora U, Shukla R, Poddar A, Shanmugam RK, White LJ, Mattocks MM, Raut R, Perween A, Tyagi P, de Silva AM (2018) A tetravalent virus-like particle vaccine designed to display domain III of dengue envelope proteins induces multi-serotype neutralizing antibodies in mice and macaques which confer protection against antibody dependent enhancement in AG129 mice. *PLoS Negl Trop Dis* 12:e0006191
36. Seo JY, Chung HJ, Kim TJ (2013) Codon optimized expression of fish iridovirus capsid protein in yeast and its application as an oral vaccine candidate. *J Fish Dis* 36:763–768
37. Zhou Y, Shen C, Zhang C, Zhang W, Wang L, Lan K, Liu Q, Huang ZY (2016) Yeast-produced recombinant virus-like particles of coxsackievirus A6 elicited protective antibodies in mice. *Antiviral Res* 132:165–169
38. Fazlalipour M, Keyvani H, Monavari SH, Mollaie HR (2015) Expression, purification and

- immunogenic description of a hepatitis C virus recombinant CoreE1E2 protein expressed by yeast *Pichia pastoris*. *Jundishapur J Microbiol* 8 (4):e17157
39. Pietrzak M, Maciola A, Zdanowski K, Protas-Klukowska AM, Olszewska M, Śmietanka K, Minta Z, Szewczyk B, Kopera E (2016) An avian influenza H5N1 virus vaccine candidate based on the extracellular domain produced in yeast system as subviral particles protects chickens from lethal challenge. *Antiviral Res* 133:242–249
 40. Wasilenko JL, Sarmento L, Spatz S, Pantin-Jackwood M (2010) Cell surface display of highly pathogenic avian influenza virus hemagglutinin on the surface of *Pichia pastoris* cells using α -agglutinin for production of oral vaccines. *Biotechnol Prog* 26:542–547
 41. Remarque EJ, Faber BW, Kocken CH, Thomas AW (2008) A diversity-covering approach to immunization with *Plasmodium falciparum* apical membrane antigen 1 induces broader allelic recognition and growth inhibition responses in rabbits. *Infect Immunity* 76:2660–2670
 42. Jacob D, Ruffie C, Combredet C, Formaglio P, Amino R, Ménard R, Tangy F, Sala M (2017) Yeast lysates carrying the nucleoprotein from measles virus vaccine as a novel subunit vaccine platform to deliver *Plasmodium circumsporozoite* antigen. *Malaria J* 16:1–4
 43. Gimenez AM, Françaço KS, Ersching J, Icimoto MY, Oliveira V, Rodriguez AE, Schnittger L, Florin-Christensen M, Rodrigues MM, Soares IS (2016) A recombinant multi-antigen vaccine formulation containing *Babesia bovis* merozoite surface antigens MSA-2a 1, MSA-2b and MSA-2c elicits invasion-inhibitory antibodies and IFN- γ producing cells. *Parasite Vectors* 9:1–3
 44. Boulangé AF, Khamadi SA, Pillay D, Coetzer TH, Authié E (2011) Production of congopain, the major cysteine protease of *Trypanosoma (Nannomonas) congolense*, in *Pichia pastoris* reveals unexpected dimerisation at physiological pH. *Protein Expr Purif* 75:95–103
 45. Dux MP, Huang J, Barent R, Inan M, Swanson ST, Sinha J, Ross JT, Smith LA, Smith TJ, Henderson I, Meagher MM (2011) Purification of a recombinant heavy chain fragment C vaccine candidate against botulinum serotype C neurotoxin [rBoNTC (Hc)] expressed in *Pichia pastoris*. *Protein Expr Purif* 75:177–185
 46. Ebrahimi SM, Tebianian M, Toghiani H, Memarnejadian A, Attaran HR (2010) Cloning, expression and purification of the influenza A (H9N2) virus M2e antigen and truncated *Mycobacterium tuberculosis* HSP70 as a fusion protein in *Pichia pastoris*. *Protein Expr Purif* 70:7–12
 47. Kohama H, Umemura M, Okamoto Y, Yahagi A, Goga H, Harakuni T, Matsuzaki G, Arakawa T (2008) Mucosal immunization with recombinant heparin-binding haemagglutinin adhesin suppresses extrapulmonary dissemination of *Mycobacterium bovis* bacillus Calmette-Guerin (BCG) in infected mice. *Vaccine* 26:924–932
 48. Hartwig DD, Bacelo KL, de Oliveira PD, Oliveira TL, Seixas FK, Amaral MG, Hartleben CP, McBride AJ, Dellagostin OA (2014) Mannosylated LigANI produced in *Pichia pastoris* protects hamsters against leptospirosis. *Curr Microbiol* 68:524–530
 49. Cheng W, Curti E, Rezende WC, Kwityn C, Zhan B, Gillespie P, Plieskatt J, Joshi SB, Volkin DB, Hotez PJ, Middaugh CR (2013) Biophysical and formulation studies of the *Schistosoma mansoni* TSP-2 extracellular domain recombinant protein, a lead vaccine candidate antigen for intestinal schistosomiasis. *Hum Vaccin Immunother* 9:2351–2361
 50. Damasceno L, Ritter G, Batt GA (2017) Process development for production and purification of the *Schistosoma mansoni* Sm14 antigen. *Protein Expr Purif* 134:72–81
 51. Bolhassani A, Muller M, Roohvand F, Motevalli F, Agi E, Shokri M, Rad MM, Hosseinzadeh S (2014) Whole recombinant *Pichia pastoris* expressing HPV16 L1 antigen is superior in inducing protection against tumor growth as compared to killed transgenic *Leishmania*. *Hum Vaccin Immunother* 10:3499–3508
 52. Wang M, Jiang S, Wang Y (2016) Recent advances in the production of recombinant subunit vaccines in *Pichia pastoris*. *Bioengineered* 7:155–165
 53. Karbalaee M, Rezaee SA, Farsiani H (2020) *Pichia pastoris*: A highly successful expression system for optimal synthesis of heterologous proteins. *J Cell Physiol* 235(9):5867–5881
 54. Hartner FS, Ruth C, Langenegger D, Johnson SN, Hyka P, Lin-Cereghino GP, Lin-Cereghino J, Kovar K, Cregg JM, Glieder A (2008) Promoter library designed for fine-tuned gene expression in *Pichia pastoris*. *Nucleic Acids Res* 36:e76
 55. Li P, Anumanthan A, Gao XG, Ilangovan K, Suzara VV, Düzgüneş N, Renugopalakrishnan V (2007) Expression of recombinant proteins in *Pichia pastoris*. *Appl Biochem Biotechnol* 142:105–124

56. Damasceno LM, Huang CJ, Batt CA (2012) Protein secretion in *Pichia pastoris* and advances in protein production. *Appl Microbiol Biotechnol* 93:31–39
57. Zhang J, Liu CB, Li RC, Li YM, Zheng YJ, Li YP, Luo D, Pan BB, Nong Y, Ge SX, Xiong JH (2009) Randomized-controlled phase II clinical trial of a bacterially expressed recombinant hepatitis E vaccine. *Vaccine* 27:1869–1874
58. Wu T, Li SW, Zhang J, Ng MH, Xia NS, Zhao Q (2012) Hepatitis E vaccine development: a 14 year odyssey. *Hum Vaccin Immunother* 8:823–827
59. Zhu FC, Zhang J, Zhang XF, Zhou C, Wang ZZ, Huang SJ, Wang H, Yang CL, Jiang HM, Cai JP, Wang YJ (2010) Efficacy and safety of a recombinant hepatitis E vaccine in healthy adults: a large-scale, randomised, double-blind placebo-controlled, phase 3 trial. *Lancet* 376:895–902
60. Zhang J, Zhang XF, Huang SJ, Wu T, Hu YM, Wang ZZ, Wang H, Jiang HM, Wang YJ, Yan Q, Guo M (2015) Long-term efficacy of a hepatitis E vaccine. *N Engl J Med* 372:914–922
61. Sehgal D, Malik PS, Jameel S (2003) Purification and diagnostic utility of a recombinant hepatitis E virus capsid protein expressed in insect larvae. *Protein Expr Purif* 27:27–34
62. Zhang M, Emerson SU, Nguyen H, Engle R, Govindarajan S, Blackwelder WC, Gerin J, Purcell RH (2002) Recombinant vaccine against hepatitis E: duration of protective immunity in rhesus macaques. *Vaccine* 20:3285–3291
63. Emerson SU, Nguyen H, Graff J, Stephany DA, Brockington A, Purcell RH (2004) In vitro replication of hepatitis E virus (HEV) genomes and of an HEV replicon expressing green fluorescent protein. *J Virol* 78:4838–4846

Part III

Vaccine Adjuvants



Developments in Vaccine Adjuvants

Farrhana Ziana Firdaus, Mariusz Skwarczynski, and Istvan Toth

Abstract

Vaccines, including subunit, recombinant, and conjugate vaccines, require the use of an immunostimulator/adjuvant for maximum efficacy. Adjuvants not only enhance the strength and longevity of immune responses but may also influence the type of response. In this chapter, we review the adjuvants that are available for use in human vaccines, such as alum, MF59, AS03, and AS01. We extensively discuss their composition, characteristics, mechanism of action, and effects on the immune system. Additionally, we summarize recent trends in adjuvant discovery, providing a brief overview of saponins, TLRs agonists, polysaccharides, nanoparticles, cytokines, and mucosal adjuvants.

Key words Vaccination, Adjuvants, Immune stimulators, Delivery systems, Innate and adaptive immunity, Subunit vaccines, Nanoparticles

1 Introduction

Vaccination has been the most efficient medical invention to counter infectious diseases to date. The strategy has reduced mortality, with estimates suggesting that vaccines save approximately three million lives across the globe each year [1, 2]. Generally, vaccines are biological substances that resembles a disease-causing microorganism [2]. They work by stimulating the body to produce memory immune responses against a pathogen, allowing for rapid pathogen elimination if the body is exposed to it again in the future [3]. Over the years, vaccines have become increasingly popular, with over 20 licensed vaccines against infectious diseases widely used in mass vaccinations and approximately 24 new vaccines in the pipeline, as reported by the World Health Organization (WHO) in 2019. Vaccines have been able to prevent the spread of many infectious diseases, including smallpox, pertussis, poliomyelitis, measles, mumps, rubella, and influenza [1, 4].

Despite the success of vaccination for some diseases, numerous other infectious diseases and cancers could potentially be managed

and controlled by vaccines, but effective composition has remained elusive [5]. Diseases such as malaria, AIDS, and COVID-19 are caused by microorganisms with highly variable structure and complex pathogenesis, and they often have the ability to evade the human immune system, resulting in high mortality rates [6, 7]. Novel vaccine designs are required to induce a strong and suitable immune response against such challenging pathogens, emerging infections, and cancers [8].

Traditional vaccines are prepared based on whole live-attenuated, weakened, inactivated, or killed pathogens [9]. Pathogens prepared in these ways maintain most of their immunogenicity, mimicking natural infection and inducing long-lasting immunity [10]. However, the use of whole pathogens has significant drawbacks, including the risk of inducing undesirable side effects, such as autoimmune, reactogenic, and allergic responses [11]. These adverse effects result from the administration of unnecessary and potentially harmful microorganism components and the presence of contamination from the pathogen culturing medium [12, 13]. Other disadvantages of traditional vaccines include: (1) the possibility of the attenuated pathogen to revert back to its virulent state, especially in immunocompromised individuals [14]; (2) the pathogen can shed to the environment during production or infect production personnel [13]; (3) difficulties in culturing certain pathogens in large quantities; and (4) the requirement for cold chain transport, which affects the cost of immunization programs [7]. The shortcomings of conventional vaccines have led to the emergence of subunit vaccines. These are often known as modern-day or non-living vaccines [2].

Subunit vaccines contain selected, purified fragments of a pathogen (used as an antigen) with preservatives and stabilizers [15]. Proteins, toxoids, peptides, polysaccharides, and virus sections may all be included as antigen in subunit vaccines [2]. There are many benefits to using purified antigens as vaccine components, including (1) low to no adverse reactions observed, even in immunocompromised individuals, due to the removal of the pathogenic features of the microorganism [15]; (2) high vaccine viability [11]; (3) relatively easy large-scale manufacturing and production; and (4) less demanding transport and storage conditions [5]. Nevertheless, subunit vaccines have disadvantages; one of which is that typical antigens are poorly immunogenic due to their lack of pathogenic components, which are needed to activate innate immunity [13]. Therefore, these vaccines require the use of an adjuvant (immune stimulator) and multiple immunizations (boosts) in order to induce strong, long-lasting immune responses [16].

2 Introduction to Adjuvants

The word adjuvant comes from the Latin word *ad* (“towards”) and *juvo* (“help”). Adjuvants have been incorporated into almost all recently developed vaccines (Table 1). The aims of adding adjuvant to a vaccine system are: (1) to enhance vaccine efficiency by increasing seroconversion rate in both the general and hyporesponsive populations (infants, immunocompromised, and elderly) [17]; (2) to reduce the amount of antigen/vaccine dosage and the number of immunizations needed to elicit a protective immune response [18]; and (3) to improve vaccine stability by making the vaccine less susceptible to degradation [17]. However, many of the adjuvants tested have limited potency, issues with formulation stability, are non-biodegradable, expensive to produce, and/or are not well-tolerated in the general population [8, 19]. They may also present safety issues and cause adverse side effects (local and systemic), especially those built from bacterial components [19, 20]. Additionally, adjuvants can present manufacturing difficulties in terms of formulation reproducibility (due to their complexity) and stability [21]. As a result, unfortunately, only a limited number of adjuvants have been approved, or even tested in clinical trials, for human vaccines (Fig. 1) [22].

Adjuvants were first discovered in the 1920s by Gaston Ramon, a veterinarian who was able to increase antibody production against diphtheria and tetanus. He injected a combination of lecithin, starch, and tapioca with inactivated diphtheria toxin, and achieved more effective antibody production [23]. Then, in 1926, Alexander Glenny and colleagues revealed that diphtheria toxoid precipitated with aluminum salts showed an improved immune response against the toxoid [24]. A few years later, aluminum salts were introduced as the first human adjuvant, and they were incorporated into vaccines against diphtheria, tetanus, and pertussis [23]. Conventionally, adjuvants were designed to form a depot of antigen at the injection site to allow its controlled release, mimicking local infection [25]. However, it is now known that they are able to trigger innate immunity by interaction with antigen-presenting cells (APCs) in order to direct the adaptive immune system to produce specific and effective immune responses against the antigen. Therefore, besides the depot effect, a variety of other adjuvanting mechanisms have been discovered and utilized to maximize adjuvant efficacy and reduce adverse effects [26–28].

Table 1
Approved adjuvants in human vaccines

Adjuvant	Vaccine for disease	Vaccine trade name	Vaccine type
Aluminum hydroxide	Anthrax	Biothrax	Subunit
	Diphtheria, tetanus toxoid, and acellular pertussis	Infanrix	Toxoid and inactivated
	Diphtheria, tetanus toxoid, and acellular Pertussis	KINRIX	Toxoid
	Hepatitis A	Havrix	Inactivated
	Meningococcal group C	Menjugate	Conjugate
	Meningococcal group C and tetanus toxoid	Neisvac-C	Conjugate
	Meningococcal group C CRM-197	Menjugate	Conjugate
	<i>Neisseria meningitidis</i> serogroup B	Bexsero	Recombinant
	Hepatitis A	Avaxim	Inactivated
	Hepatitis B	Engerix-B	Subunit
	Diphtheria, tetanus toxoids, acellular pertussis, hepatitis B (recombinant), Poliomyelitis (inactivated) and <i>Haemophilus influenzae</i> type b (adsorbed conjugated)	Infanrix-hexa	Subunit and inactivated
	Purified Vi polysaccharide typhoid and inactivated hepatitis A	ViVaxim	Subunit and inactivated
	Hepatitis B	GeneVac-B	Recombinant
	Hepatitis B <i>Japanese encephalitis</i>	Shanvac-B IXIARO	Recombinant Inactivated
Aluminum potassium sulfate	Anthrax	Anthrax vaccine precipitated	N/A
	Diphtheria and tetanus toxoid (DT)	No tradename	Toxoid and inactivated
	Diphtheria, tetanus toxoid, and acellular pertussis (DTaP)	Tripedia	Toxoid
	Tetanus and diphtheria toxoids (adsorbed)	Decavac	Toxoid
	Tetanus toxoid (adsorbed)	No tradename	Toxoid
Aluminum phosphate	Diphtheria, tetanus toxoid, and acellular pertussis (DTaP)	DAPTACEL	Toxoid
	Diphtheria, tetanus toxoids, acellular pertussis (adsorbed), poliovirus (inactivated) and <i>Haemophilus influenzae</i> type b (conjugate)	Pentacel	Subunit and inactivated
	Diphtheria, tetanus toxoids and acellular pertussis (adsorbed) combined with poliomyelitis (inactivated)	Quadracel	Subunit and inactivated
	Diphtheria, tetanus toxoids, acellular pertussis (adsorbed) and <i>Haemophilus influenzae</i> type b (conjugate)	Actacel	Subunit
	Tetanus toxoid, diphtheria toxoid (reduced) and acellular pertussis (adsorbed)	Adacel	Toxoid
	Tetanus toxoid, diphtheria toxoid (reduced) and acellular pertussis vaccine (adsorbed) combined with poliomyelitis (inactivated)	Adacel-Polio	Toxoid, subunit, and inactivated

(continued)

Table 1
(continued)

Adjuvant	Vaccine for disease	Vaccine trade name	Vaccine type
	Tetanus toxoid, diphtheria toxoid (reduced) and acellular pertussis (adsorbed)	Boostrix	Toxoid
	Diphtheria, tetanus and polio (adsorbed)	DT Polio (Adsorbed)	Subunit and inactivated
	Tetanus and diphtheria toxoids (adsorbed)	Td (Adsorbed)	Toxoid
	Tetanus and diphtheria toxoids (adsorbed) and poliomyelitis (inactivated)	Td Polio (Adsorbed)	Subunit and inactivated
	Tetanus toxoid (adsorbed)	No Tradename	Toxoid
	Pneumococcal 13-valent	Prevnar 13	Conjugate
	Meningococcal group B	TRUMENBA	Recombinant
	Tetanus toxoid and diphtheria (adsorbed)	TdVax	Toxoid
	Tetanus toxoid and diphtheria (adsorbed)	TENIVAC	Toxoid
Aluminum hydroxide and aluminum phosphate	Diphtheria, tetanus toxoid, acellular pertussis (adsorbed) and poliomyelitis (inactivated)	Boostrix-Polio	Toxoid, subunit, and inactivated
	Diphtheria, tetanus toxoid and acellular pertussis (adsorbed), hepatitis B (recombinant) and poliovirus (inactivated)	Pediarix	Toxoid and inactivated
	Hepatitis A and B	Twinrix	Inactivated
Amorphous aluminium hydroxyphosphate sulfate	<i>Haemophilus influenzae</i> type b	PedvaxHIB	Conjugate
	<i>Haemophilus influenzae</i> type b (meningococcal protein conjugate) and hepatitis B (recombinant)	COMVAX	Conjugate
	Hepatitis B	Recombivax HB	Subunit
	Hepatitis A	VAQTA	Inactivated
	Human papillomavirus quadrivalent (type 6, 11, 16, and 18)	Gardasil	Subunit
	Human papillomavirus 9-valent (type 6, 11, 16, 18, 31, 33, 45, 52, and 58)	Gardasil 9	Subunit
MF59	Influenza H5N1 (pre-pandemic)	Aflunov	Inactivated
	Influenza (trivalent)	Flud	Inactivated
	Influenza H1N1v	Focetria	Inactivated
AS04	Human papillomavirus bivalent (type 16 and 18)	Cervarix	Recombinant
AS03	Influenza H1N1 (pandemic)	AREPANRIX H1N1	Inactivated
	Influenza H1N1 (pandemic)	Pandemrix	Inactivated
CpG1018	Hepatitis B	HEPLISAV-B	Recombinant
AS01B	Varicella zoster	SHINGRIX	Recombinant

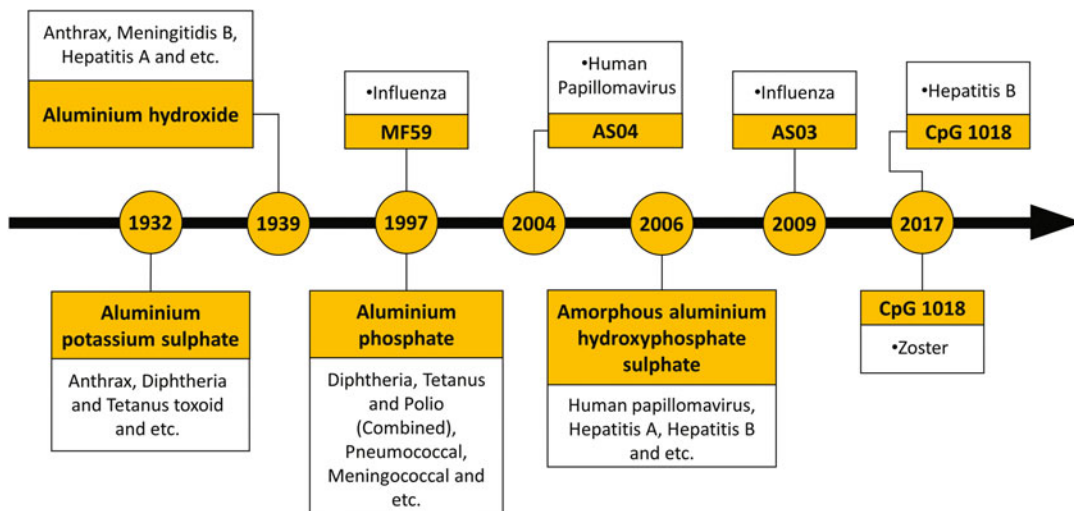


Fig. 1 Timeline of licensed adjuvants discovery

3 Adjuvants Used in Licensed Vaccines

3.1 Mineral Salt-Based Adjuvants

3.1.1 Aluminum Salts

Aluminum salt-based adjuvants (alum) were the first, and only adjuvants approved for use in human vaccines for over 90 years [29]. They have been used in vaccines containing inactivated, weakened, or killed pathogens to induce stronger immune responses [30]. Currently, alum is included in vaccines against diphtheria, tetanus, pertussis, hepatitis A and B, Japanese encephalitis, human papillomavirus (HPV), and many more [31]. Despite the singular term, “alum,” many versions of this adjuvant system exist [32]. Aluminum hydroxide was the first vaccine adjuvant introduced, followed by aluminum phosphate; incidentally, these still remain as the major forms of alum used for human vaccines [33].

Two methods are employed for alum preparation: (1) in situ precipitation of aluminum compounds in the presence of antigens, and (2) adsorption of antigens onto preformed aluminum gel/particles; the latter is the preferred method as it provides a more reproducible formulation [32, 34]. Adsorption of antigen to alum forms nanoparticles. Aluminum hydroxide adjuvant (AH) has elongated nanoparticles ($4 \times 2 \times 10$ nm), while aluminum phosphate adjuvant (AP) forms plate-like particles with a diameter of 50 nm [35]. The adsorption of antigens to alum salt occurs through electrostatic, hydrophobic, or ligand exchange mechanisms, to name a few, depending on the physicochemical properties of the antigen [32, 36]. Manufacturing alum adjuvant is not a simple process; therefore, a standard was created, Alhydrogel[®], to prevent the production of batch disparities and non-reproducibility from

using different aluminum compounds [37]. In addition, Rehydrgel[®] and Adju-Phos[®] were created to match differences in the charge of antigens [38]. Among all of the different alum forms, three have been clinically approved: (1) aluminum oxyhydroxide-based Alhydrogel[®], (2) aluminum hydroxyphosphate-based Adju-Phos[®], and (3) amorphous aluminum hydroxyphosphate sulfate adjuvant, which is used in the vaccine against HPV [39, 40].

The mechanism of alum adjuvanticity was first described in 1926 by Alexander Glenny and colleagues, who suggested that alum forms a “depot” effect [16, 24]. They observed higher antibody production in guinea pigs injected with precipitate of the toxoid and aluminum potassium sulfate compared to those administered with just the toxoid [41]. Adjuvants’ mechanisms of action of are often explained by their interactions with APCs [41]. It has been found that alum functions through intracellular pattern recognition receptors present on APCs and NOD-like receptors (NLRs). NLRs increase pro-inflammatory cytokine production (interleukin-1 β (IL-1 β) and interleukin-18 (IL-18)) [42, 43], induce the recruitment of immune cells (neutrophils, eosinophils, monocytes, and dendritic cells (DCs)) to the injection site, increase the expression of MHC class II (major histocompatibility class II) [44], and increase the production of antigen-specific IgG1 [42, 45]. Alum also interacts with cell membrane lipids, which activates signaling pathways, such as PI3-K (phosphoinositide 3-kinase) [46] and calcineurin-NFAT (nuclear factor of activated T-cells) [47], and leads to the secretion of cytokine, IL-2 (interleukin-2) [33, 48]. Furthermore, alum triggers the release of DAMPs (danger-associated molecular patterns), such as uric acid [49], and host DNA by producing necrotic cells at the site of injection [50, 51].

Alum can activate humoral and (rather weak) cellular immune responses [52–54]. It is inexpensive and effective and has been incorporated into many licensed vaccines that are administered to millions of people annually. However, it also induces side effects, which include skin irritation (formation of granulomas) at the site of injection and allergic reactions (increased production of immunoglobulin E responses (IgE)) [19, 55]. Alum’s high efficacy is limited to whole pathogen-based vaccines, as it is a relatively weak immune stimulator for subunit vaccines [29]. Unsurprisingly, therefore, the development of modern vaccines built based on pathogen fragments has triggered the search for stronger alternative adjuvants.

3.1.2 Calcium Phosphate

Calcium phosphate (CAP) was developed by the Pasteur Institute in the hydroxyapatite form ($\text{Ca}_{10}(\text{PO}_4)_6(\text{OH})_2$), but was initially described as tricalcium phosphate ($\text{Ca}_3(\text{PO}_4)_2$) in the patent filed in 1975 [56]. The formulation was used as an adjuvant for diphtheria, pertussis, tetanus, and polio vaccines, but was later substituted by

alum in the 1980s. However, CAP still remains as an approved adjuvant by WHO for human vaccines [56, 57]. Like with alum, there are two methods for preparing CAP: (1) in situ co-precipitation of disodium hydrogen phosphate, calcium chloride, and antigen to form a gel or (2) direct absorption of antigen onto preformed gel [58]. Commercial CAP has a mean particle size distribution of 40 nm to 5 μ m, but in fact particles between 100 and 400 nm are responsible for the main immune-stimulating properties [59]. There are many other forms of CAP, depending on the ratio of calcium and phosphate ions (Ca:P ratio) [58, 60]. Additionally, the quality of the gel depends on the concentration and mixing rate of the reactants, which in turn affects the physicochemical characteristics and adsorption of the antigen onto the gel [56]. The adsorption capacity of the antigen can be affected by charge, the presence of a hydroxyl group [61], and surface area [62]. The adsorption of antigen onto CAP can occur through electrostatic interaction, ligand exchange, or hydrophobic attractive forces, similar to alum salts [61, 63].

Calcium phosphate was initially developed as a substitution for alum-based adjuvants, mostly due to the safety concerns with using alum salts in vaccines. However, it failed to replace popular alum-based adjuvants, and therefore, no intensive mechanistic studies were performed on CAP [56]. However, it was demonstrated that (1) CAP forms a depot effect and triggers a balanced Th1/Th2 immune response [64]; (2) CAP particles of 100–400 nm elicited higher antibody production than larger particles [62]; and (3) CAP can activate NLRP-3 inflammasomes, which are protein complexes responsible for initiating cell death and the release of pro-inflammatory cytokines (e.g., IL-1 β) by macrophages [65, 66].

3.1.3 AS04

AS04 is considered to be an adjuvant system, as it contains more than one adjuvant. It consists of 3-*O*-desacyl-4'-monophosphoryl lipid A (MPLA) adsorbed on aluminum hydroxide or aluminum phosphate. The clinical grade form of AS04 is known as MPL adjuvantTM [67]. MPLA is a mixture of monophosphorylated lipopolysaccharides derived from *Salmonella minnesota* endotoxin—particularly its lipid A fragment [68]. In the 1970s, Edgar Ribi modified lipid A chemically to form MPLA by removing one phosphoryl moiety to retain most of the immunomodulatory properties while reducing the toxicity by 1000-fold [68, 69]. MPLA is recognized by toll-like receptor 4 (TLR-4) and has the ability to induce both humoral and cellular immune responses and promote the stimulation of Th-1-type T-helper cells [70]. AS04 has been approved for use as an adjuvant for human papillomavirus (HPV) (CervarixTM) and hepatitis B virus (HBV) (FENDrixTM), both developed by GlaxoSmithKline [67].

FENDrix™, which contains HBV surface antigen produced in *Saccharomyces cerevisiae* (HBsAg), was created to improve the efficacy of HBV alum-based vaccine (Engerix-B™) in immunocompromised populations [71]. The vaccine, adjuvanted with AS04, induced the production of long-term protective antibodies and enhanced cell-mediated immune responses after fewer vaccinations than the alum-adjuvanted HBV vaccine [71, 72]. Cervarix™ contains HPV-type 16 and 18 major capsid protein, L1, as antigen with AS04 as the adjuvant [67]. The vaccine elicits a long-term immune response and high levels of functional antibodies in female subjects 10–55 years old. It has been shown to provide 100% protection against persistent HPV infections (type 16 and 18) [73, 74] and was also 100% effective in preventing the manifestation of HPV-related precancerous lesions [75]. Additionally, AS04 was used as an adjuvant for vaccines against herpes simplex virus (HSV), respiratory syncytial virus (RSV), and Epstein–Barr virus (EBV) [67].

3.2 Emulsion-Based Adjuvants

The word emulsion describes the dispersions of immiscible phases of two liquids (usually oil and water). There are two types of emulsion, water in oil (W/O) and oil in water (O/W). Emulsions are unstable; they require the use of a surfactant to stabilize the mixture by forming a more rigid film at the interface [76]. There are two commonly used surfactants, polysorbates (e.g., Tween 20), used for O/W emulsions, and sorbitan esters (e.g., Span 20), used for W/O emulsions [77]. The physicochemical characteristics of emulsions rely on droplet size and the viscosity of the mixture, which is controlled by the type and concentration of surfactant used, the ratio of the dispersed phases, and the method of emulsion preparation. Stability, sterility, and viscosity are important parameters to consider for the use of emulsions as adjuvant [78].

An emulsion was used for the first time as an adjuvant in the 1930s; Jules Freund developed Freund's complete adjuvant (CFA), which is a W/O emulsion [79]. CFA consists of paraffin oil combined with heat-killed *Mycobacterium tuberculosis*. It is a highly effective “gold standard” adjuvant, but it is also highly toxic and reactive as it commonly induces the formation of granulomas, abscesses, and necrosis at the site of immunization [80]. Therefore, CFA was never approved for general human use. Freund's incomplete adjuvant (IFA) was subsequently developed in an effort to reduce the toxicity through the omission of bacterial material [80]. IFA was first used in influenza vaccines tested in animals in 1950s. It triggered higher and long-lasting antibody production in comparison to non-adjuvanted vaccine formulation [81]. However, IFA still produced severe side effects when used in human vaccines, so ultimately was approved only for veterinary purposes [80].

IFA further evolved into Montanide ISAs, a class of well-tolerated adjuvants that enhance antigen-specific cytotoxic

T-lymphocyte (CTL) responses. They convey relatively minor side effects of local discomfort at the site of immunization, fever, headache, and flu-like symptoms [82]. Montanide ISA™ 51 is a mixture of mineral oil and mannide monooleate surfactant [83]. The mineral oil causes the vaccine to stay at the injection site, with approximately just 30% of the oil dissolving during the first month after immunization [84]. It has been used in clinical trials for vaccines against malaria [83], human immunodeficiency virus (HIV), and influenza [84]. It has also been licensed for lung cancer therapeutic vaccine in Cuba [85]. Montanide ISA™ 720 comprises non-mineral vegetable oil and mannide monooleate surfactant. The oil is well-tolerated and can be easily metabolized and eliminated from the injection site; however, it induces weak and transient inflammation [82]. It has been used in vaccine trials for malaria [86] and AIDS [84].

3.2.1 MF59

MF59 is an O/W emulsion that consists of squalene oil (a naturally occurring component of certain plants and animals), two surfactants (Tween 80 and Span 85, commonly sourced from plants), and citrate buffer (trisodium citrate and citric acid). Therefore, it is biodegradable and biocompatible [77, 78]. MF59 is an altered version of IFA and CFA emulsions. There are two generations of MF59, which differ by the presence of citrate emulsion stabilizer. The individual components of MF59 do not induce an immune response, but combined, the emulsion is immunostimulatory [87].

Initially, antigen depot at the site of injection was considered to be the MF59 mechanism of action [88, 89]. However, similar to alum, this was recently refined. First, at the site of injection, MF59 activates resident immune cells (monocytes, macrophages, and DCs), which results in the production of a gradient of chemokines (CCL4, CCL2, CCL5, CXCL8). More phagocytic immune cells are then recruited, increasing antigen uptake to the lymph nodes. MF59 also upregulates the differentiation of monocytes to DCs and facilitates the migration of naïve T cells to draining lymph nodes [76, 82, 90].

MF59 was introduced in 1977; it was the first approved novel adjuvant since alum, 70 years earlier [87]. In preclinical mouse trials, influenza vaccine adjuvanted with MF59 showed full protection against intranasal influenza challenge at a lower antigen dose [76]. It was approved as an adjuvant for influenza vaccine for the elderly (≥ 65 years), and marketed as FLUAD® (Novartis Vaccines and Diagnostics Inc., MA, USA). While first licensed in Italy, it is now available in 30 countries [76]. MF59 is used as an adjuvant for seasonal trivalent influenza vaccines (TIVs) based on clinical trials composed of 20,000 elderly subjects. These showed that MF59-adjuvanted vaccine was more immunogenic and better-tolerated than non-adjuvanted vaccine. MF59 was also approved for use in individuals as young as 6 months during the H1N1 pandemic [91].

MF59 has an excellent safety profile; it has shown no sign of inducing autoimmune syndromes, chronic diseases, neurological conditions, or death [92]. Furthermore, vaccines adjuvanted with MF59 reduced the incidence of hospitalization for elderly individuals with pneumonia, acute coronary syndrome, or cerebrovascular syndrome at the peak of virus circulation [93]. A more recent large, randomized study ($n = \sim 170,000$ individuals) on MF59-adjuvanted flu vaccine demonstrated a 23% reduction in influenza- and pneumonia-related hospitalization rates in individuals 65 years and older [94].

In addition to influenza, MF59 has been tested in preclinical trials for a range of other vaccines, including HIV, HSV, and HBV [95]. However, Phase III trials on MF59-adjuvanted vaccine against HSV-2 infection failed to demonstrate protective efficacy of the vaccine [96]. MF59-adjuvanted HIV and HBV vaccines induced the production of high levels of antigen-specific antibody titers; however, no vaccine emerged from these studies [97, 98].

3.2.2 AS03

AS03 is an O/W emulsion-based adjuvant (≤ 200 nm) composed of two biodegradable oils, squalene and D,L- α -tocopherol (a form of vitamin E), and polysorbate 80 surfactant [99]. Thus, AS03 differs from MF59 by the presence of D,L- α -tocopherol. The addition of the novel oil to the emulsion resulted in the generation of higher antibody responses [82]. D,L- α -Tocopherol also modulated the expression of cytokines (CCL2, CCL3, CSF3, CXCL1) and enhanced antigen loading by monocytes [100]. AS03 is used as an adjuvant for monovalent influenza vaccines, H1N1 vaccines (Pandemrix™ and Arepanrix™), and H5N1 vaccines (Q-Pan H5N1 and Prepandrix™, or Pandemic Influenza Vaccine) developed by GlaxoSmithKline Biologicals. It was licensed in Europe in 2009 and also used for the pre-pandemic H5N1 influenza vaccine developed for the pandemic preparedness effort. When the H1N1 pandemic was declared in 2009, AS03 was chosen as an adjuvant for the H1N1 vaccine [101, 102].

The pre-pandemic influenza vaccine (Prepandrix™) contained H5 hemagglutinin (surface glycoprotein) with the flu strain A/VietNam/1194/2004 (H5N1)-like strain (NIBRG-14) adjuvanted with AS03 [103]. A randomized trial administered two doses of the vaccine to volunteers (18–60 years) 21 days apart. The adjuvanted vaccine was more immunogenic than the non-adjuvanted vaccine, and lower H5N1 antigen doses were able to induce significant antibody titers against the virus, and these titers exceeded immunogenicity licensing criteria [104, 105]. Similar results were observed in nonclinical models, such as mice and ferrets [99, 106]. AS03-adjuvanted H5N1 vaccines were also assessed in elderly populations (61–88 years) and showed higher seroprotection rates in individuals immunized with

adjuvanted vaccines compared to nonadjuvanted vaccines [107]. Similar studies were performed with the H1N1 version of the vaccines Pandemrix™ and Arepanrix™, which showed high efficacy in adults and children. As of 2018, only Q-Pan H5N1, Prepandrix™, and AS03-adjuvanted influenza vaccines are still in use, while other flu vaccines are nonadjuvanted or use alum [108].

AS03 has also been used in malaria and HIV vaccines. In a challenge trial with malaria-naïve individuals, AS03-adjuvanted vaccine was able to postpone the onset of malaria after the challenge [109, 110]. When the adjuvant was tested with HIV vaccine, it was able to elicit potent neutralizing antibodies. However, further observation indicated that other adjuvants (e.g., AS02 and AS01, discussed in detail below) elicited greater cellular immune responses than AS03; therefore, AS03 was not chosen for further development [111–113].

3.3 Liposome-Based Adjuvants

Liposomes were discovered in the 1960s by Alec Bangham and have been intensively researched as a drug delivery system ever since [114]. They were first described as a lamella of swollen lipids with the ability to act as a model membrane system [115]. Liposomes are spherically shaped amphiphilic lipid bilayer vesicles (20 nm to 10 µm) with an aqueous core. They possess a unique ability to entrap a range of compounds, allowing them to act as a carrier system [116, 117]. Hydrophobic compounds can be implanted within the lipid bilayer, while hydrophilic compounds are encapsulated within the core of the vesicles [118]. The physicochemical properties of liposome vesicles—shape, size, surface charge, permeability, and stability—rely on the lipids used in preparation. These properties, in turn, affect antigen loading and release, biological behavior, and the ability to act as a drug/vaccine delivery system [119, 120]. Delivery systems based on liposomes can significantly increase a formulation's therapeutic index, stability, and absorption, while reducing toxicity and prolonging the biological half-life of the encapsulated compound [117, 118].

Liposomes are one of the most widely investigated self-adjuvanting vaccine delivery systems [121]. Antigens encapsulated within the liposomes are protected against degradation in vivo and are preferably taken up by APCs. Following liposome endocytosis, antigen is accumulated, processed, and presented on MHC class II molecules. This results in the activation of CD4+ T-cells, B-cells, and the production of antigen-specific antibodies. However, certain types of liposomes allow antigen to escape from endosomes to the cytoplasm, or they deliver antigen directly to the cytoplasm. This results in the presentation of processed antigen to MHC class I molecules, and the stimulation of CTLs. Thus, liposomes have the capacity to induce both humoral and cellular immune responses [119, 122, 123].

3.3.1 Virosomes

Virosomes were first described by Almeida and colleagues in 1975 as liposomes modified with influenza surface proteins (haemagglutinin and neuraminidase) [124]. Influenza virus was the first virus used in the preparation of a virosome formulation, but over the years, other enveloped viruses have been utilized, including sendai virus, vesicular stomatitis virus, Epstein–Barr virus, HIV, respiratory syncytial virus, and HSV [125–127]. Virosomes, in the same manner as classical liposomes, have the ability to encapsulate a wide range of antigens, which includes peptides, protein, carbohydrates, and nucleic acids [128, 129]. Virosome vesicles possess similar structure and versatility to liposomes, but can fuse with cellular membranes far more effectively due to the presence of viral membrane proteins. Virosomes can be prepared *in vitro* in three steps: (1) dissolving the inactivated and purified virus in detergent; (2) separation of the envelope fraction of the virus (containing the membrane viral proteins) from the internal proteins and genetic materials; and (3) removal of the detergent, which triggers the formation of the empty membrane vesicles [125, 130]. Phospholipids are often added to the solubilized envelope fraction of the virus to produce robust and scalable particles and minimize the loss of the viral proteins during step 3 [124, 131]. Virosomes were found to be stable when stored at 2–8 °C. They can maintain their fusion activity at a broad range of temperatures, and lyophilization of the particles has been shown to stabilize the encapsulated antigens [129, 132]. The physicochemical properties of virosomes can be moderated by the amount and type of phospholipids used in the formulation [123, 133, 134]. Like in liposomes, antigen placement affects the immune response produced. When the antigen of interest is (1) displayed on the surface of the vesicle (anchored to the lipid bilayer), the antigen is presented to B-cells inducing antibody production, or (2) encapsulated in the core/lumen, it is delivered to APC cytoplasm and presented on MHC class I, resulting in the activation of CTLs [132, 135, 136]. In both cases, antigen is also processed through the endosomal pathway and presented by T-helper cells. Despite the use of different enveloped viruses in the formulation of virosome vesicles, only influenza virosomes are approved for use in human vaccines (Epaxal™ for hepatitis A virus (HAV), and Inflexal™ V and Nasalflu™ for influenza virus) [119, 130].

Historically, vaccines against HAV, including Havrix™, Vaqta™, and Avaxim™, used inactivated HAV adsorbed onto alum adjuvant (aluminum hydroxide) [137]. In 1994, a new strategy was introduced by Crucell, in which HAV antigen (formalin-inactivated and purified HAV virions) was adsorbed to the surface of the virosome producing Epaxal™ [138]. A single dose of Epaxal™ displayed 98–100% seroprotection rates in adults (≤ 50 years) [139]. Lower immune responses were observed in older

individuals (60–73 years) [140, 141]. In children and infants, 2 doses of the vaccine provided 100% seroprotection against HAV [142, 143].

A similar vaccine was created against influenza. Inflexal™ V contains a virosomal preparation of three virus strains (H1N1, H3N2, and B) and is delivered with the help of virosomes [131]. The vaccine was shown to be effective, safe, and well-tolerated in children [144, 145], adults [144], the elderly [146–148], and immunocompromised individuals [149, 150]. Nasalflu™, marketed in 2000 by Berna Biotech, was also developed as a virosomal influenza vaccine. The vaccine contained two strains of influenza A and B (inactivated and purified), grown individually in fertilized hen eggs, and heat labile toxin derived from *Escherichia coli* as an additional mucosal adjuvant [130, 151]. However, the vaccine was withdrawn from use due to the association of the heat labile toxin with Bell's palsy [152].

3.3.2 AS01

AS01 is a liposome-based adjuvant containing two immunostimulants (MPLA and QS-21). The standardized form of AS01 consists of liposomes (containing dioleoyl phosphatidylcholine (DOPC) and cholesterol), MPLA, and QS-21 with vesicle size ranging between 50 and 100 nm [153, 154]. QS-21 is a derivative of the saponin, QuilA (isolated from the bark of *Quillaja saponaria* Molina, a tree found in South America) [155]. QS-21 alone induced high antigen-specific antibodies [156], CD8+ T-cell responses [157, 158], cytotoxic T-lymphocytes (CTLs), Th1 cytokines, the production of cytokines (IL-2 and IFN- γ), and equal production of IgG1 and IgG2a [158–160] when tested in mice. As an adjuvant, AS01 induces the activation of APCs, especially DCs and monocytes; the presence of MPLA and QS-21 results in increased antigen-specific responses. AS01 showed increased cellular immune responses and induced antibody isotype switching through the activation of the interferon (IFN) cell signaling pathway [156, 161, 162]. Furthermore, it was observed that AS01-adjuvanted vaccines increased the production of antigen-specific antibodies and CD4+ T-cell responses [163]. AS01 is used as an adjuvant vaccines against malaria (RTS, S/AS01 or Mosquirix™) and shingles (HZ/su or SHINGRIX™) [102].

RTS,S/AS01 vaccine contains fused antigen: a fragment of *Plasmodium falciparum* protein fused to HBsAg, encapsulated in AS01_E (containing 25 μ g of MPLA and 25 μ g of QS-21) as the adjuvant [102]. In a study with rhesus monkeys, AS01-adjuvanted vaccine was able to elicit higher levels of RTS,S-specific antibodies and high levels of IFN- γ -producing cells compared to AS02 adjuvant (O/W emulsion with MPL and QS-21), indicating improved T-cell response [164]. In Phase III clinical trials, three doses of RTS,S/AS01 reduced infection and increased CD4+ T-cell

responses in infants (6–12 weeks old) and toddlers (5–17 months) from seven sub-Saharan African countries [165]. When AS01 was tested with a specific merozoite stage surface protein (MSP1), it induced high levels of Th1-biased antibody responses [166].

In 2006, Zostavax™ (live-attenuated vaccine) was made available to prevent varicella-zoster virus (VZV) infections in adults (≤ 50 years), but its protective efficacy decreases with age [167]. SHINGRIX™ was developed as a result. It consists of glycoprotein E (gE) from VZV and AS01_B (containing 50 μg of MPLA and 50 μg of QS-21) [168]. The vaccine was able to prevent the reactivation of shingles for up to 4 years post-vaccination (vaccine efficacy: 97% in ≥ 50 years and 90% in ≥ 70 years) in clinical trials [169]. It induced strong and long-lasting IgE-specific antibodies (humoral immune responses) and the production of CD4+ T-cells expressing pro-inflammatory cytokines (IFN- γ , IL-2, TNF- α) [169, 170].

3.4 Virus-Like Particles (VLP) as Adjuvants

Virus-like particles (VLPs) are viral structural proteins that self-assemble into particles. These particles (20–200 nm) mimic the geometric arrangement of the native virus, but do not contain any of the viral genetic material and, therefore, cannot be infectious [172]. VLPs have the ability to encapsulate and deliver many different molecules, including siRNA, RNA, proteins, and peptides [173]. Alternatively, VLP structural proteins can be modified with desired antigen sequences. VLPs are produced through gene expression systems (e.g., bacteria, yeast, mammalian cells, plant cell culture) via recombinant DNA technology [174, 175]. The structure resembles microbial (especially viral) antigen presentation, with repetitive displays of the antigen, which is easily detected by the mammalian immune system. Strong B- and T-cell responses are produced as a result [176, 177]. VLPs trigger immune responses in a similar manner to virosomes.

The first VLP-based vaccine was produced in 1981 by Kleid and colleagues by cloning the polypeptide (VP3) from foot-and-mouth disease virus in *Escherichia coli* as a vaccine for animals [178]. VLP-based vaccines have been acknowledged as highly effective, safe, and scalable for mass production [175]. Today, there are several licensed VLP-based vaccines for HBV (Engerix-B™, Recombivax HB™, GenHevac B™, FENDrix™), HPV (Gardasil™, Gervarix™), hepatitis E virus (HEV) (Heclin™), and influenza (Inflexal™, Epaxal™) [179]. VLPs can be considered as a delivery system, carrier, or adjuvant and are often administered with an additional adjuvant (e.g., Engerix-B™ with alum, Cervarix™ and FENDrix™ with AS04, and Inflexal™ and Epaxal™ as virosomes).

3.5 Toll-Like Receptors Agonists as Adjuvants

Toll-like receptors (TLR) were first identified in the 1990s as a type of pattern recognition receptor (PRR). PRR functions as the first line of defense against pathogens, as they recognize the molecular signatures found on the microbes [180]. TLRs are highly conserved across different species, and they are closely involved in the activation of innate immune responses. There are several human TLRs that recognize different ligands/agonists, such as TLR3 (which recognizes double-stranded RNA), TLR4 (bacterial lipopolysaccharides), TLR5 (bacterial flagellin), TLR7&8 (single-stranded RNA), and TLR9 (CpG DNA motifs) [181]. Several TLR agonists have been tested as vaccine adjuvants in humans. For example, MPLA, a TLR4 agonist, has been incorporated as a component of several of the adjuvants described above.

3.5.1 Cytosine Phosphate Guanosine Oligodeoxynucleotides

Cytosine phosphate guanosine (CpG) oligodeoxynucleotides (ODN) are short, single-stranded synthetic DNA molecules. CpG motifs are often observed in bacterial and viral DNA, and recognized by TLR9 [182]. TLR9 is localized in the cytoplasm, and, therefore, is associated with cellular immune responses and the MHC I/Th1 activation pathway [183]. Moreover, CpG ODNs directly activate B-cells and plasmacytoid dendritic cells due to their interaction with TLR9 [184]. CpG ODN triggers the expression of proteins (MHC, CD40, CD86, pDCs), in turn increasing antigen presentation and processing [185], induces the production of IFN- γ , and strongly activates CTLs [186], but also induces antigen-specific humoral immune responses [183, 187].

CpG ODN 1018 (5'-TGACTGTGAACGTTTCGAGATGA-3') was the first TLR agonists-based adjuvant approved for HBV. The product, HEPLISAV-B™, is comprised of HBsAG and CpG ODN 1018 in liquid form (20 μ g HBsAG and 3 mg CpG1018) [183]. This vaccine was compared with the older alternative, Engerix-B™, in clinical trials. All (100%) of the HEPLISAV-B recipients produced protective antibodies against HBV antigens 1 week after the second dose and long-lasting seroprotection against HBV, regardless of age [188, 189]. Meanwhile, individuals that received Engerix-B™ required a third dose to show protective antibody responses [190]. HEPLISAV-B™ was also able to induce high seroprotective rates in smokers, obese individuals, and individuals vulnerable to HBV infection (chronic kidney disease patients), who are known to be hypo-responsive to Engerix-B™ [191–193]. However, there is some concern that CpG motifs could promote autoimmune reactions, which was highlighted in a clinical trial for HBV vaccine when one of the participants developed Wegener's granulomatosis, an autoimmune disease caused by inflammation of the blood vessels [194].

4 Other Adjuvants

In addition to the adjuvants detailed above, a large number of other adjuvants are being developed or are undergoing preclinical investigation (Fig. 2). This is the result of the high demand for new adjuvants that are nontoxic, well-tolerated in the general population, have high potency and provide long-lasting immune responses, preferably after a single dose.

Saponins are natural glycosides of the steroid triterpene with a diverse range of pharmacological effects. These include anti-inflammatory, antitumor, immunomodulatory, and antiviral activity, among others [159]. QuilA, a well-known saponin, is a heterogeneous mixture of saponins with 23 different saponin peaks detectable on RP-HPLC. QuilA can stimulate both humoral and cellular immunity, but is mostly used for veterinary vaccines and in preclinical trials because it is highly toxic and, therefore, not suitable for human vaccines. However, QuilA has been used in co-formulation with aluminum salts, liposomes, emulsions, and immunostimulatory complex (ISCOMS), which has reduced its

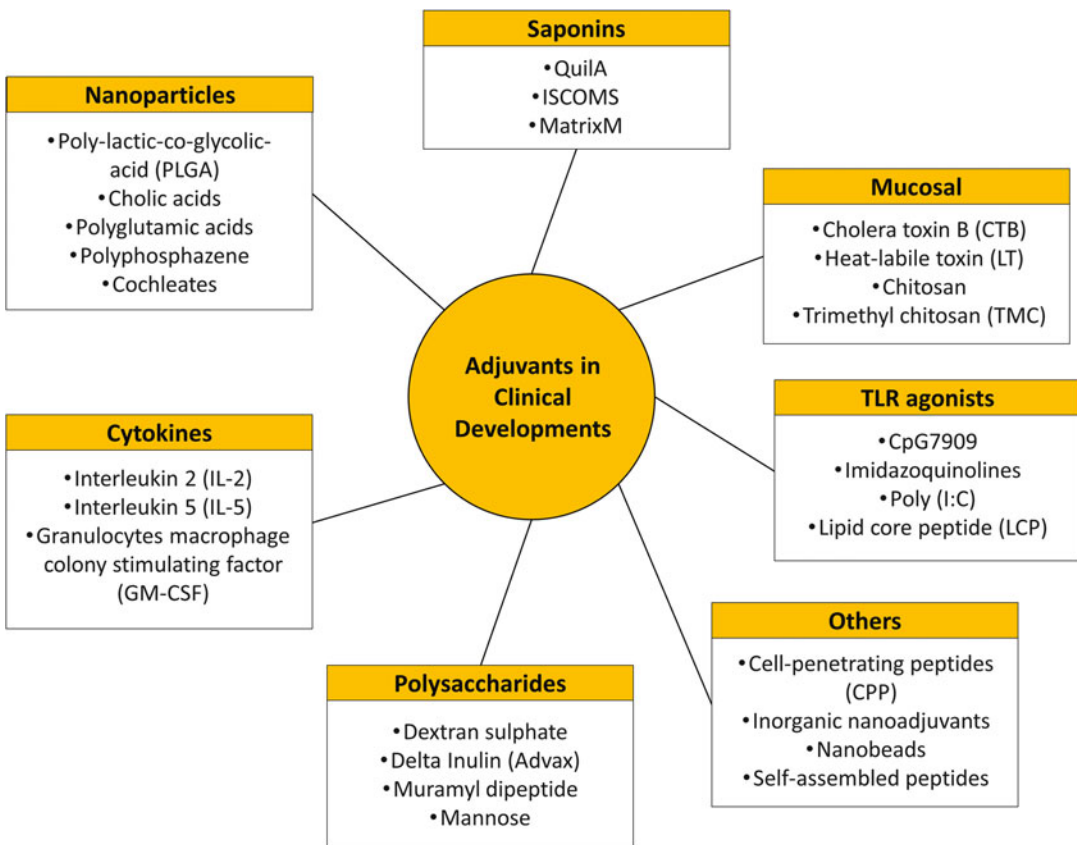


Fig. 2 Examples of adjuvants in preclinical developments

toxicity [153]. ISCOMATRIX[®] is a particulate antigen delivery system (40 nm) composed of phospholipids, cholesterol, and saponin (QuilA); upon antigen incorporation, it is known as ISCOM [195]. ISCOM produces strong antigen-specific humoral and cellular immune responses in animals and is typically more immunogenic than liposomes and micelle-based systems [196]. These delivery systems have been used in vaccines against bacteria (*Helicobacter pylori*, *Mycobacterium tuberculosis*, *Streptococcus pyogenes*), parasites (*Neospora caninum*, *Toxoplasma gondii*), and in cancer immunotherapeutics [197]. Matrix MTM, a system derived from ISCOM, is a homogenous mixture of stable nanoparticles consisting of semi-purified and fractionated saponins [82]. Matrix M has been used in clinical trials for pandemic influenza vaccine [198] and seasonal influenza vaccines for older populations (65–75-year-olds) [199].

Many other TLR-based adjuvants exist (than mentioned in previous section), but have not been applied in human applications. For example, CpG 7909 (PF-3512676 or ODN2006), a 24-mer-B-Class CpG ODN and known TLR9 agonists, can induce the production of TNF- α and stimulate and proliferate B-cells to induce the production of IgM [180]. It has been used in vaccines for anthrax, influenza [201], HBV [200], and cancer immunotherapeutics (melanoma) [202]. Imidazoquinolines are structures that mimic single-stranded RNAs (ssRNAs) and are recognized by TLR7/8. They can activate Th1 cellular responses to aid in viral clearance and stimulate the proliferation of B-cells to induce the production of antibodies and pro-inflammatory cytokines [80]. Imiquimod (R837) has been approved in experimental vaccines against influenza, HBV, and varicella zoster [80]. Additionally, Resiquimod (R848) was examined in clinical trials to treat lesions formed from herpes simplex virus (HSV) infections [203] and in prophylactic vaccines against allergic rhinitis, HBV, and influenza [80]. Flagellin, the main component of bacterial flagella, which is recognized by TLR5, was incorporated into a vaccine against *Yersinia pestis*, a bacterium that causes the plague, and influenza vaccines [204]. Poly (I:C) (polyinosinic-polycytidylic acid) is a synthetic double-stranded RNA (dsRNA) recognized by TLR3 [80]. It has been used in clinical trials for vaccines against HIV [205], dengue [206], and malaria [207]. Poly-IC₁₂U, a derivative of Poly (I:C), was developed to overcome the toxicity issues related to Poly (I:C) [80]. It has been used in clinical trials for HIV vaccines [208], chronic fatigue syndrome (CFS) [209], and cancer immunotherapeutics [210]. TLR2 agonists Pam2Cys (dipalmitoyl-S-glyceryl cysteine) and Pam3Cys (tripalmitoyl-S-glyceryl cysteine) stimulated both humoral and cellular immune responses [7]. They have been used in preclinical trials for vaccines against tuberculosis (TB) [211] and group A streptococcus (GAS) [212]. Lipid core peptide (LCP), a system that mimics Pam2Cys/Pam3Cys and is

recognized by TLR2 [213], has been extensively studied in experimental vaccines against GAS [214], hookworm [215], *Chlamydia trachomatis* [216], and *Schistosoma* [217]. Glucopyranosyl lipid adjuvant (GLA), the analog of Lipid A, a TLR4 agonist, can encapsulate various biologically active agents, such as DNA and fatty acids, and can increase both humoral and cellular immune responses [82]. GLA was included in vaccine formulations against pandemic influenza (H5N1) [218], HIV [219], TB, schistosomiasis, and leishmaniasis [220].

Polysaccharides are naturally occurring polymers consisting of carbohydrate monomers that are glycosidically linked. They can be recognized by carbohydrate receptors (C-type lectins) present on APCs. As an adjuvant, they activate B- and T-lymphocytes, macrophages, and natural killer (NK) cells, and elicit antigen-specific immune responses [21]. For example, dextran sulfate derived from *Saccharomyces cerevisiae* was reported to induce lymphocyte proliferation, increase the production of IL-2 and IFN- γ , and enhance antibody titers in the serum against Newcastle disease [221]. β -Glucan, a biologically active compound with antitumor and anti-infection activity, can be recognized by TLRs, dectin-1, and complement receptor 3 (CR3) [222]. It has been used experimentally, where it helped to provide protection against infection with *Candida albicans* [223], *Staphylococcus aureus* [224], *E. coli* [225], and *Bacillus anthracis* [226]. Acetal dextran (Ac-DEX) was used as a delivery system to encapsulate imiquimod. It increased the potency of the TLR agonist and induced the production of pro-inflammatory cytokines (IL-1 β , IL-6, TNF- α) [227]. Delta inulin (AdvaxTM), a polysaccharide found in fruits and vegetables [228], increased antigen presentation, stimulated a balanced Th1 and Th2 immune response, increased the production of antibody titers against influenza [229], Japanese encephalitis virus [230], *Mycobacterium tuberculosis* [231], HIV [232], HBV [233], and West Nile virus [234]. Muramyl dipeptide (MDP), a component of peptidoglycan, which can activate nucleotide-binding oligomerization domain-containing protein 2 (NOD2), and increased the production of pro-inflammatory cytokines and the secretion of nitric acid [235]. It was used in a clinical trial as a part of a HIV vaccine [236]. Mannose monosaccharide can be used as a conjugate with antigen, or as part of a delivery system (liposomes and nanoparticles). It effectively activates innate immunity and stimulates Th1 and Th2 immune responses [222]. It has been used in experimental studies for vaccine candidates against malaria [237], TB [238], HIV [239], group B streptococci (GBS), leishmaniasis, *N. meningitidis*, and cancer [240]. The linear mucopolysaccharide, hyaluronic acid (hyaluronan, HA), has mainly been used for transdermal immunization, as it can bind to HA receptors, dermal DCs, and TLR 2 and 4 [241]. It has been used in vaccines against HBV [242], *Yersinia pestis* [243], and as transdermal immunotherapy for

Duchenne's muscular dystrophy [244]. Upon conjugation with antigen, nontoxic and biocompatible polyacrylates, which have often been used in biomedical applications [245], can self-assemble into nanoparticles. These constructs have been utilized for vaccine delivery against influenza [246], HIV [247], GAS [248], and HPV [249].

Nanoparticles are structures composed of polymers, lipids, and peptides. They can be pre-formed or self-assembled, and act as delivery systems for subunit vaccines [250, 251]. Extensive investigation has shown that the immune responses resulting from nanoparticle vaccination are particle-size-dependent [252]. For example, it has been shown that small nanoparticles (<100 nm) can travel in the lymphatic system and are preferably taken up by APCs. Thus, many self-adjuvanting delivery systems have been developed based on nanocarriers. For example, poly-lactic-*co*-glycolic-acid (PLGA) and its derivatives have often been used to form nanoparticles [253]. They are currently used in several marketed non-vaccine products, such as Atridox[®], which is a periodontal treatment, and Sandostin[®] and Lupron Depot, which are cancer treatments [254]. PLGA has been used to deliver a variety of antigens, producing vaccine candidates against GAS [255], *Chlamydia trachomatis* [256], HIV, leishmaniasis, brucellosis, and dengue [254].

Poly-hydrophobic amino acids, which can form fully biodegradable nanoparticles, were tested as vaccine carriers in mice, where they successfully cleared GAS infection [257]. Polyglutamic acid has been included in experimental vaccine candidates against HIV [258], Japanese encephalitis virus [259], influenza [260], HBV [261], GAS [262], and antitumor vaccines [263].

Cholic acid, a human bile salt, was reported to form nanoparticles upon conjugation to peptide antigen and triggered strong humoral immune responses [264]. Polyphosphazene polyelectrolyte increased the secretion of pro-inflammatory cytokines and chemokines at the injection site and increased the production of IgG and IgA antibodies [265]. It was used in vaccines to deliver antigens from influenza [266], tetanus toxoid, HBV, HSV, HIV, and cholera [267]. Cochleates, which are lipid-based cylindrical structures [268], have been utilized in a HIV vaccine [269].

Most adjuvants can induce a wide range of cytokines, such as type 1 IFNs, IFN- γ , IL-2, IL-12, and IL-18. These cytokines are essential to the induction of innate immune responses and promote adaptive immunity [270]. Therefore, cytokines have also been tested as potential adjuvants. Interleukin 2 (IL-2), a T-cell growth factor responsible for the clonal expansion of T-cells and one that is required for the survival of FoxP3⁺ regulatory T-cells [270], has been used as an adjuvant for HIV vaccines [271], HSV type-1 (HSV-1) [272], influenza [273], and metastatic solid tumors [274]. Interleukin 5 (IL-5), which is essential in the activation of

T-cells and NK cells and the proliferation of CD8+ T-cells [270], has been included in experimental vaccine candidates against HIV [275], Staphylococcus enterotoxin B [276], HBV [277], influenza [278], foot-and-mouth disease virus [279], and HSV [280]. Granulocyte macrophage colony-stimulating factor (GM-CSF), known to recruit and induce the maturation of DCs and enhance antigen-specific CD8+ T-cell responses, has been included as an adjuvant in a DNA vaccine against pseudorabies virus [281].

While most pathogens enter the body through mucosal surfaces, most vaccines are delivered systemically, and therefore, mucosal immune responses are not generated and hosts are not protected from the initial infection [282]. In addition to providing first-line protection, mucosal vaccination (e.g., intranasal, oral) is also beneficial due to the elimination of needle-associated risks, improved patient compliance, and importantly, because it elicits both systemic (i.e., IgG, and/or CTL) and mucosal (i.e., IgA) immune responses. However, many “systemic” vaccine adjuvants are not compatible with mucosal delivery. As such, several adjuvants have been evaluated primarily to enable mucosal vaccine administration [283]. The most widely used experimental mucosal adjuvant is cholera toxin subunit B (CTB), which is the nontoxic subunit of cholera toxin (CT). CTB has shown affinity to monosialotetrahexosylganglioside (GM1), which is distributed in epithelial cells and APCs [284]. As an adjuvant, it can induce the activation of DCs, stimulate the production of long-lived CD4+ T-cells, and enhance B- and T-cell responses [285]. It has been used in experimental vaccines against influenza [286], *Helicobacter pylori* [287], *Bordetella pertussis* [288], and *Streptococcus pneumoniae* [289]. It has also been approved for human use in a killed whole-cell monovalent vaccine (WC-rBS) against cholera (Dukoral®) first licensed in Sweden in 1991 [290]. It needs to be noted that cholera bacterium is a naturally secreting cholera toxin; therefore, CTB is not exactly an external adjuvant in this vaccine formulation.

Heat-labile toxin (LT) expressed by enterotoxigenic *Escherichia coli* strains, which are homologous to CT, was also examined [180]. It promoted multifaceted antigen-specific responses, induced antigen-specific IgA antibodies and long-lasting immune responses [291]. LT has been used in influenza vaccine [292] and in a vaccine trial against gastroenteritis-causing enterotoxigenic *E. coli* [293]. Chitosan, a polysaccharide polymer obtained through the deacetylation of chitin [294], has been tested for vaccines against HBV, *Mycobacterium tuberculosis*, influenza A, *Helicobacter pylori*, and poliovirus [295]. Despite its advantages, chitosan is limited by poor solubility [296]. Therefore, chitosan derivatives were developed. The derivative trimethyl chitosan (TMC) has improved solubility and can form nanoparticles. It has been tested for intranasal delivery of vaccines against influenza [297], TB [298], and GAS [262]. TMC has also been used for orally delivered

vaccines against *Brucella melitensis* [299] and HBV [300], and dermally delivered vaccines for diphtheria toxoid [301] and inactivated poliovirus [302].

Alginate (algin or alginic acid), a water-soluble polymer, has been used for the delivery of antigens to mucosal tissues in conjugate- and nanogel forms. Intranasally delivered alginate has been used in vaccines against rotavirus [303], HBV [304], and HAV [305]. It has also been used as a hydrogel for subcutaneous vaccine delivery for *Helicobacter pylori* [306]. Polyelectrolytes are macromolecules consisting of electrolyte groups (e.g., chitosan, heparin, sodium alginate) with polymers made of opposing charges [307]. They have been used in a variety of experimental vaccines, including GAS [308] and *Yersinia pestis* [243].

A variety of other classes of adjuvants have also been tested in animal models, including: (1) cell-penetrating peptides (CPP), short peptides with the ability to cross cell membranes to deliver antigens via both endocytic and non-endocytic pathways [309]; (2) inorganic nanoadjuvants (e.g., mesoporous silica, zinc oxide, gold), which can stabilize vaccine formulations, enhance the quality and longevity of induced immune responses and prolong the effects of the vaccine [310]; (3) nanobeads, which can efficiently deliver antigen to APCs and stimulate potent humoral and CD8+ T-cell immunity [311]; (4) self-assembled peptide (e.g., Q11), which upon conjugation to antigen can form nanoparticles [312]; and (5) immunostimulatory peptides [5]. Unfortunately, many of these will not reach clinical trials, due to limited efficacy, toxicity, poor cost-effectiveness, or even limited availability or lack of funding for further development.

5 Conclusion

Adjuvants have been an essential component of modern-day vaccines for more than a century. While only a few adjuvants are currently available for human vaccines, many others are under clinical investigation, as highlighted in this chapter. Ideal adjuvants have a broad range of effects on the immune system so that they can effectively activate both humoral and cellular immune responses but remain safe and well-tolerated for use within the general population. Problematically, strong adjuvanting activity, which is required especially for single-dose vaccines, often inflicts some degree of toxicity. Thus, further understanding of how adjuvants act and their effects on the immune system and normal tissues is required. Structure–activity relationship studies need to be performed more often to develop safe and efficient adjuvant formulations for the future. Screening of natural product libraries, often performed for the exploration of new drugs, could present alternative strategies for adjuvant discovery. For over 60 years, essentially

only one adjuvant was employed in vaccine constructs for human use. The addition of several new human-use-approved adjuvants in just the last two decades, and the huge leap in knowledge relating to others, therefore, provides reason for excitement for future advances in the field.

References

1. Delany I, Rappuoli R, De Gregorio E (2014) Vaccines for the 21st century. *EMBO Mol Med* 6(6):708–720
2. Vetter V et al (2018) Understanding modern-day vaccines: what you need to know. *Ann Med* 50(2):110–120
3. Sompayrac LM (2019) How the immune system works. Wiley, New York
4. Tognotti E (2010) The eradication of smallpox, a success story for modern medicine and public health: what lessons for the future? *J Infect Dev Ctries* 4(05):264–266
5. Nevagi RJ, Toth I, Skwarczynski M (2018) Peptide-based vaccines. In: Koutsopoulos S (ed) *Peptide applications in biomedicine, biotechnology and bioengineering*. Woodhead Publishing, Cambridge, pp 327–358
6. Koff WC et al (2013) Accelerating next-generation vaccine development for global disease prevention. *Science* 340(6136):1232910
7. Bartlett S, Skwarczynski M, Toth I (2020) Lipids as activators of innate immunity in peptide vaccine delivery. *Curr Med Chem* 27(17):2887–2901
8. Reed SG, Orr MT, Fox CB (2013) Key roles of adjuvants in modern vaccines. *Nat Med* 19(12):1597–1608
9. Levine MM, Sztein MB (2004) Vaccine development strategies for improving immunization: the role of modern immunology. *Nat Immunol* 5(5):460–464
10. Cunningham AL et al (2016) Vaccine development: from concept to early clinical testing. *Vaccine* 34(52):6655–6664
11. Li W et al (2014) Peptide vaccine: progress and challenges. *Vaccines (Basel)* 2(3):515–536
12. Moyle PM, Toth I (2013) Modern subunit vaccines: development, components, and research opportunities. *ChemMedChem* 8(3):360–376
13. Skwarczynski M, Toth I (2016) Peptide-based synthetic vaccines. *Chem Sci* 7(2):842–854
14. Carapetis JR et al (2005) The global burden of group A streptococcal diseases. *Lancet Infect Dis* 5(11):685–694
15. Azmi F et al (2014) Recent progress in adjuvant discovery for peptide-based subunit vaccines. *Hum Vaccin Immunother* 10(3):778–796
16. Coffman RL, Sher A, Seder RA (2010) Vaccine adjuvants: putting innate immunity to work. *Immunity* 33(4):492–503
17. Schijns VE, Lavelle EC (2011) Trends in vaccine adjuvants. *Expert Rev Vaccines* 10(4):539–550
18. O’Hagan DT (2015) New-generation vaccine adjuvants. In: eLS. Wiley, New York, pp 1–7
19. Petrovsky N, Aguilar JC (2004) Vaccine adjuvants: current state and future trends. *Immunol Cell Biol* 82(5):488–496
20. Allison AC, Byars NE (1991) Immunological adjuvants: desirable properties and side-effects. *Mol Immunol* 28(3):279–284
21. Mbow ML et al (2010) New adjuvants for human vaccines. *Curr Opin Immunol* 22(3):411–416
22. Dubensky TW Jr, Reed SG (2010) Adjuvants for cancer vaccines. *Semin Immunol* 22(3):155–161
23. Christensen D (2016) Vaccine adjuvants: why and how. *Hum Vaccin Immunother* 12(10):2709–2711
24. Di Pasquale A et al (2015) Vaccine adjuvants: from 1920 to 2015 and beyond. *Vaccines (Basel)* 3(2):320–343
25. Del Giudice G, Rappuoli R, Didierlaurent AM (2018) Correlates of adjuvanticity: a review on adjuvants in licensed vaccines. *Semin Immunol* 39:14–21
26. Moyer TJ, Zmolek AC, Irvine DJ (2016) Beyond antigens and adjuvants: formulating future vaccines. *J Clin Invest* 126(3):799–808
27. Ho NI et al (2018) Adjuvants enhancing cross-presentation by dendritic cells: the key to more effective vaccines? *Front Immunol* 9:2874
28. Perez O et al (2013) Adjuvants are key factors for the development of future vaccines: lessons from the finlay adjuvant platform. *Front Immunol* 4:407

29. Kool M, Fierens K, Lambrecht BN (2012) Alum adjuvant: some of the tricks of the oldest adjuvant. *J Med Microbiol* 61 (Pt 7):927–934
30. Clapp T et al (2011) Vaccines with aluminum-containing adjuvants: optimizing vaccine efficacy and thermal stability. *J Pharm Sci* 100 (2):388–401
31. Principi N, Esposito S (2018) Aluminum in vaccines: does it create a safety problem? *Vaccine* 36(39):5825–5831
32. HogenEsch H, O’Hagan DT, Fox CB (2018) Optimizing the utilization of aluminum adjuvants in vaccines: you might just get what you want. *NPJ Vaccines* 3:51
33. Oleszycka E, Lavelle EC (2014) Immunomodulatory properties of the vaccine adjuvant alum. *Curr Opin Immunol* 28:1–5
34. Gupta RK (1998) Aluminum compounds as vaccine adjuvants. *Adv Drug Deliv Rev* 32 (3):155–172
35. Burrell LS et al (2000) Aluminium phosphate adjuvants prepared by precipitation at constant pH. Part II: physicochemical properties. *Vaccine* 19(2-3):282–287
36. Rabe M, Verdes D, Seeger S (2011) Understanding protein adsorption phenomena at solid surfaces. *Adv Colloid Interface Sci* 162 (1-2):87–106
37. Hem SL, White JL (1995) Structure and properties of aluminum-containing adjuvants. In: *Vaccine design*. Springer, Berlin, pp 249–276
38. Al-Shakhshir RH et al (1995) Contribution of electrostatic and hydrophobic interactions to the adsorption of proteins by aluminium-containing adjuvants. *Vaccine* 13(1):41–44
39. Mold M, Shardlow E, Exley C (2016) Insight into the cellular fate and toxicity of aluminium adjuvants used in clinically approved human vaccinations. *Sci Rep* 6:31578
40. Lee SH (2012) Detection of human papillomavirus (HPV) L1 gene DNA possibly bound to particulate aluminum adjuvant in the HPV vaccine Gardasil. *J Inorg Biochem* 117:85–92
41. Wen Y, Shi Y (2016) Alum: an old dog with new tricks. *Emerg Microbes Infect* 5:e25
42. Eisenbarth SC et al (2008) Crucial role for the Nalp3 inflammasome in the immunostimulatory properties of aluminium adjuvants. *Nature* 453(7198):1122–1126
43. Hornung V et al (2008) Silica crystals and aluminum salts activate the NALP3 inflammasome through phagosomal destabilization. *Nat Immunol* 9(8):847–856
44. Kool M et al (2008) Cutting edge: alum adjuvant stimulates inflammatory dendritic cells through activation of the NALP3 inflammasome. *J Immunol* 181(6):3755–3759
45. Li H et al (2008) Cutting edge: inflammasome activation by alum and alum’s adjuvant effect are mediated by NLRP3. *J Immunol* 181(1):17–21
46. Mori A et al (2012) The vaccine adjuvant alum inhibits IL-12 by promoting PI3 kinase signaling while chitosan does not inhibit IL-12 and enhances Th1 and Th17 responses. *Eur J Immunol* 42(10):2709–2719
47. Khameneh HJ et al (2017) The Syk-NFAT-IL-2 pathway in dendritic cells is required for optimal sterile immunity elicited by alum adjuvants. *J Immunol* 198(1):196–204
48. Flach TL et al (2011) Alum interaction with dendritic cell membrane lipids is essential for its adjuvanticity. *Nat Med* 17(4):479–487
49. Kool M et al (2011) An unexpected role for uric acid as an inducer of T helper 2 cell immunity to inhaled antigens and inflammatory mediator of allergic asthma. *Immunity* 34(4):527–540
50. Marichal T et al (2011) DNA released from dying host cells mediates aluminum adjuvant activity. *Nat Med* 17(8):996–1002
51. Ghimire TR (2015) The mechanisms of action of vaccines containing aluminum adjuvants: an in vitro vs in vivo paradigm. *SpringerPlus* 4:181
52. Ulanova M et al (2001) The common vaccine adjuvant aluminum hydroxide up-regulates accessory properties of human monocytes via an interleukin-4-dependent mechanism. *Infect Immun* 69(2):1151–1159
53. Rose WA 2nd et al (2015) IL-33 released by alum is responsible for early cytokine production and has adjuvant properties. *Sci Rep* 5:13146
54. Oleszycka E et al (2018) The vaccine adjuvant alum promotes IL-10 production that suppresses Th1 responses. *Eur J Immunol* 48 (4):705–715
55. He Q et al (2000) Calcium phosphate nanoparticle adjuvant. *Clin Diagn Lab Immunol* 7 (6):899–903
56. Masson JD et al (2017) Calcium phosphate: a substitute for aluminum adjuvants? *Expert Rev Vaccines* 16(3):289–299
57. Sesardic D, Rijpkema S, Patel BP (2007) New adjuvants: EU regulatory developments. *Expert Rev Vaccines* 6(5):849–861
58. Gupta RK et al (1995) Adjuvant properties of aluminum and calcium compounds. In: *Vaccine design*. Springer, Berlin, pp 229–248

59. Ginebra MP, Driessens FC, Planell JA (2004) Effect of the particle size on the micro and nanostructural features of a calcium phosphate cement: a kinetic analysis. *Biomaterials* 25(17):3453–3462
60. Relyveld EH (1977) Calcium phosphate gel for adsorbing vaccines. Google Patents
61. Jiang D et al (2004) Structure and adsorption properties of commercial calcium phosphate adjuvant. *Vaccine* 23(5):693–698
62. Hayashi M et al (2016) Optimization of physiological properties of hydroxyapatite as a vaccine adjuvant. *Vaccine* 34(3):306–312
63. Seeber SJ, White JL, Hem SL (1991) Predicting the adsorption of proteins by aluminium-containing adjuvants. *Vaccine* 9(3):201–203
64. Jones S et al (2014) Protein coated microcrystals formulated with model antigens and modified with calcium phosphate exhibit enhanced phagocytosis and immunogenicity. *Vaccine* 32(33):4234–4242
65. Yang Y et al (2019) Recent advances in the mechanisms of NLRP3 inflammasome activation and its inhibitors. *Cell Death Dis* 10(2):128
66. Pazar B et al (2011) Basic calcium phosphate crystals induce monocyte/macrophage IL-1 β secretion through the NLRP3 inflammasome in vitro. *J Immunol* 186(4):2495–2502
67. Garçon N, Chomez P, Van Mechelen M (2007) GlaxoSmithKline Adjuvant Systems in vaccines: concepts, achievements and perspectives. *Expert Rev Vaccines* 6(5):723–739
68. Casella CR, Mitchell TC (2008) Putting endotoxin to work for us: monophosphoryl lipid A as a safe and effective vaccine adjuvant. *Cell Mol Life Sci* 65(20):3231–3240
69. Ribi E et al (1979) Peptides as requirement for immunotherapy of the guinea-pig line-10 tumor with endotoxins. *Cancer Immunol Immunother* 7(1):43–58
70. Didierlaurent AM et al (2009) AS04, an aluminium salt- and TLR4 agonist-based adjuvant system, induces a transient localized innate immune response leading to enhanced adaptive immunity. *J Immunol* 183(10):6186–6197
71. Kundi M (2007) New hepatitis B vaccine formulated with an improved adjuvant system. *Expert Rev Vaccines* 6(2):133–140
72. Tong NK et al (2005) Immunogenicity and safety of an adjuvanted hepatitis B vaccine in pre-hemodialysis and hemodialysis patients. *Kidney Int* 68(5):2298–2303
73. Harper DM et al (2004) Efficacy of a bivalent L1 virus-like particle vaccine in prevention of infection with human papillomavirus types 16 and 18 in young women: a randomised controlled trial. *Lancet* 364(9447):1757–1765
74. Harper DM et al (2006) Sustained efficacy up to 4.5 years of a bivalent L1 virus-like particle vaccine against human papillomavirus types 16 and 18: follow-up from a randomised control trial. *Lancet* 367(9518):1247–1255
75. Gall S, et al (2007) Substantial impact on precancerous lesions and HPV infections through 5.5 years in women vaccinated with the HPV-16/18 L1 VLP AS04 candidate vaccine. In: AACR
76. O'Hagan DT, Wack A, Podda A (2007) MF59 is a safe and potent vaccine adjuvant for flu vaccines in humans: what did we learn during its development? *Clin Pharmacol Ther* 82(6):740–744
77. O'Hagan DT et al (2013) The history of MF59((R)) adjuvant: a phoenix that arose from the ashes. *Expert Rev Vaccines* 12(1):13–30
78. Ott G et al (2000) The adjuvant MF59: a 10-year perspective. Springer, Berlin, pp 211–228
79. Opie EL, Freund J (1937) An experimental study of protective inoculation with heat killed tubercle bacilli. *J Exp Med* 66(6):761
80. Apostolico Jde S et al (2016) Adjuvants: classification, modus operandi, and licensing. *J Immunol Res* 2016:1459394
81. Salk JE, Laurent AM (1952) The use of adjuvants in studies on influenza immunization. I. Measurements in monkeys of the dimensions of antigenicity of virus-mineral oil emulsions. *J Exp Med* 95(5):429–447
82. Shi S et al (2019) Vaccine adjuvants: understanding the structure and mechanism of adjuvanticity. *Vaccine* 37(24):3167–3178
83. Wu Y et al (2008) Phase I trial of malaria transmission blocking vaccine candidates Pfs25 and Pvs25 formulated with montanide ISA 51. *PLoS One* 3(7):e2636
84. Aucouturier J et al (2002) Montanide ISA 720 and 51: a new generation of water in oil emulsions as adjuvants for human vaccines. *Expert Rev Vaccines* 1(1):111–118
85. van Doorn E et al (2016) Safety and tolerability evaluation of the use of Montanide ISA51 as vaccine adjuvant: a systematic review. *Hum Vaccin Immunother* 12(1):159–169
86. Saul A et al (2005) A human phase I vaccine clinical trial of the *Plasmodium falciparum* malaria vaccine candidate apical membrane

- antigen 1 in Montanide ISA720 adjuvant. *Vaccine* 23(23):3076–3083
87. El Sahly H (2010) MF59™; as a vaccine adjuvant: a review of safety and immunogenicity. *Expert Rev Vaccines* 9(10):1135–1141
 88. Herbert W (1966) Antigenicity of soluble protein in the presence of high levels of antibody: a possible mode of action of the antigen adjuvants. *Nature* 210(5037):747–748
 89. Awate S, Babiuk LA, Mutwiri G (2013) Mechanisms of action of adjuvants. *Front Immunol* 4:114
 90. O'Hagan DT et al (2012) The mechanism of action of MF59—an innately attractive adjuvant formulation. *Vaccine* 30(29):4341–4348
 91. Vesikari T et al (2009) Enhanced immunogenicity of seasonal influenza vaccines in young children using MF59 adjuvant. *Pediatr Infect Dis J* 28(7):563–571
 92. Puig-Barbera J et al (2007) Effectiveness of MF59-adjuvanted subunit influenza vaccine in preventing hospitalisations for cardiovascular disease, cerebrovascular disease and pneumonia in the elderly. *Vaccine* 25(42):7313–7321
 93. Job A et al (2005) Evidence of increased clinical protection of an MF59-adjuvant influenza vaccine compared to a non-adjuvant vaccine among elderly residents of long-term care facilities in Italy. *Epidemiol Infect* 133(4):687–693
 94. Mannino S et al (2012) Effectiveness of adjuvanted influenza vaccination in elderly subjects in northern Italy. *Am J Epidemiol* 176(6):527–533
 95. Podda A, Del Giudice G (2003) MF59-adjuvanted vaccines: increased immunogenicity with an optimal safety profile. *Expert Rev Vaccines* 2(2):197–203
 96. Corey L et al (1999) Recombinant glycoprotein vaccine for the prevention of genital HSV-2 infection: two randomized controlled trials. *JAMA* 282(4):331–340
 97. Nitayaphan S et al (2000) A phase I/II trial of HIV SF2 gp120/MF59 vaccine in seronegative Thais. *Vaccine* 18(15):1448–1455
 98. Heineman TC et al (1999) A randomized, controlled study in adults of the immunogenicity of a novel hepatitis B vaccine containing MF59 adjuvant. *Vaccine* 17(22):2769–2778
 99. Garçon N, Vaughn DW, Didierlaurent AM (2012) Development and evaluation of AS03, an adjuvant system containing alpha-tocopherol and squalene in an oil-in-water emulsion. *Expert Rev Vaccines* 11(3):349–366
 100. Morel S et al (2011) Adjuvant system AS03 containing alpha-tocopherol modulates innate immune response and leads to improved adaptive immunity. *Vaccine* 29(13):2461–2473
 101. Jacob L et al (2015) Comparison of Pandemrix and Arepanrix, two pH1N1 AS03-adjuvanted vaccines differentially associated with narcolepsy development. *Brain Behav Immun* 47:44–57
 102. Laupeze B et al (2019) Adjuvant systems for vaccines: 13years of post-licensure experience in diverse populations have progressed the way adjuvanted vaccine safety is investigated and understood. *Vaccine* 37(38):5670–5680
 103. Carter NJ, Plosker GL (2008) Prepandemic influenza vaccine H5N1 (split virion, inactivated, adjuvanted) [Prepandrix™]. *BioDrugs* 22(5):279–292
 104. Treanor JJ et al (2006) Safety and immunogenicity of an inactivated subvirion influenza A (H5N1) vaccine. *N Engl J Med* 354(13):1343–1351
 105. Bresson J-L et al (2006) Safety and immunogenicity of an inactivated split-virion influenza A/Vietnam/1194/2004 (H5N1) vaccine: phase I randomised trial. *Lancet* 367(9523):1657–1664
 106. Hampson AW (2006) Ferrets and the challenges of H5N1 vaccine formulation. *J Infect Dis* 194(2):143–145
 107. Langley JM et al (2011) Dose-sparing H5N1 A/Indonesia/05/2005 pre-pandemic influenza vaccine in adults and elderly adults: a phase III, placebo-controlled, randomized study. *J Infect Dis* 203(12):1729–1738
 108. Tregoning JS, Russell RF, Kinnear E (2018) Adjuvanted influenza vaccines. *Hum Vaccin Immunother* 14(3):550–564
 109. Stoute J et al (1998) Long-term efficacy and immune responses following immunization with the RTS, S malaria vaccine. *J infect Dis* 178(4):1139–1144
 110. Sun P et al (2003) Protective immunity induced with malaria vaccine, RTS,S, is linked to Plasmodium falciparum circumsporozoite protein-specific CD4+ and CD8+ T cells producing IFN-gamma. *J Immunol* 171(12):6961–6967
 111. McElrath MJ, Haynes BF (2010) Induction of immunity to human immunodeficiency virus type-1 by vaccination. *Immunity* 33(4):542–554
 112. Li Y et al (2006) Characterization of antibody responses elicited by human immunodeficiency virus type 1 primary isolate trimeric

- and monomeric envelope glycoproteins in selected adjuvants. *J Virol* 80(3):1414–1426
113. Group, r.H.V.S (2005) Placebo-controlled phase 3 trial of a recombinant glycoprotein 120 vaccine to prevent HIV-1 infection. *J Infect Dis* 191(5):654–665
 114. Bozzuto G, Molinari A (2015) Liposomes as nanomedical devices. *Int J Nanomed* 10:975–999
 115. Bangham A, Standish MM, Watkins JC (1965) Diffusion of univalent ions across the lamellae of swollen phospholipids. *J Mol Biol* 13(1):238–IN27
 116. Sharma A, Sharma US (1997) Liposomes in drug delivery: progress and limitations. *Int J Pharm* 154(2):123–140
 117. Çağdaş M, Sezer AD, Bucak S (2014) Liposomes as potential drug carrier systems for drug delivery. In: *Application of nanotechnology in drug delivery*. IntechOpen, London
 118. Akbarzadeh A et al (2013) Liposome: classification, preparation, and applications. *Nano-scale Res Lett* 8(1):102
 119. Wang N, Chen M, Wang T (2019) Liposomes used as a vaccine adjuvant-delivery system: from basics to clinical immunization. *J Control Release* 303:130–150
 120. Euliss LE et al (2006) Imparting size, shape, and composition control of materials for nanomedicine. *Chem Soc Rev* 35 (11):1095–1104
 121. Gregoriadis G, Florence AT (1993) Liposomes in drug delivery. *Drugs* 45(1):15–28
 122. Schwendener RA (2014) Liposomes as vaccine delivery systems: a review of the recent advances. *Ther Adv Vaccines* 2(6):159–182
 123. Felnerova D et al (2004) Liposomes and virosomes as delivery systems for antigens, nucleic acids and drugs. *Curr Opin Biotechnol* 15 (6):518–529
 124. Almeida J et al (1975) Formation of virosomes from influenza subunits and liposomes. *Lancet* 306(7941):899–901
 125. Gluck R, Burri KG, Metcalfe I (2005) Adjuvant and antigen delivery properties of virosomes. *Curr Drug Deliv* 2(4):395–400
 126. Stegmann T et al (2010) Lipopeptide-adjuvanted respiratory syncytial virus virosomes: a safe and immunogenic non-replicating vaccine formulation. *Vaccine* 28(34):5543–5550
 127. Datta SA, Rein A (2009) Preparation of recombinant HIV-1 gag protein and assembly of virus-like particles in vitro. *Methods Mol Biol* 485:197–208
 128. Correale P et al (2008) Anti-angiogenic effects of immune-reconstituted influenza virosomes assembled with parathyroid hormone-related protein derived peptide vaccine. *Cancer Lett* 263(2):291–301
 129. Wilschut J et al (2007) Preservation of influenza virosome structure and function during freeze-drying and storage. *J Liposome Res* 17 (3-4):173–182
 130. Moser C, Amacker M, Zurbriggen R (2011) Influenza virosomes as a vaccine adjuvant and carrier system. *Expert Rev Vaccines* 10 (4):437–446
 131. Mischler R, Metcalfe IC (2002) Inflaxal® V a trivalent virosome subunit influenza vaccine: production. *Vaccine* 20:B17–B23
 132. Kammer AR et al (2007) A new and versatile virosomal antigen delivery system to induce cellular and humoral immune responses. *Vaccine* 25(41):7065–7074
 133. Khoshnejad M et al (2007) Modified influenza virosomes: recent advances and potential in gene delivery. *Curr Med Chem* 14 (29):3152–3156
 134. Mallick AI et al (2012) Vaccination with CpG-adjuvanted avian influenza virosomes promotes antiviral immune responses and reduces virus shedding in chickens. *Viral Immunol* 25(3):226–231
 135. Angel J et al (2007) Virosome-mediated delivery of tumor antigen to plasmacytoid dendritic cells. *Vaccine* 25(19):3913–3921
 136. Bungener L et al (2005) Virosome-mediated delivery of protein antigens in vivo: efficient induction of class I MHC-restricted cytotoxic T lymphocyte activity. *Vaccine* 23 (10):1232–1241
 137. Wiedermann G et al (1990) Safety and immunogenicity of an inactivated hepatitis A candidate vaccine in healthy adult volunteers. *Vaccine* 8(6):581–584
 138. Bovier PA (2008) Epaxal®: a virosomal vaccine to prevent hepatitis A infection. *Expert Rev Vaccines* 7(8):1141–1150
 139. Bovier PA et al (2010) Predicted 30-year protection after vaccination with an aluminum-free virosomal hepatitis A vaccine. *J Med Virol* 82(10):1629–1634
 140. Genton B et al (2006) Hepatitis A vaccines and the elderly. *Travel Med Infect Dis* 4 (6):303–312
 141. D’Acremont V, Herzog C, Genton B (2006) Immunogenicity and safety of a virosomal hepatitis A vaccine (Epaxal®) in the elderly. *J Travel Med* 13(2):78–83

142. Usonis V et al (2003) Antibody titres after primary and booster vaccination of infants and young children with a virosomal hepatitis A vaccine (Epaxal®). *Vaccine* 21 (31):4588–4592
143. Dagan R et al (2000) Immunization against hepatitis A in the first year of life: priming despite the presence of maternal antibody. *Pediatr Infect Dis J* 19(11):1045–1052
144. Herzog C et al (2009) Eleven years of Inflexal V-a virosomal adjuvanted influenza vaccine. *Vaccine* 27(33):4381–4387
145. Kunzi V et al (2009) Safe vaccination of children with a virosomal adjuvanted influenza vaccine. *Vaccine* 27(8):1261–1265
146. Boon AC et al (2002) Influenza A virus specific T cell immunity in humans during aging. *Virology* 299(1):100–108
147. de Bruijn IA et al (2004) Virosomal influenza vaccine: a safe and effective influenza vaccine with high efficacy in elderly and subjects with low pre-vaccination antibody titers. *Virus Res* 103(1-2):139–145
148. de Bruijn IA et al (2005) Clinical experience with inactivated, virosomal influenza vaccine. *Vaccine* 23(Suppl 1):S39–S49
149. Amendola A et al (2001) Influenza vaccination of HIV-1-positive and HIV-1-negative former intravenous drug users. *J Med Virol* 65(4):644–648
150. Gaeta GB et al (2002) Immunogenicity and safety of an adjuvanted influenza vaccine in patients with decompensated cirrhosis. *Vaccine* 20:B33–B35
151. Glück R (2002) Intranasal immunization against influenza. *J Aerosol Med* 15 (2):221–228
152. Mutsch M et al (2004) Use of the inactivated intranasal influenza vaccine and the risk of Bell's palsy in Switzerland. *N Engl J Med* 350(9):896–903
153. Zhu D, Tuo W (2016) QS-21: a potent vaccine adjuvant. *Nat Prod Chem Res* 3(4):e113
154. Vandepapeliere P (2018) Vaccine compositions comprising a saponin adjuvant. Google Patents
155. Kensil CR, Kammer R (1998) QS-21: a water-soluble triterpene glycoside adjuvant. *Expert Opin Investig Drugs* 7(9):1475–1482
156. Garçon N, Van Mechelen M (2011) Recent clinical experience with vaccines using MPL and QS-21-containing adjuvant systems. *Expert Rev Vaccines* 10(4):471–486
157. Song X, Hu S (2009) Adjuvant activities of saponins from traditional Chinese medicinal herbs. *Vaccine* 27(36):4883–4890
158. Singh M, O'Hagan DT (2003) Recent advances in veterinary vaccine adjuvants. *Int J Parasitol* 33(5-6):469–478
159. Sun HX, Xie Y, Ye YP (2009) Advances in saponin-based adjuvants. *Vaccine* 27 (12):1787–1796
160. Liu G et al (2002) QS-21 structure/function studies: effect of acylation on adjuvant activity. *Vaccine* 20(21-22):2808–2815
161. Dendouga N et al (2012) Cell-mediated immune responses to a varicella-zoster virus glycoprotein E vaccine using both a TLR agonist and QS21 in mice. *Vaccine* 30 (20):3126–3135
162. Vandepapeliere P et al (2008) Vaccine adjuvant systems containing monophosphoryl lipid A and QS21 induce strong and persistent humoral and T cell responses against hepatitis B surface antigen in healthy adult volunteers. *Vaccine* 26(10):1375–1386
163. Didierlaurent AM et al (2017) Adjuvant system AS01: helping to overcome the challenges of modern vaccines. *Expert Rev Vaccines* 16(1):55–63
164. Stewart VA et al (2006) Pre-clinical evaluation of new adjuvant formulations to improve the immunogenicity of the malaria vaccine RTS,S/AS02A. *Vaccine* 24 (42-43):6483–6492
165. RTS,S Clinical Trials Partnership (2015) Efficacy and safety of RTS,S/AS01 malaria vaccine with or without a booster dose in infants and children in Africa: final results of a phase 3, individually randomised, controlled trial. *Lancet* 386(9988):31–45
166. Pichyangkul S et al (2004) Pre-clinical evaluation of the malaria vaccine candidate *P. falciparum* MSP1(42) formulated with novel adjuvants or with alum. *Vaccine* 22 (29-30):3831–3840
167. Keating GM (2016) Shingles (Herpes Zoster) vaccine (zostavax((R))): a review in the prevention of herpes zoster and postherpetic neuralgia. *BioDrugs* 30(3):243–254
168. Lecrenier N et al (2018) Development of adjuvanted recombinant zoster vaccine and its implications for shingles prevention. *Expert Rev Vaccines* 17(7):619–634
169. Levin MJ, Oxman MN, Zhang JH, Johnson GR, Stanley H, Hayward AR, ... Weinberg A (2008) Varicellazoster virus-specific immune responses in elderly recipients of a herpes zoster vaccine. *J Infect Dis* 197(6):825–835
170. Cunningham AL et al (2018) Immune responses to a recombinant glycoprotein E herpes zoster vaccine in adults aged 50 years or older. *J Infect Dis* 217(11):1750–1760

171. Lal H, Zahaf T, Heineman TC (2013) Safety and immunogenicity of an AS01-adjuvanted varicella zoster virus subunit candidate vaccine (HZ/su): a phase-I, open-label study in Japanese adults. *Hum Vaccin Immunother* 9 (7):1425–1429
172. Chackerian B (2007) Virus-like particles: flexible platforms for vaccine development. *Expert Rev Vaccines* 6(3):381–390
173. Rohovie MJ, Nagasawa M, Swartz JR (2017) Virus-like particles: next-generation nanoparticles for targeted therapeutic delivery. *Bioeng Transl Med* 2(1):43–57
174. Zhao Q et al (2013) Virus-like particle-based human vaccines: quality assessment based on structural and functional properties. *Trends Biotechnol* 31(11):654–663
175. Kushnir N, Streatfield SJ, Yusibov V (2012) Virus-like particles as a highly efficient vaccine platform: diversity of targets and production systems and advances in clinical development. *Vaccine* 31(1):58–83
176. Bachmann MF, Zinkernagel RM (1997) Neutralizing antiviral B cell responses. *Annu Rev Immunol* 15(1):235–270
177. Fifis T et al (2004) Size-dependent immunogenicity: therapeutic and protective properties of nano-vaccines against tumors. *J Immunol* 173(5):3148–3154
178. Roldao A et al (2010) Virus-like particles in vaccine development. *Expert Rev Vaccines* 9 (10):1149–1176
179. Cimica V, Galarza JM (2017) Adjuvant formulations for virus-like particle (VLP) based vaccines. *Clin Immunol* 183:99–108
180. De Gregorio E, Caproni E, Ulmer JB (2013) Vaccine adjuvants: mode of action. *Front Immunol* 4:214
181. Hussein WM et al (2014) Toll-like receptor agonists: a patent review (2011–2013). *Expert Opin Ther Pat* 24(4):453–470
182. Bode C et al (2011) CpG DNA as a vaccine adjuvant. *Expert Rev Vaccines* 10 (4):499–511
183. Vollmer J, Krieg AM (2009) Immunotherapeutic applications of CpG oligodeoxynucleotide TLR9 agonists. *Adv Drug Deliv Rev* 61(3):195–204
184. Krieg AM et al (1995) CpG motifs in bacterial DNA trigger direct B-cell activation. *Nature* 374(6522):546–549
185. Krieg AM (2002) CpG motifs in bacterial DNA and their immune effects. *Annu Rev Immunol* 20(1):709–760
186. Lipford GB et al (2000) CpG-DNA-mediated transient lymphadenopathy is associated with a state of Th1 predisposition to antigen-driven responses. *J Immunol* 165 (3):1228–1235
187. Klinman DM (2004) Immunotherapeutic uses of CpG oligodeoxynucleotides. *Nat Rev Immunol* 4(4):249–258
188. Heyward WL et al (2013) Immunogenicity and safety of an investigational hepatitis B vaccine with a Toll-like receptor 9 agonist adjuvant (HBsAg-1018) compared to a licensed hepatitis B vaccine in healthy adults 40–70 years of age. *Vaccine* 31 (46):5300–5305
189. Jilg W, Schmidt M, Deinhardt F (1988) Persistence of specific antibodies after hepatitis B vaccination. *J Hepatol* 6(2):201–207
190. Halperin SA et al (2006) Comparison of the safety and immunogenicity of hepatitis B virus surface antigen co-administered with an immunostimulatory phosphorothioate oligonucleotide and a licensed hepatitis B vaccine in healthy young adults. *Vaccine* 24(1):20–26
191. Janssen JM et al (2015) Immunogenicity of an investigational hepatitis B vaccine with a Toll-like receptor 9 agonist adjuvant (HBsAg-1018) compared with a licensed hepatitis B vaccine in subpopulations of healthy adults 18–70 years of age. *Vaccine* 33 (31):3614–3618
192. Janssen RS et al (2013) Immunogenicity and safety of an investigational hepatitis B vaccine with a toll-like receptor 9 agonist adjuvant (HBsAg-1018) compared with a licensed hepatitis B vaccine in patients with chronic kidney disease. *Vaccine* 31(46):5306–5313
193. Janssen JM et al (2015) Immunogenicity and safety of an investigational hepatitis B vaccine with a Toll-like receptor 9 agonist adjuvant (HBsAg-1018) compared with a licensed hepatitis B vaccine in patients with chronic kidney disease and type 2 diabetes mellitus. *Vaccine* 33(7):833–837
194. DeFrancesco L (2008) Dynavax trial halted. *Nat Biotechnol* 26(5):484
195. Pearse MJ, Drane D (2005) ISCOMATRIX adjuvant for antigen delivery. *Adv Drug Deliv Rev* 57(3):465–474
196. Sanders MT et al (2005) ISCOM-based vaccines: the second decade. *Immunol Cell Biol* 83(2):119–128
197. Sun HX, Xie Y, Ye YP (2009) ISCOMs and ISCOMATRIX. *Vaccine* 27(33):4388–4401
198. Madhun AS et al (2009) Intramuscular Matrix-M-adjuvanted virosomal H5N1 vaccine induces high frequencies of multifunctional Th1 CD4+ cells and strong antibody

- responses in mice. *Vaccine* 27 (52):7367–7376
199. Bengtsson KL (2013) Matrix M adjuvant technology. In: *Novel immune potentiators and delivery technologies for next generation vaccines*. Springer, Berlin, pp 309–320
 200. Cooper CL et al (2004) Safety and immunogenicity of CPG 7909 injection as an adjuvant to Fluarix influenza vaccine. *Vaccine* 22 (23-24):3136–3143
 201. Cooper C et al (2004) CpG 7909, an immunostimulatory TLR9 agonist oligodeoxynucleotide, as adjuvant to Engerix-B® HBV vaccine in healthy adults: a double-blind phase I/II study. *J Clin Immunol* 24 (6):693–701
 202. Shirota H, Klinman DM (2017) CpG oligodeoxynucleotides as adjuvants for clinical use. In: *Immunopotentiators in modern vaccines*. Elsevier, Amsterdam, pp 163–198
 203. Fife KH et al (2008) Effect of resiquimod 0.01% gel on lesion healing and viral shedding when applied to genital herpes lesions. *Antimicrob Agents Chemother* 52(2):477–482
 204. Cui B et al (2018) Flagellin as a vaccine adjuvant. *Expert Rev Vaccines* 17(4):335–349
 205. Apostolico Jde S et al (2016) HIV envelope trimer specific immune response is influenced by different adjuvant formulations and heterologous prime-boost. *PLoS One* 11(1):e0145637
 206. Henriques HR et al (2013) Targeting the non-structural protein 1 from dengue virus to a dendritic cell population confers protective immunity to lethal virus challenge. *PLoS Negl Trop Dis* 7(7):e2330
 207. Tewari K et al (2010) Poly(I:C) is an effective adjuvant for antibody and multi-functional CD4+ T cell responses to Plasmodium falciparum circumsporozoite protein (CSP) and alphaDEC-CSP in non human primates. *Vaccine* 28(45):7256–7266
 208. Thompson K et al (1996) Results of a double-blind placebo-controlled study of the double-stranded RNA drug polyI: PolyC 12 U in the treatment of HIV infection. *Eur J Clin Microbiol Infect Dis* 15(7):580–587
 209. Strayer DR et al (2012) A double-blind, placebo-controlled, randomized, clinical trial of the TLR-3 agonist rintatolimod in severe cases of chronic fatigue syndrome. *PLoS One* 7(3):e31334
 210. Jasani B, Navabi H, Adams M (2009) Ampligen: a potential toll-like 3 receptor adjuvant for immunotherapy of cancer. *Vaccine* 27 (25-26):3401–3404
 211. Gowthaman U et al (2011) Promiscuous peptide of 16 kDa antigen linked to Pam2Cys protects against Mycobacterium tuberculosis by evoking enduring memory T-cell response. *J Infect Dis* 204(9):1328–1338
 212. Moyle PM et al (2014) Site-specific incorporation of three Toll-like receptor 2 targeting adjuvants into semisynthetic, molecularly defined nanoparticles: application to group A streptococcal vaccines. *Bioconjug Chem* 25 (5):965–978
 213. Zhong W, Skwarczynski M, Toth I (2009) Lipid core peptide system for gene, drug, and vaccine delivery. *Aust J Chem* 62 (9):956–967
 214. Zaman M et al (2014) Group A Streptococcal vaccine candidate: contribution of epitope to size, antigen presenting cell interaction and immunogenicity. *Nanomedicine* 9 (17):2613–2624
 215. Bartlett S et al (2020) Lipopeptide-based oral vaccine against hookworm infection. *J Infect Dis* 221(6):934–942
 216. Zhong G et al (1993) Immunogenicity evaluation of a lipidic amino acid-based synthetic peptide vaccine for Chlamydia trachomatis. *J Immunol* 151(7):3728–3736
 217. Fuaad AAA et al (2015) The use of a conformational cathepsin D-derived epitope for vaccine development against Schistosoma mansoni. *Bioorg Med Chem* 23 (6):1307–1312
 218. Carter D et al (2018) The adjuvant GLA-AF enhances human intradermal vaccine responses. *Sci Adv* 4(9):eaas9930
 219. Arias MA et al (2012) Glucopyranosyl Lipid Adjuvant (GLA), a synthetic TLR4 agonist, promotes potent systemic and mucosal responses to intranasal immunization with HIVgp140. *PLoS One* 7(7):e41144
 220. Reed SG et al (2018) Correlates of GLA family adjuvants' activities. *Semin Immunol* 39:22–29
 221. Wang M et al (2014) Sulfated glucan can improve the immune efficacy of Newcastle disease vaccine in chicken. *Int J Biol Macromol* 70:193–198
 222. Sun B et al (2018) Polysaccharides as vaccine adjuvants. *Vaccine* 36(35):5226–5234
 223. Bacon J, Farmer V (1968) The presence of a predominantly beta (1-6) component in preparations of yeast glucan. *Biochem J* 110 (3):34P
 224. Liang J et al (1998) Enhanced clearance of a multiple antibiotic resistant Staphylococcus aureus in rats treated with PGG-glucan is

- associated with increased leukocyte counts and increased neutrophil oxidative burst activity. *Int J Immunopharmacol* 20 (11):595–614
225. Rasmussen LT, Seljelid R (1990) Dynamics of blood components and peritoneal fluid during treatment of murine *E. coli* sepsis with β -1, 3-D-polyglucose derivatives: I. Cells. *Scand J Immunol* 32(4):321–331
 226. Vetvicka V (2011) Glucan-immunostimulant, adjuvant, potential drug. *World J Clin Oncol* 2(2):115–119
 227. Li P, Wang F (2015) Polysaccharides: candidates of promising vaccine adjuvants. *Drug Discov Ther* 9(2):88–93
 228. Cooper PD, Petrovsky N (2011) Delta inulin: a novel, immunologically active, stable packing structure comprising beta-D-[2 \rightarrow 1] poly(fructo-furanosyl) alpha-D-glucose polymers. *Glycobiology* 21(5):595–606
 229. Rodriguez-Del Rio E et al (2015) A gold glyco-nanoparticle carrying a Listeriolysin O peptide and formulated with Advax delta inulin adjuvant induces robust T-cell protection against listeria infection. *Vaccine* 33 (12):1465–1473
 230. Lobigs M et al (2010) An inactivated Vero cell-grown Japanese encephalitis vaccine formulated with Advax, a novel inulin-based adjuvant, induces protective neutralizing antibody against homologous and heterologous flaviviruses. *J Gen Virol* 91(Pt 6):1407–1417
 231. Counoupas C et al (2017) Delta inulin-based adjuvants promote the generation of poly-functional CD4(+) T cell responses and protection against *Mycobacterium tuberculosis* infection. *Sci Rep* 7(1):8582
 232. Cristillo AD et al (2011) Induction of mucosal and systemic antibody and T-cell responses following prime-boost immunization with novel adjuvanted human immunodeficiency virus-1-vaccine formulations. *J Gen Virol* 92 (Pt 1):128–140
 233. Saade F et al (2013) A novel hepatitis B vaccine containing Advax, a polysaccharide adjuvant derived from delta inulin, induces robust humoral and cellular immunity with minimal reactogenicity in preclinical testing. *Vaccine* 31(15):1999–2007
 234. Petrovsky N et al (2013) An inactivated cell culture Japanese encephalitis vaccine (JE-ADVAX) formulated with delta inulin adjuvant provides robust heterologous protection against West Nile encephalitis via cross-protective memory B cells and neutralizing antibody. *J Virol* 87(18):10324–10333
 235. Dzierzbicka K, Wardowska A, Trzonkowski P (2011) Recent developments in the synthesis and biological activity of muramylpeptides. *Curr Med Chem* 18(16):2438–2451
 236. Bahr GM et al (2003) Clinical and immunological effects of a 6 week immunotherapy cycle with murabutide in HIV-1 patients with unsuccessful long-term antiretroviral treatment. *J Antimicrob Chemother* 51 (6):1377–1388
 237. Giddam AK et al (2016) A semi-synthetic whole parasite vaccine designed to protect against blood stage malaria. *Acta Biomater* 44:295–303
 238. Geijtenbeek TB et al (2003) Mycobacteria target DC-SIGN to suppress dendritic cell function. *J Exp Med* 197(1):7–17
 239. Geijtenbeek TB et al (2000) DC-SIGN, a dendritic cell-specific HIV-1-binding protein that enhances trans-infection of T cells. *Cell* 100(5):587–597
 240. Irache JM et al (2008) Mannose-targeted systems for the delivery of therapeutics. *Expert Opin Drug Deliv* 5(6):703–724
 241. Nevagi RJ, Skwarczynski M, Toth I (2019) Polymers for subunit vaccine delivery. *Eur Polym J* 114:397–410
 242. Moon SH et al (2015) Evaluation of hyaluronic acid-based combination adjuvant containing monophosphoryl lipid A and aluminum salt for hepatitis B vaccine. *Vaccine* 33 (38):4762–4769
 243. Fan Y et al (2015) Cationic liposome-hyaluronic acid hybrid nanoparticles for intranasal vaccination with subunit antigens. *J Control Release* 208:121–129
 244. Kong WH et al (2016) Self-adjuvanted hyaluronate—antigenic peptide conjugate for transdermal treatment of muscular dystrophy. *Biomaterials* 81:93–103
 245. Bettencourt A, Almeida AJ (2012) Poly (methyl methacrylate) particulate carriers in drug delivery. *J Microencapsul* 29 (4):353–367
 246. Kreuter J, Speiser PP (1976) New adjuvants on a polymethylmethacrylate base. *Infect Immun* 13(1):204–210
 247. Voltan R et al (2007) Preparation and characterization of innovative protein-coated poly (methylmethacrylate) core-shell nanoparticles for vaccine purposes. *Pharm Res* 24 (10):1870–1882
 248. Skwarczynski M et al (2010) Polyacrylate dendrimer nanoparticles: a self-adjuvanting vaccine delivery system. *Angew Chem Int Ed Engl* 49(33):5742–5745

249. Liu TY et al (2013) Self-adjuvanting polymer-peptide conjugates as therapeutic vaccine candidates against cervical cancer. *Biomacromolecules* 14(8):2798–2806
250. Skwarczynski M, Toth I (2014) Recent advances in peptide-based subunit nanovaccines. *Nanomedicine* 9(17):2657–2669
251. Zhao G et al (2017) The application of self-assembled nanostructures in peptide-based subunit vaccine development. *Eur Polym J* 93:670–681
252. Skwarczynski M, Toth I (2011) Peptide-based subunit nanovaccines. *Curr Drug Deliv* 8(3):282–289
253. Gutjahr A et al (2016) Biodegradable polymeric nanoparticles-based vaccine adjuvants for lymph nodes targeting. *Vaccines (Basel)* 4(4):34
254. Lü J-M et al (2014) Current advances in research and clinical applications of PLGA-based nanotechnology. *Expert Rev Mol Diagn* 9(4):325–341
255. Marasini N et al (2016) Lipid core peptide/poly (lactic-co-glycolic acid) as a highly potent intranasal vaccine delivery system against Group A streptococcus. *Int J Pharm* 513(1–2):410–420
256. Taha MA, Singh SR, Dennis VA (2012) Biodegradable PLGA85/15 nanoparticles as a delivery vehicle for Chlamydia trachomatis recombinant MOMP-187 peptide. *Nanotechnology* 23(32):325101
257. Skwarczynski M et al (2020) Poly (amino acids) as a potent self-adjuvanting delivery system for peptide-based nanovaccines. *Sci Adv* 6(5):eaax2285
258. Akagi T et al (2007) Protein direct delivery to dendritic cells using nanoparticles based on amphiphilic poly(amino acid) derivatives. *Biomaterials* 28(23):3427–3436
259. Okamoto S et al (2012) Poly-gamma-glutamic acid nanoparticles and aluminum adjuvant used as an adjuvant with a single dose of Japanese encephalitis virus-like particles provide effective protection from Japanese encephalitis virus. *Clin Vaccine Immunol* 19(1):17–22
260. Chowdhury MYE et al (2017) Mucosal vaccination of conserved sM2, HA2 and cholera toxin subunit A1 (CTA1) fusion protein with poly gamma-glutamate/chitosan nanoparticles (PC NPs) induces protection against divergent influenza subtypes. *Vet Microbiol* 201:240–251
261. Wang H et al (2018) Single dose HBsAg CS-gamma-PGA nanogels induce potent protective immune responses against HBV infection. *Eur J Pharm Biopharm* 124:82–88
262. Nevagi RJ et al (2018) Polyglutamic acid-trimethyl chitosan-based intranasal peptide nano-vaccine induces potent immune responses against group A streptococcus. *Acta Biomater* 80:278–287
263. Yoshikawa T et al (2008) Nanoparticles built by self-assembly of amphiphilic gamma-PGA can deliver antigens to antigen-presenting cells with high efficiency: a new tumor-vaccine carrier for eliciting effector T cells. *Vaccine* 26(10):1303–1313
264. Azuar A et al (2019) Cholic acid-based delivery system for vaccine candidates against Group A Streptococcus. *ACS Med Chem Lett* 10(9):1253–1259
265. Payne LG et al (1998) Poly [di (carboxylatophenoxy) phosphazene] (PCPP) is a potent immunoadjuvant for an influenza vaccine. *Vaccine* 16(1):92–98
266. Eng NF et al (2009) Polyphosphazenes enhance mucosal and systemic immune responses in mice immunized intranasally with influenza antigens. *Open Vaccine J* 2(1):134–143
267. Eng NF et al (2010) The potential of polyphosphazenes for delivery of vaccine antigens and immunotherapeutic agents. *Curr Drug Deliv* 7(1):13–20
268. Pawar A et al (2015) An insight into cochleates, a potential drug delivery system. *RSC Adv* 5(99):81188–81202
269. Kersten G, Hirschberg H (2004) Antigen delivery systems. *Expert Rev Vaccines* 3(4):453–462
270. Tovey MG, Lallemand C (2010) Adjuvant activity of cytokines. In: *Vaccine adjuvants*. Springer, Berlin, pp 287–309
271. Kovacs JA et al (1996) Controlled trial of interleukin-2 infusions in patients infected with the human immunodeficiency virus. *N Engl J Med* 335(18):1350–1356
272. Osorio Y, Ghiasi H (2003) Comparison of adjuvant efficacy of herpes simplex virus type 1 recombinant viruses expressing TH1 and TH2 cytokine genes. *J Virol* 77(10):5774–5783
273. Henke A et al (2006) Co-expression of interleukin-2 by a bicistronic plasmid increases the efficacy of DNA immunization to prevent influenza virus infections. *Intervirology* 49(4):249–252
274. Rosenberg SA et al (1985) Observations on the systemic administration of autologous lymphokine-activated killer cells and

- recombinant interleukin-2 to patients with metastatic cancer. *N Engl J Med* 313 (23):1485–1492
275. Bolesta E et al (2006) Increased level and longevity of protective immune responses induced by DNA vaccine expressing the HIV-1 Env glycoprotein when combined with IL-21 and IL-15 gene delivery. *J Immunol* 177(1):177–191
 276. Saikh KU et al (2008) Interleukin-15 increases vaccine efficacy through a mechanism linked to dendritic cell maturation and enhanced antibody titers. *Clin Vaccine Immunol* 15(1):131–137
 277. Kwissa M et al (2003) Cytokine-facilitated priming of CD8+ T cell responses by DNA vaccination. *J Mol Med (Berl)* 81(2):91–101
 278. Kutzler MA et al (2005) Coimmunization with an optimized IL-15 plasmid results in enhanced function and longevity of CD8 T cells that are partially independent of CD4 T cell help. *J Immunol* 175(1):112–123
 279. Wang X et al (2008) Interleukin-15 enhance DNA vaccine elicited mucosal and systemic immunity against foot and mouth disease virus. *Vaccine* 26(40):5135–5144
 280. Toka FN et al (2005) Rescue of memory CD8+ T cell reactivity in peptide/TLR9 ligand immunization by codelivery of cytokines or CD40 ligation. *Virology* 331 (1):151–158
 281. Yoon HA et al (2006) Cytokine GM-CSF genetic adjuvant facilitates prophylactic DNA vaccine against pseudorabies virus through enhanced immune responses. *Microbiol Immunol* 50(2):83–92
 282. Shakya AK et al (2016) Mucosal vaccine delivery: current state and a pediatric perspective. *J Control Release* 240:394–413
 283. Skwarczynski M, Toth I (2020) Non-invasive mucosal vaccine delivery: advantages, challenges and the future. *Expert Opin Drug Deliv* 17(4):435–437
 284. Stratmann T (2015) Cholera toxin subunit B as adjuvant—an accelerator in protective immunity and a break in autoimmunity. *Vaccines (Basel)* 3(3):579–596
 285. Hou J et al (2014) Cholera toxin B subunit acts as a potent systemic adjuvant for HIV-1 DNA vaccination intramuscularly in mice. *Hum Vaccin Immunother* 10(5):1274–1283
 286. Li J et al (2014) Intranasal immunization with influenza antigens conjugated with cholera toxin subunit B stimulates broad spectrum immunity against influenza viruses. *Hum Vaccin Immunother* 10(5):1211–1220
 287. Li Y et al (2016) Antibody production and Th1-biased response induced by an epitope vaccine composed of cholera toxin B unit and *Helicobacter pylori* Lpp20 epitopes. *Helicobacter* 21(3):234–248
 288. Olivera N et al (2014) Immunization with the recombinant Cholera toxin B fused to Fimbrin 2 protein protects against *Bordetella pertussis* infection. *Biomed Res Int* 2014:421486
 289. Wiedinger K, Pinho D, Bitsaktsis C (2017) Utilization of cholera toxin B as a mucosal adjuvant elicits antibody-mediated protection against *S. pneumoniae* infection in mice. *Ther Adv Vaccines* 5(1):15–24
 290. WHO Organization (2010) Cholera vaccines: WHO position paper. *Wkly Epidemiol Rec* 85 (13):117–128
 291. Clements JD, Norton EB (2018) The Mucosal Vaccine Adjuvant LT(R192G/L211A) or dmLT. *mSphere* 3(4):e00215–e00218
 292. Valli E et al (2019) LTA1 is a safe, intranasal enterotoxin-based adjuvant that improves vaccine protection against influenza in young, old and B-cell-depleted (muMT) mice. *Sci Rep* 9(1):15128
 293. Pizza M et al (2000) LTK63 and LTR72, two mucosal adjuvants ready for clinical trials. *Int J Med Microbiol* 290(4–5):455–461
 294. Dodane V, Vilivalam VD (1998) Pharmaceutical applications of chitosan. *Pharm Sci Technol Today* 1(6):246–253
 295. Malik A et al (2018) Novel application of trimethyl chitosan as an adjuvant in vaccine delivery. *Int J Nanomed* 13:7959–7970
 296. Mourya VK, Inamdar NN (2008) Chitosan-modifications and applications: opportunities galore. *React Funct Polym* 68(6):1013–1051
 297. Hagenaaers N et al (2010) Role of trimethylated chitosan (TMC) in nasal residence time, local distribution and toxicity of an intranasal influenza vaccine. *J Control Release* 144 (1):17–24
 298. Amini Y et al (2017) Development of an effective delivery system for intranasal immunization against *Mycobacterium tuberculosis* ESAT-6 antigen. *Artif Cells Nanomed Biotechnol* 45(2):291–296
 299. Abkar M et al (2017) Oral immunization of mice with Omp31-loaded N-trimethyl chitosan nanoparticles induces high protection against *Brucella melitensis* infection. *Int J Nanomed* 12:8769–8778
 300. Farhadian A, Dounighi NM, Avadi M (2015) Enteric trimethyl chitosan nanoparticles containing hepatitis B surface antigen for oral

- delivery. *Hum Vaccin Immunother* 11 (12):2811–2818
301. Schipper P et al (2017) Diphtheria toxoid and N-trimethyl chitosan layer-by-layer coated pH-sensitive microneedles induce potent immune responses upon dermal vaccination in mice. *J Control Release* 262:28–36
 302. van der Maaden K et al (2015) Layer-by-layer assembly of inactivated poliovirus and N-trimethyl chitosan on pH-sensitive microneedles for dermal vaccination. *Langmuir* 31 (31):8654–8660
 303. Kim B et al (2002) Mucosal immune responses following oral immunization with rotavirus antigens encapsulated in alginate microspheres. *J Control Release* 85 (1-3):191–202
 304. Saraf S et al (2020) Lipopolysaccharide derived alginate coated Hepatitis B antigen loaded chitosan nanoparticles for oral mucosal immunization. *Int J Biol Macromol* 154:466–476
 305. AbdelAllah NH et al (2020) Alginate-coated chitosan nanoparticles act as effective adjuvant for hepatitis A vaccine in mice. *Int J Biol Macromol* 152:904–912
 306. Leonard M et al (2004) Hydrophobically modified alginate hydrogels as protein carriers with specific controlled release properties. *J Control Release* 98(3):395–405
 307. Zhao L, Skwarczynski M, Toth I (2019) Polyelectrolyte-based platforms for the delivery of peptides and proteins. *ACS Biomater Sci Eng* 5(10):4937–4950
 308. Zhao L et al (2020) Development of polyelectrolyte complexes for the delivery of peptide-based subunit vaccines against Group A *Streptococcus*. *Nanomaterials (Basel)* 10(5):823
 309. Yang J et al (2019) Cell-penetrating peptides: efficient vectors for vaccine delivery. *Curr Drug Deliv* 16(5):430–443
 310. Li X, Wang X, Ito A (2018) Tailoring inorganic nanoadjuvants towards next-generation vaccines. *Chem Soc Rev* 47(13):4954–4980
 311. Aguilar JC, Rodriguez EG (2007) Vaccine adjuvants revisited. *Vaccine* 25 (19):3752–3762
 312. Lin LC et al (2018) Advances and opportunities in nanoparticle- and nanomaterial-based vaccines against bacterial infections. *Adv Healthc Mater* 7(13):e1701395



Adjuvants: Engineering Protective Immune Responses in Human and Veterinary Vaccines

Bassel Akache, Felicity C. Stark, Gerard Agbayani, Tyler M. Renner, and Michael J. McCluskie

Abstract

Adjuvants are key components of many vaccines, used to enhance the level and breadth of the immune response to a target antigen, thereby enhancing protection from the associated disease. In recent years, advances in our understanding of the innate and adaptive immune systems have allowed for the development of a number of novel adjuvants with differing mechanisms of action. Herein, we review adjuvants currently approved for human and veterinary use, describing their use and proposed mechanisms of action. In addition, we will discuss additional promising adjuvants currently undergoing preclinical and/or clinical testing.

Key words Vaccine, Adjuvant, Immunomodulatory, Human, Veterinary

1 Introduction

Since the advent of the first successful vaccine against smallpox by Edward Jenner in 1796 [1], vaccines have become our principal weapon in the battle against infectious disease (e.g., smallpox, polio, hepatitis). Their ability to prevent disease and protect the most vulnerable segments of the population (i.e., infants, elderly) is a major cause for the decrease in mortality and the increase in life expectancy worldwide in the past century [2, 3]. As our understanding of microbial pathogenesis and the immune system has evolved, so have methods to develop safer and more effective vaccines. While generally highly efficacious, many of the early vaccines based on whole-killed or live attenuated pathogens had safety concerns, and therefore protein subunit vaccines rose to prominence in the twentieth century as a safer alternative [4]. Subunit vaccines were shown to mediate protection against many diseases while eliminating the risk of major side effects (e.g., viral reversion to an infectious state as with the polio vaccine) [5]. Whereas live

vaccines rely on the original pathogen's characteristics (e.g., infectious cycle, molecular patterns) to provoke an immune response, subunit vaccines based on a single or few types of protein/sugar molecules may be unable to independently induce sufficient protective immunity from infection by the target pathogen. As such, adjuvants (from the Latin word to help: "adjuvare") have become critical tools in the development of novel vaccines to fight disease and improve health, for both humans and animals.

Adjuvants are components included in vaccine formulations to augment the immune response to the vaccine antigen(s) [4, 6]. The antigen in turn is a part or mimetic of the pathogen that has been included to induce targeting by a recipient's immune response. As opposed to a live or whole killed vaccine approach, a subunit vaccine requires some rational design to select the optimal antigen [7]. The selection of a specific antigen to include in a vaccine formulation is based not only on its ability to induce an immune response but also on its biology. In considering whether an immune response to a particular antigen would prevent infection, the vaccine developer may also consider its role in infection (e.g., mediating internalization by binding to receptor molecule), accessibility to circulating antibodies, ability to generate T-cell responses, and/or ability to prevent infection in preclinical challenge models. The same rational approach must be taken for the adjuvant.

Adjuvants can serve many functions, such as (a) enhancement of an immune response; (b) dose sparing (generation of sufficient immunity through a lower antigen dose, increasing vaccine accessibility and/or reducing production costs); (c) orientation toward a humoral (antibody-based) and/or cellular immune response. As discussed below, there are different classes of vaccine adjuvants with different safety profiles and capabilities to induce antigen-specific antibodies and/or T cells. For example, mineral salts (e.g., aluminum phosphate, aluminum hydroxide, calcium phosphate) or emulsions (e.g., oil-in-water, water-in-oil, or multiphasic water-in-oil-in-water) are generally more proficient in stimulating an increase in the antigen-specific antibody response and accompanying T-helper (Th) type 2 response, whereas toll-like receptor (TLR) agonists (e.g., 3-deacylated monophosphoryl Lipid A (MPL), CpG oligodeoxynucleotides (ODN)) are more capable of inducing a Th1 and cytotoxic CD8⁺ T-cell response [4, 6]. Combination adjuvant formulations, where adjuvants of different classes are combined (e.g., aluminum salts with MPL), have also been employed to generate a more balanced Th1/Th2 response.

When selecting an adjuvant for a specific application, many factors must be considered such as the nature of the pathogen and whether the vaccine is to be used for a prophylactic/therapeutic application. Certain applications may require the generation of neutralizing antibodies capable of binding pathogens or toxins to prevent infection or disease, while others might require a cellular

response to eliminate the cells within which the infection is persisting. In addition, the safety profile and track record of a particular adjuvant in the target population (e.g., infant, elderly, pregnant) will need to be taken into account [8]. Considering the impact of the disease on a patient or the population at large, there may be different degrees of tolerance to side effects. While many vaccine adjuvants have utility in both humans and animals, for veterinary use cost also becomes a critical factor. This review discusses the different types of adjuvants already approved for human/veterinary use, as well as some promising research being conducted preclinically/clinically to develop novel adjuvants.

2 Adjuvants in Approved Human Vaccines

Considering the long history of vaccine use, relatively few adjuvants have been incorporated into commercialized human vaccines, and most of these have been in recent years. While the primary objective of any vaccine adjuvant is to enhance protection from disease, factors such as (a) compatibility with antigen, (b) safety/reactogenicity, and (c) feasibility of large-scale production are important criteria when selecting an adjuvant at the commercial scale. In this section, we will describe the qualities of commercialized vaccine adjuvants, their mechanisms of action, and the vaccines they are included in (summarized in Table 1).

2.1 Aluminum Salts

Aluminum salts (alum) have a long history of use in vaccine formulations; they were the first-approved vaccine adjuvant in humans and have been in use for over 80 years. Most notably, alum was the only licensed vaccine adjuvant in use up until 1997 when the oil-in-water emulsion MF-59 (see below) was also approved for use in the Fludax[®] influenza vaccine [4]. From their use in tetanus and diphtheria toxoid vaccines in the 1930s to modern day vaccines that protect against influenza, human papillomavirus (HPV), pneumococcus and meningococcus, hepatitis A and B, tetanus, diphtheria, pertussis, and polio [4, 9], aluminum salts have been a reliable, safe, easy to produce, and common vaccine ingredient. While early aluminum containing vaccines were made by precipitating antigen with insoluble aluminum salts [11], alum containing vaccine formulations have been refined over time for better reproducibility and are now typically prepared by the adsorption of antigen to preformed aluminum gels [12, 13]. While the term “alum” is often used without further description, there are multiple types of aluminum salts used in vaccine formulations, the most common of which are aluminum hydroxide (AlHy) and aluminum phosphate (AlP) [14]. Less common formats such as aluminum hydroxyphosphate sulfate are also found in approved vaccines (e.g., Gardasil) [15]. Several important physicochemical differences between AlHy

Table 1
Adjuvants approved for use in licensed vaccines

Adjuvant	Components	Mechanism of action and effect on immunity	Approved for use against	Select brand names [9, 10]
Alum	Aluminum hydroxide, aluminum phosphate, aluminum hydroxyphosphate sulfate	Provides antigen depot effect. Promotes release of DAMPs. Promotes Th2 type immune responses and enhances antibody responses	Diphtheria, tetanus, pertusis, polio, <i>Hemophilus influenzae</i> type B, hepatitis A, hepatitis B, meningococcal type B, pneumococcal disease, anthrax, human papillomavirus (HPV), influenza	Td Adsorbed [®] , Boostrix [®] , Adacel [®] , Adacel-polio [®] , Kinrix [®] , Havrix [®] , Infanrix [®] hexa or IPV/HiB, Quadracel [®] , Bexsero [®] , Prevnar [®] 13, Avaxim [®] , Vivaxim [®] , Pediacil [®] , Pentacel [®] , Menjugate [®] , Vaqta [®] , Engerix [®] - B, Recombivax HB [®] , Gardasil [®] , Ixiaro [®]
CpG	Synthetic unmethylated cytosine-guanine oligonucleotides	TLR9 agonist. Plasmacytoid DC (pDC) maturation, B- and T-cell activation. Promotes mixed Th1/Th2 responses	Hepatitis B	Heplisav-B [®]
MF59	Squalene-based oil-in-water nanoemulsion	Emulsion causes the activation of macrophages and DCs. Activation of B and effector CD8 ⁺ T cells	Influenza	Fluad [®]
AS04	MPL adsorbed onto aluminum hydroxide or aluminum phosphate	Enhances antigen uptake and immune activation through TLR4 signaling. Activation of T- and B-cell responses, mixed Th1/Th2 responses	Hepatitis B, human papillomavirus	Fendrix [®] , Cervarix [®]

(continued)

Table 1
(continued)

Adjuvant	Components	Mechanism of action and effect on immunity	Approved for use against	Select brand names [9, 10]
AS03	Squalene oil-in-water emulsion with Tween 80 and vitamin E	Enhances antigen uptake, increases cytokine and chemokine expression. Enhances antibody responses, supports Th2 CD4 ⁺ T cells	Pandemic influenza strains	Pandemrix [®] Arepanrix [®]
AS01	QS-21, MPL, and cholesterol-based DOPC liposomes	Activation of APCs, costimulation of T cells. Pro-inflammatory, mixed Th1/Th2 immune responses	Herpes zoster, malaria	Shingrix [®] Mosquirix [™]
Virosomes	Reconstituted influenza virosomes	Enhances APC activation and uptake. Stimulates antibody responses, CD8 ⁺ T-cell responses and a balanced Th1/Th2 CD4 ⁺ T-cell response	Hepatitis A	Epaxal [®]

APC antigen-presenting cell, DAMP damage-associated molecular pattern, DC dendritic cell, DOPC dioleoylphosphatidylcholine, MPL monophosphoryl lipid A, Th T helper cell

and AIP must be considered when deciding how to pair a particular vaccine antigen with alum. First, AlHy and AIP have differing points of zero charge: 11 and 4.0–5.5, respectively. As such, at neutral pH (typical of commercial formulations), they have different surface charges (positive and negative, respectively); since molecules typically bind better to oppositely charged salts, a vaccine protein antigen would likely have a stronger affinity to one or the other based on its own charge [14, 16]. Second, the choice of buffer can also reduce the adsorptive surface of alum. For example, AlHy has a strong affinity for phosphate and fluoride, a moderate affinity to sulfate, and a low affinity for chloride and nitrate [13, 17]; therefore, buffers containing these could affect protein adsorption. In the case of AIP, using a non-phosphate solution will reduce the number of surface phosphate groups and increase the point of zero charge [13, 18], reducing the adsorptive rate of positively charged protein antigens. Finally, differing manufacturing conditions can impact the degree of alum crystallinity affecting antigen adsorption and downstream immunogenicity

[19]; therefore, it is best to commit to one source when using alum-based adjuvants.

Alum's long history of use in vaccines has provided strong evidence of a generally positive safety profile and is likely partially responsible for the lack of initial investigation into alum's mechanism of action. More recently, there has been a renewed interest to decipher alum's mechanism of action, especially as alum has been found to act synergistically with other immunostimulants and has been included in new combinatorial adjuvant formulations, such as in AS04 [20] and with CpG [21, 22] (see below). It was originally thought that the adjuvant activity of alum was due simply to the physical adsorption of antigen to alum, resulting in an antigen depot effect where antigen was retained at the injection site and released slowly over time. Indeed, this was supported by studies comparing adsorbed versus nonadsorbed formulations. For example, adsorption of three *Streptococcus pneumoniae* (Sp) vaccine antigens to AlHy induced higher antibody concentrations than when antigens were administered with AlP with no stable interactions [23]. However, it also appears that there are other mechanisms involved in the adjuvanticity of aluminum salts. Thus far, there have been no receptors identified through which alum can directly signal through, but recent studies have revealed that alum promotes local necrosis in vaccinated muscle tissue [24]. It has been widely reported that after vaccination an alum granuloma can form which promotes short-term inflammation and cell death [25]. The resulting cell death is thought to release endogenous danger signals, such as uric acid crystals [26] and host DNA [27, 28]. These damage-associated molecular patterns (DAMPs) are known to contribute to pro-inflammatory responses and immune cell recruitment that can promote the induction of Th2-type responses, typical of alum containing vaccine formulations. Nalp3 inflammasomes have been identified as essential to the adjuvanticity of alum and can be activated by crystalline uric acid [29]. NALP3 inflammasomes regulate the release of pro-Th2 cytokines IL-1 and IL-33 which can explain why alum favors the induction of Th2 responses [29–31]. Multiple studies demonstrate that inclusion of an alum adjuvant will generally induce an overall improvement in humoral responses to the antigen, resulting in an enhancement of antigen-specific antibody responses and a skewing of CD4⁺ T-cell responses toward a Th2 phenotype [32, 33]. While Th2-skewed immune responses are proficient in protecting against extracellular infection and parasites, they are often not sufficient to protect against intracellular infections which require the activation of cellular immune responses. Accordingly, combination adjuvant approaches, where alum is combined with Th1-inducing molecules such as MPL or CpG, have been employed to generate more balanced Th1/Th2 immune responses thought to be necessary for protection against intracellular pathogens [21, 22].

2.2 Oil-in-Water Emulsion MF59

MF59 is a squalene-based oil-in-water nanoemulsion vaccine adjuvant originally developed by Chiron Corporation and then acquired by Novartis in 2006. It was first approved in Europe in 1997 as part of the influenza vaccine, Flud[®]. Generally considered to be the second vaccine adjuvant (after alum) approved for use in humans and the first approved oil-in-water human vaccine adjuvant; the successful use of MF59 during the 2009 influenza pandemic (Focetria[®] by Novartis) solidified its good safety profile, and as such, it is now approved and licensed for use in influenza vaccines in 38 countries [34, 35]. In the US and Canada, Flud[®] is currently licensed for those over the age of 65 years who are most at risk of morbidity and mortality due to influenza and has been found to be 51% effective in reducing influenza-related hospital admissions in this age group [36]. In some countries including Canada, MF59-adjuvanted influenza vaccines (e.g., Flud Pediatric[®]) are also available to another high risk cohort: children aged 6 months to 2 years. While not currently approved for use in Canada and the US for those aged 2–65 years, a meta-analysis by Yang et al. suggests there is evidence that the MF59-adjuvanted flu vaccine confers better immunogenicity compared to non-adjuvanted inactivated flu vaccines in those aged 7–64 years [37]. MF59 is an oil-in-water formulation containing the biodegradable oil squalene and the nonionic surfactants Tween 80 and Span 85, as well as trisodium citrate dihydrate [34, 38]. It was initially developed as a safe alternative to the highly reactogenic Freund's complete/incomplete adjuvants, through the use of the naturally occurring biodegradable oil squalene, as well as less toxic nonionic surfactants. By opting for an oil-in-water formulation, the designers were also able to reduce the amount of oil in the formulation compared to the water-in-oil emulsion found in Freund's adjuvants. In addition, the use of small droplets in the formulation reduced viscosity and improved stability [38]. Squalene is a triterpene hydrocarbon (C₃₀H₅₀) with a complex structure that is found to be naturally occurring in humans as part of the steroid hormone biosynthetic pathway as a direct precursor for cholesterol [34]. It is also a common component of the human diet and thus can be readily metabolized. MF59 is made by dispersing Span 85 in squalene and Tween 80 in aqueous buffer. The oil and water solutions are then mixed and passed through a microfluidizer to form an oil-in-water emulsion with uniform droplets of 160 nm [34]. Since the individual components of MF59 do not have adjuvant activity, it is the resulting oil-in-water emulsion that confers the adjuvant effect of MF59 [34]. MF59 enhances the immune response through the activation of tissue resident macrophages and dendritic cells (DCs) at the injection site. Following the release of chemokines, there is enhanced immune cell (including monocytes/macrophages) recruitment to the injection site, that in turn increases the transport of antigen to the draining lymph nodes leading to the activation of T and B cells [39]. MF59 allows for dose

sparing [40], enhances protective immunity against antigenically drifted viruses [41], and is also proven to drive strong and broad memory B- and T-cell responses [42, 43]. In 2000, there were reports that MF59 containing vaccines may be linked to “Gulf War syndrome,” through the induction of anti-squalene responses [44]. These reports have since been disproven; while many people naturally have low levels of anti-squalene antibodies, MF59 was found to neither enhance nor induce anti-squalene titers [45]. MF59 is also currently being investigated in clinical trials as a vaccine adjuvant for the prevention of HIV [46], Pandemic H5N1 [47], and SARS-CoV-2 [48].

2.3 CpG Oligodeoxynucleotides

With the approval of the second-generation hepatitis B vaccine, Heplisav-B[®], in 2017, synthetic CpG ODN became the latest adjuvant class to be approved by the FDA. Heplisav-B[®] utilizes the CpG-based ISS 1018 adjuvant to augment responses to hepatitis B surface antigen and was shown to be more immunogenic following two immunizations than the previously approved alum-adjuvanted vaccine formulation Engerix[®]-B following a three-dose vaccination regimen [49]. Despite only recently gaining approval for use in a vaccine, CpG ODNs have long been demonstrated to induce potent immunostimulatory responses as they have been designed to mimic bacterial DNA through the inclusion of unmethylated C-G dinucleotides [50, 51]. Unlike eukaryotic DNA, prokaryotic DNA is known to contain substantial amounts of unmethylated C-G dinucleotides, which is recognized as a pathogen-associated molecular pattern (PAMP) in humans and other mammals. When bacterial DNA is released during an infection, the unmethylated CpG motifs bind the TLR9 protein found in the endosome of certain innate immune cells triggering a cascading protective immune response [52]. Synthetic CpG oligodeoxynucleotides (ODNs) consisting of 20–30 bases of single-stranded DNA containing unmethylated C-G dinucleotides were developed for use as single agents for cancer immunotherapy or as vaccine adjuvants. Four classes have been described thus far: A, B, C, and P. Each type differs structurally and triggers disparate immune responses. A-type CpG ODNs (also known as D-type) possess a mixed phosphodiester/phosphorothioate backbone and contain a single CpG motif flanked by palindromic sequences and poly G tails at both the 3' and 5' ends [53]. The phosphorothioate backbone helps to protect the ODNs from degradation by nucleases. A-type ODNs trigger the maturation of plasmacytoid dendritic cells (pDCs) and secretion of IFN- α but do not have an effect on B cells [54]. B-type CpG ODNs (also known as K-type) include ISS 1018 (found in Heplisav-B[®]) and CPG 7909 (included in the third-generation anthrax vaccine, NuThrax[™] currently in phase 3 clinical trials). B-type CpG ODNs contain multiple CpG motifs on a phosphorothioate backbone and have been shown to

trigger the production of TNF- α by pDCs, the proliferation of B cells and the production of IgM [52, 55]. C-type CpG ODNs resemble B-type in that the backbone is composed entirely of phosphorothioate nucleotides, but they also contain the palindromic CpG motifs present in A-type CpG ODNs. As such, the activation profile of C-type CpGs includes the stimulation of B cells to produce IL-6 (similar to B-type CpG) and pDCs to produce IFN- α (similar to A-type CpG) [52, 56, 57]. The fourth class of CpG, P class, with two palindromic sequences and a propensity to form multimeric units, has also been described. Partially combining the effects of the other three CpG ODN types, P class ODNs activate both B cells and pDCs and stimulate more IFN- α than C-Class ODNs [58]. CpG ODNs are also being investigated as therapeutic agents against multiple cancer indications [59, 60], and in vaccines against malaria [61], hookworm [62], and SARS-CoV-2 [22, 63, 64]. The combination of CpG and alum has been shown in multiple preclinical studies to have potent synergistic activity [65–67], as a result this combination was chosen by Valneva SE [22], Sichuan Clover Biopharmaceuticals Inc. [63], and Medigen Inc. [64] for evaluation in their vaccine formulations against SARS-CoV-2.

2.4 Adjuvant Systems by GlaxoSmithKline (GSK)

With the discovery of new immunostimulants and a better understanding of their mechanism of action, it became possible to develop combination adjuvants that achieve additive and even synergistic responses not possible with a single adjuvant. The Adjuvant Systems concept was pioneered in the 1990s by GlaxoSmithKline (GSK) when classical adjuvants such as alum, liposomes, and oil-in-water emulsions were combined with relatively newer immunomodulators such as MPL, QS-21 (a saponin derived from the soap bark tree *Quillaja saponaria*), or CpG [68]. During their development, these Adjuvant Systems were evaluated based on their (a) ability to induce stronger immune responses compared to antigen alone or alum-adjuvanted formulations; (b) safety profile and local reactogenicity; and (c) ease to manufacture in a highly reproducible manner [68]. Ten Adjuvant System families were created over 5 years through combining adjuvants and establishing stable formulations; it was noted early on that the formulation method was just as important as choice of adjuvant for the creation of an effective Adjuvant System [68]. Of the ten adjuvant families, three have been licensed for use in human vaccines, thus far including AS01, AS03, and AS04.

2.4.1 AS04

AS04 was the first Adjuvant System candidate approved for use in humans by the European Medicine Agency in 2005 as part of the Hepatitis B vaccine, Fendrix[®]. In the US and Canada, AS04-adjuvanted vaccine formulations were first approved in 2009–2010 with the HPV vaccine, Cervarix[®]. AS04 is formulated

by adsorbing the water-insoluble MPL onto either AlHy as is found in Cervarix[®] or onto AlP in the case of Fendrix[®]. MPL is a detoxified derivative of bacterial lipopolysaccharide (LPS), isolated from *Salmonella minnesota* R595 strain [69–71]. During manufacturing, the MPL is first adsorbed onto alum before addition of the antigen. This overcomes MPL's insolubility in water and also enhances the manufacturing reproducibility by ensuring that similar amounts of MPL are bound to each alum particle. As MPL is a derivative of LPS, it retains some of the latter's ability to signal through the pattern recognition receptor (PRR) TLR4 [72–76], albeit to a weaker degree (likely due to the absence of the 1-phosphate molecule on MPL) [77]. MPL is the main driver of AS04's ability to enhance immune responses by inducing local inflammation, enhanced antigen uptake by antigen-presenting cells (APCs) and activation of T- and B-cell responses [20]. While alum-adjuvanted vaccines induce a predominant Th2 response, the addition of MPL shifts the response to more of a Th1 bias [38], which supports the activation of the CD4⁺ and CD8⁺ T-cell responses involved in efficacious anti-viral immune responses. In addition to addressing MPL's solubility issues, alum helps provide an antigen depot effect thought to prolong immune responses as described above.

2.4.2 AS03

AS03 gained widespread approval in influenza vaccines due to their successful use as part of the response to the 2009 H1N1 and H5N1 influenza pandemic as a component of the Pandemrix[®] and Arepanrix[®] vaccines [78]. Similar to MF59, AS03 is a squalene-based oil-in-water emulsion made with Tween 80 and also the immune-enhancer alpha-tocopherol (vitamin E). AS03 was selected among many tested oil-in-water emulsion-based formulations based on its strong adjuvanting properties as well as its stability profile and manufacturing reproducibility [68]. Vitamin E was included in AS03 because of its known immune-stimulating properties, which include increased antigen uptake by monocytes and induction of cytokine/chemokine expression [79, 80]. AS03 is a good option for antigen dose sparing as it enhances antibody responses by activating Th2 cells that in turn support B-cell responses [80]. AS03's use in the 2009 influenza pandemic vaccines was due to (a) its ability to induce high antibody responses, considered a correlate of protection for influenza; and (b) its relative ease to produce using components that are readily sourced. After the mass vaccinations campaigns of this pandemic, it was reported that narcolepsy was associated with one of the vaccine formulations, Pandemrix[®], but not Arepanrix[®]. Further investigation by the Swedish Medical Products Agency and the Finnish National Institute for Health and Welfare determined that the association between Pandemrix[®] vaccination and narcolepsy was valid with a 12.7-fold

increase in cases of narcolepsy among vaccinated children [81, 82]. Multiple factors were considered to help better understand the link between the increased incidence of narcolepsy and the vaccine, in addition to the difference in safety profiles between the two AS03-adjuvanted formulations. As the Pandemix[®] vaccine was approved for use in Europe while the wild-type H1N1 virus was still in circulation; it was possible that recently infected persons received that vaccine. In contrast, the Arepanrix[®] vaccine, which was approved for use and manufactured in Canada, was deployed later when the wild-type virus was no longer circulating as extensively. It was theorized that antigen mimicry (due to similarity in H1N1 and hypocretin-derived peptides) may have played a role in the induction of narcolepsy. Specifically, H1N1-specific CD8⁺ T cells induced from natural infection may have become reactivated during vaccination and attacked the hypocretin producing neurons, leading to symptoms similar to narcolepsy [81]. While the European Medicines Agency concluded there was still a favorable benefit–risk profile for the continued use of Pandemix[®], it has since been withdrawn by GSK [78]. It should be noted that AS03 was not found to be the direct cause of the observed narcolepsy, rather its intrinsic ability to induce antigen-specific immune responses that could have led to a recall of hypocretin-reactive memory CD8⁺ T cells. As such, AS03 is still considered a useful adjuvant in particular for vaccines that require strong antibody responses; as such, it is currently under investigation in multiple active phase 2/3 clinical trials for SARS-CoV-2 vaccines [63, 83, 84].

2.4.3 AS01

The AS01-based adjuvant system was approved for use in Europe in 2015 as part of a malaria vaccine, Mosquirix[®] (AS01). It was first approved in the US and Canada in 2017 as a component of the first non-live shingles vaccines, Shingrix[®] (AS01_B). AS01 and AS01_B are made by combining QS-21, MPL (as in AS04), and cholesterol-based dioleoyl phosphatidylcholine (DOPC) liposomes. QS-21 is a highly complex triterpene glycoside (saponin) with branched sugar chains and is acylated at the 4-hydroxyl position on fucose with two ester-linked 3,5-dihydroxy-6-methyl-octanoic acids [85]. AS01 and AS01_B contain identical components (MPL, QS-21, DOPC, and cholesterol), only the amount of each differs in the final adjuvant formulations [86]. QS-21 is known to induce pro-inflammatory Th1/Th2 immune responses, yet its mechanism of action is complex and has not been fully elucidated. QS-21 is thought to activate macrophages and DCs via the NLRP3 inflammasome. However, QS-21 still induced high antigen-specific T-cell and antibody responses in NLRP3-deficient mice [87], suggesting another mechanism of action for its adjuvanticity must be present. QS-21 does not cause an antigen depot effect, and it does migrate

from the injection site independently of antigen. It can be found at draining lymph nodes, where it may provide direct co-stimulation for T-cell activation [88, 89]. It was once thought that the immune-stimulating properties of QS-21 were mediated through its lytic ability to form pores in the cell membrane. As these lytic properties were also shown to induce hemolysis, there was concern that they could contribute to severe reactogenicity at the injection site. As such, AS01 was formulated with cholesterol-based liposomes that quenched the lytic function of QS-21, while maintaining its adjuvant effect. The quenched QS-21 was also found to be more stable at higher pH and at temperatures above 37 °C when compared to the unquenched version [68]. While AS01 is a relatively new addition to the approved adjuvant arsenal, it was one of the first Adjuvant Systems created, initially for use in a potential HIV vaccine. It is now currently being assessed in numerous Phase 2/3 clinical trials for various indications, including *Mycobacterium tuberculosis* [90], malaria [91–94], and glioblastoma multiforme [95].

2.5 Virosomes

Virosomes were first approved for use as a vaccine adjuvant in 1996 as part of a hepatitis A vaccine Epaxal[®] [4, 96] which was registered for use in most countries of the EU, the Americas, and Asia. Notably, it was the first adjuvanted vaccine to be approved that did not contain alum. Epaxal[®] is made with a whole-virus preparation of formalin-inactivated hepatitis A virus (HAV) (strain RG-SB) adsorbed to reconstituted influenza virosomes (IRIVs) isolated from the influenza A/Singapore H1N1 strain [97]. Epaxal[®] induces potent anti-HAV immune responses within 10 days of immunization [98] and is considered more tolerable than conventional alum adsorbed vaccine formulations [99, 100]. Recently, a 20-year follow-up study of healthy vaccinated participants revealed that two doses of Epaxal[®] provided protection against hepatitis A infection for at least 30 years [101]. While still recommended for use by the WHO and approved for use in many countries, the production of Epaxal[®], now owned by Janssen-Cilag, has been discontinued [102].

3 Adjuvants in Approved Veterinary Vaccines

As with humans, vaccination is an effective and widely used approach to control and prevent disease in multiple animal species. While adjuvants may work equally well in animals and humans due to similarities in our immune systems, they may be employed to different degrees in human vs. veterinary vaccines. This is due to many factors, but in general, different tolerances for cost and safety will influence whether an adjuvant is suitable for human and/or veterinary vaccines. Human vaccine candidates are generally

required to go through formal toxicity studies in animals followed by several phases of clinical trials (I, II, III) involving increasingly larger numbers of human participants to properly demonstrate vaccine safety and efficacy in the target population. In contrast, licensure of veterinary vaccines is routinely granted upon providing more limited safety and vaccine efficacy data, typically generated through challenge studies involving much smaller cohorts [103]. Due at least in part to cost constraints but also to a lower concern for rare side effects, cohort sizes in animal vaccination studies are typically much smaller than those seen in human trials. As there are frequently lower ethical concerns with regard to conducting infectious challenge studies in veterinary applications, it is possible to demonstrate vaccine efficacy more efficiently by directly administering the target pathogen to the animal trial test subjects. As the development costs of human vaccines are higher, it is not surprising that the marketed product would generally need to be more expensive if the developer is looking to recuperate these costs and generate a profit. In fact, the cost of human and animal vaccines can vary by several orders of magnitude [103]. Another factor influencing veterinary vaccine pricing is the inherent value to the end user. For example, the nature of the animal (e.g., companion animal vs. livestock) will influence the amount the owner is willing to spend on a vaccine. In the case of livestock, if the cost of a prospective vaccine was found to be higher than the expected profit to be gained from the particular animal, it would be a non-starter in the marketing/deployment of the vaccine [103]. As such, there is more focus on the use of relatively inexpensive and stable ingredients, including adjuvants, when developing many veterinary vaccines. With regard to vaccine safety, short-term impacts on overall animal health may be more acceptable with veterinary vaccines and adjuvants. In addition, other parameters, such as the impact of vaccine formulations on the quality of meat, may be important to consider when developing vaccines for livestock [104]. If the value of the animals to the owner (i.e., pets) or impact of the disease (necessitating a mass culling of infected or exposed livestock) is more substantial, more expensive formulations may be viable [105]. A recent example of high commercial cost of an infectious disease outbreak is the culling of mink farms to minimize the spread of new mutant strains of SARS-CoV-2 [106]. Another consequence of veterinary vaccines' lower price/profit margin is a lower level of investment in the characterization of veterinary vaccines. Generally, there is more focus on simply demonstrating efficacy (e.g., mortality/abortion rates of a vaccinated vs. unvaccinated herd, etc.) than, for example, on defining specific correlates of protection [103]. Overall, this results in less available information on veterinary vaccines and/or adjuvants, which may be reflected in some of the sections below.

3.1 Mineral Salts

As with human vaccines above, aluminum salts have been used extensively in veterinary vaccines for many years. Their relatively low cost and immunostimulatory properties have led to their use in many commercially licensed vaccines either alone or in combination with oil/polymers (Table 2). In addition, calcium phosphate and uric salts have also been used as effective adjuvants in vaccine models of relevant diseases, such as equine, swine, and highly pathogenic avian influenza virus strains [107–109].

3.2 Emulsions

Emulsion-based adjuvants have been used extensively within veterinary vaccines due to their ability to induce robust immune activation, while requiring relatively simple and low-cost production methods. As discussed above with MF59 and AS03, adjuvant emulsions are typically formed by the mixing of immiscible solvents (i.e., oil and water) with the assistance of a surfactant, usually a gentle detergent. Owing to the amphipathic nature of a surfactant, it will generate a micellar solution to stabilize the emulsion. This will result in differing effects depending on the formulation of the emulsion.

Water-in-oil emulsions are composed of a majority oil and minority water components. Emulsifying this type of solution will result in water droplets surrounded by an oil phase. Given the aqueous solubility of vaccine components (i.e., nucleic acids, proteins, inactivated pathogens, etc.), most antigens will be entrapped within these water droplets. Consequently, the mechanism of action of water-in-oil emulsions is hypothesized to be a depot effect, where antigen is slowly released from the injection site over time [111]. The water-in-oil emulsion-based Freund's adjuvant has been used for decades in research, but is not in any approved human or veterinary vaccines due to its high reactogenicity and potential to generate lesions and granulomas [112]. The company Seppic SA offers alternative water-in-oil emulsions under the Montanide™ brand, which display lower reactogenicity, while maintaining some of the potency of Freund's adjuvants [113]. There are a multitude of these Montanide™ formulations that are either being tested clinically for human use (*see* Subheading 4.1) or marketed specifically as veterinary adjuvants. The latter includes the more synthetic water-in-lipophilic polymer emulsions, such as Montanide™ ISA 760VG. These adjuvants have been successfully employed in the field in a variety of animals and pathogens [108, 114, 115].

As their namesake suggests, oil-in-water emulsions are a majority aqueous solution with a minority oil component that results in the micellar component being oil-based. Consequently, the surrounding water phase contains the water-soluble immunostimulatory materials that are released immediately post-administration of the vaccine. As mentioned above, studies with the MF59 adjuvant suggest that their adjuvant activity relies on the rapid attraction of

Table 2
Licensed veterinary vaccines that contain aluminum salt-based adjuvants^a

Adjuvant	Vaccine	Type	Pathogen (# of species)	Animal
Aluminum hydroxide	Bar Somnus 2P™	Inactivated bacteria	<i>Haemophilus</i> , <i>Mannheimia</i> , <i>Pasteurella</i>	Cattle
	Biocom®-P	Killed virus and inactivated bacteria/toxoid	Mink enteritis virus, <i>Clostridium</i> and <i>Pseudomonas</i>	Mink
	Biovac®	Killed virus	Mink enteritis virus	Mink
	Botumink®	Inactivated bacteria/toxoid	<i>Clostridium</i>	Mink
	Bovib-Lepto 5	Inactivated bacteria	<i>Campylobacter</i> , <i>Leptospira</i> (5)	Cattle
	Campylobacter Fetus-Jejuni	Inactivated bacteria	<i>Campylobacter</i> (2)	Sheep
	Bacterin-Ovine			
	CattleMaster® 4+VL5	Modified live and killed virus, inactivated bacteria	Bovine rhinotracheitis/diarrhea virus, parainfluenza-3-respiratory syncytial virus, <i>Campylobacter</i> , <i>Leptospira</i>	Cattle
	Durvac Past HM	Inactivated bacteria	<i>Mannheimia</i> , <i>Pasteurella</i>	Cattle/ sheep/ goats
	Essential 1, 2(+P), 4	Inactivated bacteria	<i>Clostridium</i> (4), <i>Mannheimia</i> , <i>Pasteurella</i>	Cattle/ sheep/ goats
	Haemo Shield® P	Inactivated bacteria	<i>Actinobacillus</i> , <i>Pasteurella</i>	Swine
	Mannheimia Haemolytica-Pasteurella Multocida Bacterin	Inactivated bacteria	<i>Mannheimia</i> , <i>Pasteurella</i>	Cattle/ sheep/ goats
	Para Shield™	Inactivated bacteria	<i>Haemophilus</i>	Swine
	Parapleuro Shield® P	Inactivated bacteria	<i>Actinobacillus</i> , <i>Haemophilus</i> , <i>Pasteurella</i>	Swine
	Parvo Shield™ L5E	Killed virus and inactivated bacteria	Parvovirus, <i>Erysipelothrix</i> , and <i>Leptospira</i> (5)	Swine
	Porcine Pili Shield™	Inactivated <i>Escherichia coli</i>	<i>Escherichia</i> (4)	Swine
	Resvac® 4/Somubac®	Modified live and killed virus, inactivated bacteria	Bovine rhinotracheitis/diarrhea virus, parainfluenza-3-respiratory syncytial virus, <i>Haemophilus</i>	Cattle
			Swine	

(continued)

Table 2
(continued)

Adjuvant	Vaccine	Type	Pathogen (# of species)	Animal
	Rhini Shield™ TX4	Inactivated bacteria/ toxoid	<i>Bordetella</i> , <i>Erysipelothrix</i> , <i>Pasteurella</i>	
	Salmonella Dublin- Typhimurium Bacterin	Inactivated bacteria	<i>Salmonella</i> (2)	Cattle
	Scourmune®-C	Inactivated bacteria/ toxoid	<i>Clostridium</i> , <i>Escherichia</i>	Swine
	Serpens Species Bacterin	Inactivated bacteria	<i>Aquaspirillum</i>	Cattle
	Somnu Shield™	Inactivated bacteria	<i>Haemophilus</i>	Cattle
	Somubac®	Inactivated bacteria	<i>Haemophilus</i>	Cattle
	Strepvax® II	<i>Streptococcus</i> <i>equi</i> extract	<i>Streptococcus</i>	Horses
Potassium alum	Bar Vac® 7/Somnus	Inactivated bacteria/ toxoid	<i>Clostridium</i> (6), <i>Haemophilus</i>	Cattle
	Tasvax® 8	Inactivated bacteria/ toxoid	<i>Clostridium</i> (8)	Cattle/ sheep
Emunade® (oil-in- water emulsion and aluminum hydroxide combination)	M+PAC®	Inactivated bacteria	<i>Mycoplasma</i>	Swine
	MaxiVac Excell® 5.0	Killed virus	Swine influenza virus (2)	Swine
Aluminum hydroxide and DEAE-dextran combination (polymer)	Vepured®	<i>Escherichia coli</i> subunit	<i>Escherichia</i>	Swine
Aluminum hydroxide and oil combination	Endovac-Porci® with Immuneplus®	Inactivated bacteria/ toxoid	<i>Salmonella</i>	Swine

^aDerived from compendium for veterinary products approved for use in Canada and USA [110]. This may be a partial list as the majority of licensed veterinary vaccines did not disclose the nature of the adjuvant used

monocytes and macrophages, leading to differentiation and maturation toward antigen-presenting cell functions [116, 117]. Multiple manufacturers have developed their own versions of oil-in-water emulsions for veterinary applications including Seppic, which also has a variety of oil-in-water emulsions (similarly under the Montanide™ brand). MVP adjuvants has several versions of Emulsigen®

adjuvants, while Amphigen[®] (mineral oil/soy lecithin) and MetaStim[®] (squalene) are used within licensed Zoetis vaccines such as FluSure[®] Pandemic, RespiSure-One[®] and FarrowSure[®] Gold which immunize pigs against pandemic H1N1 influenza, *Mycoplasma hyopneumoniae*, and a combinatorial vaccine against porcine parvovirus and bacterial leptospirosis and erysipelas, respectively. It is unclear how the specific ingredients of these various adjuvant compositions differ due to the proprietary and/or undisclosed nature of these patented formulations. Some of the different types of emulsions used in commercially licensed veterinary vaccines are listed in Table 3. While most of these vaccines utilize a single emulsion-based adjuvant, there are examples of emulsions being combined successfully with other adjuvant types.

A more complex preparation method was investigated to create water-in-oil-in-water emulsions that may combine the immunostimulatory effects of both water-in-oil and oil-in-water emulsions. In this preparation, water droplets exist within oil droplets which are surrounded by a phase of aqueous solution, allowing for immediate and slow release of antigen. This type of adjuvant was identified to reduce the adverse effects of water-in-oil emulsions, while maintaining a robust immune response [118]. There are several of these emulsions offered by Seppic that are commercially available for veterinary vaccine research: both Montanide[™] ISA 201 and 206 water-in-oil-in-water emulsions have been used in multiple studies, displaying different degrees of effectiveness [115, 119–121]. The more limited use of these types of adjuvants in commercial vaccines may be indicative of the lower stability of the multi-emulsion system.

3.3 Liposomes

The generation of liposomes in solution is similar to the principle of generating an oil-in-water emulsion. The main structural difference being that the emulsion contains micelles with a lipid monolayer, whereas a liposome will be composed of droplets with lipid bilayers, not unlike that of a cellular membrane. Depending on the nature of the lipid, the polar head group can be either positively or negatively charged, which allows for the potential of electrostatic attraction or repulsion of liposomes with cell membranes, respectively. Furthermore, liposomes can be generated to include nucleic acid, lipid, or protein molecules in the interior or on the surface of the vesicle [122]. This allows for liposomes to be used as both an adjuvant and/or a delivery tool, which has been shown to elicit an effective immune response with subunit and DNA vaccines in livestock [123, 124]. The effective use of liposomes is illustrated by the use of cationic lipids to deliver live Newcastle disease virus of a commercial vaccine (La Sota[®]), leading to an enhanced immune response in chickens when compared to the liposome free vaccine [125]. Additionally, Victrio[™] and Zelrate[®] are liposomal

Table 3
Licensed veterinary vaccines that contain emulsion-based adjuvants^a

Adjuvant	Vaccine	Type	Pathogen (# of species)	Species
Amphigen [®]	ER Bac Plus [®]	Inactivated bacteria	<i>Erysipelothrix</i>	Swine
	FluSure [®] XP [™]	Inactivated virus	Swine influenza virus	Swine
	Respisure (-One [®] /ER Bac Plus [®])	Inactivated bacteria	<i>Erysipelothrix</i> , <i>Mycoplasma</i>	Swine
DD-2 [™]	Alpha-7/MB-1 [®]	Inactivated bacteria/toxoid	<i>Clostridium</i> (6), <i>Moraxella</i>	Cattle
	Alpha-CD [™]	Toxoid	<i>Clostridium</i> (2)	Cattle
Emulsigen [®]	Emulsibac [®] APP	Inactivated bacteria	<i>Actinobacillus</i> (3)	Swine
Emulsigen [®] D	Nuplura [™] PH	Inactivated bacteria/toxoid	<i>Mannheimia</i>	Cattle
MetaStim [®]	Core EQ Innovator [®] + V	Killed virus and inactivated bacteria/toxoid	Encephalomyelitis virus, rabies virus/West Nile virus, <i>Clostridium</i>	Horse
	Equivac [®] Innovator EHV-1/4	Killed virus	Equine herpes virus 1/4	Horse
	Fluvac Innovator [®] (1-6)	Killed virus and inactivated bacteria/toxoid	Encephalomyelitis virus, rhinopneumonitis-influenza viruses, <i>Clostridium</i>	Horse
	Fostera [®] PCV MetaStim [®]	Killed virus	Porcine circovirus	Swine
	Lepto EQ Innovator [®]	Inactivated bacteria	<i>Leptospira</i>	Horse
	Pyramid [®] 3/5 (+ Presponse [®] SQ)	Modified live virus (/toxoid)	Bovine rhinotracheitis/diarrhea virus, parainfluenza-3-respiratory syncytial virus, <i>Mannheimia</i>	Cattle
	Tetanus Toxoid	Inactivated bacteria/toxoid	<i>Clostridium</i>	Horse, Sheep, Swine
	West Nile-Innovator [®] (VEWT)	Killed virus (and inactivated bacteria/toxoid)	Encephalomyelitis virus, West Nile virus, <i>Clostridium</i>	Horse
Mineral oil	Campylobacter Fetus Bacterin-Bovine	Inactivated bacteria	<i>Campylobacter</i>	Cattle
	Chlamydia Abortus Bacterin	Inactivated bacteria	<i>Chlamydia</i>	Sheep

(continued)

Table 3
(continued)

Adjuvant	Vaccine	Type	Pathogen (# of species)	Species
Oil-based emulsion	Avian Influenza Vaccine	Killed virus	Avian influenza virus	Chicken
	Bovilis [®] J-5	Inactivated bacteria	<i>Escherichia</i>	Cattle
	Breedervac-(IV [®] /Reo)-Plus	Killed virus	Infectious bursal disease virus, Newcastle disease virus, infectious bronchitis disease virus and reovirus	Chicken
	Bron-Newcavac [™] -SE	Killed virus and inactivated bacteria	Newcastle disease virus, infectious bronchitis virus, <i>Salmonella</i>	Chicken
	Bursa Guard (Reo/N-B-R)	Killed virus	Infectious bursal disease virus, Newcastle disease virus, infectious bronchitis disease virus and reovirus	Chicken
	Circovac [®]	Killed virus	Porcine circovirus	Swine
	Circuvent [®] PCV (-M G2)	Killed virus (and inactivated bacteria)	Porcine circovirus, <i>Mycoplasma</i>	Swine
	Corvac-3 [®]	Inactivated bacteria	<i>Haemophilus</i> (3)	Chicken
	Endovac-(Beef [®] /Dairy [®]) with ImmunePlus [®]	Inactivated bacteria	<i>Salmonella</i>	Cattle
	Forte Micro [™]	Inactivated bacteria	<i>Aeromonas</i> , <i>Vibrio</i> (3)	Salmonid
	Forte V II [™]	Killed virus and inactivated bacteria	Infectious salmon anemia virus, <i>Aeromonas</i> , <i>Vibrio</i> (3)	Salmonid
	Gallimune [®] NC-BR	Killed virus	Newcastle disease virus, bronchitis virus	Chicken
	J-5 <i>Escherichia coli</i> Bacterin	Inactivated bacteria	<i>Escherichia</i>	Cattle
	Layermune [®] (SE/3/5/ND)	Inactivated bacteria (and/or killed virus)	<i>Salmonella</i> , infectious bursal disease virus, Newcastle disease virus, infectious bronchitis disease	Chicken
	MG-Bac [®]	Inactivated bacteria	<i>Mycoplasma</i>	Chicken/ turkey
	Multimune [®] K5	Inactivated bacteria	<i>Pasteurella</i> (4)	Chickens/ turkeys
	Piliguard [®] Pinkeye TriView [®]	Inactivated bacteria	<i>Moraxella</i>	Cattle
	Piliguard [®] Pinkeye-1 Trivalent	Inactivated bacteria	<i>Moraxella</i> (3)	Cattle
	Poulvac [®] Pabac [®] IV	Inactivated bacteria	<i>Pasteurella</i>	Chicken/ turkey
	SE Guard [™]	Inactivated bacteria	<i>Salmonella</i>	Chicken

(continued)

Table 3
(continued)

Adjuvant	Vaccine	Type	Pathogen (# of species)	Species
	Staybred™ VL5	Inactivated bacteria	<i>Campylobacter, Leptospira</i> (5)	Cattle
	Streptococcus Uberis Bacterin	Inactivated bacteria	<i>Streptococcus</i>	Cattle
Paraffin oil	Emulsibac® APP	Inactivated bacteria	<i>Actinobacillus</i> (3)	Swine
	Hiprabovis® Somni/Lkt	Inactivated bacteria/toxoid	<i>Histophilus, Mannheimia</i>	Cattle
SuprImm™	Fusogard™	Inactivated bacteria	<i>Fusobacterium</i>	Cattle
Unspecified emulsion	Salmonella Vetovax™ SRP®	Bacterial extract	<i>Salmonella</i>	Cattle
Water-in-oil-in-water	Cevac® Salmune TEK	Inactivated bacteria	<i>Salmonella</i> (3)	Chicken
Emunade® (oil-in-water emulsion and aluminum hydroxide combination)	M+Pac®	Inactivated bacteria	<i>Mycoplasma</i>	Swine
	MaxiVac Excell® 5.0	Killed virus	Swine influenza virus	Swine
Aluminum hydroxide and oil combination	Endovac-Porci® WITH Immuneplus®	Inactivated bacteria/toxoid	<i>Salmonella</i>	Swine
Combination of Amphigen® and undisclosed ingredient	Cattlemaster® Gold FP® 5 (L5)	Modified live and killed virus (and inactivated bacteria)	Bovine rhinotracheitis/diarrhea virus, parainfluenza-3-respiratory syncytial virus, <i>Leptospira</i> (5)	Cattle
	ER Bac® Plus/Leptoferm-5®	Inactivated bacteria	<i>Erysipelothrix, Leptospira</i> (5)	Swine
	ER Bac®/L5 Gold	Inactivated bacteria	<i>Erysipelothrix, Leptospira</i> (5)	Swine
	Farrowsure® (Plus/Gold) (B)	Killed virus and inactivated bacteria	Parvovirus, <i>Erysipelothrix, Leptospira</i> (6)	Swine
Montanide ISA 907.1 mg and MPL combination	Top-Ubac®	<i>Streptococcus uberis</i> subunit	<i>Streptococcus</i>	Cattle
Paraffin oil and LPS combination	Hyogen®	Inactivated bacteria	<i>Mycoplasma</i>	Swine

^aDerived from compendium for veterinary products approved for use in Canada and USA. [110]. This may be a partial list as the majority of licensed veterinary vaccines did not disclose the nature of the adjuvant used

formulations containing DNA immunostimulants that have been licensed to prevent bacterial infection in chicken and cattle, respectively.

3.4 Polymers

Polymers are another class of adjuvants characterized by large molecules with repeating subunits that have been used within veterinary medicine. These compounds are generally recognized to induce minimal adverse events, are readily biodegradable, and can be customized to react to specific biological stimuli, such as pH or oxidative stress [126]. Similar to the lipids mentioned previously, natural or synthetic polymers can be amphiphilic, which allows them to encapsulate antigen. This feature allows for a targeted delivery of antigen, while enhancing vaccine stability [127]. Some polymers have been recognized as biologically inert, precipitating around delivered antigen to create a depot effect [128]. The use of polymers continues to be investigated within the veterinary vaccine field due to their ability to enhance immune responses and protection rates within livestock species [108, 129–131]. A number of polyacrylate-based polymer adjuvants are available for veterinary applications: Carbigen[®] (carbomer-based, Carbopol 934P) and Polygen[®] (low molecular weight co-polymer) from MVP adjuvants and several compounds are available from Seppic under the Montanide[™] (i.e., Gel 01 PR and Gel 02 PR). As an example of a licensed product, VEPURED[®] uses a dextran polymer adjuvant in its *E. coli* subunit vaccine for pigs.

Polymers based on a repeating polyphosphazene structure have also been demonstrated to have adjuvant activity in multiple animal species. Poly-dicarboxylato-phenoxy-phosphazene (PCPP) and poly-disodiumcarboxylatoethyl-phenoxy-phosphazene (PCEP) induce immune cell recruitment and secretion of cytokines/chemokines at the injection site, leading to enhancement of adaptive immune responses [132]. While increasing antigen stability and half-life, polyphosphazene polymers have been shown to enhance antigen-specific antibody titers, leading to dose-sparing and protection from influenza when administered intramuscularly or intradermally in ferrets and pigs, respectively [133–135]. Interestingly, phosphazene polymers are also compatible with combinatorial adjuvant approaches, with PCEP displaying enhanced immune responses when combined with TLR agonists such as CpG ODNs [136].

3.5 Saponins and Immunostimulatory Complexes (ISCOMs)

The immunostimulatory activity of saponins has been known for nearly a century, though the initially impure compounds, isolated from *Quillaja Saponaria* bark extracts, were shown to cause localized toxicities [137]. Quillaic acid, or Quil-A, is a commonly used heterogenous saponin mixture, while QS-21 is a purified saponin from within this extract that is used in the human adjuvant system AS01 (see above). While the direct mechanism of action of saponin compounds is not entirely known, one hypothesis is that their

affinity for cholesterol allows them to integrate within the membranes of APCs, thereby delivering antigen [138]. It is this activity that is also thought to mediate some of the adverse effects of saponin such as cell lytic activity, although more recently, the amphipathic structures of these compounds have been linked with their adjuvanticity [139]. Vaccine formulations with more homogeneous saponin extracts have been successfully used in veterinary vaccines for decades with fewer adverse reactions [140]. For example, the feline leukemia virus vaccine (FELOCELL[®] FeLV, Zoetis) includes a saponin-based compound, marketed as Gentle Safe-Quil[™], while the livestock anthrax vaccine (Anthrax Spore Vaccine, Colorado Serum) and swine pneumonia vaccine (Myco Shield[™]) contain saponin and Quil-A, respectively.

Immunostimulatory complexes (ISCOMs) are liposomes that contain saponin, which along with cholesterol and phospholipid moieties act as structural components [141]. As with traditional liposomes, antigen can be internalized within the ISCOM liposomes. An antigen-free preparation is commercially available as ISCOMATRIX[®], enabling custom vaccine formulations for any subunit antigen [142]. Simply mixing this adjuvant preparation with soluble antigen provides immunostimulation without the necessity of antigen internalization; however, depending on the antigen, there may be direct interactions or even aggregate formation with ISCOMATRIX[®] [142–144]. The exact mechanism of these complexes remains unclear, though these complexes are significantly more potent adjuvants than the saponin monomers [145]. It is believed that the affinity of this adjuvant for cellular membranes enables an efficient delivery of antigen to the internal compartments of cells, allowing for both MHC class I and class II processing [146]. As with AS01 above, the cholesterol quenching of saponin within these complexes seems to drastically reduce its cell lytic activity and observed side effects [147]. The ability to stimulate both the innate and adaptive arms of the immune response has proven effective at protecting animals from viral infections, such as equine influenza [148]. This particular vaccine was commercialized and is available from Zoetis as Equip FT[®]. In cattle, efficacious vaccines against bovine viral diarrhea virus also contain ISCOMs [149, 150]. Altogether, ISCOMs act as an effective antigen delivery tool with strong immunostimulatory effects and fewer side effects than earlier generations of saponin compounds.

3.6 Pathogen-Associated Molecular Patterns (PAMPs)

As discussed above, MPL and CpG are PAMPs that mimic bacterial components to stimulate the immune system through TLRs 4 and 9, respectively. Several vaccines listed in Table 3 include TLR4 agonists (MPL or LPS) along with an emulsion-based adjuvants. There are other TLRs and several classes of PRRs capable of detecting PAMPs (i.e., Nod-like receptors, intracellular sensors, etc.), which have been utilized to activate the immune response by adjuvants. For example, Pam₃CSK₄ is a synthetic lipopeptide that

mimics similar compounds found within bacterial membranes. It functions as a TLR1/2 agonist and has been used in pigs in an inactivated vaccine against porcine reproductive and respiratory syndrome virus [151]. Similarly, a lipoprotein isolated from *Pseudomonas aeruginosa*, OprI, stimulates both TLR2 and TLR4 and was shown to have adjuvanting properties in a subunit vaccine against classical swine fever virus [152]. A synthetic ligand for TLR2, TLR4, TLR6, and a NOD2-like receptor, referred to as CVC1302, showed strong immune stimulating effects in a pig vaccine for foot-and-mouth disease virus [153]. CpG ODNs have also been widely used in veterinary applications in a variety of animals [52].

3.7 Chemokines and Cytokines

Administration of an effective adjuvant will generally result in a measurable increase in the production cytokines and chemokines, the messenger proteins used by immune cells to communicate. For several decades now, researchers have been investigating the possibility of bypassing the production step and supplying chemokines or cytokines directly within a vaccine [154]. As of yet, no commercially available vaccine has disclosed use of these compounds as an adjuvant. However, their activity within experimental veterinary vaccines has been demonstrated. For example, in fish, the chemokines CK6 and CXCL12 have been shown to enhance responses against infectious pancreatic necrosis virus and viral hemorrhagic septicemia virus, respectively [155, 156]. There are other examples of cytokines being used as vaccine adjuvants in a variety of hosts, mainly for viral vaccines [157]. One major drawback of these biologic-type molecules is their increased production costs, when compared to other effective adjuvants.

3.8 Combinations

As with the adjuvant systems described above for human vaccines, combinatorial approaches have been evaluated in veterinary vaccine development (see examples in Tables 2 and 3). A more natural example of this is highlighted by the generation of bacterial ghosts, which are nonliving cells with preserved surface PAMPs and membrane antigens, cleared of the cytosolic components, and any potential pathogenicity [158]. These cells are easily modifiable for drug or antigen delivery and their effectiveness has already been illustrated with a variety of experimental vaccines in livestock species [159]. There are numerous examples of other combinatorial approaches that take advantage of some of the aforementioned adjuvants in the previous sections [160]. The combination of emulsions or liposomes with a direct immune stimulant, such as cytokines or TLR ligands, are commonly used in experimental vaccines. Notably, Emulsigen[®] combined with CpG illustrated synergistic protective effects in cattle against a bovine herpesvirus 1 challenge [161]. Other combinations, such as saponins mixed with emulsions or aluminum salts have also shown promise [162, 163].

4 Adjuvants in Clinical/Preclinical Testing

While major advances in adjuvant development have been made in recent years with a number of clinically approved adjuvants, there is still an ongoing need for novel adjuvants. The use/availability of a number of adjuvants, especially the more novel formulations, is restricted due to their proprietary nature. In addition, the main correlate of protection for many of the vaccines mentioned above is antigen-specific antibodies. While many approved adjuvants are quite proficient at inducing antigen-specific antibodies, novel adjuvants capable of inducing strong CD8⁺ T-cell responses may be required for vaccines targeting certain viral diseases or used therapeutically for cancer. Herein, we review some vaccine adjuvants that are currently being evaluated in clinical trials, as well as others that have been evaluated in a pre-clinical setting. Due to the large number of experimental adjuvants, our selection below was based on their advanced clinical use or the novelty of their structure/mechanism of action (as compared to adjuvant types described above).

4.1 *Water-in-Oil Emulsion Montanide™ ISA 51*

Montanide™ ISA 51 is a water-in-oil emulsion developed by Seppic for human indications. It has been used extensively (alone or in combination with other adjuvants) in various human clinical trials of different types of cancer vaccines (see below). It was approved by Cuba in 2013 as a component of the CIMAvax-EGF vaccine [164] for the treatment of lung cancer [165]. Similar to incomplete Freund's adjuvant, Montanide™ ISA 51 is one of a set of incomplete Seppic adjuvants (ISAs) and contains highly purified Drakeol 6 VR light mineral oil and the surfactant mannide monooleate [166, 167]. The emulsion is made at the time of immunization by blending via either two-syringe mixing, vortexing, or homogenizing [168]; the two-syringe mixing method was shown to be the most efficacious to create stable emulsions and, in comparison to vortexing, caused less local adverse events after immunization [165]. Montanide™ ISA 51 has been shown to increase both antigen-specific antibody titers as well as CD8⁺ T-cell responses [169]. In providing an antigen depot effect as well as causing local inflammation at the site of immunization, Montanide™ ISA 51 has been shown to cause the activation and recruitment of APCs to the injection site and is considered a strong inducer of long-lasting cell-mediated immune responses. It is currently being heavily investigated in numerous active Phase 2/3 clinical trials for multiple indications including breast cancer [170, 171], melanoma [170, 172, 173], lung cancer [174, 175], multiple myeloma [176], leukemia [177], prostate cancer [178], glioblastoma [179–181], multiple sclerosis [182], and other cancer types [183–187].

4.2 Adjuvant System 15 (AS15)

AS15 is an experimental adjuvant system developed by GSK that is comprised of the main components of AS01 (QS-21 and MPL immunostimulants with liposomes) and a TLR9 agonist (CPG7909). When compared to the other Adjuvant Systems from GSK, AS15 is unique in its inclusion of CpG. CPG7909 is a B class CpG and has been shown to promote antigen-specific antibody production, human B-cell proliferation, IFN- α /IL-10 expression, and NK cell activity [188]. The immunostimulatory activity of AS15 has been evaluated in combination with the MAGE-A3 protein in melanoma and non-small-cell lung cancer therapies [189–192]. MAGE-A3 is a cancer-testis antigen that is overexpressed in a wide range of tumors and can be presented by both HLA class I and class II [193]. AS15 has been shown to induce higher anti-MAGE-A3 antibody titers and CD4⁺ T-cell responses compared to AS02B (QS-21, MPL in an oil-in-water emulsion) [194]. However, MAGE-A3-AS15 treatment did not significantly improve survival of patients with MAGE-A3-positive surgically resected NSCLC or melanoma [191, 192, 195]. Induction therapy with MAGE-A3-AS15 plus high-dose interleukin-2 (HDIL-2), followed by maintenance therapy with MAGE-A3-AS15 has shown encouraging antitumor responses in patients exhibiting disease control [190]. Currently, AS15 is being evaluated in a therapeutic vaccine for patients with non-metastatic, HER2-negative localized breast cancer at high-risk of relapse [196].

4.3 Matrix-M™

Matrix-M™ (developed by Isonova AB, Uppsala, Sweden) is an ISCOM technology-based nanoparticle formulation comprised of cholesterol, phospholipids, and a mixture of purified fractions of *Quillaja* saponins (Matrix-A™ and Matrix-C™ at 85:15 ratio) [197, 198]. It promotes potent immunostimulatory properties in the absence of antigen, including immune cell recruitment to local and distant tissues, activation of APCs and inflammatory cytokine production [198]. Vaccines adjuvanted with Matrix-M™ have been shown to induce potent cellular and humoral responses in various preclinical and clinical models of viral infection [199–204]. Recent focus has been given to the adjuvant potential of Matrix-M™ in a recombinant SARS-CoV-2 nanoparticle vaccine, being developed by Novavax, comprised of the trimeric full-length SARS-CoV-2 spike glycoproteins (NVX-CoV2373). Preclinical evaluation of this vaccine formulation in mouse and nonhuman primate models showed robust induction of antigen-specific T cells, and antibodies that blocked spike protein receptor binding and neutralized the virus [205]. Phase I–II trials of the NVX-CoV2373 showed a similar immunogenicity profile to the preclinical studies, particularly a Th1-biased cellular response [206]. Viral-vectored malaria vaccine formulations adjuvanted with Matrix-M™ have also been evaluated in a recent phase I trial, where they were shown to significantly improve vaccine-specific T-cell responses compared

to unadjuvanted formulations [207, 208]. Several other clinical trials evaluating malaria vaccines using the Matrix-M™ platform are also ongoing/being planned [209–212].

4.4 Imidazoquinoline TLR7/8 Agonists

Agonists of TLR7/TLR8 have also been investigated for use as vaccine adjuvants due to their differential and wide-ranging induction of inflammatory responses. TLR7 stimulation promotes the expression of IFN- α and other inflammatory cytokines by pDCs, antibody production by B cells and Th1-polarizing responses [213–216]. In contrast, TLR8 activation leads to the production of NF- κ B-dependent inflammatory cytokines primarily by myeloid immune cells [213]. While TLR7/8 are PRRs for single-stranded RNA, a class of synthetic small molecules, imidazoquinolines, have also been shown to exhibit strong TLR7- or TLR8-specific or 7/8 bispecific activity. Major types of imidazoquinolines include imiquimod (R-837) and resiquimod (R-848). The adjuvant and immunotherapeutic activities of imidazoquinolines against cancer are well-documented, with imiquimod approved for use as a monotherapy immunomodulator when applied topically for genital warts [217]. As with many other novel adjuvants, imidazoquinolines are also being evaluated as adjuvants in SARS-CoV-2 vaccine formulations. The BBV152 vaccine is composed of a whole-virion inactivated SARS-CoV-2 adjuvanted with Algel-IMDG, a TLR7/8 agonist molecule adsorbed to alum [218]. It has been shown to induce antigen-specific antibodies as well as Th1-biased cellular responses with mild to moderate reactogenicity in a recent Phase I trial [218]. In mouse models, a recombinant spike protein vaccine formulation with a novel amphiphilic imidazoquinoline (IMDQ-PEG-CHOL) has been demonstrated to enhance immune cell recruitment and activation in the draining lymph node, induce neutralizing antibody titers and provide protective immunity [219]. Novel lipidated imidazoquinoline adjuvants (i.e., UM-3003, -3004, and -3005) have also been shown to induce influenza-virus specific antibody and Th1- and Th17-polarized cellular responses [220].

4.5 TLR3 Agonist Poly(I:C) and Derivatives

Poly(I:C) is a double-stranded RNA composed of polyinosinic: polycytidylic acid with strong immunostimulatory properties exerted through activation of TLR3 and MDA5. It has been evaluated not only as a vaccine adjuvant but also as a monotherapy for cancer or viral disease indications [221, 222]. It has been suggested that the potent ability of Poly(I:C) to increase MHC class I expression in both immune and nonimmune cells and, consequently, promote self-antigen presentation could lead to tolerance impairment and autoimmunity [223, 224]; however, additional studies are needed to verify this. Poly(I:C) is also susceptible to nuclease degradation which can result in lowered cellular uptake in vivo, possibly limiting its use as a vaccine adjuvant [225]. Two

promising Poly(I:C) derivatives, Poly-ICLC (Hiltonol[®], Oncovir, Inc.) and Poly-IC12U (Ampligen[®], Hemispherx), are currently being evaluated for clinical use. Poly-ICLC similarly targets MDA-5 and TLR3 receptors as conventional Poly(I:C), but is more stable in vivo due to increased resistance to nucleolytic hydrolysis [226, 227]. In contrast, Poly-IC12U signals exclusively through TLR3 and exhibits reduced toxicity due to a shortened half-life in vivo [226, 228]. Both Poly(I:C) derivatives promote enhanced antibody and Th1-biased cellular responses in multiple preclinical and/or clinical models [226, 229]. Poly-ICLC has been shown to induce robust tumor antigen-specific antibody and CD8⁺ T-cell responses in combination with synthetic overlapping long peptides (OLP) from a human tumor self-antigen and Montanide ISA 51 in a phase I clinical trial [230]. Poly-IC12U can also promote human DC maturation in vitro, which may prove beneficial in the induction of tumor-specific T-cell responses in cancer patients [231, 232]. While Poly(I:C) derivatives are interesting vaccine adjuvant candidates, recent clinical trials have also focused on their therapeutic potential as non-antigen- and antigen-specific immunotherapies against various solid (i.e., glioma, colon, breast, prostate head and neck) and hematologic (i.e., leukemia, lymphoma) tumors [233–237].

4.6 TLR4 Agonist Glucopyranosyl Lipid Adjuvant

Glucopyranosyl lipid adjuvant (GLA) is a synthetic TLR4 agonist with immunostimulatory activity similar to MPL. It promotes an increase in cytokine/chemokine production, DC activation and maturation, and Th1-mediated cellular responses, without the associated physiologic toxicity of classic LPS [238]. In contrast to MPL, GLA can be synthesized in pure form and is highly modifiable, providing enhanced ease of production and characterization [238, 239]. GLA is being licensed by Avanti Polar Lipids as Phosphorylated HexaAcyl Disaccharide (PHAD[®]) for use as an adjuvant in human vaccines. Variants of PHAD[®] include 3D-PHAD[®] and 3D(6-acyl) PHAD[®]. 3D-PHAD[®] is a highly pure, homogeneous equivalent of 3-deacylated MPL with reduced pyrogenicity [240, 241]. 3D(6-acyl) PHAD[®] shares structural similarities with MPL found in the GSK adjuvant systems AS01 and AS04 [242]. Despite differences in composition, both variants exhibit equivalent adjuvant activity as the original PHAD[®] [243]. They have also been shown to promote synergistic effects on antibody responses in mice when formulated in human papillomaviruses (HPV) and hepatitis B virus (HBV) vaccine formulations with alum [244]. A second-generation GLA-based adjuvant (referred to as SLA-TLR4 in this review) has also been developed with enhanced affinity/activity potential for the human receptor [245]. The safety and immunogenicity of GLA or SLA-TLR4 alone and in vaccine formulations against infectious diseases, including influenza, malaria, leishmania, and schistosomiasis have

been evaluated in multiple clinical trials in the past decade [246–249]. Recent results from the first in-human trial of a tuberculosis vaccine formulation with GLA in squalene emulsion (ID93 + GLA-SE) showed an acceptable safety profile and the robust induction of vaccine-specific humoral (IgG1 and IgG3) and Th1-biased cellular responses [250, 251]. A phase 2a clinical trial is also currently evaluating the safety, immunogenicity, and efficacy of ID93 + GLA-SE in BCG-vaccinated healthy healthcare workers [252]. As a cancer immunotherapeutic, GLA-SE in combination with a recombinant NY-ESO-1 protein (G305) has been shown to induce tumor protein-specific antibody and T-cell responses in patients with advanced NY-ESO-1-expressing solid tumors [253, 254].

4.7 Army Liposome Formulations

Army liposome formulations (ALFs) are liposome-based adjuvants comprised of a synthetic version of MPL/GLA (e.g., 3D-PHAD[®]), cholesterol, and saturated phospholipids. ALF in combination with other common adjuvants such as aluminum hydroxide (ALFA), QS-21 (ALFQ), and ALFQ + aluminum hydroxide (ALFQA) have also been developed to improve immunogenicity and address the limited availability of adjuvants approved for human use [255]. These formulations exhibit little to no detectable adjuvant activity in the absence of MPL, indicating a central role for TLR4 signaling in their mechanism of action [255]. While the ALFQ and AS01 are similar in that they both contain QS-21 and a TLR4 agonist, each features a distinct liposome composition. ALFQ is comprised of saturated dimyristoyl fatty acids with a 55% cholesterol/phospholipid molar ratio, in contrast to the unsaturated dioleoyl fatty acids, and 33.7% cholesterol/phospholipid ratio in AS01 [255]. In addition, the doses of QS-21 and MPL are two- to fourfold higher in ALFQ than in AS01_B. ALF saw its early use in malaria vaccines, inducing potent antigen-specific antibody responses [256–258]. ALF-based formulations have also been shown to promote enhanced HIV-1 antigen-specific antibody and cellular responses compared to alum or MPL alone [259]. While ALF formulations initially involved liposome encapsulation of antigen, it was later discovered that simply mixing the antigen with liposomes could provide equivalent or enhanced responses [255]. A novel malaria vaccine formulation containing ALFQ and the *P. falciparum* protein 013 (FMP013) is currently being evaluated in a Phase I clinical trial [260]. Recent preclinical evaluation of this vaccine formulation showed high reactivity of serum antibodies against the malaria circumsporozoite protein (CSP) and a Th1-biased cytokine response with minimal adverse reactions in rhesus macaques [261]. A Phase I clinical trial evaluating the impact of delayed boosting with a HIV vaccine adjuvanted with ALFQ on antibody production by healthy, HIV-uninfected participants is also set to begin in 2021 [262].

4.8 Polyacrylates

Polyacrylates (PAAs) are a class of adjuvant-active polymers that can be formulated in a wide range of polymer sizes, formulations, and doses with a favorable safety profile [263]. Major types of PAAs that have been evaluated in various experimental and commercial veterinary vaccines include: (1) simple, non-crosslinked polymers; (2) dendrimers; (3) alkyl esters; and (4) crosslinked polymers (e.g., Carbomers™ and Carbopols™) [263–268]. Currently, the adenovirus-based cocaine vaccine dAd5GNE co-delivered with the Adjuplex™ (Advanced BioAdjuvants LLC) platform, which is based on purified lecithin and carbomer homopolymer, is being evaluated in a Phase I clinical study [269–272]. SPA09, a novel vaccine adjuvant based on high molecular weight straight PAA, is also being developed by Sanofi Pasteur for evaluation in clinical trials [263, 273, 274]. It provides the key advantages of ease of synthesis and quality control, as well as cost-effectiveness over other PAA-based formulations due to its simple structure and the commercial availability of straight PAAs [263]. SPA09 has been shown to induce robust Th1-biased cellular and humoral responses in combination with various antigens, particularly the recombinant cytomegalovirus glycoprotein B (CMV-gB) and a *Staphylococcus aureus* polysaccharide conjugate in mice [274]. A similar effect was recently observed in cynomolgus macaques upon immunization with SPA09 in combination with respiratory syncytial virus (RSV) nanoparticulate prefusion F model antigen [273].

4.9 Heat-Labile Toxins

Heat-labile toxins (LTs) are a family of enterotoxins derived from *Escherichia coli* and *Vibrio cholerae*. They have been shown to induce strong antigen-specific immune responses, in particular when administered via mucosal routes [275]. LTs can be classified into types I and II subfamilies, according to biochemical properties and antigenic capacity [276, 277]. Type I LTs consist of *E. coli* heat-labile enterotoxin (LT-I) and cholera toxin (CT), which typically promote a mixed Th1/Th2/Th17 response, and IgG1 and IgG2a antibody responses when administered with antigen to mice [278–280]. In contrast, type II LTs such as LT-IIa, LT-IIb and LT-IIc predominantly induce Th1 and IgG2a responses [278, 281]. Both LT types share a similar AB5 oligomeric structure but differ in B subunit amino acid sequences, leading to distinct target specificities [281]. Despite exhibiting potent immunostimulatory properties, LT-based adjuvants have not been approved for human use due to inherent toxicity linked to their ADP-ribosylating enzymatic activity [278]. Oral and intranasal administration of LT-based formulations have also been linked to adverse effects such as diarrhea and Bell's palsy (temporary facial paralysis or weakness), respectively [282, 283]. Modified LTs such as mLT (R192G: glycine to arginine at position 192), which exhibits reduced toxicity but equivalent adjuvanticity as native LT, also saw limited success in clinical trials. Oral mLT at 25µg dose was

well-tolerated but induced self-limited, mild diarrhea when combined with killed whole-cell bacterial vaccines [284]. The double-mutant dmLT (R192G and L211A: leucine 211 to alanine in the A1-A2 activation loop on the A2 domain) was shown to have further reduced toxicity and has been/is being currently evaluated in several human clinical trials [285]. Recent Phase I studies have examined the adjuvant potential of dmLT when administered orally or intradermally with inactivated polio vaccine formulations [286, 287].

The CT-based CTA-1DD is also being developed for use as a vaccine adjuvant. It is comprised of the CTA1-subunit of cholera toxin (CT) linked to a dimer of the D-domain from *S. aureus* protein A, effectively reducing physiologic toxicity associated with CT [288]. CTA-1DD specifically targets B cells and promotes germinal center reactions, leading to enhanced development of long-lived plasma cells and memory B cells [289, 290]. It also exhibits equivalent adjuvant properties as native CT, including potent induction of systemic and mucosal antibody and CD4⁺ T-cell responses when co-administered with various antigens in mice and nonhuman primates [288, 289, 291, 292]. Mucosal immunization of adult mice with a CTA1-DD-adjuvanted influenza vaccine formulation was shown to confer protection from lethal viral challenge [293]. Recently, CTA1-DD was demonstrated to induce follicular DC maturation and germinal center formation upon systemic or mucosal immunization of neonatal mice [294]. Oral prime and intranasal boost immunizations with a novel CTA1-DD-adjuvanted influenza vaccine increased antigen-specific antibody responses and CD4⁺ T-cell proliferation, leading to enhanced protection from infection.

4.10 Archaeosomes

Archaeosomes are liposomes formed with archaeal-derived lipids (i.e., total polar lipids (TPLs) from Archaea, or semi-synthetic archaeal-derived glycolipids). Archaeal-based lipids have unique adaptations when compared to their bacterial/eukaryotic counterparts, namely the presence of (a) ether instead of the ester linkages between the glycerol backbone and the lipid tails and (b) lipid tails named phytanyl chains, which are composed of branched 5-carbon repeating units [295]. Traditional archaeosome formulations possess key advantages over conventional liposomes, including enhanced immunostimulatory properties, decreased proton permeability, and high thermal and pH stability [296]. When used to entrap/encapsulate antigen, traditional archaeosome formulations induce robust antigen-specific humoral and cell-mediated responses [296]. The enhanced immunogenicity of these formulations as compared to traditional liposomes was thought to be due to their increased stability and their promotion of endocytosis/MHC class I cross-presentation through the phosphatidylserine receptor [297]. TPL formulations based on the lipids from

Methanobrevibacter smithii were particularly immunogenic in pre-clinical models of infectious disease and cancer [298–304]. However, the complex and diverse lipid composition of traditional archaeosome formulations presented challenges in formulation characterization. Variations in antigen entrapment efficiency (5–40%) could also lead to antigen loss and increased production costs [304–306]. These challenges have been addressed through the development of an archaeosome formulation comprised of a single semi-synthetic archaeal lipid (SLA, sulfated lactosyl archaeol). SLA archaeosomes retain the robust adjuvant activity of traditional archaeosome formulations in various animal models of infection and cancer [307–310]. They also offer equivalent or enhanced immunostimulatory and antigen-specific responses as established adjuvants such as aluminum hydroxide, TLR3/4/9 agonists, oil-in-water, and water-in-oil emulsions [65]. Recently, SLA was shown to generate equivalent/superior antigen-specific responses when antigen was simply admixed with, instead of encapsulated within the archaeosomes [305, 307, 310]. This has provided a simplified vaccine formulation with minimal antigen loss. As these adjuvants seem to retain their immunostimulatory potential with non-encapsulated antigen, their mechanism of action may differ than that observed with the TPL formulations. Admixed SLA does increase antigen retention at the injection site, while inducing increased cytokine/chemokine expression and immune cell recruitment/antigen uptake [310]. In addition, SLA has been shown to synergize with certain TLR agonists (e.g., Poly (I:C), CpG) in mice, inducing superior antigen-specific responses than those obtained with either adjuvant alone [311]. The specific molecular pathways responsible for immunostimulation by SLA remain to be elucidated.

4.11 α -Galactosylceramide

α -Galactosylceramide (α -GalCer), originally identified in extracts from the marine sponge *Agelas mauritianus*, is a glycolipid that is able to activate natural killer T cells with invariant T-cell receptors (iNKT cells) via the CD1d receptor found on APCs [312]. CD1d-restricted iNKT activation promotes the induction and proliferation of various immune cells, including NK cells, DCs, and T cells [313–316]. Deficiencies in the number and function of iNKT cells are associated with poor responses against solid (i.e., prostate, head and neck) and hematologic (i.e., acute myeloid leukemia) cancers [317]. A synthetic analog, KRN7000, has been developed for use as an immunotherapy/adjuvant. KRN7000 alone or in combination with other immunomodulators (i.e., TLR agonist, cytokine) has been shown to enhance antitumor and antimicrobial responses when co-administered with antigen in various murine models of infection and cancer [315, 318, 319]. Several clinical trials have also evaluated the impact of KRN7000 when administered alone or pulsed into various APC platforms on tumor immunity within the

last two decades [320–330]. Recently, a Phase II clinical study demonstrated the safety and survival benefit of KRN7000-pulsed APCs comprised primarily of immature and mature HLA-DR⁺ and CD86⁺ monocyte-derived DCs (MoDCs) as a second-line treatment for advanced non-small-cell lung cancer (NSCLC) [331].

4.12 Polysaccharides

Chitosan is a polysaccharide derivative of chitin, a major component of arthropod exoskeletons and fungal cell walls [332]. Due to its nontoxic and biocompatible properties, it has been used in a wide range of medical and pharmacological applications such as drug delivery, vaccines, wound healing, and antimicrobial procedures [333–335]. Chitosan exhibits various immunostimulatory properties, including DC maturation via type I IFN induction and Th1-mediated cellular responses in a type I IFN receptor-dependent manner [336]. While chitosan is not currently being evaluated as a vaccine adjuvant in clinical trials, it has shown promising safety profiles and immunostimulatory activities in multiple preclinical and clinical studies in the past. A Norwalk VLP vaccine containing chitosan and MPL has been shown to induce VLP-specific antibodies and antibody-secreting cells (ASCs) that express mucosal and peripheral lymphoid tissue homing molecules in Phase I clinical studies [337, 338]. Influenza vaccine formulations with chitosan are also well-tolerated and effective in promoting high antibody titers in both humans and mice [339, 340].

Advax™ (Vaxine Pty Ltd) is a plant-based adjuvant platform developed from delta inulin polysaccharides. While inulin is not immunologically active in its native soluble form, its crystallization into delta inulin particles confers adjuvant activity [341]. Advax™ formulations that have been evaluated in preclinical and/or clinical studies include: Advax-1 (delta inulin alone); Advax-2 (delta inulin and a TLR9 agonist); Advax-3 (TLR9 agonist CpG55.2 and aluminum hydroxide); Advax-4 (delta inulin and a TLR7/8 agonist); and Advax-5 (delta inulin and a TLR4 agonist) [342–344]. Vaccine formulations containing Advax™ have been shown to promote potent humoral and/or cellular immune responses against multiple models of murine infection, including severe acute respiratory syndrome (SARS) coronavirus, hepatitis B, influenza, RSV, and *M. tuberculosis* [341, 344, 345]. Recently, VLP-based malaria vaccines adjuvanted with Advax™ formulations have been shown to be highly immunogenic and promote long-lasting, antigen-specific (*P. falciparum* CSP) antibodies in murine and nonhuman primate models [342]. In clinical studies, Phase I trials evaluating the safety and immunogenicity of Advax™-adjuvanted vaccine formulations against hepatitis B and influenza have been recently completed [346–348]. A SARS-CoV-2 recombinant protein vaccine adjuvanted with Advax-2 is also currently being evaluated in a Phase I trial in response to the current COVID-19 pandemic [349].

5 Concluding Remarks

Our ability to harness the power of the immune system through vaccines has allowed us to directly improve our quality of life, either directly through prevention of human disease or indirectly by preserving the health of our companion animals and livestock on which we rely. As our understanding of the innate and adaptive immune systems has increased, so have the number of different adjuvants available for scientists to generate novel vaccines capable of inducing protective and/or therapeutic immune responses. This has been highlighted in the recent SARS-CoV-2 pandemic, where many different adjuvants and antigen platforms are being evaluated to offer us a broader range of potential vaccine candidates. Surely, established as well as novel experimental adjuvants will be integral parts of future vaccines, helping us address existing health challenges or new diseases as they arise.

References

1. Jenner E (1799) History of the inoculation of the cow-pox: further observations on the variolæ vaccinae, or cow-pox. *Med Phys J* 1:313–318
2. Pollard AJ, Bijker EM (2021) A guide to vaccinology: from basic principles to new developments. *Nat Rev Immunol* 21:83–100. <https://doi.org/10.1038/s41577-020-00479-7>
3. Doherty M, Buchy P, Standaert B, Giaquinto C, Prado-Cohrs D (2016) Vaccine impact: benefits for human health. *Vaccine* 34:6707–6714. <https://doi.org/10.1016/j.vaccine.2016.10.025>
4. Pasquale D, Alberta SP, Da Silva FT, Garçon N (2015) Vaccine adjuvants: from 1920 to 2015 and beyond. *Vaccines* 3:320–343. <https://doi.org/10.3390/vaccines3020320>
5. Pliaka V, Kyriakopoulou Z, Markoulatos P (2012) Risks associated with the use of live-attenuated vaccine poliovirus strains and the strategies for control and eradication of paralytic poliomyelitis. *Expert Rev Vaccines* 11:609–628. <https://doi.org/10.1586/erv.12.28>
6. McKee AS, Marrack P (2017) Old and new adjuvants. *Curr Opin Immunol* 47:44–51. <https://doi.org/10.1016/j.coi.2017.06.005>
7. Rueckert C, Guzmán CA (2012) Vaccines: from empirical development to rational design. *PLoS Pathog* 8:e1003001. <https://doi.org/10.1371/journal.ppat.1003001>
8. Petrovsky N (2015) Comparative safety of vaccine adjuvants: a summary of current evidence and future needs. *Drug Saf* 38:1059–1074. <https://doi.org/10.1007/s40264-015-0350-4>
9. Public Health Agency of Canada (2020) Contents of immunizing agents available for use in Canada: Canadian Immunization Guide. Education and awareness; guidance. aem, January 30.
10. Adjuvants and vaccines | vaccine safety | CDC (2020), August 14
11. Glennly AT, Barr M (1931) The precipitation of diphtheria toxoid by potash alum. *J Pathol Bacteriol* 34:131–138. <https://doi.org/10.1002/path.1700340203>
12. Gupta RK (1998) Aluminum compounds as vaccine adjuvants. *Adv Drug Deliv Rev* 32:155–172. [https://doi.org/10.1016/S0169-409X\(98\)00008-8](https://doi.org/10.1016/S0169-409X(98)00008-8)
13. HogenEsch H, O'Hagan DT, Fox CB (2018) Optimizing the utilization of aluminum adjuvants in vaccines: you might just get what you want. *npj Vaccines* 3:51. <https://doi.org/10.1038/s41541-018-0089-x>
14. Jones LTS, Peek LJ, Power J, Markham A, Yazzie B, Middaugh CR (2005) Effects of adsorption to aluminum salt adjuvants on the structure and stability of model protein antigens. *J Biol Chem* 280:13406–13414. <https://doi.org/10.1074/jbc.M500687200>

15. Bryan JT (2007) Developing an HPV vaccine to prevent cervical cancer and genital warts. *Vaccine* 25:3001–3006. <https://doi.org/10.1016/j.vaccine.2007.01.013>
16. Seeber SJ, White JL, Hem SL (1991) Predicting the adsorption of proteins by aluminium-containing adjuvants. *Vaccine* 9:201–203. [https://doi.org/10.1016/0264-410x\(91\)90154-x](https://doi.org/10.1016/0264-410x(91)90154-x)
17. Hsu PH (1989) Aluminum hydroxides and oxyhydroxides. In: *Minerals in soil environments*. Wiley, Hoboken, pp 331–378. <https://doi.org/10.2136/sssabookser1.2ed.c7>
18. Al-Shakhshir RH, Lee AL, White JL, Hem SL (1995) Interactions in model vaccines composed of mixtures of aluminum-containing adjuvants. *J Colloid Interface Sci* 169:197–203. <https://doi.org/10.1006/jcis.1995.1020>
19. Cain DW, Sanders SE, Cunningham MM, Kelsoe G (2013) Disparate adjuvant properties among three formulations of “alum.”. *Vaccine* 31:653–660. <https://doi.org/10.1016/j.vaccine.2012.11.044>
20. Didierlaurent AM, Morel S, Lockman L, Giannini SL, Bisteau M, Carlsen H, Kielland A et al (2009) AS04, an aluminum salt- and TLR4 agonist-based adjuvant system, induces a transient localized innate immune response leading to enhanced adaptive immunity. *J Immunol* 183:6186–6197. <https://doi.org/10.4049/jimmunol.0901474>
21. Richmond P, Hatchuel L, Dong M, Ma B, Hu B, Smolenov I, Li P et al (2021) Safety and immunogenicity of S-Trimer (SCB-2019), a protein subunit vaccine candidate for COVID-19 in healthy adults: a phase 1, randomised, double-blind, placebo-controlled trial. *Lancet* 397(10275):682–694. [https://doi.org/10.1016/S0140-6736\(21\)00241-5](https://doi.org/10.1016/S0140-6736(21)00241-5)
22. Valneva Austria GmbH (2021) A phase I/II randomized, two parts, dose-finding study to evaluate the safety, tolerability and immunogenicity of an inactivated, adjuvanted Sars-Cov-2 virus vaccine candidate (VLA2001), against Covid-19 in healthy subjects. Clinical trial registration NCT04671017. clinicaltrials.gov
23. Levesque PM, Foster K, de Alwis U (2006) Association between immunogenicity and adsorption of a recombinant *Streptococcus pneumoniae* vaccine antigen by an aluminium adjuvant. *Hum Vaccines* 2:74–77. <https://doi.org/10.4161/hv.2.2.2645>
24. Goto N, Kato H, Maeyama J, Shibano M, Saito T, Yamaguchi J, Yoshihara S (1997) Local tissue irritating effects and adjuvant activities of calcium phosphate and aluminium hydroxide with different physical properties. *Vaccine* 15:1364–1371. [https://doi.org/10.1016/S0264-410x\(97\)00054-6](https://doi.org/10.1016/S0264-410x(97)00054-6)
25. Ghimire TR (2015) The mechanisms of action of vaccines containing aluminum adjuvants: an in vitro vs in vivo paradigm. *SpringerPlus* 4:181. <https://doi.org/10.1186/s40064-015-0972-0>
26. Kool M, Soullié T, van Nimwegen M, Willart MAM, Muskens F, Jung S, Hoogsteden HC, Hammad H, Lambrecht BN (2008) Alum adjuvant boosts adaptive immunity by inducing uric acid and activating inflammatory dendritic cells. *J Exp Med* 205:869–882. <https://doi.org/10.1084/jem.20071087>
27. Marichal T, Ohata K, Bedoret D, Mesnil C, Sabatel C, Kobiyama K, Lekeux P et al (2011) DNA released from dying host cells mediates aluminum adjuvant activity. *Nat Med* 17:996–1002. <https://doi.org/10.1038/nm.2403>
28. Oleszycka E, Lavelle EC (2014) Immunomodulatory properties of the vaccine adjuvant alum. *Curr Opin Immunol* 28:1–5. <https://doi.org/10.1016/j.coi.2013.12.007>
29. Eisenbarth SC, Colegio OR, O’Connor W, Sutterwala FS, Flavell RA (2008) Crucial role for the Nalp3 inflammasome in the immunostimulatory properties of aluminium adjuvants. *Nature* 453:1122–1126. <https://doi.org/10.1038/nature06939>
30. Kaye J, Gillis S, Mizel SB, Shevach EM, Malek TR, Dinarello CA, Lachman LB, Janeway CA (1984) Growth of a cloned helper T cell line induced by a monoclonal antibody specific for the antigen receptor: interleukin 1 is required for the expression of receptors for interleukin 2. *J Immunol* 133:1339–1345
31. Dunne A, O’Neill LAJ (2003) The interleukin-1 receptor/Toll-like receptor superfamily: signal transduction during inflammation and host defense. *Sci STKE* 2003:re3. <https://doi.org/10.1126/stke.2003.171.re3>
32. Grun JL, Maurer PH (1989) Different T helper cell subsets elicited in mice utilizing two different adjuvant vehicles: the role of endogenous interleukin 1 in proliferative responses. *Cell Immunol* 121:134–145. [https://doi.org/10.1016/0008-8749\(89\)90011-7](https://doi.org/10.1016/0008-8749(89)90011-7)
33. Del’Guidice T, Lepetit-Stoffaès J-P, Bordeleau L-J, Roberge J, Théberge V, Lauvaux C, Barbeau X et al (2018) Membrane permeabilizing amphiphilic peptide delivers recombinant transcription factor and CRISPR-Cas9/

- Cpfl ribonucleoproteins in hard-to-modify cells. *PLoS One* 13:e0195558. <https://doi.org/10.1371/journal.pone.0195558>
34. O'Hagan DT, Ott GS, Van Nest G, Rappuoli R, Del Giudice G (2013) The history of MF59[®] adjuvant: a phoenix that arose from the ashes. *Expert Rev Vaccines* 12:13–30. <https://doi.org/10.1586/erv.12.140>
 35. Adjuvanted Flu Vaccine | CDC (2020)
 36. Domnich A, Arata L, Amicizia D, Puig-Barberà J, Gasparini R, Panatto D (2017) Effectiveness of MF59-adjuvanted seasonal influenza vaccine in the elderly: a systematic review and meta-analysis. *Vaccine* 35:513–520. <https://doi.org/10.1016/j.vaccine.2016.12.011>
 37. Yang J, Zhang J, Han T, Liu C, Li X, Yan L, Yang B, Yang X (2020) Effectiveness, immunogenicity, and safety of influenza vaccines with MF59 adjuvant in healthy people of different age groups. *Medicine* 99:e19095. <https://doi.org/10.1097/MD.00000000000019095>
 38. Shi S, Zhu H, Xia X, Liang Z, Ma X, Sun B (2019) Vaccine adjuvants: understanding the structure and mechanism of adjuvanticity. *Vaccine* 37:3167–3178. <https://doi.org/10.1016/j.vaccine.2019.04.055>
 39. O'Hagan DT, Ott GS, De Gregorio E, Seubert A (2012) The mechanism of action of MF59—an innately attractive adjuvant formulation. *Vaccine* 30:4341–4348. <https://doi.org/10.1016/j.vaccine.2011.09.061>
 40. Atmar RL, Keitel WA, Patel SM, Katz JM, She D, El Sahly H, Pompey J, Cate TR, Couch RB (2006) Safety and immunogenicity of nonadjuvanted and MF59-adjuvanted influenza A/H9N2 vaccine preparations. *Clin Infect Dis* 43:1135–1142. <https://doi.org/10.1086/508174>
 41. Stephenson I, Bugarini R, Nicholson KG, Podda A, Wood JM, Zambon MC, Katz JM (2005) Cross-reactivity to highly pathogenic avian influenza H5N1 viruses after vaccination with nonadjuvanted and MF59-adjuvanted influenza A/Duck/Singapore/97 (H5N3) vaccine: a potential priming strategy. *J Infect Dis* 191:1210–1215. <https://doi.org/10.1086/428948>
 42. Galli G, Hancock K, Hoschler K, DeVos J, Praus M, Bardelli M, Malzone C et al (2009) Fast rise of broadly cross-reactive antibodies after boosting long-lived human memory B cells primed by an MF59 adjuvanted pre-pandemic vaccine. *Proc Natl Acad Sci U S A* 106:7962–7967. <https://doi.org/10.1073/pnas.09031811106>
 43. Galli G, Medini D, Borgogni E, Zedda L, Bardelli M, Malzone C, Nuti S et al (2009) Adjuvanted H5N1 vaccine induces early CD4+ T cell response that predicts long-term persistence of protective antibody levels. *Proc Natl Acad Sci U S A* 106:3877–3882. <https://doi.org/10.1073/pnas.0813390106>
 44. Asa PB, Cao Y, Garry RF (2000) Antibodies to squalene in Gulf War Syndrome. *Exp Mol Pathol* 68:55–64. <https://doi.org/10.1006/exmp.1999.2295>
 45. Giudice D, Giuseppe EF, Bugarini R, Hora M, Henriksson T, Palla E, O'hagan D, Donnelly J, Rappuoli R, Podda A (2006) Vaccines with the MF59 adjuvant do not stimulate antibody responses against squalene. *Clin Vaccine Immunol* 13:1010–1013. <https://doi.org/10.1128/0191-06>
 46. National Institute of Allergy and Infectious Diseases (NIAID) (2020) A pivotal phase 2b/3 multisite, randomized, double-blind, placebo-controlled clinical trial to evaluate the safety and efficacy of ALVAC-HIV (vCP2438) and bivalent subtype C gp120/MF59 in preventing HIV-1 infection in adults in South Africa. Clinical trial registration NCT02968849. clinicaltrials.gov
 47. Seqirus (2020) A phase 2, randomized, observer-blind, multicenter study to evaluate the immunogenicity and safety of several doses of antigen and MF59 adjuvant content in a monovalent H5N1 pandemic influenza vaccine in healthy pediatric subjects 6 months to < 9 years of age. Clinical trial registration NCT04669691. clinicaltrials.gov
 48. The University of Queensland (2020) A phase 1, randomised, double-blind, placebo-controlled, dosage-escalation, single centre study to evaluate the safety and immunogenicity of an adjuvanted SARS-CoV-2 sclamp protein subunit vaccine in healthy adults aged 18 to 55 years old and healthy older adults, aged 56 years and over. Clinical trial registration NCT04495933. clinicaltrials.gov
 49. Champion CR (2020) Heplisav-B: a hepatitis B vaccine with a novel adjuvant. *Ann Pharmacother* 55(6):783–791. <https://doi.org/10.1177/1060028020962050>
 50. McCluskie MJ, Weeratna RD, Payette PJ, Davis HL (2001) The use of CpG DNA as a mucosal vaccine adjuvant. *Curr Opin Investig Drugs* 2:35–39
 51. Klinman DM (2003) CpG DNA as a vaccine adjuvant. *Expert Rev Vaccines* 2:305–315. <https://doi.org/10.1586/14760584.2.2.305>

52. Bode C, Zhao G, Steinhagen F, Kinjo T, Klinman DM (2011) CpG DNA as a vaccine adjuvant. *Expert Rev Vaccines* 10:499–511. <https://doi.org/10.1586/erv.10.174>
53. Verthelyi D, Ishii KJ, Gursel M, Takeshita F, Klinman DM (2001) Human peripheral blood cells differentially recognize and respond to two distinct CPG motifs. *J Immunol* 166:2372–2377. <https://doi.org/10.4049/jimmunol.166.4.2372>
54. Krug A, Rothenfusser S, Hornung V, Jahrsdörfer B, Blackwell S, Ballas ZK, Endres S, Krieg AM, Hartmann G (2001) Identification of CpG oligonucleotide sequences with high induction of IFN- α/β in plasmacytoid dendritic cells. *Eur J Immunol* 31:2154–2163. [https://doi.org/10.1002/1521-4141\(200107\)31:7<2154::AID-IMMU2154>3.0.CO;2-U](https://doi.org/10.1002/1521-4141(200107)31:7<2154::AID-IMMU2154>3.0.CO;2-U)
55. Capolunghi F, Cascioli S, Giorda E, Rosado MM, Plebani A, Auriti C, Seganti G et al (2008) CpG drives human transitional B cells to terminal differentiation and production of natural antibodies. *J Immunol* 180:800–808. <https://doi.org/10.4049/jimmunol.180.2.800>
56. Hartmann G, Battiany J, Poeck H, Wagner M, Kerkmann M, Lubenow N, Rothenfusser S, Endres S (2003) Rational design of new CpG oligonucleotides that combine B cell activation with high IFN-alpha induction in plasmacytoid dendritic cells. *Eur J Immunol* 33:1633–1641. <https://doi.org/10.1002/eji.200323813>
57. Marshall JD, Fearon K, Abbate C, Subramanian S, Yee P, Gregorio J, Coffman RL, Van Nest G (2003) Identification of a novel CpG DNA class and motif that optimally stimulate B cell and plasmacytoid dendritic cell functions. *J Leukocyte Biol* 73:781–792. <https://doi.org/10.1189/jlb.1202630>
58. Samulowitz U, Weber M, Weeratna R, Uhlmann E, Noll B, Krieg AM, Vollmer J (2010) A novel class of immune-stimulatory CpG oligodeoxynucleotides unifies high potency in type I interferon induction with preferred structural properties. *Oligonucleotides* 20:93–101. <https://doi.org/10.1089/oli.2009.0210>
59. Rizzieri D (2020) A randomized phase II trial to evaluate progression-free survival rates in patients receiving NK cell-enriched donor cell infusions when administered alone or administered with the TLR9 agonist, DUK-CPG-001, from a 4-6/8 HLA-matched related or 7-8/8 HLA-matched donor following reduced intensity or non-ablative allogeneic stem cell transplantation. Clinical trial registration NCT02452697. clinicaltrials.gov
60. Meijerink MR (2020) Irreversible electroporation and nivolumab combined with intratumoral administration of a Toll-like receptor ligand as a means of in vivo vaccination for oligometastatic pancreatic ductal adenocarcinoma. Clinical trial registration NCT04612530. clinicaltrials.gov
61. Ezoe S, Palacpac NMQ, Tetsutani K, Yamamoto K, Okada K, Taira M, Nishida S et al (2020) First-in-human randomised trial and follow-up study of Plasmodium falciparum blood-stage malaria vaccine BK-SE36 with CpG-ODN(K3). *Vaccine* 38:7246–7257. <https://doi.org/10.1016/j.vaccine.2020.09.056>
62. Bottazzi ME (2020) Phase 2 study to assess the safety, efficacy and immunogenicity of Na-GST-1/alhydrogel co-administered with different Toll-like receptor agonists in hookworm-naïve Adults. Clinical trial registration NCT03172975. clinicaltrials.gov
63. Clover Biopharmaceuticals AUS Pty Ltd (2021) A double-blind, randomized, controlled, phase 2/3 study to evaluate the efficacy, immunogenicity, and safety of SCB 2019, a recombinant SARS-CoV-2 trimeric S protein subunit vaccine for the prevention of COVID-19 in participants aged 18 years and older. Clinical trial registration NCT04672395. clinicaltrials.gov
64. Medigen Vaccine Biologics Corp (2021) A phase II, prospective, double-blinded, multicenter, multi-regional study to evaluate the safety, tolerability, and immunogenicity of the SARS-CoV-2 vaccine candidate MVC-COV1901. Clinical trial registration NCT04695652. clinicaltrials.gov
65. Akache B, Stark FC, Jia Y, Deschatelets L, Dudani R, Harrison BA, Agbayani G et al (2018) Sulfated archaeol glycolipids: comparison with other immunological adjuvants in mice. *PLoS One* 13:e0208067
66. McCluskie MJ, Thorn J, Gervais DP, Stead DR, Zhang N, Benoit M, Cartier J et al (2015) Anti-nicotine vaccines: comparison of adjuvanted CRM197 and Qb-VLP conjugate formulations for immunogenicity and function in non-human primates. *Int Immunopharmacol* 29:663–671. <https://doi.org/10.1016/j.intimp.2015.09.012>
67. Wang H, Huang W, Gao H, Liu TT (2020) NY-ESO-1 protein vaccine combining alum, CpG ODN, and HH2 complex adjuvant induces protective and therapeutic anti-tumor responses in murine multiple myeloma.

- OncoTargets Ther 13:8069–8077. <https://doi.org/10.2147/OTT.S255713>
68. Garçon N, Di Pasquale A (2016) From discovery to licensure, the adjuvant system story. *Hum Vaccin Immunother* 13:19–33. <https://doi.org/10.1080/21645515.2016.1225635>
 69. Qureshi N, Takayama K, Ribí E (1982) Purification and structural determination of non-toxic lipid A obtained from the lipopolysaccharide of *Salmonella typhimurium*. *J Biol Chem* 257:11808–11815
 70. Baldrige JR, McGowan P, Evans JT, Cluff C, Mossman S, Johnson D, Persing D (2004) Taking a Toll on human disease: Toll-like receptor 4 agonists as vaccine adjuvants and monotherapeutic agents. *Expert Opin Biol Ther* 4:1129–1138. <https://doi.org/10.1517/14712598.4.7.1129>
 71. Casella CR, Mitchell TC (2008) Putting endotoxin to work for us: monophosphoryl lipid A as a safe and effective vaccine adjuvant. *Cell Mol Life Sci* 65:3231–3240. <https://doi.org/10.1007/s00018-008-8228-6>
 72. Hirschfeld M, Ma Y, Weis JH, Vogel SN, Weis JJ (2000) Cutting edge: repurification of lipopolysaccharide eliminates signaling through both human and murine toll-like receptor 2. *J Immunol* 165:618–622. <https://doi.org/10.4049/jimmunol.165.2.618>
 73. Tapping RI, Akashi S, Miyake K, Godowski PJ, Tobias PS (2000) Toll-like receptor 4, but not toll-like receptor 2, is a signaling receptor for *Escherichia* and *Salmonella* lipopolysaccharides. *J Immunol* 165:5780–5787. <https://doi.org/10.4049/jimmunol.165.10.5780>
 74. Evans JT, Cluff CW, Johnson DA, Lacy MJ, Persing DH, Baldrige JR (2003) Enhancement of antigen-specific immunity via the TLR4 ligands MPL adjuvant and Ribí.529. *Expert Rev Vaccines* 2:219–229. <https://doi.org/10.1586/14760584.2.2.219>
 75. Martin M, Michalek SM, Katz J (2003) Role of innate immune factors in the adjuvant activity of monophosphoryl lipid A. *Infect Immun* 71:2498–2507. <https://doi.org/10.1128/iai.71.5.2498-2507.2003>
 76. Tiberio L, Fletcher L, Eldridge JH, Duncan DD (2004) Host factors impacting the innate response in humans to the candidate adjuvants RC529 and monophosphoryl lipid A. *Vaccine* 22:1515–1523. <https://doi.org/10.1016/j.vaccine.2003.10.019>
 77. Park BS, Song DH, Kim HM, Choi B-S, Lee H, Lee J-O (2009) The structural basis of lipopolysaccharide recognition by the TLR4–MD-2 complex. *Nature* 458:1191–1195. <https://doi.org/10.1038/nature07830>
 78. Laupèze B, Hervé C, Di Pasquale A, Da Silva FT (2019) Adjuvant systems for vaccines: 13 years of post-licensure experience in diverse populations have progressed the way adjuvanted vaccine safety is investigated and understood. *Vaccine* 37:5670–5680. <https://doi.org/10.1016/j.vaccine.2019.07.098>
 79. Garçon N, Vaughn DW, Didierlaurent AM (2012) Development and evaluation of AS03, an adjuvant system containing α -tocopherol and squalene in an oil-in-water emulsion. *Expert Rev Vaccines* 11:349–366. <https://doi.org/10.1586/erv.11.192>
 80. Morel S, Didierlaurent A, Bourguignon P, Delhaye S, Baras B, Jacob V, Planty C et al (2011) Adjuvant system AS03 containing α -tocopherol modulates innate immune response and leads to improved adaptive immunity. *Vaccine* 29:2461–2473. <https://doi.org/10.1016/j.vaccine.2011.01.011>
 81. Edwards K, Lambert P-H, Black S (2019) Narcolepsy and pandemic influenza vaccination: what we need to know to be ready for the next pandemic. *Pediatr Infect Dis J* 38:873–876. <https://doi.org/10.1097/INF.0000000000002398>
 82. Nohynek H, Jokinen J, Partinen M, Vaarala O, Kirjavainen T, Sundman J, Himanen S-L et al (2012) AS03 adjuvanted AH1N1 vaccine associated with an abrupt increase in the incidence of childhood narcolepsy in Finland. *PLoS One* 7:e33536. <https://doi.org/10.1371/journal.pone.0033536>
 83. Medicago (2020) Randomized, observer-blind, placebo-controlled, phase 2/3 study to assess the safety, efficacy, and immunogenicity of a recombinant coronavirus-like particle COVID-19 vaccine in adults 18 years of age or older. Clinical trial registration NCT04636697. clinicaltrials.gov
 84. Medicago (2020) A randomized, observer-blind, placebo-controlled study to assess the safety, efficacy, and immunogenicity of a recombinant coronavirus-like particle COVID-19 vaccine in adults 18 years of age or older (United States—Phase 2). Clinical trial registration NCT04662697. clinicaltrials.gov
 85. Soltysik S, Wu J-Y, Recchia J, Wheeler DA, Newman MJ, Coughlin RT, Kensil CR (1995) Structure/function studies of QS-21 adjuvant: assessment of triterpene aldehyde and glucuronic acid roles in adjuvant function. *Vaccine* 13:1403–1410. [https://doi.org/10.1016/0264-410X\(95\)00077-E](https://doi.org/10.1016/0264-410X(95)00077-E)

86. European Medicines Agency: Shingrix public assessment report (2018) https://www.ema.europa.eu/en/documents/assessment-report/shingrix-epar-public-assessment-report_en.pdf. European Medicines Agency
87. Marty-Roix R, Vladimer GI, Pouliot K, Weng D, Buglione-Corbett R, West K, John D, MacMicking, et al. (2016) Identification of QS-21 as an inflammasome-activating molecular component of saponin adjuvants. *J Biol Chem* 291:1123–1136. <https://doi.org/10.1074/jbc.M115.683011>
88. Fernández-Tejada A, Chea EK, George C, Pillarsetty NVK, Gardner JR, Livingston PO, Ragupathi G, Lewis JS, Tan DS, Gin DY (2014) Development of a minimal saponin vaccine adjuvant based on QS-21. *Nat Chem* 6:635–643. <https://doi.org/10.1038/nchem.1963>
89. Marciari DJ (2003) Vaccine adjuvants: role and mechanisms of action in vaccine immunogenicity. *Drug Discov Today* 8:934–943. [https://doi.org/10.1016/s1359-6446\(03\)02864-2](https://doi.org/10.1016/s1359-6446(03)02864-2)
90. Bill & Melinda Gates Medical Research Institute (2020) A randomized, placebo-controlled, observer-blind, phase 2 study to evaluate safety and immunogenicity of the investigational M72/AS01E Mycobacterium tuberculosis (Mtb) vaccine in virally suppressed, antiretroviral-treated participants with human immunodeficiency virus (HIV). Clinical trial registration NCT04556981. clinicaltrials.gov
91. PATH (2020) A phase 2b randomized, open-label, controlled, single center study in Plasmodium falciparum-infected and uninfected adults age 18–55 years old in Kenya to evaluate the efficacy of the delayed, fractional dose RTS,S/AS01E malaria vaccine in subjects treated with artemisinin combination therapy plus primaquine. Clinical trial registration NCT04661579. clinicaltrials.gov
92. London School of Hygiene and Tropical Medicine (2020) Seasonal vaccination with the RTS,S/AS01 malaria vaccine given with or without seasonal malaria chemoprevention: extension of a randomised, double-blind phase 3 trial until children reach the age of five years. Clinical trial registration NCT04319380. clinicaltrials.gov
93. National Institute of Allergy and Infectious Diseases (NIAID) (2020) Safety, immunogenicity and efficacy of Pfs230D1M-EPA/AS01 vaccine, a transmission blocking vaccine against Plasmodium falciparum, in an age de-escalation trial of children and a family compound trial in Mali. Clinical trial registration NCT03917654. clinicaltrials.gov
94. GlaxoSmithKline (2020) Efficacy, safety and immunogenicity study of GSK biologicals' candidate malaria vaccine (SB257049) evaluating schedules with or without fractional doses, early dose 4 and yearly doses, in children 5–17 months of age. Clinical trial registration NCT03276962. clinicaltrials.gov
95. VBI Vaccines Inc (2020) A two-part, phase I/IIA dose-escalation study to define the safety, tolerability, and optimal dose of candidate GBM vaccine VBI-1901 with subsequent extension of optimal dose in recurrent GBM subjects. Clinical trial registration NCT03382977. clinicaltrials.gov
96. Bovier PA (2008) Epaxal: a virosomal vaccine to prevent hepatitis A infection. *Expert Rev Vaccines* 7:1141–1150. <https://doi.org/10.1586/14760584.7.8.1141>
97. Glück R, Metcalfe IC (2002) New technology platforms in the development of vaccines for the future. *Vaccine* 20:B10–B16. [https://doi.org/10.1016/S0264-410X\(02\)00513-3](https://doi.org/10.1016/S0264-410X(02)00513-3)
98. Der Wielen V, Marie AV, Froesner G, Ibáñez R, Hunt M, Herzog C, Van Damme P (2007) Immunogenicity and safety of a pediatric dose of a virosome-adjuvanted hepatitis A vaccine: a controlled trial in children aged 1–16 years. *Pediatr Infect Dis J* 26:705–710. <https://doi.org/10.1097/INF.0b013e31806215c8>
99. Wiedermann G, Kundi M, Ambrosch F (1998) Estimated persistence of anti-HAV antibodies after single dose and booster hepatitis A vaccination (0–6 schedule). *Acta Tropica* 69:121–125. [https://doi.org/10.1016/s0001-706x\(97\)00120-4](https://doi.org/10.1016/s0001-706x(97)00120-4)
100. Holzer BR, Hatz C, Schmidt-Sissolak D, Glück R, Althaus B, Egger M (1996) Immunogenicity and adverse effects of inactivated virosome versus alum-adsorbed hepatitis A vaccine: a randomized controlled trial. *Vaccine* 14:982–986. [https://doi.org/10.1016/0264-410x\(96\)00042-4](https://doi.org/10.1016/0264-410x(96)00042-4)
101. Chappuis F, Farinelli T, Deckx H, Sarnecki M, Go O, Salzgeber Y, Stals C (2017) Immunogenicity and estimation of antibody persistence following vaccination with an inactivated virosomal hepatitis A vaccine in adults: a 20-year follow-up study. *Vaccine* 35:1448–1454. <https://doi.org/10.1016/j.vaccine.2017.01.031>
102. Epaxal—summary of product characteristics (SmPC)—(emc) (2021) <https://www.medicines.org.uk/emc/product/4035/smpc>. Accessed Jan 10

103. Knight-Jones TJ, Edmond K, Gubbins S, Paton DJ (2014) Veterinary and human vaccine evaluation methods. *Proc Biol Sci* 281 (1784):20132839. <https://doi.org/10.1098/rspb.2013.2839>
104. Willson PJ, Rossi-Campos A, Potter AA (1995) Tissue reaction and immunity in swine immunized with *Actinobacillus pleuropneumoniae* vaccines. *Can J Vet Res* 59 (4):299–305
105. te Beest DE, Hagenaars TJ, Stegeman JA, Koopmans MP, van Boven M (2011) Risk based culling for highly infectious diseases of livestock. *Vet Res* 42(1):81. <https://doi.org/10.1186/1297-9716-42-81>
106. Frutos R, Devaux CA (2020) Mass culling of minks to protect the COVID-19 vaccines: is it rational? *New Microbes New Infect* 38:100816. <https://doi.org/10.1016/j.nmni.2020.100816>
107. Horohov DW, Dunham J, Liu C, Betancourt A, Stewart JC, Page AE, Chambers TM (2015) Characterization of the in situ immunological responses to vaccine adjuvants. *Vet Immunol Immunopathol* 164 (1–2):24–29. <https://doi.org/10.1016/j.vetimm.2014.12.015>
108. Lone NA, Spackman E, Kapczynski D (2017) Immunologic evaluation of 10 different adjuvants for use in vaccines for chickens against highly pathogenic avian influenza virus. *Vaccine* 35(26):3401–3408. <https://doi.org/10.1016/j.vaccine.2017.05.010>
109. Dhakal S, Cheng X, Salcido J, Renu S, Bondra K, Lakshmanappa YS, Misch C et al (2018) Liposomal nanoparticle-based conserved peptide influenza vaccine and monosodium urate crystal adjuvant elicit protective immune response in pigs. *Int J Nanomed* 13:6699–6715. <https://doi.org/10.2147/IJN.S178809>
110. Vetarylix. Compendium of veterinary products
111. Herbert WJ (1968) The mode of action of mineral-oil emulsion adjuvants on antibody production in mice. *Immunology* 14 (3):301–318
112. Stills HF Jr (2005) Adjuvants and antibody production: dispelling the myths associated with Freund's complete and other adjuvants. *ILAR J* 46(3):280–293. <https://doi.org/10.1093/ilar.46.3.280>
113. Johnston BA, Eisen H, Fry D (1991) An evaluation of several adjuvant emulsion regimens for the production of polyclonal antisera in rabbits. *Lab Anim Sci* 41(1):15–21
114. Jaafar RM, Chettri JK, Dalsgaard I, Al-Jubury A, Kania PW, Skov J, Buchmann K (2015) Effects of adjuvant Montanide ISA 763 A VG in rainbow trout injection vaccinated against *Yersinia ruckeri*. *Fish Shellfish Immunol* 47(2):797–806. <https://doi.org/10.1016/j.fsi.2015.10.023>
115. Ibrahim Eel S, Gamal WM, Hassan AI, Sel DM, Hegazy AZ, Abdel-Atty MM (2015) Comparative study on the immunopotentiator effect of ISA 201, ISA 61, ISA 50, ISA 206 used in trivalent foot and mouth disease vaccine. *Vet World* 8(10):1189–1198. <https://doi.org/10.14202/vetworld.2015.1189-1198>
116. Seubert A, Monaci E, Pizza M, O'Hagan DT, Wack A (2008) The adjuvants aluminum hydroxide and MF59 induce monocyte and granulocyte chemoattractants and enhance monocyte differentiation toward dendritic cells. *J Immunol* 180(8):5402–5412. <https://doi.org/10.4049/jimmunol.180.8.5402>
117. Dupuis M, Denis-Mize K, LaBarbara A, Peters W, Charo IF, McDonald DM, Ott G (2001) Immunization with the adjuvant MF59 induces macrophage trafficking and apoptosis. *Eur J Immunol* 31 (10):2910–2918. [https://doi.org/10.1002/1521-4141\(200110\)31:10<2910::aid-immu2910>3.0.co;2-3](https://doi.org/10.1002/1521-4141(200110)31:10<2910::aid-immu2910>3.0.co;2-3)
118. Kimura J, Nariuchi H, Watanabe T, Matuhasi T, Okayasu I, Hatakeyama S (1978) Studies on the adjuvant effect of water-in-oil-in-water (w/o/w) emulsion of sesame oil. I. Enhanced and persistent antibody formation by antigen incorporated into the water-in-oil-in-water emulsion. *Jpn J Exp Med* 48(2):149–154
119. Barnett PV, Pullen L, Williams L, Doel TR (1996) International bank for foot-and-mouth disease vaccine: assessment of Montanide ISA 25 and ISA 206, two commercially available oil adjuvants. *Vaccine* 14 (13):1187–1198. [https://doi.org/10.1016/s0264-410x\(96\)00055-2](https://doi.org/10.1016/s0264-410x(96)00055-2)
120. Cox SJ, Barnett PV, Dani P, Salt JS (1999) Emergency vaccination of sheep against foot-and-mouth disease: protection against disease and reduction in contact transmission. *Vaccine* 17(15–16):1858–1868. [https://doi.org/10.1016/s0264-410x\(98\)00486-1](https://doi.org/10.1016/s0264-410x(98)00486-1)
121. Bouguyon E, Goncalves E, Shevtsov A, Maisonnasse P, Remyga S, Goryushev O, Deville S, Bertho N, Ben Arous J (2015) A new adjuvant combined with inactivated

- influenza enhances specific CD8 T cell response in mice and decreases symptoms in swine upon challenge. *Viral Immunol* 28 (9):524–531. <https://doi.org/10.1089/vim.2014.0149>
122. Tandrup Schmidt S, Foged C, Korsholm KS, Rades T, Christensen D (2016) Liposome-based adjuvants for subunit vaccines: formulation strategies for subunit antigens and immunostimulators. *Pharmaceutics* 8(1):7. <https://doi.org/10.3390/pharmaceutics8010007>
 123. Li W, Watarai S, Iwasaki T, Kodama H (2004) Suppression of *Salmonella enterica* serovar Enteritidis excretion by intraocular vaccination with fimbriae proteins incorporated in liposomes. *Dev Comp Immunol* 28 (1):29–38. [https://doi.org/10.1016/s0145-305x\(03\)00086-7](https://doi.org/10.1016/s0145-305x(03)00086-7)
 124. Hiszczynska-Sawicka E, Li H, Boyu Xu J, Akhtar M, Holec-Gasior L, Kur J, Bickerstaffe R, Stankiewicz M (2012) Induction of immune responses in sheep by vaccination with liposome-entrapped DNA complexes encoding *Toxoplasma gondii* MIC3 gene. *Pol J Vet Sci* 15(1):3–9. <https://doi.org/10.2478/v10181-011-0107-7>
 125. Onuigbo EB, Okore VC, Ofokansi KC, Okoye JO, Nworu CS, Esimone CO, Attama AA (2012) Preliminary evaluation of the immunoenhancement potential of Newcastle disease vaccine formulated as a cationic liposome. *Avian Pathol* 41(4):355–360. <https://doi.org/10.1080/03079457.2012.691154>
 126. Colson YL, Grinstaff MW (2012) Biologically responsive polymeric nanoparticles for drug delivery. *Adv Mater* 24(28):3878–3886. <https://doi.org/10.1002/adma.201200420>
 127. Petersen LK, Phanse Y, Ramer-Tait AE, Wannemuehler MJ, Narasimhan B (2012) Amphiphilic polyanhydride nanoparticles stabilize *Bacillus anthracis* protective antigen. *Mol Pharm* 9(4):874–882. <https://doi.org/10.1021/mp2004059>
 128. Shakya AK, Nandakumar KS (2013) Applications of polymeric adjuvants in studying auto-immune responses and vaccination against infectious diseases. *J R Soc Interface* 10 (79):20120536. <https://doi.org/10.1098/rsif.2012.0536>
 129. Park ME, Lee SY, Kim RH, Ko MK, Lee KN, Kim SM, Kim BK, Lee JS, Kim B, Park JH (2014) Enhanced immune responses of foot-and-mouth disease vaccine using new oil/gel adjuvant mixtures in pigs and goats. *Vaccine* 32(40):5221–5227. <https://doi.org/10.1016/j.vaccine.2014.07.040>
 130. Gong X, Chen Q, Ferguson-Noel N, Stipkovits L, Szathmary S, Liu Y, Zheng F (2020) Evaluation of protective efficacy of inactivated *Mycoplasma synoviae* vaccine with different adjuvants. *Vet Immunol Immunopathol* 220:109995. <https://doi.org/10.1016/j.vetimm.2019.109995>
 131. Yang Y, Xing R, Liu S, Qin Y, Li K, Yu H, Li P (2020) Chitosan, hydroxypropyltrimethyl ammonium chloride chitosan and sulfated chitosan nanoparticles as adjuvants for inactivated Newcastle disease vaccine. *Carbohydr Polym* 229:115423. <https://doi.org/10.1016/j.carbpol.2019.115423>
 132. Magiri R, Mutwiri G, Wilson HL (2018) Recent advances in experimental polyphosphazene adjuvants and their mechanisms of action. *Cell Tissue Res* 374:465–471. <https://doi.org/10.1007/s00441-018-2929-4>
 133. Andrianov AK, Decollibus DP, Marin A, Webb A, Griffin Y, Webby RJ (2011) PCPP-formulated H5N1 influenza vaccine displays improved stability and dose-sparing effect in lethal challenge studies. *J Pharm Sci* 100:1436–1443. <https://doi.org/10.1002/jps.22367>
 134. Andrianov AK, DeCollibus DP, Gillis HA, Kha HH, Marin A, Prausnitz MR, Babiuk LA, Townsend H, Mutwiri G (2009) Poly[di(carboxylatophenoxy)phosphazene] is a potent adjuvant for intradermal immunization. *Proc Natl Acad Sci U S A* 106:18936–18941. <https://doi.org/10.1073/pnas.0908842106>
 135. Magiri R, Lai K, Chaffey A, Zhou Y, Pyo H-M, Gerds V, Wilson HL, Mutwiri G (2018) Intradermal immunization with inactivated swine influenza virus and adjuvant polydi(sodium carboxylatoethylphenoxy) phosphazene (PCEP) induced humoral and cell-mediated immunity and reduced lung viral titres in pigs. *Vaccine* 36:1606–1613. <https://doi.org/10.1016/j.vaccine.2018.02.026>
 136. Dar A, Lai K, Dent D, Potter A, Gerds V, Babiuk LA, Mutwiri GK (2012) Administration of poly[di(sodium carboxylatoethylphenoxy)]phosphazene (PCEP) as adjuvant activated mixed Th1/Th2 immune responses in pigs. *Vet Immunol Immunopathol* 146:289–295. <https://doi.org/10.1016/j.vetimm.2012.01.021>
 137. Campbell JB, Peerbaye YA (1992) Saponin. *Res Immunol* 143(5):526–530. [https://doi.org/10.1016/0923-2494\(92\)80064-r](https://doi.org/10.1016/0923-2494(92)80064-r)
 138. Bangham AD, Horne RW, Glauert AM, Dingle JT, Lucy JA (1962) Action of saponin on

- biological cell membranes. *Nature* 196:952–955. <https://doi.org/10.1038/196952a0>
139. Oda K, Matsuda H, Murakami T, Katayama S, Ohgitani T, Yoshikawa M (2003) Relationship between adjuvant activity and amphipathic structure of soyasaponins. *Vaccine* 21 (17-18):2145–2151. [https://doi.org/10.1016/s0264-410x\(02\)00739-9](https://doi.org/10.1016/s0264-410x(02)00739-9)
 140. Marciani DJ, Kensil CR, Beltz GA, Hung CH, Cronier J, Aubert A (1991) Genetically-engineered subunit vaccine against feline leukaemia virus: protective immune response in cats. *Vaccine* 9 (2):89–96. [https://doi.org/10.1016/0264-410x\(91\)90262-5](https://doi.org/10.1016/0264-410x(91)90262-5)
 141. Lovgren K, Morein B (1988) The requirement of lipids for the formation of immunostimulating complexes (iscoms). *Biotechnol Appl Biochem* 10(2):161–172
 142. Pearce MJ, Drane D (2005) ISCOMATRIX adjuvant for antigen delivery. *Adv Drug Deliv Rev* 57(3):465–474. <https://doi.org/10.1016/j.addr.2004.09.006>
 143. Windon RG, Chaplin PJ, McWaters P, Tavarnesi M, Tzatzaris M, Kimpton WG, Cahill RN et al (2001) Local immune responses to influenza antigen are synergistically enhanced by the adjuvant ISCOMATRIX. *Vaccine* 20:490–497. [https://doi.org/10.1016/s0264-410x\(01\)00332-2](https://doi.org/10.1016/s0264-410x(01)00332-2)
 144. Maraskovsky E, Sjölander S, Drane DP, Schnurr M, Le Thuy TT, Mateo L, Luft T et al (2004) NY-ESO-1 protein formulated in ISCOMATRIX adjuvant is a potent anti-cancer vaccine inducing both humoral and CD8+ T-cell-mediated immunity and protection against NY-ESO-1+ tumors. *Clin Cancer Res* 10:2879–2890. <https://doi.org/10.1158/1078-0432.CCR-03-0245>
 145. Ronnberg B, Fekadu M, Morein B (1995) Adjuvant activity of non-toxic Quillaja saponaria Molina components for use in ISCOM matrix. *Vaccine* 13(14):1375–1382. [https://doi.org/10.1016/0264-410x\(95\)00105-a](https://doi.org/10.1016/0264-410x(95)00105-a)
 146. Villacres MC, Behboudi S, Nikkila T, Lovgren-Bengtsson K, Morein B (1998) Internalization of iscom-borne antigens and presentation under MHC class I or class II restriction. *Cell Immunol* 185(1):30–38. <https://doi.org/10.1006/cimm.1998.1278>
 147. Morein B, Hu KF, Abusugra I (2004) Current status and potential application of ISCOMs in veterinary medicine. *Adv Drug Deliv Rev* 56(10):1367–1382. <https://doi.org/10.1016/j.addr.2004.02.004>
 148. Paillot R, Grimmett H, Elton D, Daly JM (2008) Protection, systemic IFN γ , and antibody responses induced by an ISCOM-based vaccine against a recent equine influenza virus in its natural host. *Vet Res* 39 (3):21. <https://doi.org/10.1051/vetres:2007062>
 149. Carlsson U, Alenius S, Sundquist B (1991) Protective effect of an ISCOM bovine virus diarrhoea virus (BVDV) vaccine against an experimental BVDV infection in vaccinated and non-vaccinated pregnant ewes. *Vaccine* 9(8):577–580. [https://doi.org/10.1016/0264-410x\(91\)90245-2](https://doi.org/10.1016/0264-410x(91)90245-2)
 150. Basqueira NS, Ramos JS, Torres FD, Okuda LH, Hurley DJ, Chase CCL, Gomes ARC, Gomes V (2020) An assessment of secondary clinical disease, milk production and quality, and the impact on reproduction in holstein heifers and cows from a single large commercial herd persistently infected with bovine viral diarrhoea virus type 2. *Viruses* 12(7):760. <https://doi.org/10.3390/v12070760>
 151. Vreman S, McCaffrey J, Popma-de Graaf DJ, Nauwynck H, Savelkoul HFJ, Moore A, Rebel MJM, Stockhofe-Zurwieden N (2019) Toll-like receptor agonists as adjuvants for inactivated porcine reproductive and respiratory syndrome virus (PRRSV) vaccine. *Vet Immunol Immunopathol* 212:27–37. <https://doi.org/10.1016/j.vetimm.2019.04.008>
 152. Rau H, Revets H, Cornelis P, Titzmann A, Ruggli N, McCullough KC, Summerfield A (2006) Efficacy and functionality of lipoprotein OprI from *Pseudomonas aeruginosa* as adjuvant for a subunit vaccine against classical swine fever. *Vaccine* 24(22):4757–4768. <https://doi.org/10.1016/j.vaccine.2006.03.028>
 153. Chen J, Yu X, Zheng Q, Hou L, Du L, Zhang Y, Qiao X, Hou J, Huang K (2018) The immunopotentiator CVC1302 enhances immune efficacy and protective ability of foot-and-mouth disease virus vaccine in pigs. *Vaccine* 36(52):7929–7935. <https://doi.org/10.1016/j.vaccine.2018.11.012>
 154. Taylor CE (1995) Cytokines as adjuvants for vaccines: antigen-specific responses differ from polyclonal responses. *Infect Immun* 63 (9):3241–3244. <https://doi.org/10.1128/IAI.63.9.3241-3244.1995>
 155. Duan K, Hua X, Wang Y, Wang Y, Chen Y, Shi W, Tang L, Li Y, Liu M (2018) Oral immunization with a recombinant *Lactobacillus* expressing CK6 fused with VP2 protein

- against IPNV in rainbow trout (*Oncorhynchus mykiss*). *Fish Shellfish Immunol* 83:223–231. <https://doi.org/10.1016/j.fsi.2018.09.034>
156. Choi MG, Kim MS, Choi TJ, Kim KH (2019) Effect of CXCL12-expressing viral hemorrhagic septicemia virus replicon particles on leukocytes migration and vaccine efficacy in olive flounder (*Paralichthys olivaceus*). *Fish Shellfish Immunol* 89:378–383. <https://doi.org/10.1016/j.fsi.2019.04.018>
 157. Asif M, Jenkins KA, Hilton LS, Kimpton WG, Bean AGD, Lowenthal JW (2004) Cytokines as adjuvants for avian vaccines. *Immunol Cell Biol* 82(6):638–643. <https://doi.org/10.1111/j.1440-1711.2004.01295.x>
 158. Hajam IA, Dar PA, Appavoo E, Kishore S, Bhanuprakash V, Ganesh K (2015) Bacterial ghosts of *Escherichia coli* drive efficient maturation of bovine monocyte-derived dendritic cells. *PLoS One* 10(12):e0144397. <https://doi.org/10.1371/journal.pone.0144397>
 159. Hajam IA, Dar PA, Won G, Lee JH (2017) Bacterial ghosts as adjuvants: mechanisms and potential. *Vet Res* 48(1):37. <https://doi.org/10.1186/s13567-017-0442-5>
 160. Mutwiri G, Gerdt S, van Drunen Littel-van den Hurk S, Auray G, Eng N, Garlapati S, Babiuk LA, Potter A (2011) Combination adjuvants: the next generation of adjuvants? *Expert Rev Vaccines* 10(1):95–107. <https://doi.org/10.1586/erv.10.154>
 161. Ioannou XP, Griebel P, Hecker R, Babiuk LA, van Drunen Littel-van den Hurk S (2002) The immunogenicity and protective efficacy of bovine herpesvirus 1 glycoprotein D plus Emulsigen are increased by formulation with CpG oligodeoxynucleotides. *J Virol* 76(18):9002–1010. <https://doi.org/10.1128/jvi.76.18.9002-9010.2002>
 162. Chang YF, Appel MJ, Jacobson RH, Shin SJ, Harpending P, Straubinger R, Patrican LA, Mohammed H, Summers BA (1995) Recombinant OspA protects dogs against infection and disease caused by *Borrelia burgdorferi*. *Infect Immun* 63(9):3543–3549. <https://doi.org/10.1128/IAI.63.9.3543-3549.1995>
 163. Khorasani A, Madadgar O, Soleimanjahi H, Keyvanfar H, Mahravani H (2016) Evaluation of the efficacy of a new oil-based adjuvant ISA 61 VG FMD vaccine as a potential vaccine for cattle. *Iran J Vet Res* 17(1):8–12
 164. Saavedra D, Crombet T (2017) CIMAvax-EGF: a new therapeutic vaccine for advanced non-small cell lung cancer patients. *Front Immunol* 8:269. <https://doi.org/10.3389/fimmu.2017.00269>
 165. van Doorn E, Liu H, Huckriede A, Hak E (2015) Safety and tolerability evaluation of the use of Montanide ISATM51 as vaccine adjuvant: a systematic review. *Hum Vaccin Immunother* 12:159–169. <https://doi.org/10.1080/21645515.2015.1071455>
 166. Ascarateil S, Puget A, Koziol M-E (2015) Safety data of Montanide ISA 51 VG and Montanide ISA 720 VG, two adjuvants dedicated to human therapeutic vaccines. *J Immunother Cancer* 3:P428. <https://doi.org/10.1186/2051-1426-3-S2-P428>
 167. Moss RB, Savary JR, Diveley JP, Jensen F, Carlo DJ (2002) Maternal and newborn immunization with a human immunodeficiency virus-1 immunogen in a rodent model. *Immunology* 106:549–553. <https://doi.org/10.1046/j.1365-2567.2002.01464.x>
 168. Koh YT, Higgins SA, Weber JS, Kast WM (2006) Immunological consequences of using three different clinical/laboratory techniques of emulsifying peptide-based vaccines in incomplete Freund's adjuvant. *J Transl Med* 4:42. <https://doi.org/10.1186/1479-5876-4-42>
 169. Yamshchikov GV, Barnd DL, Eastham S, Galavotti H, Patterson JW, Deacon DH, Teates D et al (2001) Evaluation of peptide vaccine immunogenicity in draining lymph nodes and peripheral blood of melanoma patients. *Int J Cancer* 92:703–711. [https://doi.org/10.1002/1097-0215\(20010601\)92:5<703::AID-IJC1250>3.0.CO;2-5](https://doi.org/10.1002/1097-0215(20010601)92:5<703::AID-IJC1250>3.0.CO;2-5)
 170. University of Arkansas (2020) A combined phase II efficacy study of a carbohydrate mimotope-based vaccine with MONTANIDETM ISA 51 VG combined with neoadjuvant chemotherapy in triple negative breast cancer. Clinical trial registration NCT02938442. clinicaltrials.gov
 171. University of Arkansas (2020) A combined phase I/II feasibility-and-efficacy study of a carbohydrate mimotope-based vaccine with MONTANIDETM ISA 51 VG combined with neoadjuvant chemotherapy. Clinical trial registration NCT02229084. clinicaltrials.gov
 172. Slingluff CL Jr (2020) Evaluation of safety and durable immunogenicity of melanoma vaccination, with or without systemic CDX-1127, in patients with stage II-IV melanoma. Clinical trial registration NCT03617328. clinicaltrials.gov
 173. Slingluff CL Jr (2020) Open label, randomized, phase I/II study of a long peptide vaccine plus TLR agonists for resected stage

- IIB-IV melanoma (MEL60). Clinical trial registration NCT02126579. clinicaltrials.gov
174. University of Arkansas (2020) "Vaccination of advanced-stage lung cancer patients" a phase I/II study of a carbohydrate mimotope based vaccine with MONTANIDETM ISA 51 VG ST adjuvant. Clinical trial registration NCT02264236. clinicaltrials.gov
175. Centre Hospitalier Universitaire de Besancon (2020) Anticancer therapeutic vaccination using telomerase-derives universal cancer peptides in metastatic non small cell lung cancer: a phase I/II study. Clinical trial registration NCT02818426. clinicaltrials.gov
176. Knudsen LM (2020) Phase IIa trial of PD-L1 peptide vaccination as monotherapy in high risk smoldering multiple myeloma. Clinical trial registration NCT03850522. clinicaltrials.gov
177. Pedersen LM (2020) Peptide vaccination with PD-L1(IO103) and PD-L2(IO120) peptides in untreated chronic lymphatic leukemia. Clinical trial registration NCT03939234. clinicaltrials.gov
178. RhoVac APS (2021) A phase 2, double-blind, placebo controlled study of RV001V in men with biochemical failure following curatively intended therapy for localized prostate cancer (BRaVac). Clinical trial registration NCT04114825. clinicaltrials.gov
179. Roswell Park Cancer Institute (2020) A phase II study of the safety and efficacy of SVN53-67/M57-KLH (SurVaxM) in survivin-positive newly diagnosed glioblastoma. Clinical trial registration NCT02455557. clinicaltrials.gov
180. Centre Hospitalier Universitaire de Besancon (2020) Anticancer therapeutic vaccination using telomerase-derived universal cancer peptides in glioblastoma. Clinical trial registration NCT04280848. clinicaltrials.gov
181. Ahluwalia M (2020) Phase II study of pembrolizumab plus SurVaxM for glioblastoma at first recurrence. Clinical trial registration NCT04013672. clinicaltrials.gov
182. Immune Response BioPharma, Inc (2020) A phase II study of NeuroVaxTM, a therapeutic TCR peptide vaccine for SPMS of multiple sclerosis. Clinical trial registration NCT02057159. clinicaltrials.gov
183. Roswell Park Cancer Institute (2020) A phase I/II basket trial of the EGF vaccine CIMAvax in combination with anti-PD1 therapy in patients with advanced NSCLC or squamous head and neck cancer. Clinical trial registration NCT02955290. clinicaltrials.gov
184. Svane IM (2019) Dual vaccine trial in myeloproliferative neoplasms. Clinical trial registration NCT04051307. clinicaltrials.gov
185. Centre Hospitalier Universitaire de Besancon (2020) A phase II study evaluating the interest to combine UCPVax a CD4 TH1-inducer cancer vaccine and atezolizumab for the treatment of human papillomavirus positive cancers. Clinical trial registration NCT03946358. clinicaltrials.gov
186. Imugene Limited (2020) A phase 1b/2 open-label study with randomization in phase 2 of IMU-131 HER2/Neu peptide vaccine plus standard of care chemotherapy in patients with HER2/Neu overexpressing metastatic or advanced adenocarcinoma of the stomach or gastroesophageal junction. Clinical trial registration NCT02795988. clinicaltrials.gov
187. GERCOR - Multidisciplinary Oncology Cooperative Group (2020) A randomized non-comparative phase II study of maintenance therapy with OSE2101 vaccine alone or in combination with nivolumab, or FOLFIRI after induction therapy with FOLFIRINOX in patients with locally advanced or metastatic pancreatic ductal adenocarcinoma (TEDOPaM - D17-01 PRODIGE 63 Study). Clinical trial registration NCT03806309. clinicaltrials.gov
188. CpG 7909: PF 3512676, PF-3512676 (2006) *Drugs in R&D* 7:312–316. <https://doi.org/10.2165/00126839-200607050-00004>.
189. Kruit WHJ, Suciú S, Dreno B, Mortier L, Robert C, Chiarion-Sileni V, Maio M et al (2013) Selection of immunostimulant AS15 for active immunization with MAGE-A3 protein: results of a randomized phase II study of the European Organisation for Research and Treatment of Cancer Melanoma Group in Metastatic Melanoma. *J Clin Oncol* 31:2413–2420. <https://doi.org/10.1200/JCO.2012.43.7111>
190. McQuade JL, Homsí J, Torres-Cabala CA, Bassett R, Popuri RM, James ML, Vence LM, Hwu W-J (2018) A phase II trial of recombinant MAGE-A3 protein with immunostimulant AS15 in combination with high-dose Interleukin-2 (HDIL2) induction therapy in metastatic melanoma. *BMC Cancer* 18:1274. <https://doi.org/10.1186/s12885-018-5193-9>
191. Vansteenkiste JF, Cho BC, Vanakesa T, De Pas T, Zielinski M, Kim MS, Jassem J et al (2016) Efficacy of the MAGE-A3 cancer immunotherapeutic as adjuvant therapy in

- patients with resected MAGE-A3-positive non-small-cell lung cancer (MAGRIT): a randomised, double-blind, placebo-controlled, phase 3 trial. *Lancet* 17:822–835. [https://doi.org/10.1016/S1470-2045\(16\)00099-1](https://doi.org/10.1016/S1470-2045(16)00099-1)
192. Dreno B, Thompson JF, Smithers BM, Santinami M, Jouary T, Gutzmer R, Levchenko E et al (2018) MAGE-A3 immunotherapeutic as adjuvant therapy for patients with resected, MAGE-A3-positive, stage III melanoma (DERMA): a double-blind, randomised, placebo-controlled, phase 3 trial. *Lancet Oncol* 19:916–929. [https://doi.org/10.1016/S1470-2045\(18\)30254-7](https://doi.org/10.1016/S1470-2045(18)30254-7)
 193. Keshavarz-Fathi M, Rezaei N (2019) Chapter 8—Peptide and protein vaccines for cancer. In: Rezaei N, Keshavarz-Fathi M (eds) *Vaccines for cancer immunotherapy*. Academic Press, New York, pp 101–116. <https://doi.org/10.1016/B978-0-12-814039-0.00008-4>
 194. Kruit WH, Suciú S, Dreno B, Chiarion-Sileni V, Mortier L, Robert C, Maio M, Brichard VG, Lehmann F, Keilholz U (2008) Immunization with recombinant MAGE-A3 protein combined with adjuvant systems AS15 or AS02B in patients with unresectable and progressive metastatic cutaneous melanoma: a randomized open-label phase II study of the EORTC Melanoma Group (16032-18031). *J Clin Oncol* 26:9065–9065. https://doi.org/10.1200/jco.2008.26.15_suppl.9065
 195. Peled N, Oton AB, Hirsch FR, Bunn P (2009) MAGE A3 antigen-specific cancer immunotherapeutic. *Immunotherapy* 1:19–25. <https://doi.org/10.2217/1750743X.1.1.19>
 196. Institut Pasteur (2020) An open label first-in-human adjuvant phase I study of a synthetic multiple antigenic glycopeptide displaying a tri Tn glycotop (MAG-Tn3) plus AS15, as a therapeutic vaccine candidate in patients with non metastatic, HER2 negative localized breast cancer at high-risk of relapse. Clinical trial registration NCT02364492. clinicaltrials.gov
 197. Bengtsson KL, Morein B, Osterhaus AD (2011) ISCOM technology-based Matrix MTM adjuvant: success in future vaccines relies on formulation. *Expert Rev Vaccines* 10:401–403. <https://doi.org/10.1586/erv.11.25>
 198. Reimer JM, Karlsson KH, Lövgren-Bengtsson K, Magnusson SE, Fuentes A, Stertman L (2012) Matrix-MTM adjuvant induces local recruitment, activation and maturation of central immune cells in absence of antigen. *PLoS One* 7(7):e41451. <https://doi.org/10.1371/journal.pone.0041451>
 199. Radošević K, Rodriguez A, Mintardjo R, Tax D, Bengtsson KL, Thompson C, Zambon M, Weverling GJ, UytdeHaag F, Goudsmit J (2008) Antibody and T-cell responses to a virosomal adjuvanted H9N2 avian influenza vaccine: Impact of distinct additional adjuvants. *Vaccine* 26:3640–3646. <https://doi.org/10.1016/j.vaccine.2008.04.071>
 200. Cox RJ, Pedersen G, Madhun AS, Svindland S, Sævik M, Breakwell L, Hoschler K et al (2011) Evaluation of a virosomal H5N1 vaccine formulated with Matrix MTM adjuvant in a phase I clinical trial. *Vaccine* 29:8049–8059. <https://doi.org/10.1016/j.vaccine.2011.08.042>
 201. Madhun AS, Haaheim LR, Nilsen MV, Cox RJ (2009) Intramuscular Matrix-M-adjuvanted virosomal H5N1 vaccine induces high frequencies of multifunctional Th1 CD4+ cells and strong antibody responses in mice. *Vaccine* 27:7367–7376. <https://doi.org/10.1016/j.vaccine.2009.09.044>
 202. Pedersen GK, Sjørnsen H, Nøstbakken JK, Jul-Larsen Å, Hoschler K, Cox RJ (2014) Matrix MTM adjuvanted virosomal H5N1 vaccine induces balanced Th1/Th2 CD4+ T cell responses in man. *Hum Vaccin Immunother* 10:2408–2416. <https://doi.org/10.4161/hv.29583>
 203. Bengtsson KL, Song H, Stertman L, Liu Y, Flyer DC, Massare MJ, Xu R-H et al (2016) Matrix-M adjuvant enhances antibody, cellular and protective immune responses of a Zaire Ebola/Makona virus glycoprotein (GP) nanoparticle vaccine in mice. *Vaccine* 34:1927–1935. <https://doi.org/10.1016/j.vaccine.2016.02.033>
 204. Magnusson SE, Altenburg AF, Bengtsson KL, Bosman F, de Vries RD, Rimmelzwaan GF, Stertman L (2018) Matrix-MTM adjuvant enhances immunogenicity of both protein- and modified vaccinia virus Ankara-based influenza vaccines in mice. *Immunol Res* 66:224–233. <https://doi.org/10.1007/s12026-018-8991-x>
 205. Tian J-H, Patel N, Haupt R, Zhou H, Weston S, Hammond H, Logue J et al (2021) SARS-CoV-2 spike glycoprotein vaccine candidate NVX-CoV2373 immunogenicity in baboons and protection in mice. *Nat Commun* 12:372. <https://doi.org/10.1038/s41467-020-20653-8>
 206. Keech C, Albert G, Cho I, Robertson A, Reed P, Neal S, Joyce S, Plested, et al. (2020) Phase 1–2 trial of a SARS-CoV-2 recombinant spike protein nanoparticle vaccine. *N Engl J Med* 383(24):2320–2332.

- <https://doi.org/10.1056/NEJMoa2026920>
207. Venkatraman N, Anagnostou N, Bliss C, Bowyer G, Wright D, Lövgren-Bengtsson K, Roberts R et al (2017) Safety and immunogenicity of heterologous prime-boost immunization with viral-vectored malaria vaccines adjuvanted with Matrix-MTM. *Vaccine* 35:6208–6217. <https://doi.org/10.1016/j.vaccine.2017.09.028>
 208. University of Oxford (2015) Safety and immunogenicity of ChAd63 ME-TRAP/MVA ME-trap heterologous prime boost malaria vaccination adjuvanted with Matrix MTM. Clinical trial registration NCT01669512. clinicaltrials.gov
 209. University of Oxford (2020) A phase I/IIa clinical trial to assess the safety, immunogenicity and efficacy of the blood-stage *Plasmodium vivax* malaria vaccine candidate PvDBPII in Matrix M1 in healthy adults living in the UK. Clinical trial registration NCT04201431. clinicaltrials.gov
 210. University of Oxford (2020) A phase Ib/IIb randomised controlled trial of the safety, immunogenicity and efficacy of a candidate malaria vaccine, R21 adjuvanted with Matrix-M (R21/MM), in 5-17 month old children in Nanoro, Burkina Faso. Clinical trial registration NCT03896724. clinicaltrials.gov
 211. University of Oxford (2020) A phase Ib clinical trial to assess the safety and immunogenicity of the blood-stage *Plasmodium falciparum* malaria vaccine candidate RH5.1/Matrix-M in healthy adults and infants in tanzania. Clinical trial registration NCT04318002. clinicaltrials.gov
 212. University of Oxford (2021) A phase III randomized controlled multi-centre trial to evaluate the efficacy of the R21/Matrix-M vaccine in African children against clinical malaria. Clinical trial registration NCT04704830. clinicaltrials.gov
 213. Bender AT, Tzvetkov E, Pereira A, Wu Y, Kasar S, Przetak MM, Vlach J, Niewold TB, Jensen MA, Okitsu SL (2020) TLR7 and TLR8 differentially activate the IRF and NF- κ B pathways in specific cell types to promote inflammation. *ImmunoHorizons* 4:93–107. <https://doi.org/10.4049/immunoHorizons.2000002>
 214. Browne EP (2012) Regulation of B-cell responses by Toll-like receptors. *Immunology* 136:370–379. <https://doi.org/10.1111/j.1365-2567.2012.03587.x>
 215. Pone EJ, Xu Z, White CA, Zan H, Casali P (2012) B cell Toll-like receptors and immunoglobulin class-switch DNA recombination. *Front Biosci* 17:2594–2615
 216. Dowling DJ (2018) Recent advances in the discovery and delivery of TLR7/8 agonists as vaccine adjuvants. *ImmunoHorizons* 2:185–197. <https://doi.org/10.4049/immunoHorizons.1700063>
 217. Adams S (2009) Toll-like receptor agonists in cancer therapy. *Immunotherapy* 1:949–964. <https://doi.org/10.2217/imt.09.70>
 218. Ella R, Vadrevu KM, Jogdand H, Prasad S, Reddy S, Sarangi V, Ganneru B et al (2021) Safety and immunogenicity of an inactivated SARS-CoV-2 vaccine, BBV152: a double-blind, randomised, phase 1 trial. *Lancet Infect Dis* 21(5):637–646. [https://doi.org/10.1016/S1473-3099\(20\)30942-7](https://doi.org/10.1016/S1473-3099(20)30942-7)
 219. Jangra S, De Vrieze J, Choi A, Rathnasinghe R, Laghali G, Uvyn A, Van Herck S et al (2021) Sterilizing immunity against SARS-CoV-2 infection in mice by a single-shot and lipid amphiphile imidazoquinoline TLR7/8 agonist-adjuvanted recombinant spike protein vaccine. *Angew Chem Int Ed Engl* 60(17):9467–9473. <https://doi.org/10.1002/anie.202015362>
 220. Miller SM, Cybulski V, Whitacre M, Bess LS, Livesay MT, Walsh L, Burkhardt D, Bazin HG, Evans JT (2020) Novel lipidated imidazoquinoline TLR7/8 adjuvants elicit influenza-specific Th1 immune responses and protect against heterologous H3N2 influenza challenge in mice. *Front Immunol* 11:406. <https://doi.org/10.3389/fimmu.2020.00406>
 221. Bianchi F, Pretto S, Tagliabue E, Balsari A, Sfondrini L (2017) Exploiting poly(I:C) to induce cancer cell apoptosis. *Cancer Biol Ther* 18:747–756. <https://doi.org/10.1080/15384047.2017.1373220>
 222. Jin B, Sun T, Yu X-H, Liu C-Q, Yang Y-X, Lu P, Shan-Feng F, Qiu H-B, Yeo AET (2010) Immunomodulatory effects of dsRNA and its potential as vaccine adjuvant. *J Biomed Biotechnol* 2010:690438. <https://doi.org/10.1155/2010/690438>
 223. Comberlato A, Paloja K, Bastings MMC (2019) Nucleic acids presenting polymer nanomaterials as vaccine adjuvants. *J Mater Chem B* 7:6321–6346. <https://doi.org/10.1039/C9TB01222B>
 224. Lang KS, Recher M, Junt T, Navarini AA, Harris NL, Freigang S, Odermatt B et al (2005) Toll-like receptor engagement converts T-cell autoreactivity into overt autoimmune disease. *Nat Med* 11:138–145. <https://doi.org/10.1038/nm1176>

225. Smole A, Krajnik AK, Oblak A, Pirher N, Jerala R (2013) Delivery system for the enhanced efficiency of immunostimulatory nucleic acids. *Innate Immunity* 19:53–65. <https://doi.org/10.1177/1753425912450346>
226. Martins KAO, Bavari S, Salazar AM (2015) Vaccine adjuvant uses of poly-IC and derivatives. *Expert Rev Vaccines* 14:447–459. <https://doi.org/10.1586/14760584.2015.966085>
227. Levy HB, Baer G, Baron S, Buckler CE, Gibbs CJ, Iadarola MJ, London WT, Rice J (1975) A modified polyribonucleoside-polyribocytidylic acid complex that induces interferon in primates. *J Infect Dis* 132:434–439. <https://doi.org/10.1093/infdis/132.4.434>
228. Gowen BB, Wong M-H, Jung K-H, Sanders AB, Mitchell WM, Alexopoulos L, Flavell RA, Sidwell RW (2007) TLR3 is essential for the induction of protective immunity against Punta Toro Virus infection by the double-stranded RNA (dsRNA), poly(I:C12U), but not Poly(I:C): differential recognition of synthetic dsRNA molecules. *J Immunol* 178:5200–5208. <https://doi.org/10.4049/jimmunol.178.8.5200>
229. Stahl-Hennig C, Eisenblätter M, Jasny E, Rzehak T, Tenner-Racz K, Trumppheller C, Andres M, Salazar, et al. (2009) Synthetic double-stranded RNAs are adjuvants for the induction of T helper 1 and humoral immune responses to human papillomavirus in rhesus macaques. *PLOS Pathog* 5:e1000373. <https://doi.org/10.1371/journal.ppat.1000373>
230. Sabbatini P, Tsuji T, Ferran L, Ritter E, Sedrak C, Tuballes K, Jungbluth AA et al (2012) Phase I trial of overlapping long peptides from a tumor self-antigen and poly-ICLC shows rapid induction of integrated immune response in ovarian cancer patients. *Clin Cancer Res* 18:6497–6508. <https://doi.org/10.1158/1078-0432.CCR-12-2189>
231. Adams M, Navabi H, Jasani B, Man S, Fiander A, Evans AS, Donninger C, Mason M (2003) Dendritic cell (DC) based therapy for cervical cancer: use of DC pulsed with tumour lysate and matured with a novel synthetic clinically non-toxic double stranded RNA analogue poly [I]:poly [C12U] (Ampligen®). *Vaccine* 21:787–790. [https://doi.org/10.1016/S0264-410X\(02\)00599-6](https://doi.org/10.1016/S0264-410X(02)00599-6)
232. Navabi H, Jasani B, Reece A, Clayton A, Tabi Z, Donninger C, Mason M, Adams M (2009) A clinical grade poly I:C-analogue (Ampligen®) promotes optimal DC maturation and Th1-type T cell responses of healthy donors and cancer patients in vitro. *Vaccine* 27:107–115. <https://doi.org/10.1016/j.vaccine.2008.10.024>
233. Dietrich P-Y (2020) Pembrolizumab in association with the multi-peptide vaccine IMA950 adjuvanted with poly-ICLC for relapsing glioblastoma: a randomized phase I/II trial. Clinical trial registration NCT03665545. clinicaltrials.gov
234. Nayak A (2020) A phase I/II trial of pembrolizumab (MK-3475) and poly-ICLC in patients with metastatic mismatch repair-proficient (MRP) colon cancer. Clinical trial registration NCT02834052. clinicaltrials.gov
235. Brody J (2020) In situ vaccination with Flt3L, radiation, and poly-ICLC combined with pembrolizumab in patients with non-Hodgkin's lymphoma, metastatic breast cancer, and head and neck squamous cell carcinoma. Clinical trial registration NCT03789097. clinicaltrials.gov
236. Tewari AK (2020) Phase I study of in situ autologous vaccination against prostate cancer with intratumoral and systemic Hiltonol® (Poly-ICLC) prior to radical prostatectomy. Clinical trial registration NCT03262103. clinicaltrials.gov
237. Roswell Park Cancer Institute (2020) A phase I study of DEC205mAb-NY ESO 1 fusion protein (CDX-1401) given with adjuvant poly-ICLC in conjunction with 5-Aza-2'-deoxycytidine (Decitabine) and nivolumab in patients with MDS or low blast count AML. Clinical trial registration NCT03358719. clinicaltrials.gov
238. Coler RN, Bertholet S, Moutaftsi M, Guderian JA, Windish HP, Baldwin SL, Elsa M, Laughlin, et al. (2011) Development and characterization of synthetic glucopyranosyl lipid adjuvant system as a vaccine adjuvant. *PLoS One* 6:e16333. <https://doi.org/10.1371/journal.pone.0016333>
239. Johnson DA, Sowell CG, Johnson CL, Livesay MT, Keegan DS, Rhodes MJ, Ulrich JT, Ward JR, Cantrell JL, Brookshire VG (1999) Synthesis and biological evaluation of a new class of vaccine adjuvants: aminoalkyl glucosaminide 4-phosphates (AGPs). *Bioorg Med Chem Lett* 9:2273–2278. [https://doi.org/10.1016/S0960-894X\(99\)00374-1](https://doi.org/10.1016/S0960-894X(99)00374-1)
240. Disaccharide synthetic lipid compounds and uses thereof—patent US-9241988-B2—PubChem. 2021. <https://pubchem.ncbi.nlm.nih.gov/patent/US-9241988-B2#section=Priority-Date>. Accessed 5 Feb
241. 3D-PHAD® (2021) Avanti polar lipids. <https://avantilipids.com/product/699852>. Accessed 5 Feb

242. 3D(6-acyl) PHAD® (2021) Avanti polar lipids. <https://avantilipids.com/product/699855>. Accessed 5 Feb
243. MPLA (PHAD®) (2021) Avanti polar lipids. <https://avantilipids.com/product/699800>. Accessed 5 Feb
244. Taleghani N, Bozorg A, Azimi A, Zamani H (2019) Immunogenicity of HPV and HBV vaccines: adjuvant activity of synthetic analogs of monophosphoryl lipid A combined with aluminum hydroxide. *APMIS* 127:150–157. <https://doi.org/10.1111/apm.12927>
245. Carter D, Fox CB, Day TA, Guderian JA, Liang H, Rolf T, Vergara J et al (2016) A structure-function approach to optimizing TLR4 ligands for human vaccines. *Clin Transl Immunol* 5:e108. <https://doi.org/10.1038/cti.2016.63>
246. Rockefeller University (2013) A randomized, blinded, placebo-controlled phase I study to evaluate the safety and immunogenicity of GLA in healthy volunteers. Clinical trial registration NCT01397604. clinicaltrials.gov
247. IDRI (2016) A phase I, open-label clinical trial to evaluate the safety, tolerability, and immunogenicity of the LEISH-F3 + SLA-SE vaccine compared to LEISH-F3 + GLA-SE vaccine in healthy adult subjects. Clinical trial registration NCT02071758. clinicaltrials.gov
248. Oswaldo Cruz Foundation (2016) Phase I study to evaluate the safety of the vaccine prepared sm14 against schistosomiasis. Clinical trial registration NCT01154049. clinicaltrials.gov
249. Spertini F (2018) Safety and immunogenicity of novel candidate blood-stage malaria vaccine P27A with Alhydrogel® or GLA-SE as adjuvant: a staggered, antigen and adjuvant dose-finding, randomized, multi-centre phase Ia/Ib trial. Clinical trial registration NCT01949909. clinicaltrials.gov
250. Coler RN, Day TA, Ellis R, Piazza FM, Beckmann AM, Vergara J, Rolf T et al (2018) The TLR-4 agonist adjuvant, GLA-SE, improves magnitude and quality of immune responses elicited by the ID93 tuberculosis vaccine: first-in-human trial. *npj Vaccines* 3:1–9. <https://doi.org/10.1038/s41541-018-0057-5>
251. IDRI (2017) A phase I, randomized, dose-escalation study to evaluate the safety and immunogenicity of the ID93 + GLA-SE vaccine at two dose levels of the ID93 antigen and the GLA-SE adjuvant in healthy adults. Clinical trial registration NCT01599897. clinicaltrials.gov
252. Quratis Inc (2019) A phase 2a, randomized, double-blind, placebo-controlled study to evaluate the safety and explore the immunogenicity and efficacy of ID93+GLA-SE vaccine in BCG-vaccinated healthy healthcare workers. Clinical trial registration NCT03806686. clinicaltrials.gov
253. Mahipal A, Ejadi S, Gnjatich S, Kim-Schulze S, Lu H, Ter Meulen JH, Kenney R, Odunsi K (2019) First-in-human phase I dose-escalating trial of G305 in patients with advanced solid tumors expressing NY-ESO-1. *Cancer Immunol Immunother* 68:1211–1222. <https://doi.org/10.1007/s00262-019-02331-x>
254. Immune Design (2017) A phase I open label, multicenter, multiple ascending dose trial evaluating the safety, tolerability and immunogenicity of intramuscular recombinant NY-ESO-1 protein with GLA-SE adjuvant in patients with unresectable or metastatic cancer. Clinical trial registration NCT02015416. clinicaltrials.gov
255. Alving CR, Peachman KK, Matyas GR, Rao M, Beck Z (2020) Army liposome formulation (ALF) family of vaccine adjuvants. *Expert Rev Vaccines* 19:279–292. <https://doi.org/10.1080/14760584.2020.1745636>
256. Alving CR, Richards RL, Moss J, Alving LI, Clements JD, Shiba T, Kotani S, Wirtz RA, Hockmeyer WT (1986) Effectiveness of liposomes as potential carriers of vaccines: applications to cholera toxin and human malaria sporozoite antigen. *Vaccine* 4:166–172. [https://doi.org/10.1016/0264-410x\(86\)90005-8](https://doi.org/10.1016/0264-410x(86)90005-8)
257. Fries LF, Gordon DM, Richards RL, Egan JE, Hollingdale MR, Gross M, Silverman C, Alving CR (1992) Liposomal malaria vaccine in humans: a safe and potent adjuvant strategy. *Proc Natl Acad Sci U S A* 89:358–362. <https://doi.org/10.1073/pnas.89.1.358>
258. Heppner DG, Gordon DM, Gross M, Welde B, Leitner W, Krzych U, Schneider I et al (1996) Safety, immunogenicity, and efficacy of *Plasmodium falciparum* repeatless circumsporozoite protein vaccine encapsulated in liposomes. *J Infect Dis* 174:361–366. <https://doi.org/10.1093/infdis/174.2.361>
259. McElrath MJ (1995) Selection of potent immunological adjuvants for vaccine construction. *Semin Cancer Biol* 6:375–385. [https://doi.org/10.1016/1044-579x\(95\)90007-1](https://doi.org/10.1016/1044-579x(95)90007-1)
260. U.S. Army Medical Research and Development Command (2020) Phase I clinical trial

- with controlled human malaria infection (CHMI) for safety, protective efficacy, and immunogenicity of *Plasmodium falciparum* malaria protein (FMP013) administered intramuscularly with ALFQ healthy malaria-naïve adults. Clinical trial registration NCT04268420. clinicaltrials.gov
261. Cawlfeld A, Genito CJ, Beck Z, Bergmann-Leitner ES, Bitzer AA, Soto K, Zou X et al (2019) Safety, toxicity and immunogenicity of a malaria vaccine based on the circumsporozoite protein (FMP013) with the adjuvant army liposome formulation containing QS21 (ALFQ). *Vaccine* 37:3793–3803. <https://doi.org/10.1016/j.vaccine.2019.05.059>
 262. U.S. Army Medical Research and Development Command (2020) Randomized, double blind evaluation of late boost strategies with IHV01 (FLSC in aluminum phosphate) and A244 with or without ALFQ for HIV-uninfected participants in the HIV vaccine trial RV306/WRAIR 1920. Clinical trial registration NCT04658667. clinicaltrials.gov
 263. Garinot M, Piras-Douce F, Probeck P, Chambon V, Varghese K, Liu Y, Luna E, Drake D, Haensler J (2020) A potent novel vaccine adjuvant based on straight polyacrylate. *Int J Pharm X* 2:100054. <https://doi.org/10.1016/j.ijpx.2020.100054>
 264. Zaman M, Simerska P, Toth I (2010) Synthetic polyacrylate polymers as particulate intranasal vaccine delivery systems for the induction of mucosal immune response. *Curr Drug Deliv* 7(2):118–124
 265. Zaman M, Skwarczynski M, Malcolm JM, Urbani CN, Jia Z, Batzloff MR, Good MF, Monteiro MJ, Toth I (2011) Self-adjuvanting polyacrylic nanoparticulate delivery system for group A streptococcus (GAS) vaccine. *Nanomed Nanotechnol Biol Med* 7:168–173. <https://doi.org/10.1016/j.nano.2010.10.002>
 266. Hilgers LA, Ghenne L, Nicolas I, Fochesato M, Lejeune G, Boon B (2000) Alkyl-polyacrylate esters are strong mucosal adjuvants. *Vaccine* 18:3319–3325. [https://doi.org/10.1016/s0264-410x\(00\)00114-6](https://doi.org/10.1016/s0264-410x(00)00114-6)
 267. Mair KH, Koinig H, Gerner W, Höhne A, Bretthauer J, Kroll JJ, Roof MB, Saalmüller A, Stadler K, Libanova R (2015) Carbopol improves the early cellular immune responses induced by the modified-life vaccine Ingelvac PRRS® MLV. *Vet Microbiol* 176:352–357. <https://doi.org/10.1016/j.vetmic.2015.02.001>
 268. Mumford JA, Wilson H, Hannant D, Jessett DM (1994) Antigenicity and immunogenicity of equine influenza vaccines containing a Carbomer adjuvant. *Epidemiol Infect* 112:421–437
 269. Weill Medical College of Cornell University (2020) Phase I randomized, double-blind, placebo control study for an anti-cocaine vaccine. Clinical trial registration NCT02455479. clinicaltrials.gov
 270. Havlicek DF, De B, Rosenberg J, Pagovich O, Sondhi D, Kaminsky S, Crystal R (2016) 36. Translation of an adenovirus-based cocaine vaccine dAd5GNE to a clinical trial. *Mol Ther* 24:S16. [https://doi.org/10.1016/S1525-0016\(16\)32845-3](https://doi.org/10.1016/S1525-0016(16)32845-3)
 271. Hicks MJ, Kaminsky SM, De BP, Rosenberg JB, Evans SM, Foltin RW, Andrenyak DM et al (2014) Fate of systemically administered cocaine in nonhuman primates treated with the dAd5GNE anticocaine vaccine. *Hum Gene Ther* 25:40–49. <https://doi.org/10.1089/humc.2013.231>
 272. Maoz A, Hicks MJ, Vallabhjousula S, Synan M, Kothari PJ, Dyke JP, Ballon DJ et al (2013) Adenovirus capsid-based anti-cocaine vaccine prevents cocaine from binding to the nonhuman primate CNS dopamine transporter. *Neuropsychopharmacology* 38:2170–2178. <https://doi.org/10.1038/npp.2013.114>
 273. Pavot V, Bisceglia H, Guillaume F, Montano S, Zhang L, Boudet F, Haensler J (2021) A novel vaccine adjuvant based on straight polyacrylate potentiates vaccine-induced humoral and cellular immunity in cynomolgus macaques. *Hum Vaccin Immunother* 17(7):2336–2348. <https://doi.org/10.1080/21645515.2020.1855956>
 274. Rigaut G, Parisot AGAL, De Luca K, Andreoni CMP, Remolue L, Garinot M, Cotte J-F et al (2017) Novel immunogenic formulations comprising linear or branched polyacrylic acid polymer adjuvants. Patent WO2017218819A1
 275. Holmgren J, Harandi AM, Lebens M, Sun J-B, Anjuère F, Czerkinsky C (2006) 14—Mucosal adjuvants based on cholera toxin and *E. coli* heat-labile enterotoxin. In: Schijns VEJC, O'Hagan DT (eds) *Immunopotentiators in modern vaccines*. Academic Press, London, pp 235–252. <https://doi.org/10.1016/B978-012088403-2/50015-0>
 276. Liang S, Hajishengallis G (2010) Heat-labile enterotoxins as adjuvants or anti-inflammatory agents. *Immunol Investig* 39:449–467
 277. Duan Q, Xia P, Nandre R, Zhang W, Zhu G (2019) Review of newly identified functions associated with the heat-labile toxin of enterotoxigenic *Escherichia coli*. *Front Cell*

- Infect Microbiol 9:292. <https://doi.org/10.3389/fcimb.2019.00292>
278. Harandi AM, Lycke N (2017) Chapter 19—Toxin-based mucosal adjuvants. In: Schijns VEJC, O'Hagan DT (eds) Immunopotentiators in modern vaccines, 2nd edn. Academic Press, London, pp 377–397. <https://doi.org/10.1016/B978-0-12-804019-5.00019-0>
279. Fromantin C, Jamot B, Cohen J, Piroth L, Pothier P, Kohli E (2001) Rotavirus 2/6 virus-like particles administered intranasally in mice, with or without the mucosal adjuvants cholera toxin and Escherichia coli heat-labile toxin, induce a Th1/Th2-like immune response. *J Virol* 75:11010–11016. <https://doi.org/10.1128/JVI.75.22.11010-11016.2001>
280. Brereton CF, Sutton CE, Ross PJ, Iwakura Y, Pizza M, Rappuoli R, Lavelle EC, Mills KHG (2011) Escherichia coli heat-labile enterotoxin promotes protective Th17 responses against infection by driving innate IL-1 and IL-23 production. *J Immunol* 186:5896–5906. <https://doi.org/10.4049/jimmunol.1003789>
281. Hajishengallis G, Connell TD (2013) Type II heat-labile enterotoxins: structure, function, and immunomodulatory properties. *Vet Immunol Immunopathol* 152:68–77. <https://doi.org/10.1016/j.vetimm.2012.09.034>
282. Michetti P, Kreiss C, Kotloff KL, Porta N, Blanco J-L, Bachmann D, Herranz M et al (1999) Oral immunization with urease and Escherichia coli heat-labile enterotoxin is safe and immunogenic in Helicobacter pylori-infected adults. *Gastroenterology* 116:804–812. [https://doi.org/10.1016/S0016-5085\(99\)70063-6](https://doi.org/10.1016/S0016-5085(99)70063-6)
283. Mutsch M, Zhou W, Rhodes P, Bopp M, Chen RT, Linder T, Spyr C, Steffen R (2004) Use of the inactivated intranasal influenza vaccine and the risk of Bell's palsy in Switzerland. *N Engl J Med* 350:896–903. <https://doi.org/10.1056/NEJMoa030595>
284. Kotloff KL, Sztein MB, Wasserman SS, Losonsky GA, DiLorenzo SC, Walker RI (2001) Safety and Immunogenicity of oral inactivated whole-cell Helicobacter pylori vaccine with adjuvant among volunteers with or without subclinical infection. *Infect Immun* 69:3581–3590. <https://doi.org/10.1128/IAI.69.6.3581-3590.2001>
285. Clements JD, Norton EB (2018) The mucosal vaccine adjuvant LT(R192G/L211A) or dmLT. *mSphere* 3:e00215–e00218. <https://doi.org/10.1128/mSphere.00215-18>
286. PATH (2020) A phase I randomized study to examine the safety, tolerability, and immunogenicity of inactivated poliovirus vaccine (IPV) with or without E.Coli double mutant heat labile toxin (dmLT) and impact on poliovirus shedding post-bOPV challenge in healthy IPV-primed adult subjects. Clinical trial registration NCT04232943. clinicaltrials.gov
287. Cowan K (2020) Phase I evaluation of the safety, reactogenicity and immunogenicity of fractional-dose inactivated polio vaccine (fIPV) given intradermally with double mutant [LT(R192G/L211A)] enterotoxigenic Escherichia coli heat labile toxin (dmLT) adjuvant. Clinical trial registration NCT03922061. clinicaltrials.gov
288. Agren LC, Ekman L, Löwenadler B, Lycke NY (1997) Genetically engineered nontoxic vaccine adjuvant that combines B cell targeting with immunomodulation by cholera toxin A1 subunit. *J Immunol* 158:3936–3946
289. Ågren L, Sverremark E, Ekman L, Schön K, Löwenadler B, Fernandez C, Lycke N (2000) The ADP-ribosylating CTA1-DD adjuvant enhances T cell-dependent and independent responses by direct action on B cells involving anti-apoptotic Bcl-2- and germinal center-promoting effects. *J Immunol* 164:6276–6286. <https://doi.org/10.4049/jimmunol.164.12.6276>
290. Bemark M, Bergqvist P, Stensson A, Holmberg A, Mattsson J, Lycke NY (2011) A unique role of the cholera toxin A1-DD adjuvant for long-term plasma and memory B cell development. *J Immunol* 186:1399–1410. <https://doi.org/10.4049/jimmunol.1002881>
291. Helgeby A, Robson NC, Donachie AM, Beackock-Sharp H, Lövgren K, Schön K, Mowat A, Lycke NY (2006) The combined CTA1-DD/ISCOM adjuvant vector promotes priming of mucosal and systemic immunity to incorporated antigens by specific targeting of B cells. *J Immunol* 176:3697–3706. <https://doi.org/10.4049/jimmunol.176.6.3697>
292. Sundling C, Schön K, Mörner A, Forsell MNE, Wyatt RT, Thorstenson R, Karlsson Hedestam GB, Lycke NY (2008) CTA1-DD adjuvant promotes strong immunity against human immunodeficiency virus type 1 envelope glycoproteins following mucosal immunization. *J Gen Virol* 89:2954–2964. <https://doi.org/10.1099/vir.0.2008/005470-0>
293. Fan XT, Wang YL, Qiu Dong S, Qiu F, Yi Y, Jia ZY, Wang DY et al (2019) Intranasal immunization using CTA1-DD as a mucosal

- adjuvant for an inactivated influenza vaccine. *Biomed Environ Sci* 32:531–540. <https://doi.org/10.3967/bes2019.070>
294. Schussek S, Bernasconi V, Mattsson J, Wenzel UA, Strömberg A, Gribonika I, Schön K, Lycke NY (2020) The CTA1-DD adjuvant strongly potentiates follicular dendritic cell function and germinal center formation, which results in improved neonatal immunization. *Mucosal Immunol* 13:545–557. <https://doi.org/10.1038/s41385-020-0253-2>
 295. Kates M (1977) The phytanyl ether-linked polar lipids and isoprenoid neutral lipids of extremely halophilic bacteria. *Prog Chem Fats Other Lipids* 15:301–342. [https://doi.org/10.1016/0079-6832\(77\)90011-8](https://doi.org/10.1016/0079-6832(77)90011-8)
 296. Haq K, Jia Y, Krishnan L (2016) Archaeal lipid vaccine adjuvants for induction of cell-mediated immunity. *Expert Rev Vaccines* 15:1557–1566. <https://doi.org/10.1080/14760584.2016.1195265>
 297. Gurnani K, Kennedy J, Sad S, Sprott GD, Krishnan L (2004) Phosphatidylserine receptor-mediated recognition of archaeosome adjuvant promotes endocytosis and MHC class I cross-presentation of the entrapped antigen by phagosome-to-cytosol transport and classical processing. *J Immunol* 173:566–578. <https://doi.org/10.4049/jimmunol.173.1.566>
 298. Salmani AS, Aghasadeghi MR, Nategh R, Mokhtari-Azad T, Siadat SD (2013) Methanobrevibacter smithii archaeosomes-entrapped mzNL4-3 virus-like particles induce specific T helper 1-oriented cellular and humoral responses against HIV-1. *Curr HIV Res* 11(6):491–497
 299. Alavi SE, Mansouri H, Esfahani MKM, Movahedi F, Akbarzadeh A, Chiani M (2014) Archaeosome: as new drug carrier for delivery of paclitaxel to breast cancer. *Indian J Clin Biochem* 29:150–153. <https://doi.org/10.1007/s12291-013-0305-4>
 300. Aghasadeghi MR, Delbaz SA, Sadat SM, Siadat SD, Ardestani MS, Rahimi P, Bolhassani A et al (2014) Induction of strong and specific humoral and T-helper 1 cellular responses by HBsAg entrapped in the methanobrevibacter smithii archaeosomes. *Avicenna J Med Biotechnol* 6:238–245
 301. Krishnan L, Deschatelets L, Stark FC, Gurnani K, Sprott GD (2010) Archaeosome adjuvant overcomes tolerance to tumor-associated melanoma antigens inducing protective CD8+ T cell responses. *Clin Dev Immunol* 2010:578432. <https://doi.org/10.1155/2010/578432>
 302. Sprott GD, Subash S, Perry Fleming L, DiCaire CJ, Patel GB, Krishnan L (2003) Archaeosomes varying in lipid composition differ in receptor-mediated endocytosis and differentially adjuvant immune responses to entrapped antigen. *Archaea* 1:151–164
 303. Conlan JW, Krishnan L, Willick GE, Patel GB, Dennis Sprott G (2001) Immunization of mice with lipopeptide antigens encapsulated in novel liposomes prepared from the polar lipids of various Archaeobacteria elicits rapid and prolonged specific protective immunity against infection with the facultative intracellular pathogen, *Listeria monocytogenes*. *Vaccine* 19:3509–3517. [https://doi.org/10.1016/S0264-410X\(01\)00041-X](https://doi.org/10.1016/S0264-410X(01)00041-X)
 304. Krishnan L, Dicaire CJ, Patel GB, Sprott GD (2000) Archaeosome vaccine adjuvants induce strong humoral, cell-mediated, and memory responses: comparison to conventional liposomes and alum. *Infect Immun* 68:54–63. <https://doi.org/10.1128/iai.68.1.54-63.2000>
 305. Jia Y, Akache B, Deschatelets L, Qian H, Dudani R, Harrison BA, Felicity C. Stark, et al. (2019) A comparison of the immune responses induced by antigens in three different archaeosome-based vaccine formulations. *Int J Pharm* 561:187–196. <https://doi.org/10.1016/j.ijpharm.2019.02.041>
 306. Sprott GD, Yeung A, Dicaire CJ, Yu SH, Whitfield DM (2012) Synthetic archaeosome vaccines containing triglycosylarchaeols can provide additive and long-lasting immune responses that are enhanced by archaeidylserine. *Archaea* 2012:513231. <https://doi.org/10.1155/2012/513231>
 307. Stark FC, Agbayani G, Sandhu JK, Akache B, McPherson C, Deschatelets L, Dudani R et al (2019) Simplified admix archaeal glycolipid adjuvanted vaccine and checkpoint inhibitor therapy combination enhances protection from murine melanoma. *Biomedicines* 7:91. <https://doi.org/10.3390/biomedicines7040091>
 308. Stark FC, Akache B, Ponce A, Dudani R, Deschatelets L, Jia Y, Sauvageau J et al (2019) Archaeal glycolipid adjuvanted vaccines induce strong influenza-specific immune responses through direct immunization in young and aged mice or through passive maternal immunization. *Vaccine* 37:7108–7116. <https://doi.org/10.1016/j.vaccine.2019.07.010>
 309. Akache B, Deschatelets L, Harrison BA, Dudani R, Stark FC, Jia Y, Landi A et al (2019) Effect of different adjuvants on the longevity and strength of humoral and

- cellular immune responses to the HCV envelope glycoproteins. *Vaccines* 7(4):204. <https://doi.org/10.3390/vaccines7040204>
310. Agbayani G, Jia Y, Akache B, Chandan V, Iqbal U, Stark FC, Deschatelets L et al (2020) Mechanistic insight into the induction of cellular immune responses by encapsulated and admixed archaeosome-based vaccine formulations. *Hum Vaccin Immunother* 16:2183–2195. <https://doi.org/10.1080/21645515.2020.1788300>
311. Jia Y, Akache B, Agbayani G, Chandan V, Dudani R, Harrison BA, Deschatelets L et al (2021) The synergistic effects of sulfated lactosyl archaeol archaeosomes when combined with different adjuvants in a murine model. *Pharmaceutics* 13(2):205. <https://doi.org/10.3390/pharmaceutics13020205>
312. Kobayashi E, Motoki K, Uchida T, Fukushima H, Koezuka Y (1995) KRN7000, a novel immunomodulator, and its antitumor activities. *Oncol Res* 7:529–534
313. Carnaud C, Lee D, Donnars O, Park S-H, Beavis A, Koezuka Y, Bendelac A (1999) Cutting edge: cross-talk between cells of the innate immune system: NKT cells rapidly activate NK cells. *J Immunol* 163:4647–4650
314. Fujii S-i, Shimizu K, Smith C, Bonifaz L, Steinman RM (2003) Activation of natural killer T cells by α -galactosylceramide rapidly induces the full maturation of dendritic cells in vivo and thereby acts as an adjuvant for combined CD4 and CD8 T cell immunity to a coadministered protein. *J Exp Med* 198:267–279. <https://doi.org/10.1084/jem.20030324>
315. Hermans IF, Silk JD, Gileadi U, Salio M, Mathew B, Ritter G, Schmidt R, Harris AL, Old L, Cerundolo V (2003) NKT cells enhance CD4+ and CD8+ T cell responses to soluble antigen in vivo through direct interaction with dendritic cells. *J Immunol* 171:5140–5147. <https://doi.org/10.4049/jimmunol.171.10.5140>
316. Hoya M, Nagamatsu T, Fujii T, Schust DJ, Oda H, Akiba N, Iriyama T, Kawana K, Osuga Y, Fujii T (2018) Impact of Th1/Th2 cytokine polarity induced by invariant NKT cells on the incidence of pregnancy loss in mice. *Am J Reprod Immunol* 79:e12813. <https://doi.org/10.1111/aji.12813>
317. Waldowska M, Bojarska-Junak A, Roliński J (2017) A brief review of clinical trials involving manipulation of invariant NKT cells as a promising approach in future cancer therapies. *Cent Eur J Immunol* 42:181. <https://doi.org/10.5114/cej.2017.69361>
318. Gableh F, Saecidi M, Hemati S, Hamdi K, Soleimanjahi H, Gorji A, Ghaemi A (2016) Combination of the toll like receptor agonist and α -Galactosylceramide as an efficient adjuvant for cancer vaccine. *J Biomed Sci* 23:16. <https://doi.org/10.1186/s12929-016-0238-3>
319. Ko S-Y, Ko H-J, Chang W-S, Park S-H, Kweon M-N, Kang C-Y (2005) α -Galactosylceramide can act as a nasal vaccine adjuvant inducing protective immune responses against viral infection and tumor. *J Immunol* 175:3309–3317. <https://doi.org/10.4049/jimmunol.175.5.3309>
320. Giaccone G, Punt CJA, Ando Y, Ruijter R, Nishi N, Peters M, von Blomberg BME et al (2002) A phase I study of the natural killer T-cell ligand α -galactosylceramide (KRN7000) in patients with solid tumors. *Clin Cancer Res* 8:3702–3709
321. Nieda M, Okai M, Tazbirkova A, Lin H, Yamaura A, Ide K, Abraham R, Juji T, Macfarlane DJ, Nicol AJ (2004) Therapeutic activation of α 24+ β 11+ NKT cells in human subjects results in highly coordinated secondary activation of acquired and innate immunity. *Blood* 103:383–389. <https://doi.org/10.1182/blood-2003-04-1155>
322. Ishikawa A, Motohashi S, Ishikawa E, Fuchida H, Higashino K, Otsuji M, Iizasa T, Nakayama T, Taniguchi M, Fujisawa T (2005) A phase I study of α -galactosylceramide (KRN7000)-pulsed dendritic cells in patients with advanced and recurrent non-small cell lung cancer. *Clin Cancer Res* 11:1910–1917. <https://doi.org/10.1158/1078-0432.CCR-04-1453>
323. Nicol AJ, Tazbirkova A, Nieda M (2011) Comparison of clinical and immunological effects of intravenous and intradermal administration of α -galactosylceramide (KRN7000)-pulsed dendritic cells. *Clin Cancer Res* 17:5140–5151. <https://doi.org/10.1158/1078-0432.CCR-10-3105>
324. Chang DH, Osman K, Connolly J, Kukreja A, Krasovsky J, Pack M, Hutchinson A et al (2005) Sustained expansion of NKT cells and antigen-specific T cells after injection of α -galactosyl-ceramide loaded mature dendritic cells in cancer patients. *J Exp Med* 201:1503–1517. <https://doi.org/10.1084/jem.20042592>
325. Richter J, Neparidze N, Lin Z, Nair S, Monesmith T, Sundaram R, Miesowicz F, Dhodapkar KM, Dhodapkar MV (2013) Clinical regressions and broad immune activation following combination therapy targeting human NKT cells in myeloma. *Blood*

- 121:423–430. <https://doi.org/10.1182/blood-2012-06-435503>
326. Motohashi S, Nagato K, Kunii N, Yamamoto H, Yamasaki K, Okita K, Hanaoka H et al (2009) A phase I-II study of alpha-galactosylceramide-pulsed IL-2/GM-CSF-cultured peripheral blood mononuclear cells in patients with advanced and recurrent non-small cell lung cancer. *J Immunol* 182:2492–2501. <https://doi.org/10.4049/jimmunol.0800126>
327. Uchida T, Horiguchi S, Tanaka Y, Yamamoto H, Kunii N, Motohashi S, Taniguchi M, Nakayama T, Okamoto Y (2008) Phase I study of alpha-galactosylceramide-pulsed antigen presenting cells administration to the nasal submucosa in unresectable or recurrent head and neck cancer. *Cancer Immunol Immunother* 57:337–345. <https://doi.org/10.1007/s00262-007-0373-5>
328. Kurosaki M, Horiguchi S, Yamasaki K, Uchida Y, Motohashi S, Nakayama T, Sugimoto A, Okamoto Y (2011) Migration and immunological reaction after the administration of α GalCer-pulsed antigen-presenting cells into the submucosa of patients with head and neck cancer. *Cancer Immunol Immunother* 60:207–215. <https://doi.org/10.1007/s00262-010-0932-z>
329. Nagato K, Motohashi S, Ishibashi F, Okita K, Yamasaki K, Moriya Y, Hoshino H et al (2012) Accumulation of activated invariant natural killer T cells in the tumor microenvironment after α -galactosylceramide-pulsed antigen presenting cells. *J Clin Immunol* 32:1071–1081. <https://doi.org/10.1007/s10875-012-9697-9>
330. Yamasaki K, Horiguchi S, Kurosaki M, Kunii N, Nagato K, Hanaoka H, Shimizu N et al (2011) Induction of NKT cell-specific immune responses in cancer tissues after NKT cell-targeted adoptive immunotherapy. *Clin Immunol* 138:255–265. <https://doi.org/10.1016/j.clim.2010.11.014>
331. Toyoda T, Kamata T, Tanaka K, Ihara F, Takami M, Suzuki H, Nakajima T et al (2020) Phase II study of α -galactosylceramide-pulsed antigen-presenting cells in patients with advanced or recurrent non-small cell lung cancer. *J Immunother Cancer* 8:e000316. <https://doi.org/10.1136/jitc-2019-000316>
332. Smith A, Perelman M, Hinchcliffe M (2014) Chitosan. *Hum Vaccin Immunother* 10:797–807. <https://doi.org/10.4161/hv.27449>
333. Malik A, Gupta M, Gupta V, Gogoi H, Bhatnagar R (2018) Novel application of trimethyl chitosan as an adjuvant in vaccine delivery. *Int J Nanomed* 13:7959–7970. <https://doi.org/10.2147/IJN.S165876>
334. Li X, Min M, Nan D, Ying G, Hode T, Naylor M, Chen D, Nordquist RE, Chen WR (2013) Chitin, chitosan, and glycosylated chitosan regulate immune responses: the novel adjuvants for cancer vaccine. *Clin Dev Immunol* 2013:387023. <https://doi.org/10.1155/2013/387023>
335. Dai T, Tanaka M, Huang Y-Y, Hamblin MR (2011) Chitosan preparations for wounds and burns: antimicrobial and wound-healing effects. *Expert Rev Anti Infect Ther* 9:857–879. <https://doi.org/10.1586/eri.11.59>
336. Carroll EC, Jin L, Mori A, Muñoz-Wolf N, Oleszycka E, Moran HBT, Mansouri S et al (2016) The vaccine adjuvant chitosan promotes cellular immunity via DNA sensor cGAS-STING-dependent induction of type I interferons. *Immunity* 44:597–608. <https://doi.org/10.1016/j.immuni.2016.02.004>
337. El-Kamary SS, Pasetti MF, Mendelman PM, Frey SE, Bernstein DI, Treanor JJ, Ferreira J et al (2010) Adjuvanted intranasal norwalk virus-like particle vaccine elicits antibodies and antibody-secreting cells that express homing receptors for mucosal and peripheral lymphoid tissues. *J Infect Dis* 202:1649–1658. <https://doi.org/10.1086/657087>
338. LigoCyte Pharmaceuticals, Inc (2015) Randomized double-blind placebo-controlled phase I, safety and immunogenicity study of two dosages of intranasal norwalk virus-like particle vaccine (norwalk VLP antigen, MPL®, chitosan, mannitol, and sucrose) compared to adjuvant/excipients (MPL®, chitosan, mannitol, and sucrose) and to placebo (empty device). Clinical trial registration NCT00806962. clinicaltrials.gov
339. Read RC, Naylor SC, Potter CW, Bond J, Jabbal-Gill I, Fisher A, Illum L, Jennings R (2005) Effective nasal influenza vaccine delivery using chitosan. *Vaccine* 23:4367–4374. <https://doi.org/10.1016/j.vaccine.2005.04.021>
340. Chang H, Li X, Teng Y, Liang Y, Peng B, Fang F, Chen Z (2010) Comparison of adjuvant efficacy of chitosan and aluminum hydroxide for intraperitoneally administered inactivated influenza H5N1 vaccine. *DNA Cell Biol* 29:563–568. <https://doi.org/10.1089/dna.2009.0977>

341. Petrovsky N, Cooper PD (2015) AdvaxTM, a novel microcrystalline polysaccharide particle engineered from delta inulin, provides robust adjuvant potency together with tolerability and safety. *Vaccine* 33:5920–5926. <https://doi.org/10.1016/j.vaccine.2015.09.030>
342. Jelínková L, Jhun H, Eaton A, Petrovsky N, Zavala F, Chackerian B (2021) An epitope-based malaria vaccine targeting the junctional region of circumsporozoite protein. *npj Vaccines* 6:1–10. <https://doi.org/10.1038/s41541-020-00274-4>
343. Hess JA, Zhan B, Torigian AR, Patton JB, Petrovsky N, Zhan T, Bottazzi ME et al (2016) The immunomodulatory role of adjuvants in vaccines formulated with the recombinant antigens Ov-103 and Ov-RAL-2 against *Onchocerca volvulus* in mice. *PLOS Negl Trop Dis* 10:e0004797. <https://doi.org/10.1371/journal.pntd.0004797>
344. Wong TM, Petrovsky N, Bissel SJ, Wiley CA, Ross TM (2016) Delta inulin-derived adjuvants that elicit Th1 phenotype following vaccination reduces respiratory syncytial virus lung titers without a reduction in lung immunopathology. *Hum Vaccin Immunother* 12:2096–2105. <https://doi.org/10.1080/21645515.2016.1162931>
345. Counoupas C, Pinto R, Nagalingam G, Britton WJ, Petrovsky N, Triccas JA (2017) Delta inulin-based adjuvants promote the generation of dysfunctional CD4⁺ T cell responses and protection against *Mycobacterium tuberculosis* infection. *Sci Rep* 7:8582. <https://doi.org/10.1038/s41598-017-09119-y>
346. Vaxine Pty Ltd (2019) Phase I randomized, controlled, double-blind study to compare the safety and effectiveness of hepatitis B vaccines in individuals with renal impairment, diabetes mellitus or age greater than 40 years. Clinical trial registration NCT01951677. clinicaltrials.gov
347. Vaxine Pty Ltd (2019) A randomised, controlled, blinded phase I study to evaluate the immunogenicity and safety of a pandemic avian H5 influenza vaccine in adults. Clinical trial registration NCT02335164. clinicaltrials.gov
348. National Institute of Allergy and Infectious Diseases (NIAID) (2020) A phase I study to assess the safety, reactogenicity and immunogenicity of two quadrivalent seasonal influenza vaccines (Fluzone(R) or Flublok(R)) with or without one of two adjuvants (AF03 or Advax-CpG55.2) in healthy adults 18-45 years of age. Clinical trial registration NCT03945825. clinicaltrials.gov
349. Vaxine Pty Ltd (2020) A randomised, controlled, phase I study to evaluate the safety and immunogenicity of a candidate adjuvanted recombinant protein SARS-COV-2 vaccine in healthy adult subjects. Clinical trial registration NCT04453852. clinicaltrials.gov



Cationic Nanostructures as Adjuvants for Vaccines

Ana Maria Carmona-Ribeiro, Beatriz Ideriha Mathiazzi,
and Yunys Pérez-Betancourt

Abstract

Spherical or discoidal lipid polymer nanostructures bearing cationic charges successfully adsorb a variety of oppositely charged antigens (Ag) such as proteins, peptides, nucleic acids, or oligonucleotides. This report provides instructions for the preparation and physical characterization of four different cationic nanostructures able to combine and deliver antigens to the immune system: (1) dioctadecyl dimethylammonium bromide (DODAB) bilayer fragments (DODAB BF); (2) polystyrene sulfate (PSS) nanoparticles (NPs) covered with one cationic dioctadecyl dimethylammonium bromide bilayer (DODAB) named (PSS/DODAB); (3) cationic NPs of biocompatible polymer poly(methyl methacrylate) (PMMA) prepared by emulsion polymerization of the methyl methacrylate (MMA) monomer in the presence of DODAB BF (PMMA/DODAB NPs); (4) antigen NPs (NPs) where the cationic polymer poly(diallyl dimethyl ammonium chloride) (PDDA) directly combined at nontoxic and low dose with the antigen (Ag); when the oppositely charged model antigen is ovalbumin (OVA), NPs are named PDDA/OVA. These nanostructures provide adequate microenvironments for carrying and delivering antigens to the antigen-presenting cells of the immune system.

Key words Polymeric NPs, Cationic lipid, Bilayer fragments or nanodisks, Cationic polymer, Model antigen ovalbumin, Poly(diallyl dimethyl ammonium) chloride, Poly(methylmethacrylate), Dioctadecyl dimethylammonium bromide, Immunoadjuvants

1 Introduction

Cationic structures of nanometric size are especially suitable to carry and deliver antigens directly to antigen-presenting cells (APC) in the lymph nodes easily overcoming anatomical barriers from the injection site [1, 2]. They can be obtained from a variety of lipids, polymers, or lipids and polymers mostly as bilayer vesicles [3], open bilayer disks [4–6], or hybrid nanoparticles (NPs) [5, 7–14]. Cationic nanostructures applied to vaccine design were recently reviewed [15].

In particular, the cationic and synthetic lipid dioctadecyldimethylammonium bromide (DODAB) self-assembles as both

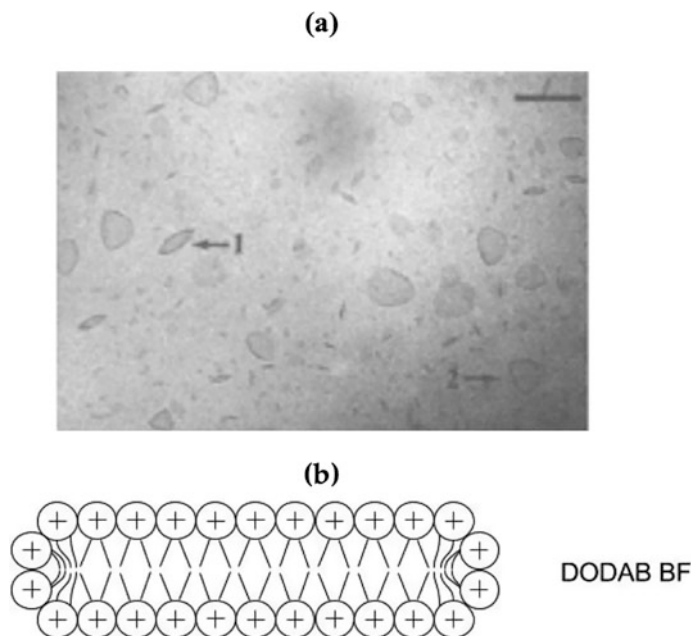


Fig. 1 (a) Bilayer fragments of dioctadecyldimethylammonium bromide (DODAB BF) visualized face-on and edge-on by cryo-transmission electron microscopy where the bar denotes 100 nm and the scheme shows a cross section of DODAB BF. The micrograph was adapted with permission from [28]. (b) Schematic representation of a DODAB BF cross section

closed and large bilayer vesicles [16, 17] or as open and cationic bilayer fragments or nanodisks (DODAB BF). The sizes of DODAB BF are below 100 nm, they are stabilized by the electrostatic repulsion, and they fuse to yield large vesicles upon addition of monovalent salt and screening of the surface potential [18]. DODAB bilayers can combine with a broad variety of antigens or enhancers of the immune response such as proteins [3, 19, 20], peptides [11, 21, 22], oligonucleotides [6, 23], mononucleotides [24, 25], or nucleic acids [26, 27] driving an enhanced cell-mediated immune response but a poor humoral response in several instances [3, 5–7]. The preparation and characterization of DODAB BF dispersions in water (Fig. 1) is stated in Subheading 3.1.

The versatile DODAB assemblies also interact with oppositely charged particles such as polystyrene sulfate (PSS) latexes [7, 11, 29–31] or silica [32–35]. Optimal deposition of DODAB bilayers on PSS NPs [7, 11, 31] or silica was achieved [34, 35] paving the way for their use as suitable immunoadjuvants and antigen carriers. Subheading 3.2 describes the preparation and characterization of PSS/DODAB NPs (Fig. 2), where a single DODAB bilayer surrounds each PSS NP [11].

The good miscibility of DODAB with the biocompatible polymer poly(methylmethacrylate) (PMMA) [8, 36] led to the

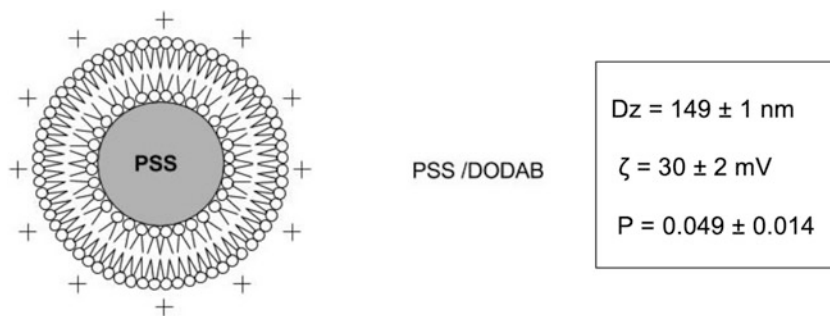


Fig. 2 Scheme of a cross section of a polystyrene sulfate nanoparticle (PSS) supporting a cationic bilayer of dioctadecyldimethylammonium bromide (DODAB). The mean hydrodynamic diameter (D_z), the zeta-potential (ζ) and the polydispersity of the dispersion in 1 mM NaCl were from ref. 11

synthesis of polymeric PMMA/DODAB NPs by emulsion polymerization of methylmethacrylate (MMA) in the presence of DODAB BF [14]. Subheading 3.3 describes this synthesis yielding the hybrid, cationic, and nanometric PMMA/DODAB NPs (Fig. 3). The cationic, hydrophilic, and antimicrobial polymer PDDA [10, 37, 38] combined by electrostatic attraction with oppositely charged biopolymers such as bovine serum albumin (BSA) [39] and ovalbumin (OVA) also yielded cationic NPs [13]. This led to the proposition of PDDA as a suitable immunoadjuvant combined with antigens; at low PDDA doses, its toxicity was nondetectable. Furthermore, PDDA/antigen NPs (Fig. 4) enhanced the humoral response to levels even higher than those elicited by the classical adjuvant alum [13]. Subheading 3.4 of the protocol details the PDDA/ovalbumin (OVA) NP preparation.

2 Materials

Prepare all solutions using analytical grade reagents and ultrapure water (prepared by purifying deionized water to attain a sensitivity of $18 \text{ M } \Omega \text{ cm}$ at $25 \text{ }^\circ\text{C}$). All reagents should be prepared at room temperature unless indicated otherwise. DODAB dispersions should be freshly prepared and used within 1–2 days after dispersion. Polymeric microspheres should be stored refrigerated at $4 \text{ }^\circ\text{C}$ to avoid microbial growth.

2.1 Preparation and Characterization of DODAB BF

1. 1 mM NaCl solution in water.
2. DODAB BF: add 32.0 mg of the DODAB powder in 25 mL of a 1 mM NaCl solution in water. Make fresh on the day of the experiment (*see* Notes 1 and 2).
3. 10 mM $\text{Hg}(\text{NO}_3)_2/0.04 \text{ M HNO}_3$ stock solution. Store in a dark vessel to protect this solution from light.
4. 0.01N HCl solution: prepare by diluting standard solution of 0.1N HCl tenfold (*see* Note 3).

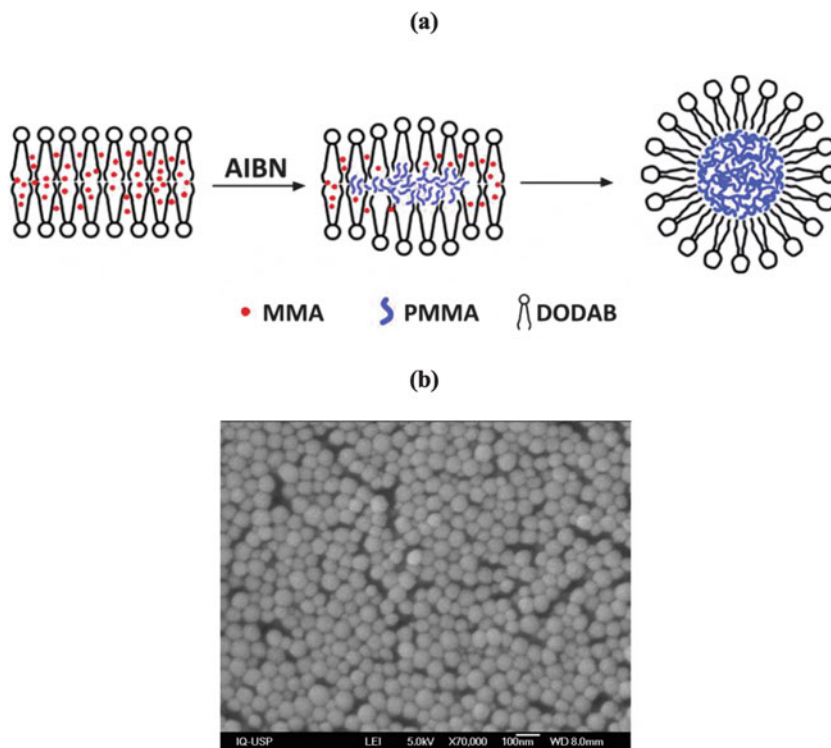


Fig. 3 (a) Scheme illustrating the polymerization of methyl methacrylate (MMA) in the presence of DODAB BF using AIBN as initiator. (b) The PMMA/DODAB hybrid NPs in 1 mM NaCl are shown in the scanning electron micrograph. From DLS, in 1 mM NaCl aqueous solution, these NPs exhibited $D_z = 75 \pm 1$ nm, $\zeta = 49 \pm 4$ mV, and $P = 0.037 \pm 0.005$ [14]

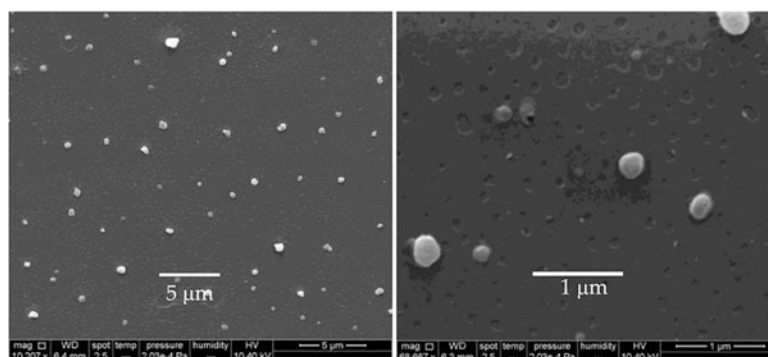


Fig. 4 Scanning electron micrographs of PDDA/OVA NPs under low and high magnification. NPs were obtained at 0.01 mg/mL PDDA and 0.1 mg/mL OVA in pure water. The mean diameter (D) of dry NPs evaluated from the micrographs using the ImageJ software was 234 ± 42 nm. The same NPs dispersion evaluated by DLS in pure water yielded $D_z = 170 \pm 4$ nm, $\zeta = 30 \pm 2$ mV, and $P = 0.11 \pm 0.01$ [13]

5. 1 mM $\text{Hg}(\text{NO}_3)_2$ in 0.04 M HNO_3 : make 1:10 dilution of 10 mM $\text{Hg}(\text{NO}_3)_2$ in 0.04 M HNO_3 (*see Note 4*).
6. 0.01 mg/mL diphenylcarbazone ethanolic solution: dissolve 50 μg of diphenylcarbazone in 5 mL ethanol (*see Note 5*).
7. Macrotip probe powered by an ultrasound source at a nominal output of 90 W (*see Note 6*).
8. High speed refrigerated centrifuge capable of $20,000 \times g$, e.g., Model SCR20B.
(Hitachi) equipped with a RPR20-2-3079 rotor (*see Note 7*).
9. DLS and Zeta-potential Analyzer for particle sizing, zeta-potential analysis, and determination of polydispersity (*see Notes 8 and 9*). Cuvettes with four transparent faces for DLS instrument.

2.2 Preparation and Characterization of PSS/DODAB NPs

1. 5.97×10^{13} particles/mL PSS dispersion of polymeric particles (Interfacial Dynamics Corporation) with nominal diameters around 140 nm (*see Note 10*).
2. DODAB BF at 2 mM DODAB prepared as in the protocol 3.1 coming in Methods.
3. Combine PSS NPs and DODAB BF in the following order:
 - (i) 0.2 mL of the stock PSS dispersion.
 - (ii) 2.5 mL of the 2 mM DODAB BF dispersion.
 - (iii) 2.3 mL of 1 mM NaCl solution.

Allow the components to interact for 1 h at 25 °C (*see Note 11*).

4. DLS and Zeta-potential Analyzer for particle sizing, zeta-potential analysis, and determination of polydispersity (*see again Notes 8 and 9*). Cuvettes with four transparent faces for DLS instrument.
5. High-speed refrigerated centrifuge capable of $20,000 \times g$, e.g., Model SCR20B.
(Hitachi) equipped with a RPR20-2-3079 rotor.
6. Sonicator macroprobe (1 cm diameter).

2.3 Preparation and Characterization of PMMA/DODAB NPs

2.3.1 Preparation of DODAB BF Dispersion at 10 mM in 1 mM NaCl

1. 1 mM NaCl solution in water.
2. 10 mM DODAB BF dispersion: add 160.0 mg of the DODAB powder in 25 mL of a 1 mM NaCl solution in water. Make fresh on the day of the experiment (*see again Notes 1 and 2*).
3. 10 mM $\text{Hg}(\text{NO}_3)_2/0.04$ M HNO_3 stock solution. Store in a dark vessel to protect this solution from light.
4. 0.01N HCl solution: Prepare by diluting standard solution of 0.1N HCl tenfold (*see again Note 3*).

5. 1 mM $\text{Hg}(\text{NO}_3)_2$ in 0.04 M HNO_3 : make 1:10 dilution of 10 mM $\text{Hg}(\text{NO}_3)_2$ in 0.04 M HNO_3 (*see again Note 4*).
6. 0.01 mg/mL diphenylcarbazone ethanolic solution: dissolve 50 μg of diphenylcarbazone in 5 mL ethanol (*see again Note 5*).
7. Macrotip probe powered by an ultrasound source at a nominal output of 90 W (*see again Note 6*).
8. High-speed refrigerated centrifuge capable of $20,000 \times g$, e.g., Model SCR20B.
(Hitachi) equipped with a RPR20-2-3079 rotor (*see again Note 7*).
9. DLS and Zeta-potential Analyzer for particle sizing, zeta-potential analysis and determination of polydispersity (*see again Notes 8 and 9*). Cuvettes with four transparent faces for DLS instrument.

2.3.2 *Synthesis of PMMA/DODAB NPs by Emulsion Polymerization*

1. 1 mM NaCl solution in water.
2. MMA at least 99% pure.
3. Initiator AIBN powder.
4. Glass assay tube of 28 mL closed with a cap.
5. Vortex.
6. Magnetic stirrer with a hot plate.
7. Water bath at 80 °C suitable for using with the magnetic stirrer.
8. Cellulose acetate dialysis membranes with a molecular weight cut-off around 12,400 g/mol.
9. DLS and Zeta-potential Analyzer for particle sizing, zeta-potential analysis and determination of polydispersity (*see Notes 8 and 9*). Cuvettes with four transparent faces for DLS instrument.
10. High-speed refrigerated centrifuge capable of $20,000 \times g$, e.g., Model SCR20B.
(Hitachi) equipped with a RPR20-2-3079 rotor (*see again Note 7*).
11. 10 mM $\text{Hg}(\text{NO}_3)_2/0.04$ M HNO_3 stock solution. Store in a dark vessel to protect this solution from light.
12. 0.01N HCl solution: Prepare by diluting standard solution of 0.1N HCl tenfold (*see again Note 3*).
13. 1 mM $\text{Hg}(\text{NO}_3)_2$ in 0.04 M HNO_3 : make 1:10 dilution of 10 mM $\text{Hg}(\text{NO}_3)_2$ in 0.04 M HNO_3 (*see again Note 4*).
14. 0.01 mg/mL diphenylcarbazone ethanolic solution: dissolve 50 μg of diphenylcarbazone in 5 mL ethanol (*see again Note 5*).

2.4 Preparation and Characterization of PDDA/OVA NPs.

1. Stock solution of PDDA 10 mg/mL: Dilute 0.262 mL of PDDA and complete up to 10 mL of Milli Q water, mix thoroughly on vortex. Store solution at room temperature.
2. Stock solution of OVA 10 mg/mL: Dissolve 10 mg of OVA in 1 mL of Milli Q water, stir the mixture at low rpm and room temperature during 30 min. OVA stock solution must be prepared on the day of the experiment.
3. Vortex.
4. DLS and Zeta-potential Analyzer for particle sizing, zeta-potential analysis and determination of polydispersity (*see* **Notes 8** and **9**). Cuvettes for DLS instrument.
5. Stirrer.

3 Methods

3.1 Preparation and Characterization of DODAB BF

1. To make a dispersion of DODAB BF, sonicate the freshly prepared DODAB/1 mM NaCl solution with a macrotip probe at a nominal output of 90 W for 20 min. Maintain the temperature at 60 °C.
2. Centrifuge the dispersion for 60 min at $10,000 \times g$ and 4 °C in order to eliminate residual titanium particles ejected from the macrotip probe. Discard the dark titanium pellet by withdrawing the supernatant of DODAB BF with a Pasteur pipette.
3. Determine DODAB analytical concentrations in the dispersion by halide microtitration using the analytical solution of Hg(NO₃)₂ and two or three droplets of the ethanol diphenyl carbazone solution as indicator of endpoint.
4. Adjust DODAB concentration in the DODAB BF dispersion to 2 mM. Aliquots of this dispersion will be used for combination with antigen.

3.2 Preparation and Characterization of PSS/DODAB NPs

1. To prepare the DODAB BF dispersions, sonicate DODAB powder in the 1 mM NaCl water solution with a macrotip for 15 min (80–90 mW).
2. To precipitate titanium residues ejected from the macrotip, centrifuge the sonicated DODAB dispersion at $10,000 \times g$ in a refrigerated centrifuge for 40 min at 15 °C.
3. Determine DODAB and NaCl analytical concentrations in the dispersion by halide microtitration using the analytical solution of Hg(NO₃)₂ and two or three droplets of the ethanolic diphenylcarbazon solution as indicator of endpoint.
4. Combine PSS NPs and DODAB BF in the following order:

Table 1

Physical properties of cationic nanostructured adjuvants dispersed in water as determined by DLS. Mean hydrodynamic diameter (Dz), zeta-potential (ζ), and polydispersity (P) of the adjuvant dispersions were determined by DLS following Subheading 3.1–3.4

Subheading	Adjuvant	Dz (nm)	ζ (mV)	P	References
3.1	DODAB BF	73 ± 4	41 ± 3	0.29 ± 0.03	[5]
3.2	PSS/DODAB	149 ± 1	30 ± 2	0.05 ± 0.01	[11]
3.3	PMMA/DODAB	75 ± 1	49 ± 5	0.04 ± 0.01	[14]
3.4	PDDA/OVA	170 ± 4	30 ± 2	0.11 ± 0.01	[13]

- (i) 0.2 mL of the stock PSS dispersion.
 - (ii) 2.5 mL of the 2 mM DODAB BF dispersion.
 - (iii) 2.3 mL of 1 mM NaCl solution.
5. Allow the components to interact for 1 h at 25 °C (*see Note 11*).
 6. Determine zeta-average diameters, zeta-potentials and polydispersities for all dispersions using DLS instrument. Follow manufacturer procedures to conduct DLS measurements. Results should be very similar to those in Table 1 (*see Note 12*).

3.3 Preparation and Characterization of PMMA/DODAB NPs

3.3.1 Preparation of DODAB BF Dispersion at 10 mM in 1 mM NaCl

1. To make a dispersion of DODAB BF, sonicate the freshly prepared DODAB/1 mM NaCl solution with a macrotip probe at a nominal output of 90 W for 20 min. Maintain the temperature at 60 °C.
2. Centrifuge the dispersion for 60 min at 10,000 × g and 4 °C in order to eliminate residual titanium particles ejected from the macrotip probe. Discard the dark titanium pellet by withdrawing the supernatant of DODAB BF with a Pasteur pipette.
3. Determine DODAB analytical concentrations in the dispersion by halide microtitration using the analytical solution of Hg (NO₃)₂ and two or three droplets of the ethanol diphenyl carbazone solution as indicator of endpoint.

3.3.2 Synthesis of PMMA/DODAB NPs by Emulsion Polymerization

1. Prepare a heating system using the magnetic stirrer with a hot plate and a magnet into the water bath at 80 °C.
2. In the glass assay tube of 28 mL with a cap, transfer 2 mL of 10 mM DODAB BF dispersion and 7.57 mL of 1 mM NaCl solution in water.
3. Apply a flow of nitrogen gas for 1 min to the contents of the tube in order to eliminate oxygen.

4. Add 0.43 mL of MMA 99%, close the tube with a cap and mix using vortex for 30 s.
5. Add 3.6 mg of AIBN powder and vortex again.
6. Place the assay tube containing the reaction mixture in the water bath and keep it at 80 °C for 1 h, vortexing every 2 min.
7. Withdraw the assay tube containing the reaction mixture from the water bath and allow the reaction system to reach room temperature.
8. Transfer the contents of the tube in the dialysis bag and purify by dialysis against 2 L of ultrapure water (3×) for 24 h.
9. For particle characterization after dialysis, use dilutions of 20–30 times of the original dispersions.
10. Transfer 2 mL of the diluted PMMA/DODAB dispersion into a DLS cuvette for determining its zeta-average diameter and zeta-potential. Follow manufacturer procedures to conduct DLS measurements. These should yield small cationic particles with zeta-potential around +49 mV and the diameter around 75 nm.
11. Centrifuge the original dispersion for 60 min at $10,000 \times g$ and 4 °C before the analytical determination of the DODAB concentration in the supernatant by halide microtitration. Withdraw the supernatant with a Pasteur pipette for determining DODAB concentration.
12. Determine DODAB concentration in the PMMA/DODAB NPs by halide microtitration of the supernatant, using the analytical solution of $\text{Hg}(\text{NO}_3)_2$ and two or three droplets of the ethanol diphenyl carbazone solution as indicator of endpoint.

3.4 Preparation and Characterization of PDDA/OVA NPs

1. To prepare 10 mL of PDDA/OVA NPs, combine the stock solutions as follows:
 - (i) In a tube containing 9.89 mL of Milli Q water, add 0.01 mL of PDDA stock solution and vortex thoroughly.
 - (ii) Into the solution obtained in (i), add 0.1 mL of stock solution of OVA and vortex for 30 s (*see Note 13*).
2. Transfer 2 mL of the PDDA/OVA dispersion into a DLS cuvette for determining zeta-average diameter and zeta-potential of the dispersion. Follow manufacturer procedures to conduct DLS measurements. These should yield small cationic particles with zeta-potential around 30 mV and the diameter around 170 nm.

4 Notes

1. This should yield 2 mM DODAB final concentration.
2. DODAB dispersions should be always prepared above the mean gel-to-liquid crystalline phase transition temperature of the DODAB bilayer that is around 45 °C [40]. Thus, DODAB should be dispersed in 1 mM NaCl aqueous solution always at temperatures above 50 °C. Sonication will raise the temperature above 50 °C, so further heating the sample is not required. Other important property to note is the low stability of the BFs in moderate to high ionic strength solutions. Above 10 mM concentrations of monovalent salts, DODAB BFs will fuse to yield larger assemblies [18].
3. This solution will be used for titrating the previous solution and determining its analytical $\text{Hg}(\text{NO}_3)_2$ concentration.
4. This solution will be used to microtitrate bromide (in DODAB dispersions) or chloride (in 1 mM NaCl solution). Details on the microtitration procedure where the mercury cation forms a complex with halides can be found on refs. 41–43.
5. This solution allows determining the endpoint of the halide microtitration where the indicator changes color at the end point.
6. This will disperse the DODAB powder in the 1 mM NaCl solution for 20 min to yield the BFs dispersion.
7. This will centrifuge the sonicated DODAB dispersion aiming at precipitation of titanium microparticles ejected from the tip of the macro-probe.
8. We used a ZetaPlus Zeta-potential Analyzer (Brookhaven Instruments Corporation, Holtsville, NY) equipped with a 677-nm laser and dynamic light scattering at 90°.
9. Mean hydrodynamic diameters should be obtained by fitting intensity of light scattered to log-normal size distributions which do not discriminate between one, two, or more different populations and consider all scattering particles as belonging to one single Gaussian population. On the other hand, for the size distribution data, fitting should be done using the non-negatively constrained least squares (NNLS) algorithm available from the light scattering apparatus, which is a model-independent technique allowing to achieve multimodal distributions [44]. ζ is usually determined from electrophoretic mobility μ in 1 mM NaCl and the Smoluchowski's equation: $\zeta = \mu\eta/\epsilon$, where η is the medium viscosity and ϵ the medium dielectric constant: this is also provided by the apparatus software. The electrode of the apparatus should be used only over a

low range of ionic strength (0–5 mM monovalent salt). High conductivities can damage the electrode.

10. The PSS original particles purchased from Interfacial Dynamics Corporation have their particle number density, size, surface charge density, and polydispersity specified in a specifications sheet provided by the supplier. In this protocol, the stock dispersion of anionic PSS NPs, nominal mean diameter from scanning electron micrographs of $0.137 \pm 0.003 \mu\text{m}$, $415,124 \text{ cm}^2/\text{g}$ of specific surface area (SSA), surface charge density of $0.79 \mu\text{C}/\text{cm}^2$, and $-43 \pm 3 \text{ mV}$ of zeta-potential were obtained from the stock dispersion containing 5.97×10^{13} particles/mL. This stock dispersion can be further diluted in 1 mM NaCl solution in order to obtain the final desired NP concentration. PSS and DODAB BF should be prepared in 1 mM NaCl because this represents an adequate ionic strength to assemble DODAB BFs as a single bilayer onto PSS particles by fusion of adsorbed and adjacent BFs [31].
11. The knowledge of the accurate concentrations of DODAB in dispersion should allow calculation of the DODAB amount required to cover all particles with one bilayer:
The final concentrations are 2.4×10^{12} particles/mL and 1 mM DODAB. This DODAB concentration is approximately the concentration required to allow coverage of each particle with a DODAB bilayer [11].
12. Note that upon coverage of each particle with a bilayer, the zeta-average diameter should increase by the equivalent of two bilayer thicknesses (one bilayer thickness is 4–5 nm).
13. Upon mixing PDDA and OVA in solution, formation of NPs is associated with the appearance of turbidity in the dispersion due to the light scattered by them.

Acknowledgments

This work was supported by grant 2019/17685-2, São Paulo Research Foundation (FAPESP) and 302758/2019-4, Conselho Nacional de Pesquisa e Desenvolvimento Tecnológico (CNPq). Y. P.-B is the recipient of a PhD fellowship from CNPq.

References

1. Xiang SD, Scholzen A, Minigo G, David C et al (2006) Pathogen recognition and development of particulate vaccines: does size matter? *Methods* 40:1–9. <https://doi.org/10.1016/j.ymeth.2006.05.016>
2. Manolova V, Flace A, Bauer M et al (2008) NPs target distinct dendritic cell populations according to their size. *Eur J Immunol* 38:1404–1413. <https://doi.org/10.1002/eji.200737984>

3. Tsuruta LR, Quintilio W, Costa MH et al (1997) Interactions between cationic liposomes and an antigenic protein: the physical chemistry of the immunoadjuvant action. *J Lipid Res* 38:2003–2011. <https://www.jlr.org/content/38/10/2003.long>
4. Carmona-Ribeiro AM (2006) Lipid bilayer fragments and disks in drug delivery. *Curr Med Chem* 13:1359–1370. <https://doi.org/10.2174/092986706776872925>
5. Lincopan N, Espindola NM, Vaz AJ et al (2009) Novel immunoadjuvants based on cationic lipid: preparation, characterization and activity in vivo. *Vaccine* 27:5760–5771. <https://doi.org/10.1016/j.vaccine.2009.07.066>
6. Rozenfeld JHK, Silva SR, Raneia PA et al (2012) Stable assemblies of cationic bilayer fragments and CpG oligonucleotide with enhanced immunoadjuvant activity in vivo. *J Control Release* 160:367–373. <https://doi.org/10.1016/j.jconrel.2011.10.017>
7. Lincopan N, Espindola NM, Vaz AJ et al (2007) Cationic supported lipid bilayers for antigen presentation. *Int J Pharm* 340:216–222. <https://doi.org/10.1016/j.ijpharm.2007.03.014>
8. Naves AF, Palombo RR, Carrasco LDM et al (2013) Antimicrobial particles from emulsion polymerization of methyl methacrylate in the presence of quaternary ammonium surfactants. *Langmuir* 29:9677–9684. <https://doi.org/10.1021/la401527j>
9. Carmona-Ribeiro AM (2014) Cationic nanostructures for vaccines. In: Guy Huynh Thien Duc GHT (ed) *Immune response activation*, 1st edn. IntechOpen, Rijeka, pp 1–45. <https://www.intechopen.com/books/immune-response-activation/cationic-nanostructures-for-vaccines>
10. Sanches LM, Petri DFS, de Melo Carrasco LD et al (2015) The antimicrobial activity of free and immobilized poly (diallyldimethylammonium) chloride in NPs of poly (methylmethacrylate). *J Nanobiotechnol* 13:58. <https://jnanobiotechnology.biomedcentral.com/articles/10.1186/s12951-015-0123-3>
11. Xavier GRS, Carmona-Ribeiro AM (2017) Cationic biomimetic particles of polystyrene/cationic bilayer/gramicidin for optimal bactericidal activity. *Nanomaterials* 7:12. <https://doi.org/10.3390/nano7120422>
12. Carmona-Ribeiro AM (2017) Nanomaterials based on lipids for vaccine development. In: Skwarczynski M, Toth I (eds) *Micro- and nano-technology in vaccine development*. Elsevier, Oxford, pp 241–257. <https://doi.org/10.1016/B978-0-323-39981-4.00013-0>
13. Perez-Betancourt Y, Tavora BCLF, Colombini M et al (2020) Simple nanoparticles from the assembly of cationic polymer and antigen as immunoadjuvants. *Vaccine* 8:105. <https://doi.org/10.3390/vaccines8010105>
14. Mathiazzi BI, Carmona-Ribeiro AM (2020) Hybrid NPs of poly (methyl methacrylate) and antimicrobial quaternary ammonium surfactants. *Pharmaceutics* 12:340. <https://doi.org/10.3390/pharmaceutics12040340>
15. Carmona-Ribeiro AM, Pérez-Betancourt Y (2020) Cationic nanostructures for vaccines design. *Biomimetics* 5:32. <https://doi.org/10.3390/biomimetics5030032>
16. Ribeiro AMC, Chaimovich H (1983) Preparation and characterization of large dioctadecyldimethylammonium chloride liposomes and comparison with small sonicated vesicles. *Biochim Biophys Acta* 733:172–179. [https://doi.org/10.1016/0005-2736\(83\)90103-7](https://doi.org/10.1016/0005-2736(83)90103-7)
17. Carmona-Ribeiro AM (1992) Synthetic amphiphile vesicles. *Chem Soc Rev* 21:209–214. <https://doi.org/10.1039/CS9922100209>
18. Carmona-Ribeiro AM, Chaimovich H (1986) Salt-induced aggregation and fusion of dioctadecyldimethylammonium chloride and sodium dihexadecylphosphate vesicles. *Biophys J* 50:621–628. [https://doi.org/10.1016/S0006-3495\(86\)83501-9](https://doi.org/10.1016/S0006-3495(86)83501-9)
19. Carvalho LA, Carmona-Ribeiro AM (1998) Interactions between cationic vesicles and serum proteins. *Langmuir* 14:6077–6081. <https://doi.org/10.1021/la980345j>
20. Lincopan N, Carmona-Ribeiro AM (2009) Protein assembly onto cationic supported bilayers. *J Nanosci Nanotechnol* 9:3578–3586. <https://doi.org/10.1166/jnn.2009.NS33>
21. Carvalho CA, Olivares-Ortega C, Soto-Arriaza MA, Carmona-Ribeiro AM (2012) Interaction of gramicidin with DPPC/DODAB bilayer fragments. *Biochim Biophys Acta* 1818:3064–3071. <https://doi.org/10.1016/j.bbame.2012.08.008>
22. Ragioto DAMT, Carrasco LDM, Carmona-Ribeiro AM (2014) Novel gramicidin formulations in cationic lipid as broad-spectrum microbicidal agents. *Int J Nanomedicine* 9:3183–3192. <https://doi.org/10.2147/IJN.S65289>
23. Rozenfeld JHK, Oliveira TR, Lamy MT et al (2011) Interaction of cationic bilayer fragments with a model oligonucleotide. *Biochim Biophys Acta* 1808:649–655. <https://doi.org/10.1016/j.bbame.2010.11.036>

24. Kikuchi IS, Viviani W, Carmona-Ribeiro AM (1999) Nucleotide insertion in cationic bilayers. *J Phys Chem A* 103:8050–8055. <https://doi.org/10.1021/jp9911090>
25. Nantes IL, Correia FM, Faljoni-Alario A et al (2003) Nucleotide conformational change induced by cationic bilayers. *Arch Biochem Biophys* 416:25–30. [https://doi.org/10.1016/S0003-9861\(03\)00280-7](https://doi.org/10.1016/S0003-9861(03)00280-7)
26. Rosa H, Petri DFS, Carmona-Ribeiro AM (2008) Interactions between bacteriophage DNA and cationic biomimetic particles. *J Phys Chem B* 112:16422–16430. <https://doi.org/10.1021/jp806992f>
27. Kikuchi IS, Carmona-Ribeiro AM (2000) Interactions between DNA and synthetic cationic liposomes. *J Phys Chem B* 104:2829–2835. <https://doi.org/10.1021/jp9935891>
28. Andersson M, Hammarstroem L, Edwards K (1995) Effect of bilayer phase transitions on vesicle structure, and its influence on the kinetics of viologen reduction. *J Phys Chem* 99:14531–14538. <https://doi.org/10.1021/j100039a047>
29. Carmona-Ribeiro AM, Midmore BR (1992) Synthetic bilayer adsorption onto polystyrene microspheres. *Langmuir* 8:801–806. <https://doi.org/10.1021/la00039a013>
30. Carmona-Ribeiro AM, de Moraes LM (1999) Interactions between bilayer membranes and latex. *Colloids Surf A Physicochem Eng Asp* 153:355–361. [https://doi.org/10.1016/S0927-7757\(98\)00532-9](https://doi.org/10.1016/S0927-7757(98)00532-9)
31. Pereira EMA, Vieira DB, Carmona-Ribeiro AM (2004) Cationic bilayers on polymeric particles: effect of low NaCl concentration on surface coverage. *J Phys Chem B* 108:11490–11495. <https://doi.org/10.1021/jp060737w>
32. Rapuano R, Carmona-Ribeiro AM (2000) Supported bilayers on silica. *J Colloid Interface Sci* 226:299–307. <https://doi.org/10.1006/jcis.2000.6824>
33. Moura SP, Carmona-Ribeiro AM (2003) Cationic bilayer fragments on silica at low ionic strength: competitive adsorption and colloid stability. *Langmuir* 19:6664–6667. <https://doi.org/10.1021/la034334o>
34. Lincopan N, Santana MR, Faquim-Mauro E et al (2009) Silica-based cationic bilayers as immunoadjuvants. *BMC Biotechnol* 9:5. <https://doi.org/10.1186/1472-6750-9-5>
35. Ribeiro RT, Braga VHA, Carmona-Ribeiro AM (2017) Biomimetic cationic NPs based on silica: optimizing bilayer deposition from lipid films. *Biomimetics* 2:20. <https://doi.org/10.3390/biomimetics2040020>
36. Pereira EMA, Kosaka PM, Rosa H et al (2008) Hybrid materials from intermolecular associations between cationic lipid and polymers. *J Phys Chem B* 112:9301–9310. <https://doi.org/10.1021/jp801297t>
37. Vieira DB, Carmona-Ribeiro AM (2008) Cationic NPs for delivery of amphotericin B: preparation, characterization and activity in vitro. *J Nanobiotechnol* 6:6. <https://doi.org/10.1186/1477-3155-6-6>
38. Melo LD, Mamizuka EM, Carmona-Ribeiro AM (2010) Antimicrobial particles from cationic lipid and polyelectrolytes. *Langmuir* 26:12300–12306. <https://doi.org/10.1021/la101500s>
39. Bohidar H, Dubin PL, Majhi PR et al (2005) Effects of protein-polyelectrolyte affinity and polyelectrolyte molecular weight on dynamic properties of bovine serum albumin-poly(diallyldimethylammonium chloride) coacervates. *Biomacromolecules* 6:1573–1585. <https://doi.org/10.1021/bm049174p>
40. Nascimento DB, Rapuano R, Lessa MM et al (1998) Counterion effects on properties of cationic vesicles. *Langmuir* 14:7387–7391. <https://doi.org/10.1021/la980845c>
41. Schales O, Schales SS (1941) A simple and accurate method for the determination of chloride in biological fluids. *J Biol Chem* 140:879–884
42. Carmona-Ribeiro AM (2012) Preparation and characterization of biomimetic nanoparticles for drug delivery. *Methods Mol Biol* 906:283–294. https://doi.org/10.1007/978-1-61779-953-2_22
43. Carmona-Ribeiro AM (2020) Biomimetic lipid polymer nanoparticles for drug delivery. *Methods Mol Biol* 2118:45–60. https://doi.org/10.1007/978-1-0716-0319-2_4
44. Grabowski E, Morrison I (1983) Particle size distribution from analysis of quasi-elastic light scattering data. In: Danecke B (ed) Measurement of suspended particles by quasi-elastic light scattering. Wiley-Interscience, New York, pp 199–236



Chapter 11

Emulsion Adjuvants for Use in Veterinary Vaccines

Rachel Madera, Yulia Burakova, and Jishu Shi

Abstract

The use of emulsion as adjuvants is widely used in veterinary vaccines. Emulsion adjuvants are inexpensive, stable, and relatively easy to prepare into vaccine formulations. Here we describe the preparation of oil-in-water emulsion adjuvant that has been shown to enhance immune responses and protect against diseases in pigs. This emulsion adjuvant and its variations could potentially be used alone or in combination with other adjuvants in veterinary vaccine formulations.

Key words Adjuvants, Antigen, Emulsion adjuvants, Oil-in-water emulsion, Surfactant, Trichosanthin, Saponins

1 Introduction

Emulsions are generated when two immiscible liquids are combined with the use of emulsifiers such as surfactants. Two of commonly used veterinary emulsion adjuvants are water-in-oil (WO) and oil-in-water (OW) emulsions (Fig. 1) [1, 2]. WO adjuvants tend to be more potent than OW adjuvants by inducing robust and long-lasting antibody responses. However, the latter has a better safety profile [3] with lower oil phase ratio (between 15% and 25%). OW emulsions are very fluid and well tolerated and induce strong short-term immune responses and therefore can be safely used for market animals such as pigs. Other important aspects in veterinary vaccines include cost effectiveness, stability, ease of use, storage convenience, and minimal impact on animal growth. Emulsion-based adjuvants embodies these criteria as a major fraction of these vaccines are used each year for livestock protection against infectious diseases. Here we describe the preparation of an OW emulsion adjuvant and its variations. The combination of OW emulsion adjuvant with another adjuvant could potentiate vaccine immunostimulatory effect. We have observed OW emulsion adjuvant to work synergistically with adjuvant Trichosanthin (TCS) [4],

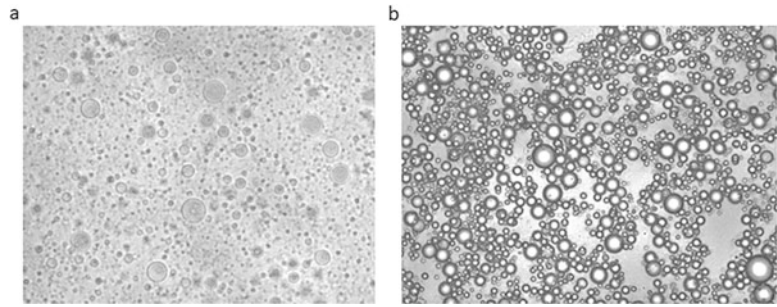


Fig. 1 Microscopic images of water-in-oil (a) and oil-in-water emulsion (b) adjuvants. Vaccines containing water-in-oil emulsion adjuvants entrap antigen (Ag) in the water phase and slowly release the Ag upon breakdown of oil, forming antigen depot at the injection site. On the other hand, oil-in-water emulsion adjuvant do not form Ag depot at the injection site. The oil droplets in aqueous phase of the emulsion induce local inflammatory responses that recruit and activate immune cells

and they lead to increased antibody responses to classical swine fever virus (CSFV), E2 glycoprotein in mice and pigs (Fig. 3a, b). A modified version of this OW emulsion adjuvant prepared with food-grade *Quillaja* saponin extract emulsifier [5] produced high levels of E2-specific antibodies (Fig. 3b) [6].

In novel vaccine formulations, it is imperative to screen for antigen and adjuvant compatibility and its efficacy in animal model systems. New vaccine technologies often get initial application within veterinary medicine [7]. The OW emulsion adjuvant preparations described in this chapter have been successfully tested in mouse and pig models. OW emulsion adjuvanted inactivated swine influenza viruses, and *Mycoplasma hyopneumoniae* vaccines could be safely administered in pigs without adverse reactions [8]. Vaccination and CSFV challenge studies of OW emulsion-based E2 subunit vaccines in pigs have provided safe and effective protection against classical swine fever disease even after single-dose vaccination [9–11].

2 Materials

The use of sterile, single-use or disposable materials such as serological pipettes and conical tubes are needed in vaccine preparation. Laboratory instrument, non-disposable containers, and other materials should be sterilized by autoclave or steam sterilizer (121 °C, 15 psi for at least 15 min). This would ensure the safety of the final product by minimizing the presence of contaminants that could cause adverse reactions. Prepare solutions using ultra-pure water (≥ 18 M Ω ·cm resistivity at 25 °C) and use reagents of high quality. Store all reagents at room temperature unless indicated otherwise.

2.1 Materials

1. Sterile glass containers.
2. Ultrapure water.
3. 70% ethanol.
4. Magnetic stir bar (*see Note 1*).

2.2 Emulsion Components

1. Emulsifier: Ticamulsion A-2010 (*see Note 2*) and *Quillaja* extract Sapnov emulsifier (*see Note 3*).
2. Oil component: Light mineral oil (NF grade) (*see Note 4*).
3. Gentamicin.
4. Combination adjuvant/vaccine additive: Trichosanthin (*see Note 5*).

2.3 Equipment

1. Magnetic stir plate with magnetic stir bar.
2. High-shear laboratory mixer (*see Note 6*).
3. Microfluidizer (*see Note 7*).
4. Vortex mixer.

3 Methods

Perform all procedures at room temperature, in aseptic or hygienic manner to maintain cleanliness of adjuvant preparations.

3.1 Oil-in-Water Emulsion

1. Dissolve Ticamulsion emulsifier in ultrapure water to a final concentration of 7.5 (w/v)% in a sterile glass container. Use a container that is at least three times the total adjuvant volume. This is to ensure enough space for mixing in the succeeding steps (*see Note 8*).
2. Stir mixture using magnetic stir plate. Stirring velocity is not crucial at this point. Depending on container used and volume to be prepared, set the magnetic stir plate at a speed that would optimally dissolve the emulsifier. Cover with parafilm or aluminum foil and let stand stirring overnight.
3. Add light mineral oil to a final concentration of 15 (v/v)%.
4. Mix coarse emulsion at $1062 \times g$ for 15 min using high-shear laboratory mixer (Fig. 2a, *see Note 9*).
5. Run emulsion through microfluidizer for five times at 10,000 psi (Fig. 2b, *see Note 10*).
6. Add 30 μ g/ml gentamicin. Mix thoroughly using vortex mixer.
7. Store oil-in-water emulsion at 4 °C until use (*see Note 11*).
8. Prepare vaccine formulations by simple hand mixing at 1:1 to 3:1 antigen to adjuvant ratio. The vaccine could also be mixed using vortex mixer for 2–3 min (*see Note 12*).

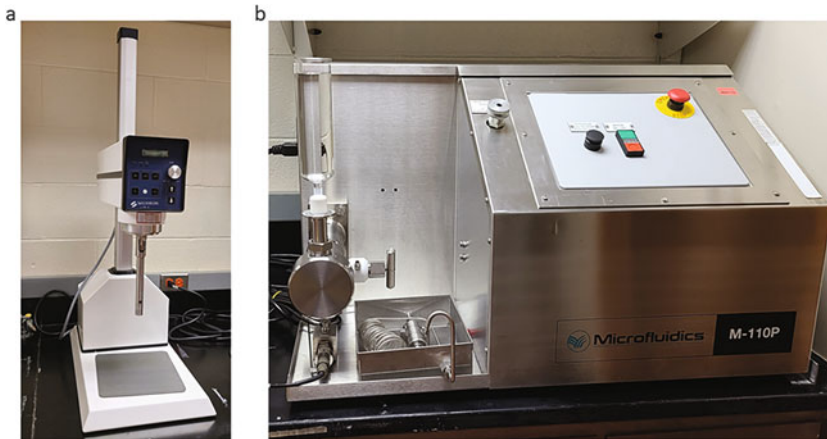


Fig. 2 Equipment for emulsion adjuvant preparation. The high-shear in-line mixer (a) is used to mix coarse oil and water emulsion at 10,000 rpm for 15 min before passing through the microfluidizer (b) for five times with continuous operating pressure at 10,000 psi

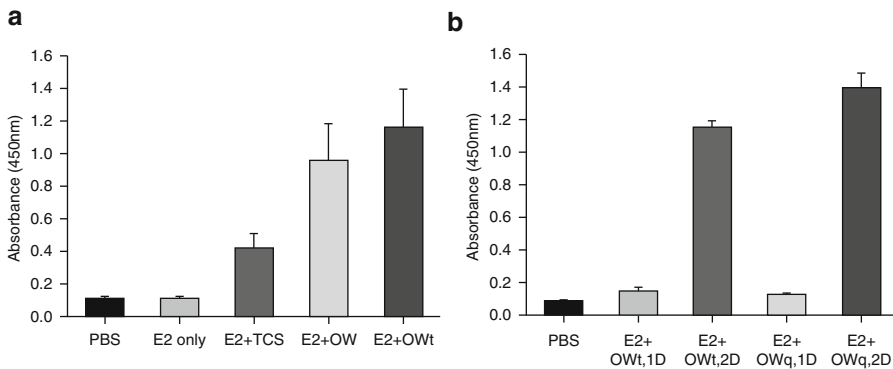


Fig. 3 Adjuvant evaluation in mice (a) and in pigs (b). Animals were immunized with classical swine fever virus E2 glycoprotein (E2) and phosphate-buffered saline (PBS) as negative control. Oil-in-water-based adjuvant (OW) elicited robust E2-specific antibodies as determined by enzyme-linked immunosorbent assay (ELISA). The combination adjuvant (OWt) composed of OW and Trichosanthin (TCS) elicited higher levels of E2-specific antibodies than single adjuvant in mice (a) and then further tested in pigs (b) in single dose (1D) and double vaccine doses (2D). The OW variant with saponin (Owq) also elicited high levels of E2-specific antibodies in pigs (b)

9. Follow recommended dose volumes for common laboratory animals [12].

3.2 Oil-in-Water Emulsion Adjuvant in Combination with Another Adjuvant/Vaccine Additive

1. Prepare oil-in-water emulsion adjuvant as described in Subheading 3.1
2. Add TCS (5–25µg per dose) (see Note 13) to antigen adjuvant mixture.
3. Continue as described in Subheading 3.1, steps 8 and 9.

3.3 Oil-in-Water Emulsion Adjuvant with Food-Grade Saponins

1. Preparation is like as described in Subheading 3.1 with component variations.
2. Dissolve Ticamulsion emulsifier in ultrapure water to a final concentration of 5 (w/v)% in a sterile glass container.
3. Stir overnight with magnetic bar.
4. Add *Quillaja* extract Sapnov emulsifier (*see Note 14*) to a final concentration of 0.5 (v/v)% and invert several times to ensure complete mixing of both emulsifiers in water.
5. Add light mineral oil to a final concentration of 15 (v/v)%.
6. Continue as described in Subheading 3.1, steps 4–8.

4 Notes

1. Sterilize magnetic stir bar by placing it in glass container that will be used for adjuvant preparation before autoclaving.
2. Ticamulsion A-2010 (TIC Gums, White Marsh, MD, USA) is a Gum Arabic plant-derived emulsifier that is commonly used in food processing including beverage, sauces, dressing, ice cream, and frozen desserts.
3. Saponins are naturally occurring triterpene glucoside compounds commonly used in animal and human vaccine research studies [13]. *Quillaja saponaria* Molina tree is a main source of saponins for vaccine adjuvants. Saponin molecules contain both hydrophobic and hydrophilic domains that can stabilize oil-in-water food emulsions [6, 14].
4. Oils commonly used in adjuvants include light mineral oil such as Drakeol V (Penreco, Karns City, PA, USA). Oil can trigger depot generation and allow the reduction of vaccine dose. Light mineral oil also stimulates local inflammation at the injection site that effectively enhance immune response.
5. Trichosanthin (TCS) is from the root tuber of *Trichosanthes kirilowii* used in traditional Chinese medicine. The gene for TCS is cloned into expression vector and protein expressed in commercial *E. coli* expression system [15, 16]. The endotoxin in the purified protein is removed using endotoxin removal spin columns from Pierce Biotechnology, Rockford, IL, USA.
6. We use high-shear laboratory mixer (L5MA Silverson Inc., East Longmeadow, MA, USA) that is suitable for mixing, emulsifying, homogenizing, disintegrating, and dissolving. It is capable to mix in-line with flow rates up to 20 l/min.
7. Microfluidization is an established technique for producing emulsion adjuvant formulations for use in vaccines. The microfluidizer (M110P, Microfluidics, Westwood, MA, USA) we use

could achieve continuous operating pressures up to 30,000 psi for the production of stable nano-dispersions and nano-emulsions.

8. Clean glass beaker or glass Erlenmeyer flask could be used. We find Erlenmeyer flask more adequate when preparing emulsion adjuvants. Care should be taken to avoid spillage during mixing.
9. Clean the high-shear laboratory mixer by running in ultrapure water for at least 5000 rpm for 2–3 min. Wipe with clean paper towel and then run in 70% ethanol at same stirring conditions. Wipe dry and run again in ultrapure water before using the equipment to mix the coarse oil and water emulsion.
10. Prepare the microfluidizer by passing through 2 l of 70% ethanol and 2 l of ultrapure water before use. Add ice to the product heat exchanger cooling coil chamber to cool down sample during processing.
11. The oil-in-water emulsion can be stored at 4 °C for 1 month. Before using in vaccine formulation, visually check for presence of contaminants. It is advisable to use the prepared emulsion adjuvant as fresh as possible.
12. We find 1:1 and 2:1 antigen to adjuvant ratio more effective in pigs [10]. Higher antigen to adjuvant ratio should be used when testing in mice.
13. TCS (~27 kD) should be as purified and concentrated as possible to minimally affect the total volume of prepared vaccine formulation. We have used 10–30 mg/ml concentration of purified TCS in our vaccine preparations. The final concentration of TCS in vaccine formulation should be determined in preliminary studies.
14. We use 65% saponin content *Quillaja* water extract Sapnov emulsifier (Naturix Inc., Chicago, IL, USA). Sapnov emulsifier is employed for emulsion stabilization as it is used as foaming agent in beverages and emulsifier in food.

Acknowledgments

This research is supported by awards from the National Bio and Agro-Defense Facility Transition Fund, the USDA National Institute of Food and Agriculture, Hatch-Multistate project (grant number 1021491), and USDA ARS Non-Assistance Cooperative Agreements (grant numbers 58-8064-8-011, 58-8064-9-007, 58-3020-9-020, 59-0208-9-222).

References

1. Aucouturier J, Dupuis L, Ganne V (2001) Adjuvants designed for veterinary and human vaccines. *Vaccine* 19:2666–2672
2. Burakova Y, Madera R, McVey S et al (2018) Adjuvants for animal vaccines. *Viral Immunol* 31:11–22
3. Shi S, Zhu H, Xia X et al (2019) Vaccine adjuvants: understanding the structure and mechanism of adjuvanticity. *Vaccine* 37:3167–3178
4. Wang Y, Mao K, Sun S et al (2009) Trichosanthin functions as th2-type adjuvant in induction of allergic airway inflammation. *Cell Res* 19:962–972
5. Silveira F, Cibulski SP, Varela AP et al (2011) Quillaja brasiliensis saponins are less toxic than Quil A and have similar properties when used as an adjuvant for a viral antigen preparation. *Vaccine* 29:9177–9182
6. Burakova Y, Madera R, Wang L et al (2018) Food-grade saponin extract as an emulsifier and immunostimulant in emulsion-based subunit vaccine for pigs. *J Immunol Res* 2018:8979838
7. Francis MJ (2018) Recent advances in vaccine technologies. *Vet Clin North Am Small Anim Pract* 48:231–241
8. Galliher-Beckley A, Pappan LK, Madera R et al (2015) Characterization of a novel oil-in-water emulsion adjuvant for swine influenza virus and *Mycoplasma hyopneumoniae* vaccines. *Vaccine* 33:2903–2908
9. Madera R, Gong W, Wang L et al (2016) Pigs immunized with a novel E2 subunit vaccine are protected from subgenotype heterologous classical swine fever virus challenge. *BMC Vet Res* 12:1–10
10. Madera R, Wang L, Gong W et al (2018) Toward the development of a one-dose classical swine fever subunit vaccine: antigen titration, immunity onset, and duration of immunity. *J Vet Sci* 19:393–405
11. Laughlin RC, Madera R, Peres Y et al (2019) Plant-made E2 glycoprotein single-dose vaccine protects pigs against classical swine fever. *Plant Biotechnol J* 17:410–420
12. IQ Consortium (2018) Recommended dose volumes for common laboratory animals. *IQ3Rs Leadersh Gr* 1:1–4
13. Marciani DJ (2018) Elucidating the mechanisms of action of saponin-derived adjuvants. *Trends Pharmacol Sci* 39:573–585
14. Yang Y, Leser ME, Sher AA, McClements DJ (2013) Formation and stability of emulsions using a natural small molecule surfactant: Quillaja saponin (Q-Naturale®). *Food Hydrocoll* 30:589–596
15. Sivashanmugam A, Murray V, Cui C et al (2009) Practical protocols for production of very high yields of recombinant proteins using *Escherichia coli*. *Protein Sci* 18:936–948
16. Studier FW (2014) Stable expression clones and auto-induction for protein production in *E. coli*. *Methods Mol Biol* 1091:17–32



Generation of a Liposomal Vaccine Adjuvant Based on Sulfated S-Lactosylarchaeol (SLA) Glycolipids

Bassel Akache, Yimei Jia, Vandana Chandan, Lise Deschatelets, and Michael J. McCluskie

Abstract

Vaccine formulations utilize adjuvants to enhance the level and breadth of the immune response to a target antigen. Liposomes composed of sulfated S-lactosylarchaeol (SLA) glycolipids can induce strong humoral and cell-mediated antigen-specific immune responses to co-administered antigens in mice. This has been demonstrated with a variety of protein antigens, where the protein is either encapsulated within or simply admixed with the archaeal liposomes (archaeosomes). In this process, a dried film of SLA glycolipid is hydrated in water or antigen solution to generate a large multilamellar (ML) liposomal suspension which is then size reduced by sonication to form unilamellar vesicles (UL) with a narrower size distribution. Herein, we describe the generation of liposomes based on the archaeal-based lipid SLA for use as an adjuvant in vaccine formulations.

Key words Vaccine, Liposome, Archaeosome, Glycolipid, Sulfated lactosyl archaeol

1 Introduction

In efforts to increase vaccine safety, most novel vaccine formulations no longer rely on the use of live attenuated disease pathogens. Instead, most novel vaccines consist of pathogen subunits (target protein or carbohydrate) formulated with an adjuvant designed to enhance the immune response to the vaccine antigen [1, 2]. While multiple vaccine adjuvants (e.g., aluminum salts, squalene-based lipid oil-in-water emulsions) are being used in licensed vaccines, they may not be suitable for novel candidate vaccines due to their inability to generate sufficiently strong or balanced (cellular vs. humoral immunity) immune responses when formulated with antigens of interest. Safety profile of a vaccine adjuvant in the target population (e.g., infant vs. adult) is also an important factor to consider when developing a novel vaccine formulation [3].

Liposomes have been utilized as delivery vehicles due to their ability to incorporate various types of payloads, including vaccine antigens, and deliver them efficiently to the interior of cells. Archaeosomes are liposomes composed of archaeal type ether lipids, which are thought to offer advantages over conventional ester lipid-based liposomes such as increased stability/lower permeability [4, 5]. This is due to adaptations found uniquely in archaeal lipids, namely the presence of (1) ether instead of the ester linkages found in eukaryotic and bacterial cells between the glycerol backbone and the lipid tails and (2) lipid tails named phytanyl chains which are composed of repeating branched 5-carbon repeating units [6]. These characteristics are thought to allow archaea to survive in the harsh environments (i.e., high temperature, high salt) where they are found.

Archaeosomes, whether constituted of total polar lipids isolated directly from archaea or semi-synthetic glycolipids, where an archaeol core is first isolated from total polar lipids and then a synthetic polar head group added, are able to induce strong immune responses specific to an entrapped antigen [5, 7–9]. However, the antigen entrapment efficiency can be low (e.g., 5–10%), the formulation process is cumbersome, and there can be variations in lipid content depending on the chemical nature of the antigen used. We have recently developed an archaeosome formulation based on a single charged glycolipid, sulfated lactosyl archaeol, which can be simply admixed with antigen, thereby greatly simplifying the formulation process, reducing antigen loss during formulation, normalizing the administered SLA dose while giving equivalent immune responses to an encapsulated antigen formulation [10]. SLA-based formulations when paired with the proper antigen, whether entrapped or admixed, have also been shown to be efficacious in various challenge models including viral influenza and tumor challenge [11, 12]. Herein, using ovalbumin as a model antigen, we describe methods to prepare SLA-based archaeosome vaccine formulations to be used with either entrapped or admixed antigen (Fig. 1). Dried lipid films are hydrated in solution in the absence or presence of antigen to generate empty and antigen-containing liposomes, respectively. Sonication is then used to generate smaller, unilamellar and more homogenous archaeosomal vesicles. This method can be adapted for the preparation of other liposome-based formulations.

2 Materials

Ultrapure water and analytical grade reagents should be used to prepare all necessary buffers/solutions. All reagents should be prepared at room temperature and stored as indicated. All glassware

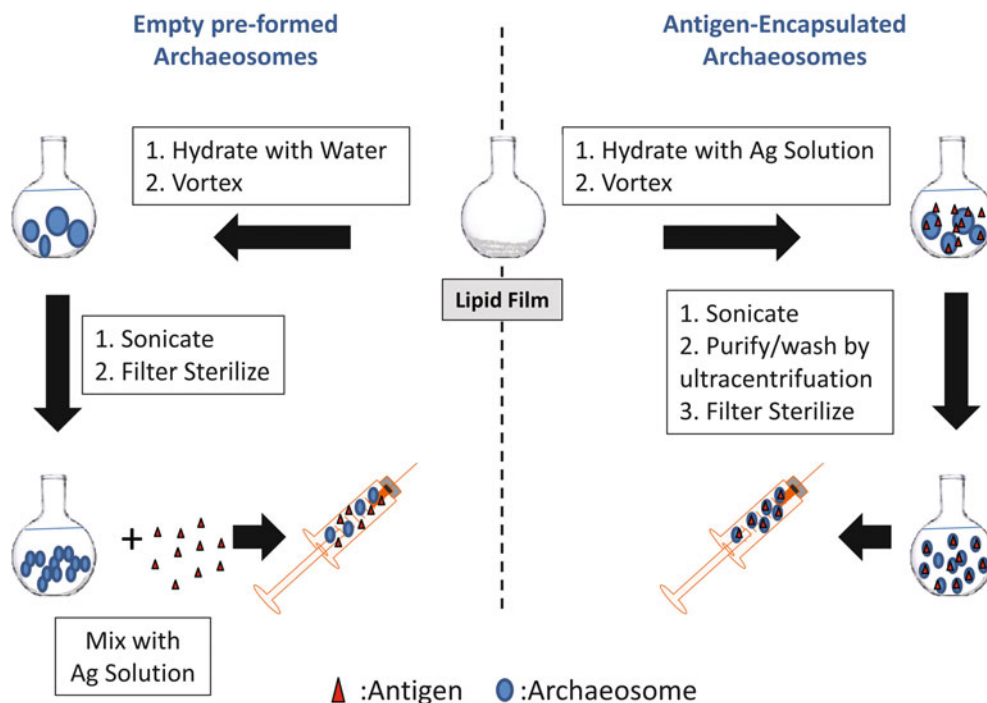


Fig. 1 Schematic overview of experimental procedures

should be pyrogen-free, i.e., pre-baked at 250 °C for 2 h, sterilized by autoclaving at 121 °C for 30 min on gravity cycle and then dried for 30 min.

2.1 Reagents and Solutions

1. Sulfated lactosyl archaeol (SLA; 6-sulfate- β -D-Galp-(1,4)- β -D-Glcp-(1,1)-archaeol): SLA was synthesized as described [13]. SLA lipid is dissolved in analytical grade chloroform and methanol mixture (2:1 v/v) at room temperature and stored at -20 °C until use (*see Note 1*).
2. 10 \times Phosphate-buffered saline (PBS pH: 7.4) without Ca²⁺ and Mg²⁺ (Dulbecco's phosphate-buffered saline).
3. Ovalbumin protein powder (OVA; type VI) (*see Note 2*).
4. Milli-Q™ water (Synergy UV Ultrapure (Type 1) Water system, Millipore Sigma).

Water and PBS can be sterilized by membrane filtration using 0.22- μ m filter unit and stored at 4 °C until use.

2.2 Equipment and Plasticware

1. Glass borosilicate vial with screw cap (autoclavable) (*see Note 3*).
2. 0.22- μ m PVDF sterile syringe-driven filter units (13 mm diameter).
3. 1-mL sterile disposable syringes.

4. 1.5-mL pyrogen-free sterile microcentrifuge tubes.
5. Ultracentrifuge with fixed rotor.
6. Ultracentrifuge plastic tubes with screw top lids.
7. P20, P200, and P1000 pipettes and sterile pipette tips.
8. Sterile Pasteur pipettes.
9. Sonic bath (e.g., Elmasonic P, Elma, Germany).
10. Sonic Dismembrator 550 (ThermoFisher Scientific, Waltham, MA, USA) (*see Note 4*).
11. Freeze Dry system (e.g., FreeZone-Plus, 4.5 liters, Labconco, Kansas City, MO, USA).
12. Magnetic stir plate.
13. Dynamic light scattering Nano ZS apparatus (Malvern Panalytical, Malvern, UK).
14. Polystyrene cuvette (10 × 10 × 45 mm) (*see Note 5*).
15. Disposable folded capillary cell DTS1070 (for Nano ZS-Malvern).
16. Vortex.
17. 37 °C Shaker incubator.
18. Positive displacement pipette.
19. Dry oven (set at 75 °C).
20. Heating blocks (capable of holding 20 mL vials) with gas manifold evaporator (e.g., Reacti-Therm1#TS18821 & Reacti-Vap1#TS-18825, ThermoFisher Scientific).
21. Nitrogen gas (in-house source or via cylinder).
22. Transmitted light microscope with up to ×1000 magnification, microscope slides, and cover slips (*see Note 6*).
23. Micro-analytical balance.
24. SDS-PAGE mini gel system.
25. Pre-stained protein molecular weight standards.

3 Methods

3.1 Preparation of Antigen Solution for Empty Preformed Archaeosomes (to Be Used in Subheading 3.5)

1. Prepare antigen solution depending on dose/amount required. For example, to prepare a 10 mg/mL ovalbumin solution, add 1 mL of sterile 1× PBS (prepared from diluting 10× PBS tenfold in water) to 10 mg of ovalbumin powder to make a 10 mg/mL solution.
2. Insert a magnetic stir bar in solution and stir the mixture on a magnetic stir plate for 2–3 h at 300 rpm at room temperature to ensure antigen is completely dissolved and solution is clear.

3. Filter sterilize the antigen stock solution by loading into a 1-mL syringe and passing through a 0.22- μ m syringe-driven 13-mm PVDF filter unit into a sterile microcentrifuge tube (*see Note 7*).

3.2 Preparation of Antigen Solution for Encapsulation in Archaeosomes (to Be Used in Subheading 3.6)

1. Prepare antigen solution depending on dose/amount required. For example, to prepare a 10 mg/mL ovalbumin solution, add 1 mL of pyrogen-free water to 10 mg of ovalbumin powder to make a 10 mg/mL solution (*see Note 8*).
2. Follow the same procedures as Subheading 3.1, steps 2 and 3.

3.3 Preparation of Dried Lipid Thin Film

1. Prepare desired amount of lipid solution using lipid stock solution. For example, for SLA lipid film, bring SLA lipid solution (*see Subheading 2.1, item 1*) to room temperature and transfer an aliquot from the SLA stock solution containing the desired amount (e.g., 20 mg) of lipid to 20-mL glass vial using positive displacement pipette (*see Notes 9–11*).
2. Place vial containing SLA solution in the 20-mL vial compartment of heating block (temperature set at $\sim 50^\circ\text{C}$) with Reacti-vap evaporator equipped with Teflon needles.
3. Dry SLA lipids under a gentle stream of nitrogen gas (*see Note 12*), until a thin uniform lipid film is formed and no visible solvent remains in the vial (typically this can take from 3 to 6 h) (*see Note 13*).
4. Place dried lipid under vacuum on a freeze dry system or lyophilizer for at least 12 h to remove any traces of organic solvent.

3.4 Preparation of Pre-formed Empty Archaeosome Formulation

1. Hydrate dried lipid film from Subheading 3.3 by adding sterile endotoxin-free water (e.g., 500 μ L for 20 mg SLA) and five to ten glass beads (3 mm diameter). Vortex the lipid suspension until a turbid, viscous, and opaque solution is formed (~ 5 min), indicating liposome formation.
2. Leave liposome solution at room temperature for 2 h and then incubate in a shaker incubator, at $37 \pm 3^\circ\text{C}$, with constant shaking at 300 rpm for 5 h. At regular intervals (e.g., every 1 h), vortex at high speed (up to 2000 rpm) to ensure complete hydration, break apart possible aggregates, and ensure a more homogenous solution.
3. Monitor the formation of liposomes, i.e., multilamellar or large unilamellar vesicles, their shape and size, under microscope under oil immersion at $1000\times$ magnification to ensure hydration is complete (Fig. 2; *see Subheading 3.7, step 1 and Note 14*).

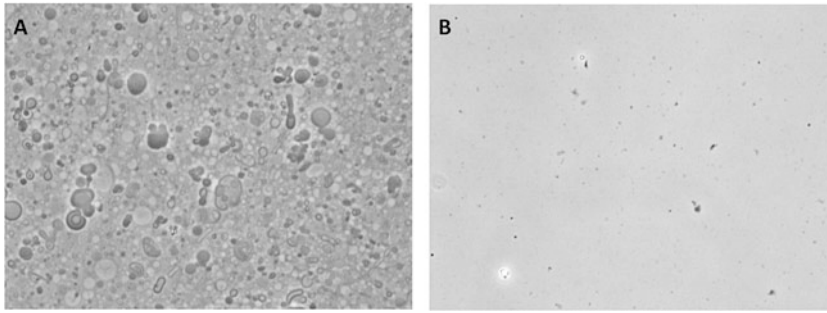


Fig. 2 Liposome appearance under oil immersion microscopy. Images of empty pre-formed archaeosomes acquired under 1000× magnification either following hydration prior to size reduction (a) or following size reduction as described in Subheading 3.4, **step 4** (b). Once target average particle size of ~100 nm is achieved, it will be difficult to observe liposomes using microscopy at this magnification

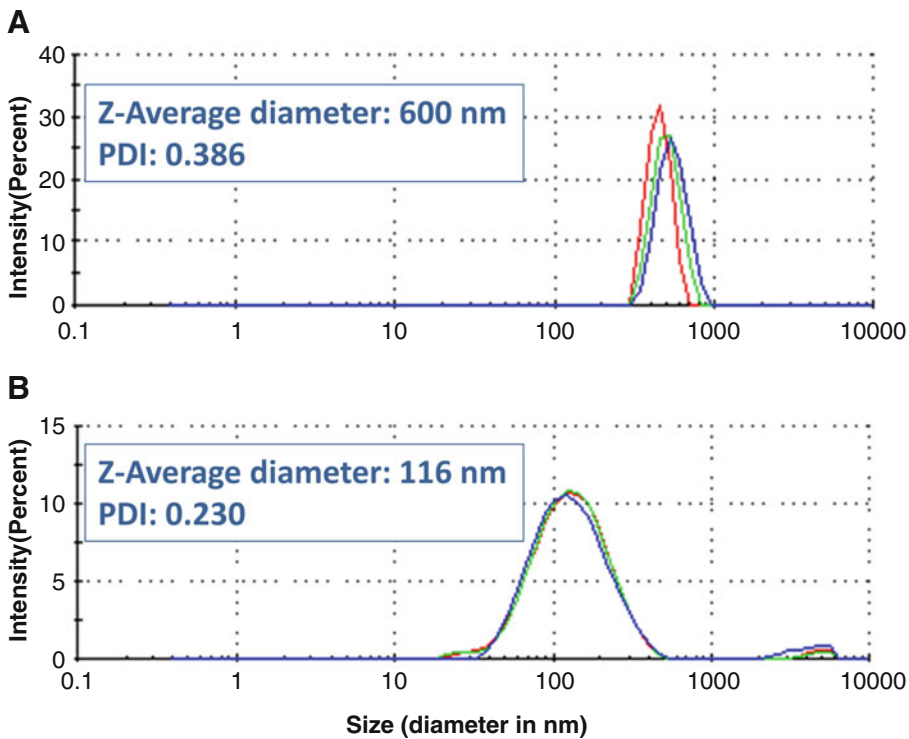


Fig. 3 Liposome particle size and size distribution. Profiles of empty pre-formed archaeosomes as determined by Malvern Zetasizer (Subheading 3.7, **step 2**) either following hydration prior to size reduction (a) or following size reduction as described in Subheading 3.4, **step 4** (b)

4. Measure particle size by using Malvern Zetasizer Nano ZS (Malvern Instruments) (*see* Subheading 3.7, **step 2**) before proceeding to size reduction. At this point, a broad range of particle size distribution is expected with vesicle size (Z-avg) of 300 nm or more (Fig. 3). To reduce the size to small unilamellar vesicles (Z-avg 100 nm ± 25 nm) bath sonication with low

intensity and/or Sonic Dismembrator 550 in bath sonication mode equipped with adjustable intensity can be used. Typically, we use setting #4 for two cycles of 3 min at room temperature with a minimum of 1 min resting between sonication cycles. Sonication is repeated until the desired Z-avg is reached (*see Note 15*). The liposome solution can then be placed at 4 °C overnight in order to allow the lipid bilayer to equilibrate and stabilize.

5. Sterilize the liposome solution by filtering through a 0.22- μ m PVDF filter (syringe-driven 13 mm diameter) into a pyrogen-free sterile glass vial (*see Note 16*). Once the lipids have passed, rinse the filter with 250 μ L of sterile pyrogen-free water and combine into same container. Measure the total volume of sterile filtrate.
6. Quantify SLA lipid in collected filtrate using dry-weight method described in Subheading 3.7, step 5.
7. Add one volume of 10 \times sterile PBS to nine volumes of the liposome solution (already in sterile water) in order to reach a final buffer solution to 1 \times PBS. The final concentration of SLA liposomes is 9/10 of the dry weight obtained above in water.
8. Characterize sterile pre-formed empty archaeosomes for their particle size (Z-avg), surface charge (zeta potential), and particle size distribution (polydispersity index, PDI) values using Malvern Nano ZS (*see Subheading 3.7, steps 2 and 3 for details*).
9. Store glass vial containing sterile SLA empty pre-formed archaeosome suspension at 4 °C.

3.5 Preparation of Vaccine Formulation by Admixing

Transfer aliquot of SLA empty archaeosomes prepared above into 1.5-mL pyrogen-free sterile Eppendorf tube, followed by the addition of previously prepared antigen solution (e.g., 10 mg/mL in 1 \times PBS) to reach desired antigen and archaeosome ratio (*see Note 17*). Mix well by vortexing or pipetting up and down for a few times immediately before immunization.

3.6 Preparation of Antigen-Encapsulated Archaeosome Formulation

1. Hydrate a known amount (e.g., 20 mg) of dried lipids from Subheading 3.3 by adding 1 mL of antigen solution (e.g., 10 mg/mL ovalbumin, *see Subheading 3.2 and Note 18*). Add five to ten glass beads to aid lipid hydration and archaeosome formation.
2. Vortex and incubate the lipid/antigen solution in a shaker incubator, at 37 \pm 3 °C, with constant shaking at 300 rpm for 5 h (*see Subheading 3.4, step 2 for details*).
3. Monitor the formation of liposomes (i.e., multilamellar/large unilamellar vesicles and their shape/size) under microscope under oil immersion at 1000 \times magnification to ensure

hydration is complete as outlined in Subheading 3.4, **step 3**. Reduce the size of the liposomes as outlined in Subheading 3.4, **step 4**. The liposome/antigen solution can then be placed at 4 °C overnight in order to allow the lipid bilayer to equilibrate and stabilize.

4. To remove untrapped antigen, carefully transfer the liposome suspension (1 mL) into 8-mL plastic ultracentrifuge tubes (pre-soaked in 70% ethanol, and then followed by air drying). Fill tube by addition of 7 mL of pyrogen-free sterile water and ultracentrifuge at $223,000 \times g$ for 2 h at 4 °C. Remove the supernatant using a sterile Pasteur pipette taking care not to disturb the pellet. Resuspend the pellet thoroughly in 7 mL of sterile pyrogen-free water by vortexing. Wash the pellet two times and finally resuspend the pellet in (400 µL) of sterile pyrogen-free water (*see Note 19*).
5. Sterilize antigen-encapsulated archaeosome solution by filtering through a 0.22-µm PVDF syringe-driven 13-mm filter unit with 1-mL syringe. Using same syringe, rinse the filter with an additional 100 µL of sterile pyrogen-free water and combine filtrates. Measure the total volume of sterile filtrate.
6. Quantify the amounts of SLA lipid and antigen-encapsulated in the collected filtrate using dry-weight and SDS-PAGE as described in Subheading 3.7, **steps 4** and **5**, respectively. Calculate lipid (SLA) to antigen (OVA-encapsulated) ratio.
7. Add 1 volume of 10× concentrated PBS to 9 volumes of the final formulation in order to bring the final concentration of archaeosome solution to 1× PBS (*see Note 20*).
8. Based on antigen concentration determined in **step 6**, adjust volume with 1× PBS to enable delivery of the desired antigen dose in the required volume (e.g., dilute to 400 µg/mL OVA final concentration to allow immunization with 20 µg OVA in 50 µL volume; *see Note 21*). Store the sterile antigen-encapsulated archaeosome suspension at 4 °C (*see Note 22*).

3.7 Archaeosome Characterization and Analytics

1. *Archaeosome morphology*: Archaeosome morphology should be monitored by transmitted light microscopy (*see Note 23*).
2. *Particle size and size distribution*: Dilute 10 µL of empty or antigen-entrapped archaeosome suspension in 1000 µL of pyrogen-free water in a disposable folded capillary cell DTS1070 (for Nano ZS-Malvern) (*see Note 24*). Measure particle size and size distribution using Malvern Zetasizer or equivalent alternative.
3. *Surface charge*: Using the same sample and capillary cell, next measure zeta potential using Malvern Zetasizer instrument settings.

4. *Quantification of encapsulated antigen (W_{Ag})*: For antigen-entrapped formulation only, entrapped antigen is quantified using densitometry on gel electrophoresis developed bands. Perform sodium dodecyl sulfate polyacrylamide gel electrophoresis (SDS-PAGE) on antigen-encapsulated archaeosomes (*see* Subheading 3.6, step 6) together with antigen calibration standards (e.g., OVA antigen alone). Prepare samples by heating known amounts of antigen (from Subheading 3.2) and a known volume of antigen-encapsulated archaeosome solution from Subheading 3.6, step 6 in SDS reducing buffer, respectively, at 100 °C for 7 min. Load samples and molecular weight standards on 12% pre-cast mini gel. Run gel in Laemmli's buffer system pH 8.3 at 200 V constant voltage at room temperature. Stain gels with Coomassie brilliant blue G250 staining solution [refer to "A Guide to polyacrylamide Gel electrophoresis" from Bio-Rad laboratories (Richmond, CA) for details]. Compare average density of bands from known amount to unknown amount of antigen (OVA) using densitometer. Calculate the final amount of antigen (OVA) present in the encapsulated archaeosome (W_{Ag}) (*see* Note 25).
5. *Lipid quantification by dry-weight method*: Label empty aluminum weighing boats and heat dry them for 12 h in the oven at 70 °C. Cool the boats for 2 min and weigh them (W_1) using a micro-analytical balance. Carefully transfer 10–50 μ L of SLA archaeosome suspension previously prepared in either Subheading 3.4 (W_2) or Subheading 3.6 (W_3) into pre-weighed empty aluminum weighing boats (W_1). Leave the samples to heat-dry for 12 h in the oven at 70 °C. Cool for 2 min and measure the final weight (*see* Notes 26 and 27). All samples are done in triplicates and average calculated.

Average weight of SLA in empty archaeosomes:

$$W_{\text{EmptyArch}} = \overline{W}_2 - \overline{W}_1$$

Average weight of SLA and OVA-encapsulated in archaeosomes: $W_{\text{EncArch}} = \overline{W}_3 - \overline{W}_1$

Average lipid weight $W_{\text{SLA}} = W_{\text{AgEncArch}} - W_{\text{Ag}}$ (from step 4)

$$\text{Antigen to lipid ratio} = W_{\text{Ag}} : W_{\text{SLA}}$$

4 Notes

1. We have selected SLA as a single glycolipid for the production of archaeosomes based on previous studies in our laboratory. Archaeosomes can also be formed using one or multiple glycolipids or using total polar lipids isolated from archaea. We typically use *Halobacterium salinarum* to generate archaeol since it can be grown aerobically and is easier to characterize.

2. We have selected ovalbumin as model antigen for this method; however, method is also appropriate for other protein antigens. Note that the current method is not suitable for DNA or RNA formulations due to the anionic nature of the SLA archaeosomes it produces. This method would need to be modified (e.g., by addition of cationic components) to effectively deliver nucleic acids.
3. We typically use a 20-mL glass vial to ensure formation of a thin lipid film. If too small a vial is used for a large amount of lipid, the lipid film will be thicker and harder to hydrate.
4. Sonic dismembrator should be used in bath sonication mode instead of with the probe sonicator.
5. Other cuvette types can also be used. For example, the capillary cell DTS 1070 can be used for both zeta potential and sizing.
6. We use an Olympus BX51 microscope equipped with camera and imaging software (Q-Imaging) although other microscopes could also be appropriate.
7. Concentration of antigen solution should be measured after filter sterilization to confirm the precise amount of antigen recovered. Antigen solution can either be used immediately or aliquoted and stored for later use depending on stability of individual antigens (e.g., we routinely aliquot ovalbumin solution in 100 μ L aliquots and store at -20 °C for up to 6 months).
8. The hydration of lipids in water (empty archaeosome) or water-based ovalbumin solution (archaeosome with encapsulated antigen) instead of a buffer such as PBS allows for more and more precise determination of lipid concentration using dry-weight method (Subheading 3.7, step 5). PBS is added afterwards to make them more suitable for administration in vivo. For the admixed vaccine formulations, the preparation of antigen in PBS ensures the administered solution maintains vehicle balance once antigen and empty archaeosomes are mixed together.
9. For a large amount of lipid, a round-bottom flask and a rotary evaporator can be used to form lipid thin film.
10. Always bring stock solution of SLA to room temperature before transferring to glass vial for drying, as this will help ensure SLA is completely in solution.
11. To ensure that we have sufficient amounts of lipid at the end of the manufacturing process, we normally include an additional 5 mg of lipid on top of what is required for our experiment [i.e., # of subjects to be immunized * # of immunizations per subject * dose (usually 1 mg/immunization in mice)] to the vial. The additional material will account for loss during

formulation/filtration and allow the user to have sufficient material for analytics. We have previously demonstrated that pre-formed empty archaeosomes are very stable (for up to 6 months at either 4 °C or 37 °C) [14], therefore quantity needed for whole experiment (e.g., prime and boost immunizations) can be prepared in advance and stored until needed.

12. A nitrogen cylinder or continuous nitrogen gas line with secondary pressure regulator attached to the evaporator in a fume hood. Nitrogen gas flow should be very gentle in order to avoid solvents from splashing and leading to an increased risk of lipid loss.
13. The amount of time required for the solvent to evaporate will depend on the quantity and nature of lipid/solvent. If using other lipid/solvent combinations, different conditions may be necessary to ensure proper removal of solvent (e.g., solvent with higher boiling point).
14. Aggregates are nonhydrated lipids or clustered large liposomes that are not spherical in shape and are usually bigger than hydrated single liposomes. If aggregates are observed under microscope, sonicate liposome suspension and reassess under microscope until hydration is complete, and uniform liposomes are observed. At this stage, it is helpful to take a picture using the camera attached to the microscope/Q-Imaging software to document the liposome appearance. Make sure water temperature stays under 40 °C during sonication.
15. When using SLA archaeosomes as a vaccine adjuvant, we typically target an average size of ~100 nm. One advantage of using particles of this size is that they are compatible with filter sterilization. Liposome particle size can influence in vivo distribution and size can be adjusted to suit individual project goals.
16. The size of the liposomes may impact the ease with which the solution can be put through the filter. Filters can be pre-flushed with sterile water to facilitate filtration. After filtration of the archaeosome solution, filters are rinsed with water and filtrate collected to increase yield.
17. For the preparation of vaccine formulations with empty archaeosomes, solutions containing antigen and SLA liposomes are simply admixed to obtain desired volume and concentration. For example, to dose five mice, we usually mix 150 μ L of 40 mg/mL empty SLA archaeosomes with 150 μ L of 800 μ g/mL OVA solution to obtain a final formulation ready for injection into mice (50 μ L injection volume containing 1 mg SLA and 20 μ g OVA). Additional solution on top of the minimum 250 μ L required for injection is prepared to account for any loss during transfer and the syringe's dead

volume. For more immunogenic antigens such as influenza hemagglutinin (HA), we usually immunize with 2 μg of antigen and would therefore prepare an 80 $\mu\text{g}/\text{mL}$ HA solution to mix at a 1:1 ratio with 40 mg/mL empty SLA archaeosomes.

18. In the case of ovalbumin, we use a ratio of 2:1 (w/w) of lipid to antigen to achieve higher entrapment of antigen in archaeosomes. This ratio can vary depending on the chemical nature of antigen being used and its availability.
19. After ultracentrifugation to remove non-entrapped antigen (OVA), make sure pellet gets thoroughly suspended into the water before every step. Supernatants and washes can be collected and re-centrifuged to increase yield.
20. The dilution effect of the archaeosome/antigen dry weight should also be considered as done with the empty archaeosome formulation in Subheading 3.4, step 7.
21. Depending on the entrapment efficiency, the lipid to antigen ratio can differ from batch-to-batch. As such, different amounts of lipid may be administered when basing dosing amounts on antigen concentration. While we have seen strong adjuvant activity with formulations containing 0.1–1 mg of archaeal lipid per dose, it is best to use the same batch of archaeosomes for a particular study or to use batches with similar antigen to lipid ratios.
22. Make sure liposomes are kept sterile. Storage vial should only be opened in laminar flow Bio-hood to maintain sterility of the sample. Lid should be kept tight and sealed with para-film when stored at 4 $^{\circ}\text{C}$. Both empty and encapsulated archaeosomes can be used for up to 6 months after preparation if stored at 4 $^{\circ}\text{C}$ under sterile conditions.
23. Standard microscopy techniques can be used. Using a P20 pipette, transfer 5 μL of archaeosome suspension onto a microscope slide and carefully slide a cover slip avoiding formation of bubbles. First focus the vesicles using high dry (400 \times) lens. Add a drop of immersion oil on the cover slip and carefully move oil immersion lens on the cover slip into drop of immersion oil, to get higher magnification. If possible, image should be captured at this stage using camera mounted on microscope and Q-Imaging software or suitable alternative.
24. Avoid any bubble formation when adding archaeosome solution to the cuvette/cell. Tap cuvette/cell lightly on the bench to get rid of bubbles.
25. While Coomassie Blue staining is compatible with most applications, other staining techniques can also be used (e.g., gels can be stained using SyproRed).

26. To help improve accuracy and consistency of final dry weight measurements of SLA archaeosomes, it is important to keep drying and cooling times constant.
27. The use of other analytical methods to characterize the formulations may be useful. For example, when delivering these formulations *in vivo* in a vaccine setting, it may be important to identify the levels of endotoxin in the solutions. The presence of high levels of endotoxin in the vaccine solutions could impact animal health and the magnitude of the immune response, complicating interpretation of study results. Multiple methods are available based on limulus amoebocyte lysate (LAL) test. Treating archaeosomes with detergent (e.g., <1.5% octaethylene glycol monododecyl ether) prior to conducting the test reduces interference and exposes any potential endotoxins encapsulated within the liposome.

References

1. Di Pasquale A, Preiss S, Tavares Da Silva F et al (2015) Vaccine adjuvants: from 1920 to 2015 and beyond. *Vaccine* 33:320–343
2. McKee AS, Marrack P (2017) Old and new adjuvants. *Curr Opin Immunol* 47:44–51
3. Petrovsky N (2015) Comparative safety of vaccine adjuvants: a summary of current evidence and future needs. *Drug Saf* 38:1059–1074
4. Benvegna T, Lemiègre L, Cammas-Marion S (2009) New generation of liposomes called archaeosomes based on natural or synthetic archaeal lipids as innovative formulations for drug delivery. *Recent Pat Drug Deliv Formul* 3:206–220
5. Haq K, Jia Y, Krishnan L (2016) Archaeal lipid vaccine adjuvants for induction of cell-mediated immunity. *Expert Rev Vaccines* 15:1557–1566
6. Kates M (1978) The phytanyl ether-linked polar lipids and isoprenoid neutral lipids of extremely halophilic bacteria. *Prog Chem Fats Other Lipids* 15:301–342
7. McCluskie MJ, Deschatelets L, Krishnan L (2017) Sulfated archaeal glycolipid archaeosomes as a safe and effective vaccine adjuvant for induction of cell-mediated immunity. *Hum Vaccin Immunother* 13:2772–2779
8. Sprott GD, Yeung A, Dicaire CJ et al (2012) Synthetic archaeosome vaccines containing triglycosylarchaeols can provide additive and long-lasting immune responses that are enhanced by archaetidylserine. *Archaea* 2012:513231
9. Patel GB, Sprott GD (1999) Archaeobacterial ether lipid liposomes (archaeosomes) as novel vaccine and drug delivery systems. *Crit Rev Biotechnol* 19:317–357
10. Jia Y, Akache B, Deschatelets L et al (2019) A comparison of the immune responses induced by antigens in three different archaeosome-based vaccine formulations. *Int J Pharm* 561:187–196
11. Stark FC, Agbayani G, Sandhu JK et al (2019) Simplified admix archaeal glycolipid adjuvanted vaccine and checkpoint inhibitor therapy combination enhances protection from murine melanoma. *Biomedicine* 7:91
12. Stark FC, Akache B, Ponce A et al (2019) Archaeal glycolipid adjuvanted vaccines induce strong influenza-specific immune responses through direct immunization in young and aged mice or through passive maternal immunization. *Vaccine* 37:7108–7116
13. Whitfield DM, Sprott GD, Krishnan L (2016) Sulfated-glycolipids as adjuvants for vaccines. <https://patents.google.com/patent/WO2016004512A1/en>
14. Jia Y, Chandan V, Akache B et al (2021) Assessment of stability of sulphated lactosyl archaeal archaeosomes for use as a vaccine adjuvant. *J Liposome Res* 31(3):1–9



Glucan Particles: Choosing the Appropriate Size to Use as a Vaccine Adjuvant

Mariana Colaço, João Panão Costa, and Olga Borges

Abstract

Beta-glucans are a group of polysaccharides with intrinsic immunostimulatory properties which makes the design of new particulate vaccine adjuvants based on β -glucans very promising. The size of the particles and the antigen loading method, encapsulated into particles or adsorbed on its surface, will influence the toxicological and adjuvanticity properties of the particulate adjuvant. Herein we describe the production of glucan nanoparticles (NPs) with three different sizes, approximately 150 nm, 350 nm, and microparticles as shells (GPs) with approximately 3 μ m. The association of the antigen to the particulate adjuvant is described using model protein antigens. The method can be easily adapted for real protein antigens.

Key words Glucan, Nanoparticles, Microparticles, Antigen loading, Adjuvants, Particle size

1 Introduction

Beta-glucans are found in certain organisms, such as barley, oat, fungi, and yeasts [1]. These group of polysaccharides are recognized by dectin-1, a cell receptor with high levels of expression in certain cells, including macrophages, B-lymphocytes, and dendritic cells. Dectin-1 is a pattern recognition transmembrane signaling receptor involved in innate immune responses against fungal pathogens [2]. Recently, a more complete set of receptors have been revealed to recognize β -glucans, which include complement receptor 3 (CR3) or CD5 as reviewed by Jin et al. [3]. Thus, the effects of glucans on the immune system are mainly derived from the binding to these receptors and depend on the source of the glucan used in the experiments. Some of the observed effects include the induction of production of diverse proinflammatory cytokines including IL-1 β , IL-6, and TNF- α or the least described IL-12. In addition, it is also reported to change immune cells function and shift of Th1/Th2 response bias [3], which explains the interest of these

polymers for the development of particulate vaccine adjuvants. The need to develop new adjuvants is not only for the design of prophylactic vaccines but also for therapeutic vaccines to treat infections, like chronic hepatitis B infection (CHB). In this case, CHB patients might benefit from having a therapeutic vaccine capable of inducing not only the production of interferons (IFNs), but also the IL-12, since it may reverse the induced liver immune tolerance [4].

Gary R. Ostroff's research group has been working for a long time with the porous micrometer-sized shells derived from baker's yeast (*Saccharomyces cerevisiae*) cell walls constituted mainly by β -1,3-D-glucan [5]. After obtaining glucan shells, the antigen is loaded into these microparticles by a process described by the same group [6]. Notwithstanding, in vaccinology, it is often chosen to adsorb the antigen on the surface of the nanoparticulate adjuvants. In this way, it is intended to mimic the microorganism structure, whose more immunogenic proteins are generally found on its surface. The size of particulate adjuvants is certainly an important quality attribute. Hence, our hypothesis is that if the size of glucan nanoparticles is similar to the size of the viruses, the immune system will be more easily deceived and stimulated. We must also be aware that size matters, not only for the adjuvant effect of the particles, but also for its toxicity. So, the cytotoxicity must always be evaluated. Concerning the particles described in this chapter, the immunotoxicological properties were evaluated and reported by our group elsewhere [7].

Our group developed a method to produce glucan particles, smaller than glucan shells, intended to adsorb antigen on its surface. This chapter describes the preparation of the micro size glucan shells (GPS has a size of approximately 3 μ m), a procedure similar to the one described by Mirza [6] with two nanometer glucan nanoparticles, 130 nm and 350 nm.

2 Materials

Prepare all solutions using ultrapure water and analytical grade reagents. Prepare and store all reagents at room temperature (unless indicated otherwise). Diligently follow all waste disposal regulations when disposing waste materials. Follow all safety precautions when handling hazardous reagents.

2.1 Preparation of Polymeric Delivery Systems

2.1.1 Glucan

Nanoparticles of 130 nm

1. P-CURDL; Curdlan contains >99% D-glucose essentially all of which is 1,3- β -linked (e.g., Megazyme, Bray, Ireland).
2. Curdlan solution: 0.025% (w/v) glucan solution in 2% (w/v) sodium hydroxide with 1% (w/v) Tween[®] 80 in water.
3. Acetic acid solution: 8% (v/v) in water.
4. 100-mL glass beaker.
5. Magnetic stirrer and magnetic stir bar.
6. Disposable Pasteur pipette.
7. Vivaspin 20 centrifugal concentrator (MWCO 300 kDa).
8. Centrifuge.
9. pH meter.

2.1.2 Glucan

Nanoparticles of 350 nm

1. P-CURDL; Curdlan contains >99% D-glucose essentially all of which is 1,3- β -linked (e.g., Megazyme, Bray, Ireland).
2. Curdlan solution: 0.1% (w/v) glucan solution in 2% (w/v) sodium hydroxide with 0.1% (w/v) Tween[®] 80 in water.
3. Acetic acid solution: 4% (v/v) in water.
4. 50-mL glass beaker.
5. Magnetic stirrer and magnetic stir bar.
6. Disposable Pasteur pipette.
7. Vivaspin 20 centrifugal concentrator (MWCO 300 kDa).
8. Centrifuge.
9. pH meter.

2.1.3 Glucan Shell Particle

1. Instant dried yeast—*S. cerevisiae*.
2. Sodium hydroxide solution: 1 M solution in water.
3. Hydrochloric acid solution: 12 M and 1 M solutions in water.
4. Isopropanol.
5. Acetone.
6. 600-mL beaker.
7. Water bath.
8. Overhead paddle stirrer.
9. 50-mL conical tubes.
10. Centrifuge.
11. pH meter
12. Vortex mixer.

2.2 Protein Loading

2.2.1 Protein Adsorption to Glucan Nanoparticles

1. Myoglobin from equine skeletal muscle, lysozyme chloride from chicken egg white, and albumin from bovine serum.
2. Rotating mixer.
3. Centrifuge.
4. Bicinchoninic acid (BCA) protein assay kit or other protein quantification kit to measure unbound protein.

2.2.2 Protein Encapsulation into Glucan Shell Particles

1. Myoglobin from equine skeletal muscle, lysozyme chloride from chicken egg white, and albumin from bovine serum.
2. TEN buffer: 2 mM EDTA, 0.15 M NaCl, 50 mM Tris-HCl, pH 8.0.
3. Ribonucleic acid from torula yeast (tRNA).
4. tRNA solution: Dissolve tRNA at 25 mg/mL in TEN buffer, with magnetic stirring at 50 °C. Dilute tRNA 25 mg/mL solution with TEN buffer to obtain a 10 mg/mL solution.
5. Saline solution: 0.9% in water.
6. Centrifuge.
7. Freeze-dryer.
8. Magnetic stirrer and magnetic stir bar.

3 Methods

3.1 Preparation of Polymeric Delivery Systems

3.1.1 Glucan Nanoparticles of 130 nm

Carry out all procedures at room temperature unless otherwise specified.

1. Dissolve curdlan in 2% (w/v) sodium hydroxide with 1% (w/v) Tween[®] 80 to a final concentration of 0.025% (w/v) for 3 h (*see Note 1*).
2. Place 20 mL of curdlan solution in a glass beaker and measure the pH of the solution (*see Note 2*).
3. Add dropwise 8% (v/v) acetic acid solution until reaching different pHs, where the mixture is kept under magnetic stirring during half an hour, specifically in pH 11.0, 7.0, 6.0, and 5.0 (*see Note 3*) (Fig. 1).
4. Distribute the batch over two Vivaspin 20 centrifugal concentrator (approximately 15 mL in each tube) (*see Note 4*).
5. Centrifuge the particles at $3000 \times g$, at 20 °C, until the volume reaches 1 mL (Fig. 2).
6. Preserve the filtrate in the lower part of the Vivaspin tube, to later quantify the polymer that did not contribute to produce the nanoparticles, in a 50-mL centrifuge tube, at 4 °C.

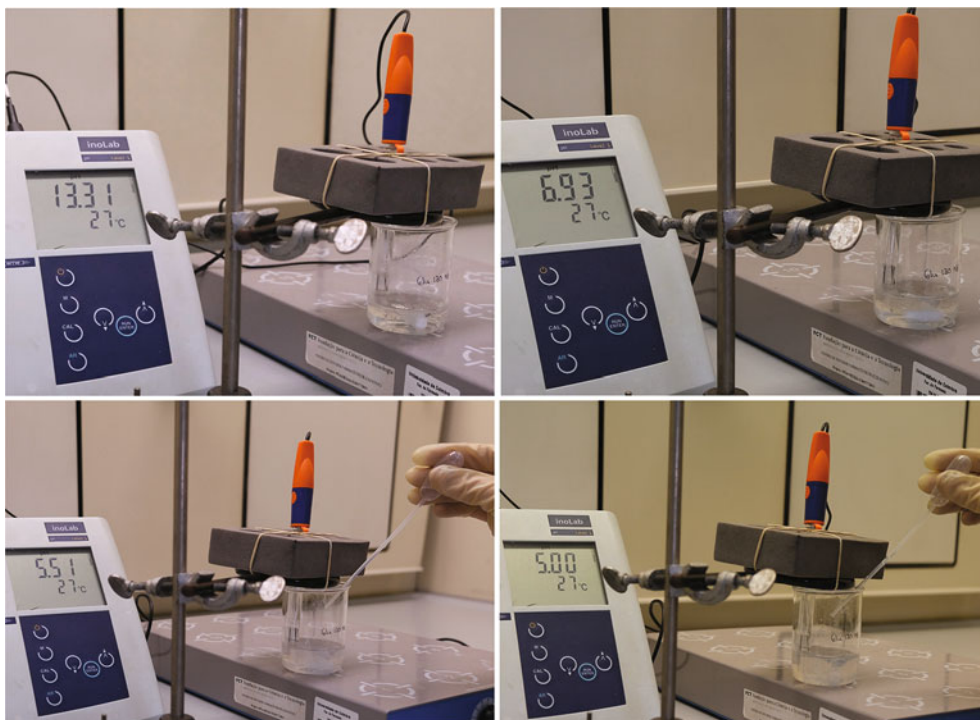


Fig. 1 Representation of the production method of 130 nm glucan nanoparticles: the solution starts at an initial pH of 13.31, then with dropwise addition of 8% (v/v) acetic acid solution the pH drops, and when it reaches pH around 7. The particles start to be produced and the suspension becomes turbid

7. Add 10 mL of ultrapure water to the upper part of the Vivaspin tube and centrifuge again at $3000 \times g$, at 20°C , until the volume reaches 0.5 mL in each tube.
8. Preserve the filtrate in the lower part of the Vivaspin tube, to later use as a solvent control in *in vitro* studies, in a 50-mL centrifuge tube, at 4°C .
9. Transfer the volume in the Vivaspin tubes to a 15-mL pyrogen-free tube and store the suspension at 4°C for further steps.
10. After nanoparticle preparation, size and zeta potential should be measured to guarantee reproducibility (*see Note 5*).

3.1.2 Glucan Nanoparticles of 350 nm

1. Dissolve curdlan in 2% (w/v) sodium hydroxide with 0.1% (w/v) Tween[®] 80 to a final concentration of 0.1% (w/v) for 3 h (*see Note 6*).
2. Place 5 mL of curdlan solution in a glass beaker and measure the pH of the solution.
3. Add dropwise 4% (v/v) acetic acid until reaching pH 5.0, where the mixture is kept under magnetic stirring during 1 h to achieve maturation (Fig. 3).



Fig. 2 130 nm glucan nanoparticle centrifugation using Vivaspin 20 centrifugal concentrator (MWCO 300KD): the nanoparticle suspension is being concentrated in the upper part of the tube (white suspension), while the bottom contains the filtrate (with no color associated)

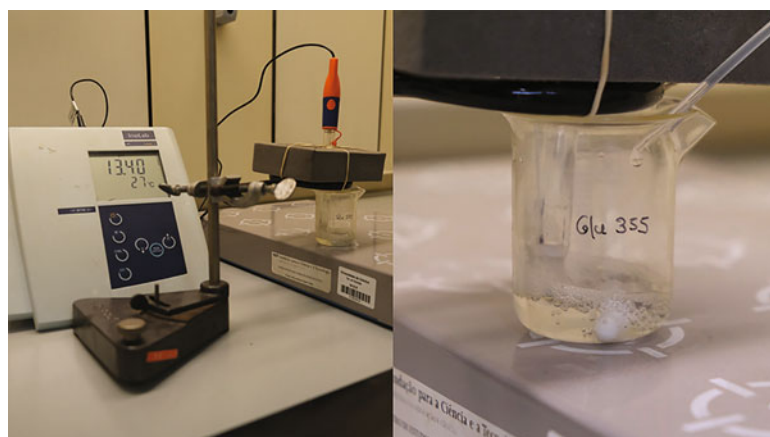


Fig. 3 Representation of the production method of 350 nm glucan nanoparticles: the solution starts at an initial pH of 13.4, then with the dropwise addition of 4% (v/v) acetic acid solution, the pH drops until 5 and the nanoparticle suspension does not become turbid, as seen in the left figure

4. Put the batch in the Vivaspin 20 centrifugal concentrator (approximately 10 mL) and centrifuge the particles at $3000 \times g$, at 20 °C, until the volume reaches 1 mL (Fig. 4).



Fig. 4 350 nm glucan nanoparticle centrifugation using Vivaspin 20 centrifugal concentrator (MWCO 300KD): the nanoparticle suspension is being concentrated in the upper part of the tube (transparent suspension), while the bottom contains the filtrate

5. Preserve the filtrate in the lower part of the Vivaspin tube, to later quantify the polymer that did not contribute to produce the nanoparticles, in a 15-mL centrifuge tube, at 4 °C.
6. Add 10 mL of ultrapure water to the upper part of the Vivaspin tube and centrifuge again at $3000 \times g$, at 20 °C, until the volume reaches 1 mL.
7. Preserve the filtrate in the lower part of the Vivaspin tube, to later use as a solvent control in in vitro studies, in a 15-mL centrifuge tube, at 4 °C.
8. Transfer the volume in the Vivaspin tubes to a 15-mL pyrogen-free tube and store the suspension at 4 °C for further steps.
9. After nanoparticle preparation, size and zeta potential should be measured to guarantee reproducibility (*see Note 5*).

3.1.3 Glucan Shell Particle

1. Add 20 g of dried yeast to 200 mL of sodium hydroxide 1 M in a 600-mL beaker.
2. Heat the suspension at 85 °C for 1 h, in water bath under rotational stirring with an overhead paddle stirrer (*see Note 7*).
3. Allow the suspension to cool down to room temperature and transfer it to 50-mL conical tubes (*see Note 8*).
4. Centrifuge the conical tubes at $3000 \times g$ for 10 min. Discard the supernatant to recover the insoluble yeast cell wall pellet (*see Note 9*).

5. Distribute 100 mL of sodium hydroxide 1 M over the conical tubes. Shake vigorously and vortex the tubes to suspend the pellet and transfer the suspension into a 600-mL beaker. Wash the conical tubes with another 100 mL of sodium hydroxide 1 M to avoid loss of insoluble material and add to the beaker.
6. Repeat **steps 2–5**.
7. Then, repeat **steps 2–4**, however, the incubation in **step 2** should last only 10 min (*see Note 10*).
8. Distribute 100 mL of ultrapure water over the conical tubes. Shake vigorously and vortex the tubes to suspend the pellet and transfer the suspension into a 600-mL beaker. Wash the conical tubes with another 100 mL of ultrapure water to avoid loss of insoluble material and add to the beaker.
11. Adjust pH with HCl to pH 4.4–4.6 (*see Note 11*).
12. Heat the suspension at 75 °C for 1 h, in water bath under rotational stirring with an overhead paddle stirrer (*see Note 7*). Allow the suspension to cool down to room temperature and transfer it to 50-mL conical tubes (*see Note 8*).
13. Centrifuge the conical tubes at $2000 \times g$ for 10 min.
14. Discard the supernatant and distribute 200 mL of ultrapure water over the conical tubes (*see Note 12*). Shake vigorously and vortex the tubes to suspend the pellet and centrifuge them at $2000 \times g$ for 10 min. Perform this step three times.
15. Repeat **step 13**, three times with 40 mL of isopropanol.
16. Repeat **step 13**, twice with 40 mL of acetone.
17. Discard the last supernatant and allow the pellet to dry in the conical tubes overnight, inside the laboratory fume hood.
18. After nanoparticle preparation, size and zeta potential should be measured to guarantee reproducibility (*see Note 5*).

3.2 Protein Loading

3.2.1 Protein Adsorption to Glucan Nanoparticles

1. Incubate a fixed particle concentration with different concentrations of proteins and keep it under rotational agitation at 20 °C for 1 h in microcentrifuge tubes.
2. After incubation, centrifuge the tubes at $21,000 \times g$ at room temperature (*see Note 13*) and collect the supernatant to measure unbound protein through bicinchoninic acid (BCA) protein assay (*see Note 14*).

3.2.2 Protein Encapsulation to Glucan Shell Particles

1. Add 100 μ L of a protein solution at the desired concentration dissolved in 0.9% saline to 10 mg of GPs (*see Note 15*).
2. Incubate for 2 h, at 4 °C, allowing protein diffusion into the hollow GP cavity.
3. Freeze-dry GPs overnight.

4. Add 100 μL of 25 mg/mL tRNA solution in TEN buffer and incubate for 30 min, at 50 °C.
5. Add 450 μL of 10 mg/mL tRNA and incubate at 50 °C for 1 h.
6. Centrifuge for 10 min at $2000 \times g$.
7. Carefully collect the supernatant with a micropipette (*see Note 16*).
8. Wash the pellet three times with 500 μL of 0.9% saline and centrifugations of 10 min at $2000 \times g$.
9. After collecting the last supernatant, add 1 mL of 0.9% saline to the pellet of GPs to obtain a 10 mg/mL GPs suspension and store at -20 °C.

3.3 Characterization of Polymeric Delivery Systems

The particles described in this chapter were characterized (Fig. 5) regarding its size and zeta potential, as well as its capacity to adsorb proteins. Protein adsorption by glucan nanoparticles was quantified by the following equations:

$$\text{Loading efficacy (\%)} = \left[\frac{(\text{total amount of protein } (\mu\text{g/mL}) - \text{unbound protein } (\mu\text{g/mL}))}{\text{total amount of protein } (\mu\text{g/mL})} \right] \times 100$$

$$\text{Loading capacity (\%)} = \left[\frac{(\text{total amount of protein } (\mu\text{g/mL}) - \text{unbound protein } (\mu\text{g/mL}))}{\text{weight of the particles } (\mu\text{g/mL})} \right] \times 100$$

The determination of protein encapsulation in GPs was not performed by BCA assay, since the presence of tRNA needed for the imprisonment of protein within the GPs interferes with the assay.

4 Notes

1. All the solutions must be prepared fresh. Curdlan is insoluble in water and suffers from poor solubility in most organic solvents. However, it is soluble in dilute alkaline solutions (>0.25 M NaOH) [8]. To be dissolved, curdlan needs 3 h in 2% (w/v) sodium hydroxide. Based on our experience, curdlan dissolution should not exceed 3 h because the polymer may precipitate again.
2. To perform this procedure in pyrogen-free and sterile conditions, all steps must be carried out inside a flow chamber and the materials needed (laboratory glassware) must be immersed in NaOH 0.5 M overnight. Remove NaOH from materials by washing thoroughly with pyrogen-free water. Moreover, depyrogenate the electrode of the pH meter by immersing it,

	Size \pm SEM (nm)	ZP \pm SEM (mV)
Glu 130	139.2 \pm 14.7	-7.9 \pm 0.8
Glu 350	380.6 \pm 38.1	-1.2 \pm 1.0
GPs	3268 \pm 425	0.39 \pm 0.09

Ratio NP Glu130:BSA	Loading Efficacy (%)	Loading Capacity (%)
1:1	100 \pm 0	100 \pm 0
1:3	81.4 \pm 7.7	244.3 \pm 23.1
1:5	53.7 \pm 4.2	268.7 \pm 20.8

Ratio NP Glu350:BSA	Loading Efficacy (%)	Loading Capacity (%)
1:1	100 \pm 0	100 \pm 0
1:3	37.2 \pm 3.4	111.6 \pm 10.1
1:5	19.7 \pm 3.6	98.3 \pm 18.1

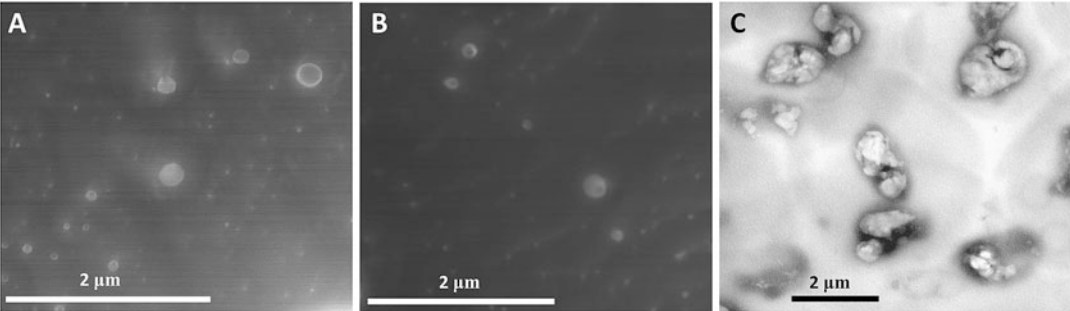


Fig. 5 Glucan particles characterization: size and zeta potential (ZP) measured in water (mean \pm SEM, $n = 8$) by dynamic light scattering and electrophoretic light scattering, respectively. Protein loading efficacy and loading capacity for Glu 130 and Glu 355 NPs, using bovine serum albumin (BSA). Data are expressed as mean \pm SEM, $n = 3$; Cryo-scanning electron microscopy images of Glu 130 NPs (a) and Glu 350 NPs (b) after being washed with Milli-Q water and concentrated using Vivaspin: scale bar, 2 μ m; Transmission electron microscopy images of GPs (c) in Milli-Q water: scale bar, 2 μ m

for 1 h, in a 0.1 M HCl solution. Nevertheless, in case of in vitro studies sensitive to pyrogens, such as lipopolysaccharide (LPS), it is necessary to pre-incubate the nanoparticles with polymyxin B sulfate salt (e.g., Sigma-Aldrich Corporation, St Louis, MO, USA) for 2 h, to guarantee a complete absence of these contaminants, which could lead to false positives [9]. Polymyxin B is required since glucan interferes with Limulus Amebocyte Lysate Assay (LAL endotoxin assay) [10].

3. The pH of the initial solution should be between values 13.0 and 13.5 and take into consideration that to reach pH 11.0 in the solution, it should be added approximately 6 mL of 8% (v/v) acetic acid. To reach pH 7.0 and 6.0, it only required a few drops of acetic acid.
4. Add a 0.1 M HCl solution to the Vivaspin tubes to depyrogenate them (for at least 2 h). Then wash the tubes with pyrogen-free water prior to the addition of nanoparticles. This procedure is only needed in pyrogen-free and sterile conditions.

5. Particle size and zeta potential should be measured to validate the production method. Dynamic light scattering (DLS) and electrophoretic light scattering (ELS) techniques can be used with this aim (e.g., Zetasizer Nano ZS instrument, Malvern Instruments, Ltd., at 25 °C and 173° angle). Nanoparticles are suspended in water or in another suitable buffer depending on their final use.
6. To dissolve this quantity of polymer, heat the solution to 30 °C during the last half an hour of the 3 h needed, to achieve total solubilization of the polymer.
7. Control the temperature inside the beaker with a thermometer. Set the temperature in the water bath in order to reach the indicated temperature inside the beaker. We find that following rigorously these conditions of temperature and time is critical to assure a good result.
8. To speed up this process, place the beaker in an ice bath.
9. The discarded supernatant should appear to be in a dark brown color with some debris material in suspension. Following the subsequent centrifugations, the supernatant should gradually become yellow/transparent with no debris visible. These characteristics may vary depending on the source or brand of your initial dried yeast material.
10. Avoid carrying out more than the described number washes/centrifugations as the increasing number of wash cycles will damage the yeast cell wall.
11. First use concentrated 12 M HCl solution to rapidly lower the starting pH to the required pH. Then use a 1 M HCl solution to avoid an abrupt drop in pH below the required pH.
12. After discarding the supernatant, vortex the pellet for 30 s to allow the pellet to better resuspend.
13. For glucan nanoparticles of 130 nm, the centrifugation time should be 1 h, and for glucan nanoparticles of 350 nm, it should be 30 min.
14. Do not use particle's concentrations above 100 µg/mL to avoid interference in the assay.
15. Drop the protein solution on top of the GP powder and let the liquid slowly spread. Do not try to homogenize.
16. Collect and store the supernatant at 4 °C for protein visualization by electrophoresis.

Acknowledgments

This work was financed by the European Regional Development Fund (ERDF), through the Centro 2020 Regional Operational Programme and through the COMPETE 2020—Operational Programme for Competitiveness and Internationalisation and Portuguese national funds via FCT – Fundação para a Ciência e a Tecnologia, under projects PROSAFE/0001/2016, POCI-01-0145-FEDER-030331 and UIDB/04539/2020 and grants SFRH/BD/139142/2018 and 2020.10043.BD.

References

- Ahmad A, Anjum FM, Zahoor T, Nawaz H, Dilshad SM (2012) Beta glucan: a valuable functional ingredient in foods. *Crit Rev Food Sci Nutr* 52:201–212
- Schorey JS, Lawrence C (2008) The pattern recognition receptor Dectin-1: from fungi to mycobacteria. *Curr Drug Targets* 9:123–129
- Jin Y, Li P, Wang F (2018) beta-glucans as potential immunoadjuvants: a review on the adjuvanticity, structure-activity relationship and receptor recognition properties. *Vaccine* 36:5235–5244
- Zeng Z, Kong X, Li F, Wei H, Sun R, Tian Z (2013) IL-12–based vaccination therapy reverses liver-induced systemic tolerance in a mouse model of hepatitis B virus carrier. *J Immunol* 191:4184–4193
- Soto E, Ostroff GR (2007) Oral macrophage mediated gene delivery system. Presented at NSTI nanotech 2007 technical proceedings
- Mirza Z, Soto ER, Dikengil F, Levitz SM, Ostroff GR (2017) Beta-glucan particles as vaccine adjuvant carriers. *Methods Mol Biol* 1625:143–157
- Colaço M, Marques AP, Jesus S, Duarte A, Borges O (2020) Safe-by-design of glucan nanoparticles: size matters when assessing the immunotoxicity. *Chem Res Toxicol* 33:915–932
- Zhang R, Edgar KJ (2014) Properties, chemistry, and applications of the bioactive polysaccharide curdlan. *Biomacromolecules* 15:1079–1096
- Colaço M, Marques AP, Jesus S, Duarte A, Borges O (2020) Safe-by-design of glucan nanoparticles: size matters when assessing the immunotoxicity. *Chem Res Toxicol* 33:915–932
- Dobrovolskaia MA, Neun BW, Clogston JD, Ding H, Ljubimova J, McNeil SE (2010) Ambiguities in applying traditional Limulus Amebocyte Lysate tests to quantify endotoxin in nanoparticle formulations. *Nanomedicine* 5:555–562

Part IV

Vaccine Delivery Systems



Use of Optical In Vivo Imaging to Monitor and Optimize Delivery of Novel Plasmid-Launched Live-Attenuated Vaccines

Sapna Sharma and Kai Dallmeier

Abstract

Plasmid-launched live-attenuated vaccines (PLLAV) are a modality of next-generation vaccines with the promise to combine the benefits of both (1) the potency of live vaccines and (2) the ease of production, quality control, and thermal stability of classical DNA vaccines. Using the live yellow fever 17D (YF17D) vaccine as paradigm, we establish a bioluminescence-based in vivo imaging approach that allows to rapidly monitor and optimize the dose and route of delivery of such PLLAV in a mouse model of YF17D immunization. Vaccine virus replication thus launched in the skin of vaccinated mice can be quantified by the light emitted, benchmarked to signals originating from a YF17D reporter virus and finally correlated to the induction of humoral immune responses to the yellow fever virus.

Key words Vaccine delivery, Optical in vivo imaging, Bioluminescence, Reporter virus, Yellow fever 17D, Plasmid-launched live-attenuated vaccine

1 Introduction

1.1 *Plasmid-Launched Live-Attenuated Vaccines*

Live-attenuated vaccines (LAV) such as the yellow fever 17D (YF17D), measles, or vaccinia vaccines are among the most efficacious vaccine modalities due to the vigorous, polyfunctional, and long-lasting immunity triggered [1]. This outstanding performance can be linked to an active replication, amplification, and finally, self-limited spread of these vaccines following inoculation. Likewise, these viruses have been applied for the design of novel live-vectored recombinant vaccines [2]. Plasmid-based production and delivery of live-attenuated vaccines, tentatively called plasmid-launched live-attenuated vaccines (PLLAV), has been proposed as a valid alternative to classical LAV [3], combining (1) the potency of the latter and (2) the ease of production, quality control, and logistics (including no need for a cold-chain) associated with

original genetic immunization using plasmid DNA. Briefly, a PLLAV (also dubbed infectious DNA or iDNA) comprises the full-length cDNA of a live-attenuated RNA virus that initiates the productive replication of the encoded vaccine after transfection into permissive mammalian cells or tissues. The vaccine viruses thus produced can amplify and spread like those originating from genuine live vaccines produced *in vitro* on a suitable cell substrate [4, 5], eventually causing a self-limiting infection and finally immunity in the vaccinated subject (for an animated video tutorial, *see* <https://youtu.be/U8-fIPTamCc>). As a consequence of this amplification of the vaccine antigen, a single-dose low-dose of PLLAV vaccines (e.g., once 1–100 µg) may be sufficient for full immunization, in stark contrast to classical DNA vaccines that generally require repeated shots of high amounts (mg) of plasmid DNA. Proof of concept of the PLLAV approach was successfully provided for yellow fever vaccination in several preclinical mouse models [6–8].

1.2 DNA Vaccine Delivery to the Skin and Subcutaneous Layers

The skin is highly populated with professional antigen-presenting cells, playing an important role in effectively inducing immune responses [9, 10]. Vaccination via the dermal route is receiving increased attention as an alternate route of immunization, next to the most frequently preferred intramuscular route (*see* for example refs. 11, 12), possibly also improving the immunogenicity of DNA vaccines in general. However, since the outer skin layers represents a significant physical barrier to the delivery of plasmid DNA [10], a variety of other routes are explored including subcutaneous, intravenous, intraperitoneal, oral, intranasal, and intravaginal. Each time, the optimal amount of DNA required to elicit vigorous antigen-specific immune responses can vary depending on the actual route (delivery methods) and animal model used [13]. A significant hurdle of DNA vaccine development toward clinical use has been translating the success of inducing protective immunity in small animal models into potent vaccines in larger animals and humans models [14–18]. Likewise, experimental approaches are needed to conveniently assess which experimental parameters (route, site of injection, dose, device, adjuvant, excipient, etc.) may positively influence DNA delivery.

1.3 In Vivo Bioluminescence Imaging (IVIS)

We have previously established that PLLAV-YF17D vaccines can readily be administered via the subcutaneous route in AG129 mice [8], resulting in the initiation of productive YF17D replication and leading consistently to seroconversion to yellow fever neutralizing antibodies and virus-specific IgG. However, testing of different dosing regimens by this means is hampered by (1) the need to use large numbers of animals and (2) a long lead time prior to serological readout. *In vivo* imaging (IVIS) is an efficient and reliable noninvasive tool to trace the delivery, amplification, and spread of viruses, including live viral vaccines, from the experimental

inoculation site to their target organs (for a comprehensive review, *see* ref. 19 and references therein). Here we take advantage of bioluminescent in vivo imaging to quantify PLLAV delivery to the mouse skin, in order to understand and optimize parameters critical for PLLAV efficacy for further preclinical and clinical testing. For that purpose, we used YF17D-based reporter viruses tagged with the small bright NanoLuciferase reporter (YF17D/NLuc) and respective PLLAV-YF17D with NanoLuciferase reporter gene (PLLAV-YF17D/NLuc) [20]. The generation of such tools has recently been described. A schematic representation of the respective constructs is depicted in Fig. 1a, b. A representative image of a single mouse 6 days post subcutaneous injection of increasing amounts of PLLAV-YF17D/NLuc is provided in Fig. 1c. The locally confined replication of YF17D (i.e., YF17D/NLuc) at the inoculation site allows to concomitantly assess multiple conditions on the back of a single mouse. In the showcased example, a 2×3 array of in total four different doses (range 0.5–62.5 μg) has been tested. Respective skin patches can be excised for ex vivo (in vitro) analysis. In parallel, blood can be sampled to correlate in vivo luminescence with yellow fever serology. By such an approach combining (1) in situ bioluminescence, (2) ex vivo luciferase activity, and (3) detection of antigen-specific antibodies rapidly large amounts of quantitative data (e.g., for dose–response, *see* Fig. 2) can be generated with a minimal number of animals to be sacrificed. Our approach can easily be adapted to study the delivery and mechanism of action of other replicating and vectored vaccine platforms, such as self-amplifying RNAs or adenovirus-vectored vaccines. Tracking of vaccine delivery based on bioluminescence imaging can readily be translated to other laboratory animals; when focusing on the ex vivo analysis, even including larger animal species, such as the pig that may better represent the human skin than small rodent animal models.

2 Materials

1. Laboratory mice (strain of choice; we use here AG129 mice) (*see* Notes 1–3).
2. Vaccine/DNA dissolved in PBS (1 mg/ml) (Fig. 1b) (*see* Note 4).
3. Reporter vaccine virus generated in tissue culture (Fig. 1a) (*see* Note 5).
4. Ear puncher.
5. Injectable anesthetics mix: (0.2 mg/kg atropine (Sterop), 40 mg/kg ketamine (Nimatek, EuroVet), and 16 mg/kg

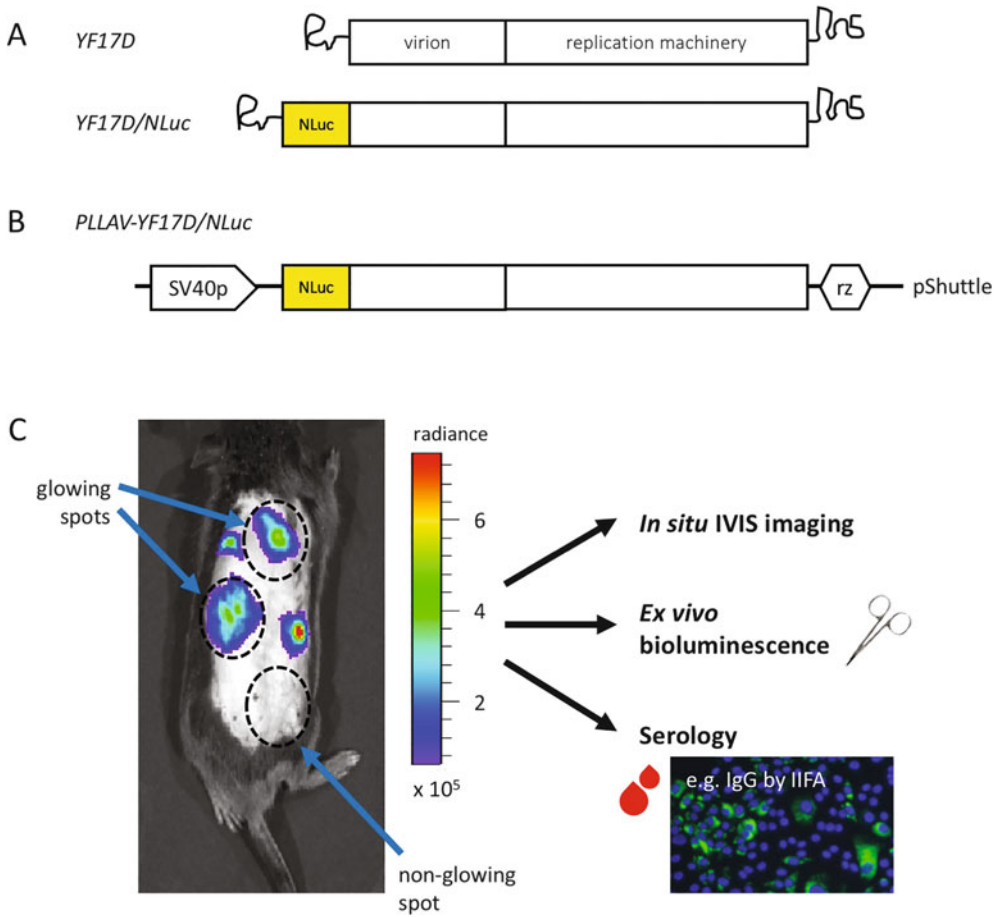


Fig. 1 Bioluminescence imaging of NanoLuciferase-tagged Plasmid-Launched Live-Attenuated Vaccine (PLLAV) delivery in mice. **(a)** Structure of the live-attenuated yellow fever 17D (YF17D) virus genome and its NanoLuciferase-tagged derivative YF17D/NLuc. **(b)** PLLAV-YF17D/NLuc expresses the reporter vaccine virus following transfection into permissive cells (Modified from Sharma et al. 2020). **(c)** In vivo imaging and ex vivo processing of biopsies. Bioluminescence image of an AG129 mouse immunized by subcutaneous injection of PLLAV-YF17D/NLuc in parallel at six spots (in a 2 × 3 grid) on its back, showing glowing and non-glowing spots resulting from locally confined YF17D (i.e., YF17D/NLuc) replication 6 days after injection. Subsequently, biopsies and blood samples are processed in vitro to quantify luciferase expression ex vivo and for serology (seroconversion to anti-yellow fever virus IgG by means of an Indirect Immune Fluorescence Assay, IIFA)

xylazine (Xyl-M, VMD) in water used for shaving (or isoflurane depending upon the availability) (*see Note 6*).

6. Pet hair trimmer (Aesculap Isis trimmer cordless hair clipper GT421).
7. Hair removal cream (Veet).
8. Heated Pad, (375 mm × 150 mm; 16 W).
9. Autoclaved water.
10. 0.5-ml insulin syringe.

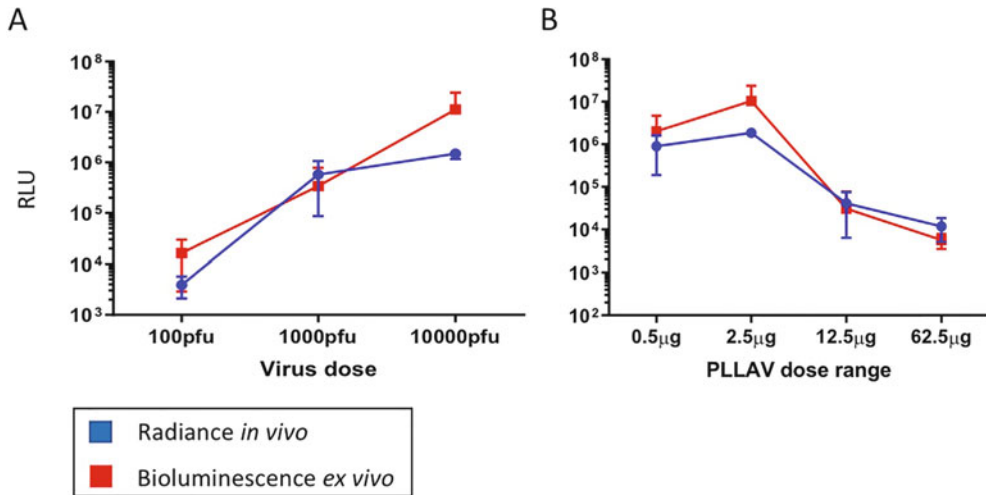


Fig. 2 Quantitative analysis of signals from in vivo imaging and in vitro testing of biopsies. (a) Bioluminescence resulting from active replication of YF17D/NLuc in the skin of mice (expressed in relative light units, RLU) increases in a dose-dependent manner for both signals originating from (1) in vivo radiance (blue) and (2) in vitro (ex vivo) luciferase activity (red). (b) YF17D/NLuc replication as initiated from subcutaneous injection of PLLAV-YF17D/NLuc shows an optimum at a dose of about 2.5 µg. The resulting RLU resembles values those obtained with a dose of 1000 PFU (plaque-forming units) of YF17D/NLuc. Data acquired 6 days (in vivo) and 8 days (ex vivo) after PLLAV injection. Means of experiments performed in triplicate with error bars indicating SEM

11. Ice bucket.
12. RAS-4 Rodent Anesthesia System.
13. IVIS spectrum, in vivo imaging system from Perkin Elmer.
14. Sodium pentobarbital (for euthanasia, 200 mg/kg of sodium pentobarbital).
15. Disposable Biopsy Punch with Plunger (4 mm), Integra Miltex.
16. Scissors.
17. Dry ice.
18. NanoGlo substrate and buffer (Nano-Glo, Promega).
19. ViewPlate-96, white 96-well microplate with clear bottom.
20. Biosafety cabinet.
21. Tissue homogenizer (bead mill).
22. Prepacked tubes for Precelly beadmill (Precellys[®] Ceramic kit 2, 8 mm, 50 × 2 ml tubes, pre-filled with ceramic beads).
23. Micro plate reader.
24. Indirect immunofluorescence assays (IIFAs) kits (Euroimmun).
25. Alexa Fluor 488 goat anti-mouse IgG.

26. ProLong antifade embedding reagent with DAPI (DAPI, 4',6-diamidino-2-phenylindole).
27. FLoid cell imaging station.

3 Methods

The methods describe the subcutaneous vaccination of AG129 mice using insulin syringe (*see Note 2*). The time required for the procedure depends on the number of mice to be prepared for vaccination.

3.1 Preparation of Animals Prior to Vaccination

1. Prior to vaccination, mice needs to be shaved (24–48 h before vaccination) (*see Notes 6 and 7*).
2. Ear tag mice and anesthetize via intramuscular injection or using isoflurane.
3. Keep mice on heating pad keeping the back of the mice in upward position. Trim fur from the desired area and completely remove residues of hair by applying small amount of epilating cream, rub the cream over the desired part for 30–40 s, and clean it using paper towel. Use clean water to remove the cream completely (*see Note 7*).
4. Put mice back in cage and monitor until animals fully recovered from anesthesia.
5. Let animal rest for roughly 48 h after removal of the fur.

3.2 Vaccination of Mice

1. Prepare dilutions of plasmid DNA in PBS. 2.5 µg DNA in 50 µl of PBS can be considered a unit dose for each spot on a mouse to be immunized (*see Notes 8 and 9*).
2. Thaw matching reporter virus (10^3 PFU in a volume of 15–50 µl per injection) and keep on ice.
3. Anesthetize mice before start of vaccination.
4. When asleep, make a grid of six spots (or depending upon the number of conditions to be tested on one mouse) on the back of the mouse using marker pen.
5. Inject the vaccine (50 µl) subcutaneously by gently lifting the skin with forceps making a small tent in each spot and inject using insulin syringe. A small bubble can be seen on the injection site to visually confirm the proper application.
6. Put animals back in cage and monitor until fully recovered from anesthesia.

3.3 Imaging

In vivo imaging of mice is done on different days post vaccination, depending upon the experiment. For PLLAV-YF17D/NLuc, we start imaging from day 3, 5, 7, and 10. However, replicating virus can further be imaged depending on the type of vaccine under study.

1. The IVIS spectrum in vivo imaging system should be turned on all time.
2. Log into computer and start the Living Image Software.
3. Initiate the system (*see Note 10*).
4. Check the charcoal filters on top of anesthesia station (XGI-8 Gas Anesthesia System) by weighing (*see Note 11*).
5. Turn on the evacuation pump.
6. Turn on the oxygen supply switch.
7. Turn on the gas switch for the imaging chamber.
8. Set the vaporizer at 0% isoflurane position. Thereafter, turn on the imaging chamber toggle valve and set at 0.25 l/min.
9. Set the vaporizer to 2.0% isoflurane (*see Note 12*).
10. Inject 10 μ l substrate (0.15 mg/g of body weight intravenously/intraperitoneally) (*see Notes 13 and 14*).
11. Weight for 5 min and thereafter put the animals (maximum five mice) in the induction chamber and turn on the induction chamber toggle valve. Keep mice in the induction chamber for 5 min.
12. Turn on the imaging chamber toggle valve.
13. Once asleep, transfer mice from induction chamber to the imaging chamber. Up to five mice can be imaged together depending upon the imaging device and needs of experiment. Put the mice in a slightly stretched prone position (on their belly) and insert their nose in nose cone. The shaved back of the mice should be exposed.
14. Turn off the induction chamber toggle.
15. Select the appropriate field of view (FOV) depending upon the number of animals being imaged together (*see Note 15*).
16. Acquire a luminescent image using predefined protocols. The protocol is set up in the Living Image software. Enable the auto save function. You can select auto exposure, manual exposure and sequence acquisition. We routinely perform auto exposure, using a setting in which the software automatically determines the binning and F/Stop settings (*see Note 16*).
17. Select bioluminescent imaging mode, check mark photograph and choose an appropriate field of view (FOV).
18. Capture images by clicking the acquire button.
19. Enter relevant image label information.
20. Take the images at different time points (1 min, 3 min, 5 min).
21. Carefully return mice to their cage. Continuously observe mice until they recover fully from anesthesia.

22. Turn off the isoflurane and keep the oxygen supply on for 5 min to clear the isoflurane in induction chamber and imaging chamber before switching off the oxygen tank.
23. Turn off toggle valves.
24. Turn off oxygen valve.
25. Turn off the evacuation pump.
26. Save your imaging data at desired folder and exit the imaging software and logout from the computer.
27. Analyze for RLU (relative light unit) and measure the ROI (region of interest) per spot using *in vivo* imaging software.
28. To quantify the amount of light emitted from glowing spots, regions of interest (ROIs) were manually defined around the glowing spot and photon flux (photons/second/square centimeter/steradian) was calculated using Living Image 4.0 software (Caliper Life Sciences, Alameda, CA, USA).
29. We normally present data by showing images of the mice with different conditions, e.g., doses along (Fig. 1c) with an accompanying graph showing quantitative data determined using ROI tool from imaging software (Fig. 2).

3.4 Serology and Ex Vivo Analysis of Biopsies from Glowing and Non-glowing Spots

1. Bleed mice before taking biopsies, through either heart puncture or submandibular puncture. Serum/plasma is collected by spinning the blood at 12,000 rpm (approximately $13,000 \times g$) for 5 min at 4 °C.
2. To determine seroconversion of animals against YF, indirect immunofluorescence assays (IIFAs) are performed as per manufacturer's instructions (Euroimmun), except for a slightly modified staining procedure: Instead of using the original secondary anti-human IgG antibody and mounting agent (glycerol), the latter two reagents are replaced by Alexa Fluor 488 goat anti-mouse IgG (dilution 1:500) and DAPI-containing mounting medium, respectively. Serum from naive non-vaccinated animals serves as negative control. Slides are visualized using a fluorescence microscope (FLoid cell imaging station) [21]. Generally, mice with glowing spots at vaccination site show seroconversion against yellow fever, confirming the functional delivery of PLLAV.
3. To analyze glowing and non-glowing spots, mark the area on the back of the mouse after imaging and euthanize mouse by giving intraperitoneal injection of 200 mg/kg of sodium pentobarbital euthanasia solution or other anesthetics at an overdose. Immediately cut the skin biopsies using biopsy punch or scissors as depicted in Fig. 1c. Collect the biopsies separately in Eppendorf tubes and put immediately on dry ice (*see Note 17*).

4. Collect the biopsies from different spots in separate tubes and mark properly.
5. Store the biopsies at -80°C for short-term storage and in liquid nitrogen for long term use until further use for analysis.
6. To analyze the biopsies, homogenize the biopsies using homogenizer (alternatively pestle and mortar), in $500\ \mu\text{l}$ lysis buffer. Centrifuge samples after homogenization (*see Note 18*).
7. Collect the supernatant in a fresh tube and perform luciferase assay by adding $100\ \mu\text{l}$ of the supernatant in 96-well white plate in triplicates. Add each $100\ \mu\text{l}$ NanoGlo substrate (premixed with luciferase buffer at the ratio of 1:50). Read the plate for luminescence after 5 min using plate reader.
8. Plot in vitro luminescence data and compare with in vivo photon flux data (*see Fig. 2*).

4 Notes

1. Any animal work requires prior ethical and biosafety approval by competent institutional and governmental authorities for the proposed experiments.
2. Wild-type mice are poorly susceptible to infection with flaviviruses, including YFV-17D infection and vaccination. Therefore, here we use AG129 mice with a combined type I and type II interferon receptor knockout as they are more permissive as compared to wild-type mice [8, 21].
3. Mice with a dark skin color absorbing emitted light (e.g., mice on a C56BL/6 background) may be less suitable for optical imaging.
4. Plasmid-launched YF17D vaccine (PLLAV-YF17D) [8] and its NanoLuciferase expressing derivative (PLLAV-YF17D/NLuc; *see Fig. 1b*) [20] have been described before. PLLAV-YF17D and PLLAV-YF17D/NLuc are grown in *E. coli* strain EPI300-T cells, purified by standard alkaline lysis using a low-endotoxin maxiprep protocol (Machinery-Nagel), dissolved in TE buffer ($10\ \text{mM}$ Tris, $1\ \text{mM}$ EDTA, pH 7.5–8) to a final concentration of $1\ \text{mg/ml}$, and stored frozen at -20°C .
5. The design, construction and use of NanoLuciferase-tagged YF17D reporter virus (YF17D/Nluc vaccine) have been described before [20, 22]. In brief, YF17D/Nluc vaccine is harvested as supernatant of VeroE6 (African green monkey kidney) cells transfected with PLLAV-YF17D/Nluc. Four to five days post transfection (when cells show a virus-induced cytopathic effect) supernatant is collected, aliquoted, and

stored frozen at $-70\text{ }^{\circ}\text{C}$ until use. Infectious content (expressed in plaque forming units per ml, PFU/ml) is titrated on BHK21/J cells as described elsewhere [21].

6. Shave animals 24–48 h before vaccination and be careful during shaving not to cut the skin. This should be done under anesthesia, either a cocktail of injectable anesthetics or isoflurane depending upon availability.
7. Use depilatory cream in small amount and remove completely, and use again if required, also wash the skin with water afterwards, because depilatory cream can irritate the skin if not removed properly and can affect the experimental outcome.
8. Dissolve plasmid DNA in PBS to make a homogenous solution and measure the DNA concentration to ensure correct concentration. Always prepare some extra volume to make sure you have sufficient material to inject, respecting syringe and vial void volumes.
9. We used different concentrations of plasmid (0.5, 2.5, 12.5, 62.5 μg) in a unit volume of 50 μl per spot for vaccination to assess dose-dependency on bioluminescence.
10. It takes few minutes to initiate the system, especially to cool down the camera to $-90\text{ }^{\circ}\text{C}$.
11. A filter weighing $>50\text{ g}$ than the original weight should be replaced to ensure good absorption of the anesthesia gas.
12. Mice should be completely anesthetized before transferring them to the imaging chamber, observe for rhythmical breathing. If mice are not completely anesthetized, isoflurane flow may be increased from 2 to 2.5 or 3% to make sure animals don't wake up during imaging.
13. Always make fresh substrate solution, by dissolving 10 μl of luciferase substrate in 90 μl of PBS and inject 100 μl per animal i.p.
14. Substrate is routinely injected intraperitoneally (i.p.), though intravenous (i.v.) injection of substrate works also very well. In latter case, animals should be anesthetized first and need to be imaged immediately (within 5 min after i.v. substrate injection) to avoid substrate depletion and thus rapid signal decay. If substrate is injected i.p., biodistribution is slower and imaging can be done after 10–12 min. Inject same amount of substrate in all mice and use mice of almost same weight, to avoid differences in luminescent signals resulting from the relative amount of substrate administered to the animals.
15. Field of view (FOV) depends on number of animals to be imaged together. FOV is the size of the stage area to be imaged. FOV A (part of 1 mouse), B (1 mouse), C (up to 3 mice), and D (up to 5 mice)

16. Exposure time: the length of the time that the shutter is open during image acquisition. Binning: controls the pixel size on the CCD camera, increasing the binning increases pixel size and sensitivity. This will reduce the spatial resolution. F/stop: defines the size of the camera lens aperture. A small aperture size results in lower sensitivity since less light is collected for the image. Small apertures produce sharp images, whereas large apertures maximize the sensitivity
17. Image the animals just before collection of biopsies and mark the area around the bioluminescence signals, called tentatively “glowing spot.” Euthanize the mice before taking the biopsy by injecting sodium pentobarbital 200 mg/kg solution intraperitoneally, and very quickly take the biopsies using biopsy punch, sometime also needing scissors to cut the skin.
18. Snap freeze the biopsies until further use. Mouse skin is very hard to homogenize. Therefore, it is better to cut in small pieces prior to addition of lysis buffer. Furthermore, suppliers provide extensive protocols how to optimizing homogenization and lysis conditions.

Acknowledgments

The authors acknowledge funding by the Flemish Research Foundation (FWO) Excellence of Science (EOS) program (No. 30981113; VirEOS project), the European Union’s Horizon 2020 research and innovation program (No 733176; RABYD-VAX consortium), the Bill and Melinda Gates Foundation (OPP1195179), and KU Leuven Internal Funds (C3/19/059; Lab of Excellence and IDN/20/011; MIRACLE).

References

1. Pulendran B et al (2013) Immunity to viruses: learning from successful human vaccines. *Immunol Rev* 255(1):243–255
2. Draper SJ, Heeney JL (2010) Viruses as vaccine vectors for infectious diseases and cancer. *Nat Rev Microbiol* 8(1):62–73
3. Pushko P et al (2016) DNA-launched live-attenuated vaccines for biodefense applications. *Expert Rev Vaccines* 15(9):1223–1234
4. Aubrit F et al (2015) Cell substrates for the production of viral vaccines. *Vaccine* 33(44):5905–5912
5. Rodrigues AF et al (2015) Viral vaccines and their manufacturing cell substrates: new trends and designs in modern vaccinology. *Biotechnol J* 10(9):1329–1344
6. Tretyakova I et al (2019) Novel DNA-launched Venezuelan equine encephalitis virus vaccine with rearranged genome. *Vaccine* 37(25):3317–3325
7. Jiang X et al (2015) Molecular and immunological characterization of a DNA-launched yellow fever virus 17D infectious clone. *J Gen Virol* 96(Pt 4):804–814
8. Kum DB et al (2019) Limited evolution of the yellow fever virus 17d in a mouse infection model. *Emerg Microbes Infect* 8(1):1734–1746
9. Kupper TS, Fuhlbrigge RC (2004) Immune surveillance in the skin: mechanisms and clinical consequences. *Nat Rev Immunol* 4(3):211–222

10. Nagao K et al (2009) Murine epidermal Langerhans cells and langerin-expressing dermal dendritic cells are unrelated and exhibit distinct functions. *Proc Natl Acad Sci U S A* 106 (9):3312–3317
11. Roukens AH et al (2008) Intradermally administered yellow fever vaccine at reduced dose induces a protective immune response: a randomized controlled non-inferiority trial. *PLoS One* 3(4):e1993
12. Young F, Marra F (2011) A systematic review of intradermal influenza vaccines. *Vaccine* 29 (48):8788–8801
13. Rosa DS et al (2015) Multiple approaches for increasing the immunogenicity of an epitope-based anti-HIV vaccine. *AIDS Res Hum Retrovir* 31(11):1077–1088
14. Zhang L et al (2008) T cell epitope-based peptide-DNA dual vaccine induces protective immunity against *Schistosoma japonicum* infection in C57BL/6J mice. *Microbes Infect* 10(3):251–259
15. Yang ZY et al (2004) A DNA vaccine induces SARS coronavirus neutralization and protective immunity in mice. *Nature* 428 (6982):561–564
16. Lee LYY, Izzard L, Hurt AC (2018) A review of DNA vaccines against influenza. *Front Immunol* 9:1568
17. Li L, Petrovsky N (2016) Molecular mechanisms for enhanced DNA vaccine immunogenicity. *Expert Rev Vaccines* 15(3):313–329
18. Zhu Y et al (2003) Protective immunity induced with 23 kDa membrane protein dna vaccine of *Schistosoma japonicum* Chinese strain in infected C57BL/6 mice. *Southeast Asian J Trop Med Public Health* 34 (4):697–701
19. Avci P et al (2018) In-vivo monitoring of infectious diseases in living animals using bioluminescence imaging. *Virulence* 9(1):28–63
20. Sharma S et al (2020) Small-molecule inhibitors of TBK1 serve as an adjuvant for a plasmid-launched live-attenuated yellow fever vaccine. *Hum Vaccin Immunother* 16(9):2196–2203
21. Mishra N et al (2020) A Chimeric Japanese encephalitis vaccine protects against lethal yellow fever virus infection without inducing neutralizing antibodies. *mBio* 11(2):e02494-19
22. Kum DB et al (2020) A chimeric yellow fever-Zika virus vaccine candidate fully protects against yellow fever virus infection in mice. *Emerg Microbes Infect* 9(1):520–533



Liposomes for the Delivery of Lipopeptide Vaccines

Jieru Yang, Armira Azuar, Istvan Toth, and Mariusz Skwarczynski

Abstract

Liposomes, which are artificial phospholipid vesicles with a bilayer membrane structure, have been developed and evaluated as a promising delivery system for vaccines. Here, we describe a procedure for the encapsulation of lipopeptide vaccines into liposomes. A liposomal formulation of lipid-core peptide was prepared via thin-film hydration followed by extrusion. The physicochemical properties of the liposomes, including their size, polydispersity, surface charge, and morphology, were analyzed using dynamic light scattering and transmission electron microscopy.

Key words Liposomes, Lipopeptides, Extrusion, Vaccine delivery

1 Introduction

Liposomes are used widely in vaccine delivery [1–4]; one example being the liposome-based vaccine against hepatitis A infection, commercialized as Epaxal[®] [5]. Vaccine delivery systems that employ liposomes have considerable advantages, including [6]:

- Liposomes are biodegradable, biocompatible, low/nontoxic, and nonimmunogenic.
- Liposomes are customizable: Their components, such as the lipid composition, can be easily altered to modify charge and fluidity/rigidity. Liposome size and vesicle layering (unilamellar or multilamellar) can also be altered.
- The concentric lipid bilayer structure allows the entrapment of hydrophilic compounds into the liposomal core and hydrophobic compounds in the membrane bilayer.
- Entrapment of antigens inside liposomes can protect against physical and biological degradation, improving vaccine stability and prolonging systemic circulation time.

- Multiple copies of the same or different antigens can be loaded into liposomes.
- Liposomes promote a strong immune response by encouraging antigen cross-presentation in antigen-presenting cell (APC) and inducing antigen-specific cytotoxic T-cell responses (CTL).

Liposomes have been used for the delivery of peptide, protein, and DNA-based vaccines. While an antigen can be simply encapsulated into liposomes, bilayer surface anchoring strategies provide higher encapsulation and loading efficacy. Thus, lipidated compounds, such as lipopeptide antigens, can be efficiently anchored into liposomes [7–10]. Lipopeptides, which have been intensively studied in the field of vaccine development for more than 30 years, have shown the ability to induce both humoral and cellular responses [11–15]. The attachment of lipids to a peptide antigen (lipidation) can improve peptide hydrophobicity, bioavailability, enzymatic stability, and recognition and uptake by antigen-presenting cells. Lipid-core peptide (LCP), a widely used lipopeptide delivery system, is composed of (a) α -amino acid bearing a long alkyl side chain (lipoamino acid, LAA) and (b) branching lysine moiety/ies, to which (c) peptide antigens are conjugated. This system has been used in peptide-based vaccine developments targeting malaria [16], group A streptococcus [10, 17], human hookworm infection [18, 19] and *Schistosoma* [20, 21]. An LCP system has been incorporated into liposomal formulations to further improve vaccine efficacy [15].

The lipopeptide LCP-1 (Fig. 1) was designed based on an LCP system consisting of two 2-amino-D,L-hexadecanoic acid (C16-LAA) compounds, a branching lysine moiety conjugated to antigenic peptide bearing a universal T-helper epitope P25 (KLIP NASLIENCTKAEL), and a conserved B-cell epitope J8 (KQAED KVKASREAKKQVEKALEQLEDKVK) derived from group A streptococcus (GAS) M protein. M protein is a highly virulent factor that resides on the surface of GAS bacteria. GAS is responsible for numerous diseases, ranging from simple pharyngitis to life-threatening illnesses, such as rheumatic fever and rheumatic heart disease [22]. Notably, LCP-1 has been successful in stimulating systemic immune responses in mice [23, 24]. The incorporation of LCP-1 into cationic liposomes induced mucosal and systemic immunity with strong antibody titers even 5 months after intranasal immunization [25].

This chapter describes the methodology to encapsulate/anchor lipopeptide (LCP-1) into liposomes using film hydration. Details of the liposomes' physicochemical properties, including size, polydispersity index (PDI), surface charge, and morphology, are also presented.

14. Kimwipes.
15. Vortex shaker.
16. Rotatory evaporator with water bath.
17. Freeze dryer.
18. Hot plate.

2.2 Liposome Characterization

1. Malvern Zetasizer.
2. Disposable folded capillary cell.
3. Transmission electron microscope.
4. Carbon-coated copper grid.
5. Filter paper.
6. 2% Phosphotungstic acid.

3 Methods

Liposomes are produced over 2 days: thin-film formation (Subheading 3.1.1, steps 1–8) on the first day, then rehydration (Subheading 3.1.2, steps 9 and 10), extrusion (Subheading 3.1.3, steps 11–23), and physiochemical characterization (Subheading 3.2) on the second day.

3.1 Liposome Formulation

3.1.1 Preparation of Thin Lipid Film

1. Rinse a 5-mL round-bottom flask and up to three glass syringes (from the mini-extruder set) with Milli-Q water (3×), methanol (3×), and chloroform (3×), then allow them to air-dry (*see Note 3*).
2. Using separate glass syringes for each solution, transfer 0.5 mL of DPPC solution, 0.2 mL of DDAB solution, and 0.1 mL of cholesterol solution to the round-bottom flask (*see Note 4*).
3. Add 1 mL of lipopeptide solution and an extra 2 mL of chloroform into the flask. Gently shake the lipid mixture at room temperature (RT) to facilitate homogenization (*see Note 5*).
4. Connect the 5-mL round-bottom flask to a rotary evaporator. Heat the water bath to 40–45 °C. During the evaporation process, keep the flask on an approximate 45° incline, with continuous rotation at 60 rpm, and above the water level.
5. Slowly reduce the pressure to gently evaporate the organic solvent (*see Note 6*).
6. Increase the pressure by 100 mbar every 30 s. The pressure should be changed slowly to avoid solvent vapor returning and dissolving the film formed. Elevate the flask from the water bath and carefully disconnect it from the rotary evaporator (Fig. 2; *see Note 7*).

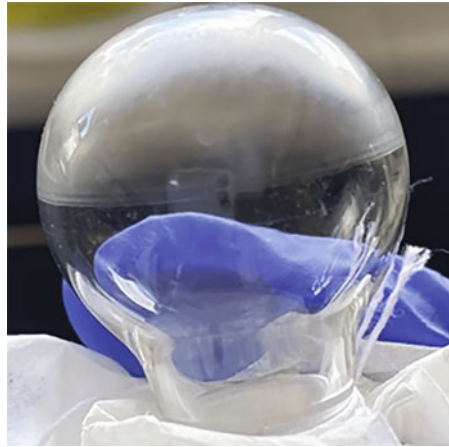


Fig. 2 Normal appearance of the thin lipid film

7. Use a piece of a kimwipe to cover the flask opening and secure it with a rubber band to avoid the entry of contaminants.
8. Keep the flask in a freeze dryer for a few hours to remove all traces of the solvents (*see Note 8*).

3.1.2 Rehydration of the Thin Lipid Film

9. Add 1 mL of water gradually to the flask containing the lipid film (*see Note 9*).
10. Transfer the rehydrated lipid suspension into a scintillation vial (*see Note 10*).

3.1.3 Extrusion of Liposomes

11. Assemble the mini-extruder based on the manufacturer guidelines (Avanti Polar Lipids, United States). The mini-extruder set includes the mini-extruder (extruder outer casing, two internal membrane supports, Teflon bearing, and retainer nut), a holder, two glass syringes, PC membranes, and filter supports (Fig. 3; *see Note 11*).
12. Lay the two internal membrane supports flat so that the O-ring seal is facing upwards. Place a pre-wetted filter support onto the surface of the internal membrane support, in the middle of the O-ring. The filter support should stick to the internal membrane support (*see Note 12*).
13. Transfer one of the internal membrane supports with filter, into the extruder outer casing with the O-ring seal still facing up. Using membrane forceps, carefully place one PC membrane above the O-ring and ensure that the PC membrane clings tightly to the O-ring without any air bubbles. The flat, white surface of the internal membrane support and O-ring should be fully covered by the PC membrane (*see Note 13*).
14. Gently place the other internal membrane support (with filter support) onto the extruder outer casing with the O-ring

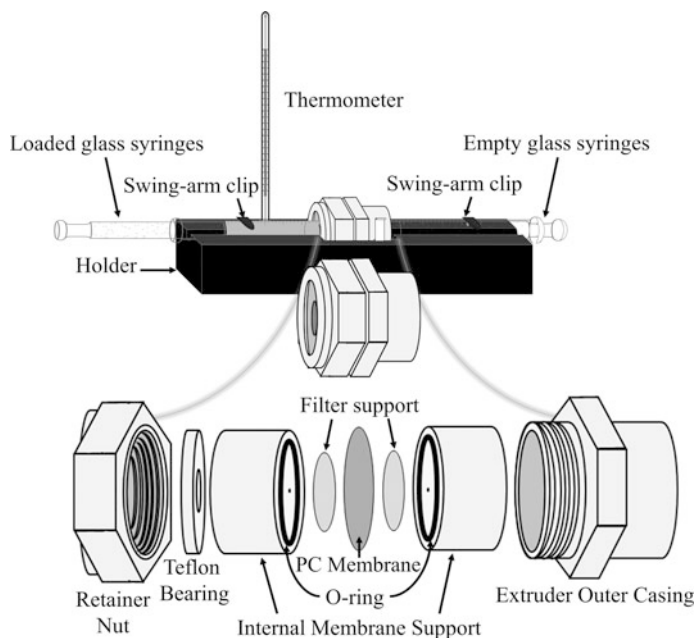


Fig. 3 The components of the mini-extruder apparatus



Fig. 4 The correct position to perform the extrusion when pushing the plunger of the loaded syringe

facing down. The two internal membrane supports should now be connected, with the PC membrane firmly held between the two filter supports (*see Note 14*).

15. Place the Teflon bearing inside the retainer nut. Fasten the retainer nut onto the threaded end of the extruder outer casing and tighten by hand until both hex nuts align with each other.
16. Secure the assembled extruder into the holder with the pointy end of the hex nut facing up. Place the holder onto a hot plate set at 50 °C. Position the thermometer in its stand on the holder to monitor the temperature (*see Note 15*).



Fig. 5 The non-extruded (red cap) liposome solution is cloudier than the extruded solution (blue cap)

17. Before extruding the prepared liposomes, test the device for leaks by extruding 1 mL of water through the extruder (as per **steps 18–22**). Remove all of the water from the syringes before continuing with the liposome sample.
18. Fill a gas-tight glass syringe with 1 mL of the liposome solution, leaving the second syringe empty. Ensure both syringe needles fit tightly into the ends of the extruder and secure them with the arm clip on the holder. Check both syringes for air bubbles and remove any present before performing the extrusion.
19. Wait 10 min to allow the temperature of the set-up to equilibrate.
20. Gently push the plunger of the loaded syringe to pass the solution through the membranes and into the second syringe. When complete, the second syringe will be full (Fig. 4, *see Note 16*).
21. Once all of the solution has been transferred into the second syringe, push the plunger of the second syringe to transfer all of the solution back to the first syringe (*see Note 17*).
22. Repeat **steps 20** and **21** to allow at least 15 passes (although 21 passes are recommended) (*see Note 18*).
23. After extrusion is complete, remove the loaded syringe from the extruder and transfer the lipid solution into a scintillation vial. The final liposome solution should be more transparent compared to the unextruded liposome solution (Fig. 5; *see Note 19*).

3.2 Liposome Characterization

3.2.1 Size, Surface Charge, and PDI

1. Open the Zetasizer analysis software and connect it with the Zetasizer Nano ZP instrument (Malvern Instrument, UK) half an hour before starting measurements.
2. Add 100 μL of liposome solution in 900 μL of water (1:10 dilution).
3. Fill the folded capillary cell with diluted liposome solution (~ 800 μL) and insert the capillary cell into the instrument. The capillary cell is used for both size and charge measurements.
4. Perform measurements (size, PDI, and surface charge) at 25 °C with a back-scattering angle of 173°. Measure each liposome solution at least five times.
5. Calculate the mean \pm standard deviation for all measurements (Table 1; see Note 20).

3.2.2 Morphology

6. Use the diluted liposome solution prepared in step 2 (see Note 21).
7. Add 5 μL of diluted liposome solution to a glow-discharged carbon-coated copper grid by pipette, and let it sit for 2 min (see Note 22).
8. Gently remove the excess liposome solution from the grid using a piece of filter paper, then air-dry the grid for 2 min (see Note 23).
9. Add 5 μL of 2% ammonium molybdate to the dried grid for 20 s to negatively stain the liposomes, then remove the excess stain solution with a piece of filter paper.
10. Air-dry the grid for 5 min before observing the liposomes using a transmission electron microscope. Take images at an accelerating voltage of 100 kV (Fig. 6).

4 Notes

1. Weight out 10 mg each of DPPC, DDAB, and cholesterol powder in separate scintillation vials. Add 1 mL of chloroform to each using a glass syringe to dissolve. Ensure the final concentration of lipid stock solutions are 10 mg/mL and that all of the lipid powders are fully dissolved. Leave the lipid stock solution at RT for 10 min to facilitate homogenization. The lipid stock solutions need to be freshly made prior to use.
2. Weight out 1 mg of lipopeptide (LCP-1 in this formulation) in a 2-mL microcentrifuge tube. Add 1 mL of methanol, then use the pipette to dissolve the lipopeptide. Gently vortex the lipopeptide solution for 2 min to ensure the lipopeptide is fully dissolved.

Table 1
Typical physicochemical characterization of the liposomal formulation of lipopeptide LCP-1

Liposome		Size by intensity (nm)	Polydispersity index (PDI)	Zeta potential (mV)
Not extruded	Blank liposome ^a	431 ± 96 3839 ± 186	0.47 ± 0.04	40 ± 2
	LCP-1-anchored liposome	621 ± 47 4162 ± 2332	0.80 ± 0.11	68 ± 1
Extruded	Blank liposome ^a	172 ± 2	0.06 ± 0.02	45 ± 1
	LCP-1-anchored liposome	171 ± 1	0.03 ± 0.01	43 ± 2

^aBlank liposome is liposome formulated without lipopeptide

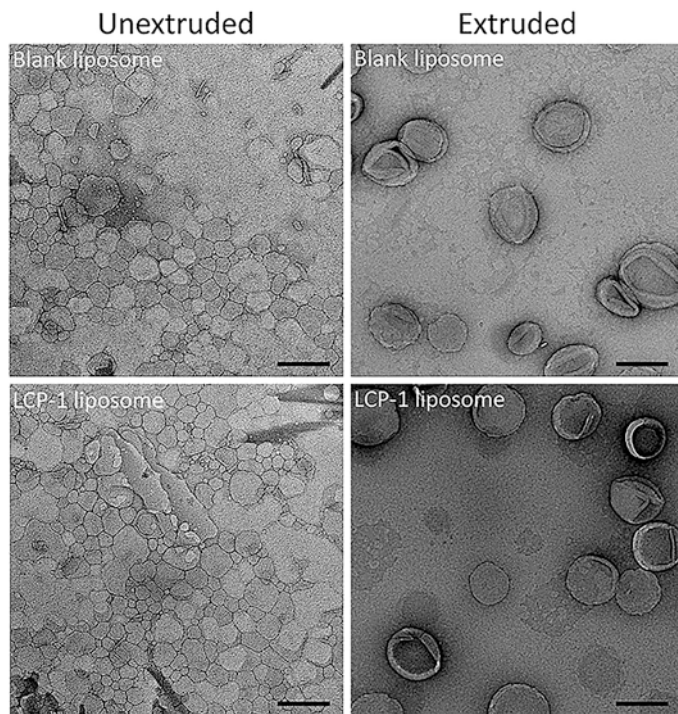


Fig. 6 Particle-imaging and morphology of the liposomes captured by transmission electron microscopy (bar 500 nm)

- Clean each of the glass syringes with chloroform (3×) and methanol (3×) after performing the thin lipid formation steps. These syringes will be used again in the extrusion steps.
- If three glass syringes are not available, a syringe can be re-used to transfer subsequent lipid stock solutions after it has been rinsed with methanol (3×) and chloroform (3×).

5. A 5:2:1:1 mass ratio of DPPC:DDAB:cholesterol:lipo peptide is used in this formulation. However, the lipid ratio in liposome formulations depends on the experimental design and can be modified to regulate liposomal fluidity (cholesterol), charge (DDAB), and antigen content (lipo peptide). Here, the final organic solvent ratio (chloroform/methanol) can range from 9:1 to 2:1, meaning every 2 mL of chloroform can be mixed with a maximum of 1 mL of methanol in this lipid mixture. Less methanol improves thin film formation, but can also result in lipo peptide insolubility in the lipid mixture.
6. Do not immediately immerse the flask in the water bath. Start the initial pressure of the rotary evaporator at 700 mbar, then reduce the pressure by 100 mbar every 2 min to finally reach 300 mbar. Then submerge the flask halfway into the preheated water bath. Continue to reduce the pressure every 5 min until the pressure reaches 100 mbar. Set the final pressure at 50 mbar for 10 min. The slow evaporation process can produce a dry lipid film with a glassy-clear appearance on the flask walls. Using the preheated water bath too early can result in fast solvent evaporation and the formation of white precipitate dots at the bottom of the flask. If this happens, re-dissolve the lipid with the chloroform/methanol mixture and repeat the evaporation step.
7. If lipid film formation is disrupted, re-dissolve the lipid with the chloroform/methanol mixture and repeat the evaporation step.
8. A vacuum desiccator can be used instead to remove solvent traces; however, this is less effective than the use of freeze dryer. If using a low vacuum desiccator, ensure the flask is placed in the desiccator for more than 12 h. It is critical to remove solvents completely because traces of solvent can interfere with liposome formulation, in addition to adding potential toxicity.
9. Start the rehydration of the lipid film by pipetting 50 μL of water onto the film, then vortex the flask on the maximum speed setting three times with 5-s intervals. This allows the water to be efficiently dispersed into the lipid film. Repeat the rehydration and vortexing step to sequentially add 50, 100, 100, 200, 200, and 300 μL (total 1 mL) of water to the flask.
10. The vesicles produced are multilamellar liposomes. Extrusion is needed to convert them into uniform-sized unilamellar liposomes.
11. The extrusion technique produces unilamellar liposomes by physically squeezing the multilamellar liposomes through polycarbonate filters (with appropriately sized pores). The structure (concentric layers) of multilamellar liposomes is physically

unstable under the extrusion pressure and temperature, which is slightly above phase transition temperature (TC). This induces membrane rupture and resealing to create uniform-sized unilamellar liposomes.

12. Ensure all parts of the extruder are thoroughly cleaned and dried before assembly. Wash the extruder kit (except PC membrane and filter supports) with mild soap and rinse three times each using water and methanol. Air-dry all cleaned materials. To pre-wet the filter supports, pipette 5 μL of water into the internal membrane support area within the O-ring before placing the dry filter supports down. Alternatively, place the filter supports directly into water, then transfer them to the correct position within the O-ring.
13. Carefully separate the PC membranes (thin and translucent disk) apart (and from the blue paper, which can be disposed of) using forceps. The PC membranes and filter supports are intended for single-use only and should not be re-used.
14. Do not twist the internal membrane support after it comes in contact with the PC membrane to avoid tearing the membrane.
15. This temperature is above the TC of DPPC and DDAB and is critical for successful extrusion. The temperature of the extruder needs to be above the TC of the composed lipids before the extrusion procedure begins.
16. Ensure both syringes are fully and tightly fitted into the extruder before pushing the plunger. Do not push faster than 1 mL in 30 s. If significant resistance occurs, reduce plunging speed to avoid breaking the membrane or syringe. Do not obstruct or pull the second plunger. Ensure the liposome solution temperature remains above the TC to avoid additional plunger resistance. It is normal for the first few pushes to present greater resistance than subsequent pushes. The smaller the size of the filter pores, the greater the resistance will be (e.g., a 100 nm PC membrane will produce greater resistance than a 400 nm PC membrane). If reverse pressure is experienced when pushing the syringe, check whether there is any air trapped in the syringe. To produce very small liposomes (below 100 nm), initial pre-extrusion of the liposome solution with a larger membrane size is advised.
17. Check how much solution has been transferred to the second syringe after each extrusion (with the aim of 1 mL). However, some dead volume (solution left inside the extruder) typically occurs following the first extrusion round. Solution lost during subsequent rounds indicates that there is a leak in the system. In this case, take apart and re-assemble the apparatus. The PC membrane and filter support need to be replaced when re-assembling the extruder. If the extruder had been assembled

correctly, then the leak likely occurred due to faulty insertion of the syringes into the extruder. When removing the syringes, pull the syringe straight out of the extruder to avoid damage and take note of the position of each syringe on the extruder. The position of these syringes cannot be switched.

18. The final pass should be made into the second syringe (the opposite syringe to the one originally filled) to reduce contamination from the original (unextruded) solution (e.g., larger liposomes that did not pass through the membrane or foreign materials). In general, the liposomes become more homogeneous with every additional pass through the membrane.
19. Disassemble and clean the extruder thoroughly after each use and before extruding new liposome formulations.
20. In general, extruded liposomes have a uniform size distribution with a PDI < 0.1.
21. Appropriate dilution is required before visualization; it is recommended that visualization starts at a 1:10 dilution. Highly concentrated solutions make the visualization of single liposomes difficult, as the liposomes are often pushed together or overlapping.
22. Use clean tweezers to hold the grid edge when adding the diluted liposome solution. Do not let the tweezer tips contact the surface of the grid.
23. Using a piece of filter paper (or kimwipe), gently touch the side of the grid to absorb excess solution. Direct contact with the grid surface is not recommended.

References

1. Giddam AK, Zaman M, Skwarczynski M, Toth I (2012) Liposome-based delivery system for vaccine candidates: constructing an effective formulation. *Nanomedicine* 7 (12):1877–1893. <https://doi.org/10.2217/nmm.12.157>
2. Nordly P, Madsen HB, Nielsen HM, Foged C (2009) Status and future prospects of lipid-based particulate delivery systems as vaccine adjuvants and their combination with immunostimulators. *Expert Opin Drug Deliv* 6 (7):657–672. <https://doi.org/10.1517/17425240903018863>
3. BenMohamed L, Wechsler SL, Nesburn AB (2002) Lipopeptide vaccines—yesterday, today, and tomorrow. *Lancet Infect Dis* 2 (7):425–431. [https://doi.org/10.1016/s1473-3099\(02\)00318-3](https://doi.org/10.1016/s1473-3099(02)00318-3)
4. Abdul Ghaffar K, Kumar Giddam A, Zaman M, Skwarczynski M, Toth I (2014) Liposomes as nanovaccine delivery systems. *Curr Top Med Chem* 14(9):1194–1208
5. Bovier PA (2008) Epaxal®: a virosomal vaccine to prevent hepatitis A infection. *Expert Rev Vaccines* 7(8):1141–1150
6. Marasini N, Ghaffar KA, Skwarczynski M, Toth I (2017) Liposomes as a vaccine delivery system. In: Skwarczynski M, Toth I (eds) *Micro and nanotechnology in vaccine development*. William Andrew, Norwich, pp 221–239
7. Bartlett S, Eichenberger RM, Nevagi RJ, Ghaffar KA, Marasini N, Dai Y, Loukas A, Toth I, Skwarczynski M (2020) Lipopeptide-based oral vaccine against hookworm infection. *J Infect Dis* 221(6):934–942. <https://doi.org/10.1093/infdis/jiz528>
8. Ghaffar KA, Marasini N, Giddam AK, Batzloff MR, Good MF, Skwarczynski M, Toth I (2017) The role of size in development of mucosal liposome-lipopeptide vaccine

- candidates against group A Streptococcus. *Med Chem* 13:22–27
9. Marasini N, Giddam AK, Ghaffar KA, Batzloff MR, Good MF, Skwarczynski M, Toth I (2016) Multilayer engineered nanoliposomes as a novel tool for oral delivery of lipopeptide-based vaccines against group A streptococcus. *Nanomedicine* 11(10):1223–1236. <https://doi.org/10.2217/nmm.16.36>
 10. Marasini N, Ghaffar KA, Giddam AK, Batzloff MR, Good MF, Skwarczynski M, Toth I (2017) Highly immunogenic trimethyl chitosan-based delivery system for intranasal lipopeptide vaccines against group A streptococcus. *Curr Drug Deliv* 14(5):701–708
 11. Nevagi RJ, Dai W, Khalil ZG, Hussein WM, Capon RJ, Skwarczynski M, Toth I (2019) Structure-activity relationship of group A streptococcus lipopeptide vaccine candidates in trimethyl chitosan-based self-adjuvanting delivery system. *Eur J Med Chem* 179:100–108. <https://doi.org/10.1016/j.ejmech.2019.06.047>
 12. Azuar A, Zhao L, Hei TT, Nevagi RJ, Bartlett S, Hussein WM, Khalil ZG, Capon RJ, Toth I, Skwarczynski M (2019) Cholic acid-based delivery system for vaccine candidates against group A streptococcus. *ACS Med Chem Lett* 10(9):1253–1259. <https://doi.org/10.1021/acsmmedchemlett.9b00239>
 13. Eskandari S, Pattinson DJ, Stephenson RJ, Groves PL, Apte SH, Sedaghat B, Chandurudu S, Doolan DL, Toth I (2018) Influence of physicochemical properties of lipopeptide adjuvants on the immune response: a rationale for engineering a potent vaccine. *Chem Eur J* 24(39):9892–9902
 14. Schulze K, Ebensen T, Chandurudu S, Skwarczynski M, Toth I, Olive C, Guzman CA (2017) Bivalent mucosal peptide vaccines administered using the LCP carrier system stimulate protective immune responses against *Streptococcus pyogenes* infection. *Nanomed Nanotechnol Biol Med* 13(8):2463–2474
 15. Bartlett S, Skwarczynski M, Toth I (2020) Lipids as activators of innate immunity in peptide vaccine delivery. *Curr Med Chem* 27(17):2887–2901. <https://doi.org/10.2174/0929867325666181026100849>
 16. Chandurudu S, Skwarczynski M, Pattinson D, Apte SH, Doolan DL, Toth I (2016) Synthesis and immunological evaluation of peptide-based vaccine candidates against malaria. *Biochem Compound* 4(1):6
 17. Hussein WM, Xu J, Simerska P, Toth I (2017) Synthesis of multicomponent peptide-based vaccine candidates against group A streptococcus. *Aust J Chem* 70(2):184–190
 18. Bartlett S, Skwarczynski M, Xie X, Toth I, Loukas A, Eichenberger RM (2020) Development of natural and unnatural amino acid delivery systems against hookworm infection. *Precision Nanomed* 3(1):471–482
 19. Fuaad AA, Pearson MS, Pickering DA, Becker L, Zhao G, Loukas AC, Skwarczynski M, Toth I (2015) Lipopeptide nanoparticles: development of vaccines against hookworm parasite. *ChemMedChem* 10(10):1647–1654. <https://doi.org/10.1002/cmdc.201500227>
 20. Dougall AM, Skwarczynski M, Khoshnejad M, Chandurudu S, Daly NL, Toth I, Loukas A (2014) Lipid core peptide targeting the cathepsin D hemoglobinase of *Schistosoma mansoni* as a component of a schistosomiasis vaccine. *Hum Vaccin Immunother* 10(2):399–409. <https://doi.org/10.4161/hv.27057>
 21. Ahmad Fuaad AA, Roubille R, Pearson MS, Pickering DA, Loukas AC, Skwarczynski M, Toth I (2015) The use of a conformational cathepsin D-derived epitope for vaccine development against *Schistosoma mansoni*. *Bioorg Med Chem* 23(6):1307–1312. <https://doi.org/10.1016/j.bmc.2015.01.033>
 22. Watkins DA, Johnson CO, Colquhoun SM, Karthikeyan G, Beaton A, Bukhman G, Forouzanfar MH, Longenecker CT, Mayosi BM, Mensah GA, Nascimento BR, Ribeiro ALP, Sable CA, Steer AC, Naghavi M, Mokdad AH, Murray CJL, Vos T, Carapetis JR, Roth GA (2017) Global, regional, and national burden of rheumatic heart disease, 1990–2015. *N Engl J Med* 377(8):713–722. <https://doi.org/10.1056/NEJMoa1603693>
 23. Abdel-Aal AB, Batzloff MR, Fujita Y, Barozzi N, Faria A, Simerska P, Moyle PM, Good MF, Toth I (2008) Structure-activity relationship of a series of synthetic lipopeptide self-adjuvanting group a streptococcal vaccine candidates. *J Med Chem* 51(1):167–172. <https://doi.org/10.1021/jm701091d>
 24. Zaman M, Abdel-Aal AB, Fujita Y, Ziora ZM, Batzloff MR, Good MF, Toth I (2012) Structure-activity relationship for the development of a self-adjuvanting mucosally active lipopeptide vaccine against *Streptococcus pyogenes*. *J Med Chem* 55(19):8515–8523. <https://doi.org/10.1021/jm301074n>
 25. Ghaffar KA, Marasini N, Giddam AK, Batzloff MR, Good MF, Skwarczynski M, Toth I (2016) Liposome-based intranasal delivery of lipopeptide vaccine candidates against group A streptococcus. *Acta Biomater* 41:161–168. <https://doi.org/10.1016/j.actbio.2016.04.012>



Current Prospects in Peptide-Based Subunit Nanovaccines

Prashamsa Koirala, Sahra Bashiri, Istvan Toth,
and Mariusz Skwarczynski

Abstract

Vaccination renders protection against pathogens via stimulation of the body's natural immune responses. Classical vaccines that utilize whole organisms or proteins have several disadvantages, such as induction of undesired immune responses, poor stability, and manufacturing difficulties. The use of minimal immunogenic pathogen components as vaccine antigens, i.e., peptides, can greatly reduce these shortcomings. However, subunit antigens require a specific delivery system and immune adjuvant to increase their efficacy. Recently, nanotechnology has been extensively utilized to address this issue. Nanotechnology-based formulation of peptide vaccines can boost immunogenicity and efficiently induce cellular and humoral immune responses. This chapter outlines the recent developments and advances of nano-sized delivery platforms for peptide antigens, including nanoparticles composed of polymers, peptides, lipids, and inorganic materials.

Key words Vaccination, Pathogens, Subunit vaccine, Peptides, Immunogenicity, Nanotechnology, Adjuvants, Nanoparticles

1 Introduction

A vaccine is a biological (or, as per recent advances, chemical) preparation that provides or enhances immunity to a particular disease in individuals. Vaccines are composed of whole pathogens or antigens that are derived from them. Upon delivery (“vaccination”), the vaccine triggers immune responses against the pathogen/antigen and generates immunological memory.

The concept of vaccination was reported for the first time in China in the tenth century [1]. It was noted that people who recovered from smallpox were subsequently immune to future infection [2]. As a result, healthy subjects were inoculated with fragments collected from dried pus or scabs of an infected person. This resulted in severe illness and a high mortality rate within the inoculated individuals. Later, Edward Jenner observed that

dairymaids were naturally immune to smallpox after being infected with cowpox [3]. To further confirm this observation, he inoculated a child with cowpox lesions, discovering a means of safely conferring immunity to smallpox. Vaccines have since been developed against several life-threatening diseases, such as rabies, polio, diphtheria, mumps, and rubella. However, vaccines are not yet available against highly variable microorganisms that require the stimulation of cell-mediated and mucosal immunity. Thus, an investigation into new classes of vaccines has moved to the forefront of medical research [4].

Traditional vaccines consist of attenuated or weakened microorganisms, which upon administration invoke immune responses without causing the actual disease. Conventional vaccines are effective in inducing immune responses; however, their application is associated with risks of infection, allergies, and autoimmune responses. In addition, difficulties around manufacturing pathogens and their limited stability have led to the development of subunit vaccines. Subunit vaccines utilize a purified antigen, such as a toxoid, subcellular fragments, proteins, and peptides. The likelihood of side effects is minimized as a variety of toxins and undesired immunogens are abolished in these vaccines [5–7].

Recently, it has been shown that not only the biochemical composition (antigen and adjuvant/immune stimulator) of the vaccine, but morphology and particle size also play important roles in providing desired immune responses. The small size, customizable surface, multifunctionality, and targeting properties of nanoparticles (NPs) can be utilized to greatly improve vaccine immunogenicity. However, an understanding of the mechanisms by which the immune system is activated is vital for developing effective nanovaccines [8–10].

2 Immune Response

The human immune system is a complex and powerful defense mechanism composed of organs, cells and molecular components designed to fight infection [11]. The immune system can be classified into two general categories, namely the innate/general resistance system and the adaptive system. The innate immune system covers all aspects of a host's immune defense mechanisms, which include physical barriers, dendritic cells, macrophages, neutrophils, and natural killer cells. Neutrophils and macrophages have the most important role during early infection [12]. They secrete highly destructive substances, including enzymes that digest proteins and reactive chemicals, such as peroxide. They then engulf and digest destructed pathogens by a process called phagocytosis. Furthermore, antigen-presenting cells (APCs), such as dendritic cells (DCs) and macrophages, recognize and bind to

pathogen-associated molecular patterns (PAMPs), known also as danger signals, which are produced by microbes [13]. Once the PAMPs are recognized, pattern recognition receptors (PRRs) signal the presence of infection to the host [14]. PRRs also detect damage-associated molecular patterns (DAMPs), which are produced by damaged or mutated host cells. After binding to their appropriate PAMP or DAMP, APCs internalize their target by initiating phagocytosis, pinocytosis, or endocytosis, then process it into peptides. The peptides are presented to major histocompatibility complexes (MHC, class I or class II) [15–17]. MHC I receptors are produced by all nucleated cells and display intracellular antigens, for example, from a viral infection, to activate CD8⁺ T-cells. These T-cells, known as killer T-cells, directly kill infected cells. In contrast, MHC II receptors are produced only by APCs and display extracellular antigens and activate CD4⁺ T-cells, which proliferate and differentiate, resulting in T-helper 1 (Th1) or Th2 cells. Th1 cells mainly activate CD8⁺ T-cells and deliver cell-mediated immunity through the release of cytokines, like interferon- γ (IFN- γ) and tumor necrosis factor- α (TNF- α). Th2 cells interact with B-cells, which further differentiate into plasma cells that secrete antibodies against specific antigens; B-cells also differentiate into memory cells that are responsible for creating immunological memory. An antigen can travel (by itself, or with the help of peripheral APCs) to lymph nodes, where most of the adaptive immune cells reside [9, 18, 19] (Fig. 1).

3 Peptide-Based Subunit Vaccines

Minimal epitopes, i.e., short peptides derived from the larger pathogenic component, such as B-cell receptors, and MHC class I and II ligands, carry all of the necessary immunological information needed to trigger adaptive immune responses when innate immunity is activated with the help of an immune stimulant/adjuvant [20, 21]. By employing such epitopes as antigens, the risk of allergic responses and cross-reactivity with human tissue can be essentially eliminated. Further, the peptide-based approach can be less expensive in terms of production and handling, and these vaccines are normally much more stable during storage and transportation [5]. Peptide antigens can be synthesized as desired by chemical synthesis and, therefore, are devoid of biological contamination. Solid-phase peptide synthesis using automatic synthesizers and the application of microwave techniques have made production easier, faster, and cost-effective. Produced antigens are stable and water-soluble, and their stability and properties can be monitored via standard physicochemical characterization methods [22, 23]. Peptide-based vaccines can consist of multiple peptide antigens, which can target several pathogen strains, giving them

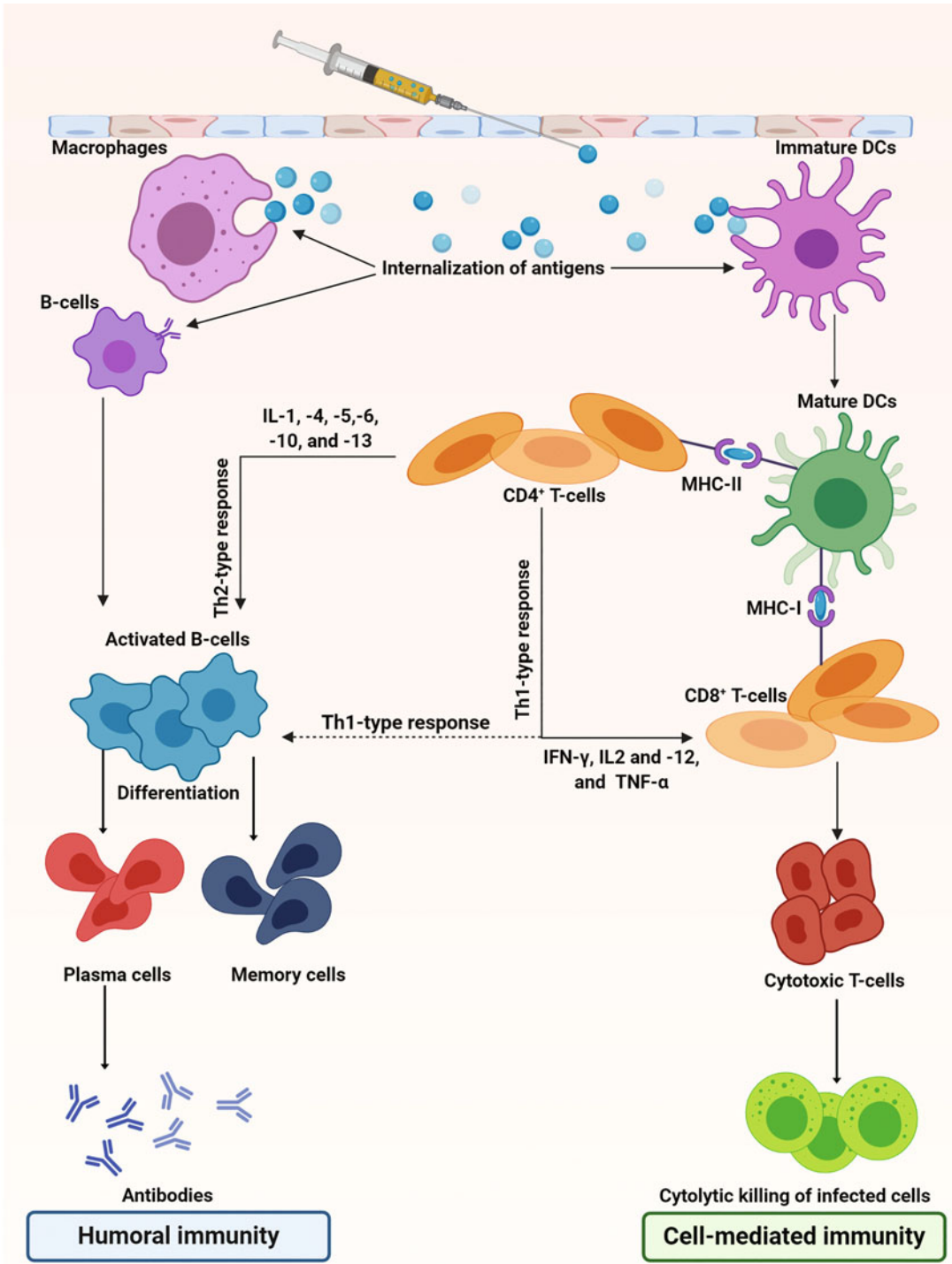


Fig. 1 Simplified diagram illustrating the main immune response pathways

wider scope in inducing immunity over a broad-spectrum of infections [24]. However, peptide antigens are very poor immunogens on their own. To boost the efficacy of peptide-based subunit vaccines, an immunostimulatory element (adjuvant and/or delivery system) is vital [25–27]. While immunostimulants can enhance immunity, their use is often associated with side-toxicity [28]. Also, some commercial adjuvants (e.g., alum) only elicit humoral immunity and are weak cellular immunostimulants. Considering the obstacles associated with peptide-based subunit vaccines, the development of new immunostimulatory elements is needed [29]. Nanoparticle-based delivery systems have recently been developed and are very effective, particularly for peptide antigens [9, 30] (Fig. 2).

4 Nanotechnology

Nanotechnology incorporates the manufacture, control, manipulation, and study of structures or devices with a size on the nanometer scale (NPs, nanorods, etc.) [31]. Either synthetically or biologically derived, nano-materials have a similar size to invading microorganisms and, therefore, can mimic some of the properties of the pathogens. The small size, surface customizability, improved solubility, and multifunctionality of NPs open new avenues for vaccine design. NPs are taken up by cells, most importantly including APCs, more efficiently than soluble molecules and large particles and, therefore, could be used as effective transport and delivery systems for antigens [32, 33].

NPs have been widely explored for drug delivery systems. Delivery systems, like lipid-based formulations, polymers, dendrimers, and inorganic NPs, are often employed in chemotherapy. They are used to increase drug concentration at a desired site in the body [34]. The ability of NPs to be picked up by phagocytic cells of the immune system (e.g., macrophages) is typically considered to be an undesirable attribute for drug delivery, as this can induce immunostimulation effects, which may promote inflammatory or autoimmune disorders and the host's susceptibility to infections and cancer. However, in contrast to drug delivery, this outcome is highly desirable for vaccines.

NPs can be designed to elicit an immune response by either direct immunostimulation of APCs (e.g., macrophages) or delivery of the antigen to a specific cellular compartment (e.g., lymph nodes). The use of NPs in vaccine formulations allows not only improved antigen stability and immunogenicity but also targeted delivery and slow release [35]. NP-based delivery systems can also reduce side-effects associated with vaccine formulations (e.g., toxicity of adjuvant) [36]. Indeed, several prophylactic nanovaccines have been approved for human use, for example, Mosquirix [37]

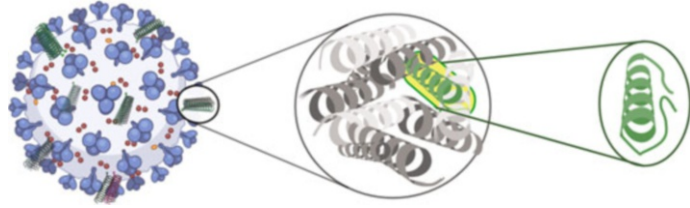


Fig. 2 Schematic diagram of the evolution of vaccine components, from traditional pathogens to protein-based subunits, then peptide-based subunits

and Inflexal [38], and others, such as Novavax [39], Norwalk [40], and various chimeric virus-like particles, are in clinical or preclinical trials. NPs are attractive system for vaccine delivery as they can (a) accommodate multiple peptide epitopes, adjuvants, and targeting moieties; (b) protect peptides from enzymatic degradation and excretion; (c) allow them to travel in the lymphatic system; (d) stimulate uptake by APCs; and (e) induce antigen cross-presentation to cytotoxic T lymphocytes (CTL) [41].

Nanosized particles can also be used for oral administration. They are capable of delivering a sufficient amount of an antigen to the target site and protecting the antigen from the extreme pH of the stomach and proteolytic degradation [42]. Nasal administration of vaccine is often desirable, though, as it increases patient compliance and triggers both mucosal and systemic immunity. NPs with mucoadhesive properties are especially effective for vaccine delivery [43]. Larger NPs incorporating antigen can exert a local depot effect, ensuring prolonged antigen presentation to immune cells [44]. Smaller NPs can be taken up by the lymphatic system and reach the lymph nodes, where most immune cells reside [45]. In addition, NPs, such as carbon nanotubes, carbon black NPs, poly (lactic-co-glycolic acid) (PLGA) and polystyrene NPs (PSNPs), have been reported to have immunomodulatory activity [46]. Thus, NPs are useful for the formulation and delivery of antigens by offering improved stability, sustained release kinetics, lower immunotoxicity, and targeting of specific immune cells (Fig. 3).

5 Polymer-Based Nanoparticles

Polymer NPs have been a focus of interest for drug/vaccine delivery due to their customizable physicochemical properties, controllable stability in vivo, relative safety, and high efficacy of cargo delivery to desired cells/tissues. These NPs can (a) have adjustable properties (size, composition, surface characteristics); (b) allow controlled drug/vaccine release; (c) be used for both therapy and imaging (theranostics); and (d) protect cargo against degradation.

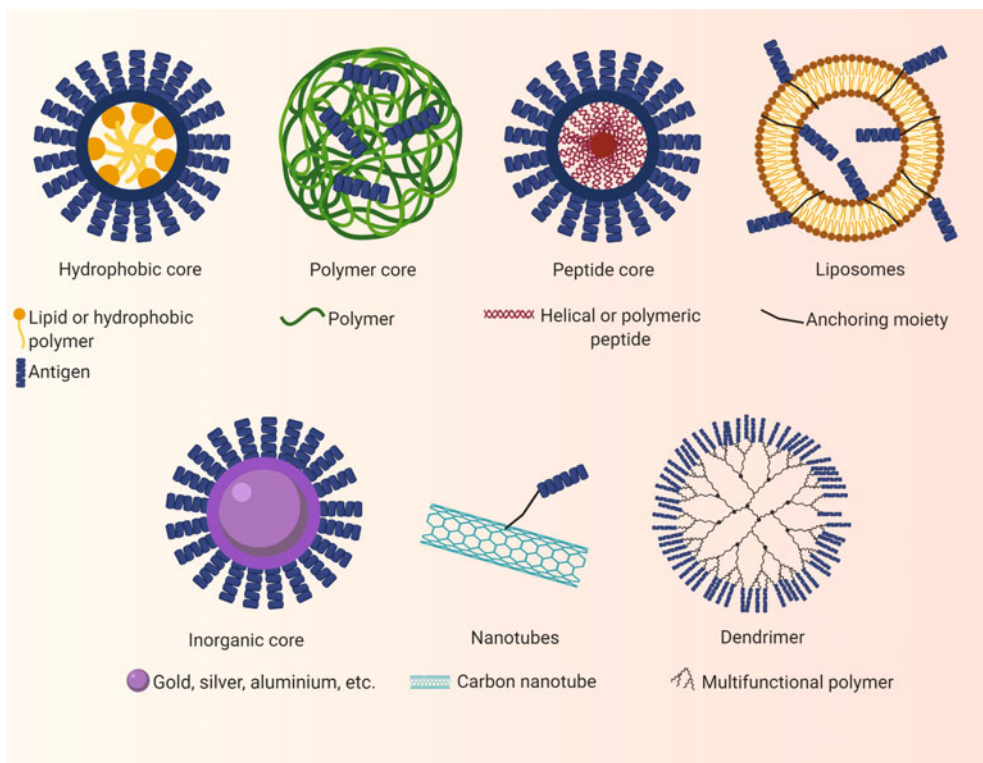


Fig. 3 Examples of nanoparticle-based antigen delivery systems

Some polymer-based nanosystems offer mucoadhesive properties that reduce rapid mucociliary clearance and provide an increased period of contact with the nasal mucosa, allowing efficient drug/antigen absorption. NPs and nanocomposites are widely used for the controlled release of active cargo at a desired time and location. Polymer-based NPs are usually 10–500 nm in diameter, with bioactive materials internalized through dissolving, wrapping, adsorption, and/or adhesion on the surface or inside the particles [47].

Plebanski and coworkers investigated polystyrene NPs (PSNPs) for vaccine delivery using ovalbumin (OVA)-derived peptide epitopes [48]. Multiple copies of OVA were conjugated to the surface of beads of different sizes (20, 40, 100, 500, 1000, and 2000 nm). PSNPs (40 nm) elicited higher antibody titers and stimulated stronger CTL responses than other nanobeads and conventional adjuvants, including alum, MPLA, and Quil A. Moreover, OVA-derived peptide epitopes were conjugated to narrow-sized beads in the range of 20, 40, 50, 70, 90, 100, and 120 nm; the 40–50 nm beads induced significantly higher IFN- γ response from CD8⁺ T-cells, while 90–120 nm PSNPs induced CD4⁺ T-cell activation and IL-4 induction [49]. The 50 nm NPs were effective in delivering vaccines against malaria [50] and cancer [51].

PLGA, a polymer ester of two α -hydroxyacids (lactic and glycolic acids), is one of the most frequently used biodegradable polymers for drug delivery. It has an excellent safety profile and has been FDA-approved for pharmaceutical formulations [52]. Silva et al. formulated PLGA NPs using long synthetic antigenic peptides (24 amino acids) to cover a CTL epitope of ovalbumin (SIINFEKL) as a model antigen. The peptide-loaded PLGA NPs were prepared by double emulsion/solvent evaporation. Sixteen different types of PLGA NPs were prepared with sizes ranging from 210 nm to 600 nm. PLGA-loaded NPs with an average size of 370 nm had the highest encapsulation efficiency and induced cellular immunity most efficiently, as demonstrated by the enhancement of CD8⁺ T-cell activation in vitro [53]. The same group also compared the immune stimulatory efficacy of the PLGA-NPs with PLGA-microparticles (MPs) [54]. PLGA NPs (average diameter 350 nm) and MPs (110 μ m) co-encapsulating OVA and poly(I:C) adjuvant, with comparable antigen release characteristics, were formulated. The NPs were efficiently taken up by DCs, generated the highest antigen-specific CTL responses, and induced balanced Th1/Th2-type antibody responses. In contrast, MPs were not taken up by APCs and failed to trigger IgG and CTL responses, suggesting that particles in the nano, rather than micro, size range are desirable for vaccine design. PLGA NPs have also been found to be effective for the delivery of anticancer vaccine [55]. STEAP326-335 peptide (DVS₃₂₆KINRTEM₃₃₅)-loaded PLGA NPs (370 nm) improved survival rate and significantly reduced tumor growth compared to STEAP peptide emulsified in incomplete Freund's adjuvant (IFA) following intravenous injection in mice. Tumor inhibition was attributed to the induction of a stronger CD8⁺ T-cell immune response when compared with controls. Kabiri and coworkers produced PLGA NPs encapsulating human T-cell lymphoma virus epitopes and Toll-like receptor (TLR)-9 agonist, CPG oligonucleotide, as an adjuvant (170 nm, -34 mV) [56]. The NPs elicited potent cell-mediated and mucosal immunity without inflammatory responses when injected in mice. The titers of IgG1, IgG2a, and sIgA antibodies, as well as IL-10 and IFN- γ cytokines, were elevated and the amount of TGF- β 1 production was reduced in comparison to PLGA nanospheres having the same particle size and charge, but lacking CPG. Therefore, the incorporation of an additional adjuvant into these NPs further improved their efficacy.

Interestingly, the method of antigen incorporation into PLGA NPs also plays an important role in efficacy. PLGA encapsulating or coated with lipopeptide vaccine LCP-1 [57] consisting of B-cell epitope derived from group A streptococcus (GAS) M protein and universal T-helper cell epitope produced NPs (200 nm, 8 mV) or (220 nm, -5 mV), respectively [58]. NPs encapsulating LCP-1 were taken up more efficiently by APCs and induced a higher

expression of maturation marker CD80 compared to the coated NPs. NPs that encapsulated antigen also induced much higher IgG and IgA titers upon intranasal administration, despite the fact that all particles carried the same amount of antigen. Unfortunately, the negative charge of PLGA particles is a disadvantage for particle uptake and the preparation process must be tailored to the properties of the antigen [59]. Further, antigen degradation may occur during preparation, storage, and release. Therefore, a variety of other polymers have been examined as alternatives to PLGA for vaccine delivery.

Chitosan, a polymer of glucosamine, is a natural, biodegradable polysaccharide with mucoadhesive properties [60]. It is usually obtained from the deacetylation of chitin. Chitosan is recognized by different receptors on APCs, including TLR-2, leukotriene B₄, and mannose receptors. Chitosan is a common nanocarrier used for the delivery of therapeutic agents [61]. Chitosan NPs have been used in numerous studies to deliver antigens to APCs and to stimulate mucosal immunity [62]. Despite the many benefits of chitosan, it is notably limited by its insolubility and precipitation at physiological pH [63]. To overcome these problems, chitosan derivatives, such as trimethyl chitosan (TMC), have been synthesized. TMC, formed by the methylation of chitosan amino groups (quaternization), has been widely investigated for vaccine delivery because of its stronger adjuvanting activity compared to chitosan, which is likely due to its permanent cationic charge and excellent water-solubility [64]. Akbari et al. loaded *Shigella flexneri*'s recombinant IpaD antigen into TMC NPs (270 nm). Following both oral [65] and intranasal [66] administration, high titers of IpaD-specific serum IgG and IgA were observed.

Polyelectrolyte (PEC)-based platforms are often used to combine positively charged chitosan derivatives with antigen [67]. Positively charged lipopeptide vaccine, LCP-1, bearing conserved B-cell epitope (J8) derived from GAS M-protein, was mixed with various anionic polymers, including alginate, chondroitin sulfate, dextran, hyaluronic acid, and heparin, to form PECs [57]. These PECs were further coated with TMC to form NPs with similar size (~200 nm) and charge (~30 mV) [68]. Among them, LCP-1 mixed with heparin and coated with TMC induced the strongest humoral immune responses, especially high IgA titers, in outbred mice. It was predicted that the negatively charged polymers assisted in eliciting immune responses, in addition to functioning as complexing agents. A TMC-based delivery system has also been combined with PLGA [69]. Four different NPs were produced by double-emulsion solvent evaporation: LCP-1/dextran (150 nm, -38 mV), LCP-1/dextran/TMC (300 nm, 39 mV), LCP-1/dextran/PLGA (190 nm, -31 mV), and LCP-1/dextran/PLGA/TMC (190 nm, 10 mV). LCP-1/dextran and LCP-1/dextran/TMC were taken up more efficiently by DCs; however, of the four NPs, only

TMC-bearing NPs, LCP-1/dextran/TMC and LCP-1/dextran/PLGA/TMC, stimulated the maturation of DCs and induced a high level of IgA and IgG titers following intranasal administration. In addition, LCP-1/dextran/TMC effectively opsonized GAS clinical isolates. Thus, NPs carrying mucoadhesive TMC and positive charge were the most effective against GAS.

TMC has also been used to develop oral vaccine delivery systems [70]. LCP-1 was anchored through its lipid moieties to liposomes, which were further coated by layers of alginate and TMC. Alginate/TMC-coated positively charged liposomes (180 nm, 27 mV) were promptly taken up by APCs, compared to negatively charged liposomes bearing alginate on the surface. Alginate/TMC liposomes produced significantly higher, long-lasting, antigen-specific mucosal IgA, and systemic IgG titers compared to lipopeptide antigen alone and NPs coated with negatively charged polymer. However, multiple oral immunizations with a high dose of antigen were required to stimulate humoral immunity.

To simplify the formulation and avoid the use of liposomes and extensive coating, antigen itself has been modified with a negatively charged inert polymer [71]. Cationic TMC-NPs (200 nm) were produced by the conjugation of a short-length anionic polymer, poly-L-glutamic acid (PGA), to GAS J8 epitope and universal T-helper epitope, PADRE, followed by assembly of the conjugate with TMC by ionic interactions. PGA-J8-PADRE/TMC NPs induced significantly higher serum IgG and mucosal IgA antibody titers against J8 antigen, compared with antigen mixed with the commercial mucosal adjuvant, cholera toxin subunit B (CTB), following intranasal immunization. The incorporation of PGA was vital for immunological activity, as simply mixing epitopes with TMC did not elicit strong immune responses. Moreover, it was demonstrated that (a) the optimal length of PGA was 10 units; (b) glutamic acid can be replaced with aspartic acid; (c) fungal TMC was most effective; (d) lipidation of antigen further enhanced humoral immune responses; and (e) rod NPs were more efficient than spherical NPs [72, 73].

Recently, particle self-assembly has been widely applied for vaccine delivery [74]. Self-assembled nanoarchitectures can improve biocompatibility and provide stability against enzymatic degradation, encapsulation of hydrophobic drugs, sustained drug release, shear-thinning viscoelastic properties, and/or adjuvanting properties [75]. The first example of self-assembled, self-adjuvanting polymer peptide antigen conjugate was reported in 2010 [76]. Hydrophobic dendritic poly(*tert*-butyl acrylate) was conjugated with hydrophilic B-cell epitope J14 derived from GAS M-protein. The resulting amphiphilic conjugate was self-assembled into NPs (20 nm), which triggered the production of high levels of opsonic J14-specific IgG antibody titers similar to those triggered by the delivery of J14 epitope adjuvanted with CFA, following both

subcutaneous and intranasal immunizations [77]. It was also demonstrated that (a) single immunization was efficient to stimulate high antibody titers; (b) smaller particles (20 nm) were much more effective than larger particles (400 nm) [78]; and (c) an exchange of dendritic polymer to star, branched, or linear polyacrylate did not significantly reduce the immunogenicity of conjugates [79]. Importantly, PADRE-J8 polyacrylate conjugate (146 nm) was able to induce the production of high levels of opsonic antibody titers following single oral low-dose immunization [42].

The above strategy was also applied for the design of therapeutic vaccine against cervical cancer [79]. 8Qmin peptide epitope derived from human papillomavirus (HPV)-6 E7 oncogenic protein containing CTL epitope and T-helper cell epitope was conjugated to a variety of poly(*tert*-butyl acrylate) forming microparticles (~10 μ m) [80, 81]. All conjugates stimulated therapeutic immunity in tumor-bearing mice. Vaccination significantly improved mouse survival and reduced tumor growth when compared with 8Qmin emulsified with commercial adjuvant, Montanide (humanized version of IFA). In addition, all conjugates were efficiently taken up by DCs and macrophages and stimulated significant CD8⁺ and CD4⁺ T-cell activation [82]. The dendritic polyacrylate was more effective than branched or linear versions. Vaccine candidates lost their efficacy when used to treat more advanced tumors; however, this efficacy was restored when the conjugates were incorporated into liposomes [83]. The enhanced efficacy of the liposomal formulation was most likely related to its smaller size (~130 nm) compared to the self-assembled conjugate, itself (~10 μ m) [84].

Polyacrylates are considered to be safe polymers; however, they are not biodegradable and have undefined stereochemistry and number of units per polymer. To overcome these shortcomings, fully defined and biodegradable polymers built from natural hydrophobic amino acids (HAAs) were synthesized using simple automated solid-phase peptide synthesis [85]. J8-PADRE was incorporated into a polyHAA sequence built based on valine, phenylalanine, and leucine. The resulting amphiphilic compounds were self-assembled into nanoparticles (10–30 nm), which aggregated in larger chain-like aggregates. NPs based on leucine induced the maturation of APCs *in vitro* and triggered the production of high titers of opsonic antibodies in mice. In addition, they greatly reduced the bacterial burden in mice challenged with the M1 GAS strain without inducing potentially damaging soluble inflammatory mediators. Upon conjugation to hookworm epitope, the poly-leucine system (~100 nm) was also effective in inducing protective immune responses in orally vaccinated, hookworm-challenged mice [86].

6 Self-assembled Peptides

Self-assembled peptides offer the advantages of compatible, multi-valent nanomaterials with lower toxicity, and the ability to adopt desired conformations [74]. For example, valine-rich peptides, or polyvalines, are known to adopt β -sheet conformation and aggregate into fibrils. Valine-rich peptide containing serine moieties linked with amino acids by ester bond (depsipeptide, isopeptide) was conjugated by azide alkyne cycloaddition with B-cell peptide epitope [87]. The conjugates were able to adopt β -sheet conformation and self-assembled to form fibrils upon pH-triggered intramolecular acyl migration, while their O-acyl isoforms were stable in the non-aggregative form. This strategy addressed potential issues related to over-aggregation, precipitation, and changes in other properties during storage of fibril-based vaccines.

Colliers and coworkers examined nanofibers, NPs, and gels that were stabilized by non-covalent forces (hydrophobic interactions, hydrogen bonding, and electrostatic interactions) for vaccine design, to avoid the use of classical, potentially toxic adjuvants [88]. Early secretory antigenic target (ESAT-6) peptide epitope derived from *Mycobacteria tuberculosis* (TB) ESAT-6 protein or OVA was conjugated with fibril-promoting sequence Q11 (QQK FQFQFEQQ) [89]. Both the self-assembled peptides (ESAT-Q11 and OVA-Q11) formed fibrils (20 nm thick and >1000 nm length) and induced elevated Ig titers and IFN- γ secretion in mice. They also demonstrated that immunogenicity is not related to specific Q11 peptide sequence, as the other fibrillizing peptide, KFE8 (FKFEFKFE), also induced high antibody responses [90]. Even in the absence of adjuvant, this system resulted in comparable antibody responses to peptide epitope delivered with CFA in mice [91].

KFE8 was also used to deliver cocaine vaccine, which assembled into β -sheet-rich nanofibers in aqueous buffers [92]. The vaccine produced high titers of anticocaine antibodies in vaccinated mice, without the need for an adjuvant. The Q11 system has also been used to treat/prevent malaria [93], influenza [94], and cancer [95]. A fibril system based on α -helical structure was also examined. α -Helical peptide Coil29 was conjugated to PADRE and cancer B-cell epitope PEPvIII to elicit durable epitope-specific antibody responses that were higher than CFA-adjuvanted formulation [96].

7 Lipid-Based Nanoparticles

Many biological structures are lipidated. Pathogen-associated lipoprotein and liposaccharide are often recognized as danger signals through the activation of APC receptors, mainly TLR-2 and TLR-4

[97]. Tripalmitoyl-S-glycerol cysteine (Pam₃Cys) is a synthetic analog of the N-terminal moiety of lipoproteins of Gram-negative bacteria. Pam₃Cys is comprised of three palmitic acid groups that are bound via glycerol ester and amide linkage to a cysteine residue [98]. Due to its poor water solubility, Pam₃Cys is usually used in conjugation with lysine solubilizing moiety as Pam₃Cys-Ser-(Lys)₄ [99]. R-configured Pam₃Cys-Ser-(Lys)₄ was shown to be more effective at inducing cytokine and antibody production in mice when administered with antigen [100]. Although showing strong adjuvanting ability, Pam₃Cys and its conjugates are poorly soluble and difficult to formulate [101]. Therefore, the hydrophilic analog of Pam₃Cys, Pam₂Cys, derived from macrophage-activating lipopeptide-2 of *Mycoplasma fermentans*, was extensively investigated [102, 103].

Pam₃Cys and Pam₂Cys were conjugated with eight GAS M protein-derived epitopes yielding two lipopolypeptides (<200 nm) [104]. Mice immunized subcutaneously with Pam₂Cys or Pam₃Cys lipopolypeptides demonstrated faster increases in serum J14-specific IgG antibody levels compared to mice immunized with alum-adjuvanted polypeptide formulation. The produced antibodies recognized a variety of clinically relevant GAS serotypes. Pam₂Cys was also conjugated to peptide epitopes derived from HPV. Only the conjugates that formed submicron sized particles (0.3–0.8 μm) triggered antitumor immune responses.

Other lipids have also been examined for immune stimulating activity. Tirrell's group showed that peptide amphiphile can form NPs with self-adjuvanting capacity [105]. J8 epitope derived from GAS M protein was covalently coupled to hydrophobic dipalmitoylglutamic acid (diC16), forming J8-diC16 amphiphilic conjugate, which self-assembled into nanofibers (approximately 5–15 nm in diameter and 0.2–2 μm in length). The nanofibers induced significantly higher IgM production compared to antigen adjuvanted with IFA. Lipopeptide J8-diC16 was not recognized by TLR-2, suggesting that nanostructure plays a crucial role in immune stimulation, but not lipid recognition by TLR. J8-diC16 was also co-self-assembled with Pam₂Cys-Ser-(Lys)₄ to form NPs (5–15 nm) that enhanced the delivery of antigens and adjuvant to the lymph nodes, significantly improving systemic and mucosal antibody responses in mice [106].

The capacity of lipopeptides, such as lipid core peptides (LCPs), to stimulate immune responses has been known for decades; however, their ability to form self-adjuvanting nanoparticles has only recently been recognized [25]. LCP systems contain a non-microbial lipopeptide adjuvant based on lipoamino acids (α-amino acids with a long alkyl side-chain) and a polylysine branching scaffold, which provides conjugation sites for the peptide epitopes [107]. LCP has been used for the delivery of a variety

of peptide-based vaccines against malaria [108], GAS [58], Schistosoma [109], and hookworm [110]. When the three different hookworm APR-1 protein-derived peptides covering the same B-cell epitope were incorporated into LCP, they self-assembled into NPs (<100 nm) [111]. These NPs induced the production of high levels of peptide-specific IgG antibodies, similar to those induced by CFA-adjuvanted peptide antigens. Importantly, only long peptides that adopted β -sheet conformation upon conjugation to LCP (<30 nm) stimulated the production of antibodies that recognized parent APR-1 protein. Thus, it was suggested that B-cell epitope conformation is crucial to stimulating proper immune responses.

The size and orientation of LCP components in nanoparticle formation and immunogenicity were also examined. LCP vaccine candidates were designed to incorporate J14 B-cell and P25 Th-cell epitopes with varying lengths of lipoamino acid C16 (2-amino-D,L-hexadecanoic acid) and C20 (2-amino-D,L-eicosanoic acid), and their spatial orientation [112]. While neither the length of lipoamino acid side chains nor their position in the conjugate influenced the size of the NPs formed (~10 nm), C20-bearing LCP induced stronger antibody responses than other LCPs and CTB-adjuvanted antigen following intranasal immunization. This enhanced adjuvanting activity may be correlated to TLR recognition of longer lipids, instead of nanoparticle size. On the other hand, the size of lipopeptide nanoparticles was reported to be crucial for the induction of strong immune responses [113]. Three lipopeptide vaccine delivery systems incorporating 88/30 and J14 GAS peptide epitopes were produced with varying particle size. The smallest NPs (10 nm) induced significantly higher antigen uptake by APCs, APC maturation, and higher J14 and 88/30 antibody titers compared to its larger analog (100 nm). In addition, these NPs induced antibody responses without the need for additional adjuvant.

LCP conjugates bearing respiratory syncytial virus F-protein-derived B-cell epitope formed nanoparticles (<200 nm) and induced strong humoral immune responses [114]. However, the antibodies produced did not neutralize the virus, reinforcing that the formation of NPs does not always correlate with vaccine efficacy. Interestingly, when LCP was replaced with the human bile salt, cholic acid (CA), to form conjugated CA-PADRE-J8 (130 nm, 21 mV), the conjugate was able to self-assemble into NPs and induced high titers of antibodies, which were opsonic against several GAS clinical isolates [115].

While lipidation is a popular strategy for inducing stronger immune responses against peptide-based antigens, liposomes are an even more popular system to deliver any type of vaccines, including peptide-, protein-, and also whole pathogen-based vaccines (e.g., malaria parasites) [116–119]. These lipid-based particles are biocompatible and biodegradable and can be recognized by

TLRs (TLR-2 or -4 recognizing lipidic ligands) [120]. The first use of liposomes to raise the immune response to loaded antigen was reported by Allison in 1974 [121]. Liposomes and liposome-derived nanovesicles, such as archaeosomes and virosomes, have become important carrier systems for antigen delivery because they can (a) protect antigen from enzymatic degradation; (b) are preferentially taken up by APCs due to their size, charge, and presence of anchoring targeting moieties/proteins; (c) carry antigen on their surface or encapsulate it; (d) incorporate adjuvants in the same particle as the antigen; (e) form a depot effect or travel in the lymphatic system; (f) form stable formulations due to lipid bilayers; and (g) overcome biological barriers, such as skin and mucosa [119].

Jaafri and coworkers demonstrated the importance of liposomal formulations in antitumor therapy for breast cancer. They conjugated [122] or encapsulated [123] the CD8⁺ epitope, P5, derived from HER2/neu protein into liposomes. HER2/neu is the growth factor receptor 2 overexpressed in 20–40% of primary breast cancers. Liposomes were composed of dimyristoylphosphatidylcholine (DMPC), dimyristoylphosphoglycerol (DMPG), and cholesterol. The liposomal formulation containing conjugated P5 and MPLA adjuvant (130 nm, -45 mV) induced higher levels of IFN- γ and higher CTL responses than liposomal formulations without MPLA. The immune responses were further enhanced when more stable liposomes were applied (built from lipids with higher phase transition temperature) [124].

To further improve the efficacy of liposomes for vaccine delivery, another delivery system was developed [125]. CAF01 is a two-component liposomal delivery system composed of a cationic liposome vehicle (dimethyldioctadecyl-ammonium bromide, DDAB) formulated with glycolipid adjuvant (trehalose 6,6-dibehenate), which is a synthetic variant of cord factor located in the mycobacterial cell wall. Mycobacterial antigens (ESAT-6 and Antigen 85B (Ag85B)) were adsorbed on CAF01. The formulation (500 nm, 60 mV) induced strong Th1-type immune responses (high levels of INF- γ and IgG2b). In clinical trials, CAF01-based vaccine induced a strong, long-lasting cellular immune response confirmed by the broad induction of Th1-associated cytokines (IFN- γ , IL-2, TNF- α , GM-CSF), and chemokines (MIG, IP-10 and MIP-1 β) [126].

Army liposome formulation (ALF) was designed following a similar strategy [127], i.e., MPLA was incorporated into liposomal membrane as an inbuilt adjuvant. Tetanus toxoid and HIV-1-derived peptides were adsorbed to aluminum hydroxide, which was then co-adsorbed to ALF (30–100 nm, respectively). The formulation induced more balanced Th1/Th2 responses, eliminating the side effects of excessive Th2 responses triggered by aluminum salt alone. ALF has been tested as a delivery system for

vaccines against shingles caused by herpes zoster, malaria, HIV-1, and *Campylobacter jejuni* causing diarrhea [128].

ISCOMATRIX is a liposome-like immunostimulatory complex formulated with saponins, cholesterol, and phospholipids under controlled conditions to construct spherical cage-like structures 40–60 nm in size (once the antigen is incorporated, it is named ISCOM). It delivers antigen to DCs and stimulates both Th1 and Th2 cytokine production, as well as antigen-specific antibody responses and long-lasting immunity [129]. A chimeric peptide vaccine was constructed bearing Tax, gp21, gp46, and gag (p19) epitopes that were connected by flexible linker, in the absence or presence of MPLA and ISCOMATRIX adjuvants for immunization against human T-cell lymphotropic virus type 1 [130]. ISCOMATRIX loaded with the antigen stimulated a higher level of IgG antibodies, especially IgG2a, compared to MPLA-adjuvanted vaccine. A higher level of IFN- γ and IL-10 cytokines were produced following subcutaneous immunization, rather than nasal. Human cancer testis antigen NY-ESO-1 (derived from New York esophageal squamous cell carcinoma-1) adjuvanted with ISCOMATRIX was tested in Phase I clinical trials [131]. The vaccine was well-tolerated and induced strong humoral and cellular immune responses. Antibody responses were observed in 100% of the vaccine recipients and CD4⁺ and CD8⁺ T-cell responses in 69% and 38%, respectively. Importantly, CD8⁺ T-cell responses were observed in individuals with and without preexisting antibodies to NY-ESO-1. Recently, a double-blind Phase II clinical trial of NY-ESO-1 vaccine with ISCOMATRIX adjuvant versus ISCOMATRIX alone in participants with high-risk resected melanoma was conducted [132]. Vaccine recipients developed strong humoral and cellular immune responses against NY-ESO-1. The vaccine was well-tolerated; however, despite inducing antigen-specific immunity, it did not affect survival endpoints.

8 Inorganic Nanoparticles

Particles including gold, aluminum, calcium phosphate, silica, and pure carbon have been intensively tested as adjuvants and antigen delivery vehicles over the last decade. They can be easily and economically produced, their modification with antigen is straightforward, and their surface can be further modified to achieve desired immune properties [133].

Aluminum salts (alum) have been used in human vaccines as adjuvants and are known to accelerate antigen-specific immune responses [134]. Alum has been included in vaccines for polio, hepatitis A and B, anthrax, pneumococcus, diphtheria, tetanus, pertussis, and others [135]. However, it is structurally complex and heterogeneous, making it difficult to characterize for quality

control, especially after being mixed with vaccine antigens. The adjuvanting capacity of aluminum salt-based materials is significantly influenced by the materials' physicochemical properties (e.g., size, shape, and crystallinity) [136]. Antigen may be adsorbed in alum-containing adjuvant through electrostatic attraction and ligand exchange [27].

One of the proposed mechanisms of alum-based adjuvants is depot formation at the injection site [137]. This allows the slow release of antigens, which are trapped in the porous spaces of alum adjuvant, over time, and efficient presentation of the antigen to the APCs and lymphocytes. Another hypothesized mechanism of alum is activation of the complement cascade and recruitment of cells from blood to create an inflammatory environment at the site of injection [138]. Recent studies have highlighted that the activation of NLRP3 inflammasomes is vital in inducing adjuvant effects that are controlled by the inherent shape and hydroxyl content of aluminum oxyhydroxide particles [139]. Another hypothesis suggests that alum triggers cytotoxicity and the release of DNA, which acts as an immune stimulator, from dying cells or damaged mitochondria [140].

However, alum is a relatively weak adjuvant, especially against poorly immunogenic antigens (proteins and peptides), does not induce strong cellular immunity, and is not free from adverse effects, such as macrophagic myofasciitis [141]. To overcome some of these problems, Orr and coworkers developed a lipid-based nanosuspension of synthetic TLR-7/8 ligand, imidazoquinoline (3M-052), which facilitated the adsorption of vaccine antigen (ID93 for tuberculosis and FLSC for HIV) to aluminum oxyhydroxide NPs (<200 nm) [142]. Mice immunized with these vaccines (the aluminum oxyhydroxide-adsorbed formulation of 3M-052 and peptide) produced enhanced antibody levels in comparison to peptide adjuvanted with Alhydrogel, and a Th1-type cellular immune response. Similarly, nanoalum (75–110 nm) was derived from the clinical adjuvant Alhydrogel (0.5–10 μm) by incorporation of polyacrylic acid polymer as a stabilizing agent [143]. The nanoalum elicited a robust Th1 immune response characterized by antigen-specific CD4⁺ T-cells expressing IFN- γ and TNF, as well as higher IgG2 titers when compared to Alhydrogel.

In another study, aluminum oxyhydroxide nanosticks were produced to determine alum adjuvanting activity [144]. OVA-bearing nanosticks (~200 nm length and ~8 nm thick) were more effective in delivering antigens to APCs, activating inflammasomes, and potentiating OVA-specific antibody responses in mice compared to Alhydrogel-formulated OVA (~1.2 μm). Despite the advantages of using alum NPs, they are reported to adsorb antigen so tightly that they can alter antigen structure, which limits efficacy and utility [145, 146]. Thus, other

inorganic particles have been intensively investigated as replacements for alum.

Calcium phosphate (CP) has been approved by the World Health Organization as an adjuvant [147] and is the only non-aluminum mineral salt adjuvant used in human vaccines. Relveld et al. demonstrated that CP-induced similar neutralizing antibodies to alum after single injection of tetanus toxoid or diphtheria tetanus in humans and animals [148]; stronger neutralizing antibody production was achieved after a booster dose with tetanus toxoid. CP NPs are bioresorbable and nontoxic and have adjuvanting properties, high antigen loading capacity, a simple preparation method, excellent biodegradation, and low cytotoxicity, making them suitable as adjuvant [149]. Preformed CP gel, to which antigen is absorbed, is available in the market, supplied by companies like Superfos Biosector, Vedbaek, Denmark. Similar to alum, CP generates a depot effect. However, unlike alum, CP is incapable of eliciting IgE [150, 151]. Knuschke and coworkers recently used CP as an adjuvant in a therapeutic anti-retroviral vaccine [152]. Immunization with CP NPs functionalized with Friend retrovirus (FV)-derived T-cell epitopes and the TLR-9 ligand, CpG, strongly activated CD4⁺ and CD8⁺ T-cells, leading to the eradication of infected cells in chronic FV infection in mice. CP NPs loaded with TLR-3 agonist, poly(I:C), coated with a silica shell and functionalized by silanization led to the presence of a thiol-terminated surface. This allowed subsequent conjugation of antibodies to CP. The NPs had a hydrodynamic diameter of 280 nm and zeta potential of +20 mV [153]. After intravenous injection, in vivo uptake was especially prominent in the lungs and liver in comparison to the spleen. Pronounced immunostimulatory effects of the NPs were found in vitro with primary liver cells. The activation of TLR-3 via poly(I:C) led to antiviral effects in a type I INF-dependent manner, so the CP NPs were speculated to be useful for the treatment of viral infections, neoplastic diseases, and other diseases that can be treated by type I interferon in the liver and lungs. Furthermore, murine xenograft colorectal cancer model mice were vaccinated with CP NPs functionalized with CpG and tumor model antigens (influenza-derived peptides: HA110-120, SVSSFERFERFEIFPKES; HA512-520, YQILAIYSTVASSLVLL) [154]. Tumor-bearing mice were vaccinated subcutaneously on day 3, 5, and 7 posttumor transplantation. The frequency of cytotoxic CD8⁺ T-cells was elevated in an IFN I-dependent manner. Tumor growth was significantly suppressed in CP NP-treated mice compared to untreated mice. However, tumor eradication was not observed.

Gold NPs have also been used for vaccine delivery. Gold NPs are biologically inert, non-toxic, and their size and shape can be easily controlled [155]. Chen et al. conjugated foot and mouth virus-associated peptide to gold NPs (2, 5, 8, 12, 17, 37, and

50 nm) [156]. Gold NPs of 8 and 12 nm were more selectively accumulating in spleen and triggered the highest antibody titers in immunized mice. Similarly, small gold NPs (10, 22 nm) have been shown to be taken up more efficiently by DCs compared to larger particles (33 nm) [157]. Spherical gold NPs (15 nm) coupled to swine transmissible gastroenteritis virus antigen activated APCs and increased the proliferative activity of splenic lymphoid (antibody-forming) cells following immunization in mice [158]. Tao and coworkers also demonstrated that small gold NPs (10 nm diameter) conjugated to M2e, the 23 amino acid extracellular domain of the influenza A virus surface, and ion channel membrane matrix protein 2, can induce strong immune responses [159]. Intranasal delivery of these NPs with soluble CpG as an adjuvant completely protected mice from lethal challenge against a broad spectrum of influenza A subtypes [160].

Mesoporous silica NPs (MSNPs) were first developed in the 1990s and have become one of the most studied nanomaterials for controlled drug delivery and release [161]. They are a promising material for vaccine delivery due to their pore structure and capacity to carry antigen, easy surface modification, and intrinsic biocompatibility. Cationic silica NPs efficiently co-loaded negatively charged oligonucleotide adjuvant (CpG) and OVA antigen through electrostatic interactions [162]. The CpG-loaded silica NPs (30–80 nm) enhanced the cellular uptake of antigen, TLR activation, and immune response against antigen *in vitro* and *in vivo*. Immunization with silica NPs potentiated the *in vivo* generation of antigen-specific cytotoxic T-cells and humoral response, which, in turn, lead to enhanced antitumor efficacy. Kim and coworkers were able to produce MSNPs in a controlled manner with NP size ranging from 100 to 200 nm, and pore size of 20–30 nm. The large pore size of MSNPs allowed enhanced loading of OVA, and CpG, as compared with conventional small-pore MSNPs (3 nm) [163]. Vaccination with MSNPs/OVA/CpG stimulated adaptive immune responses, including antigen-specific cytotoxic T-cells, and subsequently suppressed tumor growth in a prophylactic tumor model. Additionally, MSNPs stimulated the activation of CD4⁺ and CD8⁺ T-cells in the splenocytes of mice [164]. However, it must be noted that accumulation of silica in macrophages has been reported, as MSNPs are not biodegradable, causing potential long-term toxicity issues [165].

Carbon nanotubes (CNTs) are carbon sheet(s) rolled into a cylinder. These are the most extensively studied cylindrical-shaped delivery systems in the biomedical field. These nanostructures can be found in two classes: single-walled carbon nanotubes (SWNT), which are formed by a single cylindrical graphene layer; and multi-walled carbon nanotubes (MWNT) comprising several concentric layers of graphene [166]. CNTs have been designed as antigen delivery systems for enhancing immune responses against infectious

agents and cancers [167]. For example, four types of MWNT-OVA conjugates were produced: long MWNT-OVA (~390 nm, 6 mV), and three short MWNT-OVAs (~120 nm, -23, -35, or -40 mV). Short MWNT-OVA with the lowest negative charge had the highest cellular uptake and generated the strongest immune response among all other short MWNT-OVAs *in vitro* and *in vivo*. Long, positively charged MWNT-OVAs showed limited cellular uptake and OVA-specific immune responses. MWNTs were also used to co-deliver two immunoadjuvants, CpG and anti-CD40 Ig [168]. MWNTs improved the ability of co-loaded peptide with CpG to inhibit the growth of OVA-expressing B16F10 melanoma cells in subcutaneous or lung pseudo-metastatic tumor models. Likewise, recombinant subunit fish vaccine (pET32a-G) was conjugated to SWNTs [169]. The produced SWCNT-subunit vaccine induced enhanced protective immunity against spring viremia of carp virus infection in fish. Unfortunately, apart from the advantages, several challenges of CNTs, including toxicity, need to be addressed. It has been evidenced that CNTs can be toxic both *in vitro* and *in vivo*, through the production of cytotoxic reactive oxygen species, cell apoptosis, and necrosis [170].

9 Conclusion

Nanotechnology has provided a range of very promising delivery platforms for vaccines. Highly defined nanocarriers can overcome the limits and drawbacks associated with traditional vaccine formulations, which are mainly based on simple co-administration of antigen/pathogen with adjuvants. NP properties can be tuned to such an extent that the use of toxic immune stimulants/adjuvants can be omitted in vaccine formulations. NPs can be modified with respect to their size, charge, stability, biodegradation, mucoadhesion and APC-targeting properties. While particle properties often play crucial roles in nanovaccine efficacy, the other factors that also influence immune responses should not be neglected. For example, lipidic components of nanoparticles can be recognized by TLRs and play a crucial role in immune stimulation, independent of particle size or charge. Antigen loading efficiency, antigen release profile, and stability may all influence the efficacy of delivery systems. Furthermore, the route of administration also has significant influence on vaccine pharmacokinetics.

The use of suitable NPs should ultimately replace the need for adjuvants. However, surprisingly, adjuvant use is still the prevailing strategy, and in many cases, adjuvants are still added to NP-based vaccine formulations. Moreover, a large number of studies have not even used adjuvant-free nanosystems as a control. Therefore, the efficacy of adjuvant-free nanosystem is often not investigated. Instead, using a mixture of several adjuvants is often reported,

even if this creates a risk of stimulating toxic side effects. Fortunately, some nanosystems have been tested without co-administration of classical adjuvants and they still induced strong immune responses.

While several self-assembled NPs can induce protective immune responses without the need for an adjuvant, these nanovaccines still have some limitations, including potential toxicity, nonbiodegradable carriers, difficulties in scaling-up the production process, and a lack of standard regulatory guidelines. The acute and chronic toxicities of nano-sized particles have been evidenced in various clinical reports, including the toxicity of metallic NPs after prolonged exposure. Similarly, carbon-based NPs induced size-dependent toxicity. Thus, the choice of nanocarrier material is crucial.

Some nanovaccines are already approved for human use (e.g., Mosquirix, Inflexal). However, overall, nanovaccines are still at a rather early stage of development and require much more intensive research, especially in clinical trials. We can easily expect that the popularity of nano approaches in vaccine development will grow, and new nanovaccines will reach the market soon.

References

1. Boylston A (2012) The origins of inoculation. *J R Soc Med* 105(7):309–313. <https://doi.org/10.1258/jrsm.2012.12k044>
2. Belongia EA, Naleway AL (2003) Smallpox vaccine: the good, the bad, and the ugly. *Clin Med Res* 1(2):87–92. <https://doi.org/10.3121/cm.r.1.2.87>
3. Gross CP, Sepkowitz KA (1998) The myth of the medical breakthrough: smallpox, vaccination, and Jenner reconsidered. *Int J Infect Dis* 3(1):54–60. [https://doi.org/10.1016/S1201-9712\(98\)90096-0](https://doi.org/10.1016/S1201-9712(98)90096-0)
4. Stern AM, Markel H (2005) The history of vaccines and immunization: familiar patterns, new challenges. *Health Aff* 24(3):611–621. <https://doi.org/10.1377/hlthaff.24.3.611>
5. Skwarczynski M, Toth I (2016) Peptide-based synthetic vaccines. *Chem Sci* 7(2):842–854. <https://doi.org/10.1039/c5sc03892h>
6. Baxter D (2007) Active and passive immunity, vaccine types, excipients and licensing. *Occup Med* 57(8):552–556. <https://doi.org/10.1093/occmed/kqml110>
7. Scott C (2004) Classifying vaccines. *BioProcesses Inter*:14–23
8. Fujita Y, Taguchi H (2011) Current status of multiple antigen-presenting peptide vaccine systems: application of organic and inorganic nanoparticles. *Chem Cent J* 5(1):48. <https://doi.org/10.1186/1752-153X-5-48>
9. Skwarczynski M, Toth I (2014) Recent advances in peptide-based subunit nanovaccines. *Nanomedicine* 9(17):2657–2669. <https://doi.org/10.2217/nmm.14.187>
10. De Brito RCF, Cardoso JMDO, Reis LES, Vieira JF, Mathias FAS, Roatt BM, Aguiar-Soares RDDO, Ruiz JC, Resende DM, Reis AB (2018) Peptide vaccines for leishmaniasis. *Front Immunol* 9:1043–1043. <https://doi.org/10.3389/fimmu.2018.01043>
11. Nicholson Lindsay B (2016) The immune system. *Essays Biochem* 60(3):275–301. <https://doi.org/10.1042/EBC20160017>
12. Janeway CA Jr, Travers P, Walport M, Shlomchik MJ (2001) The complement system and innate immunity. In: *Immunobiology: the immune system in health and disease*, 5th edn. Garland Science
13. ten Broeke T, Wubbolts R, Stoorvogel W (2013) MHC class II antigen presentation by dendritic cells regulated through endosomal sorting. *Cold Spring Harb Perspect Biol* 5(12):a016873–a016873. <https://doi.org/10.1101/cshperspect.a016873>
14. Mogensen TH (2009) Pathogen recognition and inflammatory signaling in innate immune

- defenses. *Clin Microbiol Rev* 22(2):240. <https://doi.org/10.1128/CMR.00046-08>
15. Gaudino SJ, Kumar P (2019) Cross-talk between antigen presenting cells and T cells impacts intestinal homeostasis, bacterial infections, and tumorigenesis. *Front Immunol* 10:360. <https://doi.org/10.3389/fimmu.2019.00360>
 16. Chaplin DD (2010) Overview of the immune response. *J Allerg Clin Immunol* 125(2, Supplement 2):S3–S23. <https://doi.org/10.1016/j.jaci.2009.12.980>
 17. Bowie A, O'Neill LAJ (2000) The interleukin-1 receptor/Toll-like receptor superfamily: signal generators for pro-inflammatory interleukins and microbial products. *J Leukoc Biol* 67(4):508–514. <https://doi.org/10.1002/jlb.67.4.508>
 18. Clem AS (2011) Fundamentals of vaccine immunology. *J Glob Infect Dis* 3(1):73–78. <https://doi.org/10.4103/0974-777X.77299>
 19. Liao S, von der Weid PY (2015) Lymphatic system: an active pathway for immune protection. *Semin Cell Dev Biol* 38:83–89. <https://doi.org/10.1016/j.semcdb.2014.11.012>
 20. Nevagi RJ, Toth I, Skwarczynski M (2018) 12—Peptide-based vaccines. In: Koutsopoulos S (ed) *Peptide applications in biomedicine, biotechnology and bioengineering*. Woodhead Publishing, pp 327–358. <https://doi.org/10.1016/B978-0-08-100736-5.00012-0>
 21. Malonis RJ, Lai JR, Vergnolle O (2020) Peptide-based vaccines: current progress and future challenges. *Chem Rev* 120(6):3210–3229. <https://doi.org/10.1021/acs.chemrev.9b00472>
 22. Purcell AW, McCluskey J, Rossjohn J (2007) More than one reason to rethink the use of peptides in vaccine design. *Nat Rev Drug Discov* 6(5):404–414. <https://doi.org/10.1038/nrd2224>
 23. Moyle PM, Toth I (2013) Modern subunit vaccines: development, components, and research opportunities. *ChemMedChem* 8(3):360–376. <https://doi.org/10.1002/cmdc.201200487>
 24. Black M, Trent A, Tirrell M, Olive C (2010) Advances in the design and delivery of peptide subunit vaccines with a focus on Toll-like receptor agonists. *Expert Rev Vaccines* 9(2):157–173. <https://doi.org/10.1586/erv.09.160>
 25. Bartlett S, Skwarczynski M, Toth I (2020) Lipids as activators of innate immunity in peptide vaccine delivery. *Curr Med Chem* 27(17):2887–2901
 26. Tsoras AN, Champion JA (2019) Protein and peptide biomaterials for engineered subunit vaccines and immunotherapeutic applications. *Ann Rev Chem Biomol Eng* 10(1):337–359. <https://doi.org/10.1146/annurev-chembioeng-060718-030347>
 27. Azmi F, Ahmad Fuaad AAH, Skwarczynski M, Toth I (2014) Recent progress in adjuvant discovery for peptide-based subunit vaccines. *Hum Vaccin Immunother* 10(3):778–796. <https://doi.org/10.4161/hv.27332>
 28. Luo Y, Teng Z, Li Y, Wang Q (2015) Solid lipid nanoparticles for oral drug delivery: chitosan coating improves stability, controlled delivery, mucoadhesion and cellular uptake. *Carbohydr Polym* 122:221–229. <https://doi.org/10.1016/j.carbpol.2014.12.084>
 29. Nevagi RJ, Skwarczynski M, Toth I (2019) Polymers for subunit vaccine delivery. *Eur Polym J* 114:397–410. <https://doi.org/10.1016/j.eurpolymj.2019.03.009>
 30. Skwarczynski M, Toth I (2011) Peptide-based subunit nanovaccines. *Curr Drug Deliv* 8(3):282–289
 31. Ranzoni A, Cooper MA (2017) Chapter one—the growing influence of nanotechnology in our lives. In: Skwarczynski M, Toth I (eds) *Micro and nanotechnology in vaccine development*. William Andrew Publishing, pp 1–20. <https://doi.org/10.1016/B978-0-323-39981-4.00001-4>
 32. Angioletti-Uberti S (2017) Theory, simulations and the design of functionalized nanoparticles for biomedical applications: a soft matter perspective. *Comput Material* 3(1):48. <https://doi.org/10.1038/s41524-017-0050-y>
 33. Irvine DJ, Hanson MC, Rakhra K, Tokatlian T (2015) Synthetic nanoparticles for vaccines and immunotherapy. *Chem Rev* 115(19):11109–11146. <https://doi.org/10.1021/acs.chemrev.5b00109>
 34. Li Z, Tan S, Li S, Shen Q, Wang K (2017) Cancer drug delivery in the nano era: an overview and perspectives (Review). *Oncol Rep* 38(2):611–624. <https://doi.org/10.3892/or.2017.5718>
 35. Poland CA, Duffin R, Kinloch I, Maynard A, Wallace WA, Seaton A, Stone V, Brown S, MacNee W, Donaldson K (2008) Carbon nanotubes introduced into the abdominal cavity of mice show asbestos-like pathogenicity in a pilot study. *Nat Nanotechnol* 3(7):423

36. Casella CR, Mitchell TC (2008) Putting endotoxin to work for us: monophosphoryl lipid A as a safe and effective vaccine adjuvant. *Cell Mol Life Sci* 65(20):3231–3240. <https://doi.org/10.1007/s00018-008-8228-6>
37. Didierlaurent AM, Laupèze B, Di Pasquale A, Hergli N, Collignon C, Garçon N (2017) Adjuvant system AS01: helping to overcome the challenges of modern vaccines. *Expert Rev Vaccines* 16(1):55–63. <https://doi.org/10.1080/14760584.2016.1213632>
38. Glück R, Metcalfe IC (2002) New technology platforms in the development of vaccines for the future. *Vaccine* 20:B10–B16. [https://doi.org/10.1016/S0264-410X\(02\)00513-3](https://doi.org/10.1016/S0264-410X(02)00513-3)
39. Roldão A, Mellado MCM, Castilho LR, Carrondo MJT, Alves PM (2010) Virus-like particles in vaccine development. *Expert Rev Vaccines* 9(10):1149–1176. <https://doi.org/10.1586/erv.10.115>
40. Correia-Pinto JF, Csaba N, Alonso MJ (2013) Vaccine delivery carriers: insights and future perspectives. *Int J Pharm* 440(1):27–38. <https://doi.org/10.1016/j.ijpharm.2012.04.047>
41. Wang J, Hu X, Xiang D (2018) Nanoparticle drug delivery systems: an excellent carrier for tumor peptide vaccines. *Drug Deliv* 25(1):1319–1327. <https://doi.org/10.1080/10717544.2018.1477857>
42. Faruck MO, Zhao L, Hussein WM, Khalil ZG, Capon RJ, Skwarczynski M, Toth I (2020) Polyacrylate-peptide antigen conjugate as a single-dose oral vaccine against group A streptococcus. *Vaccines* 8(1):23
43. Köping-Höggård M, Sánchez A, Alonso MJ (2005) Nanoparticles as carriers for nasal vaccine delivery. *Expert Rev Vaccines* 4(2):185–196. <https://doi.org/10.1586/14760584.4.2.185>
44. Fredriksen BN, Grip J (2012) PLGA/PLA micro- and nanoparticle formulations serve as antigen depots and induce elevated humoral responses after immunization of Atlantic salmon (*Salmo salar* L.). *Vaccine* 30(3):656–667. <https://doi.org/10.1016/j.vaccine.2011.10.105>
45. Reddy ST, van der Vlies AJ, Simeoni E, Angeli V, Randolph GJ, O’Neil CP, Lee LK, Swartz MA, Hubbell JA (2007) Exploiting lymphatic transport and complement activation in nanoparticle vaccines. *Nat Biotechnol* 25(10):1159–1164. <https://doi.org/10.1038/nbt1332>
46. Zhu M, Wang R, Nie G (2014) Applications of nanomaterials as vaccine adjuvants. *Hum Vaccin Immunother* 10(9):2761–2774. <https://doi.org/10.4161/hv.29589>
47. Salatin S, Barar J, Barzegar-Jalali M, Adibkia K, Milani MA, Jelvehgari M (2016) Hydrogel nanoparticles and nanocomposites for nasal drug/vaccine delivery. *Arch Pharm Res* 39(9):1181–1192. <https://doi.org/10.1007/s12272-016-0782-0>
48. Fifis T, Gamvrellis A, Crimeen-Irwin B, Pietersz GA, Li J, Mottram PL, McKenzie IFC, Plebanski M (2004) Size-dependent immunogenicity: therapeutic and protective properties of nano-vaccines against tumors. *J Immunol* 173(5):3148. <https://doi.org/10.4049/jimmunol.173.5.3148>
49. Mottram PL, Leong D, Crimeen-Irwin B, Gloster S, Xiang SD, Meanger J, Ghildyal R, Vardaxis N, Plebanski M (2007) Type 1 and 2 immunity following vaccination is influenced by nanoparticle size: formulation of a model vaccine for respiratory syncytial virus. *Mol Pharm* 4(1):73–84. <https://doi.org/10.1021/mp060096p>
50. Wilson KL, Xiang SD, Plebanski M (2015) Montanide, poly I:C and nanoparticle based vaccines promote differential suppressor and effector cell expansion: a study of induction of CD8 T cells to a minimal Plasmodium berghei epitope. *Front Microbiol* 6:29. <https://doi.org/10.3389/fmicb.2015.00029>
51. Xiang SD, Wilson KL, Goubier A, Heyerick A, Plebanski M (2018) Design of peptide-based nanovaccines targeting leading antigens from gynecological cancers to induce HLA-A2.1 restricted CD8(+) T cell responses. *Front Immunol* 9:2968–2968. <https://doi.org/10.3389/fimmu.2018.02968>
52. Amjadi I, Rabiee M, Hosseini M-S (2013) Anticancer activity of nanoparticles based on PLGA and its co-polymer: in-vitro evaluation. *Iran J Pharm Res* 12(4):623–634
53. Silva AL, Rosalia RA, Sazak A, Carstens MG, Ossendorp F, Oostendorp J, Jiskoot W (2013) Optimization of encapsulation of a synthetic long peptide in PLGA nanoparticles: low-burst release is crucial for efficient CD8+ T cell activation. *Eur J Pharm Biopharm* 83(3):338–345. <https://doi.org/10.1016/j.ejpb.2012.11.006>
54. Silva AL, Rosalia RA, Varypataki E, Sibuea S, Ossendorp F, Jiskoot W (2015) Poly-(lactic-co-glycolic-acid)-based particulate vaccines: particle uptake by dendritic cells is a key parameter for immune activation. *Vaccine* 33(7):847–854. <https://doi.org/10.1016/j.vaccine.2014.12.059>

55. Chen Q, Bao Y, Burner D, Kaushal S, Zhang Y, Mendoza T, Bouvet M, Ozkan C, Minev B, Ma W (2019) Tumor growth inhibition by mSTEAP peptide nanovaccine inducing augmented CD8⁺ T cell immune responses. *Drug Deliv Transl Res* 9 (6):1095–1105. <https://doi.org/10.1007/s13346-019-00652-z>
56. Kabiri M, Sankian M, Sadri K, Tafaghodi M (2018) Robust mucosal and systemic responses against HTLV-1 by delivery of multi-epitope vaccine in PLGA nanoparticles. *Eur J Pharm Biopharm* 133:321–330. <https://doi.org/10.1016/j.ejpb.2018.11.003>
57. Skwarczynski M, Toth I (2011) Lipid-core-peptide system for self-adjuvanting synthetic vaccine delivery. In: Mark SS (ed) *Bioconjugation protocols: strategies and methods*. Humana Press, Totowa, NJ, pp 297–308. https://doi.org/10.1007/978-1-61779-151-2_18
58. Marasini N, Khalil ZG, Giddam AK, Ghaffar KA, Hussein WM, Capon RJ, Batzloff MR, Good MF, Skwarczynski M, Toth I (2016) Lipid core peptide/poly(lactic-co-glycolic acid) as a highly potent intranasal vaccine delivery system against group A streptococcus. *Int J Pharm* 513(1):410–420. <https://doi.org/10.1016/j.ijpharm.2016.09.057>
59. Silva AL, Soema PC, Slütter B, Ossendorp F, Jiskoot W (2016) PLGA particulate delivery systems for subunit vaccines: linking particle properties to immunogenicity. *Hum Vaccin Immunother* 12(4):1056–1069. <https://doi.org/10.1080/21645515.2015.1117714>
60. Li X, Min M, Du N, Gu Y, Hode T, Naylor M, Chen D, Nordquist RE, Chen WR (2013) Chitin, chitosan, and glycated chitosan regulate immune responses: the novel adjuvants for cancer vaccine. *Clin Dev Immunol* 2013:387023. <https://doi.org/10.1155/2013/387023>
61. Arca HÇ, Günbeyaz M, Şenel S (2009) Chitosan-based systems for the delivery of vaccine antigens. *Expert Rev Vaccines* 8 (7):937–953. <https://doi.org/10.1586/erv.09.47>
62. Amidi M, Mastrobattista E, Jiskoot W, Hennink WE (2010) Chitosan-based delivery systems for protein therapeutics and antigens. *Adv Drug Deliv Rev* 62(1):59–82. <https://doi.org/10.1016/j.addr.2009.11.009>
63. Mourya VK, Inamdar NN (2008) Chitosan-modifications and applications: opportunities galore. *React Funct Polym* 68(6):1013–1051. <https://doi.org/10.1016/j.reactfunctpolym.2008.03.002>
64. Snyman D, Hamman JH, Kotze JS, Rollings JE, Kotzé AF (2002) The relationship between the absolute molecular weight and the degree of quaternisation of N-trimethyl chitosan chloride. *Carbohydr Polym* 50 (2):145–150. [https://doi.org/10.1016/S0144-8617\(02\)00008-5](https://doi.org/10.1016/S0144-8617(02)00008-5)
65. Akbari MR, Saadati M, Honari H, Ghorbani HM (2019) IpaD-loaded N-trimethyl chitosan nanoparticles can efficiently protect guinea pigs against shigella flexneri. *Iran J Immunol* 16(3):212–224. <https://doi.org/10.22034/iji.2019.80272>
66. Jahantigh D, Saadati M, Fasihi Ramandi M, Mousavi M, Zand AM (2014) Novel intranasal vaccine delivery system by chitosan nanofibrous membrane containing N-terminal region of Ipad antigen as a nasal shigellosis vaccine, studies in guinea pigs. *J Drug Delivery Sci Technol* 24(1):33–39. [https://doi.org/10.1016/S1773-2247\(14\)50005-6](https://doi.org/10.1016/S1773-2247(14)50005-6)
67. Zhao L, Skwarczynski M, Toth I (2019) Polyelectrolyte-based platforms for the delivery of peptides and proteins. *ACS Biomater Sci Eng* 5(10):4937–4950. <https://doi.org/10.1021/acsbomaterials.9b01135>
68. Zhao L, Jin W, Cruz JG, Marasini N, Khalil ZG, Capon RJ, Hussein WM, Skwarczynski M, Toth I (2020) Development of polyelectrolyte complexes for the delivery of peptide-based subunit vaccines against group A streptococcus. *Nanomaterials* 10 (5):823
69. Marasini N, Giddam AK, Khalil ZG, Hussein WM, Capon RJ, Batzloff MR, Good MF, Toth I, Skwarczynski M (2016) Double adjuvanting strategy for peptide-based vaccines: trimethyl chitosan nanoparticles for lipopeptide delivery. *Nanomedicine* 11 (24):3223–3235. <https://doi.org/10.2217/nmm-2016-0291>
70. Marasini N, Giddam AK, Ghaffar KA, Batzloff MR, Good MF, Skwarczynski M, Toth I (2016) Multilayer engineered nanoliposomes as a novel tool for oral delivery of lipopeptide-based vaccines against group A streptococcus. *Nanomedicine* 11(10):1223–1236. <https://doi.org/10.2217/nmm.16.36>
71. Nevagi RJ, Khalil ZG, Hussein WM, Powell J, Batzloff MR, Capon RJ, Good MF, Skwarczynski M, Toth I (2018) Polyglutamic acid-trimethyl chitosan-based intranasal peptide nano-vaccine induces potent immune responses against group A streptococcus. *Acta Biomater* 80:278–287. <https://doi.org/10.1016/j.actbio.2018.09.037>
72. Nevagi RJ, Dai W, Khalil ZG, Hussein WM, Capon RJ, Skwarczynski M, Toth I (2019)

- Self-assembly of trimethyl chitosan and poly (anionic amino acid)-peptide antigen conjugate to produce a potent self-adjuncting nanovaccine delivery system. *Bioorg Med Chem* 27(14):3082–3088. <https://doi.org/10.1016/j.bmc.2019.05.033>
73. Nevagi RJ, Dai W, Khalil ZG, Hussein WM, Capon RJ, Skwarczynski M, Toth I (2019) Structure-activity relationship of group A streptococcus lipopeptide vaccine candidates in trimethyl chitosan-based self-adjuncting delivery system. *Eur J Med Chem* 179:100–108. <https://doi.org/10.1016/j.ejmech.2019.06.047>
 74. Zhao G, Chandrudu S, Skwarczynski M, Toth I (2017) The application of self-assembled nanostructures in peptide-based subunit vaccine development. *Eur Polym J* 93:670–681. <https://doi.org/10.1016/j.eurpolymj.2017.02.014>
 75. Eskandari S, Guerin T, Toth I, Stephenson RJ (2017) Recent advances in self-assembled peptides: implications for targeted drug delivery and vaccine engineering. *Adv Drug Deliv Rev* 110-111:169–187. <https://doi.org/10.1016/j.addr.2016.06.013>
 76. Skwarczynski M, Zaman M, Urbani CN, Lin IC, Jia Z, Batzloff MR, Good MF, Monteiro MJ, Toth I (2010) Polyacrylate dendrimer nanoparticles: a self-adjuncting vaccine delivery system. *Angew Chem* 122 (33):5878–5881
 77. Zaman M, Skwarczynski M, Malcolm JM, Urbani CN, Jia Z, Batzloff MR, Good MF, Monteiro MJ, Toth I (2011) Self-adjuncting polyacrylic nanoparticulate delivery system for group A streptococcus (GAS) vaccine. *Nanomed Nanotechnol Biol Med* 7 (2):168–173. <https://doi.org/10.1016/j.nano.2010.10.002>
 78. Ahmad Fuaad AAH, Jia Z, Zaman M, Hartas J, Ziora ZM, Lin IC, Moyle PM, Batzloff MR, Good MF, Monteiro MJ, Skwarczynski M, Toth I (2013) Polymer-peptide hybrids as a highly immunogenic single-dose nanovaccine. *Nanomedicine* 9 (1):35–43. <https://doi.org/10.2217/nmm.13.7>
 79. Chandrudu S, Bartlett S, Khalil ZG, Jia Z, Hussein WM, Capon RJ, Batzloff MR, Good MF, Monteiro MJ, Skwarczynski M, Toth I (2016) Linear and branched polyacrylates as a delivery platform for peptide-based vaccines. *Ther Deliv* 7(9):601–609. <https://doi.org/10.4155/tde-2016-0037>
 80. Liu T-Y, Hussein WM, Giddam AK, Jia Z, Reiman JM, Zaman M, McMillan NAJ, Good MF, Monteiro MJ, Toth I, Skwarczynski M (2015) Polyacrylate-based delivery system for self-adjuncting anticancer peptide vaccine. *J Med Chem* 58 (2):888–896. <https://doi.org/10.1021/jm501514h>
 81. Liu TY, Hussein WM, Jia Z, Ziora ZM, McMillan NA, Monteiro MJ, Toth I, Skwarczynski M (2013) Self-adjuncting polymer-peptide conjugates as therapeutic vaccine candidates against cervical cancer. *Biomacromolecules* 14(8):2798–2806. <https://doi.org/10.1021/bm400626w>
 82. Liu TY, Giddam AK, Hussein WM, Jia Z, McMillan NA, Monteiro MJ, Toth I, Skwarczynski M (2015) Self-adjuncting therapeutic peptide-based vaccine induce CD8⁺ cytotoxic T lymphocyte responses in a murine human papillomavirus tumor model. *Curr Drug Deliv* 12(1):3–8
 83. Hussein WM, Liu T-Y, Jia Z, McMillan NAJ, Monteiro MJ, Toth I, Skwarczynski M (2016) Multiantigenic peptide-polymer conjugates as therapeutic vaccines against cervical cancer. *Bioorg Med Chem* 24(18):4372–4380. <https://doi.org/10.1016/j.bmc.2016.07.036>
 84. Khongkow M, Liu T-Y, Bartlett S, Hussein WM, Nevagi R, Jia Z, Monteiro MJ, Wells J, Ruktanonchai UR, Skwarczynski M (2018) Liposomal formulation of polyacrylate-peptide conjugate as a new vaccine candidate against cervical cancer. *Precision Nanomed* 1 (3):186–196
 85. Skwarczynski M, Zhao G, Boer JC, Ozberk V, Azuar A, Cruz JG, Giddam AK, Khalil ZG, Pandey M, Shibu MA (2020) Poly (amino acids) as a potent self-adjuncting delivery system for peptide-based nanovaccines. *Sci Adv* 6(5):eaax2285
 86. Bartlett S, Skwarczynski M, Xie X, Toth I, Loukas A, Eichenberger RM (2020) Development of natural and unnatural amino acid delivery systems against hookworm infection. *Prec Nanomed* 3:471–482. [https://doi.org/10.33218/prnano3\(1\).191210.1](https://doi.org/10.33218/prnano3(1).191210.1)
 87. Skwarczynski M, Kowapradit J, Ziora ZM, Toth I (2013) pH-triggered peptide self-assembly into fibrils: a potential peptide-based subunit vaccine delivery platform. *Biochem Compound* 1(1)
 88. Wen Y, Collier JH (2015) Supramolecular peptide vaccines: tuning adaptive immunity. *Curr Opin Immunol* 35:73–79. <https://doi.org/10.1016/j.coi.2015.06.007>
 89. Sun T, Han H, Hudalla GA, Wen Y, Pompano RR, Collier JH (2016) Thermal stability of self-assembled peptide vaccine materials.

- Acta Biomater 30:62–71. <https://doi.org/10.1016/j.actbio.2015.11.019>
90. Rudra JS, Sun T, Bird KC, Daniels MD, Gasiorowski JZ, Chong AS, Collier JH (2012) Modulating adaptive immune responses to peptide self-assemblies. *ACS Nano* 6(2):1557–1564. <https://doi.org/10.1021/nn204530r>
 91. Rudra JS, Tian YF, Jung JP, Collier JH (2010) A self-assembling peptide acting as an immune adjuvant. *Proc Natl Acad Sci U S A* 107(2):622–627. <https://doi.org/10.1073/pnas.0912124107>
 92. Rudra JS, Ding Y, Neelakantan H, Ding C, Appavu R, Stutz S, Snook JD, Chen H, Cunningham KA, Zhou J (2016) Suppression of cocaine-evoked hyperactivity by self-adjuncting and multivalent peptide nanofiber vaccines. *ACS Chem Neurosci* 7(5):546–552. <https://doi.org/10.1021/acscchemneuro.5b00345>
 93. Rudra JS, Mishra S, Chong AS, Mitchell RA, Nardin EH, Nussenzweig V, Collier JH (2012) Self-assembled peptide nanofibers raising durable antibody responses against a malaria epitope. *Biomaterials* 33(27):6476–6484. <https://doi.org/10.1016/j.biomaterials.2012.05.041>
 94. Si Y, Wen Y, Kelly SH, Chong AS, Collier JH (2018) Intranasal delivery of adjuvant-free peptide nanofibers elicits resident CD8⁺ T cell responses. *J Control Release* 282:120–130. <https://doi.org/10.1016/j.jconrel.2018.04.031>
 95. Huang Z-H, Shi L, Ma J-W, Sun Z-Y, Cai H, Chen Y-X, Zhao Y-F, Li Y-M (2012) A totally synthetic, self-assembling, adjuvant-free MUC1 glycopeptide vaccine for cancer therapy. *J Am Chem Soc* 134(21):8730–8733. <https://doi.org/10.1021/ja211725s>
 96. Wu Y, Norberg PK, Reap EA, Congdon KL, Fries CN, Kelly SH, Sampson JH, Conticello VP, Collier JH (2017) A supramolecular vaccine platform based on α -helical peptide nanofibers. *ACS Biomater Sci Eng* 3(12):3128–3132. <https://doi.org/10.1021/acsbomaterials.7b00561>
 97. Hussein WM, Liu T-Y, Skwarczynski M, Toth I (2014) Toll-like receptor agonists: a patent review (2011–2013). *Expert Opin Ther Pat* 24(4):453–470. <https://doi.org/10.1517/13543776.2014.880691>
 98. Ignacio BJ, Albin TJ, Esser-Kahn AP, Verdoes M (2018) Toll-like receptor agonist conjugation: a chemical perspective. *Bioconjug Chem* 29(3):587–603. <https://doi.org/10.1021/acs.bioconjchem.7b00808>
 99. Buwitt-Beckmann U, Heine H, Wiesmüller K-H, Jung G, Brock R, Ulmer AJ (2005) Lipopeptide structure determines TLR2 dependent cell activation level. *FEBS J* 272(24):6354–6364. <https://doi.org/10.1111/j.1742-4658.2005.05029.x>
 100. Khan S, Weterings JJ, Britten CM, de Jong AR, Graafland D, Melief CJM, van der Burg SH, van der Marel G, Overkleeft HS, Filippov DV, Ossendorp F (2009) Chirality of TLR-2 ligand Pam3CysSK4 in fully synthetic peptide conjugates critically influences the induction of specific CD8⁺ T-cells. *Mol Immunol* 46(6):1084–1091. <https://doi.org/10.1016/j.molimm.2008.10.006>
 101. Zaman M, Toth I (2013) Immunostimulation by synthetic lipopeptide-based vaccine candidates: structure-activity relationships. *Front Immunol* 4:318. <https://doi.org/10.3389/fimmu.2013.00318>
 102. Zeng W, Ghosh S, Lau YF, Brown LE, Jackson DC (2002) Highly immunogenic and totally synthetic lipopeptides as self-adjuncting immunoc contraceptive vaccines. *J Immunol* 169(9):4905. <https://doi.org/10.4049/jimmunol.169.9.4905>
 103. Chua BY, Zeng W, Lau YF, Jackson DC (2007) Comparison of lipopeptide-based immunoc contraceptive vaccines containing different lipid groups. *Vaccine* 25(1):92–101. <https://doi.org/10.1016/j.vaccine.2006.07.012>
 104. Moyle PM, Dai W, Zhang Y, Batzloff MR, Good MF, Toth I (2014) Site-specific incorporation of three toll-like receptor 2 targeting adjuvants into semisynthetic, molecularly defined nanoparticles: application to group A streptococcal vaccines. *Bioconjug Chem* 25(5):965–978. <https://doi.org/10.1021/bc500108b>
 105. Trent A, Ulery BD, Black MJ, Barrett JC, Liang S, Kostenko Y, David NA, Tirrell MV (2015) Peptide amphiphile micelles self-adjuncting group A streptococcal vaccination. *AAPS J* 17(2):380–388. <https://doi.org/10.1208/s12248-014-9707-3>
 106. Barrett JC, Ulery BD, Trent A, Liang S, David NA, Tirrell MV (2017) Modular peptide amphiphile micelles improving an antibody-mediated immune response to group A streptococcus. *ACS Biomater Sci Eng* 3(2):144–152. <https://doi.org/10.1021/acsbomaterials.6b00422>
 107. Moyle PM, Toth I (2008) Self-adjuncting lipopeptide vaccines. *Curr Med Chem* 15(5):506–516
 108. Apte SH, Groves PL, Skwarczynski M, Fujita Y, Chang C, Toth I, Doolan DL

- (2012) Vaccination with lipid core peptides fails to induce epitope-specific T cell responses but confers non-specific protective immunity in a malaria model. *PLoS One* 7(8):e40928
109. Ahmad Fuaad AAH, Roubille R, Pearson MS, Pickering DA, Loukas AC, Skwarczynski M, Toth I (2015) The use of a conformational cathepsin D-derived epitope for vaccine development against *Schistosoma mansoni*. *Bioorg Med Chem* 23(6):1307–1312. <https://doi.org/10.1016/j.bmc.2015.01.033>
110. Bartlett S, Eichenberger RM, Nevagi RJ, Ghaffar KA, Marasini N, Dai Y, Loukas A, Toth I, Skwarczynski M (2020) Lipopeptide-based oral vaccine against hookworm infection. *J Infect Dis* 221(6):934–942. <https://doi.org/10.1093/infdis/jiz528>
111. Fuaad AAHA, Pearson MS, Pickering DA, Becker L, Zhao G, Loukas AC, Skwarczynski M, Toth I (2015) Lipopeptide nanoparticles: development of vaccines against hookworm parasite. *ChemMedChem* 10(10):1647–1654. <https://doi.org/10.1002/cmcd.201500227>
112. Chan A, Hussein WM, Ghaffar KA, Marasini N, Mostafa A, Eskandari S, Batzloff MR, Good MF, Skwarczynski M, Toth I (2016) Structure–activity relationship of lipid core peptide-based group A streptococcus vaccine candidates. *Bioorg Med Chem* 24(14):3095–3101. <https://doi.org/10.1016/j.bmc.2016.03.063>
113. Zaman M, Chandrudu S, Giddam AK, Reiman J, Skwarczynski M, McPhun V, Moyle PM, Batzloff MR, Good MF, Toth I (2014) Group A streptococcal vaccine candidate: contribution of epitope to size, antigen presenting cell interaction and immunogenicity. *Nanomedicine* 9(17):2613–2624. <https://doi.org/10.2217/nmm.14.190>
114. Jaberolansar N, Chappell KJ, Watterson D, Bermingham IM, Toth I, Young PR, Skwarczynski M (2017) Induction of high titred, non-neutralising antibodies by self-adjuvanting peptide epitopes derived from the respiratory syncytial virus fusion protein. *Sci Rep* 7(1):11130. <https://doi.org/10.1038/s41598-017-10415-w>
115. Azuar A, Zhao L, Hei TT, Nevagi RJ, Bartlett S, Hussein WM, Khalil ZG, Capon RJ, Toth I, Skwarczynski M (2019) cholic acid-based delivery system for vaccine candidates against group A streptococcus. *ACS Med Chem Lett* 10(9):1253–1259. <https://doi.org/10.1021/acsmchemlett.9b00239>
116. Giddam AK, Reiman JM, Zaman M, Skwarczynski M, Toth I, Good MF (2016) A semi-synthetic whole parasite vaccine designed to protect against blood stage malaria. *Acta Biomater* 44:295–303. <https://doi.org/10.1016/j.actbio.2016.08.020>
117. Marasini N, Ghaffar KA, Skwarczynski M, Toth I (2017) Liposomes as a vaccine delivery system. In: Skwarczynski M, Toth I (eds) *Micro- and nanotechnology in vaccine development*. William Andrew, Norwich, pp 221–239
118. Ghaffar KA, Giddam AK, Zaman M, Skwarczynski M, Toth I (2014) Liposomes as nanovaccine delivery systems. *Curr Top Med Chem* 14(9):1194–1208
119. Schwendener RA (2014) Liposomes as vaccine delivery systems: a review of the recent advances. *Ther Adv Vaccine* 2(6):159–182. <https://doi.org/10.1177/2051013614541440>
120. Pati R, Shevtsov M, Sonawane A (2018) Nanoparticle vaccines against infectious diseases. *Front Immunol* 9:2224. <https://doi.org/10.3389/fimmu.2018.02224>
121. Allison AC, Gregoriadis G (1974) Liposomes as immunological adjuvants. *Nature* 252(5480):252–252. <https://doi.org/10.1038/252252a0>
122. Shariat S, Badiie A, Jalali SA, Mansourian M, Yazdani M, Mortazavi SA, Jaafari MR (2014) P5 HER2/neu-derived peptide conjugated to liposomes containing MPL adjuvant as an effective prophylactic vaccine formulation for breast cancer. *Cancer Lett* 355(1):54–60. <https://doi.org/10.1016/j.canlet.2014.09.016>
123. Yazdani M, Amir Jalali S, Badiie A, Shariat S, Mansourian M, Arabi L, Abbasi A, Saberi Z, Reza Jaafari M (2017) Stimulation of tumor-specific immunity by p5 HER-2/neu generated peptide encapsulated in nano-liposomes with high phase transition temperature phospholipids. *Curr Drug Deliv* 14(4):492–502
124. Rastakhiz S, Yazdani M, Shariat S, Arab A, Momtazi-Borojeni AA, Barati N, Mansourian M, Amin M, Abbasi A, Saberi Z, Jalali SA, Badiie A, Jaafari MR (2019) Preparation of nanoliposomes linked to HER2/neu-derived (P5) peptide containing MPL adjuvant as vaccine against breast cancer. *J Cell Biochem* 120(2):1294–1303. <https://doi.org/10.1002/jcb.27090>
125. Davidsen J, Rosenkrands I, Christensen D, Vangala A, Kirby D, Perrie Y, Agger EM, Andersen P (2005) Characterization of cationic liposomes based on

- dimethyldioctadecylammonium and synthetic cord factor from *M. tuberculosis* (trehalose 6,6'-dibehenate)—a novel adjuvant inducing both strong CMI and antibody responses. *Biochim Biophys Acta* 1718(1):22–31. <https://doi.org/10.1016/j.bbame.2005.10.011>
126. van Dissel JT, Joosten SA, Hoff ST, Soonawala D, Prins C, Hokey DA, O'Dee DM, Graves A, Thierry-Carstensen B, Andreasen LV, Ruhwald M, de Visser AW, Agger EM, Ottenhoff THM, Kromann I, Andersen P (2014) A novel liposomal adjuvant system, CAF01, promotes long-lived *Mycobacterium tuberculosis*-specific T-cell responses in human. *Vaccine* 32(52):7098–7107. <https://doi.org/10.1016/j.vaccine.2014.10.036>
 127. Beck Z, Torres OB, Matyas GR, Lanar DE, Alving CR (2018) Immune response to antigen adsorbed to aluminum hydroxide particles: effects of co-adsorption of ALF or ALFQ adjuvant to the aluminum-antigen complex. *J Control Release* 275:12–19. <https://doi.org/10.1016/j.jconrel.2018.02.006>
 128. Alving CR, Peachman KK, Matyas GR, Rao M, Beck Z (2020) Army liposome formulation (ALF) family of vaccine adjuvants. *Expert Rev Vaccines* 19(3):279–292. <https://doi.org/10.1080/14760584.2020.1745636>
 129. Morelli AB, Becher D, Koernig S, Silva A, Drane D, Maraskovsky E (2012) ISCOMATRIX: a novel adjuvant for use in prophylactic and therapeutic vaccines against infectious diseases. *J Med Microbiol* 61(7):935–943
 130. Kabiri M, Sankian M, Hosseinpour M, Tafaghodi M (2018) The novel immunogenic chimeric peptide vaccine to elicit potent cellular and mucosal immune responses against HTLV-1. *Int J Pharm* 549(1):404–414. <https://doi.org/10.1016/j.ijpharm.2018.07.069>
 131. Davis ID, Chen W, Jackson H, Parente P, Shackleton M, Hopkins W, Chen Q, Dimopoulos N, Luke T, Murphy R, Scott AM, Maraskovsky E, McArthur G, MacGregor D, Sturrock S, Tai TY, Green S, Cuthbertson A, Maher D, Miloradovic L, Mitchell SV, Ritter G, Jungbluth AA, Chen Y-T, Gnjatich S, Hoffman EW, Old LJ, Cebon JS (2004) Recombinant NY-ESO-1 protein with ISCOMATRIX adjuvant induces broad integrated antibody and CD4+ and CD8+ T cell responses in humans. *Proc Natl Acad Sci U S A* 101(29):10697. <https://doi.org/10.1073/pnas.0403572101>
 132. Cebon JS, Gore M, Thompson JF, Davis ID, McArthur GA, Walpole E, Smithers M, Cerundolo V, Dunbar PR, MacGregor D, Fisher C, Millward M, Nathan P, Findlay MPN, Hersey P, Evans TRJ, Ottensmeier CH, Marsden J, Dalglish AG, Corrie PG, Maria M, Brimble M, Williams G, Winkler S, Jackson HM, Endo-Munoz L, Tutuka CSA, Venhaus R, Old LJ, Haack D, Maraskovsky E, Behren A, Chen W (2020) Results of a randomized, double-blind phase II clinical trial of NY-ESO-1 vaccine with ISCOMATRIX adjuvant versus ISCOMATRIX alone in participants with high-risk resected melanoma. *J Immunother Cancer* 8(1):e000410. <https://doi.org/10.1136/jitc-2019-000410>
 133. Al-Halifa S, Gauthier L, Arpin D, Bourgault S, Archambault D (2019) Nanoparticle-based vaccines against respiratory viruses. *Front Immunol* 10:22–22. <https://doi.org/10.3389/fimmu.2019.00022>
 134. Xu H, Ruwona TB, Thakkar SG, Chen Y, Zeng M, Cui Z (2017) Nasal aluminum (oxy)hydroxide enables adsorbed antigens to induce specific systemic and mucosal immune responses. *Hum Vaccin Immunother* 13(11):2688–2694. <https://doi.org/10.1080/21645515.2017.1365995>
 135. Lindblad EB (2004) Aluminium compounds for use in vaccines. *Immunol Cell Biol* 82(5):497–505. <https://doi.org/10.1111/j.0818-9641.2004.01286.x>
 136. Alshantqiti FM, Al-Masaudi SB, Al-Hejin AM, Redwan EM (2017) Adjuvants for *Clostridium tetani* and *Clostridium diphtheriae* vaccines updating. *Hum Antibodies* 25:23–29. <https://doi.org/10.3233/HAB-160302>
 137. Glennly A (1926) The antigenic value of toxoid precipitated by potassium alum. *J Pathol Bacteriol* 29:38–45
 138. Ramanathan VD, Badenoch-Jones P, Turk JL (1979) Complement activation by aluminium and zirconium compounds. *Immunology* 37(4):881–888
 139. Eisenbarth SC, Colegio OR, O'Connor W, Sutterwala FS, Flavell RA (2008) Crucial role for the Nalp3 inflammasome in the immunostimulatory properties of aluminium adjuvants. *Nature* 453(7198):1122–1126. <https://doi.org/10.1038/nature06939>
 140. Monie TP (2017) Section 5—connecting the innate and adaptive immune responses. In: Monie TP (ed) *The innate immune system*. Academic, pp 171–187. <https://doi.org/10.1016/B978-0-12-804464-3.00005-3>

141. Tomljenovic L, Shaw CA (2011) Aluminum vaccine adjuvants: are they safe? *Curr Med Chem* 18(17):2630–2637
142. Fox CB, Orr MT, Van Hoeven N, Parker SC, Mikasa TJT, Phan T, Beebe EA, Nana GI, Joshi SW, Tomai MA, Elvecrog J, Fouts TR, Reed SG (2016) Adsorption of a synthetic TLR7/8 ligand to aluminum oxyhydroxide for enhanced vaccine adjuvant activity: a formulation approach. *J Control Release* 244:98–107. <https://doi.org/10.1016/j.jconrel.2016.11.011>
143. Orr MT, Khandhar AP, Seydoux E, Liang H, Gage E, Mikasa T, Beebe EL, Rintala ND, Persson KH, Ahniyaz A, Carter D, Reed SG, Fox CB (2019) Reprogramming the adjuvant properties of aluminum oxyhydroxide with nanoparticle technology. *Vaccines* 4(1):1. <https://doi.org/10.1038/s41541-018-0094-0>
144. Li X, Hufnagel S, Xu H, Valdes SA, Thakkar SG, Cui Z, Celio H (2017) Aluminum (Oxy)-hydroxide nanosticks synthesized in bicontinuous reverse microemulsion have potent vaccine adjuvant activity. *ACS Appl Mater Interfaces* 9(27):22893–22901. <https://doi.org/10.1021/acsami.7b03965>
145. Frey A, Mantis N, Kozlowski PA, Quayle AJ, Bajardi A, Perdomo JJ, Robey FA, Neutra MR (1999) Immunization of mice with peptomers covalently coupled to aluminum oxide nanoparticles. *Vaccine* 17(23):3007–3019. [https://doi.org/10.1016/S0264-410X\(99\)00163-2](https://doi.org/10.1016/S0264-410X(99)00163-2)
146. Fox CB, Kramer RM, Barnes VL, Dowling QM, Vedvick TS (2013) Working together: interactions between vaccine antigens and adjuvants. *Ther Adv Vaccine* 1(1):7–20. <https://doi.org/10.1177/2051013613480144>
147. Masson J-D, Thibaudon M, Bélec L, Crépeaux G (2017) Calcium phosphate: a substitute for aluminum adjuvants? *Expert Rev Vaccines* 16(3):289–299. <https://doi.org/10.1080/14760584.2017.1244484>
148. Relyveld E, Bengounia A, Huet M, Kreeftenberg JG (1991) Antibody response of pregnant women to two different adsorbed tetanus toxoids. *Vaccine* 9(5):369–372. [https://doi.org/10.1016/0264-410X\(91\)90066-F](https://doi.org/10.1016/0264-410X(91)90066-F)
149. Lin Y, Wang X, Huang X, Zhang J, Xia N, Zhao Q (2017) Calcium phosphate nanoparticles as a new generation vaccine adjuvant. *Expert Rev Vaccines* 16(9):895–906. <https://doi.org/10.1080/14760584.2017.1355733>
150. Relyveld E (1980) Current developments in production and testing of tetanus and diphtheria vaccines. *Prog Clin Biol Res* 47:51
151. Relyveld E (1985) Immunological, prophylactic and standardization aspects in tetanus. In: *Proceedings of the seventh international conference on tetanus*. Gangemi, Rome, pp 215–227
152. Knuschke T, Rotan O, Bayer W, Sokolova V, Hansen W, Sparwasser T, Dittmer U, Epple M, Buer J, Westendorf AM (2016) Combination of nanoparticle-based therapeutic vaccination and transient ablation of regulatory T cells enhances anti-viral immunity during chronic retroviral infection. *Retrovirology* 13(1):24. <https://doi.org/10.1186/s12977-016-0258-9>
153. Sokolova V, Shi Z, Huang S, Du Y, Kopp M, Frede A, Knuschke T, Buer J, Yang D, Wu J, Westendorf AM, Epple M (2017) Delivery of the TLR ligand poly(I:C) to liver cells in vitro and in vivo by calcium phosphate nanoparticles leads to a pronounced immunostimulation. *Acta Biomater* 64:401–410. <https://doi.org/10.1016/j.actbio.2017.09.037>
154. Heße C, Kollenda S, Rotan O, Pastille E, Adamczyk A, Wenzek C, Hansen W, Epple M, Buer J, Westendorf AM, Knuschke T (2019) A tumor-peptide-based nanoparticle vaccine elicits efficient tumor growth control in antitumor immunotherapy. *Mol Cancer Ther* 18(6):1069. <https://doi.org/10.1158/1535-7163.MCT-18-0764>
155. Salazar-González JA, González-Ortega O, Rosales-Mendoza S (2015) Gold nanoparticles and vaccine development. *Expert Rev Vaccines* 14(9):1197–1211. <https://doi.org/10.1586/14760584.2015.1064772>
156. Chen Y-S, Hung Y-C, Lin W-H, Huang GS (2010) Assessment of gold nanoparticles as a size-dependent vaccine carrier for enhancing the antibody response against synthetic foot-and-mouth disease virus peptide. *Nanotechnology* 21(19):195101. <https://doi.org/10.1088/0957-4484/21/19/195101>
157. Kang S, Ahn S, Lee J, Kim JY, Choi M, Gujrati V, Kim H, Kim J, Shin E-C, Jon S (2017) Effects of gold nanoparticle-based vaccine size on lymph node delivery and cytotoxic T-lymphocyte responses. *J Control Release* 256:56–67. <https://doi.org/10.1016/j.jconrel.2017.04.024>
158. Staroverov SA, Volkov AA, Mezheny PV, Domnitsky IY, Fomin AS, Kozlov SV, Dykman LA, Guliy OI (2019) Prospects for the use of spherical gold nanoparticles in immunization. *Appl Microbiol Biotechnol* 103(1):437–447

159. Tao W, Gill HS (2015) M2e-immobilized gold nanoparticles as influenza A vaccine: role of soluble M2e and longevity of protection. *Vaccine* 33(20):2307–2315. <https://doi.org/10.1016/j.vaccine.2015.03.063>
160. Tao W, Hurst BL, Shakya AK, Uddin MJ, Ingrole RSJ, Hernandez-Sanabria M, Arya RP, Bimler L, Paust S, Tarbet EB, Gill HS (2017) Consensus M2e peptide conjugated to gold nanoparticles confers protection against H1N1, H3N2 and H5N1 influenza A viruses. *Antiviral Res* 141:62–72. <https://doi.org/10.1016/j.antiviral.2017.01.021>
161. Li Z, Barnes JC, Bosoy A, Stoddart JF, Zink JI (2012) Mesoporous silica nanoparticles in biomedical applications. *Chem Soc Rev* 41(7):2590–2605
162. An M, Li M, Xi J, Liu H (2017) Silica nanoparticle as a lymph node targeting platform for vaccine delivery. *ACS Appl Mater Interfaces* 9(28):23466–23475. <https://doi.org/10.1021/acsami.7b06024>
163. Cha BG, Jeong JH, Kim J (2018) Extra-large pore mesoporous silica nanoparticles enabling co-delivery of high amounts of protein antigen and toll-like receptor 9 agonist for enhanced cancer vaccine efficacy. *ACS Central Sci* 4(4):484–492. <https://doi.org/10.1021/acscentsci.8b00035>
164. Wang X, Li X, Ito A, Yoshiyuki K, Sogo Y, Watanabe Y, Yamazaki A, Ohno T, Tsuji NM (2016) Hollow structure improved anti-cancer immunity of mesoporous silica nanospheres in vivo. *Small* 12(26):3510–3515
165. Mody KT, Popat A, Mahony D, Cavallaro AS, Yu C, Mitter N (2013) Mesoporous silica nanoparticles as antigen carriers and adjuvants for vaccine delivery. *Nanoscale* 5(12):5167–5179. <https://doi.org/10.1039/C3NR00357D>
166. Versiani AF, Astigarraga RG, Rocha ESO, Barboza APM, Kroon EG, Rachid MA, Souza DG, Ladeira LO, Barbosa-Stancioli EF, Jorio A, Da Fonseca FG (2017) Multi-walled carbon nanotubes functionalized with recombinant Dengue virus 3 envelope proteins induce significant and specific immune responses in mice. *J Nanobiotechnol* 15(1):26. <https://doi.org/10.1186/s12951-017-0259-4>
167. Hassan HAFM, Smyth L, Rubio N, Ratnasothy K, Wang JTW, Bansal SS, Summers HD, Diebold SS, Lombardi G, Al-Jamal KT (2016) Carbon nanotubes' surface chemistry determines their potency as vaccine nanocarriers in vitro and in vivo. *J Control Release* 225:205–216. <https://doi.org/10.1016/j.jconrel.2016.01.030>
168. Hassan HAFM, Smyth L, Wang JTW, Costa PM, Ratnasothy K, Diebold SS, Lombardi G, Al-Jamal KT (2016) Dual stimulation of antigen presenting cells using carbon nanotube-based vaccine delivery system for cancer immunotherapy. *Biomaterials* 104:310–322. <https://doi.org/10.1016/j.biomaterials.2016.07.005>
169. Zhang C, Li L-H, Wang J, Zhao Z, Li J, Tu X, Huang A-G, Wang G-X, Zhu B (2018) Enhanced protective immunity against spring viremia of carp virus infection can be induced by recombinant subunit vaccine conjugated to single-walled carbon nanotubes. *Vaccine* 36(42):6334–6344. <https://doi.org/10.1016/j.vaccine.2018.08.003>
170. Gottardi R, Douradinha B (2013) Carbon nanotubes as a novel tool for vaccination against infectious diseases and cancer. *J Nanobiotechnol* 11(1):30. <https://doi.org/10.1186/1477-3155-11-30>



Design and Synthesis of Protein-Based Nanocapsule Vaccines

Ivana Skakic, Jasmine E. Francis, and Peter M. Smooker

Abstract

Increasing emergence of infectious diseases is driving demand for new vaccine technologies capable of improving antigen delivery and protective efficacy. Nanoparticle technology is a modern approach to antigen delivery, capable of stabilizing and increasing the amount of antigen delivered to immune cells. Protein-based nanoparticles are a biodegradable alternative to existing nanomaterials, offering a versatile and biocompatible approach to nanoparticle vaccine delivery. In this chapter, the methods for the synthesis and characterization of protein-based nanocapsule vaccines are discussed. Initially, the requirements for a suitable nanoparticle vaccine are outlined, and finally, methods for the design and synthesis of protein-based nanocapsule vaccines are explained.

Key words Nanocapsule vaccine, Nanoparticle, Protein nanoparticle, Vaccine delivery system, Silica template

1 Introduction

Traditional vaccines have thus far been unsuccessful in preventing some significant infections. Although many approaches to vaccination have been developed, the inability of conventional delivery methods to elicit appropriate immune responses is a major barrier to protection against some pathogens.

Despite the development of a range of effective vaccine strategies, infectious disease remains a significant global health burden. The emergence and evolution of deadly infectious diseases such as Ebola, Zika, dengue, Middle East respiratory syndrome (MERS), and more recently SARS-CoV-2 demonstrate the growing need for new vaccine technologies [1]. There are several key properties that an ideal vaccine should exhibit: it should be easy to administer, and it must be safe, stable, and preferably cheap to produce. An efficient antigen delivery system also needs to be able to deliver the required

antigen to immune cells and elicit a strong and appropriate immune response [2].

Due to the concerns associated with inactivated and attenuated vaccines and the reduced immunogenicity of subunit vaccines, there is a need for more efficient antigen delivery systems. Particulates in the range of 1–1000 nm, known as nanoparticles, may be the key to increasing the efficacy of subunit vaccines. They have been shown to stabilize vaccine antigens and more efficiently deliver antigen to intracellular compartments, increasing immunogenicity [3]. The field of vaccine development is increasingly looking toward nanotechnology for the development of delivery systems with increased antigen effectiveness, in terms of both increased immunogenicity and targeted delivery.

To date, nanoparticles synthesized from a range of materials, such as gold, silver, iron oxides, and synthetic polymers, have shown great promise as new vaccine and drug delivery systems [3, 4]. As these nanoparticles are in the size range of pathogens such as viruses and bacteria, dendritic cells readily take up particles of this size. However, the use of nonbiodegradable materials raises concerns regarding toxicity and bodily clearance. The use of biodegradable nanoparticles in vaccine formulations may allow for reduced toxicity and sustained antigen release [4–6].

The use of protein-based nanoparticles is an approach in which nanoparticles are synthesized from cross-linked antigen, without the use of nonbiodegradable materials. This method reduces concerns associated with bodily clearance of potentially toxic nanomaterials and offers some protection and stability to vaccine antigens. The fabrication of protein-based nanocapsules relies on a silica templating system in which antigen is infiltrated and cross-linked into mesoporous shell silica nanoparticles which are subsequently dissolved, leaving a hollow protein nanocapsule (Fig. 1).

The advantage of silica-based nanoparticle templates is that their fabrication, size, and structure are adaptable. Solid core mesoporous shell (SC/MS) silica nanoparticles can be prepared using existing preparation methods [7–10]. The shape, pore size, and surface functionalization of silica nanoparticles are controllable, allowing for modification as desired for infiltration of proteins of different size, structure, and isoelectric point.

Previous studies utilizing the SC/MS nanoparticle templating system have demonstrated the successful synthesis of protein-based nanocapsules which were readily internalized and cross-presented by murine dendritic cells [10]. This templating approach allows the use of any antigen to form protein nanocapsules against a desired target, which can be tested *in vitro*, or in an animal model. The experimental steps involved in the design and preparation of a protein-based nanocapsule vaccine is described in Fig. 2.

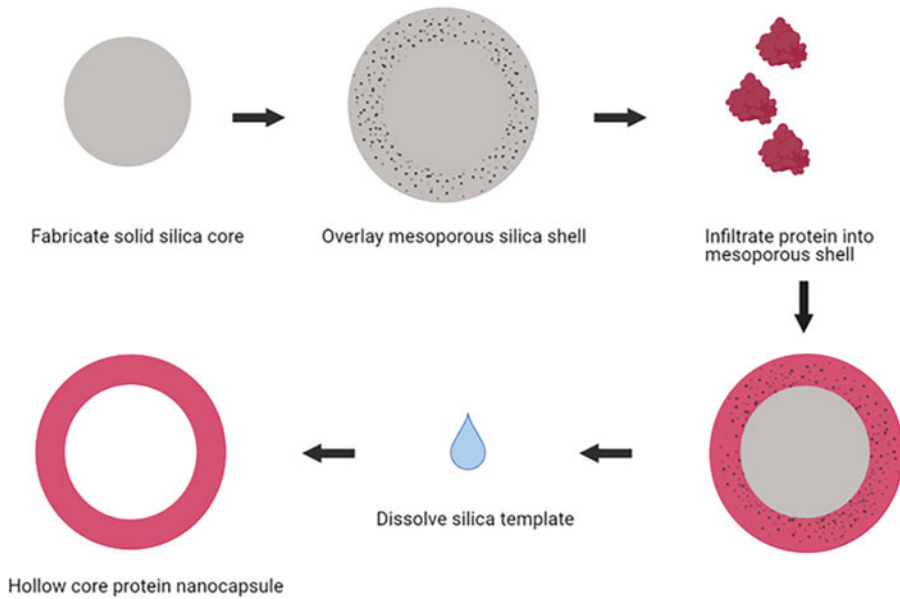


Fig. 1 Schematic diagram of synthesis of protein-based nanocapsules

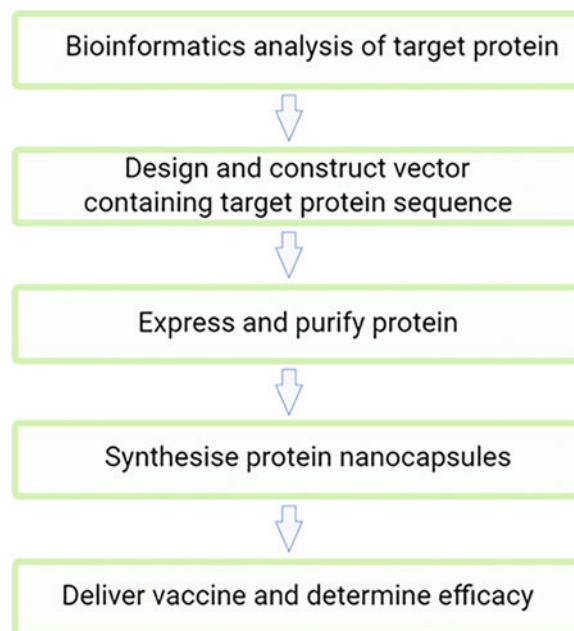


Fig. 2 Flowchart for experimental nanocapsule synthesis and vaccine delivery

In this chapter, methods for preparing protein nanocapsules, including silica template synthesis and characterization techniques are detailed. In vitro experiments to determine cellular uptake and cytotoxicity of particles are discussed.

2 Materials

2.1 Recombinant Protein Expression Vector

2.1.1 Bioinformatics Analysis and Optimization of Encoded Antigen

1. Target antigen gene sequence to be extracted from Genbank, NCBI.
2. Cloning software (such as SnapGene) for visualization of cloning strategy and final vaccine vector construct.

2.1.2 Cloning of Vector

1. Synthetic gene in standard cloning vector.
2. Empty DNA vaccine vector.
3. Restriction ligases (such as *EcoRI* and *HindIII*) and 10× buffers.
4. Chemically competent *Escherichia coli* DH5-α strain.
5. Standard cloning vector (pRSET-a) carrying ampicillin resistance marker for positive selection.
6. Agarose, nucleic acid stain (such as Sybr Red), loading dye, and 1× TAE for agarose gel electrophoresis.
7. Agarose gel electrophoresis system: for 100 mL of 1.5% agarose gel, add 1.5 g agarose powder to 100 mL 1× TAE buffer. Prepare 1 L of 10× TAE buffer by adding 48.4 g Tris base, 3.72 g di-sodium EDTA, to 1 L of ddH₂O, and adjust final pH to 8.5 with glacial acetic acid.
8. Gel imaging system.
9. QIAquick PCR Purification and Gel Extraction kits (Qiagen) for gel extraction.
10. Nanodrop or spectrophotometer for DNA quantification.
11. T4 DNA ligase and 10× buffer.
12. Working stock solution of ampicillin (100 µg/mL). To prepare 10 mL stock solution, add 1 g ampicillin to 10 mL ddH₂O and sterilize by filtering through a 0.2-µm syringe.
13. Heat block and water bath for incubation of transformed cells.
14. Mg²⁺ (2 M) buffer.
15. LB broth supplemented with 100 µg/mL ampicillin. To 1 L of ddH₂O, add 10 g NaCl, 10 g tryptone, and 5 g yeast extract. Autoclave and allow to cool to below 50 °C before adding 1 mL of ampicillin stock solution.
16. LB agar supplemented with a final concentration of 100 µg/mL ampicillin: To 1 L ddH₂O, add 10 g NaCl, 10 g tryptone, and 5 g yeast extract, followed by 15 g bacteriological agar. Autoclave and cool to below 50 °C before adding 1 mL of ampicillin stock solution. Pour into sterile petri dishes and store for up to 3 months at 4 °C.

17. Shaking incubator for broth cultures.
18. Incubator for plate cultures.

2.1.3 Confirmation of Recombinant Protein Expression in *Escherichia coli* BL21 Cells

1. Electrocompetent *Escherichia coli* BL21 cell line.
2. Vector containing inserted target gene.
3. Digital electroporator.
4. LB broth supplemented with 100 µg/mL ampicillin. To 1 L of ddH₂O, add 10 g NaCl, 10 g tryptone, and 5 g yeast extract. Autoclave and allow to cool to below 50 °C before adding 1 mL of ampicillin stock solution.
5. Shaking incubator for broth cultures.
6. Digital sonicator.
7. Sodium dodecyl-sulfate polyacrylamide gel electrophoresis (*SDS-PAGE*) system: for 1 L of 1× running buffer, add 14.4 g glycine, 3.02 g Tris base, and 1 g sodium dodecyl-sulfate to 1 L ddH₂O. To prepare 4 mL of 6% stacking gel, to 2.7 mL H₂O, add 500 µL of 1 M Tris (pH 6.8), 20 µL sodium dodecyl-sulfate (20%), 40 µL ammonium persulfate (10%), 800 µL acrylamide (30%), 4 µL TEMED. To prepare 10 mL of 10% resolving gel, to 4.1 mL H₂O, add 2.5 mL of 1.5 M tris (pH 8.8), 50 µL sodium dodecyl-sulfate (20%), 100 µL ammonium persulfate (10%), 3.3 mL acrylamide (30%), 10 µL TEMED.
8. SDS loading dye.
9. Protein standards.
10. Western blot system.
11. Fluorescently tagged antibody.
12. Tris base saline (TBS) 1×.
13. Centrifuge.

2.2 Recombinant Protein Expression and Purification Materials

2.2.1 Protein Expression

1. Ten milliliter overnight LB culture of *Escherichia coli* BL21 cells electrotransformed with selected vector.
2. LB broth supplemented with 100 µg/mL ampicillin.
3. Working stock solution of Isopropyl Thio-beta-D-Galactoside (IPTG) (1 M). To prepare 10 mL stock solution, add 2.383 g IPTG to 10 mL ddH₂O and sterilize by filtering through a 0.2-µm syringe. Aliquot and store at -20 °C.
4. Shaking incubator for broth cultures.
5. Digital sonicator.

2.2.2 Protein Purification

1. Bacterial cell lysate.
2. Imidazole stock solution (5 M). To prepare 10 mL of stock solution, add 3.403 g imidazole to 10 mL ddH₂O, dissolve and

filter through 0.45 μm filter. Store at 4 °C protected from light. Imidazole stock solution is used for preparation of equilibration and wash buffers.

3. Phosphate buffered saline (PBS) 1 \times .
4. Nickel sulfate (NiSO_4) solution (0.2 M). To prepare 10 mL of stock solution, add 0.309 g of NiSO_4 to 10 mL ddH₂O, dissolve and filter through 0.45 μm filter.
5. Iminodiacetic acid Sepharose[®] resin packed into a 1 mL gravity-flow column. To prepare resin column, pack 1 mL Iminodiacetic acid Sepharose[®] resin into column and wash with 10 mL ddH₂O. Charge resin with 500 μL of NiSO_4 working solution and wash with 10 mL ddH₂O. To prepare 10 mL of 10 mM imidazole equilibration buffer, add 20 μL of imidazole stock solution to 10 mL of 1 \times PBS. To prepare wash buffers, add required volume of imidazole working stock solution to 1 \times PBS, to obtain desired concentration.
6. Amicon ultrafiltration unit.
7. Centrifuge.

2.3 Nanoparticle Template Fabrication

1. Template stock solutions as desired; ddH₂O, ethanol, ammonia hydroxide, tetraethoxysilane (TEOS), *n*-octadecyltrimethoxysilane (TMS).
2. Vortex.
3. Magnetic stirrer.
4. Centrifuge.
5. Furnace oven, capable of heating to 550 °C.

2.4 Nanocapsule Synthesis

1. Purified protein.
2. Nanoparticle template.
3. Phosphate-buffered saline (PBS) 1 \times , pH adjusted to requirements.
4. End-over-end suspension mixer.
5. Glutaraldehyde solution, 5% (w/v) working solution.
6. Hydrofluoric acid (HF) template removal buffer: To prepare 10 mL of template removal buffer, add 2.963 g of ammonium fluoride to 10 mL of 1 \times PBS, allowing to dissolve. To the dissolved solution, add 846 μL of hydrofluoric acid (49%) (*see Note 1*).
7. Microcentrifuge.

2.5 Nanoparticle and Nanocapsule Characterization

1. Phosphotungstic acid, 1% (w/v) working solution.
2. Holey carbon grids.

2.6 *In Vitro* Characterization

2.6.1 Cell Uptake

1. HEK293 cell line and complete RPMI media.
2. Sterile six-well tissue culture plates.
3. Incubator with 5% CO₂ injection.
4. Fluorescent microscope.

2.6.2 Cell Viability

1. HEK293 cell line and complete media.
2. Sterile 96-well tissue culture plates.
3. Incubator with 5% CO₂ injection.
4. PrestoBlue cell viability reagent.
5. Microplate reader.

2.7 Mouse Vaccination

1. Female C57BL/6 mice.
2. 27 gauge needles and syringes.
3. 1 × PBS (pH 7.4).

3 Methods

3.1 Recombinant Protein Vector

3.1.1 Bioinformatics Analysis and Optimization of Encoded Antigen

1. Select the antigen of interest and download the gene sequence from Genbank, NCBI (*see Note 2*).
2. Add restriction enzyme digestion sites at both ends of the sequence, ensuring the gene will insert in the correct orientation into the desired vector.
3. Using a cloning program or software such as SnapGene, insert the antigen sequence into the insertion site of the DNA vector.
4. Ensure insertion is in frame and in the correct orientation and use the sequence for gene synthesis (*see Note 3*).
5. Order your desired gene sequence in a cloning vector from a gene synthesis service (*see Note 4*).

3.1.2 Cloning of Vector

1. Using appropriate restriction enzymes digests 1 µg of the cloning vector carrying the gene of interest and 1 µg DNA recipient vector.
2. Heat inactivate the restriction enzymes at 65 °C for 15 min.
3. Run samples on a 1.5% agarose gel and excise the fragments of the gene and vector.
4. Purify these excised fragments from the gel using the ISOLATE II PCR and Gel Kit, following manufacturer's instructions.
5. Measure the concentration of both gene and vector, then ligate the samples at a vector to insert molar ratio of 1:5 with T4 DNA Ligase enzyme.

6. Thaw chemically competent *E. coli* DH5- α cells on ice for 5 min.
7. Add 1 μg of ligation product to the cells and incubate on ice for 10 min.
8. Transform cells by heat shocking the cells at 42 °C for 50 s.
9. Keep mixture on ice for 2 min.
10. Aliquot and spread 50 μL of the mixture onto an agar plate supplemented with 100 $\mu\text{g}/\text{mL}$ ampicillin.
11. After 24 h, isolate a colony from the plate and subculture in LB broth by incubation at 200 rpm, 37 °C for 18 h.
12. Purify plasmid DNA using the ISOLATE II plasmid mini kit.
13. Confirm the presence of the antigen gene by sequencing and restriction enzyme digestion.
14. Store a glycerol stock of your sequence verified plasmid construct in *E. coli* DH5- α in 20% glycerol at -80 °C.

3.1.3 Confirmation of Recombinant Protein Expression in *Escherichia coli* BL21 Cells

1. Electrotransform the sequence-verified plasmid into electrocompetent *Escherichia coli* BL21 cells, and culture in LB broth without ampicillin for 2 h at 200 rpm, 37 °C in a shaking incubator.
2. Subculture the electrotransformed cells in LB broth supplemented with 100 $\mu\text{g}/\text{mL}$ ampicillin at 200 rpm, 37 °C, until OD₆₀₀ reaches 0.4–0.6. Induce expression by the addition of IPTG to a working concentration of 1 mM. Allow expression to proceed for at 200 rpm, 37 °C in a shaking incubator for 5 h.
3. Centrifuge the culture at 4000 $\times g$ for 10 min. Collect the cell pellet, discarding the supernatant. Wash cell pellet with 1 \times PBS, centrifuging at 4000 $\times g$ for 10 min. Discard the supernatant.
4. Resuspend cell pellet in 1 \times PBS.
5. Lyse cells with a digital sonicator, at 27% power for three intervals of 15 s power with 15 s rest (*see* **Note 5**).
6. Collect cell lysate samples and combine with SDS loading buffer as follows: combine 20 μL of protein sample with 5 μL of SDS loading buffer and denature at 100 °C for 5 min.
7. Prepare stacking gel and loading gel, unless using pre-cast SDS-PAGE gels.
8. Assemble the gel cassette and place inside the SDS-PAGE electrophoresis unit. Fill the gel tank with SDS-PAGE running buffer. Load prepared samples onto SDS-PAGE gel. Load protein standard onto gel. Run gel for 30 min at 60 V, followed by a further 60 min at 180 V.
9. Remove the gel from the gel cassette.

10. For SDS-PAGE protein staining, place gel into SDS-PAGE protein gel stain as per manufacturer's instructions.
11. For antibody probing, transfer the protein gel onto a nitrocellulose membrane using a Western blot system, according to manufacturer's instructions.
12. Following protein transfer, block the nitrocellulose membrane with 5% blocking buffer for 2 h at room temperature, 40 rpm on a platform shaker.
13. Remove blocking buffer and wash membrane three times with TBS.
14. Add diluted fluorescently tagged antibody against the antigen and incubate for 2 h at room temperature, 40 rpm on a platform shaker.
15. Remove antibody and wash membrane three times with TBS.
16. Add detection buffer and visualize, as per manufacturer's instructions.

3.2 Recombinant Protein Expression and Purification Materials

3.2.1 Protein Expression

1. Subculture the sequence verified plasmid from -80°C glycerol stock in LB broth supplemented with $100\ \mu\text{g}/\text{mL}$ ampicillin at 200 rpm, 37°C in a shaking incubator.
2. Induce expression by addition of IPTG to a working concentration of 1 mM when culture reaches OD_{600} 0.4–0.6. Allow expression to proceed for at 200 rpm, 37°C in a shaking incubator for time duration as per optimized expression protocol.

3.2.2 Protein Purification

1. Following bacterial protein expression, centrifuge the culture at $4000 \times g$ for 10 min. Collect the cell pellet, discarding the supernatant. Wash cell pellet with $1 \times$ PBS, centrifuging at $4000 \times g$ for 10 min. Discard the supernatant.
2. Resuspend cell pellet in $1 \times$ PBS.
3. Lyse cells with a digital sonicator, at 27% power for three intervals of 15 s power with 15 s rest.
4. Centrifuge the cell lysate at $4000 \times g$ for 20 min (*see Note 6*).
5. Reserve the supernatant and discard cell pellet (*see Note 7*).
6. Pack and wash the nickel-charged resin column as follows: pack 1 mL Iminodiacetic acid Sepharose[®] resin into column and wash with 10 mL ddH₂O. Charge resin with 500 μL of NiSO₄ working solution and wash with 10 mL ddH₂O.
7. Equilibrate column with 10 mL equilibration buffer.
8. Load clarified sample lysate onto column.
9. Following sample lysate loading onto the column, wash the column with a wash buffer containing the lowest concentration of imidazole.

10. Proceed to wash the column with wash buffers of increasing concentrations of imidazole, as per optimized imidazole gradient protocol (*see Note 8*).
11. Collect final eluate and load onto an Amicon Ultrafiltration unit with a membrane cut-off suitable for the target protein.
12. Centrifuge at $4000 \times g$ until the remaining volume in the reservoir is 1 mL, discard the flow-through.
13. Top up the reservoir with $1 \times$ PBS and centrifuge at $4000 \times g$ until the remaining volume in the reservoir is 1 mL, discarding the flow-through.
14. Repeat the above step until the sample concentration of imidazole is less than 0.1 mM.
15. Store the concentrated protein sample at -20°C until use.

3.3 Nanoparticle Template Fabrication

3.3.1 Fabrication of Solid Silica Particle Core

1. In a flask combine 37 mL of ethanol, 5 mL ddH₂O, and 4.2 mL of 32% ammonium hydroxide at room temperature.
2. Stir vigorously until the temperature of the solution has stabilized.
3. Add 2.8 mL of TEOS and vortex for 10 s.
4. Allow solution to sit still for 1 h for the reaction to proceed, at room temperature.

3.3.2 Overlay of Mesoporous Outer Shell onto Solid Silica Particle Core

1. To a solution containing solid silica particle core, add 2.35 mL TEOS and 0.5 mL 91.6% TMS slowly over a 20 min period while stirring.
2. Incubate the solution for 2.5 h at room temperature.
3. Following incubation, wash the solution three times with ethanol at $5000 \times g$ for 2 min.
4. Dry the particles on a Petri dish overnight at room temperature to completely remove the ethanol.
5. Heat the particles at 550°C for 6 h to remove the porogen TMS.
6. Store the particles in a dry polypropylene tube or resuspended in 96% ethanol at the required concentration until use.

3.4 Nanocapsule Synthesis

1. Prepare 3 mg of template by washing three times with PBS at $5000 \times g$ for 5 min.
2. Combine the washed template with purified protein in a 1.5-mL microfuge tube (*see Note 9*), resuspending the template in the solution.
3. Incubate the solution for 20 h at 4°C , on an end-over-end suspension mixer to allow the infiltration of the protein into the template.

4. Following incubation, centrifuge at $5000 \times g$ for 5 min to remove excess protein. Wash the particles with PBS two times.
5. To the washed particles, add 1 mL of 5%(w/v) glutaraldehyde solution and incubate for 2 h at 4 °C, on an end-over-end suspension mixer in the dark (*see Note 10*).
6. Following incubation, centrifuge at $5000 \times g$ for 5 min, resuspend the particles in 200 μ L 1 \times PBS in a microtube.
7. Store the infiltrated particles at 4 °C for up to 2 weeks, prior to template removal.
8. For template removal, add 800 μ L of hydrofluoric acid (HF) template removal buffer to the infiltrated particles, carefully inverting the tube 2–3 every 15 s for 1 min allowing the HF to dissolve the silica particle template (*see Note 1*).
9. Centrifuge at $5000 \times g$ for 5 min. Carefully remove the supernatant and discard into an appropriate HF waste receptacle.
10. Wash the nanocapsules with 1 mL 1/4 \times PBS, resuspended the pellet in the solution. Centrifuge at $5000 \times g$ for 5 min, carefully remove the supernatant and discard into an appropriate HF receptacle. Repeat wash three times.
11. Resuspend nanocapsules in 200 μ L 1 \times PBS. Store at 4 °C until use.

3.5 Nanoparticle and Nanocapsule Characterization

3.5.1 Dynamic Light Scattering

1. Measure size distribution, zeta potential, and polydispersity of template and nanocapsules by dynamic light scattering (*see Note 11*).
2. Dilute particles to a concentration of 10 μ g/mL in PBS and transfer to a DT1070 folded capillary cell and measure at 4 °C.

3.5.2 Transmission Electron Microscopy (TEM)

1. Visualize particles by transmission electron microscopy (TEM) for size and structural properties (*see Note 12*).
2. Load 10 μ g of template or nanocapsules onto a holey carbon grid and allow to air dry for 10 min.
3. Add 10 μ L of 1% phosphotungstic acid to the loaded grid and allow to air dry.
4. Once dry, loaded copper grids can be imaged on a transmission electron microscope at an accelerating voltage of 80 kV.

3.6 In Vitro Characterization

3.6.1 Cell Uptake

1. Seed HEK293 cells at 1×10^5 cells per well in a six-well plate, onto a sterile coverslip, and add 100 μ g of GA-cross-linked nanocapsules.
2. Incubate for 6 h to allow cell uptake of the nanocapsules.
3. Remove nanocapsules and wash coverslips three times with cold PBS.

4. Add 50 μL per coverslip of DAPI nuclear counterstain and incubate for 15 min, in the dark.
5. Fix cells by adding 1 mL of 4% PFA for 10 min, followed by washing cells three times with cold PBS.
6. Mount coverslip onto a slide and visualize nanocapsule uptake by imaging with a fluorescent microscope (*see Note 13*).

3.6.2 Cell Viability

1. Seed HEK293 cells at a density of 1×10^4 cells per well in a sterile 96-well tissue culture plate overnight.
2. Treat cells with increasing concentrations of nanocapsules (5–100 $\mu\text{g}/\text{mL}$) for 24, 48, or 72 h in a final well volume of 100 μL in complete RPMI media.
3. Incubate cells with PrestoBlue reagent for 45 min prior to measuring absorbance at 570 and 600 nm in a plate reader.
4. Analyze the data by subtracting the reference wavelength absorbance values (600 nm) from the 570 nm absorbance data and normalize all data to the average of the blank wells.
5. Determine cytotoxic effects (LC_{50}) of nanocapsules prior to proceeding to animal vaccinations.

3.7 Mouse Vaccinations

1. For intraperitoneal injection, prepare 100 μL of 20 $\mu\text{g}/\text{mL}$ nanocapsule vaccine in sterile $1 \times \text{PBS}$ (*see Note 14*).
2. Vaccinate 6- to 8-week old C57BL/6 mice. Analyze immune responses at appropriate times.

4 Notes

1. Hydrofluoric acid is extremely corrosive and toxic. Skin contact with hydrofluoric acid may cause severe burns and death. Hydrofluoric acid work should only be undertaken by trained persons.
2. It is important to assess suitability of the target protein for template infiltration purposes, as template pore size (diameter) may be a limiting factor in the ability of the target protein to infiltrate into the nanoparticle template. Therefore, the size as well as structure of the protein is important to consider in designing a nanocapsule vaccine.
3. Performing bioinformatics analysis of the construct is important as it confirms that the gene will be translated in frame.
4. Commercial gene synthesis services may offer the option of cloning the gene of interest into common bacterial expression vectors, such as pRSET-a. Selecting this option may allow the user to avoid the cloning steps described in this chapter. Standard gene synthesis will provide the desired gene in a standard cloning vector such as pRSET-a shown in Fig. 3.

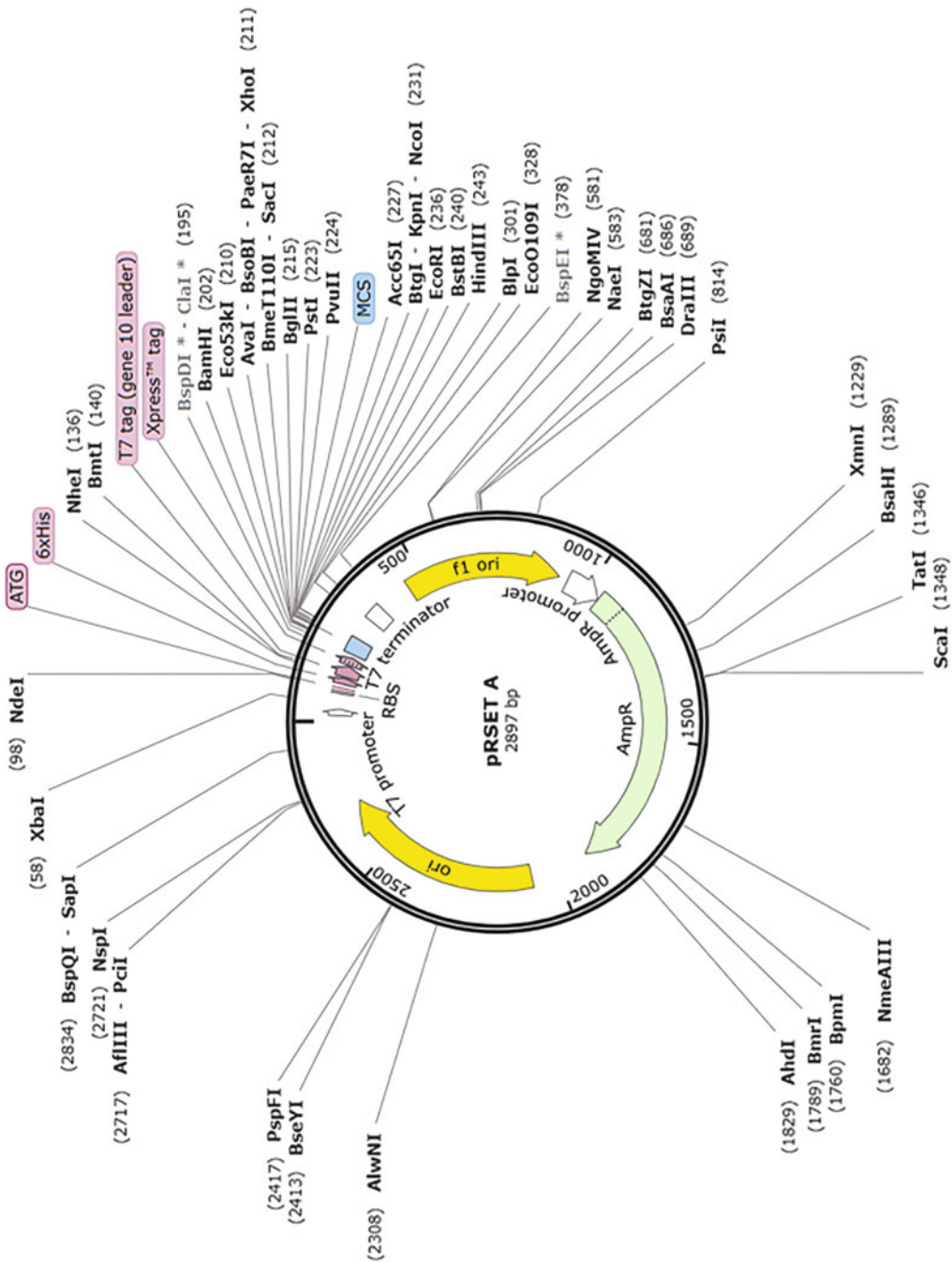


Fig. 3 Schematic representation of a standard pRSET-a expression vector. The antigen gene is cloned into the 47-base multiple cloning site (MCS) which has 18 different hexanucleotide-specific restriction enzyme sites for use in cloning or digestion. The pRSET-a vector also includes a high copy-number origin of replication (ori) for replication in *E. coli*, an AmpR gene for ampicillin resistance and an inducible LacZ operon

5. Sonication is a fast and effective method to lyse cells by ultrasound waves which transfer energy into the sample, shearing the cell wall. The process can result in a temperature increase of the sample, which may lead to denaturation of the proteins. It is recommended to place the tube containing the bacterial culture on ice during the sonication process to help keep the sample cold.
6. The cell lysate may contain small particle debris following centrifugation that may block the resin upon addition to the column. Passing the sample through a 0.45 μm membrane filter following centrifugation will eliminate most cellular debris particles.
7. Expressed proteins that are soluble will be contained within the supernatant following cell lyses. However, expressed proteins may be insoluble if they are membrane proteins, misfolding, due to overexpression, or other factors resulting in exposure of hydrophobic regions. If the target protein expresses insoluble additional steps following lysis will need to be undertaken.
8. Washes of increasing imidazole concentration are designed to eliminate most contaminants and competitive proteins without dislodging the target protein prior to elution. It is recommended to optimize wash concentrations using an imidazole gradient, 20 mM imidazole concentration increments, to establish a most suitable purification protocol for the target protein.
9. Protein infiltration efficiency should be determined before preparing nanocapsule vaccines. Infiltration at a high ratio of template to protein may result in decreased loading efficiency of protein, requiring additional infiltrations to achieve the desired amount of nanocapsules. It is recommended to use ratios between 1:1 and 1:3 of protein to template for nanocapsule synthesis.
10. Glutaraldehyde is autofluorescent when exposed to light, which may interfere with fluorescence microscopy analysis of nanocapsules. Samples should be wrapped in aluminum foil to protect from light during incubation with glutaraldehyde.
11. Dynamic light scattering is a useful technique for quick analysis of nanoparticle size, surface zeta potential, and polydispersity index (PDI). Brunauer–Emmett–Teller (BET) and Barrett–Joyner–Halenda (BJH) analysis may also be used to determine specific surface area evaluation, as well as pore area and specific pore volume, which would help guide in the selection of appropriate target proteins for template infiltration.
12. TEM analysis is a useful technique for characterizing morphological features of particles. Analysis shows protein

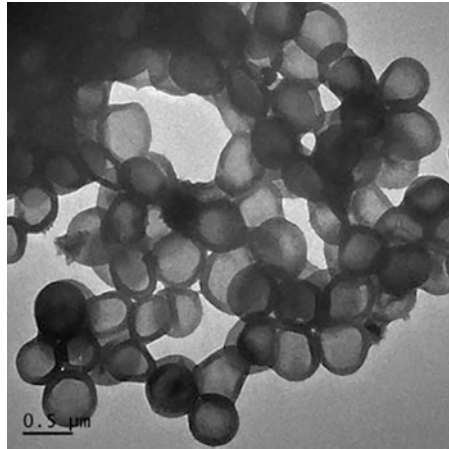


Fig. 4 Transmission electron micrograph of protein-only nanocapsules. Nanocapsules appear as hollow-core structures with a dense cross-linked protein shell

nanocapsules are homogenous in size and shape, with visible creasing and overlapping of particles indicating a hollow core structure (Fig. 4).

13. The uptake and delivery of antigen by antigen-presenting cells (APCs) is crucial to triggering the cellular immune response. Therefore, the confirmation of nanocapsule cell uptake is an important step in nanocapsule vaccine design.
14. Antigen nanocapsule vaccines can be delivered by several routes depending on the application and type of formulation used. The most common routes of nanoparticle vaccine administration include intramuscular, intradermal, subcutaneous, and mucosal. The route of administration may affect vaccine efficacy and should be considered when planning an animal trial.

References

1. Bloom DE, Cadarette D (2019) Infectious disease threats in the twenty-first century: strengthening the global response. *Front Immunol* 10:549. <https://doi.org/10.3389/fimmu.2019.00549>
2. Rappuoli R, De Gregorio E, Del Giudice G et al (2021) Vaccinology in the post-COVID-19 era. *Proc Natl Acad Sci U S A* 118(3):e2020368118. <https://doi.org/10.1073/pnas.2020368118>
3. Sahdev P, Ochyl LJ, Moon JJ (2014) Biomaterials for nanoparticle vaccine delivery systems. *Pharm Res* 31(10):2563–2582. <https://doi.org/10.1007/s11095-014-1419-y>
4. Xiao Y, Shi K, Qu Y et al (2019) Engineering nanoparticles for targeted delivery of nucleic acid therapeutics in tumor. *Mol Ther Methods Clin Dev* 12:1–18. <https://doi.org/10.1016/j.omtm.2018.09.002>
5. Danaei M, Dehghankhold M, Ataei S et al (2018) Impact of particle size and polydispersity index on the clinical applications of lipidic nanocarrier systems. *Pharmaceutics* 10(2):57
6. Penumarthi A, Basak P, Smooker P et al (2020) Hitching a ride: enhancing nucleic acid delivery into target cells through nanoparticles. In: Daima HK, Pn N, Ranjan S, Dasgupta N, Lichtfouse E (eds) *Nanoscience in medicine*,

- vol 1. Springer, Cham, pp 373–457. https://doi.org/10.1007/978-3-030-29207-2_11
7. Büchel G, Unger KK, Matsumoto A et al (1998) A novel pathway for synthesis of submicrometer-size solid core/mesoporous shell silica spheres. *Adv Mater* 10 (13):1036–1038. [https://doi.org/10.1002/\(sici\)1521-4095\(199809\)10:13<1036::aid-adma1036>3.0.co;2-z](https://doi.org/10.1002/(sici)1521-4095(199809)10:13<1036::aid-adma1036>3.0.co;2-z)
 8. Möller K, Kobler J, Bein T (2007) Colloidal suspensions of nanometer-sized mesoporous silica. *Adv Funct Mater* 17(4):605–612. <https://doi.org/10.1002/adfm.200600578>
 9. Taki A (2014) A new approach to antigen delivery using the nanoparticle templating system. RMIT University, Melbourne
 10. Taki AC, Francis JE, Skakic I et al (2020) Protein-only nanocapsules induce cross-presentation in dendritic cells, demonstrating potential as an antigen delivery system. *Nanomed Nanotechnol Biol Med* 28:102234. <https://doi.org/10.1016/j.nano.2020.102234>



Design and Preparation of Solid Lipid Nanoparticle (SLN)-Mediated DNA Vaccines

Jasmine E. Francis, Ivana Skakic, and Peter M. Smooker

Abstract

Increasing application of nucleic acid vaccines is driving demand for new delivery systems to improve stability and efficacy of DNA vaccines. Solid lipid nanoparticles (SLN) are a particulate carrier system composed of a solid lipid core and a cationic lipid surface suitable for binding negatively charged DNA. SLN delivery systems can be used to bind DNA resulting in an SLN/DNA complex (termed “lipoplex”) which can be used as a potential vaccine.

In this chapter, the methodologies associated with the use of SLNs as a DNA vaccine nanocarrier are discussed. First, requirements for an effective experimental lipoplex vaccine are discussed along with current and historical examples. Then, flowcharts for design and synthesis of lipoplex vaccines are outlined, followed by detailed materials and methods for synthesis and characterization of lipoplex vaccines.

Key words DNA vaccine, Solid lipid nanoparticle, SLN, Lipoplex, Particulate carrier systems

1 Introduction

Innovations in vaccine design have led to the development of a range of modern vaccine models, such as nucleic acid vaccines. DNA vaccines are a nucleic acid vaccine involving the transfection of mammalian cells *in vivo* with a plasmid encoding an antigenic protein, which triggers an immune response and allows the generation of immune memory against the original pathogen. This vaccine model has been found to be effective in several species, with four veterinary DNA vaccines currently licensed for use. DNA vaccines offer several advantages over traditional recombinant or whole cell vaccines in that they are easily manipulated, cheap to produce, and can be synthesized at scale with relative ease. The basic steps for experimental development of a DNA vaccine are detailed in Fig. 1.

Despite some obvious advantages to this approach, nucleic acid vaccine formulations are vulnerable to degradation by nucleases

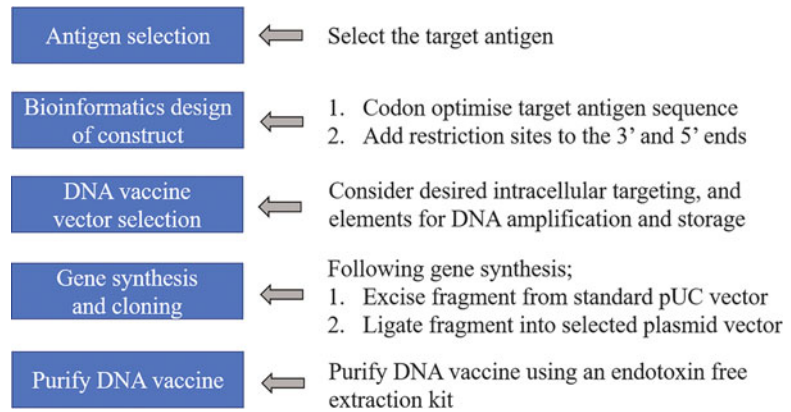


Fig. 1 Flowchart for design and synthesis of experimental DNA vaccines

and suffer rapid clearance from the body by the reticulo-endothelial system which reduces vaccine immunogenicity. Two key issues preventing the broad application of DNA vaccines are the vulnerability of naked plasmid DNA *in vivo* and the delivery of plasmid DNA to the cytoplasm of target cells [1].

One proposed solution is the application of nanoparticle technology for vaccine delivery. In terms of vaccine delivery, nanoparticles offer protection from extracellular protease degradation, increased payload stability, potential adjuvant activity, increased uptake by antigen-presenting cells (APCs), and potential cross-presentation of exogenous antigens [2–5].

Particulate carrier systems have been developed from a wide range of materials, including synthetic or organic polymers, polysaccharides, silica, iron-oxide, and lipid [6]. The ideal nanoparticle delivery system is highly effective at protecting and delivering a payload, low-cost and easy to manufacture, and highly biocompatible [7].

Solid lipid nanoparticles (SLNs) are a class of sub-micron particles composed of dense lipid and are commonly fabricated by solvent emulsification or homogenization [8]. SLNs may be synthesized from one or more lipid species with a modifiable surface for conjugation of stimulatory molecules or binding of nucleic acids [9]. SLNs typically have a solid phospholipid core and a cationic surface, capable of binding negatively charged nucleic acids, making them ideal candidates for DNA vaccine delivery [10].

SLNs offer many advantages over other nanoparticle carriers for vaccine delivery in that they are easily modifiable to include immunostimulatory lipids as a structural component of the particle itself, rather than a competing payload [11]. SLNs further offer advantages over polymeric nanoparticles due to their biocompatibility and low toxicity, and as such are the subject of interest for their potential as a DNA vaccine delivery system [12, 13].

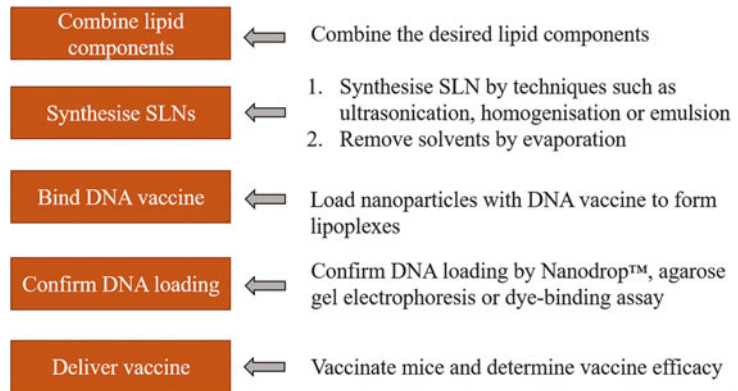


Fig. 2 Flowchart for experimental SLN synthesis and lipoplex vaccine formation

The ability of SLNs to bind plasmid DNA and transfect mammalian cells *in vitro* has been well documented [5, 10, 13, 14], and there are a growing number of studies describing the use of lipid nanomaterials as vectors for nucleic acid vaccine delivery in mice and higher mammals [15–18]. The experimental process for the development of an SLN-mediated DNA vaccine (or “lipoplex” vaccine) is described in Fig. 2.

In this chapter, methods for synthesis and characterization of solid lipid nanoparticle lipoplex vaccines are detailed. *In vitro* experiments to determine rate and pathway of cellular uptake of the particles as well as their cytotoxic and immunostimulatory properties are discussed.

2 Materials

2.1 DNA Vaccine

2.1.1 Bioinformatics Analysis and Optimization of Encoded Antigen

1. Target antigen gene sequence to be extracted from Genbank, NCBI.
2. Cloning software (such as SnapGene) for visualization of cloning strategy and final vaccine vector construct.

2.1.2 Cloning of DNA Vaccine

1. Synthetic gene in standard cloning vector.
2. Empty DNA vaccine vector.
3. Restriction ligases (such as *EcoRI* and *HindIII*) and 10× buffers.
4. Chemically competent *Escherichia coli* DH5- α strain.
5. Standard cloning vector (pUC19) and final vaccine vector carry ampicillin resistance marker for positive selection.
6. Agarose, nucleic acid stain (such as Sybr Red), loading dye, and 1× TAE for agarose gel electrophoresis.

7. Agarose gel electrophoresis system: For 100 mL of 1.5% agarose gel, add 1.5 g agarose powder to 100 mL 1× TAE buffer. Prepare 1 L of 10× TAE buffer by adding 48.4 g Tris base, 3.72 g di-sodium EDTA, to 1 L of ddH₂O, and adjust final pH to 8.5 with glacial acetic acid.
8. Gel imaging system.
9. QIAquick PCR Purification and Gel Extraction kits (Qiagen) for gel extraction.
10. Nanodrop or spectrophotometer for DNA quantification.
11. T4 DNA ligase and 10× buffer.
12. Working stock solution of ampicillin (100 µg/mL). To prepare 10 mL stock solution, add 1 g ampicillin to 10 mL ddH₂O and sterilize by filtering through a 0.2-µm syringe.
13. Heat block and water bath for incubation of transformed cells.
14. Mg²⁺ (2 M) buffer.
15. LB broth supplemented with 100 µg/mL ampicillin. To 1 L of ddH₂O add 10 g NaCl, 10 g tryptone, and 5 g yeast extract. Autoclave and allow to cool to below 50 °C before adding 1 mL of ampicillin stock solution.
16. LB agar supplemented with a final concentration of 100 µg/mL ampicillin: To 1 L ddH₂O add 10 g NaCl, 10 g tryptone, and 5 g yeast extract, followed by 15 g bacteriological agar. Autoclave and cool to below 50 °C before adding 1 mL of ampicillin stock solution. Pour into sterile petri dishes and store for up to 3 months at 4 °C.
17. Shaking incubator for broth cultures.
18. Incubator for plate cultures.

2.1.3 Confirmation of DNA Vaccine Expression in HEK293 Cells

1. HEK293 cell line.
2. Lipofectamine 3000™ reagent.
3. Dulbecco's Modified Eagle Medium (DMEM) media.
4. Penicillin-streptomycin antibiotic.
5. Heat-inactivated newborn calf serum (NCS).
6. Sterile six-well tissue culture plates.
7. Amicon ultrafiltration unit.
8. Western blot system.
9. 1× DAPI nuclear counterstain.
10. Fluorescently tagged antibody.
11. Slides and coverslips.
12. Fluorescent microscope.

2.2 Lipid Materials

2.2.1 SLN Synthesis

1. Lipid stock solutions as desired.
2. Solvents; methanol and chloroform.
3. Digital sonicator.
4. Rotary evaporator.

2.2.2 DNA Loading and Lipoplex Synthesis

1. Agarose gel equipment for confirmation of DNA loading.
2. Nanodrop or spectrophotometer.
3. Plate reader and SYBR™ Green DNA binding dye.

2.3 In Vitro Characterization

2.3.1 Cell Uptake

1. HEK293 cell line and complete RPMI media.
2. Sterile six-well tissue culture plates.
3. Incubator with 5% CO₂ injection.
4. Fluorescent microscope.

2.3.2 Cell Viability

1. HEK293 cell line and complete media.
2. Sterile 96-well tissue culture plates.
3. Incubator with 5% CO₂ injection.
4. PrestoBlue cell viability reagent.
5. Microplate reader.

2.4 Mouse Vaccination

1. Female C57BL/6 mice.
2. 27 gauge needles and syringes.
3. 1 × PBS (pH 7.4).

3 Methods

3.1 DNA Vaccine Design

3.1.1 Bioinformatics Analysis and Optimization of Encoded Antigen (See Note 1)

1. Select the antigen of interest and download the gene sequence from Genbank, NCBI.
2. Add restriction enzyme digestion sites at both ends of the sequence, ensuring the gene will insert in the correct orientation into the desired vector.
3. Using a cloning program or software such as SnapGene, insert the antigen sequence into the insertion site of the DNA vector.
4. Ensure insertion is in frame and in the correct orientation and use the sequence for gene synthesis (*see Note 2*).
5. Order your desired gene sequence in a cloning vector from a gene synthesis service (*see Note 3*).

3.1.2 Cloning of DNA Vaccine

1. Using appropriate restriction enzymes, digest 1 µg of the cloning vector carrying the gene of interest and 1 µg DNA vaccine recipient vector.

2. Heat inactivate the restriction enzymes at 65 °C for 15 min.
3. Run samples on a 1.5% agarose gel and excise the fragments of the gene and vector.
4. Purify these excised fragments from the gel using the ISOLATE II PCR and Gel Kit, following manufacturer's instructions.
5. Measure the concentration of both gene and vector, then ligate the samples at a vector to insert molar ratio of 1:5 with T4 DNA ligase enzyme.
6. Thaw chemically competent *E. coli DH5-α* cells on ice for 5 min.
7. Add 1 µg of ligation product to the cells and incubate on ice for 10 min.
8. Transform cells by heat shocking the cells at 42 °C for 50 s.
9. Keep mixture on ice for 2 min.
10. Aliquot and spread 50 µL of the mixture onto an agar plate supplemented with 100 µg/mL ampicillin.
11. After 24 h, isolate a colony from the plate and subculture in LB broth by incubation at 200 rpm, 37 °C for 18 h.
12. Purify plasmid DNA using the ISOLATE II plasmid mini kit.
13. Confirm the presence of the antigen gene by sequencing and restriction enzyme digestion.
14. Store a glycerol stock of your sequence verified plasmid construct in *E. coli DH5-α* in 20% glycerol at –80 °C.

3.1.3 Purification of Plasmid DNA for Vaccine Preparation

1. Subculture the sequence verified vaccine plasmid from –80 °C glycerol stock in LB broth overnight at 200 rpm, 37 °C.
2. Purify plasmid using an endotoxin-free plasmid prep kit.
3. Dilute the purified DNA in sterile endotoxin free 1× PBS.

3.1.4 Confirmation of DNA Vaccine Expression in HEK293 Cells

1. Revive HEK293 cells in complete RPMI media containing 10% NCS and 1% penicillin-streptomycin.
2. Seed cells at 1×10^5 cells per well in a six-well plate, onto a sterile coverslip, and add 1 mL sterile OptiMEM media.
3. In a separate tube, incubate 2.5 µg plasmid DNA with diluted Lipofectamine 2000 reagent for 5 min, before further diluting in RPMI and adding to well. Use one well of untreated cells as a negative control for expression.
4. After 6 h, change media to complete RPMI and further incubate for 72 h.
5. Remove media and wash three times with cold, sterile PBS.

6. Fix and permeabilize cells by adding 1 mL of 4% PFA and 1 mL 0.01% TritonX-100.
7. Remove solution and wash three times with cold, sterile PBS.
8. Add diluted fluorescently tagged antibody against the antigen and incubate for 2 h on ice in the dark (*see Note 4*).
9. Remove antibody and wash three times with cold, sterile PBS.
10. Mount the coverslip onto a slide and image with a fluorescent microscope to visualize expression of the encoded antigen (*see Note 5*).

3.2 Lipid Nanomaterials

3.2.1 SLN Synthesis

1. Prepare SLNs following a standard solvent-emulsification method by dissolving desired lipid components in a chloroform/methanol mixture at a ratio of 2:1 (v/v).
2. Add molecular grade H₂O to desired dilution and vortex thoroughly for 5 min.
3. Sonicate 2 mL lipid stock suspension using a digital sonicator for 3 min, 40% duty cycle and 35% power output (*see Note 6*).
4. Remove solvent from the microemulsion at 55 °C (above the melting temperature of cholesterol) using a vacuum concentrator.
5. Store at 4 °C until use.

3.2.2 SLN Characterization

Dynamic Light Scattering

1. Measure size distribution, zeta potential, and polydispersity of SLN by dynamic light scattering (*see Note 7*).
2. Dilute SLN to a concentration of 10 µg/mL in PBS and transfer to a DT1070 folded capillary cell and measure at 4 °C.

Transmission Electron Microscopy (TEM)

1. Visualize particles by transmission electron microscopy (TEM) for size and structural properties.
2. Load 10 µg SLN onto a holey carbon grid and allow to air dry for 10 min.
3. Add 10 µL of 2% ammonium molybdate to the loaded grid and allow to air dry.
4. Once dry, loaded copper grids can be imaged on a transmission electron microscope at an accelerating voltage of 80 kV.

3.2.3 DNA Loading and Lipoplex Synthesis

1. To synthesize lipoplexes, add 100 µg DNA to 1 mg SLN for a 1:10 ratio.
2. Incubate mixture for 24 h at 4 °C.
3. Confirm DNA loading by running samples on a 1.5% agarose gel at 100 V for 60 min, by visualizing the amount of unbound DNA. If a significant amount of unbound DNA is present, use a higher ratio of SLN:DNA (*see Note 8*).

3.3 *In Vitro* Characterization

3.3.1 Cell Uptake

1. Stain or tag SLN with a fluorescent dye or lipid-conjugated fluorophore.
2. Seed HEK293 cells at 1×10^5 cells per well in a six-well plate, onto a sterile coverslip, and add 100 μg of fluorescently tagged SLN.
3. Incubate for 6 h to allow cell uptake of the SLN.
4. Remove particles and wash three times with cold, sterile PBS.
5. Add 50 μL of DAPI nuclear counterstain per coverslip and incubate in the dark for 15 min.
6. Fix cells by adding 1 mL of 4% PFA for 10 min before washing three times with cold, sterile PBS.
7. Mount coverslip onto a slide and visualize SLN uptake by imaging with a fluorescent microscope (*see Note 9*).

3.3.2 Cell Viability

1. Seed HEK293 cells at a density of 1×10^4 cells per well in a sterile 96-well tissue culture plate overnight.
2. Treat cells with increasing concentrations of SLN or lipoplexes (1–100 $\mu\text{g}/\text{mL}$) for 24, 48, or 72 h to a final well volume of 100 μL in complete RPMI media.
3. At each timepoint, remove 10 μL of media and add 10 μL PrestoBlue cell viability reagent.
4. Incubate cells with PrestoBlue reagent for 30 min before measuring absorbance at 570 and 600 nm in a plate reader (*see Note 10*).
5. Analyze the data by subtracting the reference wavelength absorbance values (600 nm) from the 570 nm absorbance data and normalizing all data to the average blank wells.
6. Determine cytotoxic effects (LC_{50}) of SLN and lipoplexes before proceeding to animal vaccinations.

3.4 Mouse Vaccinations

1. For subcutaneous injection, prepare 100 μL of 100 $\mu\text{g}/\text{mL}$ lipoplex vaccine in sterile $1 \times \text{PBS}$ (*see Note 11*).
2. 6–8 week old C57BL/6 mice.

4 Notes

1. Although DNA vaccines can elicit both cellular and humoral immune responses, such responses are typically less potent than those generated by protein vaccines. There are several strategies commonly applied to increase DNA vaccine immunogenicity including the use of secretory or cytoplasmic vectors, chemokines for targeting antigen to antigen presenting cells via

chemokine receptors, encoded introns, and encoded molecular adjuvants such as the introduction of CpG motifs into the vector backbone as a Toll-like receptor 9 ligand.

2. It is important to perform bioinformatics analysis of the construct to ensure the gene will be translated in frame.
3. Commercial gene synthesis services may offer the option of cloning the gene of interest into common mammalian expression vectors such as pcDNA3.1 which can serve as a functional DNA vaccine vector. Selecting this option may allow the user to avoid the cloning steps described in this chapter. Standard gene synthesis will provide the desired gene in a standard cloning vector such as pUC19 shown in Fig. 3.
4. The antibody dilution factor is antibody dependent and should be listed on the manufacturer's website. This dilution factor occasionally requires optimization by the user and may be higher or lower than described by the manufacturer. If a tagged primary antibody is not available, an untagged primary antibody will need to be used in conjunction with a tagged secondary antibody.
5. Fluorescence microscopy is a powerful tool which can allow detection of transgene expression in real-time if live-cell imaging assays are performed. If a fluorescent microscope is not available, a Western blot is a basic and reliable method for confirming transgene expression which can be performed by probing cell lysate and supernatant from transfected cells.
6. Lipid nanoparticle synthesis parameters are dependent on several parameters (lipid species, concentration, volume of stock, vessel used for synthesis) and should be determined experimentally.
7. Dynamic light scattering is a useful technique for quick analysis of nanoparticle size, surface zeta potential, and polydispersity index (PDI). Particle size and surface charge vary significantly depending on particle composition and synthesis, but generally lipid nanocarriers fall within the range of 100–1000 nm depending on individual application. SLN designed to surface load DNA should have a positive surface charge of at least 15–30 mV to generate sufficient DNA interaction. Polydispersity is a term used to describe heterogeneity in size distribution of particles. Generally, a PDI of <0.1 indicates a monodisperse sample, while >0.7 indicates a highly polydisperse sample. For lipid nanoparticles, a PDI of <0.3 is usually considered acceptable [19].
8. Lipoplexes can be synthesized at different ratios of DNA:SLN depending on the loading capacity of the SLNs. Loading capacity is affected by surface charge of the SLNs, as the positively charged particle surface binds to negatively charged plasmid

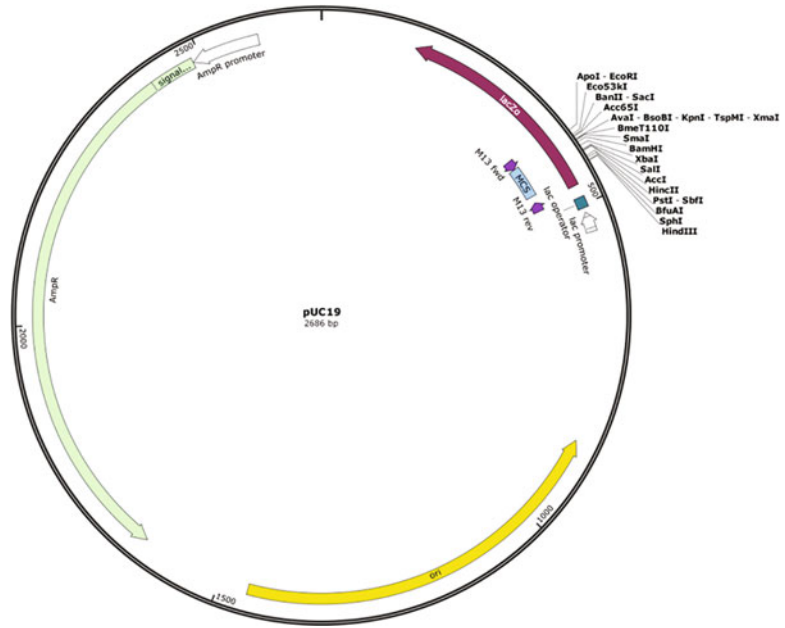


Fig. 3 Schematic representation of a standard pUC19 cloning construct. The antigen gene is cloned into the 54-base multiple cloning site (MCS) which has 13 different hexanucleotide-specific restriction enzyme sites available for selection. Other features of the construct include a high copy-number origin of replication (ori) for replication in *E. coli*, an AmpR gene conferring resistance to ampicillin, M13 sequencing primer sites, and an inducible LacZ operon

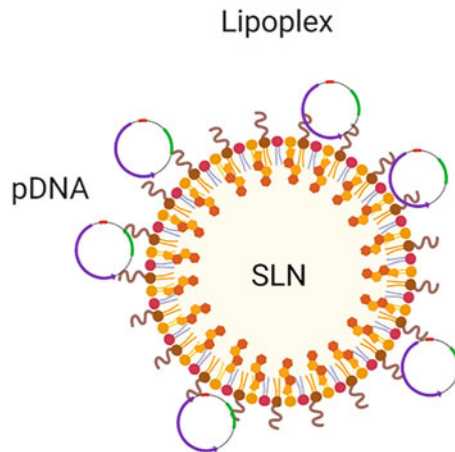


Fig. 4 Schematic representation of a lipoplex. Negatively charged plasmid DNA binds to the positively charged lipid nanoparticle surface to form a stable DNA-SLN complex

DNA (Fig. 4). Loading capacity can be determined by making samples at increasing DNA:SLN ratio and running samples on an agarose gel to visualize unbound DNA and determine the best ratio for complete DNA loading.

9. Confirmation of particle uptake by cells is an important step in lipoplex vaccine design. For antigen expression to occur, plasmid DNA to reach the nucleus for transcription and subsequent translation; therefore internalization of lipoplexes is essential for antigen expression and DNA vaccine efficacy. For quantitative analysis of particle uptake, flow cytometry can also be used to quantify the population of cells with internalized particles allowing for further statistical analysis.
10. PrestoBlue and some other cell viability reagents are reduced by live cells under standard conditions. Cells treated with PrestoBlue can be stored in the refrigerator in the dark for a further 24 h without further development of dye.
11. DNA vaccines can be delivered by several routes depending on the application and type of formulation used. The most common routes of DNA vaccine administration include intramuscular, intradermal, subcutaneous, and mucosal; however, the route of administration can affect vaccine efficacy and should be considered prior to planning an animal trial. Again, the pathogen being vaccinated against can inform this.

References

1. Ferraro B, Morrow MP, Hutnick NA et al (2011) Clinical applications of DNA vaccines: current progress. *Clin Infect Dis* 53 (3):296–302. <https://doi.org/10.1093/cid/cir334>
2. Dixon AM, Donnelly EC (2011) DNA vaccines: types, advantages, and limitations. Immunology and immune system disorders. Nova Science Publishers, New York
3. Oyewumi MO, Kumar A, Cui Z (2010) Nanomicroparticles as immune adjuvants: correlating particle sizes and the resultant immune responses. *Expert Rev Vaccines* 9 (9):1095–1107. <https://doi.org/10.1586/erv.10.89>
4. Taki A, Smooker P (2015) Small wonders—the use of nanoparticles for delivering antigen. *Vaccines (Basel)* 3(3):638–661. <https://doi.org/10.3390/vaccines3030638>
5. Penumarthi A, Parashar D, Abraham AN et al (2017) Solid lipid nanoparticles mediate non-viral delivery of plasmid DNA to dendritic cells. *J Nanopart Res* 19(6). <https://doi.org/10.1007/s11051-017-3902-y>
6. Lim M, Badruddoza AZM, Firdous J et al (2020) Engineered nanodelivery systems to improve DNA vaccine technologies. *Pharmaceutics* 12(1):30. <https://doi.org/10.3390/pharmaceutics12010030>
7. Xiao Y, Shi K, Qu Y et al (2019) Engineering nanoparticles for targeted delivery of nucleic acid therapeutics in tumor. *Mol Ther Methods Clin Dev* 12:1–18. <https://doi.org/10.1016/j.omtm.2018.09.002>
8. Mukherjee S, Ray S, Thakur RS (2009) Solid lipid nanoparticles: a modern formulation approach in drug delivery system. *Indian J Pharm Sci* 71(4):349–358. <https://doi.org/10.4103/0250-474X.57282>
9. Placzek M, Watrobska-Swietlikowska D, Stefanowicz-Hajduk J et al (2019) Comparison of the in vitro cytotoxicity among phospholipid-based parenteral drug delivery systems: emulsions, liposomes and aqueous lecithin dispersions (WLDs). *Eur J Pharm Sci* 127:92–101. <https://doi.org/10.1016/j.ejps.2018.10.018>
10. de Garibay APR, Solinís MA, del Pozo-Rodríguez A et al (2015) Solid lipid nanoparticles as non-viral vectors for gene transfection in a cell model of Fabry disease. *J Biomed Nanotechnol* 11(3):500–511. <https://doi.org/10.1166/jbn.2015.1968>
11. Azhar Shekoufeh Bahari L, Hamishehkar H (2016) The impact of variables on particle size of solid lipid nanoparticles and nanostructured lipid carriers; a comparative literature review.

- Adv Pharm Bull 6(2):143–151. <https://doi.org/10.15171/apb.2016.021>
12. Baird FJ, Taki AC, Lopata AL et al (2011) DNA vaccines: a modern-day vaccine revolution. Nova Science Publishers, New York
 13. Francis JE, Skakic I, Dekiwadia C et al (2020) Solid lipid nanoparticle carrier platform containing synthetic TLR4 agonist mediates non-viral DNA vaccine delivery. *Vaccines (Basel)* 8(3):551. <https://doi.org/10.3390/vaccines8030551>
 14. Rudolph C, Rosenecker J (2012) Formation of solid lipid nanoparticle (SLN)-gene vector complexes for transfection of mammalian cells in vitro. *Cold Spring Harb Protoc* 2012 (3):357–360. <https://doi.org/10.1101/pdb.prot068122>
 15. Hobernik D, Bros M (2018) DNA vaccines—how far from clinical use? *Int J Mol Sci* 19 (11):3605. <https://doi.org/10.3390/ijms19113605>
 16. Doroud D, Zahedifard F, Vatanara A et al (2011) Delivery of a cocktail DNA vaccine encoding cysteine proteinases type I, II and III with solid lipid nanoparticles potentiate protective immunity against *Leishmania major* infection. *J Control Release* 153(2):154–162. <https://doi.org/10.1016/j.jconrel.2011.04.011>
 17. Koriyama H, Ikeda Y, Nakagami H et al (2020) Development of an IL-17A DNA vaccine to treat systemic lupus erythematosus in mice. *Vaccine* 8(1):83
 18. Yu J, Tostanoski LH, Peter L et al (2020) DNA vaccine protection against SARS-CoV-2 in rhesus macaques. *Science* 369(6505):806–811. <https://doi.org/10.1126/science.abc6284>
 19. Danaei M, Dehghankhold M, Ataei S et al (2018) Impact of particle size and polydispersity index on the clinical applications of lipidic nanocarrier systems. *Pharmaceutics* 10(2):57



Nano-Particulate Platforms for Vaccine Delivery to Enhance Antigen-Specific CD8⁺ T-Cell Response

Jhanvi Sharma, Carcia S. Carson, Trevor Douglas, John T. Wilson, and Sebastian Joyce

Abstract

Vaccines remain the most effective way to protect populations against deathly infectious diseases. Several disadvantages associated with the traditional vaccines that use whole pathogens have led to the development of alternative strategies including the use of recombinant subunit vaccines. Subunit vaccines are, in general, safer than whole pathogens but tend to be less immunogenic due to the lack of molecular cues that are typically found on whole pathogens. To enhance immunogenicity, the subunit antigen can be administered with adjuvants that stimulate the innate immune system as a means to steer the quality and magnitude of the adaptive immune response. Novel classes of adjuvants are formulated using particle-based platforms such as virus-like particles, liposomes, and polymeric nanoparticles. These particle-based systems present antigens in ways reminiscent of whole pathogens. Such platforms offer several advantages that include co-delivery of antigen along with innate immune stimulators in a highly immunogenic format. Here we describe our recent efforts to synthesize, characterize, and validate two promising nanoparticle-based delivery systems and demonstrate their potential to induce antigen-specific CD8⁺ T cell responses, essential in clearing infection with intracellular pathogens, such as viruses and bacteria, and eradicating tumors.

Key words Nanoparticles, Virus-like particles, pH-sensitive polymeric nanoparticles, Vaccine, Antigen-specific CD8⁺ T cells, Cross-presentation

1 Introduction

Vaccine induction of a CD8⁺ T-cell response is critical for immune control and eradication of diseases caused by viruses, intracellular bacterial, and parasitic pathogens as well as cancer. Protein and peptide antigens (i.e., subunit vaccines) are attractive vaccine candidates due to their excellent safety profile, ease of manufacturability, and well-defined antigenic specificity [1]. However, peptide and protein antigens are typically weakly immunogenic when

Jhanvi Sharma and Carcia S. Carson contributed equally to this work.

administered alone and are particularly poor at generating CD8⁺ T cells [2, 3]. In order to generate a robust CD8⁺ T-cell response, antigens must either be endocytosed by specialized cross-presenting dendritic cells (DCs) or delivered to the classical cytosolic major histocompatibility complex class I (MHC-I) antigen processing pathway in the presence of additional molecular cues (i.e., type I interferons, other proinflammatory cytokines, and co-stimulation) that drive CD8⁺ T-cell expansion and differentiation [4]. However, the predominant fate of peptide and protein antigen that is endocytosed by antigen-presenting cells (APCs) is lysosomal degradation and presentation of antigen on MHC-II, with minimal presentation on MHC-I, resulting in low CD8⁺ T-cell responses. Despite this limited capacity for CD8⁺ T-cell generation, the superior safety profile of subunit vaccines continues to motivate strategies for improving their efficacy [5, 6].

The immunogenicity of subunit vaccines can be significantly enhanced by supplementing them with adjuvants.

Adjuvants can be categorized into two classes, i.e., nonspecific immunostimulatory molecules and particulate antigen delivery vehicles that present a subunit antigen in a multivalent array format reminiscent of the way in which they are naturally presented on the surface of pathogens [7]. In some cases, such as hepatitis B virus (HBV) and human papilloma virus (HPV) subunit vaccines, the target subunit antigen retains the ability to self-assemble into a noninfectious, multivalent protein cage called a virus-like particle (VLP) [8]. Because they are noninfectious and present antigens in a conformation matching that of the native virus, VLPs can serve as a safe and effective prophylactic vaccine [9]. To provide the same enhancement in immunogenicity for antigens that do not self-assemble, non-pathogen-associated VLPs can be used as a platform to display antigens at high density on their exterior interface in a multivalent fashion [10, 11]. Further, interior of the non-pathogen-associated VLPs can be used to encapsulate additional molecular cues essential for co-stimulation of antigen-specific lymphocytes [12–14].

VLPs, in addition to eliciting humoral immunity, also stimulate cell-mediated immunity and aid in eliciting a robust antigen-specific CD8⁺ T-cell response [15–20]. VLPs, although act as an exogenous antigen carrier, can feed antigen to MHC class I (MHC-I) pathway for cross-presentation [9, 12, 14]. Cross-presentation of the cargo can occur through either vacuolar or cytosolic pathway whereby antigen escapes from endosomal-lysosomal degradation pathway into the cytosol where it is processed for MHC-I antigen presentation in a proteasome-dependent pathway [21]. In this regard, VLPs closely mimic viruses that have naturally evolved to deliver genetic materials into the cytosol of host cells.

Several synthetic nanoparticle technologies are explored for efficient antigen delivery to the cytoplasm and antigen

cross-presentation [22, 23]. The majority of nanoparticle delivery systems are internalized into the endocytic pathway [24]; hence, escape from the endosomes becomes crucial and rate-limiting as endosomal entrapment results in the potential targeting of the antigen into the lysosomes for degradation. Certain particulate antigens are shown to have enhanced escape capabilities and, thus, better cross-present the cargo in comparison to their soluble counterparts [25]. Nonetheless, diverse strategies such as integration of endosome-disruptive peptides, pH sensitive polymers, fusogenic lipids into the nanoparticles have been devised to overcome entrapment and to facilitate endosomal escape and cargo delivery into the cytosol [26].

Here, we first describe the synthesis and characterization of *in vitro* assembled P22 VLPs encapsulating streptavidin as a cargo (P22-StAv), which can be utilized as a potential antigen and/or co-stimulant carrier for the induction of antigen-specific T cell response [15, 27, 28]. In second part, we describe the synthesis and characterization of pH-sensitive polymeric particles designed to enhance endosomal escape and thus antigen presentation on MHC-I for efficient induction of CD8⁺ T-cell responses [29].

2 Synthesis of P22-StAV VLP

Encapsulation of guest molecules (or cargoes) in VLP can be accomplished through *in vivo* or *in vitro* assembly. For encapsulation of cargoes in P22 VLPs, a protein-based cargo is typically fused at the N-terminus of wild-type (wtSP) or truncated Scaffold Protein (SPt) that electrostatically interacts with P22 Coat Protein (CP) through its C-terminal helix-turn-helix domain to template assembly [30, 31]. About 100–300 SP subunits come together to assemble 420 copies of CP into P22 VLPs of ~58 nm diameter in size. Fused cargo in such a construct is directed to the interior during self-assembly [32], leading to sequestration of the guest molecule. For *in vivo* cargo encapsulation, the CP and cargo-fused SP are either co-expressed or sequentially expressed in a host bacterial cell. Once assembly is completed, particles are isolated from cells and analyzed for the right product. The protocol for cargo encapsulation using *in vivo* assembly has been covered elsewhere [33]. For *in vitro* cargo encapsulation, the CP subunits and cargo-fused SP subunits are individually purified, correctly folded, and activity ascertained, and then mixed together in equal molar amounts in the presence of low concentration of a chaotropic agent. The chaotrope is dialyzed out slowly to favor folding and to ensure assembly (Fig. 1) [27]. Besides remarkable physical homogeneity of the assembled particles, *in vitro* encapsulation provides certain advantages over *in vivo* encapsulation. For example, host-associated contaminants, especially endotoxins, are potentially

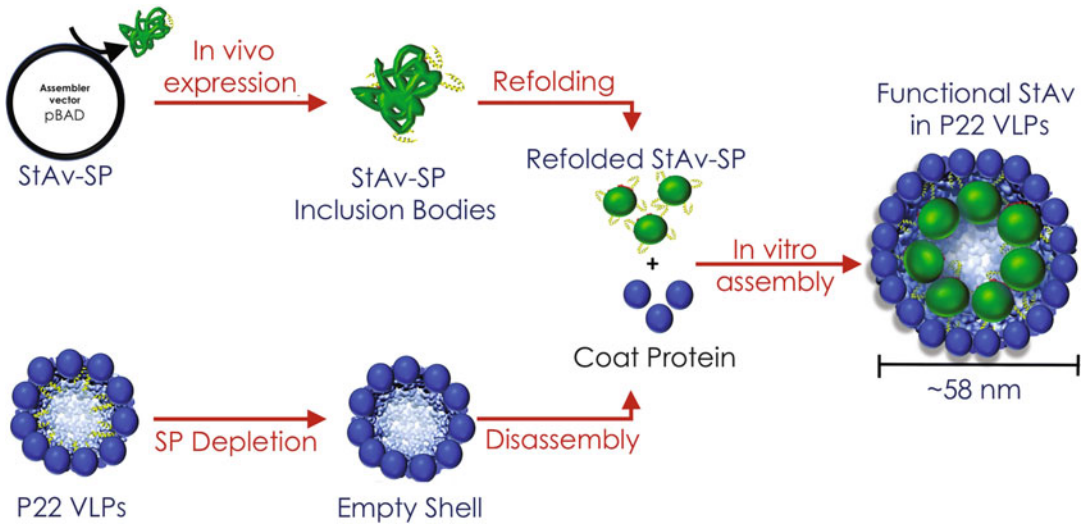


Fig. 1 Packaging of StAv in P22 VLPs using in vitro assembly. CP subunits, prepared from the disassembly of empty shells in 3 M GuHCl (the chaotrope), are mixed with refolded and independently purified SP-fused cargo (StAv-SP), such that the final concentration of GuHCl is 1.5 M. Removal of the chaotrope by dialysis results in the formation of particles with StAv directed in the interior

reduced or are removed from the VLP preparation. The low-to-no endotoxin content of in vitro assembled VLPs make them suitable for animal studies. As well, in vitro assembly provides better control over the composition of VLPs produced because the assembly is independent of host cell machinery. The control over host cell machinery is challenging because of the uncertainty of the amount of the cargo poised to encapsulate during in vivo assembly. Furthermore, the modular nature of the in vitro approach allows encapsulation of a cargo whose folding may go awry prior to encapsulation and requires external refolding to exhibit desired activity [27]. This approach can now be extended to a variety of other cargos including cages, such as ferritin, to create hierarchical multi-compartment structures [34, 35]. Encapsulation of StAv generates a non-covalent conjugation site to which biotin-tagged molecules are easily attached for interior or exterior loading. Dependent on the size of the cargo and the size-exclusion limit of the pore (~2.5 nm), VLPs can load cargo on the inside and outside of the particle shell. Combined with a targeting feature, this StAv-biotin-based coupling strategy makes VLPs a versatile delivery vehicle for controlled intracellular drug delivery or antigen delivery.

2.1 Materials

Prepare all solutions with Milli-Q water and analytical grade reagents. Media are autoclaved at 121 °C for 20 min, and buffers are filter-sterilized through 0.2 µm filter. Materials utilized herein can be replaced with analogous materials manufactured by different vendors.

2.1.1 *Expression Vectors*

1. pRSF DuetTM-1 (Novagen) vector encoding the P22 CP gene (NCBI database Gene ID: 1262831), kanamycin resistance gene, and isopropyl- β -D-1-thiogalacto-pyranoside (IPTG) inducible T7 polymerase promoter (*see Subheading 2.2.3, step 3*).
2. pET11b vector available from Dr. Paolo Arosio (University of Brescia, Italy), encoding the 6His-tagged Streptavidin gene (*see Note 1*), ampicillin resistance gene, and IPTG-inducible T7 polymerase promoter.
3. pET11a with P22 CP and wtSP (NCBI database Gene ID: 2944242) gene cloned at different multiple cloning sites (*see Note 2*) for co-expression.
4. pBAD vector (Invitrogen) containing Streptavidin-fused N-terminus truncated SP sequence, StAv-SPt (*see Note 3*), ampicillin resistance gene, and L-arabinose induced araBAD promoter (*see Subheading 2.2.3, step 4*).
5. pBAD vector encoding the Cys-6His-SP-GFP gene (*see Note 4*).

2.1.2 *Molecular Cloning*

1. DNA Primers (Eurofins MWG Operon):
 FP_{SP}: 5'-GAATTAACCATGGGTCATCATCATCATCAT
 CATGCCGGCATCACCGGC-3'.
 RP_{SP}: 5'-GAAATACAGGTTTTTCACCTGCTG
 CACCCTGCTGAACGGCGTCGAGC-3'.
2. DNA Primers (Eurofins MWG Operon):
 FP_{StAv}: 5'-GCAGGTGAAAACCTGTATTTCCA
 GAGCGGTGCGG-3'.
 RP_{StAv}: 5'-ATGATGACCCATGGTTAATTCCTCCTGT
 TAGCCCCAAAAACGG-3'.
3. HiFi DNA assembly kit (NEB Builder[®]).
4. DNA sequencing (Eurofins).
5. QuickChange Lightning kit for site-directed mutagenesis (Agilent Technologies).
6. Arktik Thermal Cycler.
7. Applied Biosystems PCR tubes and caps, RNase-free, 0.2 mL, 8-strip format.
8. Ethidium bromide.
9. TAE buffer: 40 mM Tris-base, 5 mM acetate, and 1 mM EDTA, pH 8.2.
10. 0.8% (w/v) Agarose prepared in TAE buffer.
11. Agarose gel loading dye (6 \times): Add 25 mg bromophenol blue to 3 mL glycerol and make up to 10 mL.

2.1.3 Transformation

1. BL21 (DE3) chemically competent *E. coli* cell kit (Novagen) and SOC (*see Note 5*) for propagation of recombinant vectors.
2. Aliquots (1 mL) of stock solutions of kanamycin (30 mg/mL) and ampicillin (50 mg/mL) prepared in sterile water and stored at -20°C .
3. Luria Bertani (LB) agar plates: 5 g tryptone, 5 g NaCl, 2.5 g yeast, and 7.5 g agar dissolved in 500 mL water and autoclaved. Poured in petri-plates (100 × 15 mm) with appropriate antibiotic (*see Note 6*) and stored at 4°C .
4. LB medium: 10 g tryptone, 10 g NaCl, and 5 g yeast dissolved in 1.0 L water and autoclaved.
5. 50% (v/v) glycerol.
6. Cryogenic vials (Corning).
7. Refrigerated circulating water bath.
8. Microbiological incubator.
9. Falcon™ round-bottom polypropylene test tubes with cap.
10. QIAprep spin miniprep kit.
11. QIAquick gel extraction kit.

2.1.4 Expression, Assembly, and Purification of VLPs

1. Single colony, picked up from agar plate or glycerol stock (*see Note 7*), transformed with vector(s) containing gene sequences that encode the P22 CP and SP (*see Subheading 2.2.1*).
2. Bench-top microcentrifuge.
3. Multifuge X1™ Centrifuge.
4. MaxQ 4000 Thermo Scientific Shaker.
5. IPTG: Dissolve 119.2 mg IPTG in 1.0 mL sterile water to make 0.5 M stock solution. Aliquots of 1.0 mL stock solution can be stored at -20°C .
6. Arabinose: Dissolve 2.0 g L-arabinose in 10 mL sterile water. Use 10 mL stock solution per each liter of culture. Make this solution fresh.
7. Phosphate buffer: 50 mM sodium phosphate, 100 mM sodium chloride, pH 7.0. Dissolve 2.92 g sodium phosphate monobasic monohydrate ($\text{NaH}_2\text{PO}_4 \cdot \text{H}_2\text{O}$), 7.73 g sodium phosphate dibasic heptahydrate ($\text{Na}_2\text{HPO}_4 \cdot 7\text{H}_2\text{O}$), and 5.84 g NaCl in 900 mL sterile water. Adjust pH to 7.0 using 2 M NaOH. Add water to a final volume of 1.0 L.
8. Cell lysis reagents: Dissolve 20 mg DNase, 30 mg RNase, and 15 mg lysozyme in 1.0 mL sterile water. Freeze 100 μL aliquots until use.
9. Digital sonicator with a microtip.

10. Millex Syringe filters—0.45 and 0.22 μm pores.
11. Luer Lock BD syringe with needle extension.
12. Sucrose solution (35% w/v).
13. Ultracentrifuge (Thermo Sorvall WX90), F50L-8 \times 39 Fixed-Angle Rotor (Thermo), 26.3 mL polycarbonate aluminum bottle with cap assembly (tubes).
14. Size Exclusion Column (SEC): HiPrep 16/60 Sephacryl S-500 HR (or any column with a separation range between 4×10^4 and 2×10^7 Da).
15. Fast performance liquid chromatography (FPLC): BioLogic DuoFlow Medium Pressure Chromatography Systems (or comparable).
16. Ni-NTA column (cOmplete™ His-Tag).
17. Denaturing buffer: 50 mM phosphate, 100 mM NaCl, 6 M guanidine hydrochloride, pH 7.0.
18. Wash buffer: 50 mM phosphate, 100 mM NaCl, 20 mM imidazole, pH 7.0.
19. Elution buffer: 50 mM phosphate, 100 mM NaCl, 500 mM imidazole, pH 7.0.
20. Assembly buffer: 50 mM Tris-HCl, 25 mM NaCl, 2 mM EDTA, 3 mM β -mercaptoethanol (BME), and 1% v/v glycerol, pH 7.4.
21. Pierce protease and phosphatase inhibitor tablets, EDTA free.
22. Disposable syringes, 5 mL.
23. Dialysis membrane MWCO 6–8 kDa.
24. Falcon disposable polypropylene tubes, 50 and 10 mL.
25. Polypropylene centrifuge tubes with plug seal cap, 250 mL.
26. Nalgene baffled shake flask, 2 L.
27. Eppendorf snap-cap microcentrifuge safe-lock tubes.
28. Guanidine hydrochloride.
29. Tris(2-carboxyethyl)phosphine) (TCEP).

2.1.5 Characterization and Functional Activity

1. Sodium dodecyl sulfate-polyacrylamide gel (SDS-PAGE), 15%: resolving gel, 7.5 mL 30% acrylamide/bis solution, 5 mL 1.5 M Tris, pH 8.8, 2.3 mL water, 75 μL 20% (w/v) SDS, 75 μL 10% (w/v) APS, 25 μL TEMED; stacking gel: 0.83 mL 30% acrylamide/bis solution, 0.62 mL 1.5 M Tris, pH 8.8, 3.47 mL water, 25 μL 20% (w/v) SDS, 50 μL 10% (w/v) APS, 5 μL TEMED. This recipe makes 3–4 gels with the electrophoresis system used in this protocol.
2. SDS-PAGE running buffer: 0.025 M Tris-HCl, 0.192 M glycine, 0.1% (w/v) SDS, pH 8.3.

3. Loading dye solution (4×): 2.0 mL 1 M Tris-HCl pH 6.8, 0.8 g SDS, 4.0 mL glycerol, 0.4 mL βME, 1.0 mL 0.5 M EDTA, 8 mg bromophenol blue. Make up to 10 mL with water.
4. SE250 Mini Vertical Protein Electrophoresis System.
5. Page Ruler Plus Pre-stained Protein Ladder, 10–250 kDa.
6. InstantBlue Coomassie Protein Stain.
7. UVP MultiDoc-IT Digital Imaging System.
8. 8453 UV-Vis Spectrophotometer.
9. Quartz cuvette-16.50-Q-10/Z15 (Starna) for UV-Vis.
10. NanoDrop 2000/c Spectrophotometer.
11. Agilent 1200 high-performance liquid chromatography (HPLC).
12. Electron-spray ionization mass spectrometry (ESI-LC/MS).
13. MALS/QELS/dRI, Multiangle light scattering coupled with quasi-elastic light scattering detector and differential refractive angle detector (Wyatt Technology).
14. MALS buffer: 50 mM phosphate, 100 mM NaCl, 200 ppm NaN₃, pH 7.2.
15. Transmission electron microscope.
16. For negative staining TEM: 2% uranyl acetate ready-to-use solution.
17. Carbon film-coated copper 400 mesh grid.
18. Opti-4CN detection kit.
19. 5% (w/v) Skim milk.
20. Nitrocellulose membrane.
21. Polyclonal anti-GFP rabbit antibody (Gifted by Dr. David Rudner).
22. Goat anti-rabbit HRP-conjugated secondary antibody.
23. Biotin-4-fluorescein (Biotium), make stock solution in DMSO and store at –80 °C.
24. Biotin maleimide, make stock solution in DMSO and store at –80 °C.
25. Streptavidin.
26. TBS buffer: 20 mM Tris-HCl, 150 mM NaCl, pH 7.0.

2.2 Methods

2.2.1 Construction of Expression Plasmids

The DNA sequences of P22 CP and SP can be obtained from the NCBI database. The cloning of P22 CP, wtSP, and SP_t is provided elsewhere [30, 36]; hence not elaborated here. To generate StAv_{15–159} to SP_{142–303} fusion product, amplify two amplicons 6xHis-tagged StAv_{15–159} and linker-SP_{142–303} (GAAG-

ENLYFQS-GAAG-SP₁₄₂₋₃₀₃) from plasmids pET11b and pBAD containing the corresponding genes in a reaction with high-fidelity KOD Hot Start Master Mix. The gene blocks containing the desired gene can be custom synthesized from Integrated DNA technologies (IDT). Amplify 6xHis-tagged StAv₁₅₋₁₅₉ with overhangs overlapping with pBAD vector sequence on one end and with GAAG-ENLYFQS-GAAG-SP₁₄₂₋₃₀₃ on the other with primers (forward) 5'- GAATTAACCATGGGTCATCATCATCATCATCATGCCGGCATCACCGGC -3', and (reverse) 5'- GAAATACAGGTTTTACCTGCTGCACCCTGCT GAACGGCGTCGAGC -3'. Amplify GAAG-ENLYFQS-GAAG-SP₁₄₂₋₃₀₃ (*see Note 8*) in pBAD vector backbone with overhangs that overlap with linker region (GAAG-ENLYF) on the 5' end and with 6xHis-tagged StAv₁₅₋₁₅₉ on 3' end with primers (forward) 5'- GCAGGTGAAAACCTGTATTTCCAGAGCGGTGCGG -3' and (reverse) 5'- ATGATGACCCATGGTTAATTCCTCCTGT TAGCCCAAAAACGG-3'. Verify size, yield, and linearization of insert (6xHis-tagged StAv₁₅₋₁₅₉) and linker-SP₁₄₂₋₃₀₃ containing vector by agarose (0.8% w/v) gel electrophoresis under standard conditions. Excise the desired bands using scalpel and purify by QIAquick gel extraction kit as per the manufacturer's instructions; elute the DNA into either water or EB buffer. Assemble the two PCR products with complementary overhangs into circular DNA using NEB builder HiFi DNA assembly master mix (New England Biolabs) as instructed by the manufacturer.

2.2.2 Transformation

Thaw 25 μ L aliquots of BL21 (DE3) cells on ice and add 1 μ L of purified or assembled vector (\sim 50 ng/ μ L) to cells (pipetted into 1.5 mL micro-centrifuge tube). Stir gently (*see Note 9*), and incubate on ice for 30 min. Heat shock cells for 30 s in a water bath maintained at 42 °C. Return the tube on ice for 2 min, followed by the addition of 80 μ L of recovery medium (provided in the kit) to the transformed cells. Incubate at 37 °C for 45–60 min in an orbital shaker incubator set to approximately 250 rpm. Plate on agar plate supplemented with the appropriate antibiotic (*see Note 10*) with the help of a sterilized bacterial cell spreader, invert plate, and incubate overnight at 37 °C. Store plates at 4 °C for up to 1 month.

To verify clones, isolate molecular biology grade vector using QIAprep spin miniprep kit as per vendor's protocol and confirm the insertion and sequence of gene of interest through DNA sequencing. The colony that contains gene of interest and produces protein relatively at best expression level is used for making glycerol stock. Screen colonies before scaling up protein production so as to obtain best protein expression levels (*see Note 11* and **Subheading 2.2.3**).

To prepare glycerol stock of the colonies identified as having the best protein expression, pour 3–5 mL LB medium supplemented with an appropriate antibiotic into a round-bottom

polypropylene tube. Gather a small amount of the bacteria from a colony using a pipette tip and submerge it into the medium, replace the lid and incubate at 37 °C in shaker overnight (usually 16–18 h). In a cryovial, mix 500 µL of overnight grown cell culture into 500 µL of 50% glycerol and store at –80 °C.

2.2.3 Expression, Purification, and Characterization of P22 VLPs

1. Pour 10 mL LB medium supplemented with ampicillin (50 µg/mL) into cell culture tubes using pipetboy. Inoculate medium with a colony of *E. coli* cells transformed with a plasmid that co-expresses P22 CP and SP, picked up either from agar plate or from glycerol stock. Allow the cells to grow overnight at 37 °C in shaker set at approximately 250 rpm.
2. Inoculate 1.0 L LB medium with the entire amount of overnight culture and incubate the culture at 37 °C with continuous shaking at ~250 rpm until the optical density at 600 nm ($A_{600\text{ nm}}$) reaches 0.6–0.8 (4 separate 1.0 L cultures are typically used to isolate VLPs).
3. Induce the expression of P22 CP and SP with 0.5 mM IPTG (final concentration) and continue incubation for additional 4 h.
4. Harvest cells by centrifugation at $3700 \times g$ for 20 min at 4 °C utilizing conical, 250-mL polypropylene tubes. Consolidate pellets from 2 L cultures (~5–10 g) into 50 mL falcon tubes. Resuspend the cell pellet in 30–35 mL phosphate buffer.

At this stage, cell suspension can be stored at –80 °C for later use.

5. Add 100 µL of lysis reagents per liter of resuspended cell culture, followed by incubation at room temperature for 30 min with rocking.
6. Place cells on ice water and lyse them with a macro-tip attached to the Digital Sonicator set to the following parameters: 50% amplitude, 0.3 s pulse on, 0.7 s pulse off, for total of 2 min.
7. Remove cell debris from cell lysate by centrifugation at $12,000 \times g$ for 50 min at 4 °C. Harvest the resulting supernatant with a pipetboy carefully without disturbing the cell debris layer. Filter supernatant through a 0.45-µm syringe filter.
8. Purify VLPs through sucrose cushion. Pour 20 mL of VLP containing supernatant into ultracentrifuge tubes, then carefully underlay 5 mL of 35% sucrose cushion underneath the supernatant (*see Note 12*). Pellet the particles by ultracentrifugation at 45,000 rpm, 4 °C for 50 min. Immediately, discard the supernatant completely and resuspend VLP in the sediment with 2 mL phosphate buffer. Rock at 4 °C for 1–2 h to resuspend the sediment.

Caution: Keep the pellet immersed in buffer completely during resuspension. Sediment aggregates and residual lipids, which gives pellet brownish tint, in solution by centrifugation at $17,000 \times g$ for 10 min. Recover the supernatant.

9. Column purify VLPs: Equilibrate Sephacryl S-500 HR connected to a FPLC system with 2 column volumes of phosphate buffer. Load 2 mL of VLP solution with the aid of a static loop (or dynamic loop for repetitive injections in an overlay mode) onto the column at 1 mL/min flow rate; elute with phosphate buffer in isocratic run of 120 min. Collect 3–4 mL fractions at a retention time of 60 min ($t_R = 60$ min) as P22 VLPs elute around that time. Concentrate VLPs by ultracentrifugation at 45,000 rpm for 45 min at 4 °C.
10. Assess purity and size distribution of VLPs by SDS-PAGE and transmission electron microscope (TEM) imaging. Mix VLP sample at 1–2 mg/mL with 4× loading buffer containing 100 mM DTT, heat in a boiling water bath for 10 min, sediment aggregates in a benchtop centrifuge. Separate on a 15% acrylamide gel at a constant current of 35 mA for approximately 1 h or until dye front has reached the bottom of the gel. Stain gels with an Instant Blue Protein Stain. Rinse with water and image using UVP MultiDoc-IT Digital Imaging System.
11. For TEM, apply 4 μL of VLP sample at 0.3 mg/mL to carbon-coated grids and let sit for 45 s. Wick away excess liquid with the help of filter paper and wash the grid with 5 μL water. Stain with 4 μL of uranyl acetate solution for 10 s, wick away excess liquid and image the grid on a JEOL TEM at accelerating voltage of 80 kV.

2.2.4 *In Vitro*
Reassembly of P22 CP
to Encapsulate Streptavidin

1. Deplete the P22 VLPs of the SP by treating them with 0.5 M GuHCl prepared in the backdrop of phosphate buffer. Resuspend the P22 VLPs in 1–2 mL of phosphate buffer in an ultracentrifuge tube, and then fill the tube to the brim with 0.5 M GuHCl. Rock the tube for 2 h at 4 °C, and then sediment VLPs by ultracentrifugation as in Subheading 2.2.3, step 8. Repeat this extraction process until SP is washed off completely from P22 particles, which is monitored with the aid of 15% SDS-PAGE under reducing condition (*see Note 13*).
2. Dissociate SP-depleted VLPs, referred as Empty Shell (ES), into CP subunits by adding 6 M GuHCl prepared in the backdrop of assembly buffer to reach to a final concentration of 3 M GuHCl. Incubate for 30 min at room temperature. Remove aggregates by filtration through a 0–2 μm filter. Calculate concentration of CP (mg/mL) using $A_{280 \text{ nm}}$, molar

extinction coefficient of 44,920/M/cm and molecular mass of 46,751.73 Da (*see Note 14*).

3. Concurrently, prepare the StAv-SP protein for encapsulation and assembly of CP into P22 VLPs. Induce the expression of StAv-SP with L-arabinose to a final concentration of 13 mM, when the OD₆₀₀ of the culture reaches 0.6. Continue induction for an additional 4 h (*see Note 15*). Harvest cells by centrifugation as in Subheading 2.2.3, **step 4**, resuspend sedimented cells in 30 mL phosphate buffer per 2 L starting culture; add aliquots of lysing reagents containing protease and phosphatase inhibitor tablets. Incubate for 30 min with shaking at room temperature. Sonicate the suspension using parameters described in Subheading 2.2.3, **step 6**. Discard supernatant and dissolve sediment in 6 M GuHCl made in phosphate buffer. Incubate overnight at room temperature with rocking. Filter denatured protein through 0.45 μm filter and purify by nickel-affinity chromatography. Load protein solution at 1 mg/mL flow rate onto the Ni-NTA column pre-equilibrated with denaturing buffer for 10 min at 2 mL/min to perform on-column refolding. Renature protein by running a linear reverse gradient (6–0 M GuHCl) of denaturant buffer at a flow rate of 0.25 mL/min over a 80-min period. Wash column-bound refolded protein with wash buffer at 1 mL/min over a 20 min period; elute protein with an elution buffer at a flow rate of 2 mL/min over a 20–30 min period. Collect 3 mL fractions and combine the ones containing pure protein as assessed by SDS-PAGE. Calculate concentration of StAv-SP using $A_{280\text{ nm}}$, molar extinction coefficient of 50,880/M/cm, and molecular mass of 35,252 Da (*see Note 14*). Exchange buffer with assembly buffer to facilitate in vitro assembly.
4. Mix CP subunits (~2 mg/mL) prepared in 3 M GuHCl with StAv-SP in equal molar ratio such that the amount of StAv-SP added to the CP solution results in the drop of the denaturant from 3 to 1.5 M GuHCl final concentration. Dialyze the mixture (~2 mL) against 200 mL assembly buffer overnight at room temperature (*see Note 16*) with 2–3 buffer exchanges using dialysis membrane of MWCO 6–8 kDa. Sediment to purify assembled particles by VLPs by ultracentrifugation as in Subheading 2.2.3, **step 8**.

2.2.5 Characterization of Streptavidin Encapsulated P22 VLPs

Analyze particles by SDS-PAGE and negative stain TEM to confirm encapsulation of StAv-SP and retention of spherical morphology, respectively. Filter and load 100 μL of 1 mg/mL filtered sample onto S-200 column coupled with MALS/QELS/dRI and elute with MALS buffer at 0.7 mL/min flow rate to determine MW, hydrodynamic radius (R_h) and radius of gyration (R_g). Calculate

StAv-SP copies inside a VLP by using the MW of empty shell, which is constituted of 420 copies of P22 CP, MW of P22-StAv, and the MW of StAv-SP (*see Note 17*). Calculate the concentration of encapsulated StAv from $A_{280\text{ nm}}$ and molar extinction coefficient of 215,000/M/cm (*see Note 18*) per reported literature [27].

**2.2.6 Streptavidin–
Biotin-Mediated Packaging
of a Small Molecule
(Fluorescein)**

The method used to package small cargo molecules serves two purposes: (a) to demonstrate proof-of-concept for non-covalent conjugation of ligand molecules in the interior of P22 VLPs and (b) the suggested use of biotin-4-fluorescein (B4F) acts as an efficient readout to determine the extent of ligand binding to streptavidin.

1. Titrate 100 μL aliquot of 10 μM streptavidin, solubilized in the PBS, with 400 μM B4F (*see Note 19*) in 0.5 μL increments at constant time intervals of 30s to allow reaction to reach equilibrium. Measure $A_{493\text{ nm}}$ at each titration point (*see Note 20*) and plot a graph between $A_{493\text{ nm}}$ and molar ratio of B4F:StAv monomer (*see Note 21*) to establish assay parameters. Likewise, assay the binding sites of StAv-SP and streptavidin contained in P22 VLPs in the same manner with PBS acting as a negative control. While PBS produces a single regression line, StAv/StAv-SP/StAv-P22 produces two regression lines of different slopes, intersecting each other at a point where all binding sites of streptavidin are occupied; occupancy is used to quantify ligand binding.
2. In a variation of the above step, incubate streptavidin-containing P22 (~1 mg/mL) with B4F at 1:5 molar ratio overnight either at room temperature or at 4 °C. Remove excess B4F by ultracentrifugation, followed by three rounds of dialysis in 1 L phosphate buffer. Assess molar equivalents of B4F (or another biotinylated ligand) quantitatively by monitoring concentration-dependent increase in $A_{493\text{ nm}}$, which plateaus as all sites are saturated and B4F is in excess.

**2.2.7 Streptavidin–
Biotin-Mediated Surface
Display of Large,
Pore-Excluded
Molecules (GFP)**

1. Biotinylation of Cys-SP-GFP: Treat Cys-SP-GFP (in PBS) with 20-fold molar excess of TCEP prepared in water. Rock the mixture for 30 min at room temperature. Add ten-fold molar excess of biotin-maleimide, prepared in water, to the protein solution. Incubate mixture overnight at 4 °C on a rocker and then dialyze out excess biotin-maleimide over 3–4 phosphate buffer exchanges. Assess purity using SDS-PAGE and determine the number of biotin molecules per protein unit by electron-spray ionization mass spectrometry (ESI-LC/MS). Increase in molecular weight by 453 Da indicates addition of one biotin molecule per Cys-SP-GFP.

2. Multivalent surface display: Incubate P22-StAv with fivefold molar equivalents of biotinylated (B)-SP-GFP for 2 h with continuous shaking at room temperature. Remove unbound B-SP-GFP by ultracentrifugation and three rounds of dialysis in phosphate buffer using dialysis membrane of MWCO 100 kDa. Use negative control alkylated-SP-GFP, obtained by blocking cysteine with iodoacetamide or iodoacetic acid (*see Note 22*). Analyze by SDS-PAGE and TEM as in **2.2.3.10** to ensure binding of B-SP-GFP and retention of particle morphology. Analyze by MALS/QELS/dRI and UV-Vis to determine the MW, size, and copies of surface-exposed ligand (*see Note 23*). To ensure that GFP stays on the surface of particles (P22-GFPex), conduct immunodot blot assay (*see Note 24*) where GFP-specific antibody will bind only to surface exposed GFP but not to encapsulated GFP inside the particles (P22-GFPin). This step will ascertain the location of GFP in the VLP.

3 Synthesis and Characterization of Endosome-Escape Polymer Nanoparticles

The polymer is composed of two functional blocks synthesized by reversible addition–fragmentation chain transfer (RAFT) polymerization. The first block is a hydrophilic, cationic copolymer of dimethylaminoethyl methacrylate (DMAEMA) and pyridyl disulfide ethyl methacrylate (PDSMA). The PDSMA monomer provides pyridyl disulfide functional groups on the surface of the nanoparticle for conjugation to thiolated protein or peptide antigens via a disulfide exchange reaction. DMAEMA contributes cationic charge for electrostatic complexation with a nucleic acid adjuvant. The second block is a pH-responsive, endosomolytic copolymer of propylacrylic acid (PAA), butyl methacrylate (BMA), and DMAEMA, which is hydrophobic at neutral pH and thereby drives the assembly of micellar nanoparticles. After cellular uptake and, in response to endosomal acidification, the micellar structure of the NP is disrupted and the membrane-destabilizing block (PAA-co-BMA-co-DMAEMA) becomes exposed, which promotes endosomal membrane disruption and allows the escape of antigen to the cytosol and delivery to the MHC-I pathway. The nomenclature used for the polymer is poly[(PDSMA-co-DMAEMA)-*b*-(PAA-co-DMAEMA-co-BMA)].

3.1 Materials

1. Pyridyl disulfide ethyl methacrylate (PDSMA).
2. Dimethylaminoethyl methacrylate (DMAEMA).
3. Propylacrylic acid (PAA).
4. Butyl methacrylate (BMA).

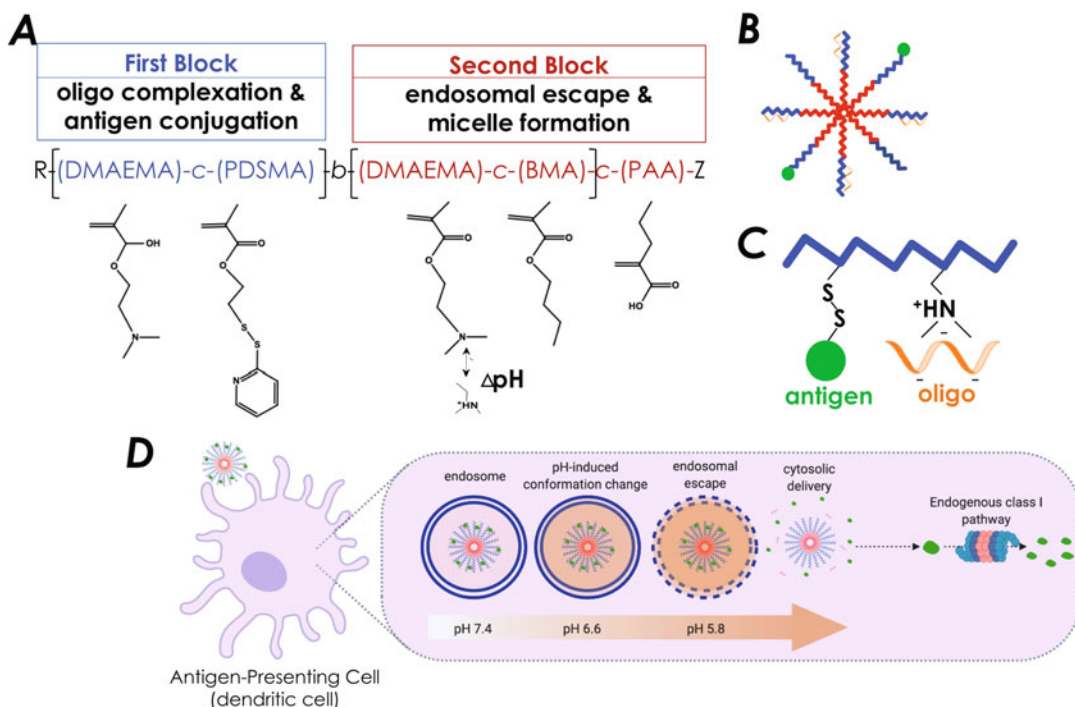
5. 2,2'-Azobis(4-methoxy-2,4-dimethylvaleronitrile) (V-70; initiator).
6. 4-Cyano-4-(ethylsulfanylthiocarbonyl) sulfanylpentanoic acid (ECT; RAFT chain transfer agent).
7. 100 mM phosphate buffer (pH 7).
8. Amicon Ultra Centrifugal Filters (3 kDa MWCO, Millipore).
9. Endotoxin-free OVA.
10. 2-Iminothiolane (Traut's Reagent).
11. Zeba Spin desalting columns (0.5 mL, 7 kDa MWCO).
12. 150 mM NaCl buffer.
13. Phosphate buffer (PB) at pH 7.4, 6.6 and 5.8. (6.6 and 5.8 need to have additional NaCl to bring to the correct ionic strength).
14. 0.1% Triton X-100.
15. DC2.4 cell culture medium: RPMI 1640, 10% FBS, 2 mM L-glutamine, 55 μ M beta-mercaptoethanol, 1 \times nonessential amino acids, 10 mM HEPES, 1 \times Pen/Strep (optional).

3.2 Methods

3.2.1 Synthesis of PDSMA-co-DMAEMA

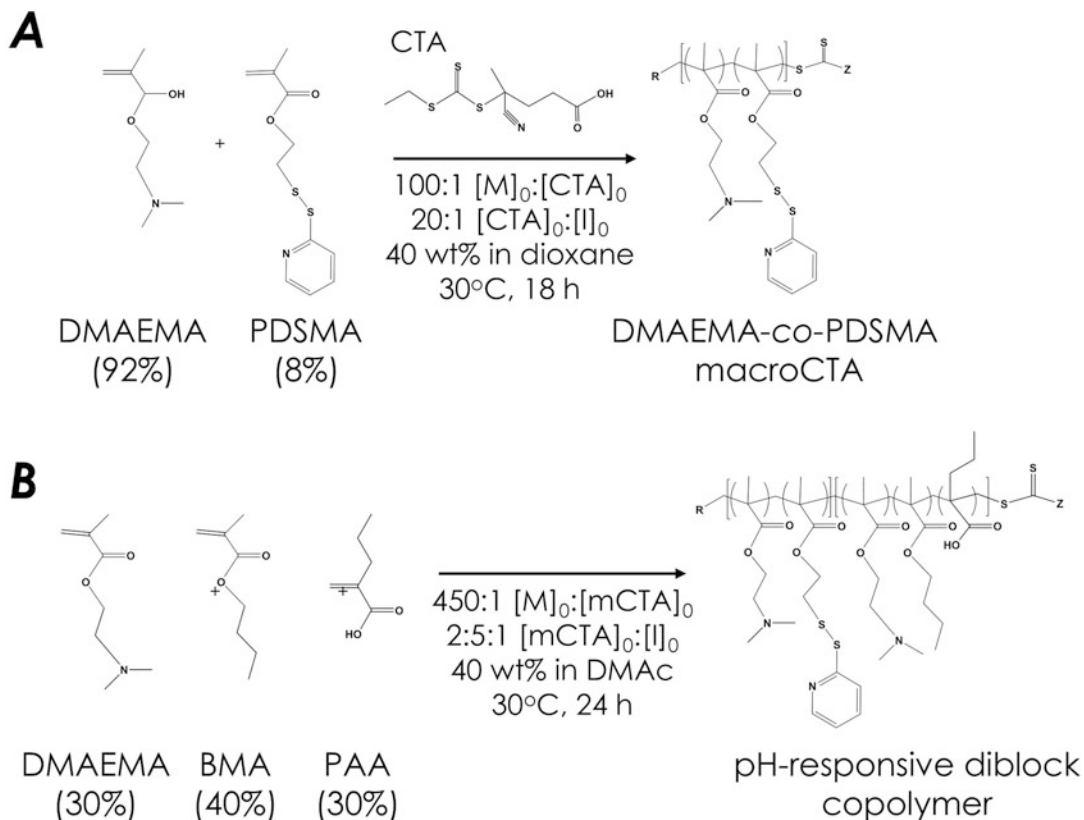
Synthesize the first block (PDSMA-co-DMAEMA) and use as the macro-chain transfer agent (macroCTA). Initial molar ratio of DMAEMA to PDSMA is 92:8 and the initial monomer ($[M]_0$) to CTA ($[CTA]_0$) to initiator ($[I]_0$) ratio is 100:1:0.05. Schemes 1 and 2 show a schematic of the relevant chemical structures and reaction conditions used in the polymerization, as well as the molecular weight (MW) and PDI of the macroCTA and final diblock copolymer.

1. For a 1.5 g scale reaction, use a clean 10 mL pear-bottom reaction vessel. Place a small magnetic stir bar in reaction vessel.
2. Filter monomer (DMAEMA) to remove inhibitor by passing through an aluminum oxide column. A simple column can be made in a pipette by stuffing glass wool (or cotton) in the bottom; fill up to a third the volume with aluminum oxide (for small-scale reactions, use small glass Pasteur pipettes and for larger-scale reactions, serological pipettes). Pour the monomer into the column and allow to flow through the column by gravity and collect in a scintillation vial.
3. Prepare initiator stock (2,2'-azobis(4-methoxy-2,4-dimethylvaleronitrile) (V-70): Make a 10 mg initiator per 1 g solvent stock (i.e., 10 mg V-70 + 990 mg dioxane).
4. Weigh out the RAFT chain transfer agent 4-cyano-4-(ethylsulfanylthiocarbonyl) sulfanylpentanoic acid (ECT) in a scintillation vial.



Scheme 1 NP vaccine formulation. (a) pH-responsive polymer synthesized via RAFT polymerization; (b) self-assembly of polymeric micelles; (c) covalently conjugate thiol-containing protein antigen to the PDSMA and electrostatically complex oligonucleotide on the micelle corona; (d) proposed mechanism of NP uptake, endosomal disruption, escape into the cytosol, and endogenous MHC class I pathway

5. Add appropriate amount of purified DMAEMA, PDSMA, CTA, and initiator stock to the reaction vessel, and dissolve in dioxane at 40 wt % monomers.
6. Seal the reaction vessel with a rubber septum.
7. Purge with N_2 for ~20 min.
Note: Highly recommended: seal the vessel with parafilm.
8. Place reaction vessel in an oil bath set at 30 °C for 18 h.
9. Stop the reaction by removing the rubber septum.
10. Purify the macroCTA via precipitation: Dissolve the macroCTA in acetone and precipitate in pentane. Perform precipitation in 50 mL conical centrifuge tubes as follows: (a) transfer reaction contents to 50-mL falcon tube; (b) add pentane to tube to crash out product; (c) Centrifuge at $5000 \times g$ for 5 min, decant pentane; (d) dissolve pellet in acetone; (e) Repeat steps (b)–(d) four times, keep the volume of acetone under 10% during the precipitation process. Finally, vacuum dry product overnight to remove residual solvent.



Scheme 2 RAFT synthesis of pH-responsive polymer for dual-delivery of protein antigen and nucleic acid adjuvant. (a) Synthesis scheme and reaction conditions for DMAEMA-co-PDSMA macro-chain transfer agent (macroCTA). (b) Synthesis of pH-responsive diblock copolymer (DMAEMA-co-PDSMA)-b-(PAA-co-DMAEMA-co-BMA)

3.2.2 Synthesis of PAA-co-BMA-co-DMAEMA

Use the purified macroCTA to chain extend via copolymerization with DMAEMA, PAA, and BMA to create pH-responsive polymer. Add DMAEMA (30%), PAA (30%), and BMA (40%) ($[M]_0/[mCTA]_0 = 450$) to macroCTA dissolved in DMAc (40 wt% monomer and mCTA) along with V-70 initiator ($[mCTA]_0/[I]_0 = 2.5$). See Schemes 1 and 2.

1. For a reaction scale of 2 g, prepare a 10 mL pear-bottom reaction vessel with small magnetic stir bar.
2. Filter monomers (DMAEMA, PAA, BMA) to remove inhibitor by passing through an aluminum oxide column as described above in Subheading 3.2.1, step 2.
3. Prepare initiator stock V-70 as described above.
4. Add appropriate amount of purified monomer, macroCTA, and initiator stock to the reaction vessel and dissolve in DMAc at 40 wt% of monomers.

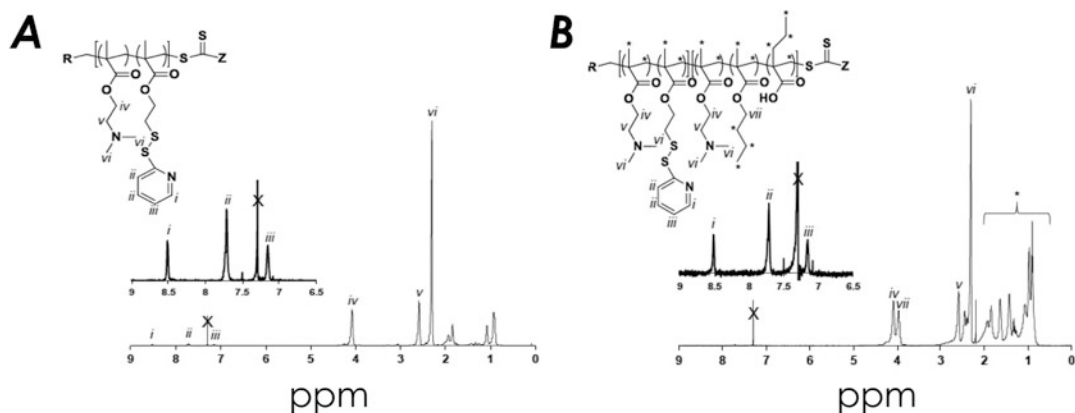


Fig. 2 Representative ^1H -NMR (CDCl_3) of (a) DMAEMA-co-PDSMA macroCTA, and (b) pH-responsive diblock copolymer. (Image adapted from our published work in ref. [6])

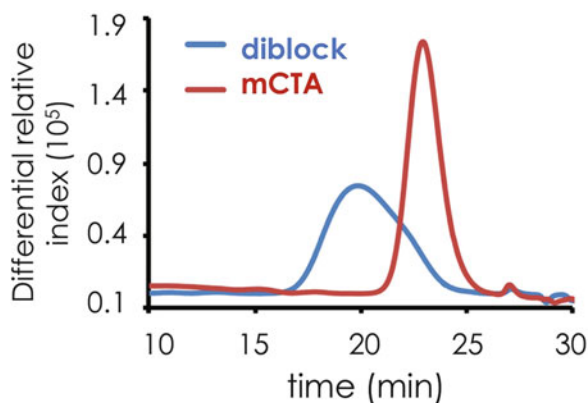


Fig. 3 Representative GPC traces of mCTA and diblock copolymer. (Image adapted from our published work in ref. [6])

5. Seal with rubber septum. Purge with N_2 as described above in Subheading 3.2.1, step 7.
6. Place reaction vessel in oil bath set at $30\text{ }^\circ\text{C}$ for 24 h.
7. Stop the reaction by removing the rubber septum.
8. Purify the polymer via dialysis against acetone three times using a 2.5 kDa MWCO membrane, followed by dialysis against deionized water.
9. Lyophilize for 72 h prior to use.

The composition and monomer conversion of both the purified macroCTA and diblock copolymer were characterized by ^1H NMR spectroscopy in CDCl_3 . Below are characteristic ^1H NMR spectra of the first block (Fig. 2a) and the full polymer (Fig. 2b) (adapted image [6]).

The molecular weight (MW) and polydispersity indices (PDI) can be obtained by gel permeation chromatography (GPC, Agilent; mobile phase HPLC grade dimethylformamide (DMF) containing 0.1% LiBr as the mobile phase) and in-line scattering (Wyatt) and refractive index (Agilent) detectors. Below are characteristic chromatograms of where MW and PDI were calculated using the ASTRA V Software (Wyatt Technology; Fig. 3). MW was determined using dn/dc values calculated previously (0.071 for macroCTA and 0.065 for diblock).

3.2.3 Micelle Assembly and Characterization

1. Dissolve lyophilized polymer at 50 mg/mL in 100% ethanol.
2. Rapidly pipette dissolved polymer into 100 mM phosphate buffer (pH 7) to a final concentration of 10 mg/mL.

Note: Highly recommended: For in vivo studies, remove ethanol by buffer exchange into PBS (pH 7.4) via three cycles of centrifugal dialysis (Amicon, 3 kDa MWCO, Millipore), and sterilize NP solutions via syringe filtration (Whatman, 0.22 μ m, GE Healthcare).

3. Polymer concentration can be determined with UV – vis spectrometry by measuring absorbance of aromatic PDSMA groups at 280 nm.

Measure the size of the NP via dynamic light scattering (DLS). Prepare NP solutions at a concentration of 0.1–0.2 mg/mL in PBS (pH 7.4), and measure the hydrodynamic radius by using a Malvern Instruments Zetasizer Nano ZS Instrument (Malvern, USA) or other particle sizing equipment.

3.2.4 OVA Protein Conjugation and Characterization

The method described here is for conjugation of a model antigen, ovalbumin (OVA), which is linked to the NP via PDS groups in a thiol-disulfide exchange reaction. The method can be adapted with minor modifications for conjugation of other protein antigens.

1. Thiolate free amines on the surface of the OVA protein by incubating with ~25-fold molar excess of 2-iminothiolane (Traut's Reagent, Thermo Fisher Scientific) in reaction buffer (100 mM phosphate buffer, pH 8, supplemented with 1 mM EDTA).

Note: Adjust the amount of 2-iminothiolane empirically for different proteins or to modify the degree of thiolation.

2. Remove unreacted 2-iminothiolane by buffer exchange of thiolated OVA into PBS (pH 7.4) by using Zeba Spin desalting columns (0.5 mL, 7 kDa MWCO).

Note: Highly recommended: For in vivo studies, sterilize thiolated OVA via syringe filtration through a 0.22- μ m filter

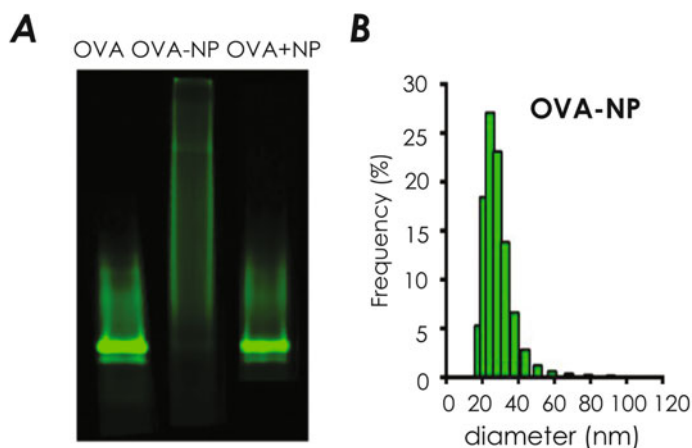


Fig. 4 Thiolated OVA protein labeled with FITC was reacted with NP made from pH-responsive polymer to form conjugates at various molar ratios of OVA: polymer. **(a)** SDS-PAGE was used to confirm antigen conjugation. Lane (1) free OVA protein; (2) OVA-NP (1:20 molar ratio); (3) OVA + NP (a physical mixture). **(b)** Representative size distribution (number average) at pH 7.4 for OVA-NP (1:5 molar ratio), as measured by DLS. (Image adapted from our published works in refs. [6, 29])

- Determine the molar ratio of thiol groups per OVA protein using Ellman's reagent following manufacturer's instructions. Typically, 3–5 thiol groups/OVA result in efficient conjugation to the NP.

Note: Determine the number of thiols required for efficient coupling of different proteins to NP as this may be different for different proteins.

- Add thiolated OVA to the NP solution in PBS at the desired molar ratios of NP:OVA (typically between 5:1 and 20:1) to form OVA-NP conjugates.
- Allow conjugation reaction to proceed overnight at room temperature.
- Verify antigen conjugation via nonreducing SDS-PAGE (Fig. 4a).
- Use dynamic light scattering to measure the size of OVA–NP conjugates (Fig. 4b).

3.2.5 Nucleic Acid Complexation and Characterization

Polymer/nucleic acid complexes can be formed by combining nucleic acid adjuvants and micelle solutions at different theoretical charge ratios (+/–). The charge ratio is defined as the molar ratio between protonated DMAEMA tertiary amines in the first block (positive charge; assuming 50% protonation at physiological pH) and phosphate groups on the nucleic acid (negative charge). Below we

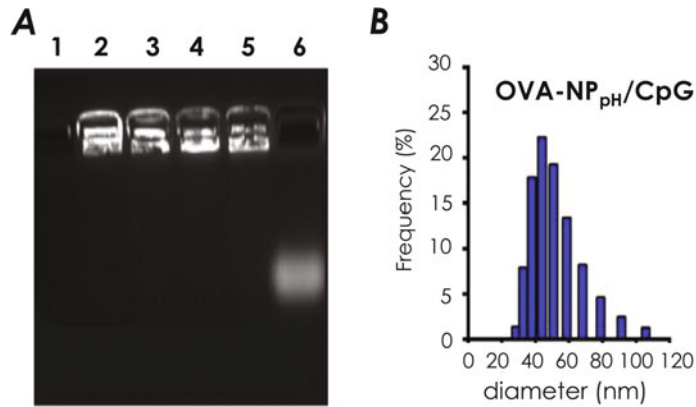


Fig. 5 CpG DNA was complexed with nanoparticles (NP) and conjugates (OVA-NP, 1:5 molar ratio) at various charge ratios of polymer:CpG (+/–). **(a)** Gel electrophoresis and GelRed staining confirmed adjuvant complexation. Lane (1) OVA-NP; (2) NP/CpG (6:1 +/-); (3) NP/CpG (4:1); (4) OVA-NP/CpG (6:1); (5) OVA-NP/CpG (4:1); (6) free CpG. Material loaded into each lane was normalized to 2.3 μ g CpG. CpG complexed with both NP and OVA-NP at both charge ratios, as shown by lack of migration from the wells of the gel (lanes 3–6). Free CpG migrated from the well due to its net negative charge (lane 7). OVA-NP did not show background staining from GelRed (lane 2). **(b)** Representative size distributions (number average) at pH 7.4 for OVA-NP/CpG (1:5 molar ratio, 6:1 charge ratio), as measured by DLS. (Image adapted from our published work in ref. [29])

describe complexation with CpG ODN 1826, a single-stranded DNA adjuvant.

1. Combine nucleic acid and conjugate (OVA-NP) in an Eppendorf tube at desired concentration and charge ratio. Add the conjugate to nucleic acid and mix vigorously via pipetting. Dilute to desired concentration in PBS at room temperature for 30 min.
2. Confirm complete complexation via an agarose gel electrophoresis. For CpG ODN 1826, use a 4% agarose gel; run at 90 V for 1 h; stain the gel with SYBR Safe nucleic acid gel stain (Invitrogen) for 20 min and visualize with a Gel Doc EZ system (Bio-Rad) (Fig. 5a).
3. Use dynamic light scattering to measure the size of the OVA–NP/CpG formulations (Fig. 5b).

3.2.6 Erythrocyte Lysis Assay

The degree to which the pH-responsive polymer was able to induce pH-dependent lysis of lipid bilayer membranes (thus leading to cytosolic delivery) was assessed via a red blood cell hemolysis assay [37].

Erythrocyte Preparation

1. Obtain 25 mL blood from anonymous donor or purchase erythrocytes from a commercial source.
2. Centrifuge blood at $500 \times g$ for 5 min, and mark the boundary between cells (red, lower layer) and plasma (yellow, top layer) on the tube.
3. Discard plasma into bleach.
4. Fill tube to marked line (original level of plasma) with 150 mM NaCl solution. Cap and invert several times to gently mix.
5. Centrifuge at $500 \times g$ for 5 min.
6. Repeat **steps 2–5** to wash blood cells. Then aspirate supernatant and resuspend cells in PBS pH 7.4. Invert to mix.
7. Split cells evenly into four tubes, corresponding to each test pH; label tubes accordingly: 7.4, 6.6, and 5.8.
8. Centrifuge tubes at $500 \times g$ for 5 min. Mark levels on tubes, then aspirate supernatant.
9. Fill each tube to the marked line with buffer of appropriate pH.
10. Label three 50-mL conical tubes, one per test pH, and pipette 49 mL of PBS of appropriate pH into each conical tube.
11. Add 1 mL of RBCs (same pH) into tube for a final dilution of 1:50 at the indicated pH buffer.

Evaluation
of pH-Responsive
Hemolysis Activity

12. Prepare stock solutions of polymers at 20-fold the desired final concentration to be tested. Assay will use 10 μ L polymer +190 μ L red blood cells, resulting in a 1:20 dilution of the original polymer concentration.
Note: Stocks of 200, 300, and 400 μ g/mL are suggested, resulting in final concentrations of 10, 15, 20 μ g/mL, respectively.
13. Pipette 10 μ L of each stock solution into a round-bottom 96-well plate.
Note: For optimal results, load each sample in triplicate or quadruplicate.
14. As positive control, add 10 μ L of 0.1% Triton X-100.
15. For negative control, add 10 μ L PBS adjusted to the test pH.
16. Pipette 190 μ L of red blood cells to each well.
17. Incubate plates at 37 °C for 1 h.
18. Centrifuge plates for 5 min at $500 \times g$ to pellet intact red blood cells.
19. Transfer 100 μ L of supernatant from each well into a clear, flat bottom 96-well plate; use a multichannel pipette.
20. Measure $A_{541 \text{ nm}}$ of supernatants using a plate reader (Synergy H1 Multi-Mode Reader, BioTek).

21. Using Microsoft Excel or a similar data analysis software, find the average of the background $A_{541\text{ nm}}$ readings from the negative control samples set up for each pH. Subtract this background absorbance value from all other samples that were measured at that pH. After background subtraction, find the average $A_{541\text{ nm}}$ of the positive control detergent-treated samples. Then normalize all experimental data points to this mean absorbance value, which should represent 100% hemolysis. Finally, multiply each well value by 100% to calculate % hemolysis that occurred in each individual well relative to the detergent control. %Hemolysis = $100 * (A_{541\text{ nm sample}} - A_{541\text{ nm buffer}}) / (A_{541\text{ nm triton}} - A_{541\text{ nm buffer}})$.

3.2.7 In Vitro Cross-Presentation Assay

The ability of polymeric nanoparticles to enhance MHC-I antigen presentation was assessed by an in vitro antigen presentation assay using DC2.4 cells as the antigen-presenting cell. This assay utilizes a specialized LacZ B3Z T cell hybridoma that produces β -galactosidase upon recognition of an immunodominant ovalbumin epitope SIINFEKL presented on mouse MHC-I H-2K^b expressed by DC2.4 cells [3].

1. Plate DC2.4 cells at 5×10^4 cells/well in 100 μL tissue culture medium in a 96-well, round-bottom plate and incubate at 37 °C in an atmosphere of 5% CO₂ for ~24 h or overnight.
2. Aspirate old medium; add 100 μL of DC2.4 culture medium; mix well, and incubate at 37 °C in an atmosphere of 5% CO₂ for 4–24 h as required. Perform assay in triplicates.
3. Remove old medium and wash thrice with DPBS.

Caution: Be careful not to remove loosely attached cells.

4. Plate B3Z cells at a density of 1×10^5 cells/well in 200 μL tissue culture medium and co-culture at 37 °C in an atmosphere of 5% CO₂ for 20–24 h.
5. Centrifuge the plate at 1500 rpm for 10 min; store supernatant (to assay for cytokines).
6. Add 150 μL lysis buffer (PBS, 100 μM 2-ME, 9 mM MgCl₂, 0.1% triton X-100, and 0.15 mM chlorophenol red- β -D-galactopyranoside) per well; mix thoroughly.

Lysis buffer (5 mL allows ~30 assays): to 4.9 mL PBS, add 9 μL β ME (55 mM) stock, 9.14 mg MgCl₂ · 6H₂O, 50 μL of 10% Triton X-100, and 8.8 μL of CPRG stock (85.4 mM, stored at –20 °C).

7. As an orange-red color develops (90 min at 37 °C), centrifuge, transfer supernatant to new 96-well plate, and read $A_{570\text{ nm}}$ using a plate reader.

4 Antigen Preparation

The protocol described here is validated for the purification of recombinant protein antigen rOVA3 (Fig. 6a; ref. [38]) that is overexpressed as inclusion bodies in *E. coli*. This protocol can be utilized to purify other protein antigens which traffic into inclusion bodies; however, the protocol must be optimized for each protein to ensure optimal yield and purity.

4.1 Materials

Note: *Buffers used in the preparation of antigen are filter sterilized using 0.2 μ m filter.*

1. *E. coli* BL21-Gold(DE3) competent cells (Agilent Technologies) transformed with plasmid encoding rOVA3 [38] protein antigen.
2. Ni-NTA Agarose resin or cobalt resin (Talon; Sigma Aldrich).
3. MgCl₂: Make 1 M stock solution; store at -20°C .
4. MnCl₂: Make 100 mM stock solution; store at -20°C .
5. DNase stock solution: 10 mg/mL DNase I, 50% v/v glycerol, 150 mM NaCl; store at -20°C .
6. RNase A, DNase and protease free, 10 mg/mL (Thermo Scientific).
7. Econo-Column Chromatography Column (BioRad).
8. Lysis Buffer: 50 mM Tris-Cl (pH 7.5) 25% w/v sucrose, 1 mM EDTA.
9. Wash Buffer: 1.0% v/v Triton X-100, 5 mM DTT (see Note 25) in 50 mM Tris-Cl (pH 7.5).
10. Detergent Buffer: 0.2 M NaCl, 1% w/v sodium deoxycholate monohydrate, 1% Nonidet P 40 (NP-40) substitute, 2 mM EDTA in 20 mM Tris-Cl (pH 7.5).
11. Solubilization buffer: 20 mM Tris-Cl, 300 mM NaCl, 8 M urea (pH 8.0).
12. Elution buffer: 20 mM Tris-Cl, 300 mM NaCl, 8 M urea, 250 mM imidazole.
13. Refolding buffer: 20 mM Tris-Cl (pH 8.0), 300 mM NaCl, 2 M (1, 0.5, or 0 M) urea, 5 mM BME, 1% glycerol.
14. Pierce high-capacity endotoxin removal spin column, 0.5 mL.
15. Endotoxin-free PBS.
16. Pierce LAL Chromogenic Endotoxin Quantification kit.
17. Slide-A-Lyzer Dialysis Cassette, 10 K MWCO, 3–12 mL.
18. Amicon Ultra-15 MWCO 10 kDa Centrifugal filter (Millipore).

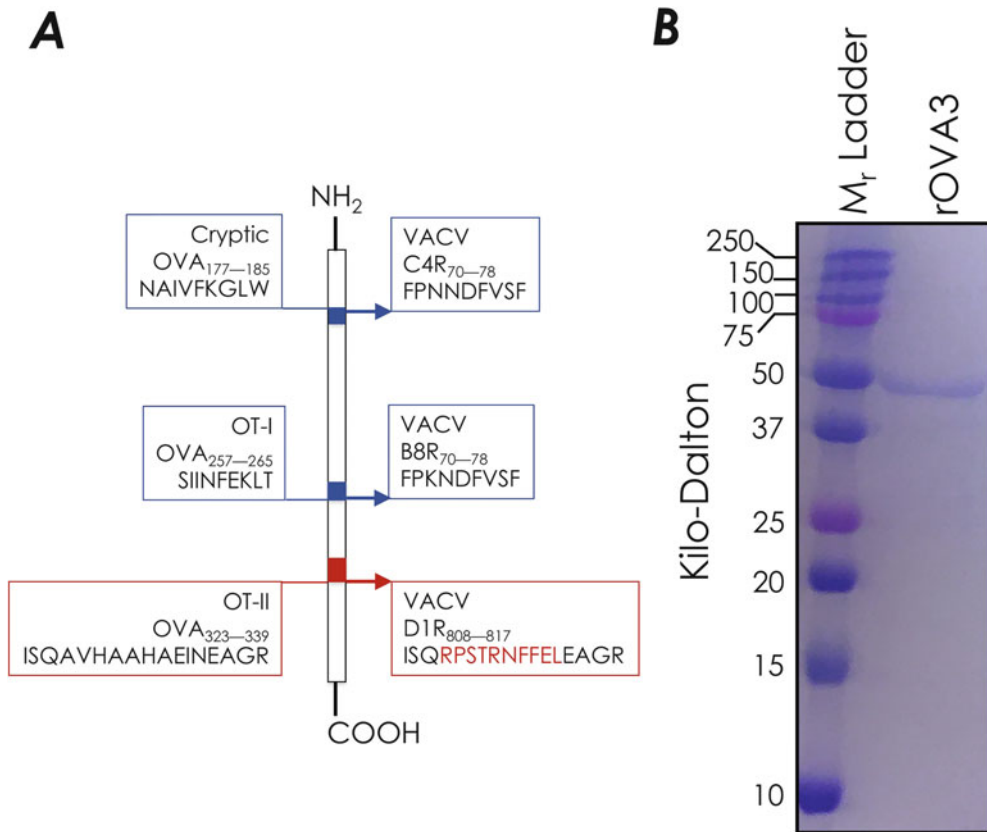


Fig. 6 Schematic rendition of rOVA3. **(a)** The original cryptic, OT-I, and OT-II epitopes within native ovalbumin protein were replaced with C4R₇₀₋₇₈, B8R₇₀₋₇₈, and D1R₈₀₈₋₈₁₇ epitopes, respectively (Adapted from ref. [38]). **(b)** rOVA3 was purified by methods described in **Subheading 4**, separated by SDS-PAGE, and detected with InstantBlue Coomassie protein stain

19. Nalgene Oak Ridge High Speed PPCO centrifuge tubes, 50 mL.
20. Branson Ultrasonics sonifier S-250A.
21. Sorvall RC-5B refrigerated centrifuge with SS-34 rotor.
22. NanoDrop One.
23. Disposable syringes, 5 mL.
24. Disposable 28-mm syringe filter, 0.45 μ m.
25. Nalgene Rapid-Flow single use sterile filtration unit, 0.2 μ m.

4.2 Methods

Note:

1. For transformation, thaw 100 μ L of competent cells on ice. Add 50 ng of the DNA to the cells and mix gently as described in Subheading 2.2.2. Incubate on ice for 30 min. Heat-pulse the cells in a 42 °C water bath for 20 s, followed by incubation on ice for 2 min. Add 900 μ L of preheated SOC medium to the

transformation reaction mixture and subsequently incubate at 37 °C for 45–60 min with shaking at 225–250 rpm. Plate 300 µL of the transformed mixture onto LB agar plate supplemented with kanamycin (50 µg/mL) using a sterile spreader. Incubate the plate overnight at 37 °C. Next, perform a colony screen (*see* **Note 11** and **Subheading 2.2.3**) to ensure that the colony contains the protein of our interest and expresses it at high level (*see* **Note 26**).

2. Inoculate 10 mL 50 µg/mL kanamycin-supplemented LB with an isolated, transformed colony. Incubate overnight at 37 °C with shaking at ~250 rpm.
3. Pour entire amount of the overnight culture as in **step 2** into 1 L of LB medium supplemented with 50 µg/mL kanamycin. Incubate at 37 °C with vigorous shaking at ~250 rpm.
4. After about 3–4 h, when $A_{600\text{ nm}}$ reaches 0.5–0.8, induce the expression of protein by adding IPTG to 0.4 mM; continue induction for additional 4 h.
5. Harvest cells by centrifugation as in **Subheading 2.2.3, step 4**.
Note: Typically, two or four separate 1 L cultures are grown, and the cell pellets obtained from two 1 L cultures are combined. Although not recommended, if necessary, store the cell pellet at –80 °C to continue later. It is best to store inclusion bodies.
6. Resuspend the cell pellet (~4–5 g from two 1 L cultures) in 8 mL lysis buffer; add 20 mg lysozyme dissolved in 2 mL lysis buffer. Incubate for 30 min at 4 °C on a rocker.
7. Add 100 µL of 100 mM MgCl₂ stock (10 mM final), 100 µL of 10 mg/mL RNase A stock, and 200 µL of 10 mg/mL DNase stock to the cell suspension. Incubate for 30 min at 4 °C on a rocker.
8. Add additional 10 mL lysis buffer and sonicate the cell suspension using Branson 250 sonifier (analog version) set at the following parameters: timer: 5 min; duty cycle: 50%; output: 5.
*Note: Before sonication, place the cell suspension in an ice water bath to avoid heat-induced protein denaturation (see **Subheading 2.2.3, step 6**).*
9. Transfer the content to Nalgene 50-mL centrifuge tubes and centrifuge at 14,000 × *g* for 20 min at 4 °C in Sorvall RC-5B refrigerated centrifuge using a SS-34 rotor.
10. Discard the supernatant; wash by adding 30 mL detergent buffer to the pellet. Resuspend the pellet and centrifuge as in **step 9**. A short sonication (1 min, 50% duty cycle) is helpful during each wash step.
11. Discard the supernatant and add 1 mL of wash solution to the pellet. Resuspend the pellet, add wash solution to 30 mL.

12. Repeat **steps 9–11** thrice or until the pellet consisting largely of inclusion bodies is whitish in color.
13. Resuspend the pellet with 30 ml of phosphate buffer containing 1 M NaCl. Centrifuge as in **step 9**. Perform a final wash with phosphate buffer to remove residual salt in the pellet. And, centrifuge again as in **step 9** to pellet purified inclusion bodies.

Note: This step will remove a lot of residual DNA and RNA from the pellet.

14. Resuspend the pellet in 10 mL solubilization buffer with the help of a short sonication (1 min, 50% duty cycle) to solubilize inclusion body. Centrifuge at $4000 \times g$ for 10 min at 4 °C to remove undissolved material.
15. Filter the supernatant through 0.45 µm filter into a 15 mL falcon (polypropylene) tube; add 5 mL Ni-NTA resin (pre-equilibrated to RT); mix well and incubate at 4 °C for 2 h on a rocker.

Note: Cobalt resin can also be used to purify rOVA3.

16. Pellet the resin at $300 \times g$ for 5 min at 4 °C; carefully remove the supernatant (*see Note 27*). Store supernatant at –80 °C until the purification of the protein and yield are confirmed.

Note: Agarose-based resins collapse with high-speed sedimentation and will form a gel. Hence, it is critical that centrifugation is performed at low speed.

17. Resuspend the resin in 15 mL solubilization buffer. Centrifuge the solution as in **step 15**; discard supernatant. Repeat this wash step once or twice more.
18. Resuspend the resin in 15 mL solubilization buffer and pour the slurry into an Econo-Column chromatography column (1.5 × 5 cm). Wash the column three times with 5–10 mL solubilization buffer.
19. Elute with 10 mL elution buffer; collect 1 mL fractions; 0.5 mL fractions are recommended. Analyze by SDS-PAGE and combine the fractions containing pure protein (*see Note 28*).
20. Remove urea from the protein sample using stepwise dialysis approach so as to enforce refolding instead of aggregation. First, dilute the sample ($\sim A_{280 \text{ nm}}$: 1.0–1.2) by twofold using refolding buffer with no urea to bring down the urea concentration to 4 M. Transfer about 5–8 mL of protein sample into a dialysis cassette of 10 K MWCO; dialyze against 1 L refolding buffer containing 2 M urea. After 2 h, transfer the cassette to 1 L refolding buffer containing 1 M urea for dialysis. Perform these dialysis steps but with refolding buffer containing 0.5 M and no urea in the dialysis buffer. Once the refolding is

completed, dialyze the sample in 1 L phosphate buffer and finally in 500 mL endotoxin-free PBS. Concentrate sample using Amicon Ultra-15 MWCO 10 kDa centrifugal filter. Filter the sample through 0.2 μm filter before use.

21. Separate purified protein by SDS-PAGE; analyze by staining with InstantBlue protein stain as per manufacturer's protocol. Figure 6b shows purified rOVA3.
22. Using manufacturer's protocol, determine the endotoxin levels in the antigen preparation. If level exceeds the acceptable limit (see ref. [39]), use endotoxin spin removal column to remove residual lipopolysaccharide (LPS) from the preparation using vendor's protocol.

Note: Endotoxin removal column will significantly lower the level of endotoxin but will not completely free the protein preparation of it.
23. Store the protein sample at 4 °C; use for immunization within 2 days (see ref. [38]).

5 Notes

1. The gene encodes for a mature StAv comprising amino acid residues 15–159.
2. CP and SP can be co-expressed or temporally expressed by placing their respective genes on one vector or on separate vectors, respectively. When using separate vectors, ensure that the origin of replication is compatible with each other for vectors to co-exist stably over generations. The staggered, temporal expression is mainly employed where cargo requires additional time to fold into mature form prior to the initiation of the encapsulation process.
3. StAv is fused at the N-terminus of truncated SP with amino acids ranging from 142 to 303. Both wt and truncated SP mediate cargo encapsulation; truncated SP, however, affords more internal space for the cargo inside the VLP.
4. Codon for Cys is inserted upstream of a previously generated 6xHis-tagged SP-GFP using QuickChange Lightning Site-Directed Mutagenesis kit, mutagenic pairs and the manufacturer's recommended protocol. The mutagenic primers can be designed using Agilent's QuickChange primer design program.
5. Novagen kit contains all reagents for transformation including cells, recovery medium, and a control plasmid. SOC from other vendors works equally well.
6. Recommended working concentration for ampicillin is 50 $\mu\text{g}/\text{mL}$ and for kanamycin 30 $\mu\text{g}/\text{mL}$.

7. Avoid freeze-thaw of glycerol stocks as this improves the storage life of bacterial stocks.
8. A linker with TEV site, GAAG-ENLYFQS-GAAG, is inserted between StAv and SP to avoid any steric hindrance biotin may experience in accessing its binding site in streptavidin.
9. Gently swirl, shake, and tap the tube; avoid mixing cells by pipetting up and down vigorously as this damages cells through shear forces generated during pipetting.
10. Add antibiotics to a final concentration of 30 µg/mL for kanamycin and 50 µg/mL for ampicillin.
11. Inoculate 3 mL of LB medium containing antibiotics for plasmid maintenance with individually grown colonies (five colonies). After overnight growth at 37 °C, transfer about 30 µL inoculum into fresh 3 mL LB cultures. Grow to an $A_{600\text{ nm}}$ of ~0.5; remove 1 mL of culture from each tube and induce the rest of the 2 mL with 2 µL of 0.5 M IPTG for 4 h. To harvest cells before and after induction, sediment 1 mL culture by centrifugation at $17,000 \times g$ for 1–2 min. Resuspend cell sediment in 1 mL PBS buffer. Take 30 µL of it, mix with 6 µL loading dye, and incubate in a 100 °C bath for 5–10 min. Sediment aggregates by 1 min centrifugation at maximum speed; separate proteins in 10 µL sample by SDS-PAGE; analyze by staining with InstantBlue protein stain as per manufacturer's protocol. Varying intensities of a recombinant protein band is a reflective of expression level.
12. Care should be taken not to mix the sucrose cushion with supernatant.
13. GuHCl is incompatible with SDS-PAGE as guanidinium causes precipitation of SDS; therefore, remove GuHCl from the samples before analyzing them by gel.
14. Protein concentration $\left(\frac{\text{mg}}{\text{mL}}\right) = \frac{A_{280\text{ nm}} \times \text{molar extinction coefficient}}{\text{Molecular weight}}$
15. Induction time may require optimization depending on the yield of the protein. To optimize expression, grow starter culture overnight and use 30 µL of it to inoculate a 3-mL culture next day. Once $A_{280\text{ nm}}$ reaches the desired level, induce for various times, e.g., 2 h, 3 h, 4 h, 6 h, 8 h, and 1 h; compare the expression levels by SDS-PAGE analysis.
16. $\text{StAv} - \text{SP} (\text{copies}) = \frac{(\text{MW of P22-StAv}) - (420 \times 46.7)}{\text{MW of StAv-SP}}$
17. Select a dialysis membrane whose MWCO is one-third the molecular mass of the macromolecule to be retained.
18. Consult references [15, 27] for detailed information on the determination of molar extinction coefficient of the cargo of choice for encapsulation.
19. B4F is used as an efficient readout for ligand binding to streptavidin. Make the working B4F in PBS. Calculate

concentration using λ_{\max} and molar extinction coefficient of 68,000/M/cm.

20. Binding of B4F to streptavidin results in the attenuation of $A_{493 \text{ nm}}$ due to a significant alteration in the molar extinction coefficient of B4F. Therefore, reduced absorbance values are observed until all sites are titrated, beyond which further addition of B4F produces a linear response with unrestrained absorbance values similar to a negative control. Such behavior of B4F yields two regression lines with different slopes. The point of intersection of these two lines represents the binding stoichiometry, thus providing a means to calculate the extent of ligand binding.
21. Piecewise linear regression model in Igor Pro was used to fit two discontinuous lines. Consult literature for more information [27].
22. For alkylation, follow the protocol that is used for biotinylation in Subheading 2.2.7, **step 1**.
23. Both MALS and densitometric analysis of SDS-PAGE can be used to obtain number of copies displayed on the surface. For densitometric analysis, prepare standards containing CP and B-linker-GFP and plot a calibration curve between band intensities and corresponding concentrations. To calculate concentration using UV-Vis spectrum, use $A_{495 \text{ nm}}$ and a molar extinction coefficient of 55,000/M/cm.
24. Apply 5 μL of standard (B-SP-GFP) and sample (P22-GFP_{in} and P22-GFP_{ex}) on nitrocellulose membrane and air dry for 5–10 min. Block membrane with 5% skim milk prepared in TBS buffer for 30 min at room temperature. Incubate membrane with polyclonal anti-GFP rabbit antibody (1:10,000 dilution in 5% milk) at room temperature on rocker; after 2 h, wash thrice with TBS, 5 min each time. Incubate membrane with goat anti-rabbit HRP-conjugated secondary antibody (1:3000 dilution in 5% milk) at room temperature; after 2 h wash above; and develop with opti-4CN substrate as per instructions provided in the kit for colorimetric method.
25. Add DTT to buffer immediately before use.
26. For every fresh batch of protein, re-transform the cells, perform colony screen, and validate the presence of our protein of interest using SDS-PAGE. Various truncation products have been observed if the glycerol stock of this protein construct is used.
27. Save an aliquot of the supernatant for gel analysis.
28. Analyze the fractions by UV-Vis spectrophotometry. A_{260}/A_{280} of 0.6 indicates the purity of protein sample, i.e., the absence of DNA contamination, which is essential for the

animal studies. A part of protein sample can be snap-frozen at this stage, and when required for a booster dose, the protein sample can be thawed and refolded quickly for administration.

29. The concentration of rOVA3 is measured using $A_{280\text{ nm}}$, MW: 46,409.98 Da, extinction coefficient: 31,775/M/cm.

Acknowledgments

SJ is a Research Career Scientist supported by IK6 BX004595 from the Department of Veterans Affairs. Supported by Vanderbilt University Discovery Grants Programs (JWT, SJ) as well as VA Merit Award (BX001444: SJ); NIH Contracts (AI040079: SJ), and Research (AI042284, HL121139: SJ; AI121626: JWT), Core (CA068485, DK058404), and Center (CA068485) grants; NSF research (CBET-1554623: JWT) and Fellowship DGE-1445197 and DGE-1937963: CSC) grants; Stand Up To Cancer Innovative Research Grant (SU2C-AACR-IRG 20-17: JWT)—a program of the Entertainment Industry Foundation administered by the American Association for Cancer Research—the scientific partner of SU2C—and Human Frontier Science Program (HFSP 4124801: TD).

References

1. Black M, Trent A, Tirrell M, Olive C (2010) Advances in the design and delivery of peptide subunit vaccines with a focus on toll-like receptor agonists. *Expert Rev Vaccines* 9:157–173
2. Fischer NO et al (2013) Colocalized delivery of adjuvant and antigen using nanolipoprotein particles enhances the immune response to recombinant antigens. *J Am Chem Soc* 135:2044–2047
3. Shae D et al (2020) Co-delivery of peptide neoantigens and stimulator of interferon genes agonists enhances response to cancer vaccines. *ACS Nano* 14:9904–9916
4. Wilson JT et al (2015) Enhancement of MHC-I antigen presentation via architectural control of pH-responsive, endosomal polymer nanoparticles. *AAPS J* 17:358–369
5. Bookstaver ML, Tsai SJ, Bromberg JS, Jewell CM (2018) Improving vaccine and immunotherapy design using biomaterials. *Trends Immunol* 39:135–150
6. Wilson JT et al (2013) pH-responsive nanoparticle vaccines for dual-delivery of antigens and immunostimulatory oligonucleotides. *ACS Nano* 7:3912–3925
7. Reed SG, Bertholet S, Coler RN, Friede M (2009) New horizons in adjuvants for vaccine development. *Trends Immunol* 30:23–32
8. Stanley M (2017) Tumour virus vaccines: hepatitis B virus and human papillomavirus. *Philos Trans R Soc Lond B Biol Sci* 372 (1732):20160268
9. Chackerian B (2007) Virus-like particles-flexible platforms for vaccine development. *Expert Rev Vaccines* 6:381–390
10. Brune KD et al (2016) Plug-and-display: decoration of virus-like particles via isopeptide bonds for modular immunization. *Sci Rep* 6:19234
11. Sharma J et al (2020) A self-adjuvanted, modular, antigenic VLP for rapid response to influenza virus variability. *ACS Appl Mater Interfaces* 12:18211–18224
12. Bachmann MF, Jennings GT (2010) Vaccine delivery: a matter of size, geometry, kinetics and molecular patterns. *Nat Rev Immunol* 10:787–796
13. Hua ZL, Hou BD (2013) TLR signaling in B-cell development and activation. *Cell Mol Immunol* 10:103–106

14. Zabel F, Kundig TM, Bachmann MF (2013) Virus-induced humoral immunity: on how B cell responses are initiated. *Curr Opin Virol* 3:357–362
15. Patterson DP, Rynda-Apple A, Harmsen AL, Harmsen AG, Douglas T (2013) Biomimetic antigenic nanoparticles elicit controlled protective immune response to influenza. *ACS Nano* 7:3036–3044
16. Schwarz B et al (2016) Viruslike particles encapsidating respiratory syncytial virus M and M2 proteins induce robust T cell responses. *ACS Biomater Sci Eng* 2:2324–2332
17. Rynda-Apple A, Patterson DP, Douglas T (2014) Virus-like particles as antigenic nanomaterials for inducing protective immune responses in the lung. *Nanomedicine* 9:1857–1868
18. Pumpens P, Grens E (2001) HBV core particles as a carrier for B cell/T cell epitopes. *Interferology* 44:98–114
19. Schafer K et al (1999) Immune response to human papillomavirus 16 L1E7 chimeric virus-like particles: induction of cytotoxic T cells and specific tumor protection. *Int J Cancer* 81:881–888
20. Ruedl C et al (2005) Virus-like particles as carriers for T-cell epitopes: limited inhibition of T-cell priming by carrier-specific antibodies. *J Virol* 79:717–724
21. Joffre OP, Segura E, Savina A, Amigorena S (2012) Cross-presentation by dendritic cells. *Nat Rev Immunol* 12:557–569
22. Gause KT et al (2017) Immunological principles guiding the rational design of particles for vaccine delivery. *ACS Nano* 11:54–68
23. Irvine DJ, Swartz MA, Szeto GL (2013) Engineering synthetic vaccines using cues from natural immunity. *Nat Mater* 12:978–990
24. Canton I, Battaglia G (2012) Endocytosis at the nanoscale. *Chem Soc Rev* 41:2718–2739
25. Graham DB et al (2010) ITAM signaling in dendritic cells controls T helper cell priming by regulating MHC class II recycling. *Blood* 116:3208–3218
26. Wan Y, Moyle PM, Toth I (2015) Endosome escape strategies for improving the efficacy of oligonucleotide delivery systems. *Curr Med Chem* 22:3326–3346
27. Sharma J, Uchida M, Miettinen HM, Douglas T (2017) Modular interior loading and exterior decoration of a virus-like particle. *Nanoscale* 9:10420–10430
28. Schwarz B et al (2015) Symmetry controlled, genetic presentation of bioactive proteins on the P22 virus-like particle using an external decoration protein. *ACS Nano* 9:9134–9147
29. Knight FC et al (2019) Mucosal immunization with a pH-responsive nanoparticle vaccine induces protective CD8(+) lung-resident memory T cells. *ACS Nano* 13:10939–10960
30. O’Neil A, Reichhardt C, Johnson B, Prevelige PE, Douglas T (2011) Genetically programmed in vivo packaging of protein cargo and its controlled release from bacteriophage P22. *Angew Chem Int Edit* 50:7425–7428
31. Padilla-Meier GP et al (2012) Unraveling the role of the C-terminal helix turn helix of the coat-binding domain of bacteriophage P22 scaffolding protein. *J Biol Chem* 287:33766–33780
32. Botstein D, Waddell CH, King J (1973) Mechanism of head assembly and DNA encapsulation in Salmonella phage p22. I. Genes, proteins, structures and DNA maturation. *J Mol Biol* 80:669–695
33. McCoy K, Douglas T (2018) In vivo packaging of protein cargo inside of virus-like particle P22. *Methods Mol Biol* 1776:295–302
34. Sharma J, Douglas T (2020) Tuning the catalytic properties of P22 nanoreactors through compositional control. *Nanoscale* 12:336–346
35. Waghvani HK et al (2020) Virus-like particles (VLPs) as a platform for hierarchical compartmentalization. *Biomacromolecules* 21:2060–2072
36. Prevelige PE Jr, Thomas D, King J (1988) Scaffolding protein regulates the polymerization of P22 coat subunits into icosahedral shells in vitro. *J Mol Biol* 202:743–757
37. Evans BC et al (2013) Ex vivo red blood cell hemolysis assay for the evaluation of pH-responsive endosomolytic agents for cytosolic delivery of biomacromolecular drugs. *J Vis Exp* e50166. <https://doi.org/10.3791/50166>
38. Kumar A et al (2020) Heterotypic immunity against vaccinia virus in an HLA-B*07:02 transgenic mousepox infection model. *Sci Rep* 10:13167
39. Brito LA, Singh M (2011) Acceptable levels of endotoxin in vaccine formulations during pre-clinical research. *J Pharm Sci* 100:34–37



PilVax: A Novel Platform for the Development of Mucosal Vaccines

Catherine (Jia-Yun) Tsai, Jacelyn M. S. Loh, and Thomas Proft

Abstract

Peptide vaccines offer an attractive strategy to induce highly specific immune responses while reducing potential side effects. However, peptides are often poorly immunogenic and unstable on their own, requiring the need for potentially toxic adjuvants or expensive chemical coupling. The novel peptide delivery platform PilVax utilizes the rigid pilus structure from Group A Streptococcus (GAS) to stabilize and amplify the peptide, and present it on the surface of the non-pathogenic food-grade bacterium *Lactococcus lactis*. Upon intranasal immunization, PilVax vaccines have proven to induce peptide-specific systemic and mucosal responses. PilVax provides an alternative method to develop mucosal vaccines that are inexpensive to produce and easy to administer.

Key words Group A Streptococcus, Pili, *Streptococcus pyogenes*, Peptide, *Lactococcus lactis*, Mucosal vaccine

1 Introduction

Peptide vaccines can be engineered to contain only the minimal necessary epitopes, therefore offer highly specific immune targets that avoid potential allergic or autoreactive reactions [1]. However, peptides on their own are often poorly immunogenic and prone to proteolytic degradation [2], thus require the addition of adjuvant or a specialized delivery system [3]. One such delivery system is the food-grade lactic acid bacterium *Lactococcus lactis*, which has been extensively investigated in the past two decades as a delivery vector for therapeutic molecules including vaccine antigens [4]. Advantages of *L. lactis* as a vaccine delivery vector include the organism's established safety profile and GRAS (generally regarded as safe) status. As a noninvasive and noncommensal organism, it is less likely to trigger immunotolerance or side effects associated with long-term use. However, the choice and mode of antigen

presentation with this vector play a critical role in the effectiveness of delivery [5].

PilVax presents a novel peptide delivery platform that utilizes a *Streptococcus pyogenes* (Group A Streptococcus, GAS) pilus structure to carry an antigenic peptide on the surface of *L. lactis* [6]. It was shown previously that fully assembled GAS pilus structures can be expressed on the surface of *L. lactis* [7, 8]. Assembly can occur due to the similar anchoring mechanisms both species use for surface protein display, namely the sortase enzyme that processes and covalently links surface-associated proteins containing the LPXTG sorting signal to the cell wall [9].

The FCT-2-type pilus produced by the M1 serotype of GAS is among the most extensively studied GAS pilus types [10–15]. The crystal structure of the backbone pilus protein Spy0128 (also known as T1 antigen) has been solved, revealing an immunoglobulin-like fold with intramolecular isopeptide bonds, which provides a rigid protein conformation that is resistant to proteases [16]. Importantly, the crystal structure also showed several flexible and surface accessible loop regions that can be used as peptide integration sites. A model peptide from ovalbumin has been successfully inserted into the β E- β F loop, β 3- β 4 loop, and β 9- β 10 loop [6] (Fig. 1). In addition, several peptides from pathogens including influenza virus, *Mycobacterium tuberculosis*, and *Staphylococcus aureus* [17] have also been successfully incorporated in the PilVax platform.

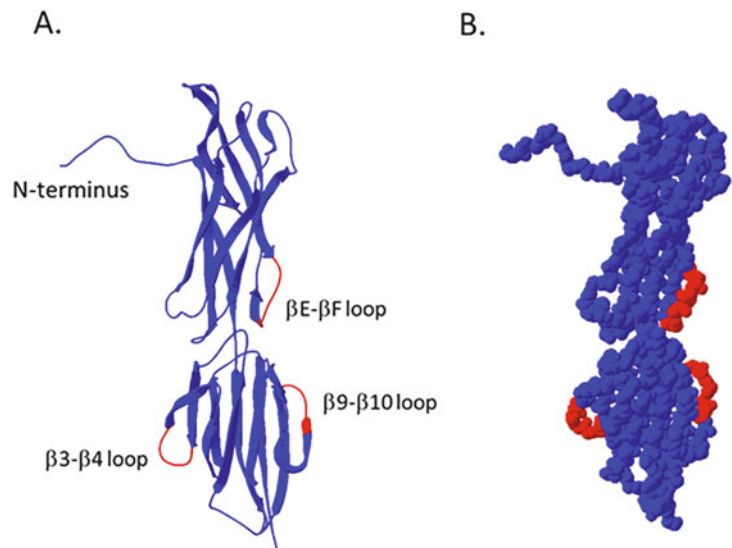


Fig. 1 Protein structure of the backbone pilin Spy0128 with peptide insertion sites labeled in red. (a) Ribbon diagram structure. (b) Accessible surface structure

The mucosal surfaces represent a primary entry route for many pathogens. Therefore, vaccination via the mucosal routes (oral, intranasal, vaginal, or rectal) may enable the establishment of specific mucosal immunity (primarily secretory IgA antibodies) to prevent infection [18]. Furthermore, mucosal vaccination is known to induce both mucosal and systemic immune responses [18]. The mucosal vaccination route also provides ease in administration, which lowers technical requirement and improves patient compliance. The prototype PilVax vaccines have been shown to elicit peptide-specific mucosal IgA and serum IgG after intranasal immunization of mice [6]. This chapter will outline the procedures from cloning PilVax constructs for generating recombinant *L. lactis* strains, to transforming and validating pilus-expressing *L. lactis*. Here we use *L. lactis* subsp. *cremoris* MG1363, the most extensively studied and commonly used strain. Other standard strains derived from MG1363 can also be used, such as the rifampicin and streptomycin-resistant derivative MG1364 [19].

2 Materials

All materials should be prepared under sterile conditions and handled with aseptic techniques. Media and buffers should be made up with ultrapure water (such as MilliQ) and sterilized by autoclaving or 0.22 μm membrane filtration.

2.1 Bacterial Culture

1. *L. lactis* strain MG1363.
2. *E. coli* strain DH5 α .
3. GM17 medium (M17 broth supplemented with 0.5% glucose).
4. GM17 agar (GM17 medium with 15 g/L agar).
5. LB medium.
6. LB agar (LB medium with 15 g/L agar).
7. Kanamycin (used at 50 $\mu\text{g}/\text{mL}$ for *E. coli*, 200 $\mu\text{g}/\text{mL}$ for *L. lactis*).
8. Sterile plastic tubes for bacterial culture.
9. Spectrophotometer for measuring culture density.

2.2 Molecular Cloning

1. An *E. coli*-*L. lactis* shuttle vector for gene expression from a strong constitutive *L. lactis* promoter such as P23 [20]. We used pLZ12km2_P23R [21, 22].
2. Restriction enzymes (*Bam*HI, *Xho*I, and *Sal*I) with appropriate buffer provided by the manufacturer.
3. DNA polymerase I, large (Klenow) fragment with appropriate buffer provided by the manufacturer.

Table 1
List of oligos required for molecular cloning

Name	Sequence (5' to 3')	Purpose
PilM1.fw	GCGGATCCGATATGATGTCACATTGAGAG	Amplification of the PilM1 pilus operon
PilM1.rev	GCGGATCCGTCGTGGGGCAATAAAAAATTC	Amplification of the PilM1 pilus operon
PilM1_βE-βF.fw	GAGAGAGACTCGAGGGTGTTCCTTATGATACAAC	Introduction of <i>XhoI</i> site into the βE-βF loop region
PilM1_βE-βF.rev	GAGAGAGACTCGAGCTCCTCAGTTACTTTG	Introduction of <i>XhoI</i> site into the βE-βF loop region
PilM1_β3-β4.fw	GAGAGAGACTCGAGCCTGTTCAAACAGAGGCTAG	Introduction of <i>XhoI</i> site into the β3-β4 loop region
PilM1_β3-β4.rev	GAGAGAGACTCGAGAGTTGTCTTCTCAATCATGAC	Introduction of <i>XhoI</i> site into the β3-β4 loop region
PilM1_β9-β10.fw	GAGAGAGACTCGAGAAAAATATCGCAGGTAATTC	Introduction of <i>XhoI</i> site into the β9-β10 loop region
PilM1_β9-β10.rev	GAGAGAGACTCGAGTTGAGGACTAACTTCCACG	Introduction of <i>XhoI</i> site into the β9-β10 loop region
peptide.fw	CCCCTCGAG[peptide sequence] (<i>see Note 1</i>)	Synthesis of peptide DNA sequence
peptide.rev	CCCGGTCGAC[peptide sequence]	Synthesis of peptide DNA sequence
Spy0128.fw	GGAGCAGCCCTAACTAGTTTT GC	Screening for successful transformants
Spy0128.rev	GAGCTCCACCAACTGCTACAATTC	Screening for successful transformants

4. High fidelity DNA polymerase, such as Phusion™ or iProof™ with appropriate buffer provided by the manufacturer.
5. T4 DNA ligase with appropriate buffer provided by the manufacturer.
6. dNTP mix (25 mM each).
7. Oligo primers for introducing peptide insertion site into *spy0128* (Table 1).
8. PCR machine.

2.3 *L. lactis* Transformation

1. Ice-cold sterile water.
2. 50 mM EDTA, ice-cold.
3. 0.3 M sucrose, ice-cold.
4. Electroporation device.
5. 2 mm quartz cuvettes.
6. 1.6-mL and 15-mL sterile plastic tubes.
7. GM17 medium and GM17 agar plates supplemented with 200 µg/mL kanamycin.

2.4 *L. lactis* Cell Wall Extraction

1. Protoplast buffer (40% sucrose, 10 mM MgCl₂, 0.1 M KPO₄ pH 6.2, 2 mg/mL lysozyme, 400 U mutanolysin, EDTA-free protease inhibitor cocktail).
2. A rotator that can be placed in a 37 °C incubator; or alternatively, a thermo-mixer.

2.5 *L. lactis* Flow Cytometry

1. Blocking buffer (PBS, 3% FBS, 5 mM EDTA).
2. FACS buffer (PBS, 1% FBS, 5 mM EDTA).
3. Rabbit anti-Spy0128 antibodies.
4. Anti-rabbit IgG FITC antibody.
5. 5-mL polystyrene tubes with caps (also known as FACS tubes).
6. 4% paraformaldehyde.
7. Water bath sonicator.
8. Small volume plastic tubes such as PCR tubes.

3 Methods

All procedures should be undertaken according to the containment regulations applicable to the laboratory. Genetically modified *L. lactis* strains should be handled according to biocontainment regulations and be disposed of according to the biohazard waste regulations.

3.1 Molecular Cloning of PilVax Constructs in *E. coli*

1. Amplify the complete pilus operon from GAS SF370 (ATCC 700294) genomic DNA by PCR using high-fidelity DNA polymerase and the primer pair PilM1.fw + PilM1.rev according to manufacturer's instruction, running 25–30 cycles in a PCR machine. The optimal annealing temperature is 53 °C, and the PCR product size is approximately 5.2 kbp.
2. Digest the purified PCR products with *Bam*HI and clone into an *E. coli*-*L. lactis* shuttle vector for gene expression in *L. lactis*, such as pLZ12Km2_P23R using T4 ligase according to manufacturer's instructions.
3. If there is an existing *Xho*I site in the expression vector (such as the case for the pLZ12Km2_P23R_PilM1 vector resulted from **step 2**), it needs to be deleted by digesting the vector with *Xho*I, end-blunting with Klenow fragment, then re-ligating the plasmid with T4 ligase. Detailed protocols are provided from the manufacturer of the enzymes.
4. Re-introduce an unique *Xho*I site into the specific loop region of the *spy0128* gene by full circle PCR using primer pairs listed in Table 1.

5. Digest the PCR products with *XhoI* and re-ligate. This creates pLZ12Km2_P23R_PilM1_βE-βF-*XhoI*, pLZ12Km2_P23R_PilM1_β3-β4-*XhoI*, or pLZ12Km2_P23R_PilM1_β9-β10-*XhoI* plasmid.
6. Amplify the peptide-encoding DNA sequence by annealing the synthetic oligos at 72 °C in the presence of dNTPs and DNA polymerase for 15 min. A sample sequence provided in **Note 1** is the 16-residue fragment of ovalbumin (Ova_{324–339}.fw + Ova_{324–339}.rev).
7. Digest the double-stranded peptide-encoding DNA sequence by *XhoI* and/or *SaII*, depending on the design of the peptide sequence according to manufacturer's instructions (*see Note 1*).
8. Clone the peptide-encoding DNA sequence into the pLZ12Km2_P23R_PilM1 plasmid containing a unique *XhoI* site in the loop region of *spy0128* using T4 DNA ligase (from **step 5**).
9. Perform diagnostic PCR to screen for positive clones that carry the inserted peptide-encoding DNA sequence in the correct orientation. The primer pairs peptide.fw + spy0128.rev or Spy0128.fw + peptide.rev can be used (*see Table 1*). Use about half of a bacterial colony as template for the PCR reaction and run for 25 cycles in a PCR machine. It is recommended to sequence the positive clones to detect possible DNA duplication or other sequence inaccuracies.

3.2 Production of Electrocompetent *L. lactis*

1. Inoculate 1 mL of overnight *L. lactis* culture in 50 mL of fresh GM17 medium, and incubate at 28 °C without aeration, until the OD_{600nm} reaches 0.4–0.6 (this takes ~2.5 h).
2. Spin down the cells by centrifugation at 5,000 × *g* for 15 min at 4 °C. Discard supernatant.
3. Wash the pellet with 4 mL of ice-cold sterile water. Spin down at 5,000 × *g* for 5 min at 4 °C.
4. Wash the pellet with 2 mL of ice-cold 50 mM EDTA. Spin down at 5,000 × *g* for 5 min at 4 °C.
5. Wash the pellet with 2 mL of ice-cold 0.3 M sucrose. Spin down at 5,000 × *g* for 5 min at 4 °C.
6. Resuspend the cells in 0.4 mL of ice-cold 0.3 M sucrose and proceed immediately to electroporation.

3.3 Electroporation of *L. lactis*

1. Add 1 μg of plasmid DNA to 40 μL of competent cells, and incubate on ice for 5 min (*see Note 2*).
2. Transfer the mixture to a pre-chilled electroporation cuvette.
3. Perform electroporation on an electroporation apparatus by applying a single pulse of 2.5 kV, resistance at 200 Ω, and capacitance at 25 μF (*see Note 2*).

4. Immediately resuspend the cells in 1 mL GM17 medium and transfer into a 1.6-mL sterile plastic tube.
5. Incubate at 28 °C without aeration for 2 h.
6. Centrifuge the culture $5,000 \times g$ for 5 min, resuspend the cell pellet in 100 μ L, and plate on GM17 agar plates supplemented with 200 μ g/mL kanamycin.
7. Use diagnostic PCR to screen for positive clones that carry the pilus gene using the primer pair spy0128.fw + spy0128.rev (*see* Table 1).

3.4 Extraction of *L. lactis* Cell Wall Proteins

1. Inoculate a single colony of *L. lactis* transformant in 15 mL GM17 medium supplemented with 200 μ g/mL kanamycin at 28 °C overnight.
2. Spin down the cells by centrifugation at $5,000 \times g$ for 15 min at 4 °C.
3. Resuspend the cell pellet in 1 mL protoplast buffer, and place on a rotator in a 37 °C incubator.
4. Spin down by centrifugation at $13,000 \times g$ for 30 min at 4 °C.
5. Store the supernatant at -20 °C until analysis by Western blot (*see* Note 3). Successful pilus assembly will show as high molecular weight laddering pattern with anti-Spy0128 antibody (*see* Note 3). Alternatively, anti-peptide antibodies can be used to detect the presentation of inserted peptide in the pilus structure (*see* Note 3).

3.5 Analysis of Pilus Expression by Flow Cytometry

This is an alternative or additional method to confirm pilus expression on the surface of *L. lactis*. This allows quantitative analysis of the expression level of each clone.

1. Grow *L. lactis* strains in 1 mL GM17 medium (supplemented with 200 μ g/mL kanamycin where appropriate) at 28 °C under static conditions overnight.
2. Measure the OD_{600nm} of the overnight culture.
3. Harvest the cells by centrifugation at $5,000 \times g$ for 5 min at RT.
4. Resuspend in blocking buffer at a concentration equivalent to an OD_{600nm} of 0.4.
5. Disperse the cells in a water bath sonicator for 2 min.
6. Incubate on ice for 30 min.
7. Centrifuge at $5,000 \times g$ for 5 min at RT to remove the blocking buffer.
8. Wash the cells once in 500 μ L FACS buffer. Centrifuge at $5,000 \times g$ for 5 min at RT to remove the supernatant.
9. Aliquot 200 μ L into a small-volume plastic tube (such as a PCR tube).

10. Centrifuge at $5,000 \times g$ for 5 min at RT. Remove the supernatant as much as possible without disturbing the pellet.
11. Add 100 μL of primary antibody (anti-Spy0128 or anti-peptide, at appropriate dilution in FACS buffer, *see* **Note 4**), incubate on ice for 30 min.
12. Add 100 μL FACS buffer, then centrifuge at $5,000 \times g$ for 5 min at RT.
13. Remove 180 μL of the supernatant and repeat **step 11** using 200 μL FACS buffer.
14. Carefully remove 200 μL of the supernatant, then resuspend in 80 μL FACS buffer containing secondary antibody.
15. Incubate on ice for 30 min.
16. Repeat **steps 11–13** to wash the cells.
17. Carefully remove 200 μL of the supernatant, then resuspend in 30 μL FACS buffer.
18. Add 50 μL 4% paraformaldehyde to fix the sample. Incubate at 37°C for 10 min.
19. Add 200 μL FACS buffer. The samples are ready to be analyzed on a flow cytometer (*see* **Note 5**).

4 Notes

1. Double-stranded DNA encompassing the peptide sequence and restriction site(s) can be synthesized by a commercial supplier. Alternatively, using the method described in Subheading **3.1 step 6** can be more economical, and the peptide-encoding oligos can also be used for diagnostic PCRs (*see* Subheading **3.1 step 9**). The restriction site *XhoI* was selected for PilVax cloning as it is not present in the PilM1 pilus operon. The compatibility between *XhoI* and *SaII* sites allow the addition of subsequent DNA fragments in the same loop region if required. It is recommended to synthesize the sense and anti-sense strand of peptide-encoding DNA sequences with an overlapping region of at least 15–20 base pairs (bp), then add the restriction site sequence (*XhoI* and/or *SaII*) at the end of the oligonucleotides. An example of the 16-residue fragment of ovalbumin-encoding DNA is as below, where the sequences shown in bold letters are the restriction sites (CTCGAG, *XhoI*; GTCGAC, *SaII*), and the underlined sequences are the overlapping region between the forward and reverse strands.

Ova_{324–399}.fw **CCCGCTCGAG**TCACAAGCTGTTTCAT
GCTGCACATGCAGAAAT

Ova_{324–399}.rev **CCCGGTCGAC** TCTACCTGCTT
 CATTAATTTCTGCATGTGCAGC

To anneal the oligonucleotides for producing double-stranded DNA, a more economical DNA polymerase without proofreading ability, such as Taq DNA polymerase and other moderately faithful enzymes can be used. These enzymes can also serve the purpose for diagnostic PCRs (Subheading 3.1 step 9 and Subheading 3.3 step 7).

2. To increase the efficiency of electroporation, all solutions and container for holding the bacterial cells should be pre-chilled on ice or cooled to 4 °C, including the centrifuge, rotor, and the electroporation cuvettes. This can be done by preparing the solutions beforehand and keeping them in the refrigerator for at least several hours, and placing the tubes and cuvettes on ice or in the fridge during the growth time of the *L. lactis* culture. In order to achieve a more stable cold temperature, a metal centrifuge rotor is preferred over a plastic one. The rotor should be placed into a fridge or cold room for several hours before use. In addition, the quality and quantity of the plasmid DNA for electroporation is critical for the success of transformation. As impurities such as proteins or salts may lower electroporation efficiency, the plasmid DNA should be purified to high standard and suspended in sterile water. High concentration of salts or air bubbles may cause arcing and lower the transformation efficiency. Another important point for consideration is the volume ratio between competent cells and the DNA sample. Ideally, the volume of the DNA solution should not exceed one tenth of the volume of the competent cells. Therefore, plasmid DNA sample at a lower concentration should be concentrated (by methods such as ethanol precipitation or commercial spin column kits) to reduce the volume required.
3. Successfully assembled pili appear as a high molecular weight (HMW) laddering pattern on the SDS-PAGE. This is due to the covalent linkage between individual pilin monomers and the varying lengths of each pilus fiber. Therefore, it is recommended to use a SDS-PAGE protein gel of less than 10%, or a gradient gel suitable for a broader range of protein sample molecular weight (such as 4–12%). A longer protein transferring time may also be required for the successful transfer of HMW proteins for Western blots. The anti-Spy0128 polyclonal antibody was raised in rabbit by immunizing the animal with purified Spy0128 protein [7]. An example of a Western blot analysis with *L. lactis* cell wall extracts using a 7.5% SDS-PAGE protein gel is shown in Fig. 2.
4. If using the antibody for the first time, a dilution series can help identify the optimal signal: background conditions. Try a simple series of dilutions (1:50, 1:100, 1:250, and 1:500, for example) to find the concentration that gives the highest signal and lowest background. A positive control, such as the M1 serotype GAS, can be used for the titration.

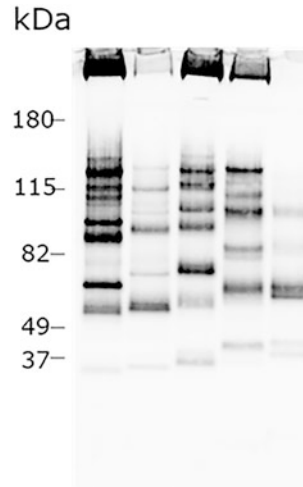


Fig. 2 The result of a Western blot analysis of the cell wall extracts of *L. lactis* expressing PiIM1 using anti-Spy0128 antibody. The high molecular weight bands are indicative of successful pilus assembly

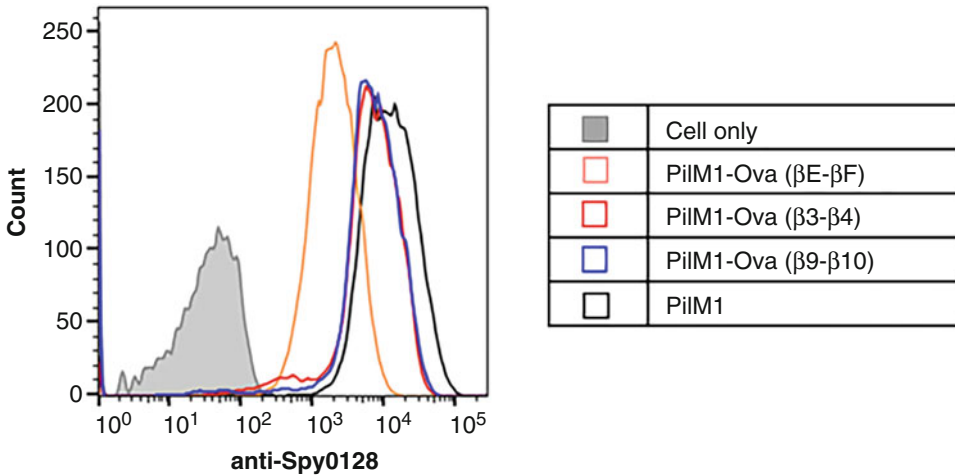


Fig. 3 The result of flow cytometry analysis of *L. lactis* expressing modified PiIM1 using anti-Spy0128 antibody. Peptide expression depends on the peptide sequence and insertion site. In case of Ova-peptide, the best expression was achieved when the peptide was introduced into the β3-β4 loop region

5. Appropriate control samples for gating on the flow cytometer should be included in the experiment. For example, for single cell gating prepare a cell-only sample by resuspending *L. lactis* cells in 200 μL FACS buffer at OD_{600nm} = 0.4. For setting the threshold of the negative cell population, prepare a secondary antibody-only sample by omitting the primary antibody staining procedures (i.e., Subheading 3.5 steps 11–13). An example of the flow cytometry analysis is shown in Fig. 3.

References

1. Clark TG, Cassidy-Hanley D (2005) Recombinant subunit vaccines: potentials and constraints. *Dev Biol (Basel)* 121:153–163
2. Purcell AW, McCluskey J, Rossjohn J (2007) More than one reason to rethink the use of peptides in vaccine design. *Nat Rev Drug Discov* 6(5):404–414. <https://doi.org/10.1038/nrd2224>
3. Bijker MS, Melief CJ, Offringa R et al (2007) Design and development of synthetic peptide vaccines: past, present and future. *Expert Rev Vaccines* 6(4):591–603. <https://doi.org/10.1586/14760584.6.4.591>
4. Bahey-El-Din M, Gahan CG, Griffin BT (2010) *Lactococcus lactis* as a cell factory for delivery of therapeutic proteins. *Curr Gene Ther* 10(1):34–45. <https://doi.org/10.2174/156652310790945557>
5. Pontes DS, de Azevedo MS, Chatel JM et al (2011) *Lactococcus lactis* as a live vector: heterologous protein production and DNA delivery systems. *Protein Expr Purif* 79(2):165–175. <https://doi.org/10.1016/j.pep.2011.06.005>
6. Wagachchi D, Tsai JC, Chalmers C et al (2018) PilVax—a novel peptide delivery platform for the development of mucosal vaccines. *Sci Rep* 8(1):2555. <https://doi.org/10.1038/s41598-018-20863-7>
7. Loh JMS, Lorenz N, Tsai CJ et al (2017) Mucosal vaccination with pili from group A *Streptococcus* expressed on *Lactococcus lactis* generates protective immune responses. *Sci Rep* 7(1):7174. <https://doi.org/10.1038/s41598-017-07602-0>
8. Tsai JC, Loh JM, Clow F et al (2017) The group A *Streptococcus* serotype M2 pilus plays a role in host cell adhesion and immune evasion. *Mol Microbiol* 103(2):282–298. <https://doi.org/10.1111/mmi.13556>
9. Fischetti VA, Pancholi V, Schneewind O (1990) Conservation of a hexapeptide sequence in the anchor region of surface proteins from gram-positive cocci. *Mol Microbiol* 4(9):1603–1605. <https://doi.org/10.1111/j.1365-2958.1990.tb02072.x>
10. Abbot EL, Smith WD, Siou GP et al (2007) Pili mediate specific adhesion of *Streptococcus pyogenes* to human tonsil and skin. *Cell Microbiol* 9(7):1822–1833. <https://doi.org/10.1111/j.1462-5822.2007.00918.x>
11. Crotty Alexander LE, Maisey HC, Timmer AM et al (2010) M1T1 group A streptococcal pili promote epithelial colonization but diminish systemic virulence through neutrophil extracellular entrapment. *J Mol Med (Berl)* 88(4):371–381. <https://doi.org/10.1007/s00109-009-0566-9>
12. Kang HJ, Coulibaly F, Clow F et al (2007) Stabilizing isopeptide bonds revealed in gram-positive bacterial pilus structure. *Science* 318(5856):1625–1628. <https://doi.org/10.1126/science.1145806>
13. Manetti AG, Zingaretti C, Falugi F et al (2007) *Streptococcus pyogenes* pili promote pharyngeal cell adhesion and biofilm formation. *Mol Microbiol* 64(4):968–983. <https://doi.org/10.1111/j.1365-2958.2007.05704.x>
14. Pointon JA, Smith WD, Saalbach G et al (2010) A highly unusual thioester bond in a pilus adhesin is required for efficient host cell interaction. *J Biol Chem* 285(44):33858–33866. <https://doi.org/10.1074/jbc.M110.149385>
15. Smith WD, Pointon JA, Abbot E et al (2010) Roles of minor pilin subunits Spy0125 and Spy0130 in the serotype M1 *Streptococcus pyogenes* strain SF370. *J Bacteriol* 192(18):4651–4659. <https://doi.org/10.1128/JB.00071-10>
16. Linke-Winnebeck C, Paterson NG, Young PG et al (2014) Structural model for covalent adhesion of the *Streptococcus pyogenes* pilus through a thioester bond. *J Biol Chem* 289(1):177–189. <https://doi.org/10.1074/jbc.M113.523761>
17. Clow F, Peterken K, Pearson V et al (2020) PilVax, a novel *Lactococcus lactis*-based mucosal vaccine platform, stimulates systemic and mucosal immune responses to *Staphylococcus aureus*. *Immunol Cell Biol* 98(5):369–381. <https://doi.org/10.1111/imcb.12325>
18. Yuki Y, Kiyono H (2009) Mucosal vaccines: novel advances in technology and delivery. *Expert Rev Vaccines* 8(8):1083–1097. <https://doi.org/10.1586/erv.09.61>
19. Fallico V, Ross RP, Fitzgerald GF et al (2012) Novel conjugative plasmids from the natural isolate *Lactococcus lactis* subspecies *cremoris* DPC3758: a repository of genes for the potential improvement of dairy starters. *J Dairy Sci* 95(7):3593–3608. <https://doi.org/10.3168/jds.2011-5255>
20. Piard JC, Hautefort I, Fischetti VA et al (1997) Cell wall anchoring of the *Streptococcus pyogenes* M6 protein in various lactic acid bacteria.

- J Bacteriol 179(9):3068–3072. <https://doi.org/10.1128/jb.179.9.3068-3072.1997>
21. Loh JM, Proft T (2013) Toxin-antitoxin-stabilized reporter plasmids for biophotonic imaging of group A streptococcus. *Appl Microbiol Biotechnol* 97(22):9737–9745. <https://doi.org/10.1007/s00253-013-5200-7>
22. Okada N, Tatsuno I, Hanski E et al (1998) Streptococcus pyogenes protein F promotes invasion of HeLa cells. *Microbiology (Reading)* 144(Pt 11):3079–3086. <https://doi.org/10.1099/00221287-144-11-3079>

Part V

Vaccine Bioinformatics



Chapter 21

Bioinformatic Techniques for Vaccine Development: Epitope Prediction and Structural Vaccinology

Peter McCaffrey

Abstract

Structural vaccinology involves characterizing the interactions between an antigen and antibodies or host immune receptors. Central to this is the task of epitope prediction, which involves describing the binding affinity and interactions of a given peptide typically to the major histocompatibility complex in the case of T-cells or to the antibodies in the case of B-cells. Several computational models exist for this purpose which we will review here. Generally, epitope predictions for MHC-I and MHC-II are substantially different tasks as well as epitope prediction for continuous versus discontinuous B-cell epitopes. Overall, these models suffer from overprediction of epitopes although general themes support both the use of neural networks as well as the incorporation of more abundant and more varied experimental annotation into model training as valuable in improving predictive performance.

Key words Structural vaccinology, Epitope prediction, Position-specific scoring matrix, Neural network

1 Introduction

Structural vaccinology (SV) aims to apply structural modeling to rationally develop more effective vaccines. This approach involves characterizing the atomic structure of an antigen or antigen–antibody complex relevant to a target disease and manufacturing an antigen or epitope that provokes a similar immune response [1]. SV offers to enhance the consistency and clinical impact of vaccine development by leveraging this structural insight to rationally improve upon a vaccine candidate by developing more specific or more immunogenic antigens than could be achieved by more traditional methods reliant upon isolation of material sampled from an infectious agent. Unsurprisingly, implementing SV requires solving non-trivial challenges many of which are experimental, such as the determination of an antigen’s structure using crystallography, and many of which are computational, such as determining which

antigens are most promising or which modifications thereof will render meaningful enhancements to vaccine performance. Here we will review a key computational pillar of structural vaccine design in the form of epitope prediction. Before moving forward, however, it is worth mentioning that there is a very active domain in the form of experimental epitope mapping which aims to identify active structural components such as antigen–antibody binding sites using experimental techniques. This is comparatively more costly than computational methods, but it exists as a synergistic aim which can inform computational epitope prediction.

Advancements in genomic sequencing technology, transcriptomics, and proteomics have made it possible to efficiently generate data representing an organism’s various coding sequences and has further enabled determination of which proteins are expressed in a given tissue or context. Further, advancements in recombinant DNA technology have made it increasingly possible to design a vaccine more directly from epitopes including the development of chimeric antigens which contain multiple epitopes selected to provoke a specific immune response. However, utilizing these various omics data to achieve such targeted outcomes requires computational prediction of which proteins and protein epitopes interact with specific immune targets. Such considerations include the conservation of epitopes across the population and lifecycle of infectious organisms, as well as the prevalence of an epitope’s target within the human population. Additionally, certain immune responses place additional constraints on valid epitopes and thus consideration of T-cell and major histocompatibility complex (MHC) targets versus B-cell targets will also guide epitope prediction [2]. Below, we will separately review epitope prediction with respect to T-cells and epitope prediction with respect to B-cells as two core examples of applied epitope prediction.

2 Prediction of T-Cell Epitopes

T-cells recognize linear epitopes that bind to MHCs, and thus, this interaction between ligands and T-cells is a fruitful aim for predictive models. This interaction is mediated by R group side chains on epitopes and binding pockets located on the floor of the MHC binding groove which has facilitated the development of several epitope mapping algorithms. MHCs exist in two primary categories: Type I, which mediates interaction with CD-8+ cytotoxic T-cells, and Type II, which mediates interaction with CD-4+ helper T-cells. This distinction is important in that MHC-I molecules bind short peptides typically from 8 to 10 residues in length and whose N- and C-terminal ends are bound within the peptide binding groove. Conversely, MHC-II molecules bind longer and more variable peptides ranging from 9 to around 22 residues in length

the N- and C-termini of which may extend beyond the peptide binding groove. As a result, the binding motifs for MHC-II are less well-defined than those for MHC-I, making MHC-II epitope prediction a more challenging task.

Currently, tools to predict epitope binding to MHC-I are quite performant with an accuracy exceeding 90% and broad allelic coverage. Among the most prevalent tools is RANKPEP which employs sequence alignment to assess the probability of an epitope binding to MHC-I. This approach relies upon the collection of known MHC-I binding epitopes typically obtained initially by elution of MHC-I although such sequences can be obtained from hosted databases such as MHCPEP which lists peptides as well as a score representing their respective binding affinities to MHC. In the case of RANKPEP, these collected epitopes were then partitioned by length and aligned to create un-gapped alignments. The result of doing this is effectively to cluster highly similar peptides, each representing known MHC binding epitopes. Finally, these multiple alignments were then used to create profiles consisting of weighted frequencies of each amino acid observed at each position of the alignment, resulting in a position-specific scoring matrix (PSSM) for each group of epitope sequences [3].

The application of PSSMs to epitope prediction involves matching a PSSM to an equivalent-length epitope candidate (e.g., 9 amino acids) and aggregating the alignment scores at each position. Effectively, this captures how much a given epitope candidate's positional residues match those of known epitopes but also applies specific penalties where mismatching occurs at a position highly conserved among known epitopes. As the name implies, RANKPEP uses these scores to rank a set of candidate epitopes according to predicted binding affinity. Validation of such an approach initially relied on testing whether known MHC binding epitopes were scored highly using these PSSMs although it has since been widely used and has established its own basis in practice. RANKPEP can be easily accessed online where it is possible to select from among several PSSMs specific to various MHC-I or MHC-II alleles. User input consists of a FASTA file containing epitope sequences or, alternatively, a pre-computed multiple alignment using CLUSTALW, and the results consist of a table wherein each row corresponds to a single-epitope amino acid sequence, and all rows are in descending order based upon the score with which that epitope would bind to the MHC target corresponding to the selected PSSM.

While such approaches based upon PSSMs are useful, they are limited to alleles which are sufficiently described in terms of known epitopes and peptide binding affinity. Given the highly polymorphic nature of the MHC genomic region, this may fail to identify many epitopes that are highly relevant to vaccine development. In response to this, efforts to predict MHC binding with broader

allelic coverage have given rise to tools such as NetMHCpan which is made available through a public web server hosted by the Technical University of Denmark. The development of netMHCpan utilizes 9-amino-acid MHC class I binding peptides obtained from the Immune Epitope Database (IEDB) accompanied by additional peptide–MHC binding data. MHC-I is represented by a “pseudo-sequence” of amino acid residues within 4.0 Å of the epitope peptide in any of a representative set of MHC structures. These sequences are used to train artificial neural networks wherein an epitope peptide sequence along with an MHC pseudo sequence are used to predict binding affinity which is then scored against known experimental data. This approach is able to assign binding affinity predictions to any MHC-I molecule including those of non-human origin. Another broad tool for MHC-I epitope prediction is nHLAPred which similarly employs artificial neural networks but also incorporates quantitative matrices generated by dividing the probability of an amino acid as a specific position in MHC binders versus non-binders for each of the 9 amino acid positions describing an MHC-I epitope [4]. Two specific versions of nHLAPred exist: ANNPred and Compred although this hybrid method is implemented by Compred.

The above methods are widely used and readily as publicly hosted servers but—even in the hybrid case—their reliance on known epitopes sequences presents a challenge when trying to predict epitopes for alleles wherein very few such epitopes have been previously discovered. It is not difficult to envision how one might end up wanting to identify epitopes with binding affinity to such lesser-known MHC alleles and so certain prediction tools have been developed to perform better in such circumstances. Among these is the Kernel-based Inter-allele peptide binding prediction SyStem (KISS) [5]. Intuition for this approach stems from previous work showing that pooling together MHC binders (i.e., epitopes known to bind to certain MHC alleles) for different alleles of the same supertype or even for all alleles improves performance for epitope prediction by allowing such models to leverage data from a far larger collection of epitope sequences. The KISS model generates separate specific predictive models for different MHC alleles but uses training data from similar alleles to enhance the power of these models. The method itself utilizes support vector machines to predict MHC binding affinity and was validated using experimentally described MHC binding epitopes obtained from the SYFPEI THI database.

Additional methods leverage insight into the biological processes surrounding MHC-I binding and antigen presentation. For example, the Transporter Associated with Antigen Processing (TAP) is associated with MHC-I restricted antigen processing. TAP is responsible for translocation of peptides across the membrane of the endoplasmic reticulum, and a portion of the

transported peptide will bind MHC-I on the cell surface. Various tools exist to predict TAP binding such as TAPPred, EpiJen, and WAPP. In the case of TAPPred, this tool is publicly hosted online and predicts binding affinity of a given epitope to the TAP transporter. EpiJen employs TAP binding affinity prediction alongside prediction of a proteasome cutoff. EpiJen is a multi-step algorithm which is applied to a set of overlapping peptides generated from a contiguous peptide sequence with a series of scoring models acting as filters for a given sequence's binding affinity to MHC. Each step employs quantitative matrices specific to each filtration aspect (e.g., proteasome cleavage, TAP binding, MHC binding, T-cell recognition) [6]. For the prediction of proteasome cleavage in particular, the algorithm views a protein as overlapping 10-mers and considers each 10-mer as containing a potential cleavage site by considering the C-terminus and its adjacent amino acid, scoring these using quantitative matrices for their probable affinity as proteasome cleavage sites. Validation for EpiJen was based initially upon known epitopes gathered from AntiJen with specific MHC allelic restriction which were then used to describe proteasome cleavage, TAP and MHC binding, and epitope selection. Using these data, EpiJen's predictions were then tested on held-out, known epitopes. Further testing involved prediction of known HIV epitopes and these results were compared to those from other tools (WAPP, SMM, and NetCTL). EpiJen recognized 62% of test epitopes, achieving higher sensitivity than the other tools. However, it should be noted that NetCTL and WAPP predictions were made using default parameters and that, for every tool, the positive predictive value for a selected epitope was low, ranging from 16 to 21% with NetCTL having the highest positive predictive value.

Much of the previous discussion has centered on MHC-I epitope prediction which, for reasons enumerated previously, is a more tractable problem for which many tools have been successful. MHC-II prediction is considerably more difficult since the MHC-II molecule is open at both ends increasing the conformational space with which it can bind an epitope. This makes it challenging to identify epitope binding motifs as the binding core cannot be as strictly localized. MHC-II epitope prediction has undergone several successive benchmarks over the past 10 years. In 2011, such benchmarking examined five MHC-II epitope prediction tools: NetMHCII, NetMHCIIpan, RANKPEP, ProPred, and EpiTOP using known binders extracted from IEDB. Single predictor performance generally demonstrated moderate sensitivity of around 50% and much more limited positive predictive value of around 10% [7]. Using ensembles across tools, it was demonstrated that up to 80% of real epitopes could be captured, but this unavoidably came at the cost of specificity, and this tradeoff was consistent across various model ensembles.

Later in 2018, a similar benchmark was performed examining six contemporary set of tools: NN-align, NetMHCIIpan, Comblib, SMM-align, TEPITOPE, and IEDB consensus [8]. NN-align and NetMHCIIpan employ neural networks while Comblib, SMM-align, and TEPITOPE use scoring matrices and, finally, IEDB consensus which represents a combination of several methods. Using a set of peptides with known MHC-II binding affinity, tools were ranked according to Area Under the receiver-operating Curve (AUC) and Spearman Rank Correlation Coefficient (SRCC). One limitation of this assessment was that many tools were not capable of evaluating a broad set of alleles, and thus, selecting a universal training set required exclusion of several data sets for which some of the measured tools may have been more performant. AUC values were observed to be as high as 0.8 which is generally attributed to an exponential increase in available, annotated epitope sequences, but it was also apparent in this work that neural network-based models such as NNAlign and NetMCHIIpan have constitutively higher performance than other methods.

This relative superiority of neural network models makes sense when one considers that many epitope modeling approaches embed flawed biological assumptions. Traditional methods examined the MHC binding pocket closely, assuming that if an epitope's side chains were occupying the binding pocket, then that epitope would be "anchored" and would therefore bind with high affinity. PSSMs offer a broader view in consideration of an entire epitope peptide, but they still discount local and non-local interactions between residues in an epitope. In fact, experimental work examining the HA306–319 peptide for the HLA-DR1 allele and altering non-anchor positions has demonstrated that conservation of "anchor" positions is insufficient to predict binding affinity in the midst of variation elsewhere in the peptide [9]. Unsurprisingly then, neural network-based models are more capable in capturing these complex interactions between amino acid residues as reflected in the 2018 benchmark and subsequent work testing prediction among known MHC-II epitopes which again demonstrated that NetMHCIIpan has superior performance in prediction binding affinity [10]. While improvements have been made, it is still generally the case that epitope prediction tools tend to overpredict, generating many false positives, and it is also true that these tools typically predict epitope binding as a proxy for immunogenicity which is a useful abstraction but, importantly, is not equivalent to functional immunogenicity of a given epitope.

Lastly, while computation is useful, experimental annotation remains critically valuable to the process of epitope prediction. An important example of this is the work of Yin et al. who examined HLA-DM, which is responsible for peptide editing and accelerates the release of prebound peptide from MHC-II, in the setting of vaccinia virus. In this work, the authors found that the kinetic

stability of a peptide-MHC-II complex in the presence of DM is a strong and independent predictor of T-cell epitopes as opposed to non-recognized peptides [11]. DM stability is not accounted for in modeling approaches, but its relevance illustrates the continued need to incorporate experimental annotation into predictive models. To this end, recent work from 2019 utilized quantitative pMHC affinity data obtained from IEDB in conjunction with a data set of in-house eluted MHC-II ligands. Authors then compared models trained using either affinity data or ligand data exclusively as opposed to incorporating both together, observing an improved AUC and F-rank (with F-rank capturing the percentile rank of positive epitope predictions with k-mers derived from source proteins) when both data sets were used together in training [12]. In general, it remains the case that, as many biological factors ultimately determine epitope immunogenicity, modeling strategies benefit from leveraging experimental data sets where possible and modeling workflows will benefit from filtering positive predictions through components of biological function such as binding affinity and antigen processing as this may purify the many overpredicted epitopes down to a more specific collection.

3 Prediction of B-Cell Epitopes

B-cell epitopes are generally predicted in continuous or discontinuous form. Continuous epitope prediction is analogous to what we have discussed with T-cell epitopes and focuses on amino acid residues residing in epitope sequences and seeks to account for properties like hydrophilicity, charge, and secondary structure. Discontinuous epitope prediction, however, represents a substantially different task and requires knowledge of an antigen's three-dimensional structure.

Linear epitope prediction tools such as Bcepred incorporate physicochemical predictions based upon reference databases of known B-cell epitopes obtained from Bcipep and negative controls sampled from SWISSPROT [13]. Bcepred incorporates multiple physicochemical properties in making its predictions, achieving accuracies ranging from 53 to 57%. As with MHC epitope prediction, neural network-based approaches such as ABCpred demonstrate improved accuracy of 66% [14], also utilizing B-cell epitopes obtained from the Bcipep database. Importantly, the approach of ABCpred is to use recurrent neural networks which maintain an awareness of contiguous subsequences of a given peptide. Much as with MHC epitope prediction, increased sensitivity can be achieved using B-cell epitope models but at the cost of significant overprediction.

Discontinuous epitope prediction leverages different tools such as DiscoTope which analyzes the 3D structure of proteins and

determines surface accessibility, assigning a score for each amino acid as a novel epitope. More specifically, this method examines the carbon backbone of a target protein using a 10 Å sphere and sums the propensity scores of residues within the sphere [15]. Such structural methods overcome many limitations of linear sequence modeling based upon predicting and composing chemical properties of constituent residues. However, a few caveats exist. One caveat is that quality structural data describing antigen–antibody structures is still relatively scarce even though more of such data is being made increasingly available. A second caveat is that most antigens have not been studied to the extent that all epitope residues are fully known, thus making it challenging to correctly determine the extent to which over prediction may occur. Third, many proteins exist as part of larger tertiary structures which are not completely characterized. Similar tools such as BEpro and SEPPA similarly examine 3D structure. SEPPA, for example, examines all surface residues of an epitope protein, considering all possible unit triangles within 15 Å, calculating a propensity index, relative Accessible Surface Area (ASA) and glycosylation ratio, and using these to assign antigenicity scores to each residue using a logistic regression model [16]. Each of these servers requires a priori structures to be provided as PDB files which describe protein macromolecular structure data derived from X-ray diffraction and NMR studies.

ElliPro is another comprehensive tool for the prediction of both linear and discontinuous epitopes which does not require structural inputs and instead accepts linear amino acid sequences. ElliPro then predicts the 3D structure of the provided sequence through homology modeling with a user-defined structural template [17]. Algorithmically, ElliPro scores residues with a protrusion index (PI) value and clusters these residues based upon their PI values to identify predicted epitopes. One attractive aspect of ElliPro is that it has relatively simple conceptual foundations, namely that regions which protrude from a globular protein likely participate more often in antibody interactions.

4 Recent Advancements

Throughout this discussion, we have mentioned that neural network models display predictive superiority in being able to capture complex interactions between amino acid residues as opposed to simply scoring and summing across residues. Recent work published in 2019 expands upon this theme with two new neural network models showing significantly improved prediction accuracy on known MHC-II epitopes compared to SMN Align and NetMHCIIpan. In both the cases, the authors examined large

data sets in excess of 50,000 MHC II-presented peptides. Chen et al. developed the MHC Analysis with Recurrent Integrated Architecture (MARIA) which incorporates gene expression data to capture interactions between peptide abundance and MHC II presentation [18]. MARIA is a deep recurrent neural network model trained on naturally occurring MHC ligands which can readily accommodate variable length sequences. MARIA takes as input three values: a peptide sequence, HLA-DR allele, and a gene name and predicts HLA-DR binding as well as peptide cleavage and uses these values to assign presentation scores for potential antigens.

Racle et al. employed a different approach relying first on MoDec, a motif de-convolution algorithm that uses convolutional filters to detect sequence motifs anywhere within the epitope peptide, learning not only the sequences of these motifs but also their preferred binding core position offsets [19]. The authors used MoDec to detect motifs from a set of HLA-II ligands, using these to train a predictor, MixMHC2pred, that combined allele-specific motifs and allele-independent N- and C-terminal motifs, peptide length and offset parameters for peptide binding cores. The accuracy of MixMHC2pred was tested in 41 samples from seven independent HLA-II peptidomics data sets, demonstrating superior predictive accuracy compared to NetMHCIIpan. Importantly, this benchmarking of MixMHC2pred encompassed known viral, bacterial, and melanoma-associated proteins for whom immunogenicity was predicted with the 30 highest-scoring epitopes being tested experimentally for their immunogenicity in two melanoma patients and one healthy donor. These publications build upon a trend of neural networks as performant modeling approaches for epitope prediction. Moreover, they also illustrate the value of training such models using multiple inputs that describe different aspects of a candidate epitope sequence.

With regard to B-cell epitopes, discontinuous epitope prediction is so critical because most B-cell epitopes take this form, and while structural information about potential epitope peptides increases predictive performance, overprediction remains a challenge. Much as with T-cell epitope prediction, this stems partly from a problem of incorrect biological assumptions. In many cases, such prediction tools assume that any protruding feature of an epitope peptide is equally immunogenic or at least that its immunogenicity is a function primarily of its protrusion. Since the human body, for example, may contain many billions of antibodies, this is true in a theoretical sense. However, in the real mechanics of immune response, the presence or relevance of the entire epitope repertoire is not a valid assumption. Thus, there is specific value in considering B-cell epitopes in light of a specific antibody or

category thereof to which epitope binding is relevant. To this end, there have been approaches which seek to predict the cognate target of a specific antibody although such approaches are typically limited by a lack of high-quality structural data describing relevant antigen-antibody complexes. Jespersen obtained a structural dataset comprising antigen-antibody complexed from IEDB-3D and combined these with antigen-antibody structures deposited in the Protein Data Bank sourced using an antibody-specific HMM followed by clustering. Several features were then derived from these structural complexes and used to calculate epitope patches. Surface patches were generated using a Monte Carlo approach. Finally, the authors defined a function for scoring epitope pairs by creating a data set of real and Monte Carlo-generated epitope-paratope pairs and assigning values to the Monte Carlo-generated pairs based upon their overlap with known pairs. Thus, a score of 1 would mean that a Monte Carlo-generated pair completely overlaps with a known pair and 0 would mean that no such overlap exists. Finally, a neural network model was trained to incorporate both epitope and paratope features, demonstrating that doing so yielded improved predictive performance when compared to using partial information obtained solely from epitopes and not paratopes and this model was evaluated on an independent test set of eight structures [20]. As we have seen previously, this work demonstrated the synergistic value of additional information to model prediction that encompasses a broader picture of the epitope and the biological task being modeled.

5 Conclusion

Epitope prediction sits at the core of structural vaccinology, and many prediction tools exist each aimed at a particular subset of epitopes. In general, linear epitopes are more easily predicted with the additional structural constraints of MHC-I resulting in several tools with useful performance. MHC-II prediction is more challenging as it must consider a far larger and more complex space of possible epitopes although recent advancements in deep learning have shown significant improvements over earlier attempts. Likewise, prediction of continuous B-cell epitopes utilizes similar model designs to MHC prediction although it must accommodate larger epitope sequences whereas discontinuous prediction represents much more its own specialized task, utilizing structural data either directly obtained or predicted from candidate epitope sequences. Overall, epitope prediction still results in overprediction of candidate epitopes and benefits greatly from the addition of experimental annotation. These annotations can lend considerable value to epitope models which often abstract away such biological details at the expense of accuracy.

References

1. Anasir MI, Poh CL (2019) Structural vaccinology for viral vaccine design. *Front Microbiol* 10:738. <https://doi.org/10.3389/fmicb.2019.00738>
2. Soria-Guerra RE, Nieto-Gomez R, Govea-Alonso DO, Rosales-Mendoza S (2015) An overview of bioinformatics tools for epitope prediction: implications on vaccine development. *J Biomed Inform* 53:405–414. <https://doi.org/10.1016/j.jbi.2014.11.003>
3. Reche PA, Glutting JP, Reinherz EL (2002) Prediction of MHC class I binding peptides using profile motifs. *Hum Immunol* 63(9):701–709. [https://doi.org/10.1016/S0198-8859\(02\)00432-9](https://doi.org/10.1016/S0198-8859(02)00432-9)
4. Bhasin M, Raghava G (2007) A hybrid approach for predicting promiscuous MHC class I restricted T cell epitopes. *J Biosci* 32(1):31–42. <http://www.imtech.res.in/raghava/nhalpred/>. Accessed 4 Oct 2020.
5. Jacob L, Vert JP (2008) Efficient peptide-MHC-I binding prediction for alleles with few known binders. *Bioinformatics* 24(3):358–366. <https://doi.org/10.1093/bioinformatics/btm611>
6. Doytchinova IA, Guan P, Flower DR (2006) EpiJen: a server for multistep T cell epitope prediction. *BMC Bioinformatics* 7(1):131. <https://doi.org/10.1186/1471-2105-7-131>
7. Dimitrov I, Flower DR, Doytchinova I (2011) Improving in silico prediction of epitope vaccine candidates by union and intersection of single predictors. *World J Vaccines* 1:15–22. <https://doi.org/10.4236/wjv.2011.12004>
8. Andreatta M, Trolle T, Yan Z, Greenbaum JA, Peters B, Nielsen M (2018) An automated benchmarking platform for MHC class II binding prediction methods. *Bioinformatics* 34(9):1522–1528. <https://doi.org/10.1093/bioinformatics/btx820>
9. Anderson MW, Gorski J (2003) Cutting edge: TCR contacts as anchors: effects on affinity and HLA-DM stability. *J Immunol* 171(11):5683–5687. <https://doi.org/10.4049/jimmunol.171.11.5683>
10. Zhao W, Sher X (2018) Systematically benchmarking peptide-MHC binding predictors: from synthetic to naturally processed epitopes. *PLOS Comput Biol* 14(11):e1006457. <https://doi.org/10.1371/journal.pcbi.1006457>
11. Yin L, Calvo-Calle JM, Dominguez-Amorocho O, Stern LJ (2012) HLA-DM constrains epitope selection in the human CD4 T cell response to vaccinia virus by favoring the presentation of peptides with longer HLA-DM-mediated half-lives. *J Immunol* 189(8):3983–3994. <https://doi.org/10.4049/jimmunol.1200626>
12. Garde C, Ramarathinam SH, Jappe EC et al (2019) Improved peptide-MHC class II interaction prediction through integration of eluted ligand and peptide affinity data. *Immunogenetics* 71(7):445–454. <https://doi.org/10.1007/s00251-019-01122-z>
13. Saha S, Raghava GPS (2004) BcePred: prediction of continuous B-cell epitopes in antigenic sequences using physico-chemical properties. *Lect Notes Comput Sci* 3239:197–204. https://doi.org/10.1007/978-3-540-30220-9_16
14. Saha S, Raghava GPS (2006) Prediction of continuous B-cell epitopes in an antigen using recurrent neural network. *Proteins Struct Funct Genet* 65(1):40–48. <https://doi.org/10.1002/prot.21078>
15. Kringelum JV, Lundegaard C, Lund O, Nielsen M (2012) Reliable B cell epitope predictions: impacts of method development and improved benchmarking. *PLoS Comput Biol* 8(12):e1002829. <https://doi.org/10.1371/journal.pcbi.1002829>
16. Zhou C, Chen Z, Zhang L et al (2019) SEPPA 3.0—enhanced spatial epitope prediction enabling glycoprotein antigens. *Nucleic Acids Res* 47(W1):W388–W394. <https://doi.org/10.1093/nar/gkz413>
17. Ponomarenko J, Bui HH, Li W et al (2008) ElliPro: a new structure-based tool for the prediction of antibody epitopes. *BMC Bioinformatics* 9:514. <https://doi.org/10.1186/1471-2105-9-514>
18. Chen B, Khodadoust MS, Olsson N et al (2019) Predicting HLA class II antigen presentation through integrated deep learning. *Nat Biotechnol* 37(11):1332–1343. <https://doi.org/10.1038/s41587-019-0280-2>
19. Racle J, Michaux J, Rockinger GA et al (2019) Robust prediction of HLA class II epitopes by deep motif deconvolution of immunopeptidomes. *Nat Biotechnol* 37(11):1283–1286. <https://doi.org/10.1038/s41587-019-0289-6>
20. Jespersen MC, Mahajan S, Peters B, Nielsen M, Marcatili P (2019) Antibody specific B-cell epitope predictions: leveraging information from antibody-antigen protein complexes. *Front Immunol* 10:298. <https://doi.org/10.3389/fimmu.2019.00298>



Immunoinformatic Approaches for Vaccine Designing for Pathogens with Unclear Pathogenesis

Naina Arora, Anand K. Keshri, Rimanpreet Kaur, Suraj Singh Rawat, and Amit Prasad

Abstract

Designing a vaccine against a pathogen has been the toughest challenge to fight against any infectious diseases. To overcome this problem, use of artificial neural network with immuno-informatics is emerging as a front runner solution. For a successful designing of a potent vaccine, prediction of T-cell/B-cell epitopes, antigen processing and presentation analysis, antigenic potential analysis of epitopes, usages of linkers, population coverage, codon optimization, allergenicity assessment, toxicity prediction of construct, and finally protein–peptide docking for stability of vaccine are important steps. To achieve this, several bioinformatics software, tools and online web servers have been developed for each application, which have their own advantages and limitations. Scientists must evaluate these parameters and should take the decision to apply more suitable and precise servers for each analysis and prediction based on their accuracy, suitability, and robustness.

Key words Immunoinformatics, B-cell epitope, T-cell epitope, In silico cloning, Genome, Pathogens

1 Introduction

The rapidly developing world has altered the microbiota and exposure of human beings to range/spectrum of pathogens. The recent pandemics including SARS, Zika, Covid-19, etc. had highlighted our limited understanding and unpreparedness to deal with microscopic organisms that shook the entire world [1]. It is incredibly difficult to predict the kind of microorganisms that can be infective to humans with the evolving climate conditions or to predict future pathogenic strains and outbreaks; and with this comes the limitation of understanding of their impact on human health. Besides that, immune system is an intricate network of fine-tuned cellular signaling that confers protection against any insult to the host [2]. It takes years of research to understand the immunopathogenesis of a disease to develop effective clinical management strategies.

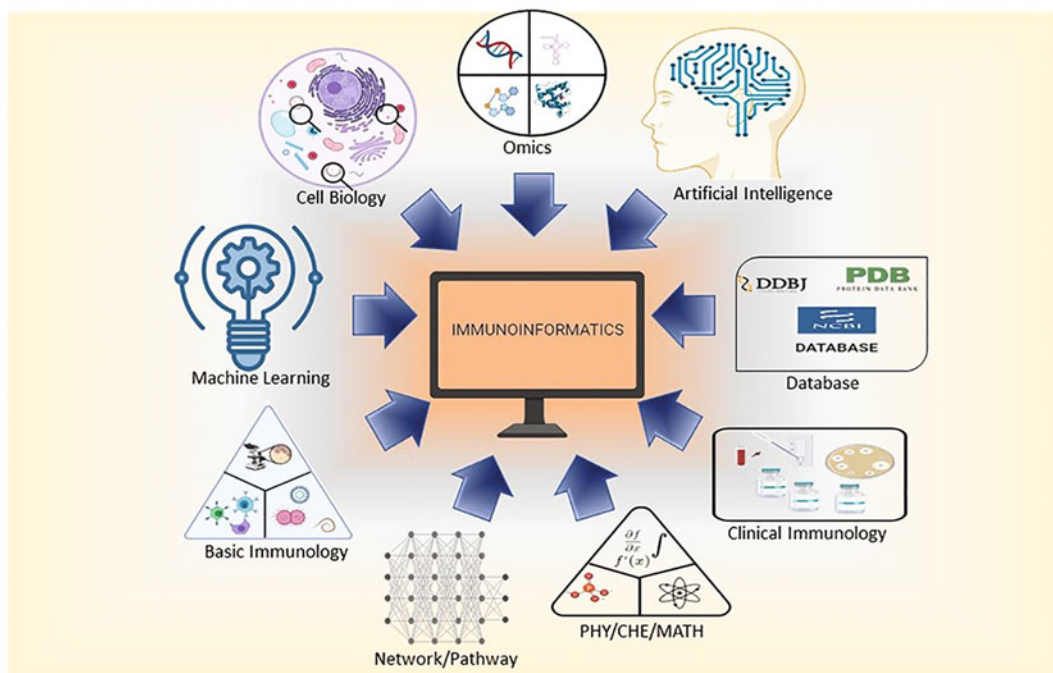


Fig. 1 Immunoinformatics hub: It integrates information from different subjects (experimental, mathematical, biological) to build layers and architecture for in silico studies to derive at best possible hits

Hence, understanding the host–pathogen interactions and producing a vaccine in response are a huge challenge to global health. Reverse vaccinology was first described and pioneered by Rino Rappuoli for vaccine against serogroup B meningococcus using whole genome [3]. Over the decades, we have seen advances in genome sequencing technologies and bioinformatics, and this has nonetheless opened wide avenues for vaccine designs, especially in scenarios where our understanding of host–pathogen interactions and immunopathogenesis is very scarce [4, 5]. Progress in bioinformatics has revolutionized our approach to address scientific hypothesis; it integrates and unifies information from various sources to address the question at hand (Fig. 1).

The wide array of prediction tools build on using informatics algorithms and mathematical models integrate with the existing cellular information to provide platform for data prediction [6, 7]. Immunoinformatics has a wide application base ranging from target prediction, drug repurposing or side effect prediction of drugs, vaccine designing, etc.

The immunoinformatic approach to vaccine design has proven to be an indispensable tool to understand complex pathogens and propose suitable future therapeutics [8, 9]. Where the traditional vaccine approach takes years (~15–20 years) time, in silico approach reduces the time period to 6–7 years (including clinical trial). Not

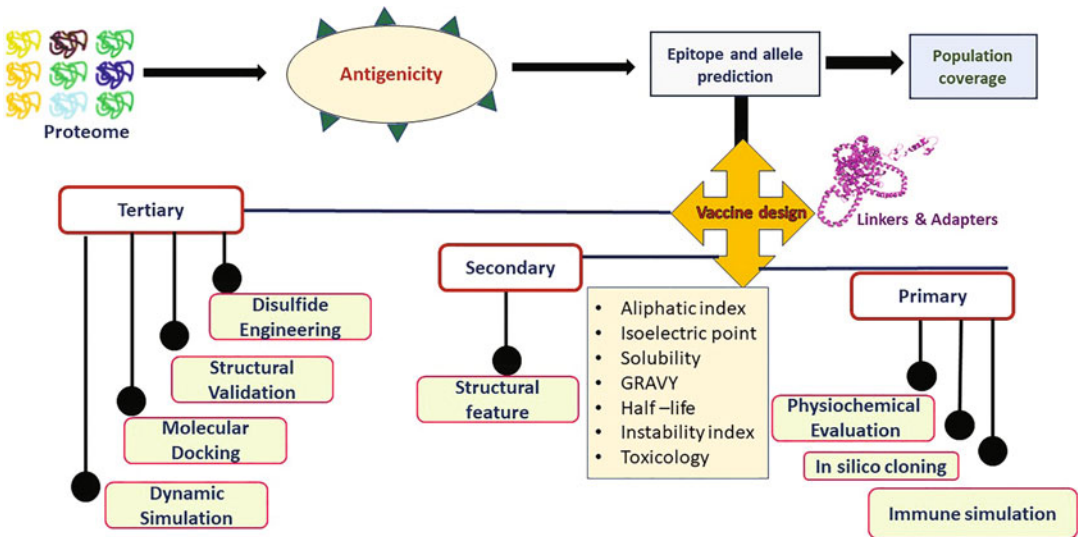


Fig. 2 Pipeline architecture: To build a reliable robust pipeline, it should be dynamic to address all the questions of hypothesis at hand, encompassing the biological information into a mathematical model and harnessing that information from a dataset

only it reduces the pace of vaccine candidate search but also helps to derive a lot of information about the pathogen like antigenic regions, the essential genes, etc. only with the help of genome sequence and identifies hot spots for immune exploration [10, 11]. Immunoinformatics is a multi-step process, building a robust and reliable pipeline as fishing target in vitro.

Thus, in silico analysis helps us to build a preliminary knowledge base about a pathogen or disease, reducing time and effort of in vitro/in vivo translation. But, a major limitation to in silico analysis is choosing the approach; with a wide array of resources and strategies available it is imperative to design a robust pipeline and take fine nuances into consideration [12]. In the absence of which in silico identified vaccine candidate will fail for sure during translational studies. In this chapter, we put forward a systematic pipeline for vaccine design, list useful resources, and talk about various challenges and considerations for immunoinformatic approach to vaccine design.

1.1 Pipeline Architecture/Framework

Immune signaling is repertoire of complex interactions; when translating live systems into in silico, it is important to encompass all the layers of cellular signaling [13, 14]. Building up a strong pipeline requires sound understanding of the immune layers and an effective strategy to bypass or filter data through these layers to get the best hits (Fig. 2). A well-defined pipeline is the first step to it. A good pipeline should be robust, reliable, and knowledge based. The tools employed in the pipeline are command line based or offer a workbench interface. The file formats are especially important, for

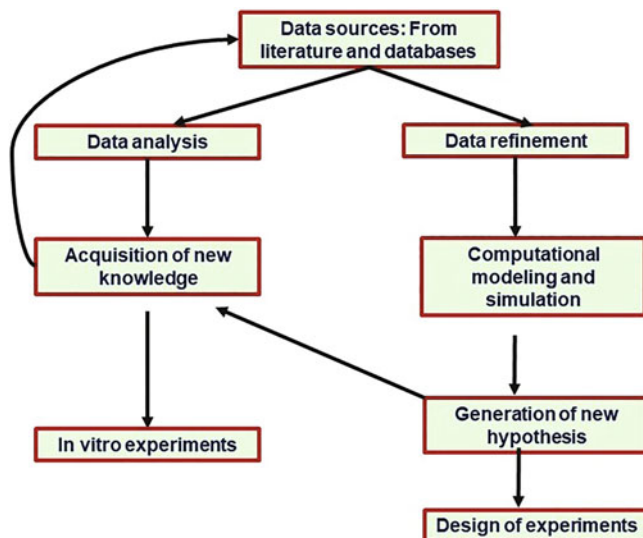


Fig. 3 In silico design of a multi-epitope vaccine candidate: Vaccine candidate fished from proteome of an organism. It evaluates the antigenicity and population coverage following a robust assessment at each structural step to have confidence in hits. As a best practice, using more than one software as prediction tool for any property helps user understand and chose hits better

sequence processing, FASTA file formats are widely used and the software and tools are very stringent to file formats to process the data. Also, a pipeline should be able to integrate different file formats.

Immunoinformatics approach for vaccine design is based on virtual screening, which is defined as searching an in silico library to identify a molecule of interest which makes it faster and speeds up the process compared to traditional approach; it allows you to screen large number of molecules in a day (Fig. 3). The pipeline make-up acts as a sieve, filtering and narrowing down the number of molecules at each step, while assaying the biological properties in silico. It filters out ~98% of unlikely molecules and leaves out limited choices of hits to be tested in vitro. Thus, reducing the cost and resources and saving time for the entire process. However, it has been seen that majority of identified compounds with virtual screening are false positives, and it happens due to imperfection in methodology or algorithm of screen program, making the entire process ineffective. Hence, it is essential to have an eye for detail, carefully defining the steps, cross checking the output at every step by employing more than one tool for same process. The online prediction tools are based on machine learning (ML) algorithms like support vector machine (SVM), random forest, or artificial neural network (ANN). The algorithm differs in the factors like number of dimension in featured space, training sets, correlated features, etc. The application of these machine learning algorithms

affect the output data, one might validate a process more effectively than other or achieve better result depending upon the data at hand.

1.2 Challenges in Immunoinformatics

In the present day world, though we are growing in terms of system biology and digital age data, the challenge lies with the credibility or reliability of the curated databases or prediction tools. There are a large number of databases that have been generated or build, but they lack a system to authenticate these data. Another limitation arises with the update of genomic data, we know that microorganisms acquire mutations under selection pressure to survive and these mutations are not frequently recorded or updated in the genomic information. There is also limitations associated with the agility to use and understand the informatics. When studying large data sets, use of command line interface, UNIX, or programming languages ease the handling of information, but most of the biologists are not well trained or versed with the use of programming languages and hence is a major limitation.

1.3 Immuno- informatic Potential

The *in silico* vaccine design approach at present is adopted for single organism at a time. But with the understanding in ML and AI, it is possible to study genome sequences of more than one organism. Taking the pathogenic groups into consideration, be it bacterial, viral, or parasitic, each group shares conserved feature for growth and development. Exploiting such conserved features with the help of artificial neural network (ANN) or QSAR approach gives tremendous scope for not only creating a multi-epitope vaccine for a pathogen but a group of similar pathogens. This strategy if translated *in vitro/in vivo*, it will accelerate the vaccine research at much faster rate with high success rate and prove to be resource efficient (Fig. 4).

2 Materials

A well-designed and curated pipeline, high-end computing power, softwares for docking studies, and molecular simulation.

3 Methods

1. **Databases:** Curate the genomic or proteomic data of the organism under study (IMGT[®], the international ImMunoGeneTics information system[®], NCBI, wormbase.org, Virus pathogen resource, etc.) or unravel the whole genome of the organism under study.
2. **Secretory vaccine:** Vaccine is a protein molecule overexpressed in animal system and purified, if it is a secreted antigenic

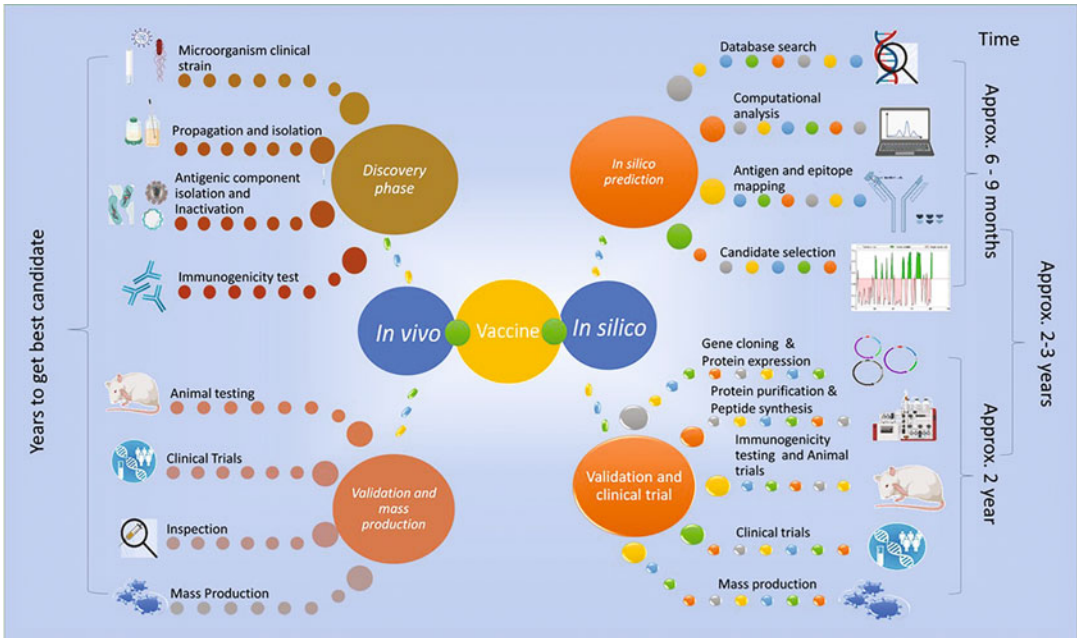


Fig. 4 Classical vs Modern vaccine design: a side-by side comparison of traditional vaccine design to modern approach combining in-silico approach for vaccine design

vaccine, it should be parsed through prediction tools to see if it carries the signal peptide or membrane binding peptide (prediction tools: SignalP, SecretomeP, TMHMM, Phobius, etc.)

3. **Epitope Prediction:** Immunogenicity of the antigen evokes the cell-mediated immunity and determine the foreignness of antigen to host. For activation of immune system for vaccination activation of cell-mediated immunity is necessary. To generate a more robust humoral response and immunological memory T-cell activation is necessary. Multi-epitope vaccine candidate should be multi-specific (i.e., has the ability to attach to suitable MHC molecule, engages in cellular antigen presentation, etc.) simultaneously activates various processes [15].

B-cell epitope prediction can be done for linear B-cell epitope or antibody-specific B-cell epitope. Linear B-cell epitope prediction can be done using different servers (BepiPred 2.0, ABCpreds, BCpreds, or SVMTrip), and recurrent hits are selected for vaccine prediction. Following this epitope prediction for T-cell is to done, this can be done in one step using EpiJen or separately for cytotoxic T lymphocytes (CTL) with NetCTL 1.2 and/or CTLPred and helper T lymphocytes with PREDIVAC and/or NETMHCII 2.2. The overlapping epitope from B-cell and T-cell epitopes are selected and in case of non overlap, unique sequences are taken forward.

4. **Population coverage:** A vaccine candidate should confer protection to all the ethnicities, and HLA phenotypes are

expressed at varying densities [16]. Hence a good vaccine should have a wide HLA coverage. The vaccine candidates with desired epitope are screened for their HLA coverage with HLAsupE or IDEB population coverage.

5. **Cytokine prediction:** Cytokine signature suggest the type of immune response generated Th1 or Th2. Vaccine candidates are mapped for their cytokine signature employing CytoPred, IFNepitope, IgPred, I110Pred, Il4 pred, or IL4IFNG.
6. **Generation of multi-epitope and use of linkers:** Once the epitopes have been shortlisted, the next step is generating the multiepitope vaccine. The B-cell and T-cell epitopes are connected using linkers or adapters like AAY or GPGPG. This helps in improving the stability of the vaccine. It is then complexed with the adjuvants like P9WHE3 or GST28 to improve vaccine performance.
7. **Primary vaccine design:**

Physicochemical properties: To achieve a robust vaccine candidate in vitro, in silico vaccine candidate is evaluated for its safety (allergenicity, as besides being B- or T-cell epitope binding, it can be allergic to humans), hydrophobicity: for delivery of vaccine candidate to host system, it should carry a net positive charge and hence cationic in nature. Its instability index tells about the stability in test tube. Thus, these properties help evaluate basic features of vaccine. A detailed list of different servers useful for T-cell, B-cell epitope prediction and antigenicity determination is given in Table 1. Physicochemical properties can be assayed with ProtPram server or combination of following:

Allergenicity: AlgPred, Allermatch, AllergenOnline, AllergenPro.

Antigenicity: VaxiJen, ANTIGENpro.

Toxicity: ToxinPred.

Autoimmunity: PeptideMatch.

Hemotoxicity: HemoPI, Hemolytik.

Immunogenicity: IEDB classI immunogenicity.

Protein Half-life: PlifePred, SprotP, ProtlifePred.

Protein solubility: SOLpro. PROSOII.

In silico vaccine cloning: To optimize the codon usage, in silico cloning is done in expression vector at java codon adaptation tool. This gives CAI score which should be between 0.8 and 1 and GC content (30–70%). This is important for DNA stability and high expression of protein.

8. **Secondary vaccine design:** The secondary structure prediction is done using PSIPRED, based on PSI-BLAST and

Table 1**List of some important multi-epitope vaccine prediction tools and application with their web address**

Database name	Applications	URL Link
<i>T-cell epitope prediction</i>		
NetMHC	Prediction of peptide–MHC class I binding	http://www.cbs.dtu.dk/services/NetMHC
NetMHCII	Predict HLA-DR, HLA-DQ, HLA-DP binding peptide	http://www.cbs.dtu.dk/services/NetMHCII/
MAPPP	MHC Class-I antigenic Peptide prediction server	www.mpiib-berlin.mpg.de/MAPPP/cleavage.html
MHCPred	Quantitative prediction of peptide–MHC binding	http://www.ddg-pharmfac.net/mhcpred/MHCPred/
BIMAS	Prediction of HLA/peptide half-time of disassociation	http://www.thr.cit.nih.gov/molbio/hla_bind
Propred	Prediction of CTL epitopes	http://www.imtech.res.in/raghava/propredI/
EpiToolKit	Prediction of MHC classes I/II ligands	http://www.epitoolkit.org
MMBPred	Prediction of atypical MHC class I binders as well as mutations that allow high-affinity binding	http://www.imtech.res.in/raghava/mmbpred/
SYFPEITHI	A database for MHC anchor motifs and binding specificity	http://www.syfpeithi.de
HLA-DR4Pred	Identification of HLA-DRB1*0401(MHC class II alleles) binding peptides	http://webs.iiitd.edu.in/raghava/hladr4pred/
TEPITOPE	Prediction of atypical class II epitopes	https://www.vaccinome.com
NetCTL	Predict of CTL/HLA super type epitopes	http://www.cbs.dtu.dk/services/NetCTL
IEDB-MHCI	MHC-I binding predictions	http://tools.immuneepitope.org/mhci/
IFNepitope	Designing of IFN- γ inducing MHC class-II binders	http://webs.iiitd.edu.in/raghava/ifnepitope/
IEDB-MHCII	MHC-II binding predictions	http://tools.immuneepitope.org/mhcii/
nHLApred	Predict peptide binding to MHC class-I based on neural network	http://www.imtech.res.in/raghava/nhlapred/
EpiVax	Prediction of classes I/II conserved and promiscuous epitopes	http://www.epivax.com
Epilen v 1.0	Use multi-step algorithm to predict of T-cell epitopes	http://www.ddg-harmfac.net/epijen/EpiJen/Epiien.htm
<i>B-cell epitope prediction</i>		
ABCpred	<i>B-cell epitope prediction using ANN</i>	http://www.imtech.res.in/raghava/abcpred/

(continued)

Table 1
(continued)

Database name	Applications	URL Link
LBtope	Predict linear B-cell epitopes	http://www.imtech.res.in/raghava/lbtope/
AlgPred	Prediction of allergenic proteins and mapping of IgE epitopes	www.imtech.res.in/raghava/algpred/
EPITOPIA	Detect immunogenic residues in a 3D structure	http://epitopia.tau.ac.il/
PEASE	Predict epitopes using antibody sequence	http://www.ofranlab.org/PEASE
PEPITOPE	Structure based B-cell epitope prediction	http://pepitope.tau.ac.il/
CBTOPE	Identification of conformational B-cell epitopes in an antigen from its primary sequence	http://webs.iitd.edu.in/raghava/cbtope/
Ellipro	Predicts linear and discontinuous antibody epitopes	http://tools.iedb.org/ellipro/
BepiPred	Predict sequential B-cell epitope	http://www.cbs.dtu.dk/services/BepiPred/
JenPep	Provide quantitative data on B- and T-cell epitopes, peptide MHC-TR complex, etc.	http://www.jenner.ac.uk/JenPep
IgPred	In silico-based models to predict B-cell epitopes	http://webs.iitd.edu.in/raghava/igpred/
EPIPRED	Predicts structural epitopes for specific antibody	http://opig.stats.ox.ac.uk/webapps/sabdab-sabpred/EpiPred.php
<i>Others databases and predictors</i>		
NetChop	Prediction of immunoproteasome/proteasome cleavage	http://www.cbs.dtu.dk/services/NetChop
Pcleavage	Prediction of immunoproteasome/proteasome cleavage	http://www.imtech.res.in/raghava/pcleavage/
TAPPred	Predict binding affinity of peptide to TAP protein	http://www.imtech.res.in/raghava/tappred/
CTLpred	Prediction of CTL epitopes using artificial neural network and support vector machines	http://www.imtech.res.in/raghava/ctlpred
TAPreg	Prediction of binding affinity of peptides to TAP*	http://imed.med.ucm.es/Tools/tapreg/
FRED	Prediction of TAP binding epitopes	http://abi.inf.unituebingen.de/Services/WAPP/information
AntigenDB	An immunoinformatics database of pathogen antigens	http://webs.iitd.edu.in/raghava/antigendb/
IMGT	A high-quality integrated resource of IG, TR, MHC, and related proteins	http://www.imgt.org
IEDB		http://www.immuneepitope.org

(continued)

Table 1
(continued)

Database name	Applications	URL Link
	A database with more than 88,382 peptidic epitopes	
PDB	MFIC/peptide/TCR combinations	https://www.rcsb.org/pdb/
Allele frequencies	HLA frequencies in worldwide population and polymorphism frequencies in immunologically	http://www.allelefrequencies.net
IMGT/HLA	A database of 5518 HLA class I and 1612 HLA class II alleles	https://www.ebi.ac.uk/ipd/imgt/hla/
<i>Antigenicity prediction</i>		
VaxiJen	Prediction of protective antigens and subunit vaccines	http://www.ddgpharmfac.net/vaxijen/VaxiJen/VaxiJen.htm
ANTIGENpro	Prediction of protein antigenicity	http://scratch.proteomics.ics.uci.edu

predicts the folds, alpha-helices, beta-sheets, coils, transmembrane topology, etc. This helps to understand steric hindrances in the structure and can be cross validated using Porter or JPred4.

9. **Tertiary vaccine design:** For docking studies, tertiary structure is required, and the number of tools can be used to generate tertiary structure. These tools generate a number of configuration, and each has its own criteria to describe most stable structure like global score or P-value (I-Tasser, Raptor, Orion, Robetta, etc.); the obtained structure is further refined: (i) Galaxy refine server and (ii) 3D refine server to get low potential energy scoring models which means better stability. Ramachandran plots are generated for the tertiary structures.
10. **Molecular docking and simulation:** Immune response is generated at the innate level, and this shapes the adaptive immune response. Innate immune cells carry pattern recognition receptors; Toll-like receptor (TLR), c-type lectin receptors (CLR), Nod-like receptor (NLR), and Rig-like receptor (RLR). Except NLR, all are involved in microbial/pathogen-derived product recognition (genomic DNA, sugars, LPS, zymosan, etc.) Thus, depending on the organism putative PRR is picked up [17–19]. PRRDB is a curated database for pattern recognition receptor and their ligands [20]. The vaccine candidate and PRR are docked in silico; clusPro, CABSdock, PatchDock. A list of computational molecular docking software and their URLs are given in Table 2. The docking software work on mathematical models like Monte Carlo

Table 2
Web server for computational molecular docking

Server	Input	URL
<i>Global docking</i>		
CABS-dock	Protein receptor structure in the PDB format or protein PDB code, and a peptide sequence	http://biocomp.chem.uw.edu.pl/CABSdock
PIPER-FlexPepDock	The structure of the receptor and the sequence of the peptide	http://piperfpd.furmanlab.cs.huji.ac.il
ClusPro	Two PDB coordinate files, one denoted as the receptor and the other as the ligand. The files may upload from computer or may input the PDB code with or without PDB chain identifiers	https://peptidock.cluspro.org/
pepATTRACT	The structure of the protein receptor in PDB format; the sequence of the peptide in FASTA format	http://bioserv.rpbs.univ-parisdiderot.fr/services/pepATTRACT/
MDockPeP	A peptide sequence and a protein structure	http://zougrouptoolkit.missouri.edu/mdockpep/
ZDOCK	The structures of a protein and ligand of interest as PDB IDs or PDB files	http://zdock.umassmed.edu
HPEPDOCK	Accepts not only structures but also sequences as input for the protein and can automatically integrate the available peptide binding information from the protein data Bank (PDB), and sequences or structures for the peptide	http://huanglab.phys.hust.edu.cn/hpepdock/
PatchDock	Protein PDB codes or uploaded protein structures	http://bioinfo3d.cs.tau.ac.il/PatchDock/
<i>Local docking</i>		
Rosetta FlexPepDock	A PDB file of the estimated complex between the receptor (first chain) and the peptide (second chain)	http://flexpepdock.furmanlab.cs.huji.ac.il/
PEP-FOLD3	Protein structure in PDB format, and the peptide sequence in FASTA format	http://bioserv.rpbs.univ-parisdiderot.fr/services/PEPFOLD3/
DINC 2.0	The structures of a protein and ligand of interest as PDB files	http://dinc.kavrakilab.org/

simulation or Fast Fourier transformation (FTT) and generate a scoring matrix of ligand receptor binding. The scoring matrices can be functional, empirical, knowledge based, or consensus. The application of scoring function is to identify ligand receptor binding hot spots, the correct scoring function can lead to the best vaccine candidate, and lead optimization to improve tightness of binding between receptor and ligand and can save synthesis cost. The ideal complex is simulated in

silico using Schrodinger's Desmond module, the stability of structure is assayed, and additional hydrogens are added to structure. Protein interactions are evaluated, and stable poses are studied for trajectories with Schrodinger's biologics module.

4 Notes

1. Vaccine candidate should be able to activate appropriate immune response and generate immunological memory [2].
2. It should cover a wide range of HLDA [2].
3. The understanding of the prediction tool algorithm (SVM, RM, or NN) is important to consider as it affects the output significantly [6, 7].
4. The purpose of in silico vaccine design is proven immunogenicity [8].
5. Every in silico step should be designed considering the actual biological events [8].
6. The prediction tools have cut-off and some default parameters; a careful choice of values have an impact on the outcome [12].

Acknowledgments

NA and RK are supported by the Indian Institute of Technology Mandi. SSR is granted a Junior Research fellowship from Department of Biotechnology, Government of India, New Delhi. AK is supported by Council for Scientific and Industrial Research, New Delhi. AP acknowledges financial support from Ramalingaswami Fellowship, Department of Biotechnology, Government of India, New Delhi.

References

1. Valencia DN (2020) Brief review on COVID-19: the 2020 pandemic caused by SARS-CoV-2. *Cureus* 12(3):e7386. <https://doi.org/10.7759/cureus.7386>. PMID: 32337113; PMCID: PMC7179986
2. Brodin P, Davis MM (2017) Human immune system variation. *Nat Rev Immunol* 17(1):21–29. <https://doi.org/10.1038/nri.2016.125>. Epub 2016 Dec 5. PMID: 27916977; PMCID: PMC5328245
3. Pizza M et al (2000) Identification of vaccine candidates against serogroup B meningococcus by whole-genome sequencing. *Science* 287:1816–1820
4. Costain G, Jobling R, Walker S, Reuter MS, Snell M, Bowdin S, Cohn RD, Dupuis L, Hewson S, Mercimek-Andrews S, Shuman C, Sondheimer N, Weksberg R, Yoon G, Meyn MS, Stavropoulos DJ, Scherer SW, Mendoza-Londono R, Marshall CR (2018) Periodic reanalysis of whole-genome sequencing data enhances the diagnostic advantage over standard clinical genetic testing. *Eur J Hum Genet* 26(5):740–744. <https://doi.org/10.1038/s41431-018-0114-6>. Epub

- 2018 Feb 16. PMID: 29453418; PMCID: PMC5945683
5. Bayliss SC, Verner-Jeffreys DW, Bartie KL, Aanensen DM, Sheppard SK, Adams A, Feil EJ (2017) The promise of whole genome pathogen sequencing for the molecular epidemiology of emerging aquaculture pathogens. *Front Microbiol* 8:121
 6. Tomar N, De RK (2010) Immunoinformatics: an integrated scenario. *Immunology* 131(2):153–168. <https://doi.org/10.1111/j.1365-2567.2010.03330.x>. Epub 2010 Aug 16. PMID: 20722763; PMCID: PMC2967261
 7. Kardani K, Bolhassani A, Namvar A (2020) An overview of in silico vaccine design against different pathogens and cancer. *Expert Rev Vaccines* 19(8):699–726. <https://doi.org/10.1080/14760584.2020.1794832>
 8. Kaur R, Arora N, Jamakhani MA, Malik S, Kumar P, Anjum F, Tripathi S, Mishra A, Prasad A (2020) Development of multi-epitope chimeric vaccine against *Taenia solium* by exploring its proteome: an in silico approach. *Expert Rev Vaccines* 19(1):105–114
 9. Arora N, Raj A, Anjum F, Kaur R, Rawat SS, Kumar R, Tripathi S, Singh G, Prasad A (2020) Unveiling *Taenia solium* kinome profile and its potential for new therapeutic targets. *Expert Rev Proteomics* 17(1):85–94
 10. Verma S, Sajid A, Singh Y, Shukla P (2020) Computational tools for modern vaccine development. *Vaccin Immunother* 16(3):723–735. <https://doi.org/10.1080/21645515.2019.1670035>
 11. Clem AS (2011) Fundamentals of vaccine immunology. *J Glob Infect Dis* 3(1):73–78. <https://doi.org/10.4103/0974-777X.77299>. PMID: 21572612; PMCID: PMC3068582
 12. Leipzig J (2017) A review of bioinformatic pipeline frameworks. *Brief Bioinform* 18(3):530–536. <https://doi.org/10.1093/bib/bbw020>. PMID: 27013646; PMCID: PMC5429012
 13. Iwasaki A, Medzhitov R (2015) Control of adaptive immunity by the innate immune system. *Nat Immunol* 16(4):343
 14. Schirle M, Weinschenk T, Stevanović S (2001) Combining computer algorithms with experimental approaches permits the rapid and accurate identification of T cell epitopes from defined antigens. *J Immunol Methods* 257(1–2):1–6. [https://doi.org/10.1016/S0022-1759\(01\)00459-8](https://doi.org/10.1016/S0022-1759(01)00459-8)
 15. Flower DR (2003) Towards in silico prediction of immunogenic epitopes. *Trends Immunol* 24(12):667–674. <https://doi.org/10.1016/j.it.2003.10.006>
 16. Seyed N, Taheri T, Vauchy C et al (2014) Immunogenicity evaluation of a rationally designed polytope construct encoding HLA-A* 0201 restricted epitopes derived from *Leishmania major* related proteins in HLA2/DR1 transgenic mice: steps toward polytope vaccine. *PLoS One* 9(10):e108848
 17. Akira S, Uematsu S, Takeuchi O (2006) Pathogen recognition and innate immunity. *Cell* 124(4):783–801
 18. Tartey S, Takeuchi O (2017) Pathogen recognition and toll-like receptor targeted therapeutics in innate immune cells. *Int Rev Immunol* 36(2):57–73
 19. Kawai T, Akira S (2010) The role of pattern-recognition receptors in innate immunity: update on toll-like receptors. *Nat Immunol* 11(5):373–384
 20. Kaur D, Patiyal S, Sharma N et al (2019) PRRDB 2.0: a comprehensive database of pattern-recognition receptors and their ligands. *Database* 2019



In Silico Identification of the B-Cell and T-Cell Epitopes of the Antigenic Proteins of *Staphylococcus aureus* for Potential Vaccines

Sunil Thomas and Irini Doytchinova

Abstract

Staphylococcus aureus is a leading cause of community-acquired, healthcare-associated, and hospital-acquired infections. *S. aureus* bacteremia is a common and serious infection with significant morbidity and mortality in older patients. The rise of antibiotic-resistant strains of *S. aureus* has resulted in substantial loss and effective treatment in hospitalized patients. Thus, there is a need in the development of a vaccine that would provide protection against *S. aureus*. The antigens of our interest include proteins that are essential for bacterial attachment and colonization (ClfA and ClfB), dermonecrosis-driven toxin (Hla), antigens that are essential for abscess formation (ExxA and ExxB), and antigens that are essential for nutrient acquisition and resistance to phagocytes killing induced by reactive oxygen species (FhuD2 and MntC). Development of a structure-based vaccine based on the antigenic protein epitopes is a novel strategy to provide protection against *S. aureus*. Using bioinformatic tools, we have determined the B-cell and T-cell epitopes of the antigenic proteins of *S. aureus*. This chapter reports identification of B-cell and T-cell epitopes of the antigenic protein that could be used in the development of effective structure-based vaccines to protect against *S. aureus*.

Key words *Staphylococcus aureus*, Bioinformatics, B-cell epitope, T-cell epitope

1 Introduction

Staphylococcus aureus is a Gram-positive, aerobic bacterium that is an important cause of infections in humans. Approximately 30% of the healthy human population are carriers of *S. aureus*. *S. aureus* can be found in the skin, rectum, vagina, gastrointestinal tract, and axilla, the anterior nares appearing as the main reservoir [1]. *S. aureus* is a major human pathogen that causes a wide range of clinical infections. It is a leading cause of bacteremia and infective endocarditis and sepsis as well as osteoarticular, skin and soft tissue, pleuropulmonary, and device-related infections [2].

Humans are daily exposed to the bacteria, but only some people are carriers over longer periods of time. With respect to *S. aureus* carriage, individuals can be categorized into three groups: persistent carriers, about 20% of the population; transient recurrent carriers, about 30% of population, and non-carriers in whom *S. aureus* is not detected over prolonged periods, comprising the remaining 50% of the population [3]. Any person is prone to *S. aureus* infection; people with chronic conditions such as diabetes, cancer, vascular disease, eczema, lung disease, and drug users are at greater risk of infection [4].

S. aureus has an incidence rate ranging from 20 to 50 cases/100,000 population per year. The morbidity and mortality rates of the pathogen vary from 15 to 60% [5]. Multiple factors influence outcomes for patients infected with *S. aureus*. The predictors of mortality include age, with older patients being twice as likely to die [6].

S. aureus is a leading cause of community-acquired, healthcare-associated, and hospital-acquired infections and has a broad spectrum of clinical syndromes, ranging from rather benign infections (e.g., folliculitis) to potentially life-threatening infections (e.g., bloodstream infection) [2, 6]. Common healthcare-associated infections caused by *S. aureus* include surgical site infections, hospital-acquired bloodstream infections, and pneumonia [2]. These are important causes of morbidity, mortality, and increased healthcare expenditure [7].

Over the years, *S. aureus* has acquired resistance to most of the antibiotics used in its treatment. The rise of methicillin-resistance in *S. aureus* strains (MRSA), as well as the emergence of vancomycin-resistant strains (VRSA), increases the complexity and cost of treatment of these infections. It is estimated that annually, ten billion dollars are spent on treating hospital-associated infections [8]. While *S. aureus* can cause disease in immunocompetent, previously healthy individuals, certain patients are at particularly increased risk. Currently, there are no effective vaccines for *S. aureus*; hence, there is an urgent need to develop effective vaccines against this debilitating disease.

The eight *S. aureus* antigenic proteins we have selected are: MntC, FhuD2, EsxA, EsxB, Csa1a, ClfA, ClfB, and Hla.

MntC is a surface protein that is an ABC (ATP-binding cassette) transporter system component. It is conserved in *S. aureus*, including MRSA and VRSA strains. MntC binds to manganese in a reversible way, by performing small changes proximal to the binding sites, composed of His, Asp, and Glu residues. MntC is reported to be immunogenic and protective against *S. aureus* [9].

S. aureus produce five different leukocidins: leukocidin ED (LukED), Pantón–Valentine leukocidin (PVL), leukocidin AB (LukAB), and γ -hemolysins AB and CB (HlgAB and HlgCB). The *S. aureus* pore-forming toxin PVL is most likely causative for

1.1 Antigenic Proteins of *S. aureus*

life-threatening necrotizing infections, which are characterized by massive tissue inflammation and necrosis. In 1932, Panton and Valentine described PVL as a virulence factor belonging to the family of synergohymenotropic toxins. These toxins form pores in the membrane of host defense cells by synergistic action of two secretory proteins, designated LukS-PV and LukF-PV, which are encoded by two co-transcribed genes of a prophage integrated in the *S. aureus* chromosome. PVL is mostly associated with community-acquired MRSA infections and distinguishable from nosocomial MRSA by non-multidrug resistance and carriage of the type IV staphylococcal chromosome cassette element [10]. *S. aureus* targets and kills DCs primarily via the activity of leukocidin LukAB [11].

FhuD2 is a large family of putative iron-binding proteins in Gram-positive bacteria. *S. aureus* possesses an ABC transporter (FhuCBG, FhuD1, FhuD2) for the import of iron(III)-hydroxamates. FhuD2 binds a variety of iron(III)-hydroxamates with differing affinities, possessing significantly higher affinity for iron(III)-ferrichrome and iron(III)-desferrioxamine [12].

Esat-6 secretion system (Ess), a specialized type VII secretion system of *S. aureus*, is required for staphylococcal virulence and persistence. Proteins secreted by the Ess, including EsxA and EsxB, are crucial virulence factors and putative vaccine candidates. Mutants that failed to secrete EsxA and EsxB displayed defects in the pathogenesis of *S. aureus* murine abscesses, suggesting that this specialized secretion system may be a general strategy of human bacterial pathogenesis [13].

Csa1A (conserved staphylococcal antigen 1a) is a lipoprotein that belongs to a family of 10–20 conserved staphylococcal antigens (Csa) classified as DUF576 [14].

S. aureus attachment to the anterior nares during colonization is facilitated by the CWA protein clumping factor B (ClfB) through high-affinity interactions with the cornified envelope. Through this interaction, ClfB has been shown to promote nasal colonization. ClfB is expressed in the early exponential phase of growth and is absent from cells in the late and stationary phase [15]. ClfA promotes bacterial adhesion to the blood plasma protein fibrinogen [16].

Alpha-toxin (Hla) is a pore-forming toxin, encoded by the *hla* gene that plays a key role in *S. aureus* pathogenesis. Hla forms heptameric pores in host cell membranes, leading to lysis of the cell. Even at sublytic levels, Hla has been shown to affect innate immune effector cells, stimulate a hyperinflammatory response characteristic of bacterial pneumonia, and disrupt epithelial and endothelial barriers [17].

Current vaccine development strategies for protection against *S. aureus* are based on recombinant proteins and/or protein–

1.2 Structure-Based Vaccines for *S. aureus*

polysaccharide conjugates. However, targeting single virulence factor has not been effective in providing protection against the pathogen; hence, a successful vaccine will need to incorporate more than a single antigen. Structure-based vaccines are more powerful than conventional vaccines in controlling infectious pathogens; hence, development of a multi-epitope structure-based vaccine may be a strategy to develop vaccines to protect against *S. aureus*.

Structural vaccinology combines elements of structural biology and bioinformatics into a promising new method for the identification of antigenic protein elements of interest based on the protein amino acid sequence and the resulting secondary and tertiary structure. The enabling principle is that the entire antigenic protein is not essential for inducing an immune response as only the epitope sequence per se actually induces the immune response. Once the epitope domains (B- and T-cell epitopes) or sites are identified and expressed in a recombinant form, they can be used as potent immunogens devoid of other regions that are irrelevant from a vaccine standpoint. Moreover, focusing in conserving epitopes shared by a group of pathogens would help the immune system to focus on mounting effective humoral and cellular responses against relevant targets. Recent studies have demonstrated that multi-epitope structure-based vaccines are more efficacious than single-epitope vaccines [18, 19]. As yet there are no structure-based vaccines commercially available. Nevertheless, structure-based vaccines have been recently developed for bacterial and viral pathogens including *Neisseria*, *Streptococci*, *Borrelia*, *Ehrlichia*, influenza virus, respiratory syncytial virus, and foot-and-mouth disease virus (reviewed in [18]). The technique of structural vaccinology thus holds considerable promise for developing broadly effective vaccines against pathogens such as *S. aureus*.

The first step in the development of *S. aureus* structure-based vaccines is the identification of the B-cell and T-cell epitopes in the antigenic proteins. Using bioinformatics tools, we determined the best B-cell and T-cell epitopes in the antigenic proteins of *S. aureus*.

2 Materials

1. UniProt program (www.uniprot.org).
2. NCBI protein database (<https://www.ncbi.nlm.nih.gov/protein/>).
3. Basic Local Alignment Search Tool (BLAST) (<https://blast.ncbi.nlm.nih.gov/Blast.cgi>).
4. DNASTAR Lasergene software.
5. Immune epitope database and analysis resource (IEDB) (iedb.org).
6. EpiTOP (<http://www.ddg-pharmfac.net/EpiTOP3/>).

3 Methods

3.1 Identification of B-Cell Antigenic Epitope

The antigenic epitopes in FASTA format was obtained from UniProt or NCBI protein database.

They were transferred to BLAST (protein BLAST) to determine whether they overlapped to other antigenic proteins.

Once the antigenic protein structure is determined as unique, they are transferred to DNASTAR Lasergene software (alternately, they could be transferred to IEDB) for B-cell epitope determination.

In this protocol, linear epitopes are identified for synthesis (*see Note 1*).

The hydrophilic regions are predominantly located on the protein surface and are potentially antigenic (*see Note 2*); hence, they are chosen as the region of choice for peptide design (Fig. 1).

We have chosen B-cell epitopes that are close to N-terminus or C-terminus because these usually represent functional epitopes with higher activities [20] (Fig. 2).

For generation of antibodies in animals, the peptides will be conjugated to KLH (*see Note 3*).

For the generation of antibodies, the animals (mice, rat, hamster, rabbit, goat) are immunized two to three times, 2–3 weeks between immunizations, and the sera collected to determine the best peptide immunogen.

3.2 Identification of T-Cell Epitopes

In order to be recognized by the T-cell receptors (TCR), the peptides generated from foreign proteins are processed in the antigen-presenting cells (APC) and form intracellular complexes with the human leukocyte antigens (HLA). The complexes are presented on the cell surface where are recognized by the TCRs. In the present study, we identified the most putative T-cell epitopes by predicting high affinity and promiscuous HLA binders. The predictions are made on the 12 most frequent HLA-DRB1 proteins (*01:01, *03:01, *04:01, *04:04, *04:05, *07:01, *08:02, *09:01, *11:01, *12:01, *13:02, *15:01) by the server EpiTOP [21]. Peptides binding to ten or more HLA proteins are selected as the most promiscuous. For EsxA are selected binders to nine HLA proteins. The most promiscuous and high affinity binders to HLA-DRB1 are given in Fig. 2.

4 Notes

1. A linear or a sequential epitope is an epitope that is recognized by antibodies by its linear sequence of amino acids, or primary structure.

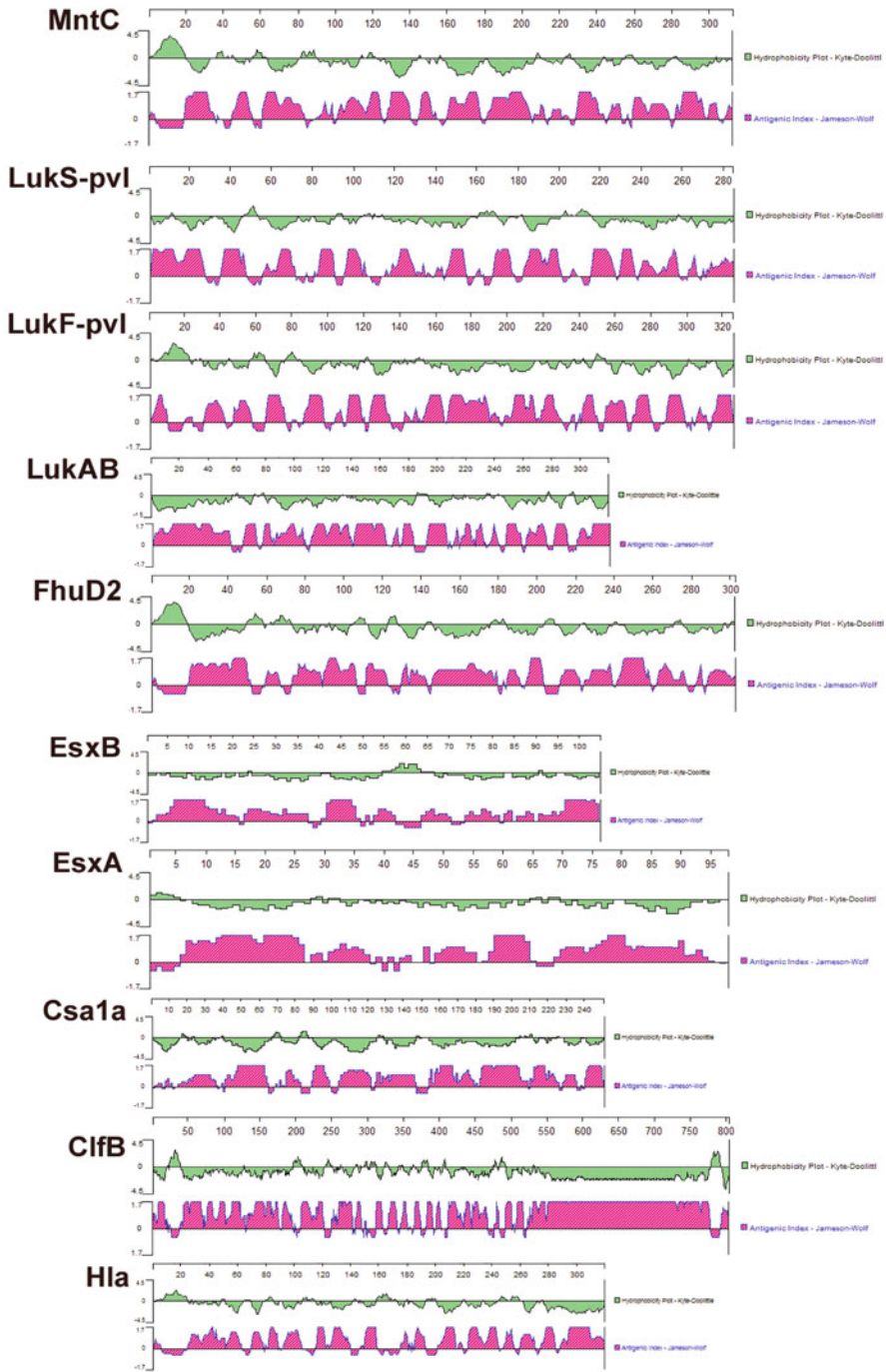


Fig. 1 Hydrophobicity plot (green) of the antigenic proteins of *S. aureus*. The antigenic index is shown in pink



Fig. 2 The *S. aureus* antigenic proteins and their epitopes for the development of structure-based vaccines. Yellow shaded: B-cell epitope. The peptides are selected based on bioinformatics analysis of available structures. The most promiscuous and high-affinity binders to HLA-DRB1 originating from the *S. aureus* antigenic proteins are shaded in green. The binders are predicted by EpiTOP. The high-affinity HLA binders are the most probable T-cell epitopes

2. The hydrophilicity of the epitope is determined based on the principle of Kyte and Doolittle [22].
3. Keyhole limpet hemocyanin (KLH) is a very large, copper-containing protein molecule derived from the hemolymph of the mollusk, *Megathura crenulata*. KLH is used as a carrier protein in the production of antibodies for immunology research. Low molecular weight peptides (haptens) are not immunogenic and require the aid of a carrier protein to stimulate an immune response. The large size of KLH makes it suitable as a carrier molecule. In addition, as KLH is derived from a mollusk, it is phylogenetically distant from mammalian proteins, thereby reducing false positives.

References

1. Sakr A, Brégeon F, Mège JL, Rolain JM, Blin O (2018) *Staphylococcus aureus* nasal colonization: an update on mechanisms, epidemiology, risk factors, and subsequent infections. *Front Microbiol* 9:2419
2. Tong SYC, Davis JS, Eichenberger E, Holland TL, Fowler VG (2015) *Staphylococcus aureus* infections: epidemiology, pathophysiology, clinical manifestations, and management. *Clin Microbiol Rev* 28:603–661
3. van Belkum A, Verkaik NJ, de Vogel CP, Boelens HA, Verveer J, Nouwen JL, Verbrugh HA, Wertheim HF (2009) Reclassification of *Staphylococcus aureus* nasal carriage types. *J Infect Dis* 199:1820–1826
4. Centers for Disease Control and Prevention (2011) *Staphylococcus aureus* in healthcare settings. <https://www.cdc.gov/hai/organisms/staph.html>
5. Cosgrove SE, Sakoulas G, Perencevich EN, Schwaber MJ, Karchmer AW, Carmeli Y (2003) Comparison of mortality associated with methicillin-resistant and methicillin-susceptible *Staphylococcus aureus* bacteremia: a meta-analysis. *Clin Infect Dis* 36:53–59
6. van Hal SJ, Jensen SO, Vaska VL et al (2012) Predictors of mortality in *Staphylococcus aureus* bacteremia. *Clin Microbiol Rev* 25:362–386
7. Klevens RM, Morrison MA, Nadle J et al (2007) Invasive methicillin-resistant *Staphylococcus aureus* infections in the United States. *JAMA* 298:1763–1771
8. Zimlichman E, Henderson D, Tamir O, Franz C, Song P, Yamin CK, Keohane C, Denham CR, Bates DW (2013) Health care-associated infections: a meta-analysis of costs and financial impact on the US health care system. *JAMA Intern Med* 173:2039–2046
9. Salazar N, Castiblanco-Valencia MM, da Silva LB, de Castro I, Monaris D, Masuda HP, Barbosa AS, Arêas AP (2014) *Staphylococcus aureus* manganese transport protein C (MntC) is an extracellular matrix- and plasminogen-binding protein. *PLoS One* 9 (11):e112730
10. Melles DC, van Leeuwen WB, Boelens HA, Peeters JK, Verbrugh HA, van Belkum A (2006) Panton-valentine leukocidin genes in *Staphylococcus aureus*. *Emerg Infect Dis* 12:1174–1175
11. Berends ETM, Zheng X, Zwack EE, Ménager MM, Cammer M, Shopsis B, Torres VJ (2019) *Staphylococcus aureus* impairs the function of and kills human dendritic cells via the LukAB toxin. *mBio* 10:e01918-18
12. Sebulsky MT, Shilton BH, Speziali CD, Heinrichs DE (2003) The role of FhuD2 in iron (III)-hydroxamate transport in *Staphylococcus aureus*. Demonstration that FhuD2 binds iron (III)-hydroxamates but with minimal conformational change and implication of mutations on transport. *J Biol Chem* 278:49890–49900
13. Burts ML, Williams WA, DeBord K, Missiakas DM (2005) EsxA and EsxB are secreted by an ESAT-6-like system that is required for the pathogenesis of *Staphylococcus aureus* infections. *Proc Natl Acad Sci U S A* 102:1169–1174
14. Schlupe C, Malito E, Marongiu A, Schirle M, McWhinnie E, Lo Surdo P, Bianucci M, Falugi F, Nardi-Dei V, Marchi S, Fontana MR, Lombardi B, De Falco MG, Rinaudo CD, Spraggon G, Nissum M, Bagnoli F, Grandi G, Bottomley MJ, Liberatori S (2013) Mining the bacterial unknown proteome: identification and characterization of a novel family of highly conserved protective

- antigens in *Staphylococcus aureus*. *Biochem J* 455:273–284
15. Lacey KA, Mulcahy ME, Towell AM, Geoghegan JA, McLoughlin RM (2019) Clumping factor B is an important virulence factor during *Staphylococcus aureus* skin infection and a promising vaccine target. *PLoS Pathog* 15(4): e1007713
 16. Herman-Bausier P, Labate C, Towell AM, Derclaye S, Geoghegan JA, Dufrene YF (2018) *Staphylococcus aureus* clumping factor A is a force-sensitive molecular switch that activates bacterial adhesion. *Proc Natl Acad Sci U S A* 115:5564–5569
 17. Tabor DE, Yu L, Mok H, Tkaczyk C, Sellman BR, Wu Y, Oganessian V, Slidel T, Jafri H, McCarthy M, Bradford P, Esser MT (2016) *Staphylococcus aureus* alpha-toxin is conserved among diverse hospital respiratory isolates collected from a global surveillance study and is neutralized by monoclonal antibody MEDI4893. *Antimicrob Agents Chemother* 60:5312–5321
 18. Thomas S, Luxon BA (2013) Vaccines based on structure-based design provide protection against infectious diseases. *Expert Rev Vaccines* 12:1301–1311
 19. Scarselli M, Aricò B, Brunelli B, Savino S, Di Marcello F, Palumbo E, Veggi D, Ciocchi L, Cartocci E, Bottomley MJ, Malito E, Lo Surdo P, Comanducci M, Giuliani MM, Cantini F, Dragonetti S, Colaprico A, Doro F, Giannetti P, Pallaoro M, Brogioni B, Tontini M, Hilleringmann M, Nardi-Dei V, Banci L, Pizza M, Rappuoli R (2011) Rational design of a meningococcal antigen inducing broad protective immunity. *Sci Transl Med* 3(91):91ra62
 20. Thomas S (2016) Development of structure-based vaccines for ehrlichiosis. *Methods Mol Biol* 1403:519–534
 21. Yordanov V, Dimitrov I, Doytchinova I (2018) Proteochemometrics-based prediction of peptide binding to HLA-DP proteins. *J Chem Inf Model* 58:297–304
 22. Kyte J, Doolittle RF (1982) A simple method for displaying the hydropathic character of a protein. *J Mol Biol* 15:105–132



Computational Mining and Characterization of Hypothetical Proteins of *Mycobacterium bovis* Toward the Identification of Probable Vaccine Candidates

Bhaskar Ganguly

Abstract

A hypothetical protein (HP) is one that is known to exist only on the basis of a corresponding gene but without any function assigned to it. Many HPs have emerged as attractive vaccine candidates against prokaryotic and eukaryotic pathogens as well as against cancers. *Mycobacterium bovis* is a serious veterinary pathogen of tremendous zoonotic importance. This protocol describes a computational workflow for the identification of the HPs of *M. bovis* with vaccine potential and their subsequent structural and functional characterization.

Key words *Mycobacterium bovis*, Tuberculosis, Hypothetical protein, Vaccine candidates, Computation, Structure, Function

1 Introduction

A newly sequenced genome is likely to contain some genes with unknown function. Further, some of these genes may code for proteins. Such proteins, which lack translational evidence and do not have any function assigned to them but are known to exist based on the presence of a corresponding gene, are known as hypothetical proteins (HPs). Since the function of a protein essentially resides in its structure, the structures of HPs are also almost always unknown. Hence, structural and functional characterization of the HPs of a pathogen not only allows a better understanding of its physiology but also bears a potential for unraveling hitherto unknown drug and vaccine targets [1]. It is, therefore, not surprising that since the turn of the current century, several HPs have emerged as attractive vaccine candidates against different prokaryotic [2–4] and eukaryotic human and veterinary pathogens [5] as well as against cancers [6].

Mycobacterium bovis (*Mb*) is an important veterinary pathogen. This aerobic bacterium causes tuberculosis in cattle as well as in a host of other animals including buffalo, goats, cats, dogs, and pigs; sheep and horses are resistant yet occasionally infected [7]. *Mb* is part of the *Mycobacterium* tuberculosis complex, which also includes *Mycobacterium tuberculosis*, and has also been reported to cause tuberculosis in more than 40 species of free-ranging, wild animals including elephants, rhinos, deer, and various species of nonhuman primates [7, 8]. *Mb*, capable of infecting humans, is also of zoonotic significance. It is accountable for causing nearly 3% of all cases of human tuberculosis in the developing countries of the world [9].

Using the *M. bovis* proteome as an example, the sections to follow present a simple computational workflow for finding the HPs and characterizing them structurally and functionally toward the identification of probable vaccine candidates. The overall schema of the computational methodology is shown in Fig. 1. The method begins with the textual mining of *M. bovis* proteome for HPs, then predicts their antigenic potential, and finally determines their structure and function.

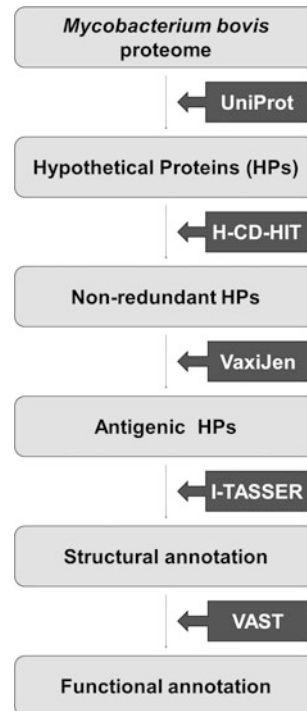


Fig. 1 Outline of the computational workflow used for the identification of the hypothetical proteins of *M. bovis* with vaccine potential and their subsequent structural and functional characterization

2 Materials

- 2.1 UniProt** The Universal Protein Resource (UniProt) [10], a freely accessible database of protein sequence and annotation data, available at <https://www.uniprot.org>, shall be used for retrieving the amino acid sequences of the hypothetical proteins of *M. bovis*.
- 2.2 CD-HIT Server** Modules from the CD-HIT suite [11], available at http://weizhong-lab.ucsd.edu/cdhit_suite/cgi-bin/index.cgi, shall be used for removing identical and closely related sequences of HPs obtained from different strains of *M. bovis*.
- 2.3 VaxiJen Server** VaxiJen [12], available at <http://www.ddg-pharmfac.net/vaxijen/VaxiJen/VaxiJen.html>, is a web server for alignment-independent prediction of protective antigens, allowing antigen classification solely based on the physicochemical properties of proteins deduced from their sequences. It will be used for the identification of potentially antigenic HPs.
- 2.4 I-TASSER Server** The Iterative Threading Assembly Refinement (I-TASSER) web server [13], available at <https://zhanglab.ccmb.med.umich.edu/I-TASSER>, consistently ranks amongst the top-performing web servers for prediction of the structure of a protein from its sequence. It will be used for computing the structure of the antigenic HPs.
- 2.5 VAST** The Vector Alignment Search Tool (VAST) [14] server, available at <https://structure.ncbi.nlm.nih.gov/Structure/VAST/vastsearch.html>, shall be used for determining the function of the HPs from their predicted structures.

3 Methods

3.1 Mining of *M. bovis* Proteome for HPs

Visit the UniProt database and in the search bar at the top of the page, click on “Advanced” to build a search query as shown in Fig. 2 (*see Note 1*). The final query generated in the search bar should appear as:

```
organism:"mycobacterium bovis" existence:"Predicted" NOT annotation:(type:function) NOT goa:(*)
```

The search should return a list of the hypothetical proteins of *M. bovis*; download and save the uncompressed Fasta file on your local drive as 1.fasta.

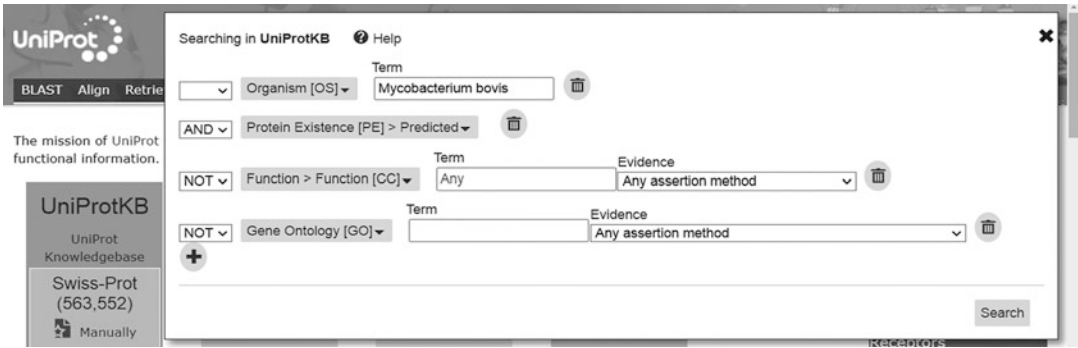


Fig. 2 Building the advanced search query in UniProt for mining the hypothetical proteins of *M. bovis* (see Note 1)

3.2 Exclusion of Identical Sequences

Visit the CD_HIT server and choose H-CD-HIT (see Note 2). Browse and load 1.fasta as the query. Set number of CD-HIT runs to 3; and sequence identity cut-offs for the three runs at 0.9, 0.7, and 0.5, respectively (see Note 3). Let all other parameters be at their default values and submit the query. Once the analyses are completed, download and save the Fasta file for the representative sequences at 50% identity, i.e., “Fasta file for representative sequences at 50% identity” locally as 2.fasta.

3.3 Identification of Potentially Antigenic HPs

Visit the VaxiJen server; browse and upload the output from CD-HIT, i.e., 2.fasta as the input. Select the appropriate target organism, i.e., bacteria for *M. bovis* and set the threshold at 1.0 (see Note 4). Submit the query. Once the analysis is completed, copy-paste, and save all the antigenic protein sequences from the output in a separate text file.

3.4 Determination of Structure

Visit the I-TASSER web server and submit the sequences of the antigenic HPs one by one for determination of structure (see Notes 5 and 6). After the results are obtained, download and save the model with the highest confidence (C-) score (see Note 7) as a .pdb file locally.

3.5 Determination of Function

Visit the VAST server, browse to upload the .pdb file downloaded from I-TASSER web server at Subheading 3.4 and submit for searching against “all of PDB.” The function of the HP can be inferred from the homologs identified by VAST (see Notes 8 and 9). Proteins with functions that demand constitutive expression are likely to serve as more attractive vaccine targets than those with inducible expression. Similarly, if the function of an HP is found to be essential, a selection pressure will operate against the occurrence of major mutations, disallowing the protein to alter significantly to an extent that may render the vaccine ineffective.

4 Notes

1. The first field of the query is the name of the organism whose proteome we wish to search. The remaining three fields are used for confining our search as per our definition of HPs. The second field of the query will limit our search to only those proteins that are “predicted” to exist and experimental evidence for their existence is lacking. By choosing the operator “NOT” and the third and fourth fields, we further restrict our search to only those true HPs that have been annotated neither for function nor for gene ontology.
2. The output from **Subheading 3.1** is likely to contain several nearly identical or very similar sequences; this is especially the case when working with organisms where many genome sequences are available from closely related subspecies. Hence, it is preferred that only representative sequences are retained for further analyses and the redundant sequences are eliminated. Although the CD-HIT module may also be used for this application, the H-CD-HIT module, which runs multiple rounds of CD-HIT on the input, is more accurate and is especially recommended when the number of sequences is high.
3. In this particular protocol, the sequence identity cut-off for the final run of CD-HIT was set at 0.5 (i.e., 50%). This means that sequences that differ from each other by more than 50% shall be treated as different sequences. This cut-off can be set at a different value depending upon the number of sequences to be analyzed, their lengths, and the computational resources available. A cut-off value ≥ 0.9 (i.e., 90%) would usually result in too many redundant sequences for downstream analyses whereas ≤ 0.3 (i.e., 30%) may cause sequences to get excluded.
4. The threshold has been arbitrarily set at 1.0 in the current protocol to allow high stringency. If a threshold is not specified and the field is left blank, the server will also determine a threshold by itself for classifying antigens and nonantigens.
5. Use of the I-TASSER web server requires prior registration with a noncommercial email address.
6. I-TASSER is capable of computing the structures of protein sequences up to 1500 residues in length. For longer sequences, the sequences may be split down into separate domains for modeling. Alternatively, other template-independent, ab initio and threading-based protein structure prediction tools may be used.
7. I-TASSER generates five models for the input sequence and sometimes the models may be very different from each other.

In such cases, if the C-scores of two or more models are comparable, all the different models may be chosen for further analyses.

8. Besides its structure, I-TASSER also computes the function for the input protein sequence. However, from the author's prior experience, the use of VAST for computing protein function is particularly advantageous due to its ability to identify very distant homologs that cannot be recognized from a comparison of sequences.
9. Although beyond the scope of this communication, the same computational approach that has been described in this protocol for the identification of vaccine targets can also be used to identify the druggability of the HPs, i.e., the potential of a HP to serve as a drug target. Essentiality of a protein for the survival of a pathogen or its pathogenesis is the foremost consideration for druggability, and the determination of the function of a HP is the keystone for determining its essentiality.

Acknowledgments

The author acknowledges the financial support received from M/s Ayurvet Limited, India, during the preparation of this manuscript. The authors of all the computational servers used in the present study are gratefully acknowledged for making their tools available freely and publicly.

References

1. Zarembinski TI, Hung LW, Mueller-Dieckmann HJ, Kim KK, Yokota H, Kim R, Kim SH (1998) Structure based assignment of the biochemical function of a hypothetical protein: a test case of structural genomics. *Proc Natl Acad Sci U S A* 95(26):15189–15193
2. Chen C, Chen D, Sharma J, Cheng W, Zhong Y, Liu K, Jensen J, Shain R, Arulanandam B, Zhong G (2006) The hypothetical protein CT813 is localized in the Chlamydia trachomatis inclusion membrane and is immunogenic in women urogenitally infected with *C. trachomatis*. *Infect Immun* 74(8):4826–4840
3. Bashir N, Kounsar F, Mukhopadhyay S, Hasnain SE (2010) Mycobacterium tuberculosis conserved hypothetical protein rRv2626c modulates macrophage effector functions. *Immunology* 130(1):34–45
4. Luo T, Patel JG, Zhang X, Walker DH, McBride JW (2020) Ehrlichia chaffeensis and E. canis hypothetical protein immunoanalysis reveals small secreted immunodominant proteins and conformation-dependent antibody epitopes. *NPJ Vaccines* 5(1):1–2
5. Zhai Q, Huang B, Dong H, Zhao Q, Zhu S, Liang S, Li S, Yang S, Han H (2016) Molecular characterization and immune protection of a new conserved hypothetical protein of Eimeria tenella. *PLoS One* 11(6):e0157678
6. Afjehi-Sadat L, Shin JH, Felizardo M, Lee K, Slavic I, Lubec G (2005) Detection of hypothetical proteins in 10 individual human tumor cell lines. *Biochim Biophys Acta* 1747(1):67–80
7. O'Reilly LM, Daborn CJ (1995) The epidemiology of Mycobacterium bovis infections in animals and man: a review. *Tuber Lung Dis* 76:1–46
8. Michel AL, Müller B, Van Helden PD (2010) Mycobacterium bovis at the animal-human interface: a problem, or not? *Vet Microbiol* 140(3):371–381

9. Cosivi O, Grange JM, Daborn CJ, Raviglione MC, Fujikura T, Cousins D, Robinson RA, Huchzermeyer HF, De Kantor I, Meslin FX (1998) Zoonotic tuberculosis due to *Mycobacterium bovis* in developing countries. *Emerg Infect Dis* 4(1):59
10. UniProt Consortium (2008) The universal protein resource (UniProt). *Nucleic Acids Res* 36(Suppl 1):D190–D195
11. Huang Y, Niu B, Gao Y, Fu L, Li W (2010) CD-HIT suite: a web server for clustering and comparing biological sequences. *Bioinformatics* 26(5):680–682
12. Doytchinova IA, Flower DR (2007) VaxiJen: a server for prediction of protective antigens, tumour antigens and subunit vaccines. *BMC Bioinformatics* 8(1):4
13. Zhang Y (2008) I-TASSER server for protein 3D structure prediction. *BMC Bioinformatics* 9(1):40
14. Gibrat JF, Madej T, Bryant SH (1996) Surprising similarities in structure comparison. *Curr Opin Struct Biol* 6(3):377–385



Recombinant Vaccine Design Against *Clostridium* spp. Toxins Using Immunoinformatics Tools

Rafael Rodrigues Rodrigues, Marcos Roberto Alves Ferreira, Frederico Schmitt Kremer, Rafael Amaral Donassolo, Clóvis Moreira Júnior, Mariliana Luiza Ferreira Alves, and Fabricio Rochedo Conceição

Abstract

The emergence of recombinant DNA technology has led to the exploration of the use of the technology to develop novel vaccines. With a fundamental role in vaccines design, several immunoinformatics tools have been created to identify isolated epitopes that stimulate a specific immune response, contributing to effective vaccines development. In the past, vaccine development projects relied entirely on animal experimentation, a relatively expensive and time-consuming process. Currently, use of immunoinformatics tools play a vital role in the antigen analysis and refinement, allowing the identification of possible protective epitopes capable of stimulating convenient humoral or cellular immune responses, in addition to facilitating time and cost reduction of vaccine production. The vaccination aimed at bacterial species of *Clostridium* spp. has been considered a promising example of use of these approaches in recent years. Based on the literature search, it is possible to understand the best immunoinformatics software used by researchers that facilitate recombinant vaccine antigens design and development. This chapter presents an overview of how these tools are supporting the antigen engineering, aiming at increasing the efficiency of inducing protective immune response in animals.

Key words Bioinformatics, Clostridiosis, Recombinant vaccines, Recombinant antigens

1 Introduction

Toxins are the major virulence factors of various species of the genus *Clostridium* [1], and they are responsible for causing diseases in humans and animals. Protective immunity against these toxins is based on the presence of preexisting neutralizing antibodies induced by vaccination [2]. The vaccines currently used for clostridiosis are produced from bacterial toxoids. However, the physical and chemical methods used for the production of a vaccine antigen

can denature important epitopes and decrease the immunogenicity of the vaccine [3]. Subunit vaccines offer a specific and safe alternative, causing less adverse reactions [4]. However, recombinant vaccines produced by traditional methods comprise whole proteins, which incorporate unnecessary antigenic loads and increase vaccine allergenicity [4, 5]. Such limitations can be overcome by purifying the antigen to identify immunodominant epitopes and direct the immune response.

The identification of neutralizing epitopes and understanding their interaction with the immune system is crucial for vaccine design and prevention of clostridiosis. The *in vitro* and *in vivo* evaluation of potential neutralizing epitopes of clostridial toxins is not practical since clostridial toxins range between 300 and 2710 amino acids, which is between pore-forming toxins (PFTs) and large clostridial glycosylating toxins (LCGTs).

Bioinformatics is an important tool used for protein structure prediction, function, and epitopes, contributing to the design of more efficient vaccines [6, 7]. This methodology decreases experimental bias, and substantially reduces experimental complexity and cost, thus increasing the chances of a successful vaccine [8, 9]. Immunoinformatics tools use statistical models, machine learning, and molecular interaction modeling, which contribute to the development of new hypotheses about the immune response induced by vaccines. The immunoinformatics tools used to design recombinant vaccines involve B-cell epitopes prediction, MHCII, T helper cells, antigenicity, allergenicity, and molecular docking, besides the three-dimensional structure stability of the antigens constructed from multiple epitopes [10]. This approach aims to direct the immune system toward the generation of neutralizing antibodies.

2 B-Cell Epitope Prediction

B-cell epitopes prediction can be performed using a wide variety of machine learning approaches, including supervised learning techniques, such as classification based on neural networks, support vector machines and tree-based models, and unsupervised methods, such as clustering. Sequence (usually in FASTA format) or structure (usually in PDB format) might be used as input depending on the tool. Here we summarized some of the most common tools used for this task, including tools designed for the prediction of linear (ABCpred, BepiPred and BCPREDS) and conformational epitopes (DiscoTope, ElliPro and CBTOPE), which are applicable when building recombinant vaccines for *Clostridium* spp.

ABCpred is a B-cell linear epitope prediction tool based on recurrent neural networks. It employs a fixed-length sliding window approach to analyze the submitted sequence and allows the user

2.1 ABCpred (Recurrent Neural Network)

2.1.1 Usage

to select the length of the window during the submission (10, 12, 14, 16, 18, or 20 amino acids) [11]. The server is available at <https://webs.iiitd.edu.in/raghava/abcpred/index.html>.

1. *Optional*: Define the sequence name.
2. Paste or update the sequence (without the FASTA header). The sequence must be written using only the standard 20 amino acid codes (ACDEFGHIKLMNPQRSTVWY) in upper or lowercase, and any other letter character will be converted to “X.” Whitespaces and numbers are ignored.
3. *Optional*: Change the threshold (value must be ≥ 0.1 and ≤ 1.0). Higher values lead to higher specificity but also decrease sensibility. 0.5, with a window length of 16, leads to specificity and sensibility of 65.93%.
4. *Optional*: Select the window length. By default, ABCpred uses a window length of 16, but the user can also select different sizes (10,12,14,16,18 or 20) from a predefined input box (10,12,14,16,18,20).
5. *Optional*: Enable or disable the epitope overlapping filtering step.
6. Finally, click in the “submit” button to run the analysis.

2.1.2 Output

After completing the analysis, whose running speed might vary depending on server load, output will be returned with summary of the epitopes that were identified, which might be visualized both in tabular form (“TABULAR RESULT”) and in a graphical form, with the epitopes displayed along the sequence (“OVERLAP DISPLAY”). An example output produced by ABCpred is shown in Fig. 1, with the predicted epitopes and their respective scores (output values of the neural network).

The available options may vary slightly in future updated versions.

2.2 BepiPred-2.0 (Random Forest)

BepiPred is a random forest-based prediction tool for B-cell epitopes, which employs a residue-level prediction followed by a rolling window average to identify regions more likely to be recognized by antibodies. The training dataset was derived from a collection of co-crystallized structures of antibodies and antigens [12]. The server is available at <http://www.cbs.dtu.dk/services/BepiPred/>.

2.2.1 Usage

1. Paste or update the sequence. The web server allows the user to submit up to 50 sequences, but the total number of amino acids must not pass 300,000. The sequences must also have a length between 10 and 6000.
2. Click in the “submit” button to run the analysis.

Rank	Sequence	Start position	Score
1	STIQTDHSTKASWDT	180	0.89
2	HHHLEGSNDIGKTTII	5	0.88
3	IKVKMERERNKYLLNW	266	0.87
3	IPDYQMSKLITGGLNP	234	0.87
3	KFTETTRGNYNLKSNN	196	0.87
4	TTTITRNKTSDGYTII	17	0.85
5	VGQVYSRLAFDTPNVD	287	0.84
5	SILNESINENVKIVDS	113	0.84
6	KQIISYQSVDSKNE	37	0.82
7	GYKIGGSIEIEENKPK	144	0.81
7	SNDIGKTTTITRNKTS	11	0.81
8	KASWDTKFTETTRGNY	190	0.80
9	EDVIKKYNLHDVTNST	87	0.79
10	TSDGYTIIITQNDKQII	25	0.78
10	STIEYVQPDFSTIQTD	170	0.78
11	TASIDARFIDDKYSSE	56	0.77
11	DSSSKNEDGFTASIDA	46	0.77
12	DVTNSTAINFPVRSYI	97	0.76
12	MFMYGRYTHVPATENI	218	0.76
13	TTLINLTGFMSSKKED	73	0.75
13	NVKIVDSIPKNTISQK	122	0.75
14	GFMSKKEDVIKKYNL	80	0.74
15	KNTISQKTVSNTMGYK	131	0.73
16	SKLITGGLNPNMSVVL	240	0.71
17	RERNKYLLNWGANV	272	0.64
17	LTAPNGTEESIIKVKM	255	0.64
18	HIFTFKINLTHKVTA	304	0.62
18	SIEIEENKPKASIESE	150	0.62
19	RLAFDTPNVDSHIFTF	293	0.60

Fig. 1 The output page (adapted), showing ABCpred prediction (tabular result) for the query sequence (Beta toxin of *C. perfringens* (CPB))

2.2.2 Output

After submitting the sequence, the user will be redirected to a loading screen which is updated every 20 s, where the results will be displayed after the algorithm execution. Alternatively, it is also possible to provide an email to receive a notification after the processing is finished.

The output page presents the amino acid sequence that were identified as epitopes (indicated with an “E”). By default, amino acids with a score of at least 0.5 are classified as potential epitopes, but this threshold might be changed by the user. Clicking on the “?” near the “*Epitope Threshold*” input provides more information about the expected sensibility and specificity for each value. Additionally, possible errors and a log of the calculations are displayed

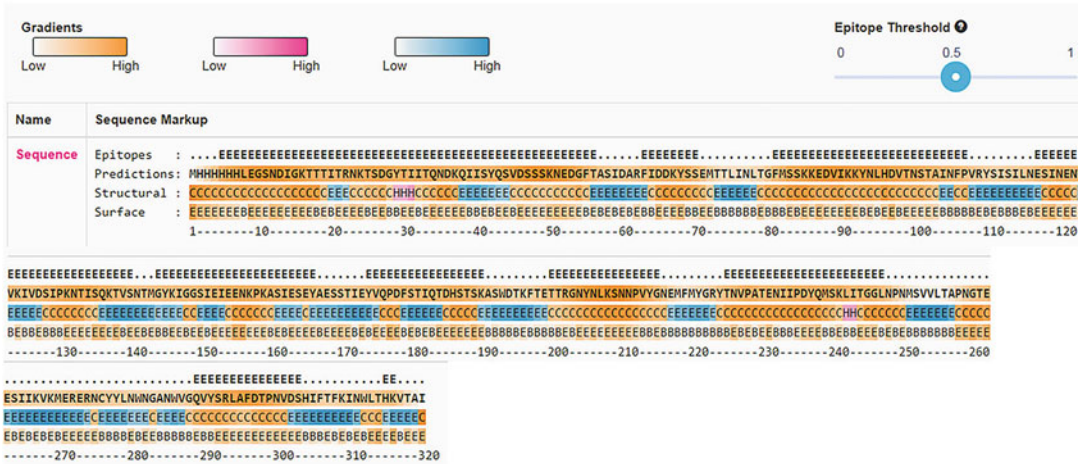


Fig. 2 The Summary output page (adapted) in Advanced Output mode, showing BepiPred-2.0 and NetSurfP prediction for the query sequence (CPB)

on the “Log” Table A detailed description of the exit page and some tips can be accessed on the “Help” tab.

Advanced visualization of the output may also be generated when clicking on the button “*Advanced Output is off;*” which includes the predictions generated by NetSurfP, a surface accessibility prediction tool. The new visualization includes the indication of structural and surface features. Structural: H—pink probability gradient (Helix), E—blue probability gradient (Sheet), and C—Orange probability gradient (Coil). Surface: B (Buried)—E (Exposed) from NetsurfP’s default threshold, and predicted relative surface accessibility (orange gradient) (Fig. 2).

The available options may vary slightly in future updated versions.

2.3 DiscoTope 2.0

This server predicts discontinuous B-cell epitopes from three-dimensional protein structures. The DiscoTope presents a new definition of spatial neighborhood and half-sphere exposure as a surface measure [13]. The server is accessible at <http://www.cbs.dtu.dk/services/DiscoTope/>.

2.3.1 Usage

1. Choose the submission method.

On the home page, you can write the file entry name in PDB format into the “PDB code” window and the chain ID into the “Chain” window or in the format “entryname_chain,” specify a file on the local disk containing a list of entries in PDB format with the identified chain ID. Also, in PDB format, you can specify a file on your local disk and chain IDs. It is important that the IDs are separated by comma, once not specified, all strings in the file will be used for forecasting.

2. Optional: Select the threshold score to identify the epitope (The default is -3.7).
The higher values allow to identify a high specificity.
3. Submit the sequence.

2.3.2 Output

4. The user will be redirected to a new page that is updated every 20 s. When the predictions are completed, the user will be automatically redirected to the output page. Optionally, the user can provide an email address, so that the results page link will be sent by email when the job is complete.
5. The results will be returned when the forecast is ready. The response time depends on the system load. The individual results are shown separately and in detail in seven columns: (1) Chain Id, (2) Residue number, (3) Amino acid, (4) Contact number, (5) Propensity score, (6) DiscoTope score, and (7) $\leq B$. Identified B-cell epitope.

The available options may vary slightly in future updated versions.

2.4 ElliPro (Structure Clustering)

This method predicts epitopes based upon solvent-accessibility and flexibility. This tool does not require training and addresses a method that is based on geometric properties. The Thornton method is applied and, together with a clustering algorithm, the MODELLER program and the Jmol visualizer project the prediction and visualization of epitopes [14]. The server is accessible at <http://tools.icdb.org/ellipro/>.

2.4.1 Usage

1. Select (using the PDB ID) or upload a PDB file containing the protein structure to be analyzed.
On this server, it is necessary to modify the corresponding PDB file to predict epitopes on a multi-chain protein, thus ensuring that all chains of interest have the same ID, as specified at <http://tools.icdb.org/ellipro/>. In some cases, residues need to be remunerated, as it avoids conflict of residences with the same numbers in the modified PDB file.
2. Select the parameters.
The minimum score: Specify an epitope prediction score (Default is 0.5).
Maximum distance (Angstrom): Specify a score to predict discontinuous epitopes (Default is 6).
3. Click “Submit.”
4. Select PDB chain(s) for calculation.
In this step, select which chains will be used to predict epitopes (in proteins containing more than one chain).
5. Click “Submit.”

6. A new page will return the results as follows: Protein sequence (s), predicted linear epitopes, and predicted discontinuous epitope (s). By selecting the “View” option in the “3D Structure” column, to the right of each predicted epitope, it is possible to view its 3D structure mapping. In the option “Click here to view the waste scores,” at the bottom of the forecast results page, it is possible to view the 2D score chart (s) of the sequence(s).

The available options may vary slightly in future updated versions.

2.5 CBTOPE (Support Vector Machine)

CBTOPE is a B-cell conformational epitope prediction based on a support vector machine (SVM) model. CBTOPE allows predicting the conformational B-cell epitope on an antigen from the primary sequence [15]. The server is accessible at <http://crdd.osdd.net/raghava/cbtope/>.

2.5.1 Usage

1. Add the protein sequence name (optional).
It can contain any letter and numbers with “-” or “_”. All other characters are not allowed.
2. E-mail address (optional).
The result can be sent by e-mail.
3. Submission and sequence format.
For submission, it is necessary to type or paste the amino acid sequence in FASTA format or specify as a file.
4. SVM Threshold and Output.
Each amino acid in the sequence gets an SVM score. It is necessary to define the limit above which the amino acid residue will be considered as an epitope, the default is -0.3 . A higher value generates high reliability and specificity. Residues are highlighted if the SVM score is greater than the specified limit.
The PSIPRED program predicts the state of the secondary structure of each residue.
5. Click on “Run prediction.”
6. The results will be returned when the forecast is ready. The response time depends on the system load. The individual results are shown separately and in detail in four columns (Fig. 3): (1) amino acid position, (2) amino acid sequence, (3) probability scale (0–9) for each amino acid (above 4 scale can be considered as epitope residue), (4) secondary structure state of each residue as predicted by ‘psipred’ standalone program. H=Helical, E = Beta Sheet, C=Coil/turns.

The available options may vary slightly in future updated versions.

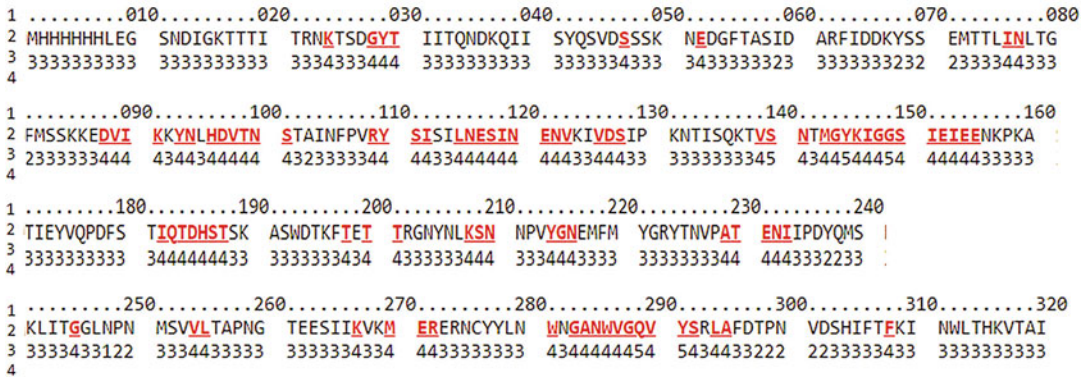


Fig. 3 The adapted output page, showing CBTOPE prediction for the query sequence (CPB)

2.6 BCPREDS

BCPREDS is a web server for B-cell epitope prediction based on string kernels, a model similar to support-vector machines (SVMs) but more specific for string-based classification tasks [16]. The server is available at <http://ailab-projects1.ist.psu.edu:8080/bcpred/predict.html>.

2.6.1 Usage

1. Paste the sequence in the input area.
2. Select one of the prediction methods: (1) amino acid pair (AAP) antigenicity scale; (2) BCPred; (3) FBCPred. For the methods AAP and BCPred, the default epitope length is 20, but it might be changed to any even value between 12 and 22. For the FBCPred, the default length is 14.
3. Select specificity. In default settings specificity is 75%.
4. Optional: select the option “report only non-overlapping epitopes.”
5. Click on the “Submit Query” button.

2.6.2 The Output

The results will be returned when the forecast is ready. The response time depends on the system load. A table indicates the position, sequence, and score of each predicted epitope, just below, the complete protein sequence is visible, with the epitopes identified in E (in red) (Fig. 4).

The available options may vary slightly in future updated versions.

3 MHC Epitope Prediction

Major histocompatibility complex (MHC) epitope prediction, both for MHC class I (MHC-I) and MHC class II (MHC-II), can be performed using the same machine learning techniques employed

BCPREDS Server 1.0

Submitted sequence: 336 amino acids
 Epitope length: 20 amino acids
 Classifier Specificity: 75%
 Prediction method: bcpred
 Use overlap filter: yes

BCPred Predictions

Position	Epitope	Score
29	DIGKTTTITRNKTS DGYTII	0.997
165	GSIEIEENKPKASIESEYAE	0.994
201	DHSTSKASWDTKFTETTRGN	0.984
237	YGRYTNVPATENIIPDYQMS	0.975
272	TAPNGTEESI IKVKMERERN	0.965
57	SYQSV DSSSKNEDGFTASID	0.944
141	IVDSIPKNTISQKT VSN TMG	0.896
303	VGQVYSRLAFDTPNVDSHIF	0.867
108	KYNLHDVTNSTAINFPVRY S	0.843
78	RFIDDKYSSEMTTLINLTGF	0.76

```

1           11           21           31           41           51           60
|           |           |           |           |           |           |
MKKKFISLVIVSSLLNGCLSPTLVYANDIGKTTTITRNKTS DGYTIIITQNDKQIISYQS 60
.....EEEEEEEEEEEEEEEEEEEE.....EEEE
VDSSSKNEDGFTASIDARFIDDKYSSEMTTLINLTGMSSKKEDVIKKYNLHDVTNSTAI 120
EEEEEEEEEEEEEEEEEEEE.EEEEEEEEEEEEEEEEEEEEE.....EEEEEEEEEEEEEE
NFPVRY SISILNESINENVKIVDSIPKNTISQKT VSN TMGKIGSGSIEIEENKPKASIES 180
EEEEEE.....EEEEEEEEEEEEEEEEEEEE.....EEEEEEEEEEEEEEEEEEEE
EYAESSTIEYVQPDFSTIQT DHSTSKASWDTKFTETTRGNYNLKSNNPVYGNEMFMYGRY 240
EEEE.....EEEEEEEEEEEEEEEEEEEE.....EEEEEEEEEEEEEEEEEEEEEEEE
TNVPATENIIPDYQMSKLITGGLNPNMSVVL TAPNGTEESI IKVKMERERNCYLWNGA 300
EEEEEEEEEEEEEEEEEEEE.....EEEEEEEEEEEEEEEEEEEE.....
NWVGQVYSRLAFDTPNVDSHIFTFKINWLTHKVTAI 336
..EEEEEEEEEEEEEEEEEEEE.....
    
```

Fig. 4 The output page, showing BCPREDS prediction for the query sequence (CPB)

for other epitope classes. For this purpose, the algorithms from the family NetMHC and its derivatives (NetMHC-II, NetMHCpan, and NetMHCIIpan) are the default choice and are all based on artificial neural networks.

3.1 NetMHC

NetMHC is a neural network-based MHC class I epitope prediction tool which comprises models for different MHC alleles for humans and other model organisms (e.g., chimpanzee, pig,

mouse), along with the possibility of the user choosing the length of the epitope to be analyzed [17]. The server is available at <http://www.cbs.dtu.dk/services/NetMHC/>.

3.1.1 Usage

1. Paste the protein(s) sequence(s) to be analyzed in FASTA format or upload a file containing them.
2. Choose the peptide length(s) to be analyzed. Multiple values may be chosen, but each one will be analyzed separately. Best results are usually observed with 9mer peptides.
3. Choose the organism and the allele profiles to be analyzed (max number: 20).
4. Optional: Define the threshold for the strong binder and weak binders % Rank. By default, these values are, respectively, 0.5 and 2.0%. The % Rank metric is the recommended reference value to be used in the identification of epitopes.
5. Optional: Select the “Sort by predicted affinity” checkbox.
6. Optional: Select the “Save output in XLS format” if you want to further analyze the results using spreadsheets or some *script* (e.g., Python, R).
7. Submit the sequence(s).

3.1.2 Output

The results of the NetMHC algorithm are presented in a tabular form. For each MHC allele and peptide length that was selected, a series of rows are included following a “sliding window” arrangement (by default), although it is also possible to sort the lines by affinity by selecting the proper setting on the input form. Along with the identification of the MHC allele and the peptide, the results also show the part of the peptide which interacts with the MHC molecule, the affinity (in both nanoMolar and log-transformed values), and %Rank metric and a flag value that is used to indicate those peptides which are predicted as weak or strong binders.

The available options may vary slightly in future updated versions.

3.2 NetMHC-II

NetMHC-II is a neural network-based MHC class II epitope prediction tool and has an interface similar to NetMHC, although only supporting the analysis of MHC alleles from humans (HLA) and mice (H-2) [18].

3.2.1 Usage

1. Paste the protein(s) sequence(s) to be analyzed in FASTA format or upload a file containing them.
2. Choose the peptide length(s) to be analyzed.
3. MHC loci and alleles to be analyzed.

4. Optional: Define the *threshold* to reduce the number of peptides returned.
5. Optional: Define the *threshold* for the strong binder and weak binders % Rank. By default, these values are, respectively, 2 and 10%. The % Rank metric is the recommended reference value to be used in the identification of epitopes.
6. Optional: Select the “Sort by affinity” checkbox.
7. Submit the sequence(s).

3.2.2 Output

The results of the NetMHC-II algorithm are presented in a tabular form and are similar to those generated by NetMHC, with a sliding window organization using by default when arranging the rows of the table. The “Identity Bind Level” attribute might be used to select those peptides with weak or strong affinity, which are respectively marked with a “WB” and “SB” flag. Thus, it is possible to select these peptides the ones that present the higher affinity (indicated with smaller nanoMolar values).

The available options may vary slightly in future updated versions.

4 Structural Vaccinology

Structural vaccinology is a rational approach used in the development of an effective and safe vaccine, which involves determining the tertiary structure of the antigen or the immune antigen–receptor complex. In addition, the projection of a stable and immunogenic vaccine antigen, composed of a single or multiepitope, must include physicochemical, immunological, and immunoinformatics knowledge. The antigen can be analyzed on different platforms based on its structural information, as shown below.

- Structural visualization of the target protein using PyMOL [19], PPM server [20], and molecular Doking [21]—PyMOL is a program written in Python programming language, which finds great application in the visualization, interpretation, and analysis of structural data. In PyMOL, it is possible to produce high-quality 3D images of small molecules and biological macromolecules, such as those generated from the analysis of the structure of target proteins, to select the immunogenic and exposed regions. The PPM Server calculates the rotational and translational positions of the transmembrane and peripheral proteins in the membranes using its 3D structure, which allows to identify the correct orientation of the protein in the cell membrane. This server is found in the Orientations of Proteins in Membranes (OPMs) database. OPMs include all structures of transmembrane proteins and some peripheral proteins and active

membrane peptides, among other data and functions. Molecular Docking allows the determination of patterns of interaction with MHC alleles by ClusPRO V.2. This server performs the task of energy minimization, calculation of the connection energy scores of the coupled complex and electrostatic complementarity/shape.

- Final molecule: The predicted epitopes can be linked to each other via rigid and flexible linkers. Flexible linkers are generally made up of nonpolar (e.g., Gly) or polar (e.g., Ser or Thr) amino acids. The reduced size of these amino acids provides flexibility and allows mobility of functional domains. The most commonly used flexible linker is GS linker (GGGGS) [22]. Rigid alpha helix (EAAAK) linkers have been used in the fusion of multi-epitope chimeras [23, 24]. The flexible ligand GS improves folding and stability in several examples of fusion proteins. Rigid ligands are preferable in cases where sufficient separation of the protein domains is necessary, as they can efficiently keep the protein portions at a distance. The insertion of the ligand may be a viable approach to improve the level of expression of fusion proteins. Both flexible and rigid ligands are stable in vivo and do not allow the separation of joined proteins.
- Evaluation of antigenicity (Vaxijen v.2) [25], allergenicity (AlgPred) [26], and physical-chemical properties with the ProtParam server [27]. Vaxijen v.2 operates by classifying antigens according to the physicochemical properties of proteins, without resorting to sequence alignment. When the results are obtained, it is possible to visualize the probability of the antigen being antigenic, demonstrating the prediction of protective antigens. AlgPred operates based on the similarity of a known epitope, which allowed the prediction of allergenic proteins. In addition, the mapping of the IgE epitope (s) characteristic allows the location of the epitope in the target protein to be located. Assessing this factor can limit the onset or development of diseases and the triggering of symptoms by proteins with high allergenicity. ProtParam is able to identify several physical-chemical parameters (isoelectric point, half-life, solubility, molecular weight, aliphatic index, and average hydrophobicity). Taken together, both the factors are essential for the rational selection of different antigens for further evaluation of immunogenicity in vivo.
- The structural modeling, refinement, and validation of the final model can be investigated using the SOPMA/Raptor-x server [28], Galaxy Refine [29], and ProSA-web server [30], respectively. Raptor-X: Determines secondary and tertiary protein structures, solvent accessibility, contact and distance map, disordered regions, functional annotation, and binding sites. In this sense, the self-optimized prediction method (SOPM)

contributes in order to improve the success rate in the prediction of the secondary structure of proteins. GalaxyRefine can improve the quality of the global and local structure. Widely used for the purpose of prediction, refinement, and related protein structure methods, it can be used to refine model structures obtained from available structure prediction methods. ProSA-web can be used to validate the structures before being submitted to the PDB. Extremely useful in the early stages of determination and refinement, as poorly bent structures are sometimes revealed after the results become available. Therefore, diagnostic tools that reveal unusual structures and problematic parts of a structure are essential in the characterization of proteins, minimizing possible limitations in the practice (in vitro, in vivo) of future research.

References

1. Popoff MR, Bouvet P (2009) Clostridial toxins. *Future Microbiol* 4:1021–1064
2. Riley TV, Lyras D, Douce GR (2019) Status of vaccine research and development for *Clostridium difficile*. *Vaccine* 37(50):7300–7306
3. Bazmara S, Shadmani M, Ghasemnejad A, Aghazadeh H et al (2019) In silico rational design of a novel tetra-epitope tetanus vaccine with complete population coverage using developed immunoinformatics and surface epitope mapping approaches. *Med Hypotheses* 130:109267
4. Ferreira MRA, Moreira GMSG, Da Cunha CEP, Mendonça M et al (2016) Recombinant alpha, beta, and epsilon toxins of *Clostridium perfringens*: production strategies and applications as veterinary vaccines. *Toxins* 8(11):340
5. Chauhan V, Singh MP (2020) Immunoinformatics approach to design a multi-epitope vaccine to combat cytomegalovirus infection. *Eur J Pharm Sci* 147:105279
6. Zhou J, Wang L, Zhou A, Lu G, Li Q, Wang Z, Zhu M, Zhou H, Cong H, He S (2016) Bioinformatics analysis and expression of a novel protein ROP48 in *Toxoplasma gondii*. *Acta Parasitol* 61:319–328
7. Wang Y (2020) Bioinformatics analysis of NetF proteins for designing a multi-epitope vaccine against *Clostridium perfringens* infection. *Infect Genet Evol* 85:2–9
8. Nazarian S, Mousavi Gargari SL, Rasooli I, Amani J et al (2012) An in silico chimeric multi subunit vaccine targeting virulence factors of enterotoxigenic *Escherichia coli* (ETEC) with its bacterial inbuilt adjuvant. *J Microbiol Methods* 90(1):36–45
9. Nosrati M, Hajizade A, Nazarian S, Amani J et al (2019) Designing a multi-epitope vaccine for cross-protection against *Shigella* spp: an immunoinformatics and structural vaccinology study. *Mol Immunol* 116:106–116
10. Kazi A, Chuah C, Majeed ABA, Leow CH et al (2018) Current progress of immunoinformatics approach harnessed for cellular- and antibody-dependent vaccine design. *Pathog Glob Health* 112(3):123–131
11. Saha S, Raghava G (2006) Prediction of continuous B-cell epitopes in an antigen using recurrent neural network. *Proteins: Structure, Function, and Bioinformatics* 65(1):40–48
12. Jespersen MC, Peters B, Nielsen M, Marcotili P (2017) BepiPred-2.0: improving sequence-based B-cell epitope prediction using conformational epitopes. *Nucl Acids Res* 45(1):24–29
13. Kringelum J V, Lundegaard C, Lund O, Nielsen M (2012) Reliable B cell epitope predictions: impacts of method development and improved benchmarking. *PLoS Comput Biol* 8(12):e1002829
14. Ponomarenko J, Bui H H, Li W, Fusseder N, Bourne P E, Sette A, Peters B (2008) ElliPro: a new structure-based tool for the prediction of antibody epitopes. *BMC Bioinform* 9(1):1–8
15. Ansari H R, Raghava G P (2010) Identification of conformational B-cell Epitopes in an antigen from its primary sequence. *Immun Res* 6(1):1–9
16. EL-Manzalawy Y, Dobbs D, Honavar V (2008) Predicting linear B-cell epitopes using string kernels. *J Mol Recognit: An Interdiscip J* 21(4):243–255

17. Andreatta M, Nielsen M (2016) Gapped sequence alignment using artificial neural networks: application to the MHC class I system. *Bioinformatics* 32(4):511–517
18. Jensen K K, Andreatta M, Marcatili P, Buus S, Greenbaum J A, Yan Z, Nielsen M (2018) Improved methods for predicting peptide binding affinity to MHC class II molecules. *Immunology* 154(3):394–406
19. DeLano W L (2002) Pymol: An open-source molecular graphics tool. *CCP4 Newslett Prot Crystallogr* 40(1):82–92
20. Lomize M A, Pogozheva I D, Joo H, Mosberg H I, Lomize A L (2012) OPM database and PPM web server: resources for positioning of proteins in membranes. *Nucl Acids Res* 40(1):370–376
21. Morris G M, Lim-Wilby M (2008) Molecular docking. In *Molecular modeling of proteins*. Humana Press 365–382
22. Chen X, Zaro J L, Shen W C (2013) Fusion protein linkers: property, design and functionality. *Adv Drug Delivery Rev* 65(10):1357–1369
23. Amet N, Lee H F, Shen W C (2009) Insertion of the designed helical linker led to increased expression of tf-based fusion proteins. *Pharma Res* 26(3):523–528
24. Bai Y, Shen W C (2006) Improving the oral efficacy of recombinant granulocyte colony-stimulating factor and transferrin fusion protein by spacer optimization. *Pharma Res* 23(9):2116–2121
25. Doytchinova I A, Flower D R (2007) VaxiJen: a server for prediction of protective antigens, tumour antigens and subunit vaccines. *BMC Bioinform* 8(1):1–7
26. Sharma N, Patiyal S, Dhall A, Pande A, Arora C, Raghava G P (2021) AlgPred 2.0: an improved method for predicting allergenic proteins and mapping of IgE epitopes. *Brief Bioinform* 22(4):bbaa294
27. Gasteiger E, Hoogland C, Gattiker A, Wilkins M R, Appel R D, Bairoch A (2005) Protein identification and analysis tools on the ExPASy server. *The Proteomics Protocols Handbook* 571–607
28. Källberg M, Wang H, Wang S, Peng J, Wang Z, Lu H, Xu J (2012) Template-based protein structure modeling using the RaptorX web server. *Nat Protoc* 7(8):1511–1522
29. Ko J, Park H, Heo L, Seo C (2012) Galaxy-WEB server for protein structure prediction and refinement. *Nucl Acids Res* 40(1):294–297
30. Wiederstein M, Sippl M J (2007) ProSA-web: interactive web service for the recognition of errors in three-dimensional structures of proteins. *Nucl Acids Res* 35(2):407–410



Searching Epitope-Based Vaccines Using Bioinformatics Studies

Marlet Martínez-Archundia, G. Lizbeth Ramírez-Salinas,
Jazmin García-Machorro, and José Correa-Basurto

Abstract

Epitope-based vaccines is one of the most recent methodologies applied in bioinformatics studies. This strategy consists of identifying regions of the protein (peptides or epitopes) which show antigen properties capable of stimulating the immune system against proteins from virus, bacteria, fungi, etc. This chapter describes a general procedure to identify epitopes to be used as epitope vaccine using bioinformatics methods including primary protein sequence analyses, epitope predictor, docking, and molecular dynamics simulations for the selection of T- and B-cell epitopes.

Key words Epitopes, Promiscuity, Super-types, Surface exposition, Conservative evolution

1 Introduction

The most widely used strategy to prevent diseases caused by pathogens (viruses, bacteria, etc.) is the use of vaccines (*see Note 1*). Vaccines contain antigens which are recognized by the immune system causing immune responses [1] The first vaccines developed for humans consist of live attenuated or killed microorganisms. These vaccines contain the whole organism which provokes long-lasting innate and adaptive immune responses. However, traditional vaccines have some disadvantages, such as the probability of allergic reactions, high reactogenicity, risk of infection due to attenuate microorganisms, as well as difficulties to vaccine production, and their low stability that require low temperatures [2].

Due to growth in scientific knowledge, it is now possible to investigate the recognition process of antigens by the immune system that allows designing new strategies for the development of vaccines such as peptide vaccines [1]. This could be possible by using immunoinformatics strategy that allow getting promising

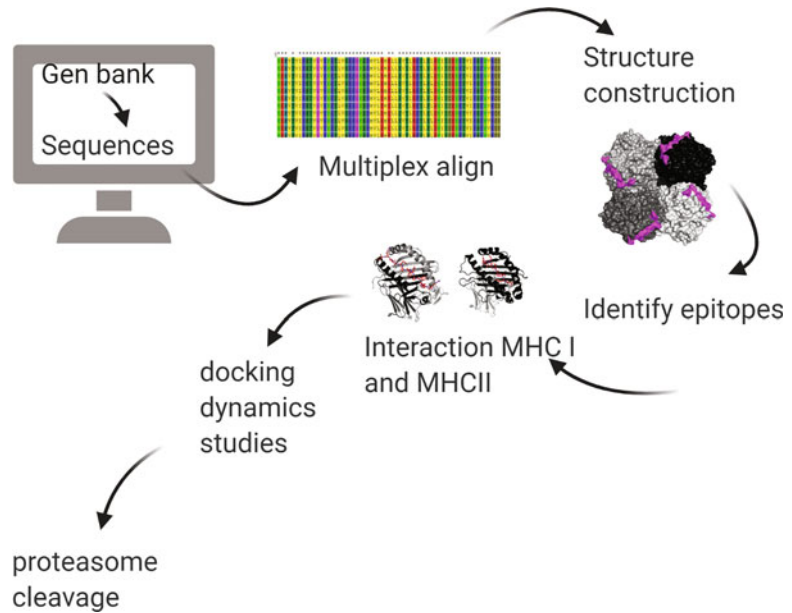


Fig. 1 Scheme of immunoinformatic strategies to get promissory immunogenic peptides that could be use as possible vaccines

epitopes in the shortest time (Fig. 1). Vaccines based on epitopes (peptides) consist of the identification of peptides that are capable of binding to proteins located on cells of the immune system. These form peptide–protein complexes are capable of inducing specific immune responses [1]. The peptide-based vaccine strategy shows several advantages compared to whole-organism-based vaccines, including lack of infectious potential, safety, ease of production, and low allergic and reactogenic responses [2]. Furthermore, peptide-based therapeutic and preventive vaccines have been developed against various cancers with satisfactory clinical results. Also, the epitope-based vaccine strategy is currently applied on immunotherapy and prophylaxis. However, the peptide-based vaccine methodology of some peptides has demonstrated that their administration alone is not active or have poor immune response. Therefore, adjuvants or peptide carriers have been developed to induce a satisfactory immune response [1].

1.1 Epitopes and Immunity

The immune response can be classified into innate immunity and adaptive immunity. Innate immunity involves barrier surfaces such as the skin or the mucosal surfaces of the respiratory and gastrointestinal tract (it is always active). While the adaptive immune system or *acquired immunity* is activated by exposure to pathogens and acquires a long-term protective immunological memory [3].

Adaptive immunity is mediated by B and T lymphocytes that are capable of recognizing molecular fragments of antigens (proteins, carbohydrates, etc.) presented by antigen-presenting cells

(APCs). The antigens are recognized by proteins located on the surface of B and T cells, in addition, the antigens are recognized by MHC-I located at intracellular T cells [3].

The recognition process of antigens by B- and T-cell receptors can activate B and T cells inducing genetic recombination events that occur during lymphocyte development, leading to the generation of millions of different lymphocyte variants in terms of antigen recognition receptors which yield humoral and cellular immune responses [3].

1.2 Identification of B-Cell Epitopes

Once the adaptive immune system has been activated, the humoral (antibodies or immunoglobulins) response forms the first line of defense against most viral and bacterial pathogens [4]. A B-cell epitope is the structural region of antigen that binds to the immunoglobulin. These epitopes include some of these molecules: lipids, carbohydrates, nucleic acids; however, most antigens are proteins [1].

The B cells recognize antigens through B-cell receptors (BCRs), which consist of membrane-bound immunoglobulins. Upon BCR activation, the B cells are able to differentiate and secrete antibodies. Antibodies from B cells have different functions such as neutralizing toxins and microorganisms and activating complement and effector cells in order to eliminate the pathogen [3].

Once antigens are bound to BCRs, the B cells can be activated in two ways: in the presence of helper T cells (Th) or independently of T cells. However, the T-cell-independent pathway does not induce a long-time B-cell response.

1.3 Identification of T-Cell Epitopes

The second line of defense in adaptive immune system is through T lymphocytes. T cells show on their cell membrane a T-cell receptor (TCR) capable of recognizing epitopes displayed on the surface of APC by the main histocompatibility complex (MHC) molecules [3, 4]. Then, the T-cell epitopes are presented by MHC class I (MHC I) and II (MHC II) molecules that are recognized by two distinct subsets of T cells, CD8 and CD4, respectively. CD8 T cells become cytotoxic T lymphocytes (CTL) after the recognition of the epitope. Meanwhile, the CD4 T cells become helper (Th) or regulatory (Treg) T cells after the recognition of the epitope [3]. Figure 2 shows MHC-epitope complexes depicting the volume of the cavity from MHC-I (Fig. 2a) and MHC-II (Fig. 2b) which explain the kind of peptides that could recognize according to their primary sequence.

Both, the CTL and the Th perform their functions in response to T-cell epitopes located on MHC. The CTL kill the infected cells whereas the T helper cells mediate growth and differentiation of both effector T cells and antibody-producing B lymphocytes [4]. Generally, the epitopes recognized by T cells are proteins [4] and can be conformational or linear epitopes [1].

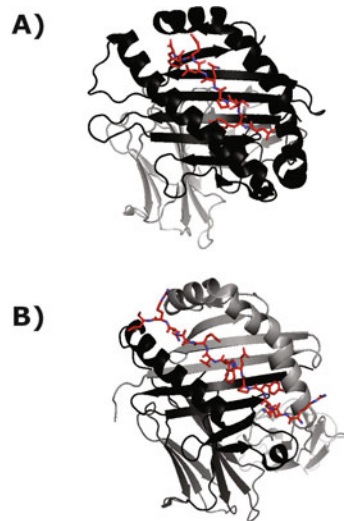


Fig. 2 Epitope-MHC complex that can be obtained by docking studies once the predicted and filtered peptides were achieved. **(a)** MHC-I-epitope complex (PDB: 4F7M). The epitope is shown in red color, and it is located in the site of recognition (groove). **(b)** The molecular recognition of the epitope in the groove of MHC-II-epitope complex (PDB: 4IS6). In both the MHC structures the groove of recognition is formed by two alpha helices and seven β -pleated sheet. One structural difference between MHC-I and MHC-II molecules, is that the groove in MHC-I is constituted by a protein subunit whereas the groove in the MHC-II molecule is constituted by two protein subunits

Thanks to the three-dimensional structural information of MHC-epitope and MCH-epitope-TCR complexes available under experimental and theoretical methods, now it is possible to apply different immunoinformatics, bioinformatics, and molecular modeling methodologies to predict structural regions of the proteins capable to bind the MHC molecules. One of the advantage of molecular modeling studies (molecular docking and molecular dynamics simulations) are due to their advantage to determine the molecular interactions and stability of the epitope-MHC complexes. These *in silico* strategies allow one to identify potential epitopes rationally faster, could be assayed by *in vitro* or *in vivo* tests and identified as potential vaccines. Additionally, by using *in silico* strategies, it is possible to develop vaccines that are capable of generating high-affinity and protective antibodies against the pathogen or disease in different populations and ethnic groups.

The development of vaccines could be carried out in different ethnic groups due to variation in MHC molecules expressed in different human races [5]. These identified MHC molecules are called super-types. Therefore, the grouping of MHC molecules into super-types is relevant for the formulation of vaccines based

on epitopes, and the selection of those epitopes that are recognized by the MHC super-types is essential; such selection will provide a wide coverage of the population [5, 6]. Among other factors that improve the efficiency of peptide-based vaccines is the promiscuity in which the epitope is capable of recognizing different MHC molecules by stimulating the immune system [7].

Another characteristic of the epitopes to be successful is the sequence evolution conservation. To this end, it is recommendable to select those epitopes located on highly conserved regions of the target protein. It is important because some point mutations could affect the epitope-MHC complex while failing during immune activation [8]. Using conserved epitopes allows to obtain long lasting immunity of the vaccine despite the appearance of constant mutations as observed in RNA viruses [8].

It is also important to consider that peptide processing by proteasomes can affect the binding on MHC I [9]. Therefore, it is necessary to submit the selected peptides to different studies including proteasome degradation *in silico*, to explore their binding properties to MHC molecules [9, 10].

2 Materials

1. Muscle/EBI server.
2. Clustal X 2.0.11 program.
3. PDB server.
4. Swiss Model server.
5. Modeller 9.27 program.
6. PDBSUM server.
7. ERRAT server.
8. NetMHC server.
9. NetMHCII server.
10. ABCpred server.
11. VMD program.
12. PCPS server.
13. CLUSPRO 2.0 server.
14. Amber 16 program.
15. NAMD 2.6 program.
16. CARMA program.
17. CPU or GPU to run Amber an NAMD programs.

3 Methods

3.1 General Protocol for the Search and Selection of Epitopes

1. Retrieve the full primary sequences of proteins reported in a certain period and consider if there are different strains, subtypes, species, etc. It is recommended to align sequences for each subtype, group, or family through the Muscle/EBI server (<http://www.ebi.ac.uk/Tools/msa/muscle/>) and the Clustal X 2.0.11 program (*see Note 2*).
2. The quaternary structure of the protein consensus sequence is modeled by using the Swiss Model server (<https://swissmodel.expasy.org/>) (*see Note 3*). It is highly recommended to use as a template; high-resolution crystal structures of proteins. Example For the H1N1 HA consensus sequence, we have used the Modeller 9.10 program [11] to build 3D models of multi-chain HA by employing a multi-trimer template HA (PDB ID: 1RUY). Their stereo-chemical qualities are also evaluated by analyzing the Ramachandran plots and using the PDBSUM (<https://www.ebi.ac.uk/thornton-srv/databases/cgi-bin/pdbsum/GetPage.pl?pdbcode=index.html>) and ERRAT servers (<https://servicesn.mbi.ucla.edu/ERRAT/>).
3. The protein consensus sequences are submit to the NetMHC 3.2 [12] (<http://www.cbs.dtu.dk/services/NetMHC-3.2/>), NetMHCII 2.2 (<http://www.cbs.dtu.dk/services/NetMHCII/>), and the ABCpred Prediction servers (<http://www.imtech.res.in/raghava/abcpred/>) are used to identify epitopes capable of interacting with MHC I, MHC II, and B cells, respectively (*see Note 4*). For this purpose, it is recommended to be focused on alleles that are deemed supertypes to MHC I (HLA-B*39:01, HLA-B*1501, HLA-A*0201, HLA-A*0301, HLA-A*2601, HLA-B*0702, and HLA-B*5801) and MHC II (HLA-DRB1*0101, HLA-DRB1*0301, HLA-DRB1*0401, HLA-DRB1*0701, HLA-DRB1*0801, HLA-DRB1*1101, HLA-DRB1*1301, and HLA-DRB1*1501).
4. We also select epitopes based on the promiscuity criteria among the subtypes, which include the degree of conservation and their surface localization on the quaternary structure of the proteins. We determine the degree of exposition of the regions by visual inspection using the VMD program [13] (Fig. 3) (*see Note 5*).
5. We predict proteasome and immunoproteasome cleavage using the Proteasome Cleavage Prediction Server, PCPS (<http://imed.med.ucm.es/Tools/pcps/index.html>) to verify epitope structural stability. The PCPS yielded fragments of peptides ranging from 9 to 21 residues in length. These peptides are

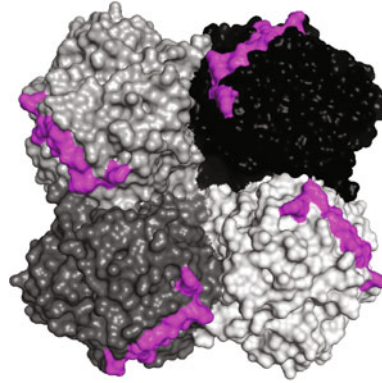


Fig. 3 Three-dimensional location of exposed epitopes on quaternary structure from neuraminidase (PDB: 4B7Q). The exposed peptides on the protein surface are colored in pink (neuraminidase peptide: 258–270, PDB: 4B7Q). It can also be observed that the tetramer of the neuraminidase in which four regions are marked in pink color, where each of the regions shows a peptide in the subunits of the protein

submitted to the NetMHC 3.2 and NetMHCII 2.2 servers to determine whether they maintained their immunogenic properties.

6. The CLUSPRO 2.0 server [14] (<https://cluspro.bu.edu/publications.php>) is used to perform the docking study of the epitope peptides on the MHC class II HLA-DR4 molecules (PDB: 1D5M) (*see Note 6*). Additionally, docking studies of the target peptides on MHC-I HLA-B5703 (PDB: 2VBQ) are performed.
7. The parameters that are used for the MHC-II/I-peptide complexes are obtained from the ff14SB force field. The topologies for the MHC-II-peptide complexes are built by the LEaP module and minimized and equilibrated through the Sander module and pmemd.cuda in Amber 16 through the use of graphical unit processors. The MHC-II/I-peptide complexes are submitted to 100-ns-long MD simulations with the MMGBSA approach to obtain their binding free energy values.
8. MD simulations are performed using NAMD 2.6 [15] with the CHARMM27 force field [16] (*see Note 7*). First, the system is embedded in a solvated water box and neutralized with 23 Na⁺ atoms. All water molecules are closer to 3.8 Å than to any atoms of the protein that did not possess hydrogen atoms. Prior to the MD simulations, the system is submitted to an equilibrium process, which started with an initial minimization, with all backbone atoms fixed. Afterward, the whole system (without structural restrictions for protein) is heated from 0 to 30 K with short MD simulations (30 steps). Then the MD simulations continued under the NTP protocol to reduce

anomalous initial contacts and to fill the empty spaces. A 30-ns-long MD simulation is performed under NTV assembly to execute the structural analyses. All simulations are performed on a Linux cluster of 19 nodes with 4 cores each. The trajectory data is saved every 2 ps and subsequently analyzed using the CARMA program [17]. All snapshots for the epitope–MHC complex are taken at 1-ns intervals, and they are then visualized using the visual molecular dynamics (VMD) program [13].

In addition, the CARMA program [13] is used to obtain root-mean-square deviations (RMSD), the root-mean-square fluctuations (RMSF), and the radius of gyration (Rg).

4 Notes

1. The first step is to identify the diseases and concentrate on pathogens such as virus, bacterium, or cancer antigens. Identify the protein target and determine three dimensional (3D) structure and protein posttranslational modifications.
2. Once the protein has been selected, a search of potential epitopes is carried out including some criteria such as external localization, residue contents, MHC-peptide affinity, etc.
3. Search for 3D structure or build the target protein including the membrane surfaces and intermonomeric structures which in some cases is difficult to find due to the lack of structure characterization.
4. Search for linear or conformational epitopes using epitope predictors that sometimes could be combined using different epitope predictors.
5. Some epitopes are excluded due to their internal localization into the protein structures, oversize to either MHC-I or MHC-II, low evolutionary conservation and low score per program.
6. Performing molecular docking studies of peptides on MHC could not yield reliable results due to the rigid structure of the MHC target.
7. Finally, performing molecular dynamics (MD) simulations of peptide-MHC complexes. Do not always rely on experimental data as parameters such as biological environments and membranes are not considered.

Acknowledgments

We gratefully acknowledge to CONACYT (Grant 312807), SIP/-COFAA-IPN.

References

1. Patronov A, Doytchinova I (2013) T-cell epitope vaccine design by immunoinformatics. *Open Biol* 3(1):120139
2. Negahdaripour M, Golkar N, Hajjighahramani N, Kianpour S, Nezafat N, Ghasemi Y (2017) Aprovechamiento de nanopartículas de péptidos autoensambladas en el diseño de vacunas de epítomos. *Biotechnol Adv* 35(5):575–596. <https://doi.org/10.1016/j.biotechadv.2017.05.002>
3. Sanchez-Trincado JL, Gomez-Perosanz M, Reche PA (2017) Fundamentals and methods for T- and B-cell epitope prediction. *J Immunol Res* 2017:2680160. <https://doi.org/10.1155/2017/2680160>
4. De Groot AS, Moise L, McMurry JA, Martin W (2008) Epitope-based immunome-derived vaccines: a strategy for improved design and safety. *Clin Appl Immunomics* 2:39–69. https://doi.org/10.1007/978-0-387-79208-8_3
5. Reche PA, Reinherz EL (2007) Definition of MHC supertypes through clustering of MHC peptide-binding repertoires. *Methods Mol Biol* 409:163–173. https://doi.org/10.1007/978-1-60327-118-9_11
6. Doytchinova IA, Guan P, Flower DR (2004 Apr 1) Identifying human MHC supertypes using bioinformatic methods. *J Immunol* 172(7):4314–4323. <https://doi.org/10.4049/jimmunol.172.7.4314>
7. Frahm N, Yusim K, Suscovich TJ et al (2007) Extensive HLA class I allele promiscuity among viral CTL epitopes. *Eur J Immunol* 37(9):2419–2433. <https://doi.org/10.1002/eji.200737365>
8. Bui HH, Sidney J, Li W, Fusseder N, Sette A (2007) Development of an epitope conservancy analysis tool to facilitate the design of epitope-based diagnostics and vaccines. *BMC Bioinformatics* 8:361
9. Diez-Rivero CM, Lafuente EM, Reche PA (2010) Computational analysis and modeling of cleavage by the immunoproteasome and the constitutive proteasome. *BMC Bioinformatics* 11:479. <https://doi.org/10.1186/1471-2105-11-479>
10. Tenzer S, Peters B, Bulik S, Schoor O, Lemmel C, Schatz MM, Kloetzel PM, Ramensee HG, Schild H, Holzhütter HG (2005) Modeling the MHC class I pathway by combining predictions of proteasomal cleavage, TAP transport and MHC class I binding. *Cell Mol Life Sci* 62(9):1025–1037. <https://doi.org/10.1007/s00018-005-4528-2>
11. Eswar N, Webb B, Marti-Renom MA, Madhusudhan MS, Eramian D, Shen MY, Pieper U, Sali A (2006) Comparative protein structure modeling using Modeller. *Curr Protoc Bioinformatics* Chapter 5:Unit-5.6. <https://doi.org/10.1002/0471250953.bi0506s15>
12. Lundegaard C, Lund O, Nielsen M (2011) Prediction of epitopes using neural network based methods. *J Immunol Methods* 374(1–2):26–34. <https://doi.org/10.1016/j.jim.2010.10.011>
13. Humphrey W, Dalke A, Schulten K (1996) VMD: visual molecular dynamics. *J Mol Graph* 14:33–38. 27–8
14. Kozakov D, Hall DR, Xia B, Porter KA, Pothorny D, Yueh C, Beglov D, Vajda S (2017) The ClusPro web server for protein-protein docking. *Nat Protoc* 12(2):255–278
15. Phillips JC, Braun R, Wang W, Gumbart J, Tajkhorshid E, Villa E, Chipot C, Skeel RD, Kalé L, Schulten K (2005) Scalable molecular dynamics with NAMD. *J Comput Chem* 16:1781–1802
16. MacKerell AD Jr, Bashford D, Bellott M, Dunbrack RL Jr, Evanseck J, Field MJ, Fischer S, Gao J, Guo H, Ha S, Joseph D, Kuchnir L, Kuczera K, Lau FTK, Mattos C, Michnick S, Ngo T, Nguyen DT, Prodhom B, Reiher IWE, Roux B, Schlenkrich M, Smith J, Stote R, Straub J, Watanabe M, Wiorkiewicz-Kuczera J, Yin D, Karplus M (1998) All-atom empirical potential for molecular modeling and dynamics studies of proteins. *J Phys Chem B* 102:3586–3616
17. Glykos NM (2006) Carma: a molecular dynamics analysis program. *J Comput Chem* 27:1765–1768

Part VI

Vaccine Safety and Regulation



The Regulatory Evaluation of Vaccines for Human Use

Norman W. Baylor

Abstract

A vaccine is an immunogen, the administration of which is intended to stimulate the immune system to prevent, ameliorate, or treat a disease or infection. A vaccine may be a live attenuated preparation of microorganisms, inactivated (killed) whole organisms, living irradiated cells, crude fractions, or purified immunogens, including those derived from recombinant DNA in a host cell, conjugates formed by covalent linkage of components, synthetic antigens, polynucleotides (such as the plasmid DNA vaccines), mRNA, living vectored cells expressing specific heterologous immunogens, or cells pulsed with immunogen. Vaccines are highly complex products that differ from small molecule drugs because of the biological nature of the source materials such as those derived from microorganisms as well as the various cell substrates from which some are derived. Regardless of the technology used, because of their complexities, vaccines must undergo extensive testing and characterization. Special expertise and procedures are required for the manufacture, control, and regulation of vaccines. Throughout their life cycle from preclinical evaluation to post-licensure lot release testing, vaccines are subject to rigorous testing and oversight by manufacturers and national regulatory authorities. In this chapter, an overview of the regulatory evaluation and testing requirements for vaccines is presented.

Key words Vaccines, Regulatory, Manufacturing, Licensing, IND, Biologics

1 Introduction

The Food and Drug Administration (FDA) is the National Regulatory Authority (NRA) in the United States responsible for assuring quality, safety, and effectiveness of all human medical products, including vaccines for human use. The Center for Biologics Evaluation and Research (CBER) within the US FDA is responsible for overseeing the regulation of therapeutic and preventative vaccines against infectious diseases. Vaccines are regulated as biologics. Authority for the regulation of vaccines resides in Section 351 of the Public Health Service Act and specific sections of the Federal Food, Drug and Cosmetic Act (FD&C). For FDA licensure, a single set of regulatory requirements applies to all vaccines, regardless of the technology used to produce them. Section 351 of the

Public Health Service Act (42 U.S.C. 262) states that a biologics license application shall be approved based on a demonstration that “... (I) the biological product that is the subject of the application is safe, pure and potent; and (II) the facility in which the biological product is manufactured, processed, packed or held meets standards designed to assure that the biological product continues to be safe, pure, and potent...” [1].

Vaccines, whether prophylactic (measles, polio, HPV, etc.) or therapeutic (HIV or other chronic infectious diseases, etc.), are subject to the same regulations as other biological products and are required to be manufactured to meet strict standards set by National Regulatory Authorities (NRA) such as the US FDA. While vaccine manufacturers have the primary legal responsibility for assuring the safety, quality, and effectiveness of the products they manufacture and distribute, it is the NRAs who have the legal authority of enforcement to ensure product quality, safety, and effectiveness. Moreover, NRAs are responsible for the review and authorization of clinical trials, approval of licensing applications and lot release, and monitoring the performance of the product throughout its life cycle. The FDA also publishes guidance documents, although not legally enforceable, which provide sponsors and manufacturers with FDA’s current thinking on various regulatory and scientific topics (Table 1).

Biological products, including vaccines, are distinguished from chemical pharmaceuticals primarily due to their derivation from living organisms with an innate molecular complexity that cannot be defined by physical or chemical means alone. In addition, the intrinsic variability of living organisms, and the potential for contamination of materials with adventitious agents, which may come from starting materials or the environment, requires special quality control and quality assurance mechanisms. Moreover, vaccines are inherently more difficult to develop, characterize, and manufacture than most pharmaceutical products.

2 Vaccine Types

Advances in vaccine research and development as well as immunology has enabled the discovery of numerous types of vaccines, many of which have been proven to be safe and elicit robust immune responses that protect against human infectious diseases. Novel vaccine strategies for the prevention of existing and emerging infectious diseases continue to be investigated. Major advances in understanding the complex interactions between microbes and their human hosts have occurred over recent decades. These insights, as well as advances in assay development, laboratory techniques, and novel technologies have also contributed to the

Table 1
Current guidance documents applicable to development, manufacture, licensure, and use of vaccines^a

Guidance documents
Emergency Use Authorization for Vaccines to Prevent COVID-19; Guidance for Industry, October 2020
Development and Licensure of Vaccines to Prevent COVID-19; Guidance for Industry CBER, June 2020
Submitting Study Datasets for Vaccines to the Office of Vaccines Research and Review; Guidance for Industry; Technical Specifications Document, 12/2019
Providing Submissions in Electronic Format—Postmarketing Safety Reports for Vaccines—Guidance for Industry, 8/2015
Guidance for Industry: General Principles for the Development of Vaccines to Protect Against Global Infectious Diseases (PDF - 57KB) ,12/2011
Guidance for Industry: Clinical Considerations for Therapeutic Cancer Vaccines, 10/2011
Guidance for Industry: Characterization and Qualification of Cell Substrates and Other Biological Materials Used in the Production of Viral Vaccines for Infectious Disease Indications, 2/2010
Guidance for Industry: Considerations for Plasmid DNA Vaccines for Infectious Disease Indications, 11/2007
Guidance for Industry: Toxicity Grading Scale for Healthy Adult and Adolescent Volunteers Enrolled in Preventive Vaccine Clinical Trials , 9/27/2007
Guidance for Industry: Clinical Data Needed to Support the Licensure of Pandemic Influenza Vaccines , 5/31/2007
Guidance for Industry: Clinical Data Needed to Support the Licensure of Seasonal Inactivated Influenza Vaccines ,5/31/2007
Guidance for Industry: Development of Preventive HIV Vaccines for Use in Pediatric Populations 5/4/2006
Guidance for Industry: Considerations for Developmental Toxicity Studies for Preventive and Therapeutic Vaccines for Infectious Disease Indications , 2/2006
Guidance for Industry: FDA Review of Vaccine Labeling Requirements for Warnings, Use Instructions, and Precautionary Information , 10/1/2004
Draft Guidance for Industry: Postmarketing Safety Reporting for Human Drug and Biological Products Including Vaccines, 3/12/2001
Guidance for Reviewers: Potency Limits for Standardized Dust Mite and Grass Allergen Vaccines: A Revised Protocol , 10/2000
Guidance for Industry: Content and Format of Chemistry, Manufacturing and Controls Information and Establishment Description Information for a Vaccine or Related Product, 1/5/1999
Guidance for Industry for the Evaluation of Combination Vaccines for Preventable Diseases: Production, Testing and Clinical Studies, 4/10/1997

^aSource: Modified from FDA Vaccine and Related Biological Product Guidances. Available at: <http://www.fda.gov/BiologicsBloodVaccines/GuidanceComplianceRegulatoryInformation/Guidances/Vaccines/>

Table 2
Summary of vaccine classification

Vaccine classification	Licensed vaccines
Live viral vaccines	Rotavirus, shingles, smallpox, polio, measles, mumps, rubella, chicken pox, influenza, yellow fever, adenovirus, Ebola Zaire, dengue
Inactivated viral vaccines	Influenza, polio, Japanese encephalitis, hepatitis A, rabies
Inactivated bacterial vaccines	Typhoid, cholera plague, diphtheria, tetanus, and pertussis toxoids
Live bacterial vaccines	BCG, cholera, typhoid
Polysaccharide and conjugated vaccines	Pneumococcal, Haemophilus influenza b, meningococcal
Subunit vaccines	Hepatitis B, HPV, acellular pertussis
Vectored vaccines	None for humans, although several in development including RSV, pandemic influenza, SARS-CoV-2
Nucleic acid vaccines (DNA, RNA, mRNA)	None for humans, although several in development, e.g., HIV, various cancer therapeutic vaccines, SARS-CoV-2

availability of new types of vaccines. Vaccines can be prophylactic or therapeutic and exist in many different forms which may contain live, attenuated virus, or inactivated microorganisms, or some unique molecular component of the organism that causes illnesses. Vaccines are generally classified as Live Attenuated, Inactivated, Subunit, Vectored, Conjugated, DNA, and RNA (Table 2). Different methods and technologies are used to manufacture and test these vaccines.

Live attenuated vaccines are developed by reducing the virulence of pathogens while maintaining their viability. Methods used to attenuate wild-type viruses or bacteria include repeated culturing in cells or culture media where the organism reproduces poorly. The resulting vaccine organisms, which retain the ability to replicate and induce immunity, usually do not cause disease. At present, most live attenuated vaccines are against viral infectious diseases. There are fewer licensed live bacterial vaccines.

Inactivated (killed) vaccines consist of either whole microorganisms or fractions of either that have been grown in culture and then killed using physical (heat or radiation) and chemical methods (usually formalin). The pathogen particles are destroyed and cannot divide, but the pathogens maintain some of their integrity to be recognized by the immune system and evoke an adaptive immune response. As for the fractional vaccines, the organism is further treated to purify only those components to be included in the vaccine (e.g., the polysaccharide capsule of pneumococcus).

Recombinant subunit vaccines contain specific highly purified antigens from infectious disease organisms or purified proteins or synthetic peptides. Subunit vaccines, like inactivated (killed)

vaccines, do not contain live components of the pathogen. Protein-based subunit vaccines present an antigen to the immune system without particles from the organism. The protein components are expressed in eukaryotic or prokaryotic expression systems (e.g., *E. coli*, yeast) using recombinant protein expression technologies.

Some vaccines against bacterial infections are based on the polysaccharides, or sugars, that form the outer coating of many bacteria. Other vaccines against bacterial illnesses, such as diphtheria and tetanus vaccines, aim to elicit immune responses against disease-causing proteins, or toxins, secreted by the bacteria. The antigens in these so-called toxoid vaccines are chemically inactivated toxins, known as toxoids.

Nucleic acid vaccines consist only of DNA, RNA, or mRNA, which is taken up and translated into protein by host cells. Nucleic acid vaccines have been widely used in infectious and malignant diseases. Unlike viruses, naked nucleic acids lack the help of essential proteins, lipids, and sugars, which are important to viral infection. To date, no RNA or DNA vaccine has been approved for humans; however, the technology has been improving, and multiple DNA vaccines have been approved for use in animals [2]. In contrast to recombinant bacteria or virus vaccines, nucleic acid vaccines consist only of DNA or RNA, which is taken up by cells and transformed into protein.

Messenger RNA (mRNA) has emerged as a novel platform technology for the development of vaccines for cancer therapeutics as well as against infectious diseases. Messenger RNA vaccines are composed of one or more nucleic acids encoding for a single or multiple vaccine antigen candidates, formulated in a delivery vehicle and then directly delivered into the host cell. These delivery vehicles may include lipid- and protein-based molecules, as well as various types of polymeric scaffolding [3]. There are several mRNA vaccines currently under clinical development against infectious diseases such as rabies and SARS-CoV-2.

Vectored vaccines use a virus or bacterium as a vector, or carrier, to introduce genetic material into cells. Several such recombinant vector vaccines are approved to protect animals from infectious diseases, including rabies and distemper; however, none are currently approved for humans. Viral vectored vaccines use live viruses to carry DNA into human cells. The DNA contained in the virus encodes antigens that, once expressed in the infected human cells, elicit an immune response. Examples of virus vector systems are retrovirus, lentivirus, vaccinia virus, adenovirus, adeno-associated virus, cytomegalovirus, and Sendai virus. Several viral vectors have been successfully used for vaccine production and gene therapy [4].

3 Vaccine Manufacturing and Testing

Vaccine manufacturing is a complex process involving analytical and formulation development to scale up the manufacturing process, finalize the formulation, and validate assays in preparation of clinical lots as well as commercial scale product (Fig. 1). A balance must be made between rapidly providing material for clinical evaluation using an interim process and delaying clinical trials until the final process, formulation, and assays are available. For each clinical trial phase, a decision must be made as to when to stop process development and establish a fixed process for the preparation of clinical materials.

The process by which a vaccine is manufactured depends on the type of antigen that makes up the vaccine. There are different vaccine-manufacturing processes depending on the specific type of antigen that makes up the vaccine. Many vaccine development processes, such as fermentation and cell culture, purification, formulation, analytical testing, and vaccine characterization, which precede the filing of an investigational new drug application (IND), may be done in parallel [5]. Process development can be divided into four interdependent categories: 1) process, analytical, and formulation development; 2) manufacture and testing of pre-clinical supplies; 3) manufacture and testing of clinical supplies (prepared according to cGMP regulations); and 4) manufacture and testing of final product for marketing authorization. In order to support clinical trials, manufacturers are expected to implement manufacturing controls that reflect product and manufacturing considerations, evolving process and product knowledge and manufacturing experience. As the process becomes better defined,

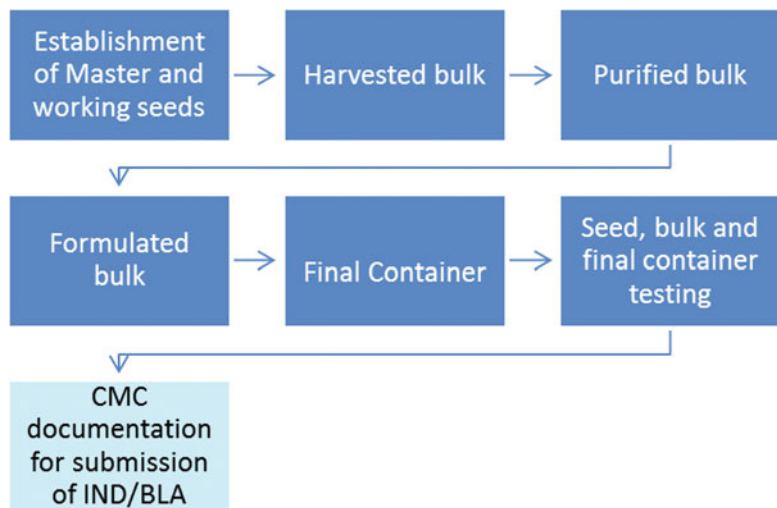


Fig. 1 Vaccine production process

critical control points are identified and experience in the process increases, and increased GMP documentation must be implemented and maintained [6].

The manufacture of most vaccines requires the growth or expression of the immunizing agent (i.e., virus, virus-like particles, recombinant proteins, etc.) in living cells. Establishing the conditions for optimization of growth and expression to obtain adequate yield is complex, and subtle changes in the process or materials can significantly affect the composition of the vaccine and its safety, effectiveness, or both. Thus, the process must be well controlled and monitored and produce a consistent, well-characterized, and reproducible product prior to its licensure. Production of the vaccine drug substance, whether by fermentation, cultivation, isolation, or synthesis, usually starts with raw materials. Subsequent steps of the procedure involve preparation, characterization, and purification of intermediates eventually resulting in the vaccine drug substance [7].

The vaccine drug substance is defined as the unformulated active (immunogenic) substance, which may be subsequently formulated with excipients to produce the drug product. The drug substance may be whole bacterial cells, viruses, or parasites (live or killed); crude or purified antigens isolated from killed or living cells; crude or purified antigens secreted from living cells; recombinant or synthetic carbohydrate, protein, or peptide antigens; polynucleotides (as in plasmid DNA vaccines); or conjugates.

The vaccine drug product is the finished dosage form of the product. The vaccine drug product contains the vaccine drug substance(s) formulated with other ingredients in the finished dosage form ready for marketing. Other ingredients, active or inactive, may include adjuvants, preservatives, stabilizers, and/or excipients. For vaccine formulation, the drug substance(s) may be diluted, adsorbed, mixed with adjuvants or additives, and/or lyophilized to become the drug product.

Upstream manufacturing responsibilities routinely include operations related to cell expansion steps starting with a single vial of frozen cells and growing these exponentially into larger systems eventually to be transferred into a large-scale terminal reactor. Downstream manufacturing, or commonly referred to as purification, is focused on the capture and isolation of a targeted molecule and the removal of impurities. This is accomplished through several different processes to include filtration, column chromatography, and tangential flow filtration.

The quality and purity of the vaccine drug substance cannot be assured solely by downstream testing but depends on proper control of the manufacturing and synthetic process as well. Proper control and attainment of minimal levels of impurities depend on full biological and physiochemical characterization such as those outlined in Table 3, as well as (1) appropriate quality and purity of

Table 3
Biological and physiochemical characterization

Biological activity	Physiochemical
<ul style="list-style-type: none"> • Specific identity testing such as Western blot analysis or ELISA • Cytometric analysis • Neurovirulence testing, if appropriate • Serotyping • Electrophoretic typing • Inactivation studies • Neutralization assays • Titrations 	<ul style="list-style-type: none"> • UV/visible or mass spectrometry • Amino acid analysis • Amino acid or nucleic acid sequencing • Peptide mapping • Determination of disulfide linkage • Sodium Dodecyl Sulfate-Polyacrylamide Gel Electrophoresis (SDS-PAGE) (reduced and nonreduced) • Isoelectric focusing (1D or 2D) • Various chromatographic methods such as HPLC, GC, LC, or thin layer chromatography • Nuclear magnetic resonance spectroscopy • Assays to detect related proteins including deamidated, oxidized, processed, and aggregated forms and other variants, such as amino acid substitutions and adducts/derivatives, and other process contaminants such as sulfhydryl reagents, urea, residual host proteins, residual DNA, and endotoxin

the starting materials, including the seed organisms, and reagents; (2) establishment and use of in-process controls for intermediates; (3) consistent adherence to validated process procedures; and (4) adequacy of the final (release) control testing of the vaccine drug substance. Even after licensure, manufacturers conduct a series of tests on the bulk, intermediate, and final vaccine products and typically are required both to meet all product and process specifications and to submit the results of key tests, along with samples of the product to CBER for evaluation prior to CBER's approval of lot release and administration of vaccine.

Regulatory requirements mandate that all licensed vaccines undergo appropriate lot testing before release. Requirements for release testing of licensed biologicals can be found in Title 21 CFR 610.27. These tests include those for bacterial and fungal sterility, general safety, purity, identity, suitability of constituent material, and potency to assess immunogenicity and/or antigen content and, depending on the nature of the vaccine and its manufacturing process, additional tests as required by the NRAs to assure vaccine safety and quality (Table 4). Depending on the product, additional testing (e.g., to ensure adequate inactivation) may be required.

A description and results of all relevant *in vivo* and *in vitro* bioassays performed on the manufacturer's reference standard lot or other relevant lots to demonstrate the potency and activity(ies) of the drug substance must also be provided, including a complete description of the protocol used for each bioassay, the control standards used, the validation of the inherent variability of the

Table 4
Lot release testing

<i>Sterility</i> —bacterial or fungal contaminants
<i>General safety test</i> —guinea pigs and mice—to detect extraneous toxic contaminants
<i>Identity test</i> —e.g., SDS SDS-PAGE, Western blot, immunologic assay, or amino acid analysis
<i>Purity</i> —e.g., % moisture, SDS SDS-PAGE, HPLC, endotoxin
<i>Potency</i> —in vivo or in vitro test to assess immunogenicity, antigen content, or chemical composition

test, and the established acceptance limits for each assay. The characteristics of specific antibodies used in immunochemical or serological assays should also be included.

Regulatory compliance in biologics manufacturing requires the implementation of a quality unit and system that is robust enough to support production throughout its clinical phase maturation. The quality unit is expected to be independent of the operations/manufacturing unit and fulfills both the quality assurance and quality control responsibilities. Their roles and responsibilities should be defined and documented. Critical roles of the quality unit are the review and approval of all quality-related documents; disposition of raw materials, intermediates, packaging, labeling materials, and the final product; conduct internal and supplier audits; review completed batch production and laboratory control records before determining disposition; approve changes that could potentially affect the intermediate and final product; and ensure the complete investigation and resolution into deviations and complaints. In biologics manufacturing, especially with Phase I material, not all critical parameters, control points, and at times raw material may all be defined or identified. Knowing this and knowing that the process will continue to grow through its clinical phases, oversight from the quality unit must ensure that the manufacturing process adheres to the foundational components of cGMPs. These foundational components are those that ensure full support of the product production and are maintained within the quality system. All components of the quality system are controlled through written and approved policies and procedures.

Vaccines, like all products that purport to be sterile, should be free of viable contaminating microorganisms to assure product safety according to FDA regulations [8]. It is not practical to demonstrate absolute sterility of a vaccine lot; however, sterility assurance is accomplished primarily by validation of the sterilization process or of the aseptic processing procedures under cGMPs. The manufacturing process must also assure that vaccines are free of extraneous material except that which is unavoidable in the manufacturing process. Testing for detection of adventitious agents should be undertaken with consideration of the possible agents

which may be present in cell substrates that may be used in the production of the vaccine. FDA regulations define purity as relative freedom from extraneous matter in the finished product, whether harmful to the recipient or deleterious to the product [9]. Final container vaccine is also required to be identified by a test specific for the product, e.g., neutralization of live viral vaccines with specific antisera. As far as constituent material, manufacturers must also ensure that all ingredients in vaccines such as preservatives, adjuvants, diluents, etc., meet generally accepted standards of purity.

Potency testing is also an important component of the manufacturing process. Potency is defined as the specific ability or capacity of a vaccine, as indicated by appropriate laboratory test or by adequately controlled clinical data obtained through the administration of the vaccine in the manner intended to effect a given result [10]. Potency is equivalent to the concept that the product must be able to perform as claimed, and if possible, this should correspond with some measurable effect in the recipient or correlate with some quantitative laboratory finding. Developing potency assays are product specific and present certain challenges due to the variety of vaccine types (Table 2), degree of purity, differing complexities, chemical heterogeneity of active moieties, and varying number of valencies or serotypes in some vaccines. Vaccine potency is only one of the tools used to ensure that a manufacturing process yields vaccines of quality consistent with that of lots proven efficacious [11].

Establishing analytical testing methods for vaccines and all intermediates is critical to assuring safety and consistency of manufacturing. Suitable analytical test methods are important components for establishing identity, quality, purity, and potency for a vaccine. Title 21 CFR 211.194(a) requires that test methods used for assessing compliance of pharmaceutical products, including vaccines, with established specifications, must meet proper standards of accuracy and reliability. While it is not necessary to have analytical methods qualified for testing process development demonstration run materials or scale-up engineering run material, all test methods need to be at least qualified for any cGMP lot material during early stages of the vaccine development and manufacturing program [6]. Validation defines the performance characteristics of an analytical procedure, based on the demonstration that the procedure is suitable for its intended purpose or use. Validation is generally performed in accordance with the relevant International Conference on Harmonization (ICH) guidelines. Process validation requires establishing documented evidence that provides a high degree of assurance that a specific process will consistently produce a product meeting its pre-determined specifications and quality characteristics.

4 Stages of Vaccine Development

The vaccine development process can be divided into two major categories, those events that are not under the regulatory authority of the FDA and are exploratory in nature and those events that are subject to regulatory authority by the FDA. Exploratory events or research and development cover basic research drug discovery processes that occur before the sponsor submits an investigational new drug application (IND) to the FDA. There are four main stages of vaccine development under the purview of regulatory authorities: preclinical, clinical (IND), licensing, and post-licensure. Throughout the vaccine life cycle from preclinical evaluation to post-licensure lot release testing, vaccines are subject to rigorous testing and oversight by manufacturers and regulatory authorities.

4.1 *Exploratory Stage*

The general stages of the development cycle of a vaccine are outlined in Table 5. The first steps are exploratory in nature. The exploratory stage involves basic laboratory research and often lasts 2–4 years [12]. The research community of academic, government, and industry scientists identifies natural or synthetic antigens that may have potential in preventing or treating a disease. These antigens could include virus-like particles, weakened viruses or bacteria, weakened bacterial toxins, or other substances derived from infectious disease pathogens. The goal of research and development at this stage is to identify and develop a viable product that is safe and immunogenic and complies with applicable regulatory requirements of the NRA of record. Research and discovery may be empirical and based on trial and error and occur in an unregulated environment (Fig. 2). If the vaccine shows promise in the exploratory phase, it moves on to animal testing or the preclinical phase. Although there is no regulatory oversight in the basic research and discovery phase, each of the product development stages beginning with the preclinical stage is impacted by the regulatory process. Once product development enters the regulated environment, there are challenges that must be overcome (Fig. 3). Preclinical studies must be completed according to GLP; chemistry, manufacturing, and control procedures must be done according to current good manufacturing practices (cGMP); and clinical studies are required to be conducted according to good clinical practices (GCP) [13].

4.2 *Preclinical Stage*

The preclinical stage consists of the development and testing of vaccines prior to the vaccine being tested in humans. Considerations for preclinical studies are evaluated on a product-specific basis, and requirements may differ depending on the type of vaccine, the manufacturing process, and the mechanism of action. Requirements for preclinical toxicity studies depend on considerations of

Table 5
Development stages of new vaccines

Exploratory/research and development
Preclinical testing:
In vitro and in vivo studies
Clinical testing:
Investigational new drug application
Manufacturing/quality control:
Chemistry, manufacturing, and control
Facility
Regulatory review and approval:
Biologics license application

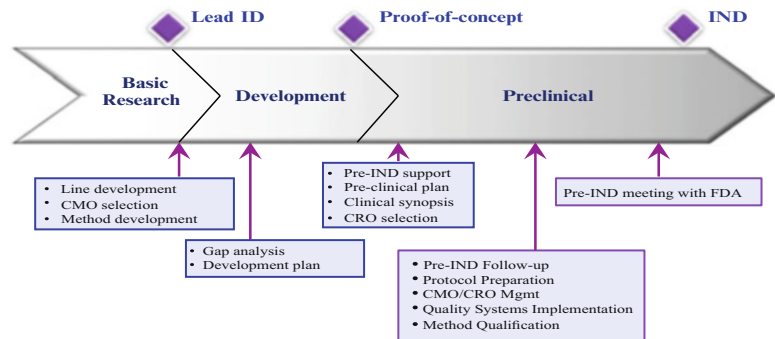


Fig. 2 Impact of the regulatory process on early product development stages. (Source: Baylor, NW. *Regulatory Approval and Compliances for Biotechnology Products in Biotechnology Entrepreneurship*, Shimasaki, C. (ed.) 2014. Elsevier)

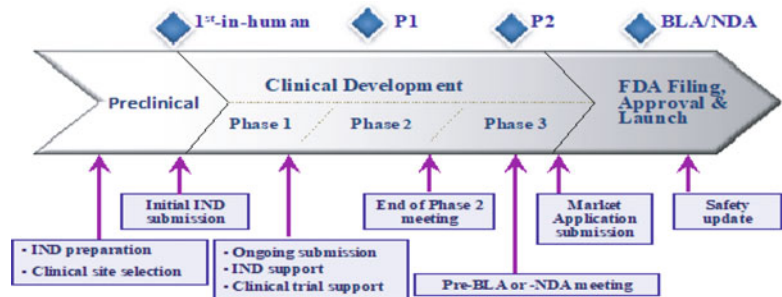


Fig. 3 Impact of regulatory process on clinical development stages. (Source: Baylor, NW. *Regulatory Approval and Compliances for Biotechnology Products in Biotechnology Entrepreneurship*, Shimasaki, C. (ed.) 2014. Elsevier)

the vaccine's potential benefit/risk, the target population, the available clinical data from the use of related products, the product features, and the availability of animal models. As product development proceeds, the FDA may request additional preclinical studies [14].

Early in the product development process, investigators test candidate vaccines *in vitro* prior to moving into animals. Preclinical studies use tissue culture or cell-culture systems and animal testing to assess the safety of the candidate vaccine and its immunogenicity. Animal subjects may include rodents and monkeys. These studies may also provide insight into the cellular responses expected in humans. Additionally, the outcome of these studies may also suggest a safe starting dose for the next phase of research as well as a safe method of administering the vaccine. Based on the clinical data, the candidate vaccine may be modified during the preclinical stage to enhance the vaccine safety and effectiveness. Although limited at the beginning of clinical development, preclinical studies should be sufficient to rule out overt toxicity and identify potential toxic effects that might occur during the clinical trial. Preclinical safety studies provide important safety data on the investigational product's effects in target organs as well as the reversibility of the toxicity. Toxicity studies should be conducted in compliance with GLP [15]. These requirements provide assurance of the validity of toxicity test results by providing a well-controlled study environment. Adequate preclinical data must be provided in the submission of an IND to the FDA for determination that the vaccine is reasonably safe to proceed with a clinical investigation.

As a consequence of more women of childbearing potential participating in clinical trials, and more preventive and therapeutic vaccines being developed for adolescents and adults, NRAs have an increasing concern about the unintentional exposure of an embryo/fetus before information is available about the risk versus benefit of a vaccine. The FDA published recommendations pertaining to the assessment of the developmental toxicity potential of preventive and therapeutic vaccines for infectious diseases indicated for females of childbearing potential and pregnant females [16].

4.3 Clinical Testing Stage

Once the preclinical data package is reviewed and accepted by the FDA, sequential phases of clinical evaluation commence. The clinical testing stage or investigational new drug (IND) stage consists of multiple phases where the investigational product is studied in human subjects under well-defined conditions and with careful monitoring. In certain cases where studies to demonstrate efficacy in humans are not ethical or feasible, sponsors may conduct studies to demonstrate efficacy of the product in appropriate animal models. The clinical development of a new vaccine begins with the sponsor requesting permission to conduct a clinical study with an investigational product through the submission of an IND application. Title 21 CFR 312 describes the content of an original IND

submission and the regulatory requirements for conducting clinical trials under the IND regulations (16). Clinical studies are governed by good clinical practices. These regulations facilitate the protection and safety of human subjects and the scientific quality of clinical studies [17].

The IND submission describes the vaccine, its manufacture and control testing for release of the vaccine, the proposed scientific rationale, available preclinical animal safety testing results, and a proposed clinical study protocol. Review of the IND submission allows the FDA to monitor the safety of clinical trial subjects and ensure that the study design permits a thorough evaluation of the vaccine's effectiveness and safety. There are typically three successive phases in the clinical evaluation of vaccine products under the IND regulations [18]. These phases can sometimes overlap, and the clinical evaluation may be highly iterative, because multiple phase I and II trials may be required as new data become available. The FDA rigorously oversees the clinical trial process. If data raise significant concerns about either safety or effectiveness, the FDA may request additional information or studies or may halt ongoing clinical studies.

Phase I studies are designed to evaluate vaccine safety and tolerability and to generate preliminary immunogenicity data. Typically, phase I studies enroll between 20 and 80 subjects who are closely monitored throughout the duration of the trial. Phase II studies, which typically enroll several hundred subjects, evaluate the immunogenicity of the vaccine and provide preliminary estimates on rates of common adverse events. Phase II studies are often designed to generate data to inform the design of phase III studies. Dose-ranging studies are also included in phase II clinical development. The phase III trial provides the critical documentation of the vaccine's safety and effectiveness needed to evaluate the benefit/risk relationship of the vaccine and to support licensure. Phase III trials for vaccines are large and typically enroll from several hundred to several thousand subjects to provide a more thorough assessment of safety as well as a definite assessment of efficacy. Manufacturing reproducibility is typically addressed during the phase III trial by evaluation of lot consistency and ensuring process validation.

The general considerations for clinical studies to support vaccine licensure include safety, immunogenicity, and efficacy (immunogenicity may be sufficient in some cases). Ideally, efficacy is demonstrated in randomized, double-blind, well-controlled studies. The end points are product specific and may be clinical disease end points or immune response end points if efficacy against clinical disease has been established. The requisite number of study participants in efficacy trials for vaccines can range from thousands to tens of thousands of subjects. This broad range depends on variables such as study design and incidence of the disease to be prevented.

4.4 Regulatory Review and Approval

The licensing stage follows the IND stage when clinical studies are completed. Regardless of the technology used to manufacture a vaccine or the targeted population or indication, the basic regulatory requirements are the same. The regulatory review of the license application begins when a vaccine manufacturer submits a biologics license application (BLA) to the US FDA. The BLA includes data from results of clinical and nonclinical studies, as well as a complete description of manufacturing methods, compliance with cGMP requirements, data establishing stability of the product through the dating period, samples representative of the product for introduction into interstate commerce, and data describing the equipment and facility of each location involved in the manufacture. The US FDA can approve the BLA once the Agency determines that the vaccine meets prescribed requirements for safety, purity, and potency. The regulations that pertain to the licensure and submission of a BLA are in 21 CFR 600 through 680.20.

The BLA is reviewed by an expert multidisciplinary group of scientists within the FDA. In addition to review of the BLA submission, important regulatory review activities support vaccine licensure. These activities help ensure the quality and safety of licensed products. Vaccine lots are subject to pre-licensure lot-release testing (Table 4). A preapproval inspection is designed as an in-depth review of the manufacturing facilities, the manufacturing process, and an assessment of the sponsor's adherence to cGMPs.

Once the FDA review committee evaluates the complete data package in the BLA, the agency generally requests that manufacturers present their data to the Vaccines and Related Biological Products Advisory Committee (VRBPAC). The VRBPAC is a standing FDA advisory committee composed of scientific experts and clinicians, consumer representatives, and a nonvoting member from industry. The VRBPAC and additional expert consultants, if needed, evaluate clinical data and comment on the adequacy of the data to support safety and efficacy in the target population. The VRBPAC's recommendations are strongly considered in the FDA's decision to license a vaccine. The VRBPAC may recommend that additional studies be performed before licensure. After FDA's review committee determines that the data in the application are satisfactory and support the safety and effectiveness of the vaccine, and manufacturing consistency is demonstrated, the vaccine may be licensed.

There are several expedited review mechanisms available to the US FDA to advance the review and/or licensure of vaccines against severe and life-threatening conditions, including accelerated approval, fast track, priority review, breakthrough therapy, and emergency use authorization (EUA) (Table 6). Designation of a vaccine under these mechanisms does not lower the required scientific/medical standards, the quality of data necessary for approval, or the length of the clinical trial period.

Table 6
US FDA expedited regulatory pathways^a

Pathway	Description of pathway ^b	Criteria	Attributes
Fast track	Program designation	Drug intended to treat a serious condition, and nonclinical or clinical data demonstrate the potential to address an unmet medical need or a product designated as a qualifying infectious disease product ^c	Actions to expedite development and review; rolling review
Breakthrough therapy	Program designation	Drug intended to treat a serious condition and <i>preliminary</i> clinical evidence indicating the drug may demonstrate substantial improvement on a clinically significant endpoint (s) over existing therapies	Intensive guidance on efficient drug development; FDA organizational commitment; rolling review
Priority review	Program designation	An application or efficacy supplement for a drug that treats a serious condition and if approved would provide a significant improvement in safety or effectiveness ^d	Shorter review clock (6 mos review time versus 10 mos for standard review)
Accelerated approval	Approval pathway	A drug that treats a serious condition and generally provides a meaningful advantage over available therapies and demonstrates an effect on a surrogate endpoint that is reasonably likely to predict clinical benefit	Approval based on an effect on a surrogate endpoint or intermediate clinical endpoint
EUA	Approval pathway	Authorization of the use of an unapproved product or the unapproved use of an approved product when an emergency or a potential emergency exists	Allows introduction of drug, device or biological into interstate commerce by the Sec. of DHHS for use in an actual or potential emergency

^aAdapted from the FDA Guidance for Industry: Expedited Programs for Serious Conditions—Drugs and Biologics

^bDescription of regulatory pathways includes regulatory programs such as fast track, breakthrough therapy and priority review. Emergency use authorization and accelerated approval are mechanisms whereby products may be approved for introduction into interstate commerce

^cTitle VI11 of FDASIA, *Generating Antibiotic Incentive Now (GAIN)*, provides incentives for the development of antibacterial and antifungal drugs for human use

^dPriority review also applies to any supplement that proposes a labeling change pursuant to 505 of the FD&C Act on a pediatric study under this section or an application for a drug that has been designated as a qualified infectious disease product (see footnote 2) or an application or supplement for a drug submitted with a priority review voucher

The fast-track mechanism is designed to facilitate the development and expedite the review of new drugs that are intended to treat serious or life-threatening conditions and that demonstrate the potential to address unmet medical needs (i.e., providing a therapy when none exists) [19]. Most drugs that are eligible for fast-track designation are likely to be considered appropriate to receive a priority-review designation. A priority-review designation is given to drugs that offer major advances in treatment or provide a treatment when no adequate therapy exists. A priority review reduces the FDA review time. The time for completing a priority review is 6 months.

Breakthrough therapy is described in Section 506(a) of the FD&C Act. Breakthrough therapy provides for the designation of a drug as a breakthrough therapy "... if the drug is intended, alone or in combination with one or more other drugs, to treat a serious or life-threatening disease or condition and preliminary clinical evidence indicates that the drug may demonstrate substantial improvement over existing therapies on one or more clinically significant endpoints, such as substantial treatment effects observed early in clinical development" [20]. The clinical evidence needed to support breakthrough designation is preliminary. In contrast to the data needed to support approval, as is the case for all drugs, FDA will review the full data submitted to support approval of drugs designated as breakthrough therapies to determine whether the drugs are safe and effective for their intended use before they are approved for marketing.

The accelerated-approval regulation allows approval based on a surrogate end point for drugs intended to treat serious diseases and that fill an unmet medical need. A surrogate end point is a marker (e.g., a laboratory measurement or physical sign) used in clinical trials as an indirect or substitute measurement that represents a clinically meaningful outcome, such as survival or symptom improvement [21]. The use of surrogate end points may shorten the FDA approval time. Approval of a drug based on such end points is given on the condition that postmarketing clinical trials verify the anticipated clinical benefit.

Emergency use authorization (EUA) is another regulatory mechanism by which the US FDA can accelerate the availability of vaccines and other pharmaceutical products [22]. Under EUA, the FDA can authorize the use of an unapproved product or the unapproved use of an approved product when an emergency or a potential emergency exists. Section 564(b)(1) of the FD&C Act allows the Secretary of the US Department of Health and Human Services (DHHS) to authorize the introduction into interstate commerce of a drug, device, or biological product intended for use in an actual or potential emergency. Once the Secretary of DHHS declares an emergency, the FDA may authorize the emergency use of a particular product such as a vaccine, if other statutory criteria and conditions are met.

The assessment of efficacy for some infectious disease vaccine candidates cannot be ethically conducted under clinical trial, such as those for certain bioterrorism agents. In 2002, the FDA amended the biological products regulations to incorporate 21 CFR 601.90, Approval of Biological Products When Human Efficacy Studies Are Not Ethical or Feasible [19]. This rule, referred to as the “animal rule,” provides that approval of certain new drug and biological products can be based on animal data when adequate and well-controlled efficacy studies in humans cannot be ethically conducted because the studies would involve administering a potentially lethal or permanently disabling toxic substance or organism to healthy human subjects. In these situations, certain new drug and biological products can be approved for marketing based on evidence of effectiveness derived from appropriate studies in animals without adequate and well-controlled efficacy studies in humans. When assessing the sufficiency of animal data, the agency may consider other data, including human data, available to the agency. Safety must be evaluated in humans as a prerequisite for approval.

5 Summary

Regardless of whether a vaccine is manufactured through traditional processes, i.e., live attenuated or inactivated (killed) whole organisms, or from well-defined materials, such as vaccines based on purified protein antigens of natural origin or produced by rDNA technology, polysaccharides, semi-synthetic poly- or oligosaccharide-protein conjugates and novel nucleic acid constructs, they all require strict adherence to regulatory requirements throughout the manufacturing process. It is critical for vaccine developers to understand the regulatory requirements in order to manufacture a consistent and reproducible vaccine that is safe and effective. Although the regulatory process does not directly impact the early or exploratory stages, developers must be cognizant of the requirements of the regulatory authorities, and develop a clear and focused regulatory strategy, even during the early stages of product development to avoid unnecessary delays in obtaining marketing authorization. Once a vaccine is licensed, the regulatory impact remains throughout the life cycle of the product.

Acknowledgments

The author would like to thank Lindsay Rinaudo for her assistance in researching and preparing this manuscript.

References

1. Public Health Service Act, July 1, 1944, Chap. 373, Title III, Sec. 351, 58 Stat. 702, currently codified at 42 U.S.C., Sec. 262
2. Rauch S, Jasny E, Schmidt KE, Petsch B (2018) New vaccine technologies to combat outbreak situations. *Front Immunol* 9:1963. <https://doi.org/10.3389/fimmu.2018.01963>
3. Poveda C et al (2019) Establishing preferred product characterization for the evaluation of RNA vaccine antigens. *Vaccines* 7:131
4. Ura T, Okuda K et al (2014) Developments in viral vector-based vaccines. *Vaccines (Basel)* 2 (3):624–641
5. Janus T, Sitrin R, LeGrow K, Aunins A, Hagen A, Thornton R, Robinett R, Howson L (2003) Integrating CMC Document preparation into the development process for vaccine INDs. Available via BioPharm International: <https://www.biopharminternational.com/view/integrating-cmc-document-preparation-development-process-vaccine-inds>. Accessed 22 Mar 2015
6. Conner J et al (2014) The biomanufacturing of biotechnology products. In: Shimasaki C (ed) *Biotechnology entrepreneurship*. Elsevier, Boston, MA, pp 351–385
7. US Food and Drug Administration. Guidance for industry: content and format of chemistry, manufacturing and controls information and establishment description information for a vaccine or related product. Available at: <http://www.fda.gov/downloads/BioLogicsBloodVaccines/GuidanceComplianceRegulatoryInformation/Guidances/Vaccines/ucm092272.pdf>
8. US Code of Federal Regulations, 21 CFR 600.3(q) 2012
9. US Code of Federal Regulations, 21 CFR 600.3(r) 2012
10. US Code of Federal Regulations, 21 CFR 600.3(s) 2012
11. Meade B, Arcinega J (2001) Assays and laboratory markers of immunological importance. Laboratory of Methods Development and Quality Control, CBER/FDA
12. Curlin G, Landry S, Bernstein J, Gorman RL, Mulach B, Hackett CJ, Foster S, Miers SE, Strickler-Dinglasan P (2011) Integrating Safety and Efficacy Evaluation Throughout Vaccine Research and Development. *Pediatrics* 127(Supplement_1):S1–S4
13. US Code of Federal Regulations, 21 CFR 312 (2010)
14. WHO Guidelines on Nonclinical Evaluation of Vaccines (2003). Available at: http://www.who.int/biologicals/publications/nonclinical_evaluation_vaccines_nov_2003.pdf
15. US Code of Federal Regulations, 21 CFR part 58 (2010)
16. US Food and Drug Administration. Guidance for industry: considerations for developmental toxicity studies for preventive and therapeutic vaccines for infectious disease indications. Available at: <http://www.fda.gov/downloads/BiologicsBloodVaccines/GuidanceComplianceRegulatoryInformation/Guidances/Vaccines/UCM092170.pdf>
17. International conference on harmonization of technical requirements for registration of pharmaceutical for human use. ICH harmonized tripartite guideline: guideline for good clinical practice E6(R1). Available at: <http://www.fda.gov/downloads/AnimalVeterinary/GuidanceComplianceEnforcement/GuidanceforIndustry/UCM052417.pdf>
18. US Code of Federal Regulations, 21 CFR part 312.21 (2010)
19. Center for Drug Evaluation and Research and Center for Biologics Evaluation and Research. Guidance for industry: fast track drug development programs—designation, development, and application review. US Department of Health and Human Services, Food and Drug Administration. Available at: http://www.msknclinnovations.org/medregulations/v1/html/Guidance/Guidance_Fast%20Track%20Development.pdf
20. Sherman RE, Li J, Shapley S, Robb M, Woodcock J (2013) Expediting drug development—The FDA’s new “breakthrough therapy” designation. *N Engl J Med* 369:1877–1880
21. US Code of Federal Regulations, 21 CFR Part 601.41 (2010)
22. Emergency Use Authorization of Medical Products. Guidance - Emergency Use Authorization of Medical Products. Available at: <http://www.fda.gov/RegulatoryInformation/Guidances/ucm125127.htm>
23. US Code of Federal Regulations, 21 CFR Part 601.90 (2009)

Part VII

Vaccine Intellectual Property



Intellectual Property Rights and Vaccines

Penny Gilbert, Richard Fawcett, Joel Coles, and William Hillson

Abstract

Over the past 20 years, there has been steady, year-on-year growth in the number of granted vaccine-related patents. It is therefore important that those involved in vaccine research should be aware of both the risks and opportunities that patents create. The aim of this chapter is to offer a brief introduction to how, and when, patent rights might become available to vaccine developers and to explain the potential risk of infringement of third-party patent rights and the potential consequences.

This chapter begins with a brief introduction to the patent application process and the international patent systems. The advantages and drawbacks of patent protection are discussed, followed by an overview of patent infringement and the various legal safe-harbors that may be available for certain research activities. Other features of the patent system which may be of particular relevance in the vaccines context are also discussed, such as compulsory licensing, sovereign states' rights to use patented inventions and voluntary technology sharing agreements. The chapter concludes with a discussion of the SARS-CoV-2 (COVID-19) pandemic and recent developments in the field of vaccine patents that have arisen as part of the international response.

Key words Vaccines, Patents, Commercialization, Infringement, Biotechnology, Legal, Intellectual property

1 Introduction

We are delighted to have been invited to contribute this chapter at a time when public interest in vaccines could not be greater. While certain parts of society reserve their right to refuse vaccination, for the vast majority the benefits are clear. Previously deadly diseases such as polio have been almost eliminated, or their impact minimized, and over the past year the unprecedentedly rapid development of the first generation of SARS-CoV-2 vaccines has emerged as the greatest hope for an eventual route back to normality after the havoc wreaked on lives and economies by the SARS-CoV-2 pandemic.

Bearing in mind the vast amounts of research time and high levels of private and governmental investment that are currently

being committed to vaccine development (and the expectation of a renewed focus on basic vaccine research and infectious disease prevention in its aftermath), it is entirely appropriate that the relevance of intellectual property rights should be a topic for consideration in this edition. The relevance of patent rights to encourage and protect innovation will doubtless be familiar to the reader: in return for investment in research, new inventions are rewarded by monopoly protection in the form of patents. The grant of a patent does not simply permit the inventor to put their own work into effect. Instead, a patent is a “negative” right that prevents others from copying or riding on the coat tails of the inventor, thereby permitting a commercial market to be reserved solely to the patent owner or, alternatively, enabling a flow of royalties from the grant of licenses. Either way, the aim is to allow investment to be recouped in order to fund future research. In return, the “patent bargain” requires that the inventor puts details of their research into the public domain by way of a patent application that provides sufficient information to enable others to understand, make, and build upon the invention once the patent term has expired.

So far, so good. But as a practical matter for anyone involved in research, the existence of patents may be a boon, in making competitor information available, or a burden in that preexisting third-party patent rights may inhibit the exploitation of a particular field.

The aim of this chapter is to explain further about how, and when, patent rights might be available. We will also consider the risk of infringement and when there may be answers available to avoid the potential blocking effect of third party patent rights upon research and upon the eventual exploitation of the fruits of that research.

While we have heard that “patents have never been a significant factor in the vaccine business” [1], it is important to dispel that fallacy.

As illustrated in Fig. 1, there has been a steady, year-on-year growth in the number of granted vaccine-related patents over the past 20 years. It is important, therefore, that those involved in vaccine research should be aware of both the risks and opportunities that patents create.

Some of the companies most active in patenting in the field of vaccine technologies over the last 20 years are shown in Fig. 2.

Patents may protect not only the vaccine product itself but also the individual vaccine components, the means by which they are made, purified, or delivered, the delivery devices themselves, the dosage regimens, and the use of the protected technology against particular disease targets. The authors are aware of United Kingdom (UK) litigation over patents for *B. pertussis* antigens [2], hepatitis B antigens [3], meningitis vaccines [4], and means of conjugating pneumococcal antigens [5], for example.

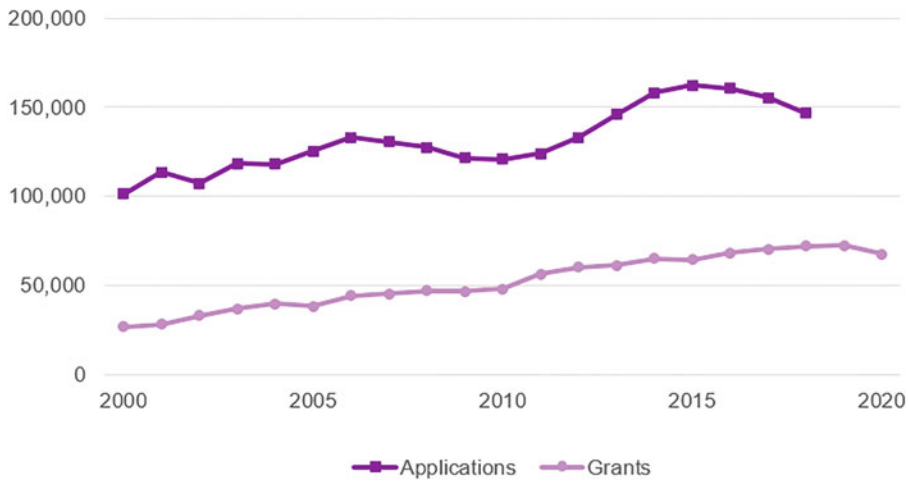


Fig 1 Grant of vaccine patents in the past 20 years. Minesoft's PatBase patent database was searched by Vaccine-related IPC code and keywords, using the search methodology described at www.tandfonline.com/doi/pdf/10.4161/hv.7.2.14004

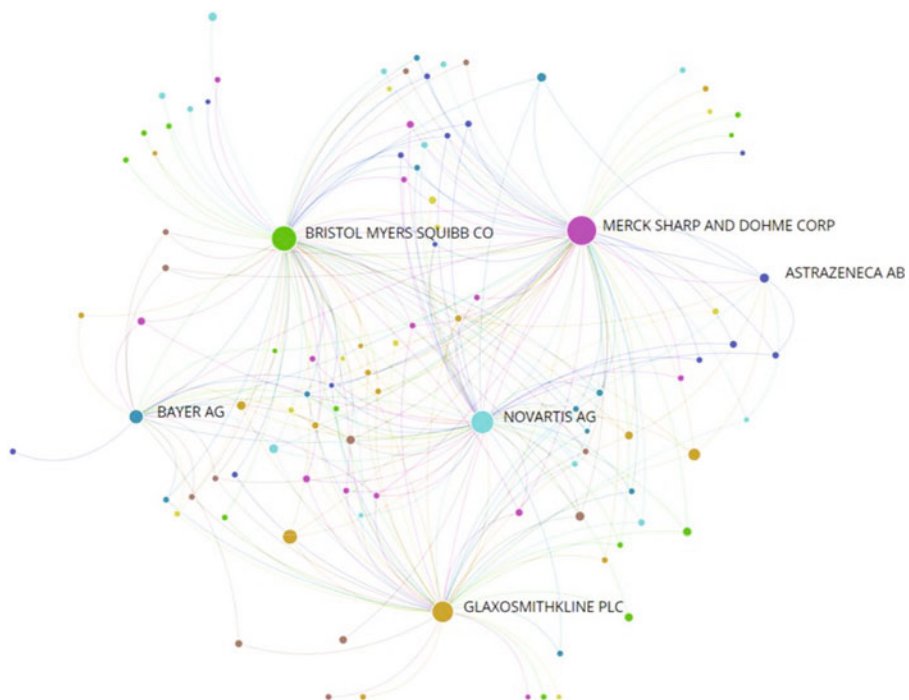


Fig 2 Network diagram showing assignees of patents, identified by searching Minesoft's PatBase patent database with vaccine-related IPC code and key words, having the most forward citations over the last 20 years

2 What Is a Patent?

A patent is a time-limited legal monopoly on an invention, which grants the owner the exclusive legal right to exploit that invention in the country of grant. This right may be sold, licensed to other parties, even given away for free or given up entirely, and for this reason, it is considered an item of personal property. The holder of a patent can, subject to a limited number of exceptions which are discussed further below, prevent any other party from using their invention, or require them to pay a royalty in order to do so.

As a result of international treaties, the lifespan of a patent is usually fixed at 20 years from the date on which the patent application was filed, although some jurisdictions may permit extensions to this in limited circumstances. In particular, patent term extension may be granted for pharmaceutical patents, including patents protecting vaccines, in order to compensate patentees for the delay in bringing a product to market as a result of the need to obtain marketing authorization before commencing sales.

3 What Can Be Patented?

Patents can be granted for both products and processes that are: (a) new; (b) inventive; and (c) serve a practical technical purpose. This latter requirement is known in Europe and some other jurisdictions as “industrial applicability” and as “utility” in the US.

It is not possible to obtain a patent for a mere discovery or idea—patent protection can only be obtained for the technical application of such discoveries in the form of products or processes.

There are also a number of specific exclusions from what can be patented, which vary between jurisdictions based on public policy considerations. For example, in the signatory states of the European Patent Convention (EPC), it is not possible to patent certain types of methods of medical treatment administered by a physician.

4 Who Can Apply for a Patent?

It is the inventor who has the right to apply for a patent for their invention. However, that right can be transferred, or assigned, to another person. In most countries, if an employee has developed an invention in the course of their usual employment then the invention (and the related patent rights) will belong to their employer. To avoid confusion and the potential for dispute, employment contracts will often specify issues of intellectual property ownership. Nevertheless, the employee may have a right to equitable

remuneration for an invention that has been particularly valuable to their employer, depending upon the particular circumstances and the relevant national laws. In any event, the employee will always retain the right to be mentioned as the inventor and that right cannot be transferred.

Since an invention may be made by a project team, or in the course of a scientific collaboration, there may be multiple inventors and, therefore, multiple applicants. The way in which shared ownership of a patent is dealt with varies according to local law.

5 Who Grants Patents?

Patents are granted by the national governments of individual countries, who are also responsible for enforcing them through the judgments of their courts. This remains the case even when countries agree by treaty to outsource some functions of their patent system to supranational organizations such as the World Intellectual Property Organization (WIPO) or European Patent Office (EPO). WIPO is a branch of the United Nations which, among other functions, allows a patent filed in one country to automatically count as having been filed on the same date in many other countries. While this can save a lot of time and money for inventors, WIPO has no power to grant patents in its own right, and they will still need to go through the granting process for each separate country. By contrast, the EPO is a centralized patent examination system, created under the EPC, which allows inventors to make a single application which, if granted, will become effective as national patents in each of the EPC member states designated by the applicant. The EPO operates a centralized opposition and amendment procedure, the effects of which take effect on all designations of a European patent across member states. The EPO is not a body of the EU, and EPC member states include a number of non-EU countries, such as Turkey, Norway, Switzerland, and (since Brexit) the UK.

Once granted, patents are inherently *national* rights, existing only within the borders of the country that grants them. There are no international patents as such, only a number of treaties between nations which streamline and coordinate various aspects of the patent application process and standardize some of the requirements for granting a patent (even though these common rules can still often be interpreted differently by different countries). This means that it is common for an inventor to file for protection of the same invention in different countries, according to where they anticipate their invention will find a market, and to receive a different scope of protection in different countries. A patent which is held valid in one state may nevertheless be held to be invalid in another due to differing national rules.

6 Why Apply for a Patent?

Patents offer a way to recoup research costs and may provide future research funding. Patents can be sold, either for a lump sum or in exchange for a royalty on future profits or sales arising from the invention. Alternatively, licenses can be granted to people who wish to use the patented invention, which can in some circumstances be a preferable option for inventors as it allows them to retain ownership and some degree of control over the patent (e.g., licenses may contain clauses to allow the patent owner to terminate the license and grant a new one to another party if the licensee fails to commercialize the technology within a reasonable amount of time). Although there are many different types of licensing arrangements, the most important distinction is between licenses which are *exclusive* (i.e., the licensee becomes the only person entitled to use or make the patented product or process, excluding even the patent owner) versus nonexclusive, in which more than one licensee may be granted the right to use the patented invention. It is possible for licenses (including exclusive licenses) to be divided by territory, or by application. For example, if a patented drug is useful in both human medicine and veterinary treatment, it is possible to grant separate exclusive licenses for the human and veterinary applications.

Patents are often a valuable asset for new startups and provide the basis for seeking investment. Likewise, patents held by academic institutions, or governmental departments, can provide a means of raising funds through license or sale of the rights. Where the patent holder does not intend on commercializing the invention of its patents itself, they may provide a bargaining chip to gain access to the patented technology of other groups or companies working in the same field, for example by way of a mutual cross-license or even by contribution to a “patent pool.”

7 How Do You Apply for Patent Protection?

The patent application process starts with the filing of what is, essentially, an early draft of the patent itself (the “priority document”) at the competent patent office, together with any necessary paperwork and a fee. The date on which this document is filed (the “priority date”) is usually the date at which validity will be assessed. Up to 1 year after this date (the “priority period”), it is possible to file updated drafts of the patent. Insofar as the invention that is eventually claimed is only disclosed and properly supported by these later drafts, then in that case the validity of the patent will be assessed from the date on which the relevant later draft is filed. This may have an impact on the patent’s validity if relevant prior art is published in the intervening period.

Ideally, a patent application should be filed as soon as possible after an invention has been made, in order to establish the right to that invention, and so that there will be less prior art with which to contend. However, this does not mean that an application should be rushed. The scope and validity of a patent will be determined by reference to the description which is filed with it. Many valuable patents for important inventions have been found to be invalid, not because of any lack of quality in the invention itself, but due to drafting errors or the omission of sufficient information to support the invention caused by the hurry to file as soon as possible. In practice, there is always a trade-off between the need to file early and the need to maximize the supporting information in the patent.

At the end of the priority period, the patent application will enter a phase known as “prosecution.” The patent office will carry out a search of its records to determine whether there are any reasons why the patent should not be granted (such as prior art which shows that the invention is not new or lacks an inventive step). There follows, in effect, a negotiation with the patent office regarding the merits of the application and the form of any claims that it is prepared to grant.

Once a patent has been granted, it will need to be actively maintained by the regular payment of renewal fees throughout its 20-year duration.

One final point to note is that due to different procedural and substantive patentability rules in different jurisdictions, it is quite possible for an identical patent application filed in two different jurisdictions to end up with significantly different sets of granted claims, once it has been through the two separate patent prosecution systems.

8 Is Patenting the Right Route?

The patent application procedure can be time-consuming and expensive, so before filing a patent application, it is worthwhile to consider whether this is the most appropriate way to protect an invention and whether the significant financial investment will be justified.

There may be good reasons for preferring alternative means of protecting an invention. In particular, the patent system is not very well-suited for protecting complex know-how or incremental technical advances, where any resulting patent claims may be highly specific and so have a narrow scope of protection, making them easy for competitors to “design around.” In some cases, it may be preferable to maintain valuable know-how (e.g., cell culture conditions or processing protocols for biological materials) as a trade secret. While this forfeits the legally enforceable monopoly of a patent, the invention will in many jurisdictions remain protected

by laws prohibiting the disclosure of confidential information. Crucially, unlike patents, which have a strict time limit, trade secrets can be maintained for as long as the secret can be kept.

At the other end of the spectrum, if the primary goal in applying for patent protection is purely defensive (i.e., to stop someone else from filing patents in a particular area of technology, so that you can continue research and development without threat), then there may be more cost-effective ways to achieve this goal, provided that maintaining confidentiality is not a concern. It is not uncommon for firms that cannot, or do not wish to, incur the cost of obtaining patent protection to engage in “defensive publishing,” in which disclosures enabling the invention (or some aspect of it) are made publicly available. This has the effect of clearing an area in which to operate, within which no patents can be filed, as they would lack novelty or be obvious in light of the published information. Such defensive publications will, however, impact upon the potential for protecting future valuable inventions of one’s own that may later emerge.

9 What Are the Consequences of Infringing Someone Else’s Patent?

The consequences of infringing a patent can be significant. A patentee may start legal proceedings in the relevant national court of the country where infringement took place. If infringement of a valid patent is proven, remedies typically include damages and an injunction to prevent further infringement for the lifetime of the patent. In some jurisdictions it is potentially possible to obtain an injunction lasting beyond expiry of the patent to prevent third parties from obtaining a so-called “springboard advantage” from infringing acts that took place during the life of the patent. It is also often possible to obtain an order to seize or destroy infringing products or equipment to remove them from the market.

Damages for patent infringement can be substantial—a patent owner may be able to obtain compensation for all lost profits, which in some cases will dwarf the profits made by the infringer. In some jurisdictions, such as the US, punitive damages may be awarded where it can be established that the infringement was willful.

It is common for companies to file large numbers of patents in a particular area resulting in so-called “patent thickets”, which may act as an obstacle to other parties attempting to develop similar technology. In many countries, there is an obligation on third parties to actively investigate whether any patents exist that are relevant to their planned activities, and seek to have them invalidated (or to obtain declarations that their technology does not infringe) before launching a commercial product. This process is known as “clearing the way” and is discussed in more detail below. Clearly such a task is particularly problematic in technology fields that are subject to patent thickets.

10 Are Research Activities Infringing?

Research activities are safeguarded from patent infringement in many jurisdictions in a variety of ways. Among the European Union (EU) states that are signatories to the EPC, a common framework was envisaged under the Community Patent Convention 1975 (CPC) to provide a range of defenses against infringement. While the CPC never entered into force, some of its provisions have nevertheless been adopted into law by member states. These are discussed below, and many are reflected, at least to some extent, in other national laws.

10.1 Private and Noncommercial Use

Research that is being carried out for non-commercial use, such as academic work, typically falls under the “private use” exemption provided that it is done in a private setting. “Private” in this context does not require confidentiality and simply means that the acts should not be performed in public.

10.2 Experimental Research Exemption

Acts that are done “for experimental purposes relating to the subject-matter of the invention” are also typically protected. This provision is intended to safeguard research whose objective is to validate the teaching of a patent or to expand knowledge in the same area, even in a commercial context. However, it has typically been construed narrowly by national courts to specifically cover experiments regarding the specific subject-matter of a patent, and so does not usually protect the use of the teaching of one patent in the development of a different product or technology, or the carrying out of commercial testing or product trials.

10.3 Exemption for Tests or Trials of Medicinal Products: The “Bolar Exemption”

In many countries, including the UK, the US, and the countries of the EU, acts done while conducting a study, test, or trial that is necessary for the purposes of obtaining a pharmaceutical marketing authorization may be subject to an exemption. This exemption is commonly known as the “Bolar exemption.”

The precise limits of this exemption vary between countries. In some places, the exemption is limited to the studies necessary to obtain generic or biosimilar approval. In other jurisdictions, the scope will extend to cover innovator clinical studies.

10.4 Extemporaneous Preparation in a Pharmacy

In keeping with the exclusion under the EPC of methods of treatment or diagnosis from patentable subject matter, acts performed in a pharmacy in connection with the preparation of a medicine in accordance with a prescription are also protected from infringement.

10.5 Right to Continue Use Begun Before Priority Date

A party that has secretly or privately used an invention prior to it being patented may not be able to show their use represents publicly available prior art (which, if proven, would result in the patent

being held to be invalid, because it was not novel or obvious). However, they are afforded some protection from patent enforcement in some jurisdictions, such as the UK and Germany, with the defense of “prior use.” This exemption is read narrowly to allow such parties only to continue doing the specific activities and use that pre-dated the patent.

11 Doctrine of “Clearing the Way”

While there are clearly a range of exemptions which can offer protections to parties performing research and testing new vaccine products, by the time a product is launched on the market, none of these exemptions are likely to apply. In some countries, such as the UK, courts place weight on whether a party has sought to “clear the way” of relevant patents in advance of a new product launch. Parties are expected to have considered what patents their product may infringe, and either seek their revocation (either by way of opposition at a patent office, or in a national court), or seek a preliminary certification that their product would not infringe, if this is available (such as a declaration of non-infringement). Should a party neglect to take either of these options, then they run the risk of being subject to a preliminary injunction to keep their product off the market pending a more detailed trial on the merits, which may take a year or longer depending on the jurisdiction.

It is therefore important at an early stage of product development to consider the patent landscape in the relevant technical field and determine what steps may need to be taken to achieve a successful product launch.

12 Can a Patentee Be Compelled to Grant a License?

Despite the protections offered by patents in restricting the use of inventions, there are circumstances where a patentee can effectively be compelled to grant a license to another party, most notably where public health or defense issues arise. Though they are not often used in practice, compulsory license provisions are a common feature in most jurisdictions, where they give effect to Article 31 of the World Trade Organization (WTO) Agreement on Trade-Related Aspects of Intellectual Property, 1994 (TRIPS). While some jurisdictions may have their own compulsory license provisions pre-dating the TRIPS Agreement, the treaty establishes a basic set of common rules to be followed by WTO member states.

In short, the TRIPS rules provide that WTO member states may authorize acts that would otherwise infringe a patent in certain circumstances. As such, they offer national authorities protection against a patentee who may have no interest, or lack the capacity, to

make an important innovative product, such as a medical technology, available in that country. Authorization is permitted in circumstances where a license has already been sought from the licensor on reasonable commercial terms and conditions, but such a license has not been granted within a reasonable period of time. A license authorized in this way should be limited to being nonexclusive, non-assignable, and restricted to the predominant purpose of supplying the market within that jurisdiction. It should also be limited in scope and duration according to the particular circumstances in which the need for it arose, and subject to periodic review.

An unwilling licensor who is compelled to grant a license can expect to receive adequate remuneration, with the amount which will be due depending on the circumstances of the case, taking into account the economic value of the compulsory license.

In the specific circumstances where a prospective licensee needs a license to an earlier (first) patent in order to exploit their own (second) patent, they can only expect a compulsory license to be authorized if the invention in the second patent represents an important technological advance of considerable economic significance in the context of the first patent. However, in return for being awarded a compulsory license, the party receiving a license to the first patent must grant a cross-license to the second patent to the licensor of the first patent.

WTO member states are allowed to impose their own stricter rules regarding compulsory licenses. In the UK, for example, the specific grounds in which a compulsory license can be sought include: (a) where demand for a patented product is not being met on reasonable terms; (b) where the establishment or development of commercial or industrial activities is being unfairly prejudiced; or (c) where the manufacture, use, etc. of associated products that themselves are not protected by the patent are being hindered. A key protection for the patentee in the UK is that they are given up to 3 years after the grant of a patent in order to commercialize it before a compulsory license can be sought by another party.

12.1 National Emergency, Extreme Urgency, or Public Noncommercial Use

The requirement for a prospective licensee to first seek a license from a licensor is waived under the TRIPS rules in circumstances of national emergency, extreme urgency, or where an authorization is only sought for public noncommercial use. This allows national authorities to grant permission immediately in emergency situations, or more generally without unnecessary delay.

In the UK, this exception is embodied in the “Crown use” exemption. A government department may be permitted to do certain acts “for the services of the Crown” which would otherwise infringe a patent, or provide written authorization for another party, usually the alleged infringer, to do so. The exemption is

intended to cover a variety of activities, but specifically includes the supply of vaccines within a more general category of drugs and medicines. A patentee is entitled to compensation to the extent that they may have missed out on being awarded a contract for provision of the relevant product, but only if, at the relevant time, they had actually been in a position to fulfil the contract their existing manufacturing capacity.

13 Are There Other Ways to Avoid Risk of Infringement?

While proprietors of patents can be compelled to grant licenses in certain circumstances, there are also ways in which third parties can be permitted to work an invention without risking infringement.

13.1 *Voluntary Licenses*

Patentees willing to grant licenses to third parties are free to advertise their patents as being available for voluntary licenses. In the UK, for example, the availability of a “license of right” can be recorded on the publicly available patent register, which entitles a patentee to pay reduced renewal fees for that patent. Licenses granted on this basis should be on commercially reasonable terms, and for reasonable remuneration, which may for example be based on the rates from existing comparable licenses.

13.2 *Patent Pools*

In mature industries, where a thicket of patents, owned by different parties, may exist, it is common for patents to be pooled and cross-licensed for the mutual benefit of all parties. Licenses to pools of patents may also be offered to third parties, particularly if the technologies are the subject of industry standards, or otherwise where there are concerns of anti-competitive behavior.

13.3 *Waivers of Patent Rights*

While it is common for inventors and innovative companies to seek financial reward for the exploitation of their intellectual property rights, patentees may of course waive their rights. By way of example, in the early stages of the 2020 SARS-CoV-2 pandemic, in the face of rapidly escalating emergency situations around the world, AbbVie took this move in relation to their HIV therapy Kaletra® (lopinavir/ritonavir) after it was, at that time, thought to show signs of potential efficacy against the novel virus.

14 Finally: Patents, Pandemics, Public Funding, and Policy Issues

As the SARS-CoV-2 pandemic has spread globally, putting unprecedented pressure on social, health, and economic systems, scientists have worked to develop vaccine candidates in record time. At the time of writing, according to the World Health Organisation there are 121 vaccines in clinical development around the world and at

least 194 preclinical vaccines in pre-clinical development [6]. The public has reacted to the announcements of efficacy for the front runner vaccine candidates with a sense of relief. The first reports of a vaccine with potentially over 90% efficacy sent the world's stock markets soaring, in the hope that there might be light at the end of the tunnel from the restrictions on daily life that have impacted global economies.

Having sunk investment into vaccine research and development, including the necessary clinical trials, it should not be surprising that companies, government agencies, and universities have filed for patent protection for their inventions. Since it may take up to 18 months for patent applications to be made public, some of the filings that may have the greatest long-term importance (for example, in fields that have recently received renewed interest such as mRNA-based vaccines) may not yet be publicly available, and the true significance of the new patent landscape will only gradually emerge.

The race to develop vaccines against SARS-CoV-2 has built upon prior research on earlier coronaviruses along with the re-purposing of delivery vehicles and adjuvants, for example, that were already being developed for other potential uses. This has enabled rapid development of novel vaccines and also created opportunities for rapid patent filing. Moderna Therapeutics, for example, is thought to have taken older patent applications relating to their work on vaccines for other coronaviruses and filed follow-on applications targeted against prevention of SARS-CoV-2.

Unsurprisingly, in an area of such significant and widespread health concern, the mere mention of patent filings has led to commentators raising concerns over public policy and access to medicines. There have been discussions as to the ethical implications of patent protection for such research, despite the recognition that patents are a necessary incentive for the development of new medicines and to permit the costs of research funding to be recouped. The World Health Organization has, for example, launched the COVID-19 Technology Access Pool (C-TAP) with the aim of encouraging patent holders to share or pool IP rights to accelerate access to COVID-19 interventions for low- and middle-income countries [7].

At the same time, questions have been raised about the role of public funding in the development of certain of the vaccines. For example, the University of Oxford has received UK government funding for the development of the vaccine that has been licensed to Astra Zeneca. However, Oxford has made public its policy for third-party access to university patents relevant to treating or preventing COVID-19 [8]. Oxford's approach has been to permit access by offering nonexclusive, royalty-free licenses to support the manufacture of free-of-charge, at-cost or cost-with-limited-margin

supply of vaccines (as appropriate) for the duration of the pandemic. Such an approach could, in theory, help ensure global, universal access.

Moderna, meanwhile, has announced that it will not enforce its COVID-19-related patents against those making vaccines during the pandemic and has indicated a willingness to license its IP for COVID-19 vaccines after the pandemic period [9].

At the time of writing, which of these vaccines will ultimately make the greatest contribution to ending the pandemic (particularly in the largely unvaccinated, remoter or less developed regions of the world where the storage requirements for the mRNA-based vaccines, that have proven so successful elsewhere, may be more challenging) remains to be seen. The first large-scale successes of some non-traditional vaccine technologies, such as the use of mRNA, in addressing COVID-19 also gives cause for optimism that they might also bring solutions to longstanding public health problems such as HIV [10]. The potential applications for these new technologies suggest that patent filing activity in the vaccine field is unlikely to slow any time soon. For now, we watch and wait for answers to some of these remaining questions on vaccine protection. In the meantime, the excitement (and in some cases controversy) that has accompanied each new development in the COVID-19 vaccine race reflects a clear appreciation among the public for the efforts and hard work of scientists in this field, and gratitude for the rapid results from the research investment that has been made.

Acknowledgments

We thank Minesoft for kindly carrying out searches for vaccine-related patents using their PatBase software and conducting the analyses shown in Figs. 1 and 2.

References

1. Jacob, R. *COVID-19 and IP* (2020) World Intellectual Property Review (published online 25 September 2020, last accessed 24 September 2021)
2. *Chiron v Evans Medical* [1997] EWHC 359
3. *Biogen v Medeva* [1996] UKHL 18
4. *GSK v Wyeth* [2016] EWHC 1045
5. *Merck v Wyeth* [2020] EWHC 2636
6. <https://www.who.int/publications/m/item/draft-landscape-of-covid-19-candidate-vaccines> (last accessed 24 September 2021)
7. <https://www.who.int/initiatives/covid-19-technology-access-pool> (last accessed 24 September 2021)
8. <https://innovation.ox.ac.uk/technologies-available/technology-licensing/expedited-access-covid-19-related-ip/> (last accessed 24 September 2021)
9. <https://investors.modernatx.com/news-releases/news-release-details/statement-moderna-intellectual-property-matters-during-covid-19> (last accessed 24 September 2021)
10. <https://clinicaltrials.gov/ct2/show/NCT05001373> (last accessed 24 September 2021)



Vaccine Intellectual Property

Ana Santos Rutschman, Joshua D. Sarnoff, and Timothy L. Wiemken

Abstract

We analyzed the intellectual property landscape surrounding currently available vaccines, with a focus on patents.

Key words Immunization, Patent, World Health Organization, U.S. Patent and Trademark Office, Vaccine technology, Affordable access

1 Introduction

From the mid-twentieth century onwards, intellectual property has become a dominant feature in the vaccine research and development (R&D) landscape [1, 2] (*see* **Notes 1–4**). The branch of intellectual property most directly relevant to vaccine development and manufacturing is patent law [3]. Utility patents provide a “grant of a property right to the inventor, issued by the United States Patent and Trademark Office” [4]. This chapter examines the conditions of patentability as applied to vaccine-related products and processes (*see* **Notes 5–15**). The chapter also delves on another area of intellectual property that may be of relevance when assessing the vaccine intellectual property landscape: trade secrecy (*see* **Notes 16–18**). The chapter further reviews the types of vaccines for which intellectual property protection is no longer relevant (*see* **Notes 19**). We conclude that available data on vaccine-related patents denote the growth and prevalence of a patent-oriented culture surrounding vaccine R&D.

2 Materials

We surveyed and examined statutory materials (United States Code Title 35), selected segments of the Manual of Patent Examining Procedure, the World Health Organization (WHO) survey of

intellectual property covering basic vaccines, and the World Intellectual Property Organization (WIPO) database of patent applications covering vaccine-related technology.

3 Methods

1. We surveyed the framework applicable to vaccine intellectual property, with a focus on patents. We described and examined the parameters of statutory subject matter eligibility (*see Notes 6–9*), novelty (*see Notes 11*), nonobviousness (*see Notes 12*), and utility (*see Notes 13*) as applied to vaccine-related patenting activity. We also surveyed the progression of patenting activity as it relates to vaccine technology (*see Notes 3 and 4*).
2. For our analysis of patenting activity, we relied on the WHO survey of intellectual property covering basic vaccines (*see Notes 19*) and on the WIPO database of patent applications covering vaccine-related technology (*see Notes 3*), which identified 11,818 patent families. A patent family is defined as a “collection of published patent documents relating to the same invention, or to several inventions sharing a common aspect, that are published at different times in the same country or published in different countries or regions” [5].

4 Notes

1. Outside the context of basic vaccines, the intellectual property landscape is considerably relevant [6]. While there is no study to date systematically reviewing vaccine-related patents granted by patent offices across the world, trends can be gleaned from vaccine-specific reviews. For example, a study on vaccines based on HPV-L1 major capsid antigen virus-like particles (sold under the trade names *Gardasil* and *Cervarix*) found that there were 81 valid U.S. patents in force in 2010—4 years after *Gardasil* and 1 year after *Cervarix* entered the market [7]. These 81 issued patents resulted from 86 applications in the United States [7]. Issued patents were distributed among 18 entities, with the largest number of patents owned by a single entity—Merck (24)—followed by GlaxoSmithKline and the United States government (eight each). Nonprofit entities owned 20 patents, while for-profit and nonprofit entities held six patents in joint ownership [7].
2. The numbers above illustrate three phenomena. First, there is a prevalence of patent-centric modes of vaccine R&D, as shown by the number of patent applications. Second, there is a high success rate between patent applications and patent grants for

vaccines that eventually enter the market. And third, there is a fragmentation of ownership of patented vaccine technology among diverse R&D players and institutions.

3. While a systematic review of *granted* vaccine-related patents is not available, a systematic information review of vaccine-related patent *applications* is available in the form of a worldwide survey conducted by the World Intellectual Property Organization (WIPO) [8]. The WIPO survey has shown that the rate of vaccine-related patent applications has increased exponentially from the 1960s onwards [8]. Until 1959, patent applications covering vaccine technology remained in the one-digit to two-digit range (e.g., nine patent applications worldwide in 1958). Applications reached the three-digit range in the mid-1980s (138 applications worldwide in 1984). In 1998, vaccine-related patent applications first surpassed the 500 mark (518). And in 2007, the 600 mark was surpassed (616) [8]. In short, patents have become a core strategy for protecting vaccines and their components.
4. While it is important to keep in mind that not all patent applications mature into granted patents, the rise in patent applications identified in the WIPO study illustrates the growth and prevalence of a patent-oriented culture surrounding vaccine R&D [2].
5. Different components of a vaccine may qualify for intellectual property protection in the form of a patent. Product patents may be granted to discrete components of a vaccine, including but not limited to isolated or manufactured DNA sequences, expression, vehicle, immunostimulants, antigens, adjuvants, excipients, and delivery devices [6]. Product patents cover one or more of these components. Additionally, one or more process patents may be granted to the method(s) of manufacturing a vaccine [6]. Patents prevent competitors from making, using, selling, or importing the protected elements, or embodiments thereof, or performing the patented processes, without authorization from the patent holder. This authorization often entails the payment of royalties for the use of the patent component.
6. A specific component of a vaccine or related manufacturing process must satisfy several conditions for a patent to be granted [9]. The threshold condition is subject matter eligibility, a requirement established by the patent statute. The statute allows for patents to be granted on “any new and useful process, machine, manufacture, or composition of matter, or any new and useful improvements thereof” [9]. The U.S. courts interpreted this language to hold that natural phenomena (including isolated DNA), laws of nature, and abstract ideas are not patent-eligible [10]. As forms of biotechnology that

modify naturally occurring products or are artificial products, components traditionally used in vaccine development and in their manufacture are, in principle, patent-eligible, as long as they satisfy additional statutory elements (subheading 4.6).

7. To illustrate the technical elements of subject matter eligibility, we now provide an example using a claim directed at vaccine-related composition of matter. A composition of matter consists of “a combination of two or more substances and includes all composite articles” [11]. Composition of matter claims can be directed at active ingredients in a vaccine, such as viral or bacterial antigens, or excipients, such as adjuvants, preservatives, or stabilizers. Products used in the manufacturing of a vaccine, such as antibiotics or yeast proteins, may also be patent-eligible.
8. Under the U.S. Supreme Court precedent, a patent eligible product may be distinguished from a product of nature when it is “markedly different” [10]. Nevertheless, other Supreme Court precedents provide that a process or product may be ineligible when the claims are “directed to” ineligible laws of nature, natural phenomena, or abstract ideas and fail to add limitations that amount to “significantly more than a patent upon the [ineligible concept] itself” [11]. Additional guidance from the United States Patent and Trademark Office (USPTO) on subject matter eligibility purports to illustrate the difference between eligible and noneligible composition of matter with specific regard to vaccines as follows:

Eligible Claim.

“Vaccine. A claim is directed to a vaccine comprising inactivated Pigeon flu virus. The virus is chemically inactivated for reduced virulence. Not found in nature. The claim is eligible” [12].

Ineligible Claim.

“A claim is directed to a vaccine comprised of Peptide F and a pharmaceutical carrier. The broadest interpretation of this claim would include a composition of Peptide F and water. Peptide F and water are both found in nature but not together. Are new properties formed by a composition of Peptide F and water? No. Does the claim contain significantly more? No. The claim is not eligible” [12].

9. Claims over composition of matter found in nature but introducing new properties are eligible for patent protection. The USPTO illustrates this case through the following formulation:

“A claim is directed to a vaccine delivery device of a microneedle array coated with Peptide F. Peptide F is found in nature but not coated on microneedles. The composition does not convey new properties. Does the claim include Significantly more? Yes. Microneedles were known but not routinely used at the time and Peptide F is confined to a particular use. The claim is eligible” [12].

10. Once determined that a specific product (be it composition of matter or other) or process is patent-eligible, a patent application has to meet three additional criteria. The claimed vaccine product(s) or process(es) must be new, nonobvious, and useful [9, 13, 14].
11. Under novelty standards, an invention will not be considered new if (among other things) it was in public use or was described in a printed publication before the patent application was filed (with certain complex exceptions that may occur up to 1 year before filing). Moreover, an invention will also not be considered new if described in a preexisting published patent or published patent application [13]. In the United States, if the applicant discloses the information before third parties who independently develop similar inventions, the applicant has up to 1 year from the public disclosure in which to file a patent application concerning the technology or set of technologies [15].
12. In addition to novelty, a patent application must also satisfy a nonobviousness standard [14]. This condition precludes the patenting of trivial improvements to a vaccine. The standard of examination is an assessment of whether the claimed invention would have been obvious at the effective time of filing “to a person having ordinary skill in the art to which the claimed invention pertains” [16].
13. Usefulness, also known as utility, is a requirement that assesses the practical application of a patented invention [9]. The standard of examination is a showing of “specific and substantial utility that is credible” [17]. This requirement is rarely a problem for vaccine technologies, as safety and human efficacy are not evaluated, but only a credible showing of potential human efficacy as a vaccine is required.
14. If granted, a patent has currently a term of 20 years from the effective filing date [18, 19]. As patent acquisition may take many years, complex rules govern whether any additional “term extension” should be provided [18, 19].
15. A patent enables the rightsholder (the original patent holder or subsequent transferees) “the right to exclude others from making, using, offering for sale, or selling” the patented invention, or importing it into the United States [19]. From a policy perspective, these exclusionary rights are given to a patent holder in exchange for the information provided as part of the application process, which otherwise might have been kept as a trade secret.
16. Nevertheless, in most cases as well as in the case of vaccines, some information relative to the product or process that is patented may nonetheless be kept secret via trade secret law

(particularly better methods of producing or practicing the invention that were not known at the time of filing) [20]. Under federal and most state laws, trade secrets are defined as “information, including a formula, pattern, compilation, program, device, method, technique, or process that: (1) derives independent economic value, actual or potential, from not being generally known to, and not being readily ascertainable by proper means by, other persons who can obtain economic value from its disclosure or use; and (2) is the subject of efforts that are reasonable under the circumstances to maintain its secrecy” [20]. Examples of vaccine components susceptible of trade secret protection include cell lines, adjuvants, genomic data, and manufacturing processes.

17. Unlike patents, trade secrecy does not confer a right to exclude competitors from the marketplace, but only prevents illegitimate acquisition, use, and dissemination of protected information. Trade secrecy is not subject to a legal term, lasting potentially indefinitely or as long as interested parties succeed in keeping it secret, and as long as it is not independently publicized or discovered through permissible reverse engineering.
18. Significantly, data generated during vaccine clinical trials are considered confidential information by the Food and Drug Administration (FDA) and are normally submitted to the FDA under a claim of trade secrecy, and thus are not made available to third parties [21].
19. A survey conducted by the World Health Organization concluded that a significant number of basic vaccines are no longer subject to patent protection as no fundamental changes to their components and manufacturing processes has occurred for over two decades [6]. Vaccines in this category include diphtheria vaccine, tetanus vaccine, whole-cell pertussis vaccine, monovalent acellular pertussis vaccine, hepatitis B vaccine, haemophilus influenzae type B vaccine, inactivated polio vaccine, oral polio vaccine, measles, mumps, rubella, yellow fever, and influenza vaccines. Among basic vaccines, only those with improved formulations or improved manufacturing processes were potentially subject to intellectual property protection. Even in these cases, it is still possible to work around the existing patents and avoid patent infringement. Work-around strategies include using older formulations or altering the dose of patented components in combination vaccines.

References

1. Stevens H, Huys I, Debackere K, Goldman M, Stevens P, Mahoney RT (2017) Vaccines: accelerating innovation and access. World Intellectual Property Organization global challenges report
2. Rutschman AS (2019) The vaccine race in the twenty-first century. *Ariz Law Rev* 61:729
3. Purvis SA (2013) Basics of patent protection, World Intellectual Property Organization
4. U.S. Patent & Trademark Office, General Information Concerning Patents (2015)
5. World Intellectual Property Organization (2013). Handbook on industrial property information and documentation: glossary of terms concerning industrial property Information and Documentation, 8.1.18
6. Friede M (2010) Intellectual property and license management with respect to vaccines. World Health Organization
7. Padmanabhan S, Amin T, Sampat B, Cook-Deegan R, Chandrasekharan S (2010) Intellectual property, technology transfer and developing country manufacture of low-cost HPV vaccines—a case study of India. *Nat Biotechnol* 28(7):671–678
8. World Intellectual Property Organization (2012) Patent landscape report on vaccines for selected infectious diseases
9. 35 U.S.C. § 101
10. Association for Molecular Pathology v. Myriad Genetics, Inc., 569 U.S. 576 (2013)
11. Alice Corp. v. CLS Bank international, 573 US 208, 217–18 (2014)
12. Laws of Nature, Natural Phenomena & Products of Nature, Manual of Patent Examining Procedure, 28
13. 35 U.S.C. § 102
14. 35 U.S.C. § 103
15. Manual of Patent Examining Procedure, 2153.01(a)
16. Manual of Patent Examining Procedure, 2141
17. Manual of Patent Examining Procedure, 2107
18. Agreement on Trade-Related Aspects of Intellectual Property Rights (1994), article 33
19. 35 U.S.C. § 154
20. Uniform Trade Secrets Act (1979, last amended 1985)
21. Kesselheim AS, Mello MM (2007) Confidentiality laws and secrecy in medical research: improving public access to data on drug safety. *Health Aff* 26(2):483–491
22. Digitech Image Techs., LLC v. Elecs. for Imaging, Inc., 758 F.3d 1344, 1349–50 (Federal Circuit, 2014)

Part VIII

Pathways to Vaccine Commercialization



Resources for Starting a Company

Ann Abraham, Jude Mathew, and Sunil Thomas

Abstract

After having painstakingly invented a new product, filed patents, published papers in peer-reviewed journals, you reach out to companies to license your product. More often, they reject the product as it is novel and risky. The next option is to sell the product through a startup company setup by yourself. Most inventors think that it is difficult to set up a company, find finance to run the company, and manage it. Fortunately, there are several government entities and private investment firms that can help you with setting up a company. This chapter provides information on resources for setting up and running a company.

Key words Discovery, Inventions, Business, Vaccine, Finance, Company, Startups, National Institutes of Health, NIH, National Science Foundation, NSF, Small Business Innovation Research, SBIR, Small business technology transfer, STTR, Angel Investment, Venture capital, Commercialization

1 Introduction

After years of research, burning the midnight oil, working diligently on multiple projects, successfully receiving patents and publications, you knock the doors of companies to license your inventions. Unfortunately, the companies do not believe in your inventions or products as they do not take risk on a product that is new to customers. Your invention will be staring at you, and you will be thinking, “now what?”

You wish that if you had enough financial resources, you would be manufacturing and marketing the product that you have painstakingly developed over the years. Unfortunately, you realize that you are short of funds and other resources to start a company. Fortunately, there are plenty of financial resources to realize your dream of being an entrepreneur so that you could manufacture your products and get it to the customer.

Your first goal is to set up a small company (startup company). Remember, every large company you see around was once a startup

company. Every founder(s) has faced difficult financial situation in their lives. You have the technical know-how to develop a product; that does not mean that you have the business acumen, manufacturing capabilities, and marketing skills to sell your product. I (ST) always encourage my students to read at least *Harvard Business Review* (hbr.org) and *McKinsey Insights* (mckinsey.com) during their studies. These business portals provide the basic business insights that may be useful later in life. This chapter provides information on government entities and private investment firms that can help you with setting up a company and providing finance and management expertise to run the company.

2 Building a Startup Company

Startups are the pioneers in innovation and in commercialization of new technologies, services, and products. Despite the eagerness for entrepreneurs to start a new business and to reel in profits very quickly, founding a successful startup is not an easy task. Entrepreneurs need to transform their business idea into a competitive product, secure funding, attract viable customers, design a market strategy, develop strong organizational structure, hire and coach talent, and make wise decisions at the right time to pivot. Failures and numerous challenges will arise and will need to be dealt with instantaneously and simultaneously. Startups are vulnerable ventures and susceptible for failure; however, with assistance from multiple resources for funding and networking, startups can grow into successful brand name companies.

There are three interacting levels of innovation and startup ecosystems that are strong forces in building a successful startup [1]. At the micro level, a startup must be based on Big Idea that will impact the market (product), a strong team, with the best and most gifted talents available that should lead the new venture, and the founders need to be able to pivot their original startup business strategy when the circumstances are evolving and changing. Startups are evaluated by its scalability, and investors fund startups according to their assessment of the product scalability. In relation to scale, entrepreneurs need to launch a scalable product to grow quickly and sell their products in volume. While scale and growth are key, a drive for impactful and practical innovation is even more significant.

Disruptive innovations redefine existing technology, outperform existing markets, and attract new customers. Once the Big Idea is established, team and talent play a crucial role in founding a startup. Founders of startups will need a team of passion-driven entrepreneurs focused on collating complementary skill sets, product development, product marketing, and sales abilities. Teams should establish goals and assume an achievement-oriented

mindset. Diverse teams with different personalities, characteristics, knowledge, skills, and abilities will have a positive effect and fare well in the beginning. Startup teams should excel in utilizing their collective resources to surpass individual competences. Some members may be experts in product development, others may be more experienced with business organization [1]. Therefore, it is a vital force to recognize a team's talent through its individual members.

Talent is a startup's capital and is a driving factor in innovation, business performance, and growth potential. Talented individuals are important in innovation; it is key to recruit highly educated and highly skilled employees who excel in combining hard skills as well as soft skills. Despite the lack of routine and unpredictability of working at a startup, startups should recruit exceptional talent based on an applicant's drive for contributing to the startup's mission and goal. Startups should seek out talent that is passionate about making an impact in society, as well as in their own job. Employees should be open to failure due to the vulnerability of a startup. It takes much effort and trials to make it work. Most startups will fail; however, a significant asset is finding a balance between upstream innovation (from idea to product) and downstream innovation (from product to market). Ideas are the seeds of startups, but in order to grow, the idea must become a product that will succeed in the market. An unresponsive market is detrimental to the success of a startup. Therefore, it is very important for startups to establish value creation, market entry, and product acceptance. Aligning upstream innovation with downstream innovation is the key to pivoting in the early stages for a new venture. Polishing the product endlessly before it reaches the market is not ideal, rather startups should "fail fast." The startup team needs to launch the product with the lowest amount of time, effort, and money while gauging customer reaction, product use, and willingness to pay. The feedback received from the initial launch will grant startups an opportunity to refine and polish the product, as well as any business plans and organizational structure [2]. The secret is to market the product in its early stages in order to pivot product adjustments and design a better product for the market. Accelerators and investors will play a major role in guiding startups with rightly timing pivots.

You can find information on starting a business at the US Small Business Administration (www.sba.gov). Entities such as legal zoom (www.legalzoom.com) could help you set up the business. After you set up the business, protect the company name by having the trademark and rights to the domain and hosting name. You could register a company as a DBA (doing business as), LLC (limited liability company), Corporation, or a nonprofit organization.

Once you have taken care of the company name and its legal status, apply for the employment identification number (EIN) from

the United States Internal Revenue Service (IRS). You may apply for an EIN online (www.irs.gov) if your principal business is located in the United States or the US Territories. The business should also have a DUNS number.

The Dun and Bradstreet D-U-N-S Number is a unique nine-digit identifier for businesses (www.dnb.com). D-U-N-S Numbers are often referenced by lenders and potential business partners to help predict the reliability and/or financial stability of the company in question. D-U-N-S, which stands for data universal numbering system, is used to maintain up-to-date and timely information on more than 330 million global businesses. The D-U-N-S Number also enables identification of relationships between corporate entities (hierarchies and linkages), another key element of Live Business Identity and commercial risk assessment practices. In addition, the company should have registration with SAM.gov, Grants.gov, eRA-Commons, and SBA Registry as soon as possible to avoid delays. It can take 4–6 weeks to complete all registrations.

You may be able to apply for funding with various government and nongovernment entities only after the registrations with the above organizations are completed.

3 Financing the Startups

Financing a startup may seem daunting at first glance; however, with the right information and tools, funding a startup comes with ease. Before approaching different avenues of financial support, it is important to prepare a well-conceived business plan, which will attract investors. Business plans reveal the clarity and objectivity of your new venture and idea. An investor is specifically interested in knowing the individuals behind the idea, the market potential for your idea and your marketing strategy, the invention's uniqueness and patent rights, and financial statements. Even if your startup's business plan is flawless, it is crucial for your startup to outline a plan for return on investments. Projecting a startup's financial returns based on rational expectations will attract more investors. The market potential, the invention's uniqueness, the growth prospects, the plan to achieve your objective, and the amount of financing needed should be evaluated and understood before presenting the information to potential investors.

3.1 *Venture Capital*

Venture Capital (VC) firms are the biggest players when it comes to startup funding. The VCs are one of the most important entities in the growth of an early stage company. Venture capital firms build companies from a simple idea to a maturing and growing organization.

Venture capitalists are institutionalized “angel investors” with access to a lot more money. They deploy their expertise to these startups in several different forms. Often, they lend money to these

early stage companies in a seed funding round or in Series A or B round of funding. There is a distinction between these levels of funding which is discussed later in the chapter. VCs invest money from financial institutions and wealthy individuals, which amounts to a minimum of three to five million dollars. Usually, these VC firms handle institutional money which can come from a wide range of sources. Most often these are wealthy individuals, hedge funds, university endowments, etc. There are also specialized firms that handle corporate funds which not only lookout for the best return on the money also cares about building strategic partnerships with smaller companies. Despite the major funding from venture capitalists, VCs particularly invest in fewer than 2% of the proposals sent to them, and they expect a minimum return of 40% annually on their investment [3]. In addition to the financial capital, these VC firms also provide valuable management skills to these young companies which can be crucial in the beginning stages of the company especially if the founders are inexperienced. Venture Capitalists do a lot of qualitative and quantitative analysis when looking for companies to invest in. They look at the management team, uniqueness of the product, and potential for the product or service in the market. The management team is the first essential factor for VCs, followed by the idea or product. Venture capitalists engage with the company providing strategic and operational guidance, linking entrepreneurs with investors and customers, acquiring a seat on the board, and hiring employees [4]. It is quite common to see VC firms take large positions in these smaller stage companies and play a big part in navigating the early stages of a company. This can be really helpful if these VC firms specialize in a particular sector and know the market for that sector pretty well.

The VC firms also equip these startups with access to the strong social network that they have in place and provide a lot of informational resources which is often referred to as social capital. Many venture-backed companies have grown into brand names and have generated millions of jobs and trillions of dollars benefiting the US economy. Five of the six largest publicly traded companies by market capitalization were funded by venture capitalists: Microsoft, Apple, Amazon, Alphabet, and Facebook. Despite the optimism for rising startups, venture capitalists are not easily accessible. VCs may even stop operations on a startup if a key member of the management team is lost or if the product's technology becomes outdated or changes unexpectedly [5].

In this field of early stage investing, the risk profile is usually high risk–high reward. There are plenty of investments backed by VC's that fail but the ones that do make it can provide an extraordinary amount of Return on Investment (ROI) for these firms. According to the National Venture Capital Association, 25–35% of venture-backed startups fail. It is important to realize that for every Facebook or Uber that turned to successful, there are

hundreds of other similar companies that did not make it through. Hence, there is competition and specialization amongst various Venture Capital firms.

3.2 Angel Investors

An angel investor (also known as a private investor, seed investor or angel funder) is a high-net-worth individual who provides financial backing for small startups or entrepreneurs, typically in exchange for ownership equity in the company. Often, angel investors are found among an entrepreneur's family and friends.

Angel Investors tend to have a specialized background and often invest in sectors that they are familiar with. They privately finance speculative ventures and add value beyond their financial capital by essentially acting as mentors to these startup founders and guiding them in key executive decisions. Angel investors are primarily used to finance the design of a product, specifically appearance, function, and design, and to acquire patent protection. They may also finance protection and exploitation of a trademark. A detailed account of angel investing has been published by Benjamin and Margulis [6].

Angel investors are not interested in giving large sums to businesses; they have the choice to place their money in a risky startup. In order to motivate an angel to invest, these five factors will be quite influential. First, angel investors desire a return on their investment within 7 years or less. Therefore, it is important to ensure the success of the startup and establish a payment agreement. Second, angels invest in a new product hoping it will reach a larger market than projected, which will potentially be bought by a domineering company. Third, angel investors are in for the high-risk investment adventure, where interesting products and motivating people stimulate a "fun ride." Fourth, a dedicated and passionate management team is a main factor that influences angels to invest in new ventures. It may even sway angel investors to invest more than a company's business plan and strategy. Lastly, the business proposal should be presented to angel investors with honest, encouraging, and reliable paperwork. Despite these factors, angels will not invest unless "due diligence" is performed on their part. Due diligence is the process by which angels investigate the facts, risks, and potential value of your business. Angels will verify the facts in your business plan and do their own research concerning the financials of the startup. They will also interview your family, friends, acquaintances, and, most importantly, colleagues you have worked with in the past. A crucial component for the investor is the structure and organization of your management team. Angel investors assure that the people at the top know what they are doing and have a successful record working in business ventures. Angels will also look into personal information, such as criminal records, debt payments, Internet background check, etc. They have the authority to examine the startup's product and

patent, in order to determine the enforceability and scope of the patent and to establish whether competitors have a chance of imitating the product innovation. Furthermore, angel investors will study the competitive landscape and the domain in which you are competing, in order to determine any future problems with distribution [6]. Angels will also investigate the current owner's and investor's interests in ownership. Before reaching out to potential angel investors, a startup should be aware of how to motivate angels to invest in their business proposal and how angel investors will research background information about your startup.

A huge difference between VC firms and Angel investors is that the latter provides their own capital to these early stage companies and hence has more of a personal relationship with the company. It is important to note that social networks in this sphere are extremely important because, in reality, many investors tend to invest based on the lead VC firm or angel investor who is also called the "anchor" for a particular startup. It is also important to have a broad range of investors as it expands the knowledge base available to the founders themselves.

3.3 Government Funding

The funding cycle of a startup varies from sector to sector. There is a certain uniqueness to the life science sector startup compared to companies that are in technology or consumer products. For an initial drug company, the financial capital requirements are substantial, and payouts are usually long-drawn and dependent on the success of clinical trials. Due to the long-term nature of payouts in the drug industry, it is not as correlated to shorter-term economic uncertainty.

3.3.1 National Institutes of Health

The National Institutes of Health (NIH), a part of the US Department of Health and Human Services, is the country's medical research agency that promotes improving health and saving lives through significant discoveries. The mission of NIH is to "seek fundamental knowledge about the nature and behavior of living systems and the application of that knowledge to enhance health, lengthen life, and reduce illness and disability." The agency aims to foster fundamental discoveries through innovative research strategies, diligently utilize human and physical resources to prevent disease, increase knowledge base in order to enhance the country's economic well-being and ensure a high return on investment in research, and to promote the highest level of scientific integrity, public accountability, and social responsibility.

NIH's goals translate aid to programs/small businesses/startups designed to improve the health of the US by conducting and supporting research on:

- Causes, diagnosis, prevention, and cure of human diseases.
- Human growth and development.

- Biological effects of environmental contaminants.
- Understanding mental, addictive, and physical disorders.
- Organizing programs for the enhancement of medical knowledge through the development and support of medical libraries and the training of health information specialists.

NIH funding is awarded for extramural research through almost 50,000 competitive grants to more than 300,000 researchers at more than 2500 universities, medical schools, and other research institutions.

4 NIH SBIR and STTR Funding

The SBIR (Small Business Innovation Research) and STTR (Small Business Technology Transfer) programs fund a diverse portfolio of startups and small businesses across technology areas and markets to stimulate technological innovation, meet Federal research and development (R&D) needs, and increase commercialization to transition R&D into impact. The major difference between the SBIR and STTR programs is that the STTR requires the small business to collaborate with a US nonprofit research institution. Although not required, small businesses receiving SBIR grants often choose to collaborate with universities and other non-profit research institutions.

STTR differs from SBIR in three different aspects:

- The small business awardee and its partnering institution are required to establish an intellectual property agreement detailing the allocation of intellectual property rights and rights to carry out follow-on research, development, or commercialization activities.
- STTR requires that the small business perform at least 40% of the R&D and a single partnering research institution perform at least 30% of the R&D.
- The STTR program allows the Principal Investigator to be primarily employed by the partnering research institution.

The SBIR/STTR programs have two phases:

- *Phase I: Feasibility and Proof of Concept*

Phase I awards are intended to establish the technical merit, feasibility, and commercial potential of the proposed research and research and development (R/R&D) efforts. These applications help determine the quality of performance of the small business prior to providing further Federal support in Phase II. Phase I awards normally do not exceed \$150,000 total costs for 6 months (SBIR) or 1 year (STTR).

- *Phase II: Research/Research and Development*
Phase II awards are intended to continue the R/R&D efforts initiated in Phase I. Funding is based on the results achieved in Phase I and the scientific and technical merit and commercial potential of the project proposed in Phase II. Only Phase I awardees are eligible for a Phase II award. SBIR Phase II awards normally do not exceed \$1,000,000 total costs for 2 years. Phase II applications are considered renewals (Type 2) in the NIH grant numbering system.
- *Fast Track*
Fast-track incorporates a submission and review process in which both Phase I and Phase II grant applications are submitted and reviewed together as one application.
- *Direct Phase II*
NIH may issue a Phase II award to a small business concern that did not receive a Phase I award for that R/R&D. This “phase flexibility” is called a “Direct-to-Phase II” SBIR award. The SBIR Direct-to-Phase II authority is not available to the STTR program.
- *Phase IIB: Continuation of Phase II*
Phase IIB awards are intended to provide follow-on funding to small businesses for projects that require extraordinary time and effort in the R&D phase and may or may not require FDA approval for the development of projects such as drugs, devices, vaccines, therapeutics, and medical implants.
- *Commercialization Readiness Program (CRP)*
The Commercialization Readiness Program (CRP) may provide up to \$three million in additional funding for Phase II SBIR/STTR projects and is not subject to the same partnering requirements that apply to SBIR or STTR awards.

4.1 National Science Foundation

The National Science Foundation (NSF) is an independent federal agency that supports basic research in order to promote the well-being of the US economy, enhance the nation’s security, and advance knowledge to sustain global leadership. NSF backs fields such as mathematics, computer science, and the social sciences. The agency funds 25% of all federal supported basic research conducted by the United States colleges and universities. Grants and cooperative agreements are given to more than 2000 colleges, universities, K-12 school systems, businesses, informal science organizations, and other research organizations. Along with support for fields of engineering and fundamental science, NSF supports “high-risk, high pay-off” ideas, novel collaborations, and many outlandish projects. NSF works as a “bottom up” operation, which continuously monitors the research across the country and the world, maintains constant contact with the research community, seeks areas of great progress, and selects the most qualified people to conduct the research.

The foundation considers proposals submitted by organizations, and recipients are chosen from those proposals asking for financial and academic support for a specific project. On the NSF website, funding opportunities are announced, and proposals may be submitted accordingly. The funding opportunities are categorized as program descriptions, program announcements, and program solicitations. Scientists and engineers can also submit unsolicited proposals for research. The proposals are evaluated fairly and competitively based on a rigorous system of merit review. A minimum of three independent reviewers (scientists, engineers, and educators who do not work at NSF) evaluate the proposal with much research, deliberation, thought, and discussion. The reviewer ensures that outstanding projects pass to the funding stage.

The NSF Proposal and Award Process:

1. *Phase I: Proposal Preparation and Submission (90 Days)*
 - (a) Opportunity Announced: Funding opportunities are announced on the NSF website. Program descriptions, program announcements, and program solicitations are ways NSF generates proposals. Unsolicited proposals may be submitted at any time.
 - (b) Proposal Submitted: The Grant Proposal Guide (GPG) can be used as a guide for preparing and submitting a proposal to NSF. It details formatting and submission requirements. The proposal can be submitted through the NSF FastLane System.
 - (c) Proposal Received: The NSF Proposal Processing Unit receives the proposals and assigns the proposals to the appropriate program for acknowledgment and for review, if NSF requirements are met. It is important to follow formatting and submission requirements in order to be submitted for review. If the requirements are not met (page limitations, formatting instructions, and electronic submission), the proposal will be returned without review.
2. *Phase II: Proposal Review and Processing (6 Months)*
 - (a) Reviewers Selected: Reviewers are selected according to specific/broad knowledge of the science and engineering fields; their broad knowledge of the infrastructure of the science and engineering enterprise; and diverse representation within the group. Proposers have the ability to suggest reviewers who they believe are well-qualified to review the proposal, as well as identify persons who they would not prefer to review the proposal.
 - (b) Peer Review: NSF proposals are reviewed based on two NSF-approved merit review criteria: intellectual merit and broader impacts. Some proposals may have additional

criteria. Analyses and evaluation of the proposal provides information to the NSF Program Officer.

- (c) Program Officer Recommendation: After scientific, technical, and programmatic review, the NSF Program Officer recommends to the Division Director whether or not the proposal should be recommended for an award or declined for funding. Dependent upon the complexity and length of proposals, additional review and processing time may prolong the process.
- (d) Division Director Review: If a proposal is declined, the organization will be notified, and the review information will be available for view in the FastLane System. If the proposal is accepted and the decision is to award the organization, the recommendation is submitted to a Grants and Agreements Officer in the Division of Grants and Agreements (DGA).

3. Phase III: Award Processing (30 Days)

- (a) Business Review: The Grants and Agreements Officer in the Division of Grants and Agreements (DGA) reviews the business, financial, and policy implications. The DGA typically awards organizations within 30 days of receiving the recommendation, unless the organization has not received prior funding, the award is a cooperative agreement, or special circumstances are involved.
- (b) Award Finalized: Finally, the organization is notified of the award notice, the budget, a proposal, applicable NSF conditions, and other documents or requirements involved are included in the agreement.

NSF is also known to support small businesses with grants and contracts. The foundation awards nearly \$190 million annually to startups and small businesses through the Small Business Innovation Research (SBIR) and the Small Business Technology Transfer (STTR) programs. The grants support research and development (R&D) transforming scientific discovery into products and services with commercial and societal impact. America's Seed Fund powered by NSF (NSF SBIR/STTR program) has aided startups with developing their ideas and bringing them to market. America's Seed Fund is focused on funding entrepreneurs with ideas for high-risk, high-impact technologies. They foster innovation and help create businesses and jobs in the US. As an innovator, your startup will be given the necessary funding to commercialize risky ideas, and you will have full control of your team, vision and business strategy, and intellectual property. America's Seed Fund does not take any equity in exchange for funding. Since NSF awards are not loans, a startup will not have to pay anything in return. In

addition, you will work hand-in-hand with a program director, who will serve as your coach. With America's Seed Fund, a startup can receive up to \$256,000 in seed capital to conduct R&D for 6–12 months. A startup will be incorporated into the NSF network and will receive training and mentorship from experienced entrepreneurs and innovators.

In order to apply for funding, a startup has to submit a Project Pitch. Within 3 weeks, NSF will inform your startup if your idea and proposal fits well with the program. If accepted, a Phase I proposal for up to \$256,000 can be submitted. Within 4–6 months, the status of your proposal will be accepted or declined. If awarded Phase I funding, your startup will be expected to explore product-market fit, determine the feasibility of your technology, design and test prototypes, identify any legal or regulatory issues, and develop a plan to scale and market your technology. During the course of the process, small businesses have the leeway to update their research plan, business model, or R&D strategy. Once a business has met Phase I requirements and is seeking to develop their technology greatly, the company is eligible for Phase II funding, which could amount to \$1,000,000 over 2 years.

4.2 Small Business Administration

The US government, in association with banks, lending institutions, and intermediaries, provide loans to startups who cannot secure financing through traditional avenues. Small Business Administration (SBA) is a federal agency that supports small businesses and entrepreneurs to pursue their startup goals and dreams. SBA offers a type of loan called 7(a) loans, which are primary governmental business loan programs. A 7(a) loan may be used for most business purposes including startup, expansion, equipment purchases, working capital and inventory or real estate acquisition. The SBA can guarantee up to \$750,000 of a private-sector loan. Interest rates for 7(a) loans are negotiated between the applicant and the lender.

- SBA Low Documentation Loans (SBA_{LowDoc}) grant a small business loan of \$150,000 or less.
- SBA Express encourages lenders to make more small loans to small businesses. Lenders approve loans of up to \$150,000. Lenders can also offer revolving lines of credit to borrowers.
- The SBA Prequalification Program offers loans to armed forces veterans, minorities, women, exporters, rural small business owners, and business owners in certain specialized industries. This program enables the SBA to pre-qualify an applicant for a 7(a) loan guarantee before the applicant goes to a bank. The maximum amount an applicant can apply for is \$250,000.
- The MicroLoan Program provides short-term loans of up to \$35,000. This program focuses on granting a loan for small-

scale financing purposes such as inventory, supplies, and working capital.

5 Types of Funding Rounds

The financial incentive for any early investor in a startup is to have a well-defined exit strategy. This is possible through a series of funding each at a different stage of a company. The following are the basic rounds of funding usually involved when funding a startup:

- **Seed Funding:** This is the very first level of funding which is usually done by the founders themselves and/or family and friends of the founders. This is at the earliest stage of a company and is at its riskiest time.
- **Series A Funding:** This is the first round of funding where outside investors would develop ties with the company. In order to qualify for this round of funding, a company has to have a Minimum Viable Product (MVP). At this stage of funding, a company has to show revenues and have a consistent user base which can be further optimized using the funding from the round. The investors of this round are given preferred stock in the company.
- **Series B funding:** This level of funding is about taking the company out of a developmental stage and jump into more growth. The most important factor to get to a Series B round is to show significant improvements using the capital infusion from the previous round of funding. Companies usually use the funds from this round to expand the business and put money into marketing, sales, tech, etc.
- **Series C funding:** At this level, the companies are already a successful business. This is the first of what is called the “later-stage” investments. There are some Venture Capitalist that specialize in later stage investments that start to come in to picture. Also, this level of funding is to set up a company to be acquired or to eventually get an Initial Public Offering (IPOs). An IPO is most likely the most profitable exit for all the early stage investors as the company would now be publicly owned.

References

1. Alexy OT, Block JH, Sandner P, Ter Wal A (2012) Social capital of venture capitalists and start-up funding. *Small Bus Econ* 39:835–851
2. Benjamin GA, Margulis JB (1999) *Angel financing: how to find and invest in private equity*. Wiley, p 336
3. Ester P (2017) *Accelerators in Silicon Valley: building successful startups*. In: *Accelerators in Silicon Valley*. Amsterdam University Press
4. Lander J (2005) *All I need is money how to finance your invention*. Nolo Press, Berkeley, CA, p 320

5. Mason C, Brown R (2014) Entrepreneurial ecosystems and growth-oriented entrepreneurship. Final Report to OECD, Paris
6. Meath P (2020) Funding strategies for life sciences startups in Today's rapidly changing

environment. Life Science Leader (Online). <https://www.lifescienceleader.com/doc/funding-strategies-for-life-sciences-startups-in-today-s-rapidly-changing-environment-0001>

Further Reading

<https://www.idea4invention.com/invention-loans.html>

<https://www.investopedia.com/articles/personal-finance/102015/series-b-c-funding-what-it-all-means-and-how-it-works.asp>

<https://www.investopedia.com/terms/v/venturecapital.asp>

<https://www.fundz.net/what-is-series-a-funding-series-b-funding-and-more#intro>

<https://sbir.nih.gov/about/what-is-sbir-sttr>

<https://sbir.nih.gov/funding>

<https://nvca.org/about-us/what-is-vc/#toggle-id-3>

<https://www.nsf.gov/about/how.jsp>

<https://seedfund.nsf.gov/about/>

INDEX

A

- Adaptive immunity 45, 164, 472
- Adjuvant 35, 36, 61–65, 75, 78, 86, 92, 123, 129, 136, 145–167, 180–211, 235, 240, 247–252, 255, 265, 266, 270, 283, 310, 311, 313–316, 318–329, 356, 363, 368, 380, 383, 386, 387, 399, 431, 472, 489, 492, 517, 520–522
- Angel Investment 532, 533, 535
- Antigen loading 155, 156, 326, 328
- Antigens 15–17, 20–22, 25, 27, 28, 30, 36, 45–49, 52, 55, 59–61, 63–65, 87, 96, 105, 117, 120–123, 146, 147, 150–160, 162–164, 166, 180–190, 192, 195, 199–203, 206–209, 211, 233–235, 239, 248–250, 252, 255, 256, 258–260, 262–266, 270, 284, 295, 296, 304, 309–311, 313–318, 321–328, 339, 340, 342, 345–347, 351, 353, 356, 357, 359–362, 364, 365, 367–370, 380, 382–384, 386, 389, 390, 394, 399, 400, 413, 414, 416, 419–422, 430, 433, 434, 441–443, 451, 453, 457–459, 463, 467, 468, 471–473, 477, 486–491, 493, 499, 506, 520, 521, 523
- Antigen-specific CD8+ T-cell responses 165
- Archaeosome 208, 209, 256, 258–267, 323
- ## B
- B-cell epitope 36, 296, 316–318, 320, 322, 419, 430, 433, 443, 473
- Bilayer fragments 234
- Bioinformatics 5, 6, 10, 13, 48, 49, 54–56, 60, 61, 64, 75, 342, 345, 350, 357, 359, 363, 426, 442, 445, 458, 474
- Biologics 373, 436, 483, 484, 491, 494, 496, 498
- Bioluminescence 285–287, 292, 293
- Biopharmaceutical 95, 96, 187
- Business 96, 506, 530–533, 535–541
- ## C
- Cationic lipid 194
- Cationic polymer 235, 380
- Cell culture 75, 95, 159, 376, 381, 488, 495, 511
- Clostridiosis 457, 458
- Commercialization 12, 530, 536, 537
- Company 4, 11, 96, 101, 192, 326, 506, 510, 512, 516, 517, 529–541
- Computation 10, 418
- Copper-catalyzed alkyne-azide cycloaddition click reaction 36
- Core genome 52, 53
- Cross-presentation 208, 296, 314, 356, 368, 389
- ## D
- Delivery systems 36, 65, 156, 159, 162–164, 271–277, 295, 296, 313, 315, 317, 318, 322, 323, 327, 328, 339, 340, 356, 369, 399
- Design-of-experiment (DoE) 96, 99, 105, 106
- Dialysis 37, 40, 43, 77, 84, 238, 241, 370, 373, 378–380, 384, 390, 393, 395
- Diocetyl dimethylammonium bromide (DODAB) 233–243
- Discovery 12, 150, 166, 187, 397, 484, 493, 508, 535, 539
- DNA vaccine 165, 194, 283, 284, 342, 355–357, 359, 362, 363, 365, 485, 487, 489
- Downstream processing (DSP) 96
- ## E
- Emulsion adjuvants 247, 248, 250–252
- Epitope 4–10, 12, 13, 16, 18–28, 30, 35, 36, 46, 49, 53–55, 58, 59, 61, 63–65, 75, 76, 86, 89, 91, 117, 118, 120, 296, 311, 314–316, 318–324, 326, 389, 391, 399, 413–422, 430–434, 442, 443, 445, 446, 458–468, 471–478
- Epitope prediction 4, 6–8, 45–66, 430, 431, 458–467
- Extrusion 298–301, 303–305

F

Finance 530, 533
 Function 4–6, 8, 23, 30, 53, 54,
 75, 92, 122, 151, 160, 180, 190, 194, 201, 209,
 269, 289, 419, 421, 422, 435, 449–454, 458,
 473, 509, 533

G

Genome 12, 48, 50–53, 61, 75,
 117–119, 286, 426–428, 449, 453
 Glucan 269–279
 Glycolipid 208, 209, 256, 263, 323
 Group A streptococcus (GAS) 27, 28, 36,
 162–166, 296, 316–319, 321, 322, 400, 403, 407

H

Human 9, 16–20, 22–26, 29,
 43, 45, 48–51, 55, 60, 65, 92, 119, 122, 146–150,
 152–154, 157, 160–162, 164–167, 179–211,
 251, 285, 296, 310, 311, 313, 316, 319, 322,
 324, 326, 329, 368, 397, 414, 425, 439, 441,
 443, 449, 450, 474, 483–500, 510, 522, 535
 Hypothetical protein (HP) 452, 454

I

Immune stimulators 146, 151, 310, 325
 Immunization 19–21, 26, 30,
 37, 39, 42, 78, 86, 120, 123, 136, 146, 147, 153,
 154, 163, 186, 190, 202, 207, 208, 260, 262,
 264, 265, 283, 284, 296, 318, 319, 322, 324,
 326, 327, 394, 443
 Immunoadjuvants 234, 235, 328
 Immunogenicity 6, 18, 22, 23, 25–27,
 29, 35, 46, 49, 54, 55, 60, 65, 75, 76, 89, 120,
 129, 136, 137, 146, 155, 183, 185, 203, 205,
 206, 208, 210, 283, 310, 313, 319, 320, 322,
 340, 356, 362, 368, 418, 419, 421, 430, 431,
 436, 458, 468, 490, 491, 495, 496
 Immunoinformatics 21, 54, 55,
 426–428, 433, 457–469, 471, 472, 474
 Immunomodulatory 152, 161, 314
 Innate immunity 45, 146,
 147, 163, 311, 472
 In silico cloning 431
 Inventions 145, 506, 508–514,
 516, 517, 520–522, 529, 532
 Investigational new drug
 (IND) 488, 493–496

L

Lactococcus lactis 399–405, 407, 408
 Licensing 155, 484, 493, 496, 510

Lipopptides 200, 296–298,
 302–304, 316–318, 321, 322
 Lipoplex 357, 361–365
 Liposomes 36, 65, 156–158,
 161–163, 183, 187, 189, 190, 194, 200, 201,
 203, 206, 208, 256, 259–262, 265–267,
 295–306, 318, 319, 322, 323

M

Mammalian cells 95, 119, 159,
 284, 355, 357
 Manufacturing 96, 146, 147, 150, 183,
 188, 264, 310, 413, 485, 488–494, 496, 499,
 516, 519–523, 529, 530
 Microparticles 36, 242, 270, 319
 Model antigen 207, 256,
 264, 316, 326, 384
 Molecular farming 95, 96
 Mucosal vaccine 165
Mycobacterium bovis (Mb) 449–454

N

Nanocapsule vaccine 340, 350, 352, 353
 Nanodisks 234
 Nanoparticles 16, 18, 23, 24,
 36, 65, 150, 162–166, 203, 233, 235, 270–279,
 310, 319, 321, 322, 328, 340, 344, 348–350,
 352, 353, 356, 363, 364, 368, 369, 380, 387, 389
 Nanotechnology 313–319, 328, 340
 National Institutes of Health (NIH) 397,
 535–541
 National Science Foundation
 (NSF) 397, 537–540
 Neural network 3–8, 10, 11, 56,
 57, 416, 418–422, 428, 432, 433, 458, 459, 465
Nicotiana benthamiana 95, 96,
 98, 99, 101, 104–108

O

Oil-in-water (OW) emulsion 65,
 153, 180, 181, 183, 185–188, 192, 194, 195,
 198, 203, 209, 255
 Optical in vivo imaging 283–293
 Ovalbumin 235, 256–260,
 264, 266, 315, 316, 384, 389, 400, 404

P

Particle size 40, 152, 260–262,
 265, 279, 310, 316, 322, 328, 363
 Particulate carrier systems 356
 Patent 151, 506, 508–524,
 529, 532, 533, 535

Pathogens	12, 16, 17, 20, 25, 28, 30, 45, 46, 48, 49, 53–55, 59–61, 64, 119, 121, 122, 145, 146, 150, 151, 160, 165, 179, 180, 184, 191, 192, 194, 198, 255, 269, 309–311, 313, 314, 328, 339, 340, 355, 365, 367, 368, 400, 401, 425–428, 433, 439, 440, 442, 449, 450, 454, 471–474, 477, 486, 487, 493	<i>Staphylococcus aureus</i>	28–30, 62, 163, 207, 208, 400, 439–446
Peptide epitopes	22, 55, 61, 64, 314, 315, 319–322	Startups	529–533, 535, 536, 538–541
Peptides	6–10, 22, 27, 36, 37, 40, 41, 43, 47, 54–58, 61–65, 79, 122, 146, 157, 159, 162, 164, 166, 189, 205, 234, 296, 310, 311, 313–316, 318–326, 328, 367–369, 380, 399, 400, 402, 404–406, 408, 414–419, 421, 430, 432–435, 443, 445, 446, 466–468, 471–477, 486, 489, 490, 521	<i>Streptococcus pyogenes</i>	27, 36, 162, 400
pH-sensitive polymeric nanoparticles	369	Structural biology	20, 442
Pili	193, 407	Structural vaccinology	15, 30, 413–422, 442, 467
Plasmid-launched live-attenuated vaccine (PLLAV)	283–287, 289	Structure-based vaccines	15–30, 441–442
Poly (diallyl dimethyl ammonium chloride) (PDDA)	36, 186, 204, 205, 209, 314, 316, 318, 319, 326, 380	Structures	6, 16–19, 21–24, 27–30, 46, 48, 54, 55, 58, 64, 65, 91, 112, 117, 146, 157, 159, 162, 164, 185, 199, 200, 202, 207, 233, 270, 286, 295, 304, 313, 320, 324, 325, 327, 340, 350, 353, 370, 380, 381, 400, 405, 413, 416, 419, 420, 422, 431, 433–436, 442, 443, 445, 449–454, 458, 459, 461–463, 467–469, 474, 476, 477, 530, 531, 533
Poly (methyl acrylate) (PMA)	36, 65, 162, 234	Subunit vaccine	20, 25, 29, 35, 59–62, 65, 96, 120, 146, 151, 164, 179, 180, 199, 201, 248, 310, 313, 340, 367, 368, 434, 458, 486, 487
Poly (methylmethacrylate) (PMMA)	234	Sulfated lactosyl archaeol (SLA)	209, 255–267
Polymeric NPs	356, 389	Super-types	474, 475
Position specific scoring matrix (PSSM)	415, 418	Surface proteins	16, 26, 27, 62, 63, 157, 159, 400, 440
Promiscuity	475, 476	Surfactant	153–155, 185, 192, 202, 247
Protein expression	96, 99, 120, 132, 133, 137, 347, 375, 487	T	
Protein nanoparticle	24	T-cell epitope	421, 430, 431
R		Transient expression	95, 96
Recombinant antigens	27, 207, 489	Trichosanthin (TCS)	247, 249–252
Regulatory	96, 164, 329, 473, 483–500, 540	Tuberculosis	59, 121, 153, 162, 163, 165, 190, 206, 210, 320, 325, 400, 450
Reporter virus	288, 291	U	
Reverse vaccinology	48–54, 61, 65, 66, 426	U.S. Patent and Trademark Office	519, 522
S		V	
Saponins	158, 161, 162, 187, 189, 199–201, 203, 248, 250–252, 324	Vaccination	19, 27–30, 36, 47, 59, 64, 145, 153, 164, 165, 184, 186, 188–191, 248, 283, 284, 288, 289, 291, 292, 309, 319, 327, 339, 350, 362, 401, 430, 457, 505
Self-assembly	39, 43, 318, 369, 382	Vaccine	4, 15, 35, 46, 75, 96, 118, 145, 179, 233, 255, 270, 295, 309, 339, 399, 413, 426, 440, 449, 457, 471, 483, 505, 519, 537
Silica template	341	candidate	12, 16, 18, 20, 28, 29, 49, 54, 76, 87, 117–138, 163–165, 190, 211, 297, 319, 322, 367, 413, 427, 430, 431, 434, 436, 441, 500, 516
Single immunization	42, 319	delivery	36, 156, 164, 166, 283, 285, 295, 314, 315, 317, 318, 322, 323, 326, 327, 356, 357, 399, 521
Small Business Innovation Research (SBIR)	536–541		
Small Business Technology Transfer (STTR)	536–541		
Solid lipid nanoparticle (SLN)	355–365		

Vaccine (*cont.*)

- delivery system36, 156, 295, 318, 322, 356
- design..... 15, 16, 19–21, 55, 146, 233, 313, 316, 320, 353, 355, 359–361, 365, 414
- technology 12, 47, 339, 506, 520, 522–524

Venture Capital (VC)..... 532–535

Veterinary153, 161, 179–211, 247–252, 355, 449, 450, 510

Veterinary vaccines161, 179–211

Virus-like particles (VLPs)..... 65, 117, 119, 120, 123, 134, 135, 137, 159, 314, 368–370, 372, 373, 376–379, 489, 493, 523

W

World Health Organization (WHO)118, 145, 152, 190, 326, 519, 520, 522

Y

Yellow fever 17D (YF17D)283, 285–287, 291